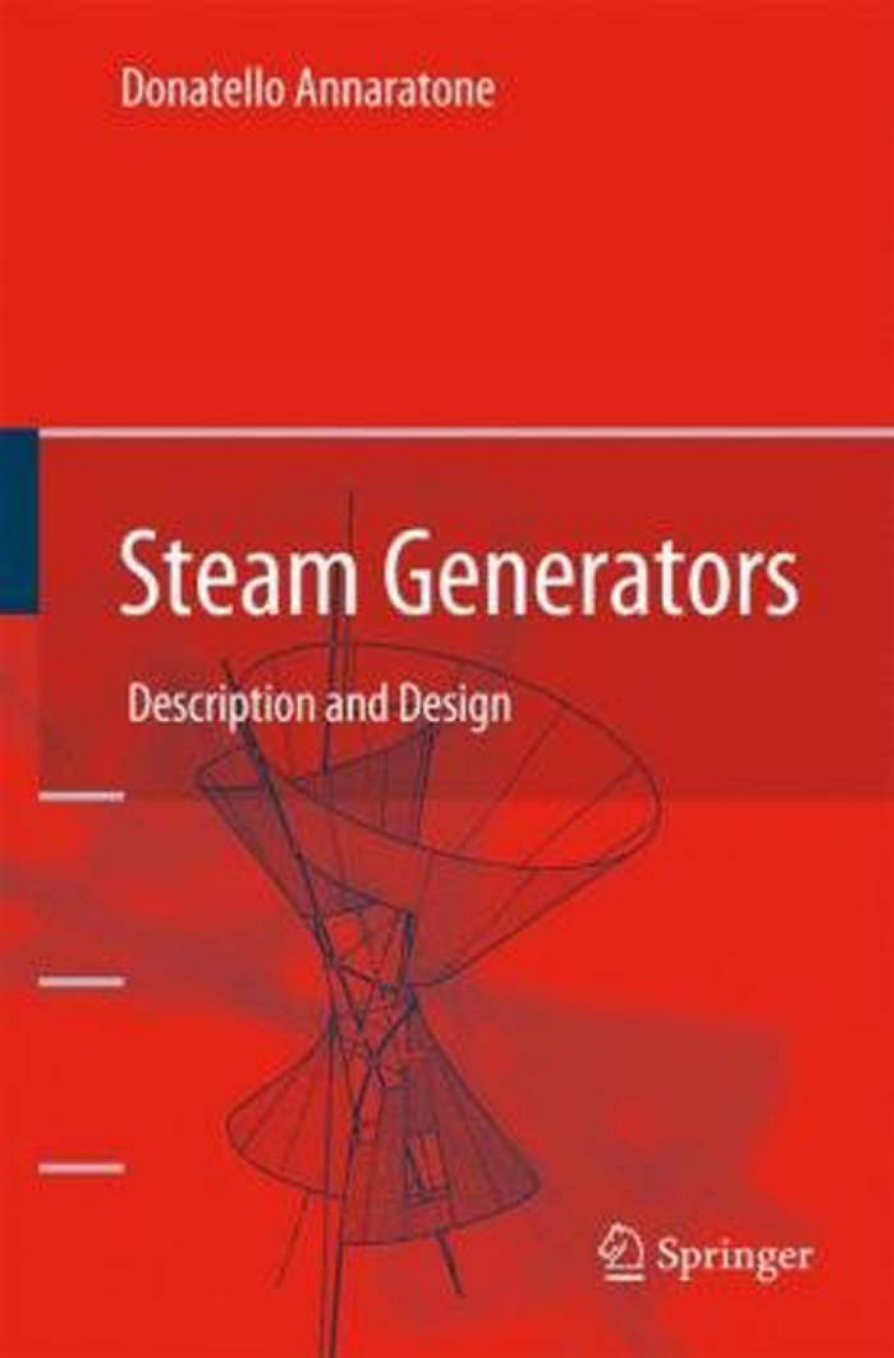
Donatello Annaratone

Steam Generators

Description and Design



Springer

Steam Generators

This page intentionally left blank

Donatello Annaratone

Steam Generators

Description and Design

Springer

Prof. Donatello Annaratone
Via Ceradini 14
20129 Milano
Italy
donatello@annaratone.eu

ISBN: 978-3-540-77714-4 e-ISBN: 978-3-540-77715-1

Library of Congress Control Number: 2008924058

© 2008 Springer-Verlag Berlin Heidelberg

This work is subject to copyright. All rights are reserved, whether the whole or part of the material is concerned, specifically the rights of translation, reprinting, reuse of illustrations, recitation, broadcasting, reproduction on microfilm or in any other way, and storage in data banks. Duplication of this publication or parts thereof is permitted only under the provisions of the German Copyright Law of September 9, 1965, in its current version, and permission for use must always be obtained from Springer. Violations are liable to prosecution under the German Copyright Law.

The use of general descriptive names, registered names, trademarks, etc. in this publication does not imply, even in the absence of a specific statement, that such names are exempt from the relevant protective laws and regulations and therefore free for general use.

Cover design: eStudio Calamar S.L.

Printed on acid-free paper

9 8 7 6 5 4 3 2 1

springer.com

Preface

The content of this book originates from 35 years of teaching “steam generators” to graduate students at the Politecnico of Milan, Milan, Italy, and from 45 years of professional activity in this area – first in industry and then as founder of a design and consulting company.

Before discussing the content of the textbook, I would like to present the rationale for the title. Boilers are machines consisting of steam-generating tubes only, that is, of internal and external tubes where water is transformed into saturated steam. Steam generators – or, simply, generators – indicate machines equipped with one or more of the following components: superheaters, reheaters, economizers, and air heaters – besides the steam-generating tubes that make up the boiler. Finally, those machines with tubes, where instead of water, a diathermic fluid flows inside, are also called boilers, for their construction is similar to that of the latter.

The above notwithstanding, the term “boiler” is used even when hot water or superheated water is produced instead of steam.

Large systems designed to produce electricity have all components indicated above in addition to the boiler. In medium size systems, some of these components are always present, whereas in small ones a regenerator is frequently and appropriately included. It is therefore justified to use “steam generators” as title, because it best matches the actual makeup of these systems.

The textbook is divided into three sections. In the first section, the different types of generators are described from a structural and functional point of view by examining them globally and then considering their various components. The different fuels being used are discussed as well. The second section is dedicated to design issues and focuses on combustion, heat transfer, generator efficiency, and fluid dynamics. Finally, the third section discusses more advanced topics and includes an Appendix.

The author particularly focuses on three fundamental design issues, that is, the physical characteristics of air and flue gas, the heat transfer in its entirety, and the computation of natural circulation. The author introduces original computation methods for these topics; this simplifies calculations and is especially useful for the development of programs, such as the ones written by the author.

- Chapter 1 examines the different possible classifications of generators, based on employed fuel, heat transfer, circulation, water content, and furnace pressure.
- Chapter 2 describes the different kinds of water-tube generators: convection generators, radiation generators, and waste-heat generators.
- Chapter 3 analyzes the different components of water-tube generators, including tube bending, tube expanding, and the danger of bursts in tubes.
- Chapter 4 deals with smoke-tube boilers, whereas Chap. 5 discusses diathermic fluid boilers.
- Chapter 6 focuses on the different fuels being used.
- Chapter 7 focuses on combustion. Specifically, the criteria to compute the required air and the resulting flue gas are discussed after a description of burners and grate stockers. The equations to compute the physical characteristics of both air and flue gas are illustrated.
- Chapter 8 is entirely devoted to heat transfer. This includes the overall heat transfer coefficient and the mean logarithmic temperature difference, the heat transfer in the furnace of water-tube generators and in the flue of smoke-tube boilers, all heat transfer coefficients relative to water, steam and diathermic fluids inside the tubes, as well as the ones relative to air and flue gas inside and outside the tubes. In addition, the heat transfer by radiation of the flue gas is also considered. Finally, the chapter examines the computation criteria for the outlet temperature of flue gas from a tube bank. This includes a comparison between in-line and staggered arrangements of tubes and the ideal layout of tubes in the second and third passage of smoke-tube boilers.
- Chapter 9 focuses on generator efficiency, including the different heat losses and ways to determine efficiency during runtime.
- Chapter 10 is about fluid dynamics. It focuses on distributed and concentrated pressure drops in tubes and ducts, as well as on pressure drops through the tube banks. This includes a description of pumps and fans and a few comments on chimneys. Special attention is given to natural circulation by presenting the required calculation criteria in detail.
- Chapter 11 discusses possible optimization criteria by considering a few significant case studies, such as a water-tube boiler, an air heater, an optimized surface division between the steam-generating bank of the generator and the heat regenerator, and a waste-heat generator.
- Chapter 12 contains a number of programming examples. The programs are in reference to a water-tube generator, a smoke-tube generator, a waste-heat generator, and an air heater. In addition, the author includes the computation of natural circulation in a simple circuit.
- The Appendix includes an in-depth analysis of a few topics discussed in previous chapters. A practically exact computation method of a steam-generating tube bank is presented together with an analysis on parallel flow and counterflow in tube coils and air heaters. Finally, computation methods for finned tubes are introduced.

In conclusion, the author has developed about 80 programs, ranging from simple to complex ones, based on the computation criteria described in the textbook. Some of these programs are used for the calculation examples in Chap. 12.

October 2, 2007 *Milan*

This page intentionally left blank

Notations

$A =$ air per fuel unit (kg/kg, $\mathrm{kg/Nm^3}$, $\mathrm{Nm^3/kg}$, $\mathrm{Nm^3/Nm^3}$), cross-sectional area ($\mathrm{m^2}$)
$B =$ black level
$C =$ carbon mass percentage (%), cost (€,$)
$c =$ specific heat (J/kgK), unitary cost
$CM =$ combustible matter (%)
$D,\ d =$ diameter (m)
$E =$ energy (J), fin efficiency
$e =$ excess air (%)
$F =$ force (N)
$G =$ flue gas per fuel unit (kg/kg, $\mathrm{kg/Nm^3}$, $\mathrm{Nm^3/kg}$, $\mathrm{Nm^3/Nm^3}$), mass velocity $(\mathrm{kg/m^2 s})$
$H =$ heat value (kJ/kg), hydrogen mass percentage (%), height (m)
$h =$ enthalpy (kJ/kg)
$k =$ thermal conductivity (W/mK)
$L =$ heat loss (%)
$l =$ length (m)
$M =$ mass (kg), mass flow rate (kg/s)
$m =$ moisture (%)
$N =$ nitrogen mass percentage (%), number of rows
$n =$ air index
$O =$ oxygen mass percentage (%)
$P =$ power (W, kW), porosity, factor for natural circulation (Pa)
$p =$ pressure (bar, Pa)
$Q =$ volumetric flow rate ($\mathrm{m^3/s}$)
$q =$ heat (kJ), heat per time unit (W, kW), thermal flux $(\mathrm{W/m^2},\ \mathrm{kW/m^2})$, thermal load $(\mathrm{kW/m^2},\ \mathrm{kW/m^3})$
$R =$ solid residues (%), circulation ratio, thermal resistance $(\mathrm{m^2 K/W})$
$r =$ radius (m)
$S =$ surface $(\mathrm{m^2})$
$s =$ pitch (m)

T = absolute temperature (K)
t = temperature ($^\circ$C)
U = overall heat transfer coefficient ($\mathrm{W/m^2K}$)
V = velocity (m/s), volume ($\mathrm{m^3}$), volatile matter (%), financial value (€, $)
v = specific volume ($\mathrm{m^3/kg}$)
x = thickness (m)
z = geodetic height (m)
Nu = number of Nusselt
Pr = number of Prandtl
Re = number of Reynolds
Δp = pressure drop (bar, Pa)
Δt = temperature difference ($^\circ$C)
Δz = geodetic height difference (m)
α = heat transfer coefficient ($\mathrm{W/m^2K}$)
ε = emissivity, relative roughness, strain
η = efficiency (%)
λ = friction factor
μ = dynamic viscosity (kg/ms)
ν = kinematic viscosity ($\mathrm{m^2/s}$, cS, $^\circ$E, SUS)
ρ = density ($\mathrm{kg/m^3}$), relative density (dimensionless)
σ = stress ($\mathrm{N/mm^2}$, MPa), constant of Stefan Boltzmann ($\mathrm{W/m^2K^4}$)
θ = time (s)
ς = factor for concentrated pressure drop
ω = angle ($^\circ$)

Superscript (for heat transfer)
$'$ = heating fluid
$''$ = heated fluid

Subscript
a = air, axial, arrangement
ad = adiabatic
b = bulk, bottom, bank, boiler
c = convection, carbon dioxide, circumferential, chimney
d = depth, drainage, downcomer, distributed
e = exit, external, electricity
f = film, fuel, furnace, flame, fix, fin
g = flue gas, gross
h = hydrogen oxide (steam), hole, heat
i = inside
in = input
l = longitudinal
m = mass, mean, miscellaneous, water–steam mix
n = net, nitrogen
o = outside, oxygen

ou = output
p = isobaric, plate, plant
r = radiation, radial, raiser, regenerator
s = steam, surface, sensible
t = tube, theoretic, transverse, total
v = volume
y = yield
w = water, wall
0 = normal conditions (for air and flue gas) or room conditions
1 = inlet (for heating or heated fluid)
2 = outlet (for heating or heated fluid)

This page intentionally left blank

Contents

1 Generator Classification 1
1.1 Classification According to the Employed Fuel 1
1.2 Classification Based on Heat Transfer 4
1.3 Classification According to Circulation 5
1.4 Classification According to Water Content 9
1.5 Classification According to Furnace Pressure 10

2 Water-Tube Generators 13
2.1 Convection Generators 13
2.2 Radiation Generators 17
2.3 Waste-Heat Generators 25

3 Components of Water-Tube Generators 29
3.1 Furnace 29
3.2 Radiated Tube Wall 33
3.3 Drum 41
3.4 Steam-Generating Tube Bank 47
3.5 Tube Bending 51
3.6 Tube Expanding 56
3.7 Superheater and Reheater 61
3.8 Economizer 70
3.9 Air Heater 75
3.10 The Danger of Tube Bursting 79
3.11 Boiler Settings 81

4 Smoke-Tube Boilers 87
4.1 Construction Characteristics 87
4.2 Running Characteristics 94
4.3 Rationalization Criteria for Construction 97

5 Diathermic Fluid Boilers 103
5.1 Employed Fluids 103
5.2 Constructive and Functional Characteristics 104
5.3 Advantages and Disadvantages in Comparison with Water-Tube Boilers 108

6 Fuels 111
6.1 Solid Fuels 111
6.2 Liquid Fuels 116
6.3 Gaseous Fuels 124

7 Combustion 129
7.1 Burners 129
7.2 Flame Characteristics 137
7.3 Grates 143
7.4 Combustion Chemistry 145
7.5 Combustion Air 147
7.6 Flue Gas 151
7.7 $|CO_2|$ and Unburned CO 157
7.8 Test of the Air Index During Runtime 162
7.9 Physical Characteristics of Air and Flue Gas 171
7.9.1 Density 171
7.9.2 Specific Isobaric Heat 172
7.9.3 Enthalpy 177
7.9.4 Thermal Conductivity 179
7.9.5 Dynamic Viscosity 183

8 Heat Transfer 187
8.1 General Considerations 187
8.2 Overall Heat Transfer Coefficient 188
8.3 Mean Logarithmic Temperature Difference 194
8.4 Heat Transfer in the Furnace of Water-Tube Generators and Diathermic Fluid Boilers 198
8.5 Heat Transfer Coefficient of Water and Steam 217
8.6 Heat Transfer Coefficient of Flue Gas and Air Inside the Tubes 225
8.7 Heat Transfer in the Flue of the Smoke-Tube Boilers 228
8.8 Heat-Transfer Coefficient of Flue Gas and Air Hitting a Tube Bank 235
8.9 Heat Radiation from Flue Gas 241
8.10 Heat Transfer Coefficient of Diathermic Fluids 250
8.11 Heat Transfer in Economizers and Air Heaters 252
8.12 Exit Gas Temperature from a Tube Bank or a Heat Regenerator . . . 255
8.13 Comparison Between Arrangement with Inline and Staggered Tubes 263
8.14 Tube Distribution in the Passages of the Smoke-Tube Boiler 265

9 Generator Efficiency 269
9.1 Efficiency Definition 269
9.2 Heat Loss by Unburned Fuel 276
9.3 Heat Loss by Unburned Carbon Monoxide 277
9.4 Loss by Sensible Heat of the Flue Gas 281
9.5 Heat Loss by External Radiation 284
9.6 Miscellaneous Heat Losses 286
9.7 Generator Efficiency Test 287

10 Fluid Dynamics 291
10.1 Distributed Pressure Drops in Tubes and in Ducts 291
10.2 Concentrated Pressure Drops 307
10.3 Pressure Drop Through the Tube Banks 314
10.4 Pressure Drop in Special Equipments 319
10.5 Pumps, Fans, and Chimneys 320
10.6 Natural Circulation 328

11 Optimization Criteria 351
11.1 General Information on Optimization of Convection Generators . . . 351
11.2 External Boiler Optimization 352
11.3 External Optimization of Air Heaters 360
11.4 Optimal Distribution of the Surfaces of the Boiler Tube Bank and of the Heat Regenerator 369
11.5 Optimized Sizing of the Waste-Heat Generator 374

12 Computation Examples 383
12.1 General Considerations 383
12.2 Water-Tube Generator 383
12.3 Smoke-Tube Generator 388
12.4 Waste-Heat Generator 391
12.5 Air Heater 396
12.6 Natural Circulation 398

Appendix 401
A.1 Accurate Calculation of the Heat Exchange in the Steam-Generating Tube Bank 401
A.2 Accurate Calculation of the Heat Exchange in both Superheaters and Economizers 404
A.3 Accurate Calculation of the Heat Exchange in the Air Heater 406
A.4 Finned Tubes 410

Bibliography 419

Index 423

This page intentionally left blank

Chapter 1
Generator Classification

1.1 Classification According to the Employed Fuel

Based on the employed fuel, generators may be classified into fuel oil, natural gas, coal (or lignite), and low-grade fuel generators.

Fuel oil generators of any kind and power are built. These generators require the installation of stocking as well as service tanks, where the oil is heated electrically for starting and through steaming at $30/40^{\circ}$C, and a pumping and heating plant to reduce viscosity at the required value to obtain good atomizing.

Viscosity varies considerably from 3–4°E at 50°C ($\approx$ 140–180 SUS at 100°F) for low-viscosity fuels up to 50°E at 50°C ($\approx$ 3500 SUS at 100°F) and more for high-viscosity fuels used in generators for thermoelectric power plants. The viscosity of oils used industrially as fuels usually goes from 25 to 50°E at 50°C ($\approx$ 1900–3500 SUS at 100°F).

Good atomizing with burners without the intervention of steam requires viscosity up to 3–4°E (100–140 SUS). In the case of steam atomizing, good results may be obtained with a viscosity of 7–10°E (240–350 SUS). Therefore, it is necessary to heat the fuel oil to a temperature that varies from 80 to 100°C. Big units are started using low-viscosity oils or gas oil.

The positioning of burners is typically horizontal. They can also be placed vertically or tilted, and in the case of big units, tiltable burners are employed to be able to vary the radiation of heat in the furnace, that is, when it is required because of output variations.

The turbulence of the air exiting the burner is quite important to obtain good combustion and to adjust the length of the flame to avoid damage of the refractory material of the burner housing with a flame that is too short, as well as the impact on refractory walls or tube walls with a flame that is too long. To this extent, the correct sizing of the furnace is crucial to ensure complete combustion before the gas exits and to avoid the impact of the flame on the walls through correct plan size dimensions.

In the case of natural gas steam generators, the latter is fed with the pressure of a few thousand pascals (Pa) (excluding special high-pressure burners with sucked

D. Annaratone, *Steam Generators*, DOI: 10.1007/978-3-540-77715-1_1,
© Springer-Verlag Berlin Heidelberg 2008

air). Therefore, it must be decompressed before it is led to the burners by the gas network. It is very important to obtain an efficient mix between air and gas.

The positioning of the burners is similar to that of fuel oil burners. Burners using oil or natural gas are often employed to be able to switch from one fuel to the other depending on availability and seasonal costs. In this case, the emissivity of the flame with combustion by fuel oil differs from that by natural gas. The heat transmission by radiation differs, as well, and so do the temperature of flue gas at the exit of the furnace and the thermodynamic conditions under which the heat exchange occurs in the convection section of the boiler, as well as in the superheater. In other words, to use both fuels it may be necessary to adopt certain measures to be able to modify the exchange conditions that will lead to the desired results in both instances. At any rate, fuel oil and natural gas are most easily interchangeable fuels, and this possibility is used the most nowadays.

In the case of natural gas, the danger of bursts is quite high, considering that this gas easily produces an explosive mix when in contact with air. This must be factored in by planning for adequate protection machinery.

Natural gas is not the only gas used for combustion even though it is the most common one. Among gas generators, we cannot forget the ones using, for example, refinery gas, coke oven gas, and blast furnace gas. The use of such fuels is obviously limited to those industries developing them as a by-product of their production processes.

In the case of coal (or lignite) generators, the coal is burned on a grate or in special burners after pulverization. In big units, it is burned as pulverized coal, frequently as an alternative to fuel oil or natural gas. The use of pulverized coal is limited to big units because these justify the costly installation of the necessary stocking, pulverization, and transportation systems.

In generators using pulverized coal, the charging hoppers fed by conveyor belts in turn feed the mills through a metering device (see Fig. 1.1), where the coal is thinly pulverized and carried to the burners through pumped air. In the furnace, secondary combustion air is added to primary air.

Combustion can also occur in a cyclone burner before the entrance into the furnace. In this case, pulverization is not required to be as thin as before.

The sizing of the furnace is very important to ensure that combustion is completed in the furnace. This depends on numerous factors, such as the turbulence of the air-pulverized coal mix at the inlet of the furnace, the position and tilt of the burners, the speed of the mix through the furnace, and the time it takes the pulverized coal to burn. The latter is in turn influenced by a number of factors and diminishes with the increase in excess air and the reduction of volatile matter. Good combustion requires the reduction of moisture in the pulverized coal and the heating of the air.

As far as the ashes, the furnace is designed with a hopper for collection in the lower part. The ashes may be scavenged in solid or melted state. In the first case, through cooling obtained through water pipes displaced as grates that solidify them; in the second case, by letting the ashes flow along the walls into a cooling container where water is kept stirring and where they are scavenged through mechanical means (conveyor belts) or pneumatic means.

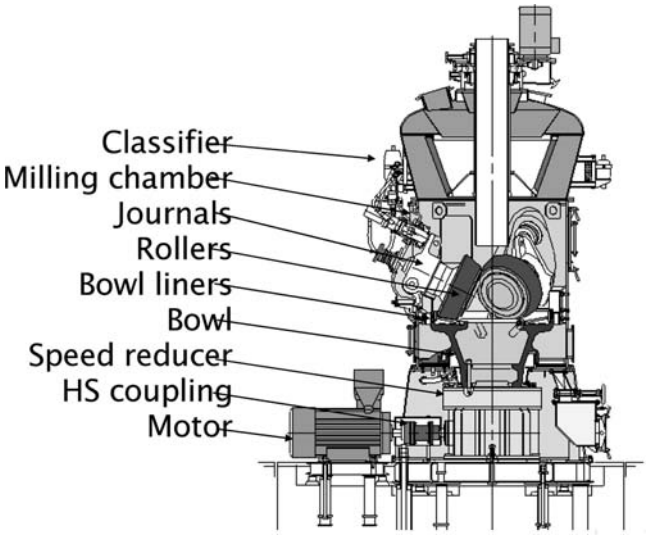


Fig. 1.1 Mill for coal pulverizing (Courtesy of Alstom)

As pointed out earlier, big generators are frequently designed to work with fuel oil, natural gas, or pulverized coal to ensure performance even when it becomes necessary or convenient to abandon one or the other fuel due to cost- or procurement-related problems. In that case, the adaptability problems of the generator to the different fuels increase with respect to the simple combustion of fuel oil and natural gas, given the combustion characteristics of coal that are sensibly different from the other two.

The dimensions of the furnace must be greater than those necessary for fuel oil and natural gas to ensure correct combustion of the coal. Given equal inlet heat in the furnace, the amount of flue gas differs in the two cases. Thus, the amount of inlet heat per mass unit of flue gas is different, as well. All this impacts the exit temperature of the flue gas from the furnace and the thermal exchange in the superheater following the furnace along the route of the flue gas. These differences must be eliminated through adequate structural measures, such as the recirculation of flue gas that is partially taken at the end of the generator and reintroduced into the furnace. We will return to this later on.

Generators using low-grade fuel generally burn it on grates. In fact, excluding special burners for the combustion of saw dust and low-grade gases, all solid low-grade fuels are burnt on grates. Of course, these are by-products of special production processes, thus they are only employed in plants that produce them in-house. By comparison, they are grape husk (by-product of the processing of grapes during production of alcohol), olive husk (by-product during the processing of olives), wooden shavings or saw dust, bagasse (by-product during the processing of sugar cane), and rice husk (by-product of rice polishing).

Moreover, it is worth mentioning the generators used to burn urban waste. The double result of eliminating it while producing steam or superheated water generally

allocated for the heating of urban homes is achieved. There are also examples of electricity production.

The grate is placed in the lower part of the furnace, or in the pre-furnace, if the presence of extended walls of refractory material that re-irradiate the fuel bed is required for correct combustion. A huge problem caused by the combustion of solid low-grade fuels is the evacuation of the high amount of ashes produced. Generally, the ashes are collected in water containers and then eliminated either hydraulically or mechanically through conveyor belts. The low-heat value of these fuels and the deriving high volumes of gas, compared to the combustion of high-grade fuels, require certain sizing criteria of the generator as far as the volume of the furnace, the cross-sectional passage areas of gas, and so on.

Finally, it is worth noting that these generators using production residues are not expected to deliver high generator efficiency, given the predominance of the installation cost during evaluation of the maximum economic goal to achieve.

1.2 Classification Based on Heat Transfer

The generators classified according to heat transfer in the boiler may be characterized by convection, radiation, or indirect heating.

First of all, note that boiler is understood to be the bulk of steam-generating tubes in its entirety, that is, the tubes where the transformation of water into saturated steam takes place. Therefore, the economizer and air heater, as well as the potential superheater and reheater, are included in the steam generator but are not part of the boiler. From this point of view, there are generators that may be correctly called radiation generators. Instead, it would be wrong to speak of convection generators, given the fact that in all generators any smaller or greater amount of heat will be transferred to the boiler through radiation.

First of all, in the furnace the heat is transmitted by radiation only (or predominantly by radiation, as is the case in the flues of smoke-tube boilers). Furthermore, even inside the bank of steam-generating tubes where the heat is mainly transmitted by convection, a part of it is transmitted by radiation from the gas itself, as described in Chap. 8 (not to be ignored if the flue gas is still very hot).

Generally, in radiation generators heat is totally or predominantly transferred through radiation, whereas in convection generators heat is mainly transmitted through convection. This is a somewhat artificial classification that aims at distinguishing some generators from others from a structural and thermodynamic point of view.

Convection generators are smoke-tube generators and most water-tube generators of small and medium power where the bank of steam-generating tubes is important in terms of heat exchange.

The radiation generators are powerful units where the steam-generating tubes are located only on the walls of the furnace, or, in some cases, there is a modest bank

of steam-generating tubes. In the first instance, it is strictly a radiation generator, in the second instance it is still an acceptable definition, given the predominance of radiated heat into the furnace.

In big units, the heat is transferred to the steam-generating tubes mainly or entirely through radiation for the following reasons. The air temperature is quite high and contributes to a temperature increase produced by combustion. Consequently, the amount of radiated heat goes up. On the other hand, these generators work under great pressure so that the heat of vaporization is rather low. The surface of the screens in the furnace is therefore sufficient to absorb all the heat required to transform the water into saturated steam. Sometimes there is excess surface and part of the furnace is screened by tubes of the superheater, as we shall see later on.

Finally, waste-heat generators cause the cooling of warm gas coming from an external source (open-hearth furnaces, glass furnaces, diesel engines, gas turbines, etc.). They can have both smoke and water tubes. In the latter case, the boiler can have a superheater in front and an economizer after it. The absence of the furnace and of the radiation from a flame is typical of these generators. Therefore, the heat is transmitted entirely by convection except for the heat radiated by gas (a modest quantity given that flue gas is usually warm but not hot).

Diathermic fluid boilers belong to the category of generators by indirect heat. Made of a furnace screened by tubes and a convection bank, there is a special fluid instead of water flowing inside it and warming up; upon leaving the boiler, it enters a heat exchanger where it warms up the water or transforms it into steam. After this cooling process, the fluid re-enters the boiler to be heated again. The nature of the fluid and the characteristics of the boiler will be discussed in Chap. 5. These fluids are heated up under atmospheric pressure in contrast to water. From a certain perspective and given the structural features, these boilers could be viewed as convection boilers. In terms of classification, though, note that the transmission of heat to the water occurs through an intermediate vector. Thus, the name indirect heating adopted for these boilers.

1.3 Classification According to Circulation

Based on the type of circulation, there are natural circulation generators, assisted circulation generators, and forced circulation generators.

In the first case, the circulation of water and of the water–steam mix (in the steam-generating tubes) occurs naturally. The specific conditions for this process to take place will be discussed in Chap. 10 on this topic. For now, it suffices to say that the circulation takes place due to the difference in density of warm water leaving the drum and feeding the lower headers of the boiler and the density of the water–steam mix returning to the drum through the steam-generating tubes and the upper headers.

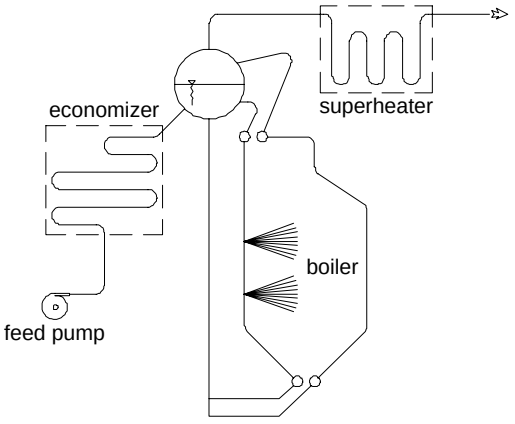


Fig. 1.2 Generator with natural circulation

The boiler is a closed circuit linked to the drum located in the highest position. The connection tubes of the potential economizer through which the pumped water is heated are also linked to the drum. In addition, the tubes carrying the saturated steam to the potential superheater start from the drum as well (see Fig. 1.2). In the absence of the economizer, the feed pump directly leads the water into the drum. In the absence of a superheater, the saturated steam goes to use right away. All generators of small and medium power and a percentage of superpower generators have natural circulation.

The generators with assisted circulation do not differ from the previous ones from a structural point of view, except for the fact that circulation in the tubes of the boiler does not occur naturally but through the help of pumps instead (see Fig. 1.3). Even in this case, the boiler consists of a closed circuit. The pump intervening with its head added to the head between the upper drum and the lower headers linked to the steam-generating tubes facilitates the circulation of water and the mix of water and steam in the circuit. This will lead to the correct functioning of the boiler, even if

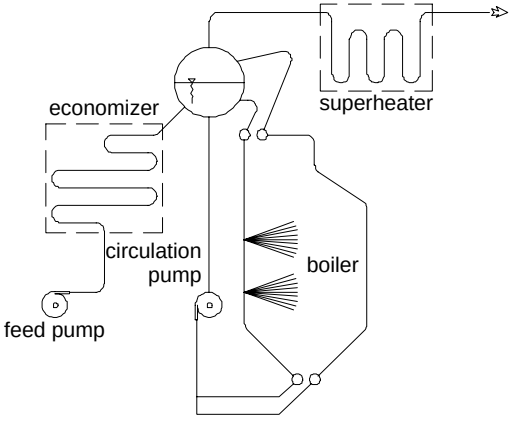


Fig. 1.3 Generator with assisted circulation

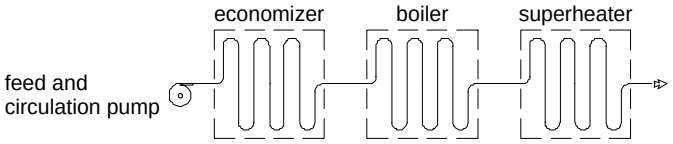


Fig. 1.4 Generators with forced circulation

the difference between the density of steam and water is small, as is the case under high pressure and as will be explained in more detail later on.

In generators with forced circulation, the pumped water is heated. Then it evaporates until the steam is superheated through a single circuit. Therefore, these are called one-through generators. In contrast to generators with natural and assisted circulation, the boiler consists of an open circuit preceded by the economizer and followed by the superheater (see Fig. 1.4). The drum is absent. With natural and assisted circulation, a huge quantity of water circulates, which is only partially transformed into steam, as will be explained later on. Instead, in the forced circulation generator, the feed pump coincides with the circulation pump and introduces the water required for the requested output, and the water is transformed into superheated steam, according to the specifications through the economizer, the boiler, and the superheater.

The necessity to abandon natural circulation in favor of assisted or forced circulation becomes real at high pressure, and this explains why all small- and medium-powered generators under low or medium pressure have natural circulation. In fact, natural circulation originates from the difference in density between the warm water in the downcomers (if the downcomers are hit by flue gas, there will be a mix of water and steam with low percentage of steam, but this will not be the case in big units) and the mix of water and steam in the steam-generating tubes. This difference decreases as the pressure increases until it disappears in correspondence of critical pressure. Figure 1.5 shows the ratio between the density of water and steam

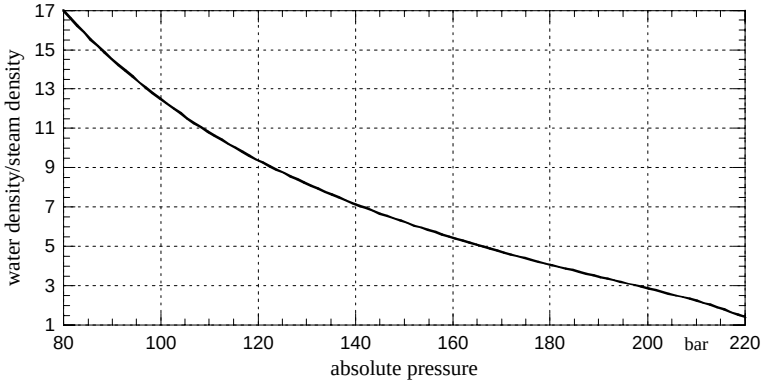


Fig. 1.5 Ratio between water density and steam density

between 80 and 220 bar. Beyond a certain level of pressure, assisted or forced circulation must replace the natural one. Generally, natural circulation is abandoned for pressures above 160 bar even though there are generators with natural circulation working at 180 bar. Some designers move to assisted circulation for pressure above 130 bar.

Assisted circulation has the following advantages. It provides the builder with more leeway as far as tube diameter, as well as the positioning of tube walls, their height, and so on. Natural circulation requires certain heads between drum and lower headers. Consequently, boilers will be narrow and tall. This greater freedom of assisted circulation generators makes it possible to design very compact units. The presence of circulation pumps makes the generator very flexible as far as quick starting and compensation for variable loads.

Moreover, it is possible to factor in more efficient steam dryers in the drum. They cause a greater pressure drop that may be neglected due to the presence of pumps. This leads to a better water-vapor ratio. The pumps also activate circulation during the starting process eliminating the danger of heat strokes and avoiding the build up of steam film on the surface of the tube that would cause it to superheat. Finally, the possibility to use tubes of smaller diameter reduces the danger in case of bursts and produces a cost reduction.

These are some of the disadvantages. Tubes with a small diameter cost less but also carry less water mass in the boiler. This leads to some instability during load variations, unless there are quite sensitive and quick automatic, hence expensive checks. In addition, these tubes require highly purified water.

Circulation pumps are responsible for greater setup and running costs, and given the fact that the water is at high temperature and pressure, they are costly and require attentive and frequent maintenance. Considering that breakdown is not admissible because it would stop the plant, there are usually back-up pumps, as well, and that necessarily increases the total cost of the plant.

If assisted circulation provides greater design flexibility on the one hand, on the other it may cause design problems to ensure the desired circulation in the different parallel circuits is fed by the pumps according to specifications.

As pointed out earlier, forced circulation does not include water recirculation, as is the case with both natural and assisted circulation. All the water entering the tubes is transformed into steam under the expected conditions.

Small diameter tubes are used, and high speed of both water–steam mix and steam is kept up to prevent superheating of the tubes and the deriving bursts where the cooling action of the water is missing. In the steam-generating tubes of well-designed natural and assisted circulation generators, the water is always present because the circulating water exceeds the produced steam.

The advantages with respect to other types of boilers are as follows:

- absence of a pressure limit, hence the design for hypercritical pressure;
- elimination of the drum and its deriving cost;
- elimination of downcomers and return tubes;
- fast lineup of steady-state condition.

The disadvantages, or rather the complications, are as follows:

- In generators with natural or assisted circulation, the sludge left by the water is removed by the drum. In this case, given that the drum is missing, the sludge must be removed by the tubes instead, and that is more complicated.
- These generators require extremely sensitive check and tuning systems.
- The temperature of the superheated steam varies quickly and sensibly upon load variations. It is worth recalling the danger of very fast evaporation of the water under reduced load, as well as the superheating and bursting of the tubes. Finally, in the area of passage from water to steam, the tube is vulnerable to corrosion.

As will be discussed in more detail further on, in diathermic fluid boilers, circulation is forced, given the necessity to keep the speed of the fluid high to prevent undesirable phenomena in the fluid and to guarantee efficient cooling of the tubes.

1.4 Classification According to Water Content

Based on the ratio between water content and heated surface, generators can be classified into high, medium, and low water content generators.

High water content generators hold between 50 and 100 kg of water for m^2 of heated surface. They allow relatively rapid starting and are not exceedingly sensitive to flame irregularities. Considering the water mass, in a way they work as steam accumulators. The smoke-tube boilers belong to this category.

The medium water mass generators hold between 20 and 50 kg water for m^2 of heated surface. They are more flexible but also more sensitive to irregularities of the flames. Variations in requested steam must rapidly be matched by variations in burnt fuel given the modest heat accumulation in the water. More accurate tuning and increased surveillance are therefore necessary during runtime. The treatment of water must be pushed further, particularly if the pressure is high. Single block, low power, transportable convection water-tube generators belong to this category.

Small water content generators have similar characteristics, fast starting time and specific requirements in terms of tuning and treatment of water. The biggest convection units and the big radiation units belong to this category.

In the case of large water content, a reserve of heat to fulfil sudden requests of steam is available, but this possibility is not to be overestimated.

The enthalpy and the density of the water at maximum allowable running pressure are indicated with h'_w and ρ'_w, respectively. Moreover, h''_w and h''_s will be the enthalpy of the water and the steam under minimum running pressure, respectively. β indicates the quantity of steam developed by $1\,m^3$ of water going from maximum to minimum pressure.

Thus,

$$\beta = \frac{h'_w - h''_w}{h''_s - h''_w}\rho'_w \tag{1.1}$$

If, for example, at $p' = 14$ bar and $p'' = 9$ bar and therefore $h'_w = 830.08\,\text{kJ/kg}$, $\rho'_w = 870.4\,\text{kg/m}^3$, $h''_w = 642.64\,\text{kJ/kg}$, and $h''_s = 2772.1\,\text{kJ/kg}$, then $\beta = 37.5\,\text{kg/m}^3$.

Let us assume a smoke-tube boiler filled with 100 kg of water for m^2 of heated surface. The boiler produces $44\,\text{kg/m}^2$ of steam. This value corresponds to specific output of these kinds of boilers. Based on the value of β and with reference to $1\,\text{m}^2$ of heated surface, $0.1 \times 37.5 = 3.75\,\text{kg/m}^2$ of steam are freed that represent 8.5% of output. Note that even though the maximum value of water content $(100\,\text{kg/m}^2)$ and a considerable reduction of pressure (5 bar) were factored in, the increase in production amounts to only 8.5%.

Finally, note that the calculation shown above is based on the assumption that the boiler is filled with water up to the normal level. In reality, as we shall discuss in Chap. 4, the boiler contains a mix of water and steam. Actually, only the water contributes to free the steam, and this is why the increase in production is definitely lower than the computed one.

1.5 Classification According to Furnace Pressure

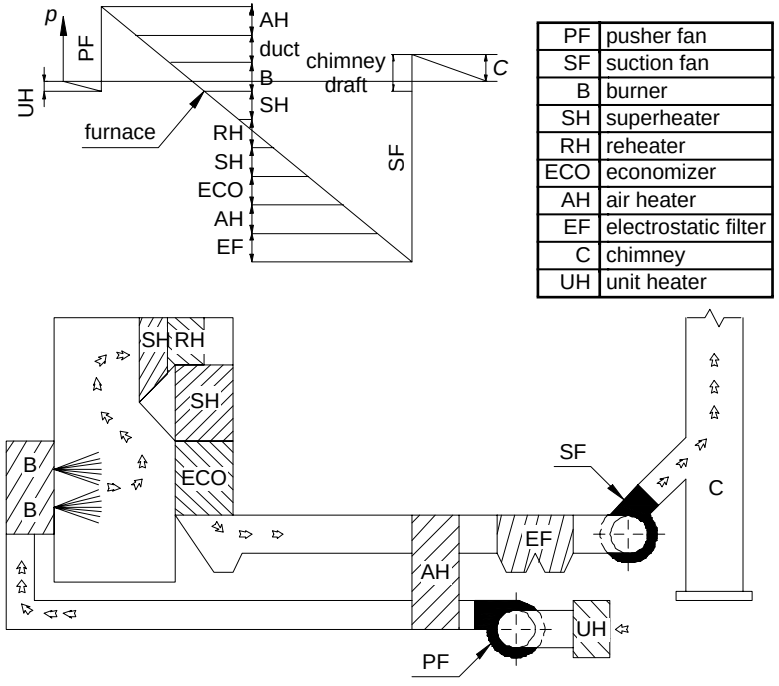
Generators may be classified as generators with a depression furnace and as pressurized generators. Initially, all generators had a depression furnace and worked through natural draught. Due to the chimney, a depression formed at its base. It would provoke the suction of flue gas from the furnace through the tube banks.

The increase in larger generators meant pressure drops of such high entity to make runtime through natural draught impossible. This increase in pressure drops did not depend on a greater number of tubes passed through by flue gas only but mostly on the opportunity to increase the speed of the gas itself to increase the value of the overall heat transfer coefficient, thus reducing exchange surfaces and costs. This led to the introduction of a suction fan placed at the base of the chimney.

The tall chimneys of thermoelectrical plants are not meant to generate totally insufficient natural draught but to keep the flue gas at the level required by ecological constraints.

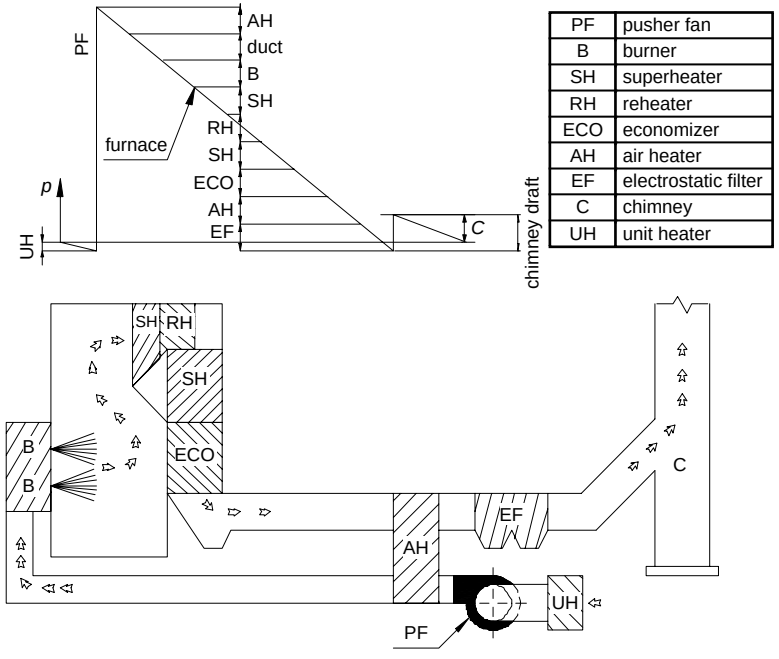
In summary, the features of a generator with a depression furnace include a suction fan for the circulation of flue gas through the generator, in addition to a pusher fan to introduce combustion air into the furnace (see Fig. 1.6). These generators with a depression furnace were once widespread. Nowadays, they are quite rare and limited to some coal generators.

The generally adopted solution consists of the so-called pressurized generator because the furnace is under pressure. Of course, the pressure is on the entire generator with value decreasing from the furnace to the exit of the generator (see Fig. 1.7). These generators have only one pusher fan or even two pusher fans in great units to control the air flow in a more rational way and to reduce the power of every fan, as well as to allow the development of at least 50–60% of the maximum generator



PF	pusher fan
SF	suction fan
B	burner
SH	superheater
RH	reheater
ECO	economizer
AH	air heater
EF	electrostatic filter
C	chimney
UH	unit heater

Fig. 1.6 Generator diagram with balanced draft



PF	pusher fan
B	burner
SH	superheater
RH	reheater
ECO	economizer
AH	air heater
EF	electrostatic filter
C	chimney
UH	unit heater

Fig. 1.7 Pressurized generator diagram

power in case of breakdown of a fan. The air sucked by the fan through a potential unit heater (steam exchanger) that increases the temperature compared to room temperature is pumped through a potential air heater into the burners and then into the furnace. The pressure is higher in this case compared to a non-pressurized generator, given that one pusher fan only must compensate for pressure drops through the generator.

Flue gas under decreasing pressure runs through the different tube banks, that is, through steam-generating banks, the superheater, the reheaters, and the economizer. At the end of the process, it may run through an air heater, and in some instances through a soot precipitator, to reach the base of the chimney.

In the case of smoke-tube generators, the fan must compensate only for the pressure drop occurring inside the tubes passed through by flue gas in addition, of course, to the pressure drop through the burner.

The pressurized generators represent the vast majority of generators for the production of energy and the totality of industrial water-tube generators of low and medium range. These have a series of advantages. Only one pusher fan is required instead of two (one of pusher type and one of suction type) that are required if the furnace is in depression. The cost is reduced even though the required power for the pusher fan is naturally higher to compensate for the pressure drops of the flue gas. This is due not only to the fact that two fans cost more than one fan as powerful as the two combined, but also because the pusher fan pumps air at low temperature and, given its smaller volume, the absorbed power is less than that required by fans of non-pressurized generators.

The smaller amount of absorbed power equals both smaller installation and maintenance costs that considerably impact the budget of large plants. In addition, the suction fan running in the presence of warm gas and soot always causes trouble because of thermal dilations and deposits on the blades of the wheel. Compared to generators with balanced draught, pressurized generators that are tight to prevent gas leaks eliminate air infiltrations that determine a reduction in efficiency. The savings obtained through pressurized generators due to a reduced power absorption by the fans, as well as the absence of infiltrations, is estimated to be about 0.5–0.7% of the cost of energy output. Finally, the presence of one fan instead of two considerably simplifies both manual and automatic tuning.

The generators of this kind also have disadvantages. In fact, besides the necessity of special attention to prevent flue gas leaks from the eyepieces and from the openings for the soot blowers and the spuds of the burners, they require a more expensive metal coating to ensure a perfect seal and the ability to withstand internal pressure.

The advantages, though, greatly exceed the disadvantages.

Chapter 2
Water-Tube Generators

2.1 Convection Generators

The most common convection generators are two-drum generators (see Fig. 2.1). Considering the most frequently adopted solution for small portable units, the following components are connected to the upper drum filled with water in the lower part and filled with steam in the upper part, and to the lower drum working as the only header of the boiler. First of all, there are the tubes building the steam-generating tube bank, where the ones on the side build a wall of the furnace and the support of the external masonry of the generator corresponding to the bank, respectively; then, the radiated tubes building the bottom wall, the side wall opposite the bank, the top wall of the furnace.

Moreover, the rear wall is partially or completely screened through tubes inserted in both drums. Finally, the front wall that carries the burners may be either completely or partially screened.

The radiated tubes in the furnace building the side walls, the bottom, and the top walls can be arranged in three ways. In the first case, they are placed side by side. The second solution involves a membrane wall consisting of tubes set apart by continuous fins between the tubes (membrane bars). Finally, the third solution consists of tubes welded together.

The bottom wall is typically covered with refractory material. This is mostly due to the necessity to reduce the heat radiated to the tubes. Given that the latter have a long path (bottom, side, and top walls), they would otherwise be in critical condition in terms of circulation compared to the other much shorter tubes connected to the drums. This solution does not include real downcomers. This task is assigned to those tubes in the bank located in the cooler areas of the flue gas. The water flowing through them from the upper to the lower drum produces a modest amount of steam because of the low gas temperature. There are also generators of this kind equipped with downcomers external to the passage of flue gas and that feed the lower drum directly.

Inside the bank, the gas runs one passage, or frequently even twice through a separation baffle plate between each passage. The baffle plate is generally made of

D. Annaratone, *Steam Generators*, DOI: 10.1007/978-3-540-77715-1_2,

© Springer-Verlag Berlin Heidelberg 2008

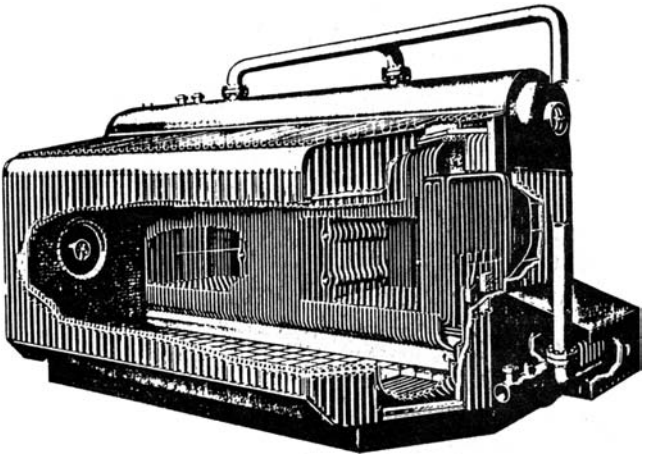


Fig. 2.1 Two-drum convection generator

refractory steel or using the same tubes equipped with fins or welded together. The flue gas runs parallel to the axis of the drums. The row of tubes close to the wall opposite the furnace (next to the bank) can be set apart, side by side, connected through membrane bars, or welded together. The burners are placed on the front wall of the generator with the axis parallel to the axis of the drums. Frequently, there is only one burner. At the most, there will be four burners.

The generator may be equipped with a superheater installed at the exit of the furnace in the area of the bank and substitutes part of the steam-generating tubes. At the exit of the generator, there may be an economizer or an air heater. These small units belong to the en-bloc type and are transportable, except for the economizer and the air heater that are a unit in themselves. They are entirely built in the workshop. The fan and often the feed water pump, the fuel oil heater, and the control board are mounted on the same structural base of the generator.

They do not require a support structure. In fact, the lower drum is placed on the structural base and works like a bearing beam of the bank and the upper drum. The tube wall of the furnace opposite the bank is supported with adequate bearings. Of course, special care is required to allow free expansion of the lower drum and the tubes. Finally, the covering walls on the side, the front wall (with the burners), and the bottom wall release their weight on the structural base.

The solution generally adopted in high power units (not transportable) is shown in Fig. 2.2. In that case, all the walls are screened, and their tubes are hooked to headers that, in turn, are connected to both drums. The burners are placed with the axis perpendicular to the axis of the drums, and the path of the gas occurs transversely to the drums. If a superheater is planned, it is located in the upper part of the furnace and sometimes separated from it by a few rows of steam-generating tubes.

The generator can be supported by a structure underneath or suspended through appropriate collars and tie rods connected to a supporting framework. This way, the expansion is free in any direction.

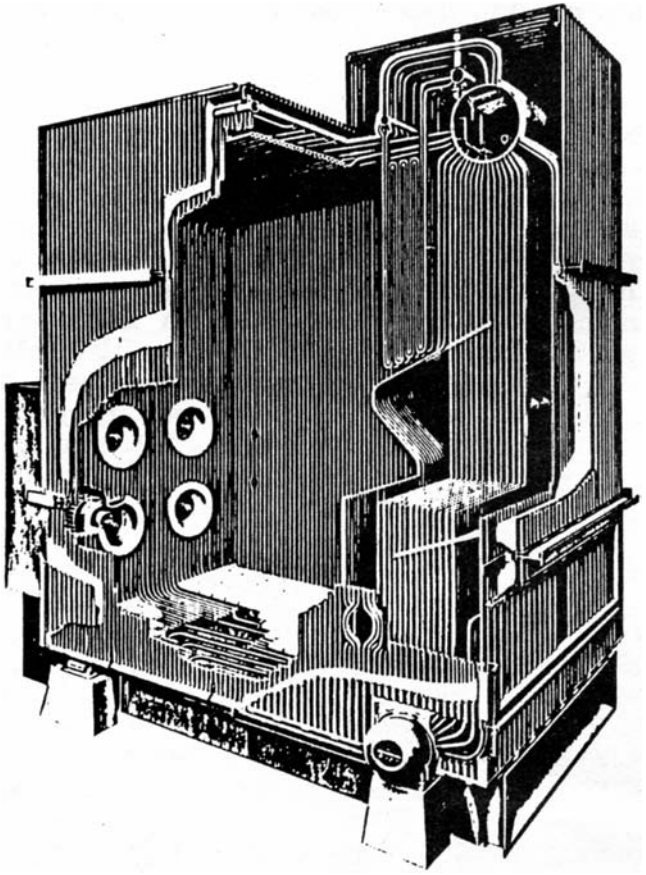


Fig. 2.2 High-power two-drum generator

The output of these generators varies from 5 t/h of steam to 50 t/h and beyond for transportable models. It reaches up to 300 t/h for models assembled in the erecting yard. The pressure is generally modest in small power units but can reach up to 120 bar in larger units.

As we mentioned before, two-drum generators are the most common ones, but they do not represent the only possible solution. Next, we will briefly illustrate two generators with a single drum that include lower headers fed by downcomers outside the flue gas path, or impacted by the heat transfer, and to which all tubes forming the screens in the furnace or the tube bank are connected. The drum is placed lengthwise and its axis parallel to the burners, centered with respect to the furnace (see Fig. 2.3), or placed laterally (see Fig. 2.4).

These generators can consist of a group of tubes connected to the headers and the drum (to the latter sometimes through return tubes). They may consist of modular elements representing an independent and self-sufficient circuit connected directly to the drum, both for water feeding and the return of the water–steam mix generated

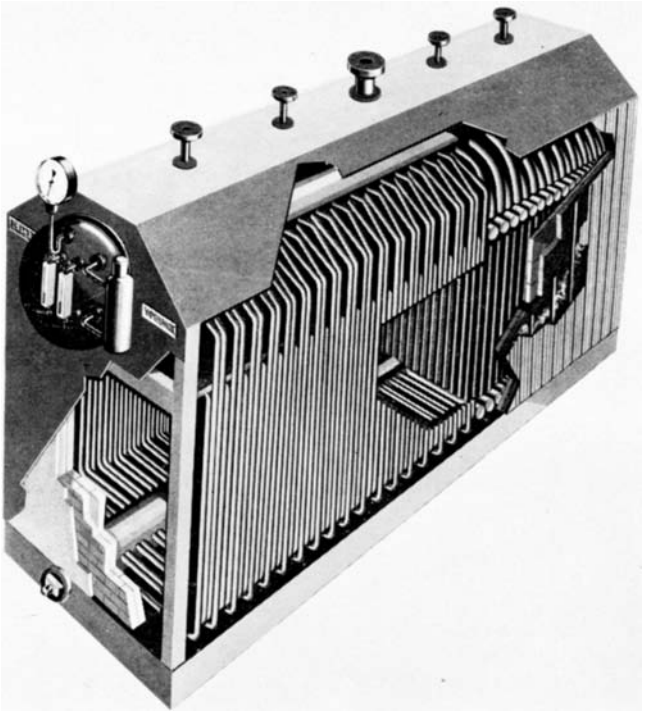


Fig. 2.3 Central drum convection generator

in the steam-generating tubes. The path of the gas can be unidirectional with the presence of baffle plates producing a certain path in the bank, or set up with partial returns in the bank toward the furnace (see Fig. 2.4).

Finally, there are examples, albeit rare, of generators with more than two drums. In the case of a generator with three drums, the two lower ones are similar conceptually to the only lower drum of the boiler with two drums. In that case, the furnace has a trapezoidal shape with the tube banks placed on the sides of the trapezoid and hit by the gas with alternating path.

All described models belong to the en-bloc transportable type. They are self-supporting and planned for modest power levels. Generally, their output ranges from 5 t/h to 30 t/h of steam with a pressure not exceeding 50 bar.

They may be designed with a superheater placed in the bank area to substitute some of the steam-generating tubes or in some instances on the walls of the furnace (radiation type). In the latter case, it forms the first section of the superheater (the second belongs to the convection type and is located inside the bank), or represents a drier, as it is meant to dry the saturated steam and to superheat it by a few dozen degrees.

This variety of convection generators is not comprehensive of all possible structural solutions. Other solutions are feasible, of course, but from a conceptual and structural point of view, they are still based on the ones described above.

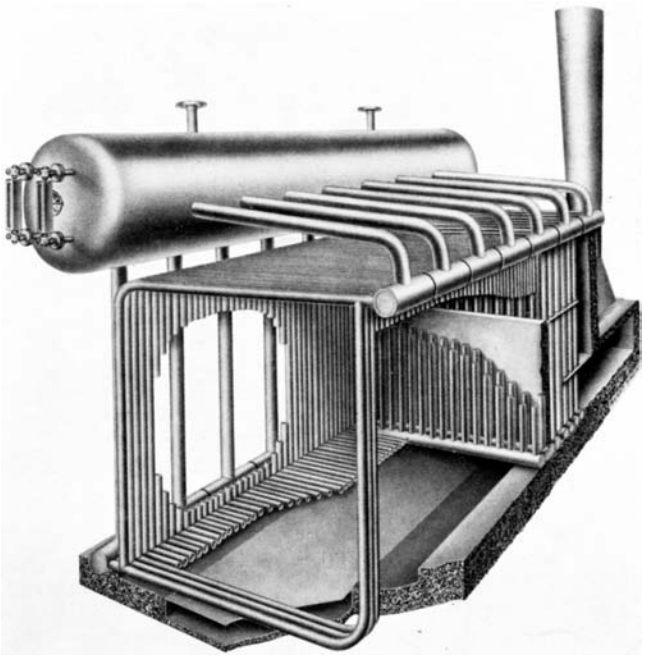


Fig. 2.4 Lateral drum convection generator

2.2 Radiation Generators

Radiation generators including the biggest units for thermoelectric power plants are characterized by the presence of a huge and fully screened furnace. As we mentioned earlier, the heat required to output saturated steam is completely or almost entirely transferred into the furnace. Therefore, the steam-generating tube bank is absent or reduced to modest size compared to the generator.

The superheater, the potential reheater, and the economizer with smooth tubes that make up one block together with the boiler are installed at the exit of the furnace or the bank, assuming the presence of one. At the exit of the economizer, the flue gas that is still warm $(350–400^{\circ}\mathrm{C})$ passes through the air heater (it will be discussed in the next chapter) where it heats the combustion air. Next it goes through the soot precipitator, and then it is sucked by the suction fan if the generator has a furnace in depression, otherwise it gets directly into the chimney if the generator is pressurized. These generators are often equipped with a recirculation fan of the flue gas that picks up some of it at the exit of the economizer to introduce it at the bottom of the furnace. A by-pass duct for cold air across the air heater may also be included. Finally, some generators are equipped with a recirculation duct for warm air that is partially picked up at the exit of the air heater and directed to the suction of the pusher fan.

Both the recirculation fan of the flue gas and the just mentioned secondary ducts modify the heat exchange in the generator. The recirculation fan is required as the load or the fuel (in the case of combustion with different fuels) varies in order to reach the desired temperature of the superheated steam. The ducts mentioned above are meant to prevent or at least keep corrosion phenomena at low temperature from occurring in the air heater under control.

To increase the temperature of the air at the suction of the pusher fan and in view of corrosion phenomena, unit heaters (steam air heaters) are installed to be used during the coldest season. Finally, air suction can be done through a duct that picks it up inside the factory building or from the upper portion of the generator where it is naturally warmer. This way, the flue gas exchanging heat with air is cooled less.

In generators with natural circulation (see Fig. 2.5) or assisted circulation (see Fig. 2.6), the drum located in the highest spot of the generator feeds the inlet headers

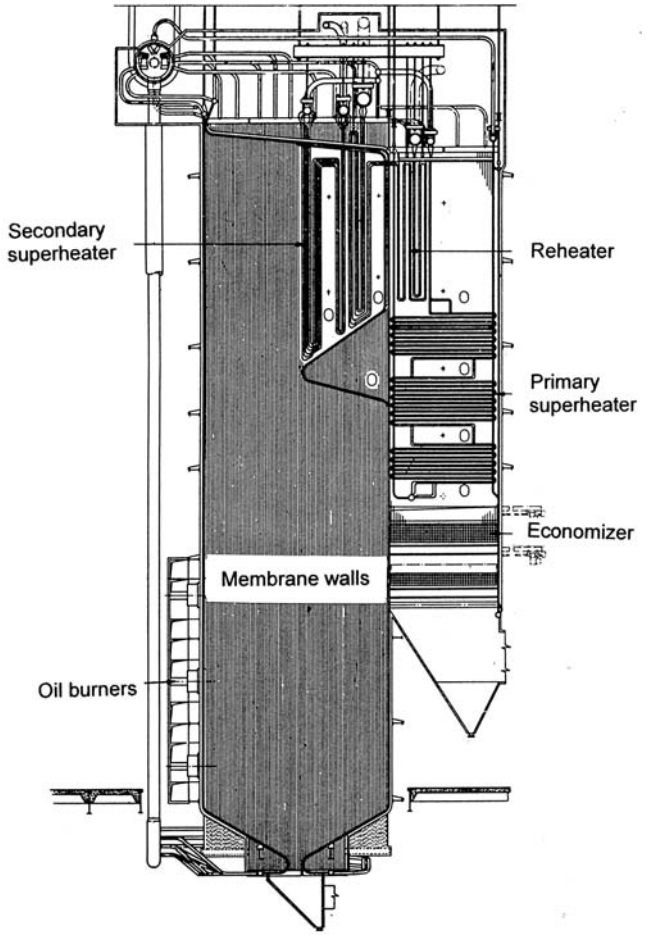


Fig. 2.5 Radiation generator with natural circulation

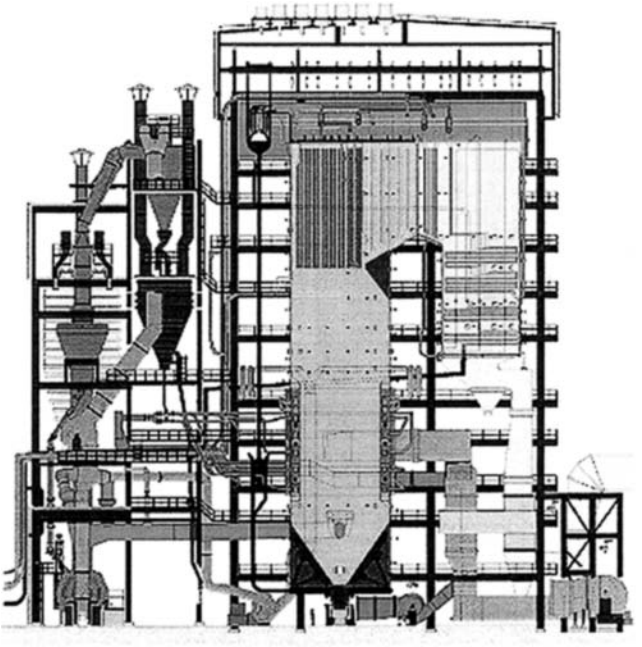


Fig. 2.6 Radiation generator with assisted circulation (Courtesy of Alstom)

of the tube walls in the furnace through huge insulated downcomers outside the path of the flue gas. If circulation is assisted, circulation pumps are inserted along the downcomers. The water–steam mix produced in the steam-generating tubes moves into the upper exit headers and comes back into the drum through return tubes.

The drum has small dimensions compared to the size of the generator (if compared with the drums of convection generators) even though its diameter can reach up to 2 m and its length up to about 15 m.

The different stages of the superheater, the reheater, and the economizer are also connected to entrance and exit headers. The one at the entrance of the economizer is fed by a feed water pump, whereas the one at the exit is connected to the drum. The header at the entrance of the first stage of the superheater (primary) gets the saturated steam from the drum while the superheated steam reaches the turbine from the one at the exit of the last stage through connection piping. Attemperators are introduced between the different stages of the superheater (Chap. 3).

The reheater gets the steam from the turbine through connection piping and the entrance header and sends it back to the turbine through additional connection piping.

Besides the walls of the furnace and the top wall, the side walls of the space containing the secondary superheater and the reheater, as well as the walls of the tunnel where the primary superheater and the economizer are installed, are screened.

Depending on the type of generator, the construction characteristics, the size, and their locations, these screens consist of steam-generating tubes (top wall of the

furnace, area of the superheaters), the primary superheater tubes (top wall of the area of the superheaters, walls of the tunnel), and the tubes of the economizer (side walls and top wall of the tunnel). Therefore, the headers at entrance and exit of the economizer and the primary superheater are not necessarily installed in correspondence of the relative tube banks.

Besides the structural solutions shown in Figs. 2.5 and 2.6, others are possible due to the presence of a reduced steam-generating tube bank, the slightly different shape of the furnace, and so on. Figure 2.7 shows a generator where the superheater, the reheater, and, of course, the economizer are set up with horizontal banks.

In generators with forced circulation, the path of the flue gas is quite similar to the other generators we discussed. Even the layout of the stages of the superheater, the reheater, and the economizer is the same as in generators with natural or assisted circulation. In fact, it fulfills requirements of maximum efficiency of the heat exchange common to any kind of generator. On the other hand, there are substantial

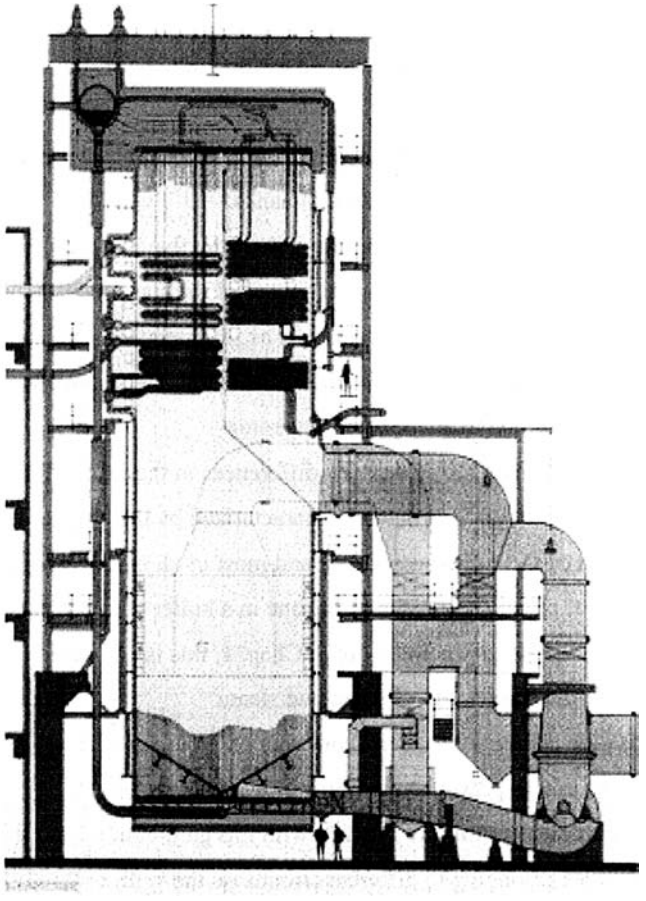


Fig. 2.7 Box-type radiation generator (Courtesy of Alstom)

differences in the realization of the boiler (steam-generating tubes). It is actually characterized by the absence of the drum (from the point of view of construction) and most of all by the completely different type of circuit compared to the one in a boiler with natural or assisted circulation. As we already pointed out in Chap. 1, this is an open circuit passed through by a reduced amount of water and steam. This implies the adoption of special construction solutions that ensure high velocity of the mix to prevent superheating of the tubes.

Even quite complex circuits are realized with this goal in mind, for instance by alternating tubes belonging to different circuits on the wall or through the adoption of screens with almost horizontal tubes placed helicoidally on the walls instead of screens with vertical tubes (see Figs. 2.8 and 2.9).

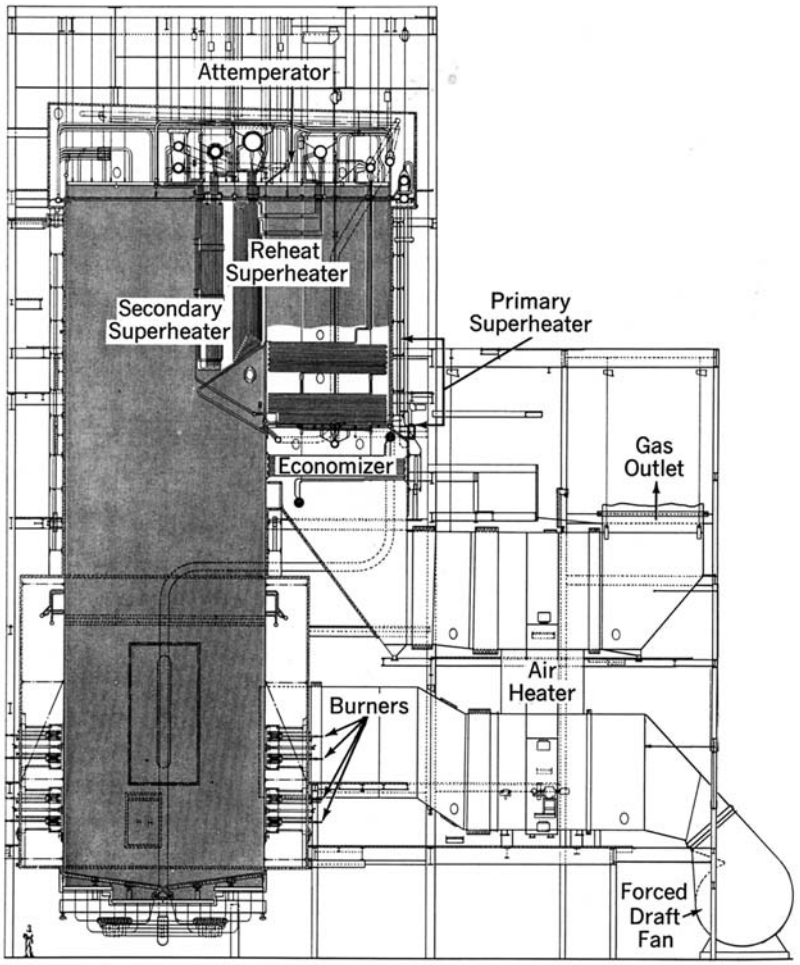


Fig. 2.8 Radiation generator with forced circulation (Courtesy of Babcock & Wilcox)

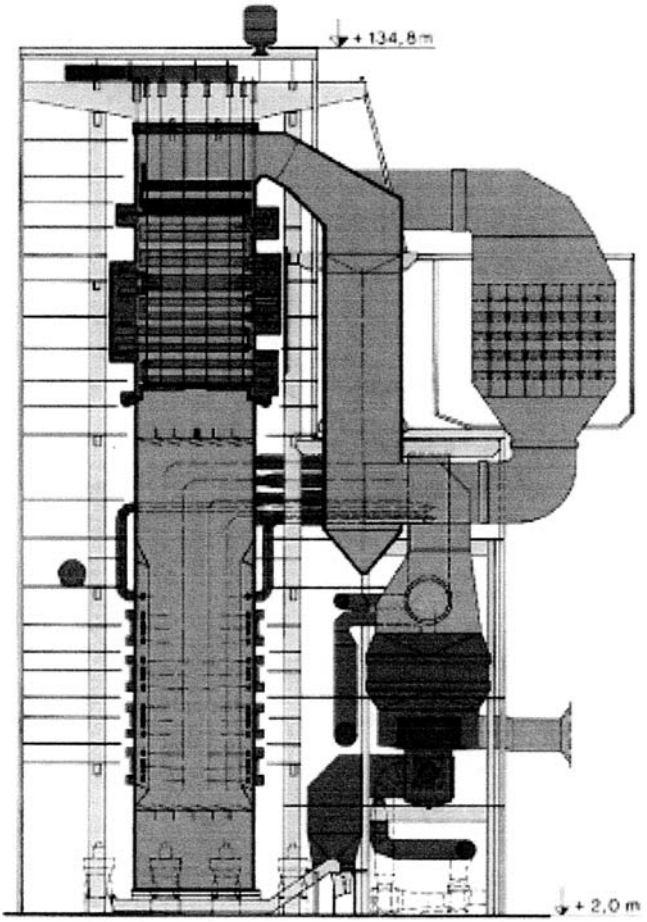


Fig. 2.9 Radiation generator with forced circulation (Courtesy of Alstom)

The uniform distribution of steam and water is of utmost importance in the various tubes in parallel flow of a circuit. In fact, an unbalance of this kind in generators with natural or assisted circulation has limited and not dangerous impact (provided it is not excessive), given that there is a huge amount of circulating water and the mix is still quite rich in water at the exit of the circuit. In generators with forced circulation, there is only a small amount of water in circulation, and all the water was transformed into saturated steam at the exit of the circuit.

Therefore, the much greater danger brought about by this unbalance is easily understood. In fact, in the tubes where circulation is reduced for whatever reason compared to those in parallel, the total transformation of water into steam occurs in advance in an area of the furnace where thermal flux can be exceedingly high. On the other hand, these unbalances are inevitable even though the tubes are identical from the point of view of construction. A different thickness of the tubes (given

the tolerance) followed by smaller internal diameter and a different roughness of the walls suffice to provoke circulation unbalances. Finally, let us not forget the constantly possible unbalances in thermal flux that may occur even between closely placed tubes.

To eliminate or at least reduce these unbalances to locally limited phenomena, generators with forced circulation are equipped with intermediate headers on the wall that work as mixers. This way, the unbalances are reduced and localized between headers. Figure 2.10 shows the scheme of a generator with forced circulation including clearly visible intermediate headers.

Another construction artifice used in generators with assisted circulation consists of including balancing valves at the base of the screens. During the set up of the generator, these valves are tuned based on the temperatures registered on screen tubes with the help of thermocouples.

In the upper area of the generator the figures show very many headers and connection tubes that must be insulated. In generators with natural and assisted circulation, the drum must be insulated, as well. It is simpler and financially more advantageous to enclose headers, piping, and drum in one single insulated penthouse, with an inside temperature identical to the saturated steam. Naturally, the piping and the headers relative to superheaters must be insulated (even though less insulation is required), given that the local temperature is higher compared to the outside.

In correspondence of the burners aligned in rows and variable number per row, depending on the power of the burner and the generator, the tube walls must be set apart through bending of the tubes and their partial overlap to create the opening

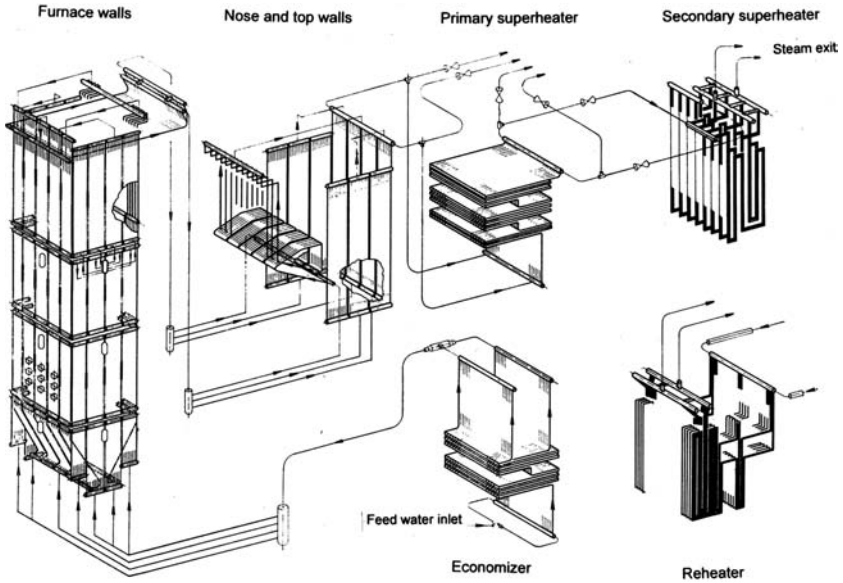


Fig. 2.10 Scheme of a generator with forced circulation

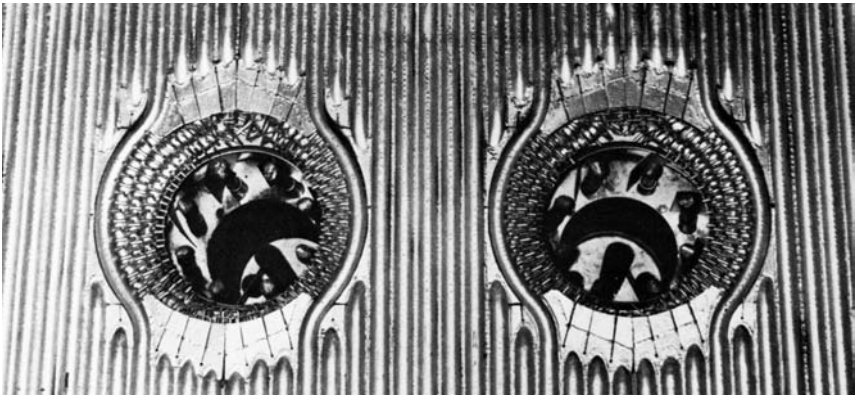


Fig. 2.11 Burner wall (Courtesy of Babcock & Wilcox)

for the burner. The tubes are equipped with studs for the anchorage of a plastic-type refractory casting (see Fig. 2.11).

The generator is equipped with soot blowers fed with steam and arranged in different locations. They can be fixed on the wall or be retractile (see Fig. 2.12). The latter kind installed outside the generator on the service gangways are introduced only during blowing. There are also eyepieces to control the generator in the different areas and inspection holes for access to the inside.

Radiation generators are suspended on a supporting framework that lets it expand in any direction. This is obtained through suspension collars (drum) and tie rods,

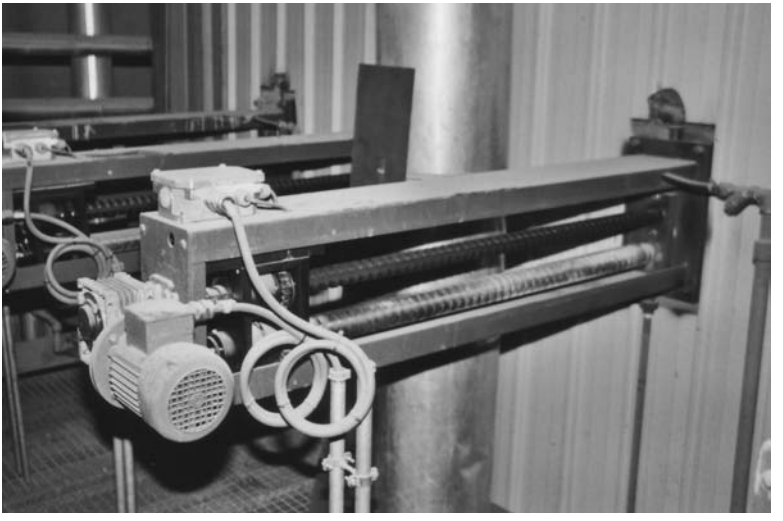


Fig. 2.12 Retractile soot blower

and sometimes with intermediate beams that support the walls and the banks, as they are directly connected to the tubes or the different headers. Collars and tie rods release the weight on a series of beams that form the upper part of the supporting framework.

Radiation generators are built for extremely high power (up to 1000 MW) and for equally high pressure. Generators with natural circulation reach a pressure limit in the reduction of the ratio between water and steam density as the pressure goes up. In generators with assisted circulation, this limitation does not exist because of the intervention of the pump. This was already discussed in Chap. 1. Generators with forced circulation are built for both sub-critical and hypercritical pressure.

As far as the temperature of the superheated and reheated steam, in general it does not exceed 540°C. This limitation allows the employment of cheaper low-alloy steel. There are several examples of generators with a steam temperature up to 600–620°C. In that case, the end coils of the superheater must be built using stabilized austenitic steel.

In high-pressure generators, the temperature of the feed water generally ranges from 200 to 250°C. This high temperature is obtained through heat exchangers fed by the steam taken from the different stages of the turbine. This is well known to improve cycle efficiency.

Radiation generators are meant for combustion using fuel oil, natural gas, and pulverized coal or pulverized lignite. Typically, at least two of these fuels will be burned in any generator. In addition, special fuels, such as coal tar oil, refinery gas, and more, are burned. Radiation generators have very small water mass. It generally decreases moving from natural circulation to assisted circulation, and finally to forced circulation.

2.3 Waste-Heat Generators

Waste-heat generators are characterized by the absence of the furnace, and for this reason, they belong to the convection category. The boiler consists of a steam-generating tube bank. It can be preceded in the path of the gas by a superheater and followed by an economizer, this way building the waste-heat generator.

From a construction point of view, the boiler generally consists of a tube bank connected to an upper and a lower drum. In other words, it consists of the convective part of a boiler with two drums (see Sect. 2.2). The gas passes perpendicular to the axis of the drums and in only one passage. The tubes are frequently finned. This provides a great heat exchange surface within a limited space. Of course, other solutions are feasible. For instance, it is possible to have only one upper drum connected to various tube-rakes tied to the drum for the water feed and the return of the water–steam mixture. The bulk of all rakes makes up the steam-generating bank. In the end, even in this case, this is the convective part of modular type boilers that were discussed in Sect. 2.2.

The boiler is installed inside the duct where the warm gas coming from the outside is flowing through, as we shall see later on. The superheater and the economizer

are installed in the same duct, as well. The former usually consists of hanging coils supported by entry and exit headers. Other solutions are possible. The latter consists of finned tubes. Generally, these are finned tubes made of cast iron or steel tubes with finned cast iron muffs (Sect. 3.8). There are also examples of steel tubes with helicoidal fins when the flue gas does not represent a risk in terms of corrosion (natural gas combustion).

The waste-heat generator is evidently quite a simple structure and does not involve either functional or implementation problems. It can exploit the sensible heat of the flue gas coming from another device where combustion takes place. For instance, it is installed at the end of a glass furnace, an open-hearth furnace, and a diesel engine. There are also numerous applications in the chemical industry to recuperate the sensible heat of the different kinds of process gas.

Finally, a more and more widespread application consists of mixed energy production through gas turbines and steam turbines (combined cycle). In that case, part of the energy is produced in the gas turbine. Its exhaust gas hits a waste-heat generator producing the steam that feeds a closed-cycle turbine (or a back-pressure turbine, if the interest lies in low-pressure steam for technological purposes).

Figure 2.13 shows a complex plant consisting of different sections that can produce steam to feed a turbine or for technological use (under different pressure levels). The first bank of coils is a superheater followed by two steam-generating banks, an economizer, a third steam-generating bank, and finally another economizer. The plant produces superheated steam at 42 bar and 385°C to feed the turbine and saturated steam at 11.5 bar, as well as 2.25 bar for technological use in a factory. The economizers are made of steel with spiral fins connected with resistance welding. Combustion occurs with natural gas. As we see, the steam-generating banks consist of two drum elements. Note that this is not the only possible solution. In

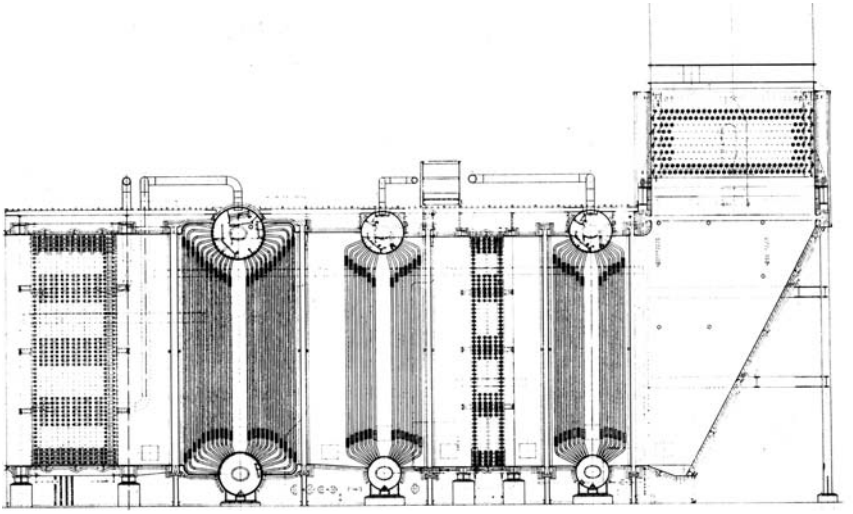


Fig. 2.13 Waste-heat generator

fact, tube banks are also built with rakes with lower headers fed by a downcomer and connected on the top to the only drum (see Fig. 2.14).

In conclusion, waste-heat water-tube generators can be used to produce electricity or to produce steam for technological purposes both directly and as release of a back-pressure turbine. The temperature at which the gas hits the generator varies from case to case, depending on the provenance. It can be relatively low (450–600°C) or considerably high (up to 1200°C). The gas may be under pressure,

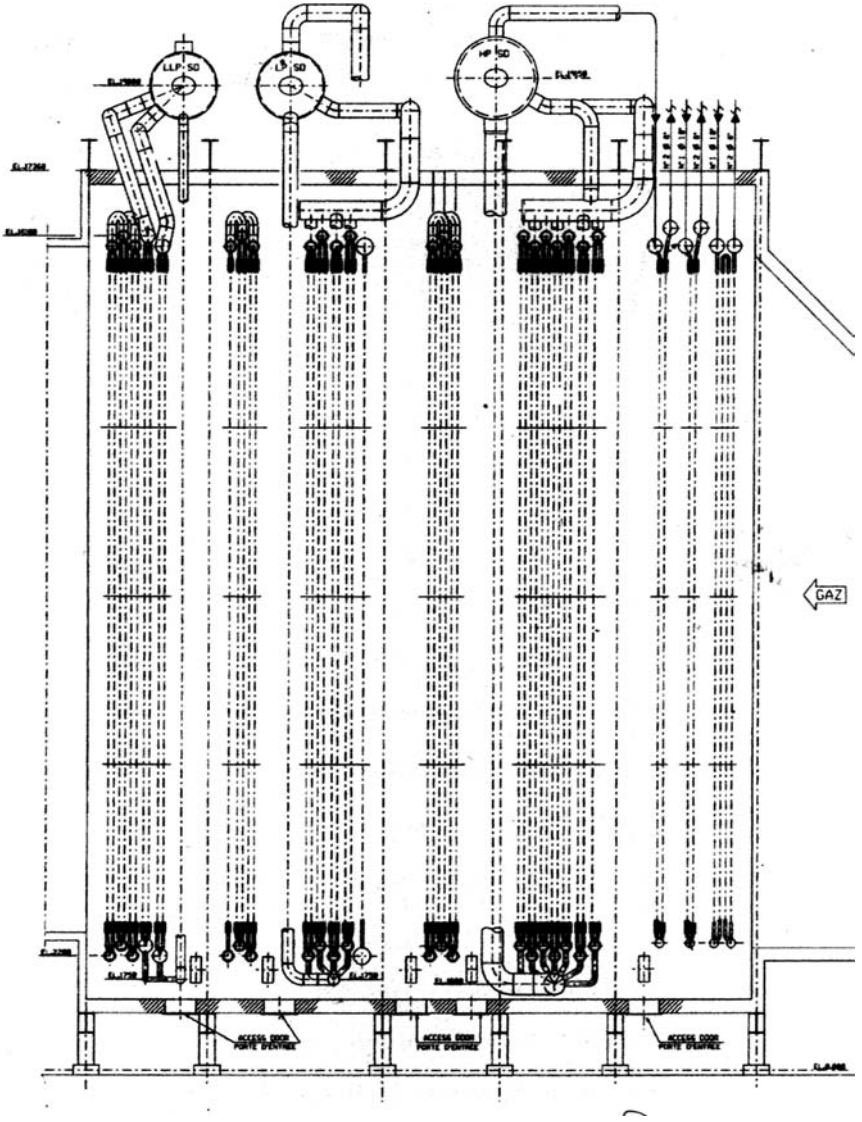


Fig. 2.14 Waste-heat generator (Courtesy of Macchi – Italy)

and in that case neither draught from the chimney nor a suction fan is required. Naturally, the duct where the generator is located must be perfectly sealed and able to withstand pressure even from the inside.

There are instances requiring a suction fan, and others where its presence is not recommended, given the highly corrosive nature of gas and its tendency to leave deposits on the wheel even though a certain amount of suction is still necessary (glass furnaces). In the latter case, the only choice is to depend on the necessarily modest draught of the chimney, if it is not very tall. Therefore, it is necessary to limit the velocity of the gas to reduce the pressure drop even though this implies a greater heat exchange surface caused by the deriving reduction in overall heat transfer coefficient.

Cleaning of the external walls of the tubes is often a problem in waste-heat generators because of the nature of the gas. Besides soot blowing through steam or compressed air, it is advisable to follow the following criteria.

The tubes should be kept quite apart from one another to prevent clogging between the tubes. There should also be hoppers to discharge the deposits, and access to the banks should be easy to perform periodical cleaning operations.

To conclude, note that besides the described models, there are waste-heat generators consisting of a variety of banks of horizontal coils piled up as a tower at the base of the chimney (the steam-generating banks are connected to a drum installed separately).

Presently, we will not discuss further possible solutions. Note that the waste-heat generator is nothing but a heat exchanger of a particular kind, provided the circulation in the boiler is natural. But this does not constitute the only solution. If circulation is forced, it is reduced to a classical gas–water or gas–steam exchanger, and evidently many other solutions can be adopted.

By the way, the water-tube boiler can be substituted with the smoke-tube boiler (Chap. 4) if circulation is natural. Of course, the goal will be to produce steam for technological purposes, as the smoke-tube boiler is unsuitable under medium and high pressure, as we shall see later on.

Chapter 3
Components of Water-Tube Generators

3.1 Furnace

Tube walls (also called screens) in a furnace can be built in three ways.

- The tubes can be placed in front of the firebrick masonry at a distance from each other or next to each other.
- Complete screening of the walls can be done through tubes that are spaced from one another, including the insertion of a continuous fin (membrane bar) to build a so-called membrane wall.
- It is also possible to place the tubes between the firebrick lining and the insulating coatings.

Among all these possible screening solutions, the first is often used in small and medium power generators. The second solution is typical of big radiation generators. The third solution is used to cool the firebrick lining without having substantial heat exchange between the flame and the tubes, for example, for the bottom of the furnace of certain small and medium power generators.

The reduction of heat exchange may at first seem illogical. Nonetheless, it is sometimes necessary to prevent a furnace from being cold, especially at reduced load, thus limiting good combustion, and also to promote circulation (natural), and obtain the desired temperature of the superheated steam. Note that any time design errors or new requirements of the generator are responsible for an increase of the exit temperature of the gas from the furnace, the easiest way is, in fact, to cover part of the screens with firebrick linings (clearly reducing generator efficiency).

The most important requirements of the furnace are as follows.

First of all, its volume must be sufficient to allow complete and regular combustion before the exit of the gas. The indicator of correct sizing of the furnace is the thermal volumetric load expressed in kW/m^3 that represents the heat developed by combustion per unit of time and per m^3 of the furnace itself.

It is impossible to provide precise numerical values not to be exceeded for that load because they depend on many factors, such as the power of the generator, the type of burner, its orientation, the type of fuel (which is crucial), the shape of the

D. Annaratone, *Steam Generators*, DOI: 10.1007/978-3-540-77715-1_3,

© Springer-Verlag Berlin Heidelberg 2008

flame, the type of screen, the shape of the furnace, the temperature of the combustion air, and so on. Generally, the load ranges from 170 to 400 kW/m^3 for big units, whereas for small power generators it will reach up to 850 kW/m^3. For combustion with pulverized coal, Rosin recommends a thermal volumetric load equal to

$$q_v = \frac{393}{z}(kW/m^3), \tag{3.1}$$

where z is the combustion time in s of the largest granule of pulverized coal. The values of z are generally greater than 1 s. In fact, the thermal load with combustion using pulverized coal generally is about 170–230 kW/m^3. Big radiation generators are also considered in reference to the thermal load with respect to the section of the furnace. Roughly, it ranges from 2900 to 9300 kW/m^2.

The furnace must have a shape that promotes a regular gas flow through the remaining portions of the generator. To this extent, note the presence of a nose on the wall opposite the burners in the generator shown in Fig. 2.5 to ensure regular flow of gas through the superheater. The shape of the furnace is usually rectangular even though great results were achieved with round or hexagonal furnaces, as well. These shapes are obviously better for pressurized boilers. The burners are installed either in front of or in the rear of the furnace, or both. In addition, they may be designed to be all around the furnace, as shown in Fig. 3.1 to achieve tangential combustion (see Fig. 3.2 for the burner). This setup is, of course, typical of furnaces with a polygonal shape.

Mostly used with coal and lignite, tangential combustion provides a more regular flame shape and a more homogeneous heat transfer toward the different tube walls.

There are also generators where the burners have a vertical axis and are placed on the bottom of the furnace.

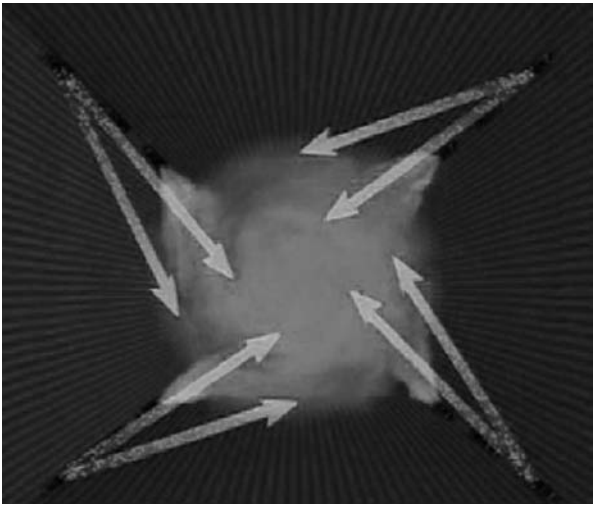
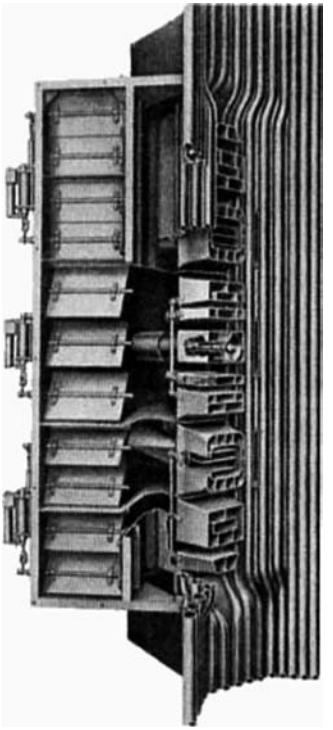


Fig. 3.1 Tangential combustion (Courtesy of Alstom)

Fig. 3.2 Tangential burner



Finally, the burners are tiltable instead of being steady. This modifies the heat transfer into the furnace.

The sizing of the furnace must be planned to ensure the necessary distance between the burners and the opposite wall. Once the fuel flow rate of the burners is known, their distribution on the wall(s) designed for them must be done respecting the required distance between them and the distance from the neighboring walls, by varying the number of burners per row, as well as the number of rows.

It is crucial to prevent the striking of the tube walls by the flame to avoid dangerous superheating of the tubes. Moreover, the different flames must not interfere with each other to ensure correct combustion. Finally, if the burners are too close to each other, there can be excessive local concentration of heat. In that case, the thermal flux through the tubes could be so high to provoke the most dangerous phenomenon of film boiling (Sect. 3.2) followed by superheating of the tubes up to their bursting.

It is impossible to provide exact rules for these distances due to the many parameters at play.

Figure 3.3 is a good reference for furnaces of small power generators with only one fuel oil or natural gas burner.

When there are several burners, $B/2$ could be the minimal distance between external burners and the walls. As far as distance Δ between the burners, the value obtained through the following equations may be used:

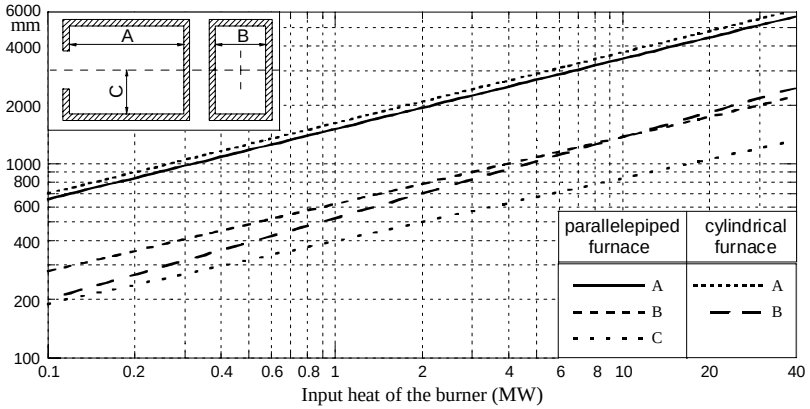


Fig. 3.3 Furnace dimensions

$$\Delta = 400 + 54q \ (\text{mm}) \tag{3.2}$$

for fuel oil burners and

$$\Delta = 550 + 54q \ (\text{mm}) \tag{3.3}$$

for gas burners. In (3.2) and (3.3), q represents the thousands of kilowatts introduced into the furnace for each burner. The sizing of the furnace must be done in such a way to achieve the desired exit temperature with respect to the superheater.

The surfaces of the furnace must be easy to clean and repair. Finally, it must be high enough to ensure natural circulation in the wall tubes if this type of circulation is the case.

The temperature reached in the furnace varies from area to area and depends on the fuel, the screens, and so on. It can range from 1000 to 1500 °C under continuous maximum load of the boiler. Exceptionally, 1800 °C may be reached. Of course, this temperature goes down under reduced load.

In big generators the exit temperature of flue gas from the furnace generally ranges around 1000–1300 °C. In some cases it goes up to 1400 °C. Small and medium size generators have temperatures ranging from 900 to 1100 °C. Naturally, these values are referred to continuous maximum generator load. The temperature in the furnace influences combustion, the value of $|CO_2|$ and the heat transferred to the walls.

The temperature at the exit of the furnace can be checked and modified through adequate measures. This is sometimes necessary to compensate for the temperature reduction of the superheated steam under reduced load in convection superheaters. This is due to the reduction of the exit temperature of the flue gas from the furnace and to the reduction of the overall heat transfer coefficient caused by the reduced speed of the flue gas. These reductions are not compensated by the reduced steam mass to be superheated.

Without appropriate measures to control the gas temperature, it is necessary to oversize the superheater, designing it for reduced load and reducing the steam

temperature under heavy load through the devices directly impacting the steam. These will be discussed in connection with superheaters. Unfortunately, this model is expensive and may cause various problems during the design phase. Therefore, it may be best to influence the exit temperature of the gas from the furnace, or at least influence this temperature as well, to increase it under reduced load. The process is as follows.

- Only the highest burners are turned on to reduce the flame radiation toward the lower areas of the furnace.
- Tiltable burners are used, and they are positioned upward under reduced load.
- By-passes of flue gas are planned.
- Part of the gas is circulated again through a fan that sucks it at the exit of the generator before entrance into the air heater and that leads it onto the bottom of the furnace.

We already mentioned the feasibility to plan to burn different fuels. Note that a furnace designed to burn natural gas is too small to deliver the same output compared to coal combustion.

Thus, combustion with different fuels requires special design characteristics.

3.2 Radiated Tube Wall

As we mentioned earlier, in generators of small and medium power, the tube walls in the furnace are sometimes built with spaced tubes, but more frequently they are equipped with tubes placed next to one another. In the first case, the tube is under direct radiation from the flame and under back radiation from the firebrick lining located behind the tubes. The heat transferred to the tubes can be computed considering an ideal surface obtained by multiplying the surface of the screened wall by the efficiency coefficient E, as shown in Sect. 8.4. If the tubes are placed next to each other, the radiated surface simply consists of the wall surface (not the external surface of the half-tubes that see the flame).

In large radiation generators, the tube walls generally consist of spaced tubes connected by a welded continuous fin (membrane bar), thus building a monolithic wall called membrane wall (see Fig. 3.4).

Panels of transportable size are built in an assembly shop through continuous and automatic welding of the fins to the tubes. The different panels are then assembled and welded together in the building yard.

Another possible solution consists of adopting tubes equipped with fins (see Fig. 3.5) that are press manufactured or cold-rolled and welded to each other. Their high cost is frequently discouraging even though there are undoubtedly advantages from the point of view of heat transfer.

In membrane walls, both the tube and the fin are under flame radiation. The fin cooled only through the welding to the tube shows increasing temperature from the welding point to the center line. These temperature differences determine a different

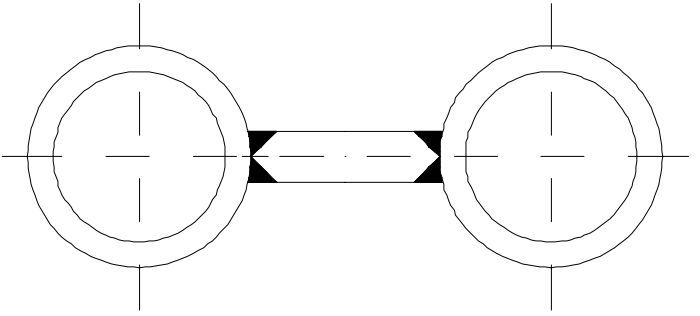


Fig. 3.4

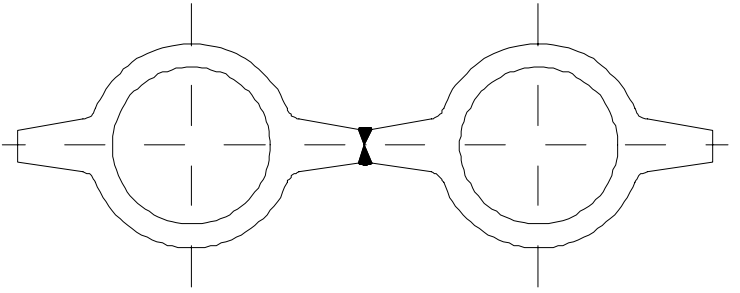


Fig. 3.5

thermal expansion of the fin from point to point, along the axis of the tube which is not compatible with the monolithic condition of the wall. Internal compression stresses occur in the central area of the fin and traction stresses in correspondence of the junction with the tube to re-establish congruence.

The value of these stresses must not exceed certain limits to prevent the disengagement of the fin or the occurrence of cracks in the welding. To that extent the temperature differences in the fin must be kept within limits. An excessive temperature of the fin also increases the risk of scaling.

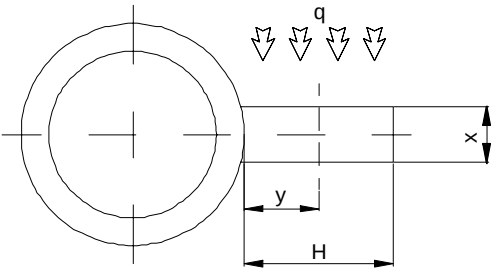
Let us now analyze how the different parameters influence the temperature of the fin. First of all, the different temperatures of the fin do practically not influence the radiated heat that can be assumed to be constant along the entire fin. Let us now consider a tube and half a fin (see Fig. 3.6) and indicate the heat per surface and time unit that hits the fin with q. The heat going through the fin at distance y from the bottom per its length unit is given by

$$q_1 = q\,(H - y)\,. \tag{3.4}$$

If x is the thickness of the fin, k the thermal conductivity, and $\mathrm{d}t/\mathrm{d}y$ the temperature gradient

$$q\,(H - y) = kx\frac{\mathrm{d}t}{\mathrm{d}y}. \tag{3.5}$$

Fig. 3.6



By integrating (3.5), we obtain

$$t = -\frac{qy^2}{2kx} + \frac{qHy}{kx} + \mathrm{C}, \tag{3.6}$$

where C is a constant.

Therefore, if t_b is the temperature at the bottom of the fin

$$t = t_\mathrm{b} + \frac{q}{kx}\left(Hy - \frac{y^2}{2}\right). \tag{3.7}$$

At the top of the fin $(y = H)$, there is a temperature t_H equal to

$$t_H = t_\mathrm{b} + \frac{qH^2}{2kx}. \tag{3.8}$$

The temperature difference Δt between the top and the bottom of the fin is given by

$$\Delta t = \frac{qH^2}{2kx}. \tag{3.9}$$

Equation (3.9) implies that this difference is directly proportional to the square of the width of the half-fin and inversely proportional to the thickness of the fin. Therefore, to limit the value of Δt it is necessary to design narrow and very thick fins. The tubes with the fins generally have fins that are 15–20 mm wide and 5–6 mm thick.

For instance, given a thermal flux equal to $290\,\mathrm{kW/m^2}$, a width of 16 mm (that corresponds to $H = 8\,\mathrm{mm}$) and a thickness $x = 6\,\mathrm{mm}$, assuming that $k = 44\,\mathrm{W/mK}$, based on (3.9) we have

$$\Delta t = \frac{290,000 \times 0.008^2}{2 \times 44 \times 0.006} = 35^\circ\mathrm{C}.$$

Moreover, the welding between the tube and the fin must absolutely belong to the full penetration type because a welding not involving the entire thickness of the fin can cause an additional temperature difference at the bottom.

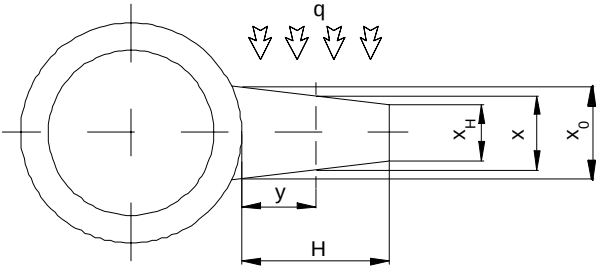


Fig. 3.7

Let us now examine the impact of the tapering of the fin in tubes equipped with fins, as shown in Fig. 3.7.

x_H is the thickness on top, x_0 the one on the bottom (see Fig. 3.7), and β their ratio, then

$$\beta = \frac{x_0}{x_H}. \tag{3.10}$$

The generic thickness x is given by

$$x = x_0 - \frac{x_0 - x_H}{H} y. \tag{3.11}$$

Applying the same process used for the fin with constant thickness,

$$q\,(H-y) = k\left(x_0 - \frac{x_0 - x_H}{H} y\right)\frac{\mathrm{d}t}{\mathrm{d}y}, \tag{3.12}$$

then

$$\mathrm{d}t = \frac{q}{k}\frac{H-y}{x_0 - \frac{x_0 - x_H}{H} y}\mathrm{d}y. \tag{3.13}$$

Integrating (3.13), we obtain

$$\Delta t = \frac{qH^2}{kx_H}\frac{1}{\frac{x_0}{x_H} - 1}\left(1 - \frac{1}{\frac{x_0}{x_H} - 1}\log_{\mathrm{e}}\frac{x_0}{x_H}\right). \tag{3.14}$$

Finally, recalling the significance of β, we have

$$\Delta t = \frac{qH^2}{kx_H}\frac{\beta - 1 - \log_{\mathrm{e}}\beta}{(\beta-1)^2}. \tag{3.15}$$

For instance, if $\beta = 2$, from (3.15) we obtain

$$\Delta t = 0.307\frac{qH^2}{kx_H}. \tag{3.16}$$

In reference to a fin with constant thickness equal to x_H, a comparison between (3.16) and (3.9) shows a reduction of Δt equal to 38.6%.

Carrying out the comparison with a fin of constant thickness equal to the average thickness of the tapered fin, based on (3.9) and factoring in that $\beta = 2$, thus $x = 1.5x_H$, this would lead to

$$\Delta t = 0.333 \frac{qH^2}{kx_H}.$$

The reduction of Δt with the tapered fin identified by the ratio 0.307/0.333 is equal to 7.8%.

Finally, note that the vertical disposition of the radiated tubes is not the only solution. Generators with forced circulation can have a helicoidal disposition with almost horizontal tubes running along the four walls of the furnace. This model more easily promotes the high speed of the fluid required for this type of circulation.

As far as the temperature of the tube with respect to the temperature of the internal fluid in terms of resistance verification, the focus lies on the average wall temperature, whereas the external temperature is crucial in terms of scaling.

The temperature difference between the fluid and the average fiber of the tube is given by

$$\Delta t = q \left(\frac{1}{\alpha} + \frac{x}{2k} \right), \tag{3.17}$$

whereas the difference between the fluid and the external wall is equal to

$$\Delta t = q \left(\frac{1}{\alpha} + \frac{x}{k} \right). \tag{3.18}$$

q stands for the thermal flux referred to the internal surface, α for the heat transfer coefficient of the evaporating water, x for the thickness, and k for the thermal conductivity of the steel.

Let us assume, for example, that $q = 290\,\mathrm{kW/m^2}$, the thickness is 5 mm, and k is equal to 44 W/mK; given that α is referred to evaporating water, the value may be assumed to be $12,000\,\mathrm{W/m^2K}$ (see Sect. 8.5).

Based on (3.17), we obtain

$$\Delta t = 290,000 \left(\frac{1}{12,000} + \frac{0.005}{2 \times 44} \right) = 41^{\circ}\mathrm{C}.$$

From (3.18), we obtain

$$\Delta t = 290,000 \left(\frac{1}{12,000} + \frac{0.005}{44} \right) = 57^{\circ}\mathrm{C}.$$

In absence of direct calculation, one can conventionally assume the temperature of the fluid plus 50 °C to be the average temperature of the wall. This small temperature difference, due to the high value of the heat transfer coefficient of the evaporating water, only occurs if the evaporation takes place by bubble enucleation. The build up of steam film on the wall of the tube leads to a sudden reduction of the heat transfer

coefficient. This is the well-known phenomenon of film boiling. Its dangerous implications are great.

As long as the thermal flux does not exceed certain values, the evaporation occurs through enucleation of steam bubbles. These detach themselves from the wall and are substituted with surrounding water. But when the flux exceeds a certain value, a film of steam builds up on the wall and considerably reduces the heat transfer coefficient compared to the one in the case of bubble enucleation. This way, there is a sudden increase in the temperature difference between wall and fluid, as is shown in Fig. 3.8 in reference to the absolute pressure of 1 bar.

Under that pressure, the critical flux is extremely high ($\approx 1000\,\mathrm{kW/m^2}$), that is, much higher than the maximum flux values that may be reached in steam generators under worst conditions. But as we shall see, the critical flux noticeably decreases as the pressure goes up, therefore impacting the generators under great pressure.

The sudden increase in temperature difference between wall and fluid leads to superheating of the wall that may be so great as to compromise the resistance of the tube up to actual bursting, especially if it is hit by a heat flux that is almost independent from the heat transfer coefficient of the fluid. This situation occurs in the furnace, by the way the only area where the phenomenon is actually possible because of the substantial thermal flux.

The quantities that condition the occurrence of this phenomenon are the water-vapor ratio (or the mass percentage of steam contained in the water-vapor mix), the pressure, the mass velocity, and the thermal flux. The latter is crucial in terms of the minor or greater danger of the phenomenon, as far as the temperature difference between the internal wall of the tube and the fluid it creates.

Figure 3.9 highlights the impact of the water-vapor ratio and the thermal flux under constant pressure and constant mass velocity.

As the flux increases, the phenomenon starts for decreasing values of the water-vapor ratio and causes increasing temperature differences. In the specific case, this difference is about proportional to the cube of the flux. This strong impact of the

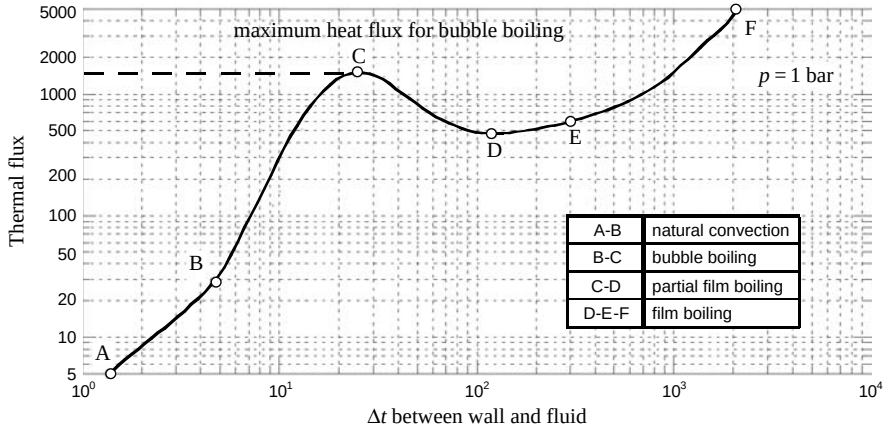


Fig. 3.8

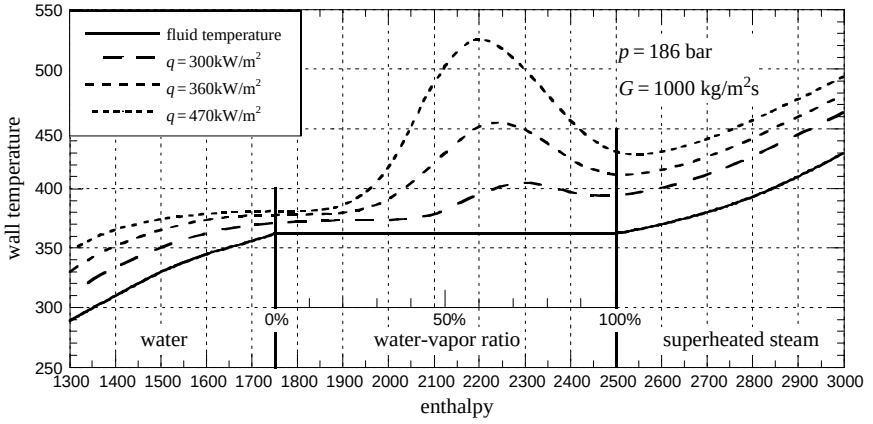


Fig. 3.9 Influence of water-vapor ratio and thermal flux on wall temperature

flux on the temperature difference is easily explainable observing that the increase in flux increases the thickness of the steam film because of the high level of evaporation. Besides the greater amount of heat to transfer through the film, there is a greater thickness to penetrate. The value of Δt is therefore influenced twice by the increase in flux. Once the maximum value is reached, Δt decreases as the water-vapor ratio increases, thus the velocity of the mix increases until it reaches the value corresponding to the heat transfer coefficient of the superheated steam.

The influence of pressure, water-vapor ratio, and flux per constant mass velocity is represented by Fig. 3.10.

The curves indicate the conditions that start film boiling. Under equal pressure, the phenomenon starts with decreasing water-vapor ratios as the flux increases, as already shown in Fig. 3.9. Under constant flux, the increase in pressure starts the film boiling with decreasing water-vapor ratios. Under high-level flux or high pressure,

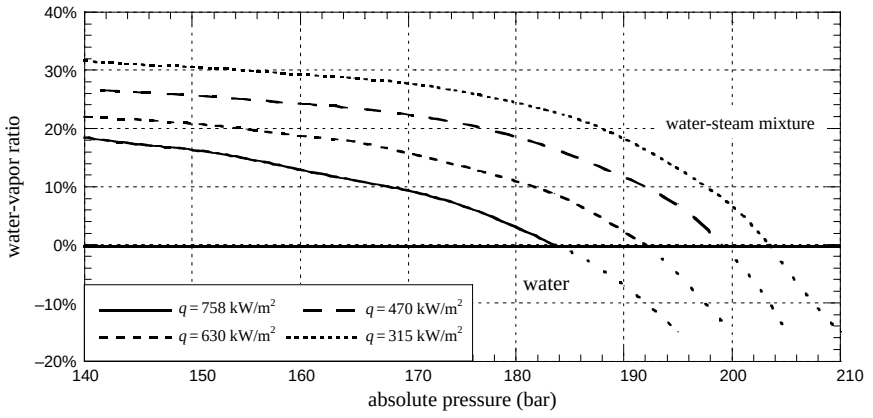


Fig. 3.10 Influence of pressure, water-vapor ratio, and thermal flux on film boiling

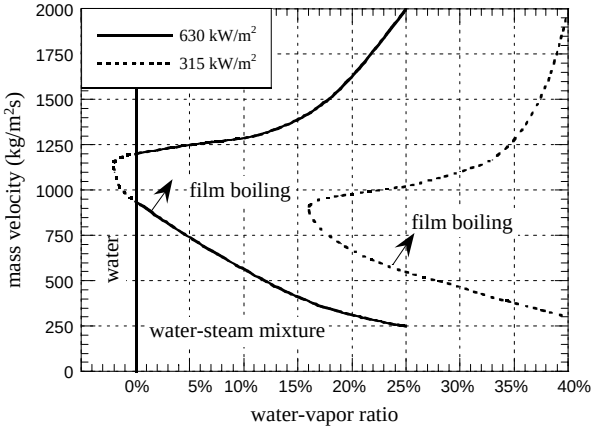


Fig. 3.11 Influence of mass velocity, water-vapor ratio, and thermal flux on film boiling

it may even occur through the mere presence of water (dotted areas of the curves). The diagram refers to a mass velocity of $830\,\mathrm{kg/m^2s}$.

The influence of mass velocity, water-vapor ratio, and flux can be examined in Fig. 3.11. The constant, absolute pressure is equal to 186 bar. Note that as the mass velocity varies, the value of the water-vapor ratio responsible for the start of the phenomenon first decreases, moving from low velocity to medium velocity to increase further if the velocity reaches high values.

The purely qualitative diagram, given that it identifies only the conditions under which the phenomenon starts to occur without quantifying its entity, may lead to mistaken conclusions. In fact, the increase in mass velocity is always favorable to push back or eliminate the danger of heavy superheating of the tube as a result of film boiling.

The phenomenon under scrutiny must be especially kept under control in the case of generators with forced circulation, both because of the high levels of pressure and most of all because all the water entering the steam-generating tubes is transformed into steam. The final part of these contains steam with a high water-vapor ratio.

Furthermore, keep in mind that the decrease in output goes hand in hand with a decrease in water and steam amount circulating in the tubes.

The generator must be designed to have high mass velocity, even under reduced load, potentially identifying structural solutions, such as almost horizontal tubes placed as a spiral along the walls we mentioned or forcing more than one path along the wall through special circuits.

In fact, if the path is longer, the heat transferred to the tube is greater and can be run through by a greater water mass to evaporate. To this extent, note that an increase in pressure reduces the heat of vaporization, thus requiring a smaller amount of heat to evaporate a given water mass. This means that the working pressure of the generator strongly influences structural characteristics.

Besides provoking high mass velocity, the design of the generator must be such that the ends of the steam-generating tubes are in an area where the thermal flux



Fig. 3.12 Ribbed tube (Courtesy of Babcock & Wilcox)

is modest. The simple presence of these parts in the upper section of the furnace, where the flame is exhausted and the gas is colder compared to the central section, provokes reduced flux. It is also possible to move the ends of the steam-generating tubes in a "quieter" area of the generator, for example, on the side walls of the area taken by the superheater and the reheater.

To reduce the danger of film boiling, it is possible to use special tubes that are ribbed on the inside (see Fig. 3.12). The tendency to film boiling can be fought by interrupting the continuity of the wall and by provoking turbulent flow in the boundary layer.

The problem is different in the case of generators with natural circulation, given that only part of the water entering the steam-generating tubes evaporates. At the exit, the mix is still rich in water. Essentially, the danger of film boiling can be avoided by intervening on the water-vapor ratio of the steam exiting the steam-generating tubes. In other words, it is a question to have a mix so rich in water to rule out the onset of the phenomenon. In fact, the previous diagrams demonstrate the crucial importance of the water-vapor ratio.

Of course, this does not rule out excessive flux and the positioning of the ends of the tubes in areas of the furnace with reduced thermal flux. In radiation generators, this is automatic considering the geometry of the tube walls.

In conclusion, natural circulation boilers require the circuits of the steam-generating tubes to be such to ensure a safe circulation ratio, that is, the ratio between the mass of the mix and the mass of steam at the exit of the steam-generating tubes (reciprocal of the water-vapor ratio).

The topic will be discussed extensively in Chap. 10 by indicating the advisable circulation ratio for the different levels of pressure.

3.3 Drum

The purpose of the drum is to separate water from steam. Its lower part is full of water. It comes from the economizer through tubes external to the boiler or if it is missing, directly from the feed pumps. The upper part is filled with steam instead taken from the main valve. If the superheater is included, the steam passes through the entry header of the latter instead.

In big radiation units, downcomers are inserted into the lower part of the drum feeding the steam-generating tubes of the bank (if there is one), as well as the screens

of the furnace. Return tubes coming from the upper headers are inserted laterally into the drum.

In small units, the downcomers can also be coupled to the lower part of the drum while the return tubes are connected to the sides. Otherwise, the tubes making up the screens of the furnace and those making up the steam-generating tubes of the bank can be coupled directly to the drum.

In generators with two drums, the lower drum is the only header of the boiler. Naturally, it is filled with water. Together with the upper drum, it is coupled with the tubes making up the radiated screens in the furnace and the steam-generating tubes of the bank.

In small power plants under low pressure, that is, up to 15–20 bar, and in the absence of a superheater, the separation of steam from the water can be achieved naturally without the intervention of special devices, counting exclusively on the difference in density of water and steam. This works as long as the intake is located at least 50 cm above the water level, to prevent huge water entrainment.

At any rate, it is always best to factor in a metal sheet in front of the main intake to force the steam to go through part of the drum before entering the external piping. Under higher pressure, it is advisable to factor in at least a few deflecting plates that force the mix of water and steam coming from the steam-generating tubes to go through a winding path to facilitate the separation of the two components in the mix.

The volume of the drum, or rather the volume of the steam chamber building up above the water surface, is of great importance too. Considering that the average water level usually coincides with the center line of the drum, the volume of the steam chamber corresponds to half the internal volume of the drum.

Figures 3.13 and 3.14 show the curves that represent the maximum and minimum values among which the values of the loads of the steam chamber under different values of pressure are usually selected.

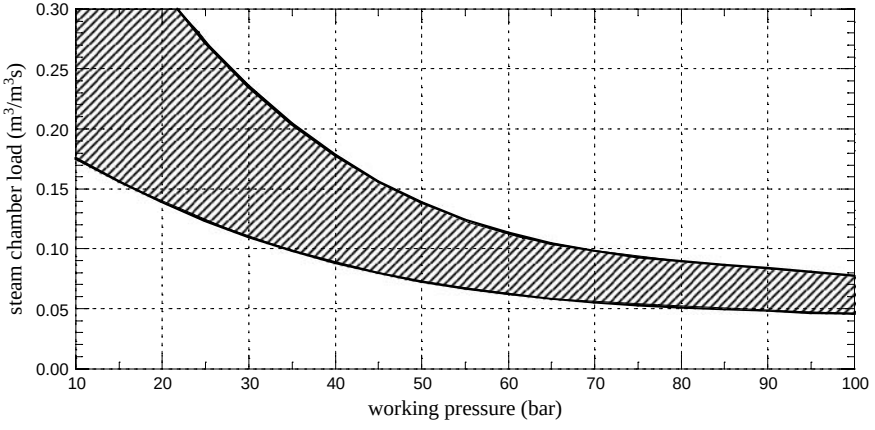


Fig. 3.13 Allowable load of steam chamber in m^3/m^3s

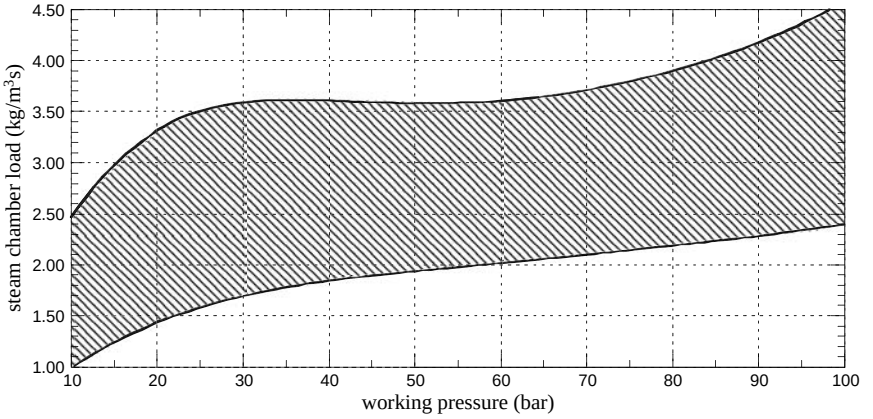


Fig. 3.14 Allowable load of steam chamber in kg/m^3s

Figure 3.13 is about the m^3/s of steam produced per m^3 of chamber, whereas Fig. 3.14 is about the kg/s of steam produced per m^3 of chamber. The choice of the value of the load is the reference to adequately size the drum.

The range is quite wide. On the other hand, it is impossible to provide more detailed instructions, considering all the factors at play, such as the location of the downcomers and the return tubes, the location of the intake, the velocity and circulation ratio of the water–steam mix, the type and shape of the deflecting plates, the presence or absence of the superheater, and so on. It is simply possible to say that minimum values are to be selected when there are low circulation ratios, an irregular distribution of the mix and not particularly efficient conveying plates. Maximum values are to be selected with high circulation ratios, good distribution, and efficient separation devices. Therefore, both Figs. 3.13 and 3.14 provide general reference material. Design and running experience only help to make the correct choices.

Without a superheater, a water-vapor ratio of 0.97 matched by a water entrainment of 3% in mass may be considered sufficient. Steam with these characteristics is commercially considered equal to saturated dry steam, even though it is not from a technical point of view.

On the other hand, if there is a superheater and especially if the pressure exceeds 50 bar, such a low water-vapor ratio is not acceptable. In fact, regardless of previous treatments in water conditioning plants, water always contains a certain amount of phosphates, sulfates, silicon dioxide, and so on that are fortunately carried through the steam only in part.

If the water was adequately treated, if there is sufficient drainage from the drum to reduce salinity, and if the water-vapor ratio is high, there will be no buildup on the tubes of the superheater and on the turbine blades.

But if the steam carries a huge amount of water, these substances dangerously increase and deposits will build up, thus provoking a temperature increase of the tubes that make up the superheater. Considering the high running temperature of the

latter, even modest deposits and relatively small temperature increases of the wall under normal conditions may suffice to trigger the burst of the superheater.

If there is a superheater, the water-vapor ratio of the steam must range from 0.98 to 0.995, depending on the pressure. Silicon dioxide is the most dangerous substance in the water because of the nature of its deposits, and its content in the superheated steam must not exceed 0.03 mg per litre. Thus, the separation of water by gravity or the deflecting plates are not enough to obtain these high water-vapor ratios under high pressure.

Special devices consisting of cyclones, drilled plates, and drying filters are used (see Figs. 3.15 and 3.16).

In this case, the mix is introduced in a series of cyclones that determine the waterfall toward the bottom through centrifugation and the output of upward steam. The latter is forced to go through driers consisting of drilled plates with staggered holes, corrugated latten, and so on where the steam frees itself from the remaining little drops collected in a lower duct and discharged on the water surface.

In this case, the volume of the drum is not tied to the necessity to limit the load of the steam chamber to a certain value, but rather to the volume of the devices located inside it instead. For instance, drums with 132 bar and a steam chamber load of $7\,\mathrm{kg/m^3 s}$ were built in reference to half the internal volume of the drum, that is, regardless of the considerable volume of the devices. Similarly, drums at 167 bar

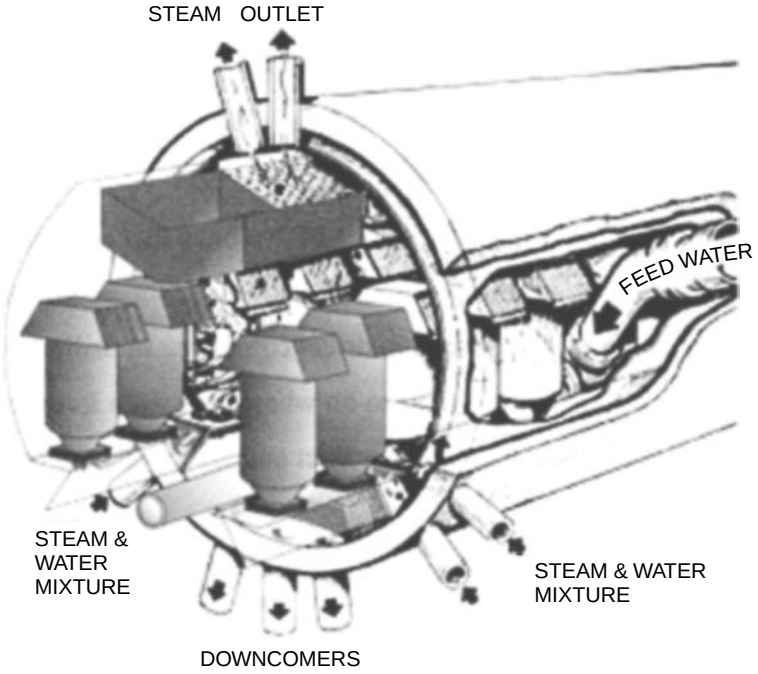


Fig. 3.15 Internal devices of the drum (Courtesy of Alstom)

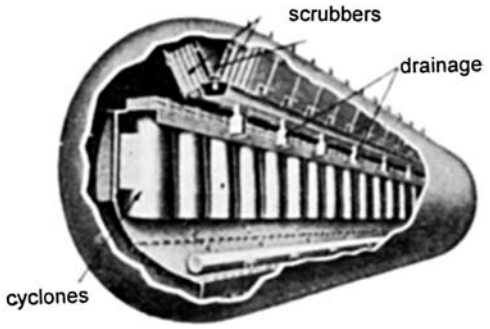


Fig. 3.16 Drum with internal devices

with a load of $10\,kg/m^3s$ were built. These very high values are made possible by the effectiveness of the devices designed to separate the water from the steam.

Without diminishing the importance of the water-vapor ratio, note that a high water-vapor ratio does not prevent superheating of the tubes of the superheater. The water in the boiler must already have a low content of silicon dioxide, especially

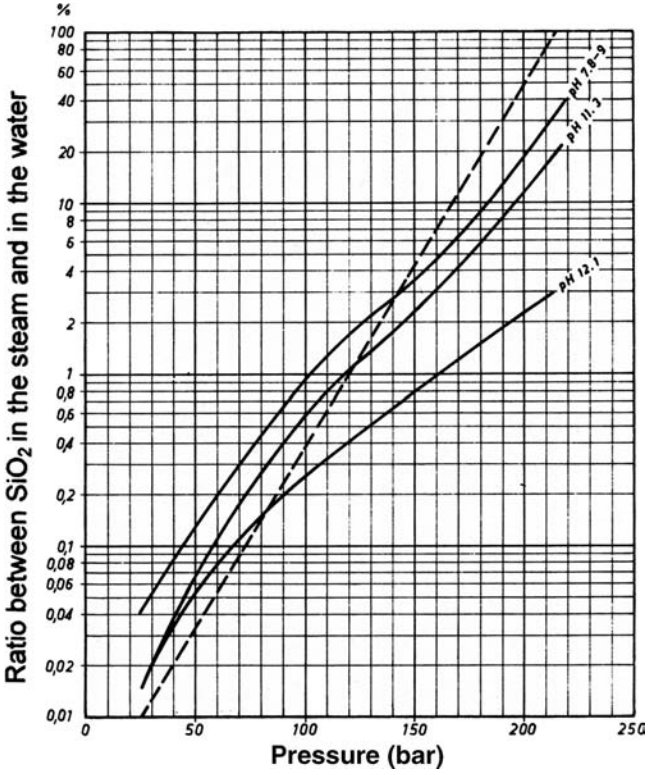


Fig. 3.17 SiO_2 in the steam and in the water

under high pressure. Figure 3.17 shows that an increase in pressure is matched by an increase of the ratio between silicon dioxide content pushed forward by the steam and the ratio of the water.

Clearly, under high pressure, even if absolutely dry steam were taken from the drum, if the content of silicon dioxide in the water were too high, the steam would drag an unacceptable amount with it.

For instance, at 150 bar, the content of silicon dioxide in the water must not exceed 1 mg/l. Generators under lower pressure will obviously have less stringent requirements. Note that for pressures below 50 bar, it is acceptable to have a water-vapor ratio of 98–99% and a content of SiO_2 in the feed water below 20 mg/l for pressures up to 15 bar, under 10 mg/l for pressures up to 25 bar, and below 5 mg/l for generators ranging from 25 to 50 bar. A content of SiO_2 in the water up to 3–4 times greater than the one indicated for feed water is tolerable.

Until now, we referred to silicon dioxide to provide significant feedback on the importance of water treatment. Of course, phosphates, sulfates, oxygen, pH, carbon dioxide levels, and so on are to be checked as well.

The treatment of water is undoubtedly of great interest for the conductivity of generators. It is not inherent to the design of generators, but on the other hand the literature includes many publications on this topic. The reader will find more in-depth information there.

Due to the reduced entrainment of impurities in the water through the steam, their concentration increases in the water contained in the drum where the so-called

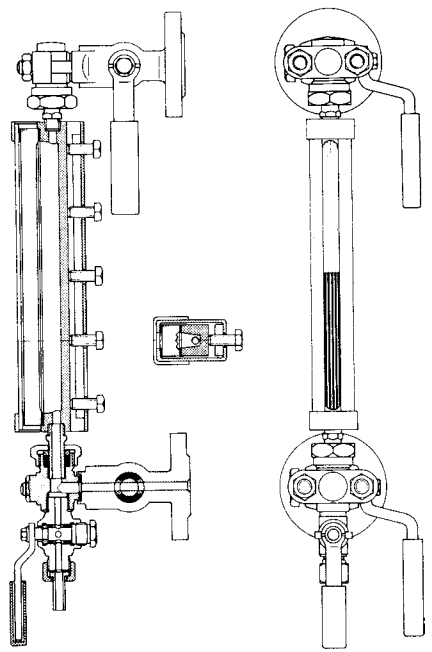


Fig. 3.18 Level gauge

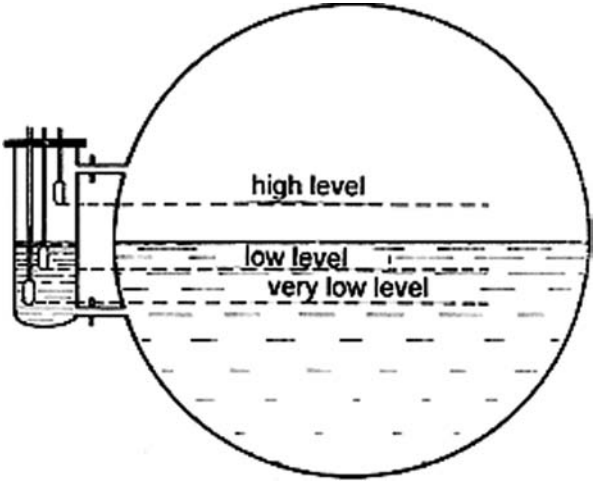


Fig. 3.19 Water level control in the drum

sludge decants on the bottom. They must be drained either periodically or continuously to keep their concentration within safety limits. In the case of on-going drainage, this may cause a significant heat loss in big plants where this is always the case. A heat exchanger will recuperate the heat.

For running safety of the drum, it is crucial to keep the water level under control.

In small power generators, two level gauges are designed to perform this function, and at least one of them must be behind glass (see Fig. 3.18). The other gauge may consist of two trial faucets. They must be clearly visible and independent from one another.

In big units, the readings are shown on the board. Moreover, a system of mirrors at maneuvering level of the stoker, that is, at one service floor of the burners, helps do this.

There are also protection devices relative to the water level. Generally, the provision is for alarm at lower and upper level and for shutdown at lowest level.

These are conduction devices that exploit the different electrical conductivity of water and steam (see Fig. 3.19).

3.4 Steam-Generating Tube Bank

Mostly missing in radiation generators, the steam-generating tube bank represents an essential part of the boiler in small- and medium-size units. Specifically, if both the superheater and the economizer are missing, or if the latter consists of cast iron finned tubes, the steam-generating bank is the only tube bank located inside the boiler block. To fully appreciate its contribution to the heat transfer, we use an example involving small power and pressure generators producing saturated steam.

Assuming combustion with fuel oil with a net heat value equal to 40,600 kJ/kg and $|CO_2|$ equal to 14% (this corresponds to excess air of 16%), the produced flue gas is 16.9 kg per kg of fuel (see Chap. 7). At conventional room temperature of 20 °C, both air and flue gas have an enthalpy of 21 kJ/kg. The introduced heat is equal to $40,600/16.9 = 2402\,\text{kJ/kg}$ of gas. The adiabatic heat content of the gas is equal to $21 + 2402 = 2423\,\text{kJ/kg}$. If the flue gas temperature at the exit of the furnace is 1000 °C with a moisture level as mass of 6%, the diagrams in Chap. 7 show that the enthalpy of the gas at the exit of the furnace is equal to 1172 kJ/kg. We assume an absolute pressure of the generator equal to 16 bar, equivalent to a steam temperature of 200 °C. To achieve acceptable generator efficiency and costs, one can assume the temperature of the flue gas at the exit of the generator to be 260 °C with an enthalpy of 279.5 kJ/kg.

In the furnace, the heat transfer corresponds to $2423 - 1172 = 1251\,\text{kJ}$ per kg of flue gas, whereas the heat transferred through the tube bank equals $1172 - 279.5 = 892.5\,\text{kJ}$ per kg of gas. The total sum amounts to 2143.5 kJ; besides losses due to external radiation and miscellaneous losses and ruling out the presence of unburned carbon monoxide, the efficiency is equal to $(2143.5/2402)100 = 89.2\%$. Thus, the heat transfer in the tube bank represents 41.6% of the total.

The steam-generating bank in two-drum generators consists of a series of tubes curved in different ways at the extremities to allow the radial insertion in drums (see Fig. 3.20); they can be in-line or staggered (see Chap. 8). The transverse pitch is selected based on different requirements, such as obtaining satisfactory heat transfer and limited pressure drop, allowing the insertion in drums with a sufficiently high transverse ligament efficiency (the closer the tubes, the greater the thickness of the drum). Moreover, it should facilitate efficient cleaning through steam blowing of the external surfaces of the tubes. The longitudinal pitch is chosen based on similar reasons even though it is less crucial in terms of either heat transfer or pressure drop. Given the persisting necessity to adopt sufficiently big pitches, especially as far as the resistance of the drums, the adoption of reduced values allows the construction of very compact units, including minor costs and ease of transportation.

Tube banks of modular-type generators have similar functional requirements. In these generators, the bank consists of different sections made of tubes inserted into tubes used as headers, in turn connected to entry and exit headers or entry only headers (the exit header tube directly connects into the upper drum), or directly connected to the drum through downcomers and return tubes (see Figs. 3.21 as well as 3.22).

From a structural point of view, there are considerable differences, depending on the type, as far as the actual construction of the bank (e.g., separate construction of the various modules in the case of modular-type generators), as well as the construction of one or two drums (where it is possible to have many holes for expanded tubes or simply few holes for the insertion of downcomers and return tubes that are either expanded or welded). Even assembly procedures in the workshop obviously vary a great deal, depending on the actual case.

Generally, the steam-generating bank is not passed through by flue gas in one step only. Two or more passages are expected, and this implies the necessity to

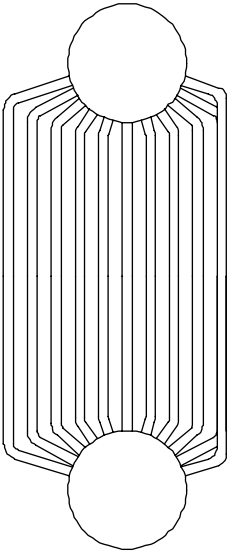


Fig. 3.20 Tube bank of two-drum generator

factor in partition baffle plates between each passage. These consist of walls of refractory tiles or refractory casting or plates made of special steel able to withstand high temperatures without scaling off (superficial oxidation).

Sometimes the seal between every passage is achieved by lining up the tubes side by side, or through finned tubes (with uninterrupted fins welded to both tubes, as with membrane walls), or by welding the tubes together. The solution with lined

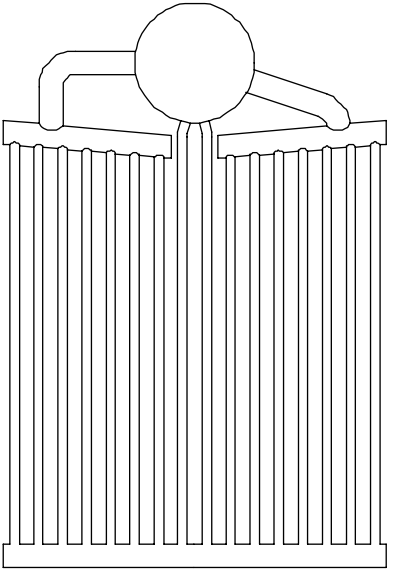


Fig. 3.21 Tube bank of a generator with central drum

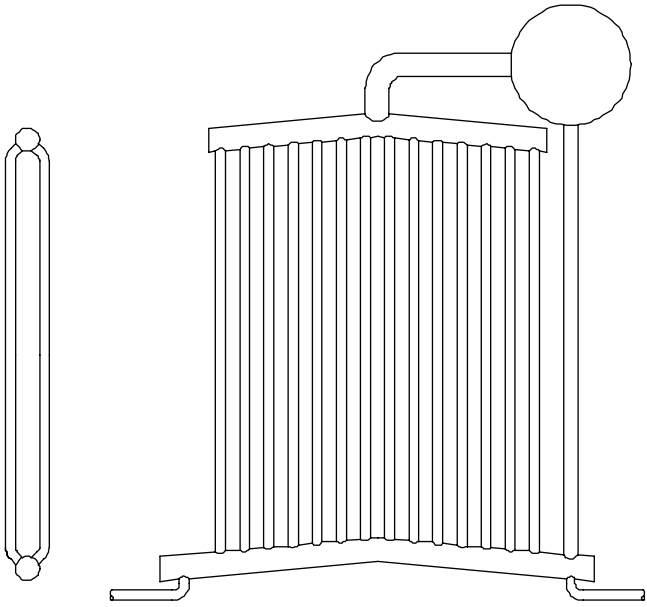


Fig. 3.22 Tube bank of a generator with lateral drum

up tubes is debatable in terms of seal. In fact, inevitable leaks between the tubes let the gas pass through.

To that extent, note the need for the diaphragms to be absolutely efficient throughout the different passages however they are set up. Otherwise, part of the gas takes a path unforeseen during the design phase. Consequently, some of the tubes in the bank are hit by a load of gas smaller than the expected one that leads to a reduction in velocity and heat exchange. A defect in the seal between the furnace and the exit of the generator can be particularly serious. It could happen, for example, in two-drum generators with two flue gas passages if the baffle plate between the two passages is inefficient (see Fig. 3.23). In that instance, part of the gas is directly conveyed to either the chimney or the economizer without hitting the bank.

As far as the temperature of the tubes, we refer to (3.17) and (3.18) that are equally used for tube walls. Assuming that the thermal flux is $70\,\mathrm{kW/m^2}$, with a thickness of $5\,\mathrm{mm}$ and heat transfer coefficient of the evaporating water equal to $12,000\,\mathrm{W/m^2K}$, in the first case, given that $k = 44\,\mathrm{W/mK}$, this means that

$$\Delta t = 70,000\left(\frac{1}{12,000} + \frac{0.005}{2\times 44}\right) = 10^{\circ}\mathrm{C}.$$

As far as the external surface

$$\Delta t = 70,000\left(\frac{1}{12,000} + \frac{0.005}{44}\right) = 14^{\circ}\mathrm{C}.$$

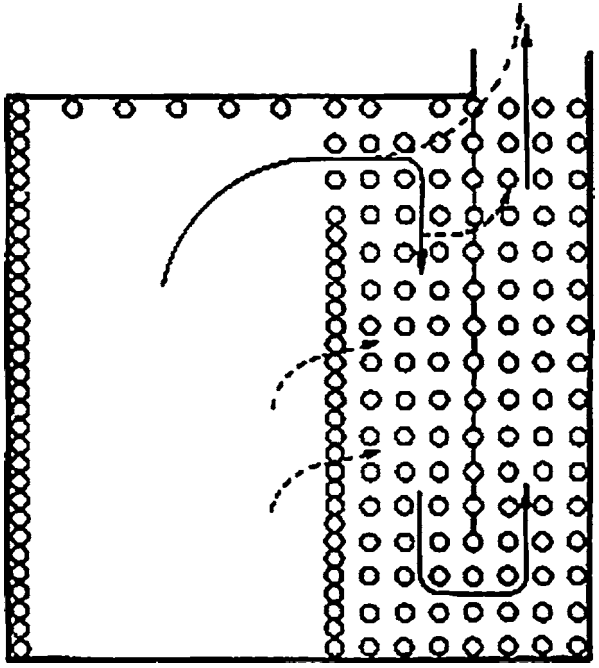


Fig. 3.23

These are evidently modest values. Even assuming that the heat transfer coefficient of the evaporating water is only $6000\,\mathrm{W/m^2K}$ (this would be the lower limit) in both cases

$$\Delta t = 16^{\circ}\mathrm{C}$$

$$\Delta t = 20^{\circ}\mathrm{C}.$$

In absence of direct calculations, one can assume a difference of $20\,^{\circ}\mathrm{C}$.

3.5 Tube Bending

Bent tubes are widely used to build the generator. The superheaters and the reheaters, the economizers in steel tubes, and in some instances the steam-generating tube bank are built through bent tubes. The screen walls of the furnace have curves for the insertion in the headers to create the nose, the top, and the bottom when they are the continuation of the vertical walls without interposition of the headers and so on. Therefore, the curvature of the tubes represents one of the most important operations in a boiler workshop.

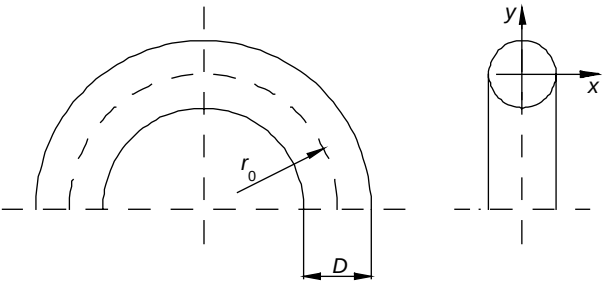


Fig. 3.24

The actual tubes of the generator, that is, the ones hit by the flue gas, are curved cold through adequately equipped machines that are able to produce even very tight curves. In fact, it is possible to curve tubes with a good success rate, even with a curvature radius referred to the axis equal to one and a half the diameter of the tube or even a curvature radius equal to its diameter.

During curvature, the external fibers (extrados) undergo elongation, whereas the internal fibers (intrados) become shorter. As a consequence, the external thickness reduces itself, whereas the internal one increases. Thus, these variations in thickness must be kept under control to prevent intolerable stresses caused by internal pressure during runtime. By applying the membrane theory to the curve (see Fig. 3.24), the hoop stress σ_c indicated with $\sigma_c{}'$ for the extrados and with $\sigma_c{}''$ for the intrados is given by

$$\sigma_c = \frac{pD}{2x}\frac{r_0+\frac{y}{2}}{r_0+y}, \tag{3.19}$$

where x is the actual thickness after curvature.

On the extrados, if the thickness is x'

$$\sigma_c{}' = \frac{pD}{2x'}\frac{r_0+\frac{D}{4}}{r_0+\frac{D}{2}}, \tag{3.20}$$

whereas on the intrados if the thickness is x''

$$\sigma_c{}'' = \frac{pD}{2x''}\frac{r_0-\frac{D}{4}}{r_0-\frac{D}{2}}. \tag{3.21}$$

Assuming that the average fiber does not elongate, the original length of the portion of the tube that was curved is equal to

$$l_0 = \pi r_0. \tag{3.22}$$

The length of the fiber on the extrados after curvature becomes

$$l' = \pi\left(r_0+\frac{D}{2}\right). \tag{3.23}$$

The elongation $\varepsilon_a{}'$ in the axial direction is therefore given by

$$\varepsilon_{\mathrm{a}}{}' = \frac{l' - l_0}{l_0} = \frac{1}{2}\frac{D}{r_0}. \tag{3.24}$$

As known, in the plastic field, deformations occur without variations in volume, and Poisson's ratio takes the value 0.5. Thus, deformations in circumferential and radial direction $\varepsilon_{\mathrm{c}}{}'$ and $\varepsilon_{\mathrm{r}}{}'$ take the following value:

$$\varepsilon_{\mathrm{c}}{}' = \varepsilon_{\mathrm{r}}{}' = -0.5\varepsilon_{\mathrm{a}}{}' = -\frac{1}{4}\frac{D}{r_0}. \tag{3.25}$$

Given that x_0 is the original thickness, the thickness on the extrados becomes

$$x' = \left(1 - \frac{1}{4}\frac{D}{r_0}\right) x_0. \tag{3.26}$$

The hoop stress $\sigma_{\mathrm{c}}{}'$ is therefore based on (3.20):

$$\sigma_{\mathrm{c}}{}' = \frac{pD}{2\left(1 - \frac{1}{4}\frac{D}{r_0}\right) x_0} \frac{r_0 + \frac{D}{4}}{r_0 + \frac{D}{2}}; \tag{3.27}$$

it can also be written as follows:

$$\sigma_{\mathrm{c}}{}' = A' \frac{pD}{2x_0}. \tag{3.28}$$

The hoop stress in the straight tube considering small thicknesses is equal to

$$\sigma_{\mathrm{c}} = \frac{pD}{2x_0}. \tag{3.29}$$

Therefore, A' represents the ratio between the value of the stress $\sigma_{\mathrm{c}}{}'$ on the extrados and the one in correspondence of the straight tube. It is given by

$$A' = \frac{1 + \frac{1}{4}\frac{D}{r_0}}{\left(1 - \frac{1}{4}\frac{D}{r_0}\right)\left(1 + \frac{1}{2}\frac{D}{r_0}\right)}. \tag{3.30}$$

From (3.30), we obtain the following values of A':

$$\begin{aligned} r_0/D &= 1.5 \qquad & A' &= 1.05 \\ &= 2 & &= 1.028 \\ &= 3 & &= 1.012 \end{aligned}$$

The hoop stress in correspondence of the extrados would visibly result to be slightly greater than the one relative to the straight tube.

By analogy, for the fiber in correspondence of the intrados we obtain

$$\varepsilon_c'' = \varepsilon_r'' = -0.5\varepsilon_a'' = \frac{1}{4}\frac{D}{r_0}. \tag{3.31}$$

The stress σ_c'' takes the following value:

$$\sigma_c'' = A''\frac{pD}{2x_0}, \tag{3.32}$$

given that

$$A'' = \frac{1-\frac{1}{4}\frac{D}{r_0}}{\left(1+\frac{1}{4}\frac{D}{r_0}\right)\left(1-\frac{1}{2}\frac{D}{r_0}\right)}. \tag{3.33}$$

From (3.33),

$$\begin{aligned} r_0/D = 1.5 \qquad & A'' = 1.07 \\ = 2 \qquad & = 1.036 \\ = 3 \qquad & = 1.015 \end{aligned}$$

The values of A' and A'' are shown in Fig. 3.25.

Even in this case, the σ_c'' relative to the intrados would evidently be greater than the one relative to the straight tube.

In reality, by taking adequate measures during construction, the value of ε_a' on the extrados is greater than the theoretical one given by (3.24), because the fiber that does not elongate is more on the inside than the average one and also because the elongation is not constant along the curve but goes down at the ends. Moreover, the

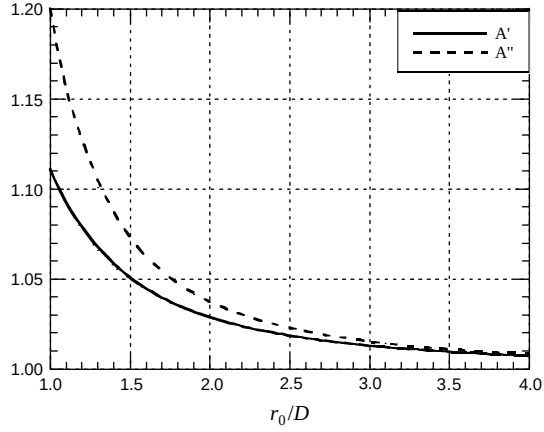


Fig. 3.25

absolute value of $\varepsilon_c{}'$ is higher than the theoretical one, but the value of $\varepsilon_r{}'$ is smaller than the theoretical one. On the intrados, the absolute value of $\varepsilon_a{}''$ is slightly smaller than the theoretical one. In addition, the value of $\varepsilon_r{}''$ is greater than the one of $\varepsilon_c{}''$ and greater than the theoretical one.

In practice, the reduction in thickness on the extrados is less than the theoretical one, whereas the increase in thickness on the intrados is greater than the theoretical one. The actual situation is therefore better than the one obtained through computation, as long as the curvature is done correctly. The curvature does not cause concern under these conditions nor does it require an increase in thickness of the tube to factor in stretching in the curve. This is what is usually done. Therefore, it is possible to request the workshop to keep variations in thickness within constraints that prevent an increase of σ_c compared to the value of the straight tube. The following equations for the allowable percentage variation in thickness (as absolute value) are obtained through steps that are not shown here.

For the extrados:

$$\frac{\Delta x}{x_0} \leq \frac{25}{\dfrac{r_0}{D} + 0.5}(\%). \tag{3.34}$$

For the intrados:

$$\frac{\Delta x}{x_0} \geq \frac{25}{\dfrac{r_0}{D} - 0.5}(\%). \tag{3.35}$$

The values of $\Delta x/x_0$ are shown in Fig. 3.26.

These limitations can actually be respected. Recalling the values of A' and A'' that do not differ much from the unity (at least for $r_0/D \geq 1.5$), the variations in thickness corresponding to the theoretical ones can exceptionally be tolerated, as long as the ratio between curvature radius and diameter is not below 1.5.

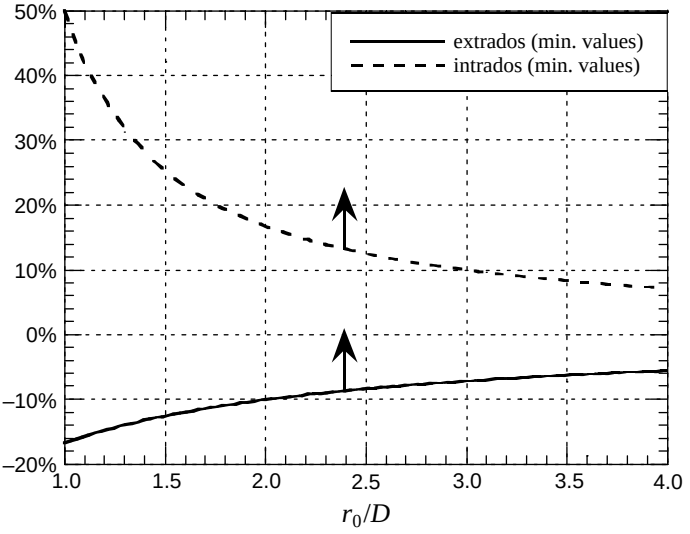


Fig. 3.26 Allowable thickness variations

Instead of (3.34) and (3.35), we obtain the following conditions.

For the extrados:

$$\frac{\Delta x}{x_0} \leq 25\frac{D}{r_0}(\%). \tag{3.36}$$

For the intrados:

$$\frac{\Delta x}{x_0} \geq 25\frac{D}{r_0}(\%). \tag{3.37}$$

Finally, when it becomes necessary to create curves with a very narrow radius, for example, $r_0/D = 1$, as is the case for some coils of the superheaters, the current technique consists of heating the tube up to a high temperature where it needs to curve, putting it under axial compression to upset it and increase the thickness, as well as curve it. This is a safeguard with respect to the reduction in thickness on the extrados; it equally promotes the increase in thickness on the intrados.

Tubes of great diameter (cold curvature is not possible in this case), such as, for example, tubes with a diameter greater than 150 mm, may be required for connections external to the flue gas passage. In that case, warm curvature must be done, if necessary in repeated steps, using intermediate heat to eliminate residual stresses due to plasticization of the material. An easy and economical execution of these curves is subject to the following constraints:

$$\frac{D}{x} \leq 35 \quad \frac{r_0}{D} \geq 3.5.$$

In exceptional instances, besides the increase in execution cost, the following limitations may be acceptable:

$$\frac{D}{x} = 40 \quad \frac{r_0}{D} = 3.5$$

or

$$\frac{D}{x} = 35 \quad \frac{r_0}{D} = 3.$$

In conclusion, note the possibility to buy ready-made curves that can be welded to the straight tube, thus avoiding the bending process.

3.6 Tube Expanding

Tube expanding consists of forcing the tube against the wall of the hole. This is done with a specific tool (see Fig. 3.27) called expander made of a body with rectangular slits that are tilted by a few degrees with respect to the axis where cone-shaped rolls are inserted (generally, the grade of the generatrixes versus the axis amounts to only 5%).

A mandrel is inserted between the rolls, and by rotating forward it forces the rolls to move radially, as well as longitudinally (see Fig. 3.28). In other words, the expander is screwed into the tube, whereas the rolls move toward the outside by pushing on the wall of the tube itself and widen it.

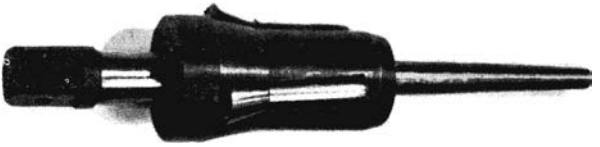


Fig. 3.27 Tube expander

The diameter of the hole is slightly more than a few tenth of a millimeter compared to the external diameter of the tube. Therefore, the expander initially yields the tube and widens it until it adheres to the wall eliminating the initial clearance.

Subsequently, the rolls roll the wall of the tube and make it thinner. This leads to axial elongation and an increase in diameter. The hole must therefore be widened, and this is done through pressure exerted by the tube on the wall of the hole, at the expense of the couple applied to the mandrel of the expander. The drilled plate is therefore subject to both radial and circumferential stresses.

The behavior of the tube–plate structure can be tied to the four phases shown in Figs. 3.29, 3.30, 3.31, and 3.32, considering that the yield strength of the steel of both tube and plate is identical.

During the first phase (Fig. 3.29), the tube is yielded by eliminating the initial clearance c between tube and plate. If expansion is interrupted at this point, nullifying the torque applied to the pin, the tube bounces back. The representative point of the external fiber of the tube goes from A to B, rebuilding a residual clearance between tube and plate c^* that is, in fact, much narrower than the initial one.

Note that point B is not on the axis of the abscissa. This is because the elastic bounce of a yielded tube generates positive residual stresses on the external fibers and negative ones on the internal fibers (the resultant is naturally zero).

The behavior of the first phase corresponds to what is normally called light expanding. It neither does generate clamping pressure between plate and tube nor does

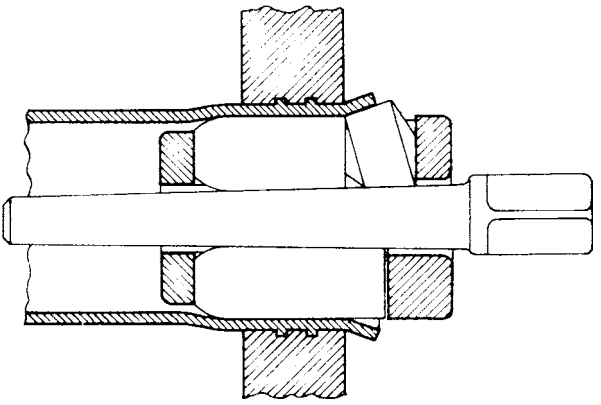
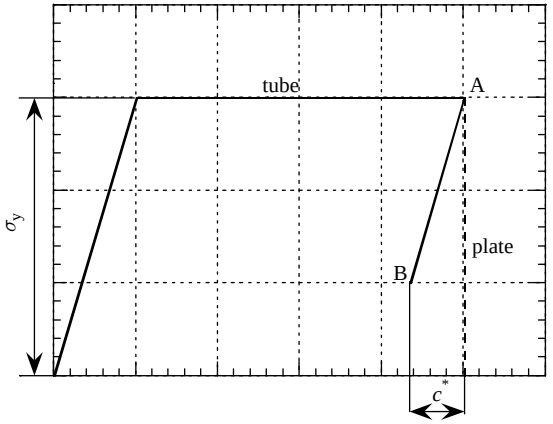


Fig. 3.28

Fig. 3.29



it completely eliminate the clearance. To eliminate the clearance, it is necessary to create stresses (in the elastic field) of a certain entity on the plate at the edge of the hole. This is described in Fig. 3.30. It shows that in order to eliminate the clearance, the radial deformation of the tube under pressure must be greater than the clearance itself. Even in this case, there is no clamping pressure. To provoke clamping, the torque applied to the mandrel must be increased further.

Figure 3.31 shows the situation taking place when the fiber of the plate at the edge of the hole is pushed to the yielding point. In the plate working in the elastic field, the released deformations nullify themselves, and the representative point moves from A to C, whereas for the tube the representative point moves from A to B, as we saw earlier. This would lead to an interference nullified by the clamping pressure generated between plate and tube. It induces compression stress in the tube, followed by a reduction of the radial deformation and the traction stress in the plate, and the deriving widening of the hole. This goes on until congruence is restored.

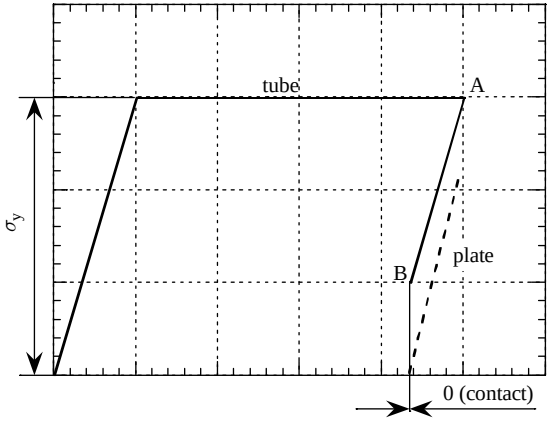
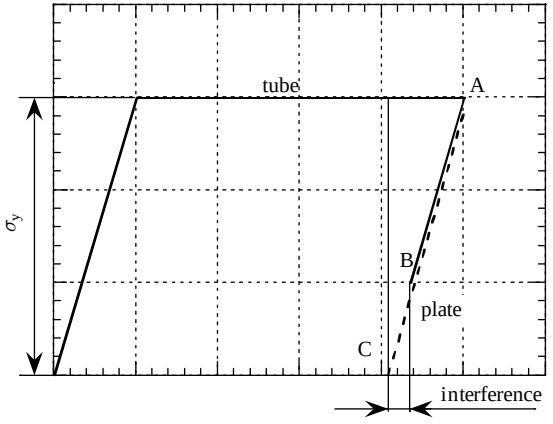


Fig. 3.30

Fig. 3.31



This type of expanding process generates insufficient clamping pressure, and this leads to the fourth phase shown in Fig. 3.32 where even the plate is partially plasticized (in the area around the hole). This way, at release, the representative point of the fiber at the edge of the hole goes from A to D (the residual stress is negative, whereas it is positive in the fibers of the plate far away from the hole), thus achieving much greater interference, followed by more clamping pressure.

The so-called light expanding process, combined with light welding to ensure the seal between tube and plate, is clearly not advisable. In fact, if the tube does not adhere to the plate, a hint of rapidly evaporating water finds its way leaving space for more water. The steam carries only a small amount of the salt contained in the water that deposits itself on the walls of the tube and the plate. Its concentration increases until it causes the well-known phenomenon of stress corrosion.

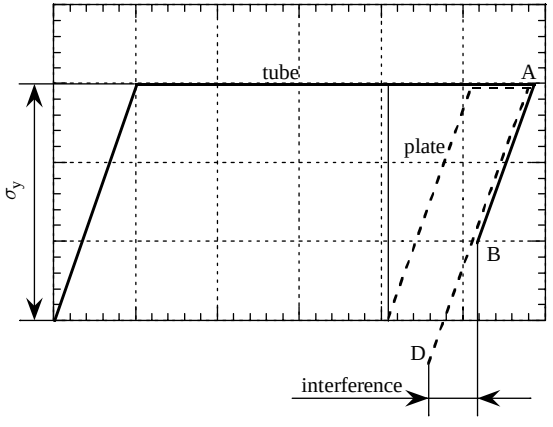


Fig. 3.32

As far as the obtainable clamping pressure, the following equation may be used to compute the maximum clamping pressure in reference to yielding by 50% of the tube sheet (plate):

$$p_{\max} = 10.4\sigma_{yt}\frac{x_t}{d_o}\left(\frac{s}{d_h}\right)^{1.5}\left[\frac{\sigma_{yp}}{\sigma_{yt}} - 1 + 0.234\left(\frac{s}{d_h}\right)^{1.3}\right]. \qquad (3.38)$$

In this equation, σ_{yt} and σ_{yp} are the yield strength of the material of both tube and plate, respectively, expressed in N/mm^2, s is the pitch between the tubes, d_o the outside diameter of the tube, d_h the diameter of the hole, and x_t the thickness of the tube; all these quantities are expressed in mm. The maximum clamping pressure is expressed in bar. The values obtained through (3.38) differ from the real ones by $\pm 9\%$ at the most, but the error is generally smaller.

The clamping pressure visibly increases with the yield strength of the tube, with the ratio between thickness and diameter, with the ratio between pitch and diameter of the hole, as well as the ratio between yield strength of plate and tube. To achieve high clamping pressure, it is therefore necessary to have sufficient thickness, large enough pitches with respect to the diameter of the hole, and preferably to the plate steel with superior mechanical characteristics compared to those of the steel of the tube. Note that with $s/d_h = 1.25$ and, based on (3.38), if the yield strength of the material of the plate is equal to 70% of that of the material of the tube, no clamping pressure will be achieved.

From a practical point of view, if the diameter of the hole increases by 1.5%, when measuring the diameter of the tube after expanding, the expanding process is generally satisfactory.

The reason for the clamping is to prevent the water from insinuating itself between tube and hole and that the axial force on the tube caused by internal pressure makes it slip out of the hole. To ensure the seal and increase the resistance to withdrawal, common practice factors in one or more grooves inside the hole, as shown in Fig. 3.33.

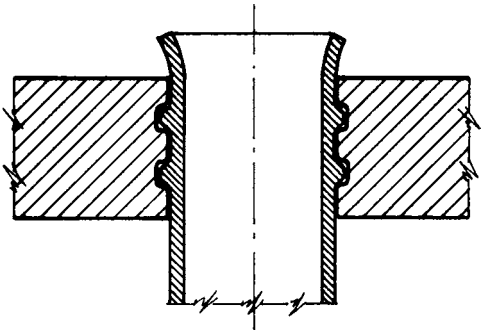


Fig. 3.33

Moreover, the tube is usually flared, as well, as shown in the figure. To that extent, all rolls except one are divided into two parts to obtain a normal expanding roll and another strongly cone-shaped roll that widens the tube protruding from the edge of the plate (see Fig. 3.28). One of the rolls is not split into two and is expected to eliminate the step that would form otherwise between the area of the tube under the normal roll and the one under the action of the more strongly cone-shaped roll.

The expanding can be done manually, for instance through an air drill, by checking the external diameter of the tube with a template. Expanding machines are also widely used to automatically interrupt the process when the applied torque reaches the value producing adequate expanding during construction.

3.7 Superheater and Reheater

Superheaters may be of convection or radiation type.

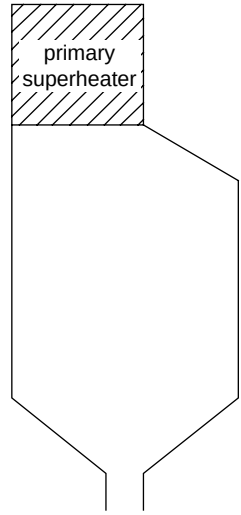
Radiation-type superheaters are those placed along the walls of the furnace. In small generators, this solution is used at times for superheaters that push up the steam temperature by a few dozen degrees above the temperature of the saturated steam. The goal is to dry the steam taken from the drum and to bring it to such a temperature that it reaches the machines it is meant for, still saturated and dry, regardless of the heat loss occurring in the external piping between generator and usage. These superheaters are done by substituting some of the steam-generating tubes on the walls of the furnace with the tubes of the superheater. The location is in the terminal part of the furnace. This way, the tubes will not *see* the flame from the front.

Superheaters placed along the walls of the furnace are used even in very large units (see Fig. 3.34). In that case, they represent the first stage of the superheater (primary superheater). This prevents the temperature of the fluid inside the tubes to increase too much.

The placement of superheaters on the wall is required in that case because, given the need for a certain volume of the furnace to achieve complete combustion, the screened walls cannot entirely be covered with steam-generating tubes (boiler), because in that case the transferred heat would exceed the required one for water evaporation, based on the required output. This situation is typical of greatest power units under very high pressure (low vaporization heat), and most of all for combustion of pulverized coal, considering the greater volume compared to other fuels that require the furnace with equal output.

Hanging superheaters of radiation-type are called SH platen, if they are placed at the exit of the furnace and consist of far apart coils (see Fig. 3.35). In fact, in this case, the heat transferred directly from the flame, or through radiation by the flue gas at high temperature, is greater than the heat transferred by convection, given the low velocity of the gas and the value of the so-called mean beam length (see Sect. 8.9).

Fig. 3.34



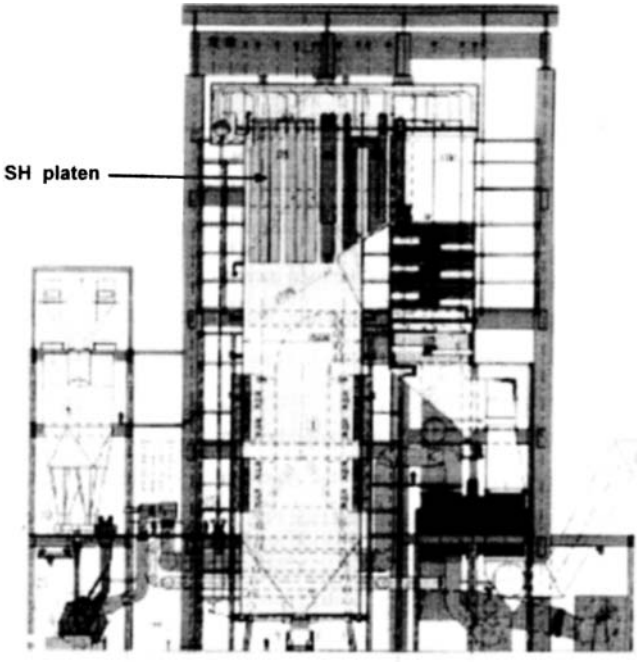


Fig. 3.35 Generator with SH platen (Courtesy of Alstom)

Convection superheaters are those consisting of a coil bank with the coils placed very close to one another in an area of the generator not radiated by the flame. In this case, there is still a quota of heat transferred by radiation by the gas (due to its high temperature), but the heat transferred by convection is greater.

The functional characteristics of superheaters by convection or radiation with regard to load variations are completely different. In fact, in convection superheaters, the temperature of the steam at the exit increases with the load (see Fig. 3.36), whereas it decreases in radiation superheaters. This behavior depends on the following causes. In convection superheaters, a load increase (it will increase the burned fuel) is matched by an increase in temperature of the flue gas that hit it. In addition, the velocity of flue gas and, by default, the overall heat transfer coefficient goes up. Therefore, the transferred heat increases considerably, prevailing on the simultaneous increase in steam to be superheated. Thus, the temperature goes up.

In radiation superheaters, the load increase will increase the temperature of both flame and flue gas. Consequently, the radiated heat goes up, but this increase does not compensate for the increase in steam to be superheated. For this reason, the temperature decreases.

By combining a convection superheater with a radiation superheater, it is possible to achieve a temperature of the superheated steam that will remain constant, regardless of load variations (see Fig. 3.37) or that will at least reduce temperature variations.

Note that radiation superheaters carry smaller costs. In fact, given equal heat absorption, the radiation superheater has a much smaller surface and is much easier to build compared to the convection superheater. On the other hand, its functioning is more delicate relative to deposits inside the tubes, as well as the danger of bursting caused by superheating of the walls, as a result of the darting of the flame (especially

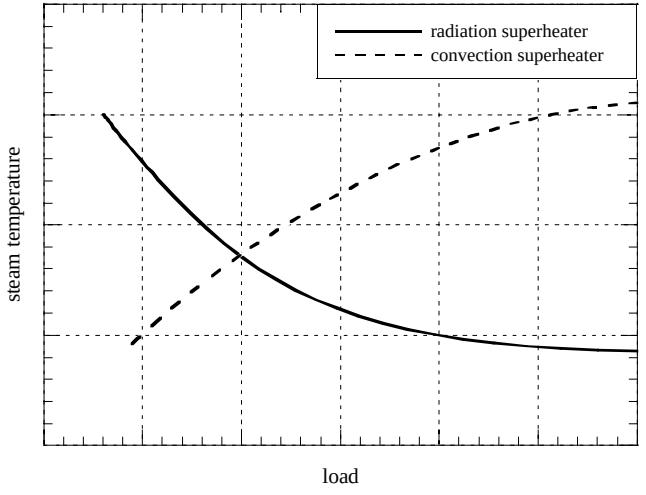


Fig. 3.36 Superheated steam temperature

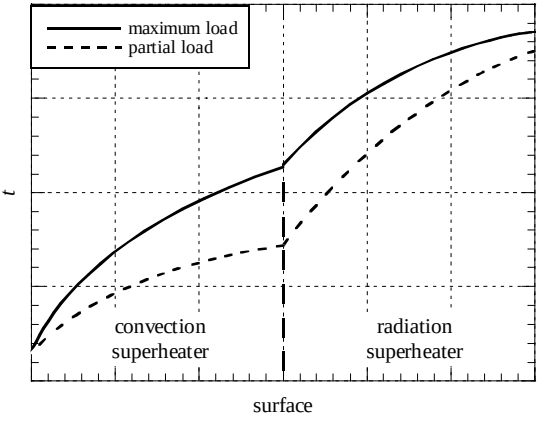


Fig. 3.37 Combination of convection superheater and radiation superheater

at starting and under low load) when the velocity of the steam is too low because of design errors or insufficient pick up of steam during starting.

Therefore, the flame must be carefully checked, the starting process initiated cautiously, and the velocity of the steam designed to have sufficient heat transfer coefficient, to guarantee enough cooling of the wall under different loads. This topic will be discussed further later on.

As far as the temperature of the superheated steam under different loads, and it is crucial to keep it as constant as possible to maintain turbine efficiency, it is feasible to intervene directly on the steam. This can be done in three ways, if we refer to a convection superheater or a group of superheaters, globally behaving like a convection superheater.

The first way consists of operating on the saturated steam before it enters the superheater. It is a question of taking heat from the steam so that the latter enters the superheater carrying more humidity than it was while exiting the drum. The reduction in enthalpy at the entrance makes the temperature at the exit decrease (see Fig. 3.38).

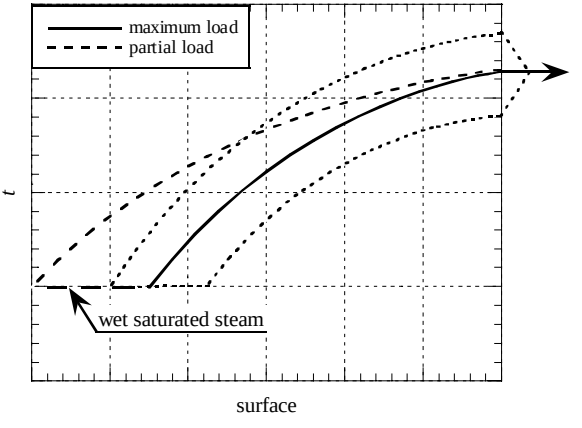


Fig. 3.38 Heat taken away at maximum load before the superheater entrance

This subtraction of heat is achieved with an exchanger where saturated steam and more or less hot water flow both inside and outside the tubes. This is a relatively small and therefore economical machine, given the high heat transfer coefficient of the condensing steam. The disadvantage of this solution, though, is an uneven distribution of the water in the steam in the various tubes that can lead to their local superheating. The dashed curves in Fig. 3.38 highlight this phenomenon.

The second method consists of desuperheating the steam at the exit of the superheater. This can be done with the help of an injection desuperheater (Fig. 3.39) by injecting water into the steam, or with a surface desuperheater which is nothing else but a heat exchanger, very similar to the one used in the previous example.

It is more expensive, though, because it must cool down steam with a much lower heat transfer coefficient compared to condensing steam. For this reason, the preference usually goes to the injection desuperheater. Note that the surface desuperheater can be fed with untreated water, whereas the former one requires either purified water or condensate. This way, the temperature of the used steam can be reduced to the desired value, but in the tubes of the superheater, it has higher values requiring the adoption of expensive materials or at least a greater thickness of the tubes. This leads to a price increase of the superheater (Fig. 3.40).

The third system is the best and works as follows. The superheater is divided into two stages. They are called primary superheater and secondary superheater, respectively. They differ both in terms of their structure, as well as their location in the generator. The injection desuperheater, called attemperator, is inserted between the stages. This reduces the temperature at the exit of the primary superheater. The steam entering the secondary one at adequately reduced temperature will exit at the desired temperature (see Fig. 3.41).

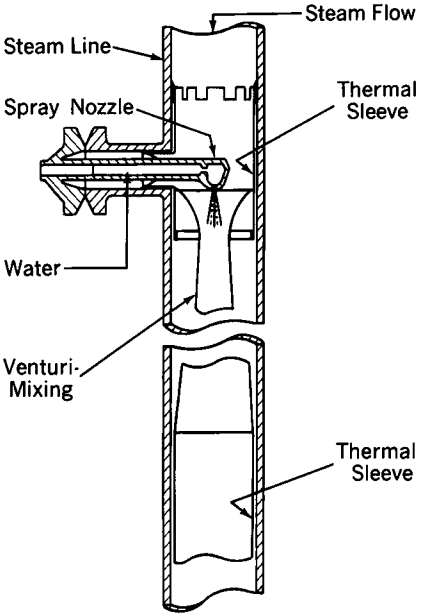


Fig. 3.39 Injection desuperheater (attemperator) (Courtesy of Babcock & Wilcox)

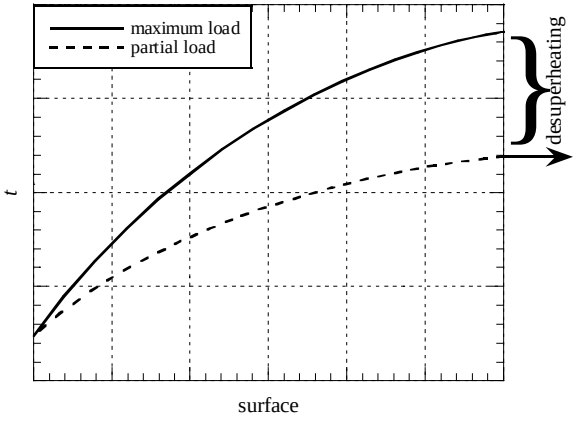


Fig. 3.40 Desuperheating after the superheater

This system, commonly used in big generators, has all the advantages of the previous one without the disadvantages. In fact, the steam temperature at the exit of the secondary superheater can be kept at the desired value without undesirable increases in temperature of the tubes as the load goes up.

In installations of modest entity, it is also customary to reduce the temperature of the steam, by making part of it go through a three-way valve in coils immersed in the water of the drum. This is a cost-effective solution because of the high overall heat transfer coefficient due to steam buildup outside the coils. The opening of the valve is controlled by a thermostat located at the beginning of the piping that leads the steam to use.

It is also possible to control the temperature of the superheated steam through recirculation of the flue gas, as we mentioned earlier. The results are shown in

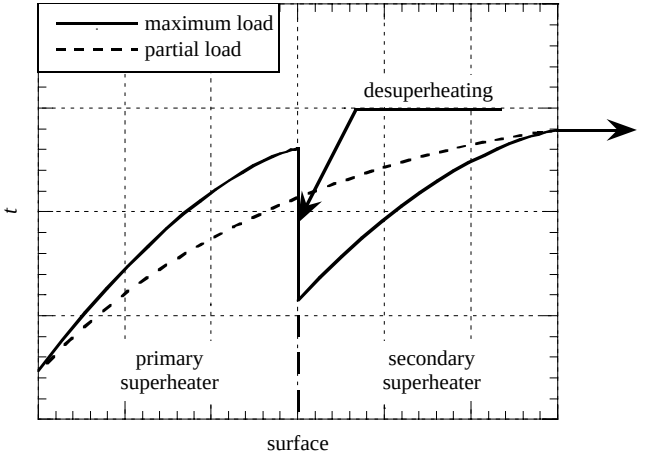


Fig. 3.41 Intermediate desuperheating

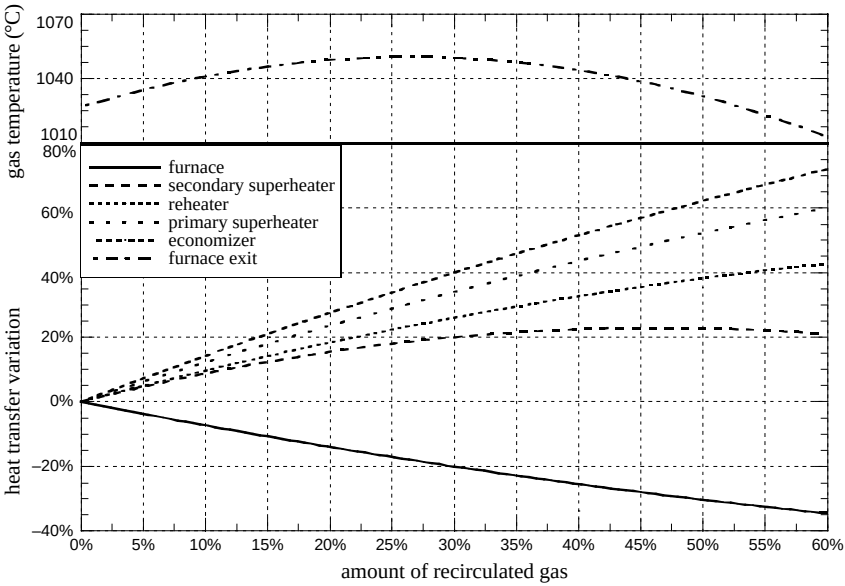


Fig. 3.42 Recirculation of flue gas

Fig. 3.42. The entry at the bottom of the furnace of a percentage of flue gas equals a reduction of the heat transferred into it that goes up with an increase in percentage of recirculated flue gas. The temperature at the exit of the furnace remains more or less constant with the tendency to increase if the load is low and to decrease if the load is high.

Consequently, the superheater, the potential reheater, and the economizer are hit by a greater mass of gas entering the secondary one at a temperature almost identical to the one obtained without recirculation. Therefore, the global heat content of the gas is greater. The velocity is higher, too. As a result, the overall heat transfer coefficient increases as well.

The heat transferred to the superheater, the reheater, and the economizer is therefore greater. Globally, the heat transfer into the furnace and to the different convection banks does not change. In the end, there is an exchange between heat transferred by radiation and by convection.

The advantages of recirculation of flue gas are shown in Fig. 3.43, where the dotted lines indicate the same temperature pattern as shown in Fig. 3.41 (without recirculation of gas).

Note that the superheater must be sized to guarantee the achievement of a certain steam temperature, including a set minimum load. Recirculation of gas under small loads will reduce the surface and the cost, as shown in Fig. 3.43. In addition, this reduces the intervention of the attemperator under full load.

There are also big units equipped with a third superheater besides the primary and the secondary one (Fig. 3.44); this one follows the secondary superheater as far as the path of both flue gas and steam.

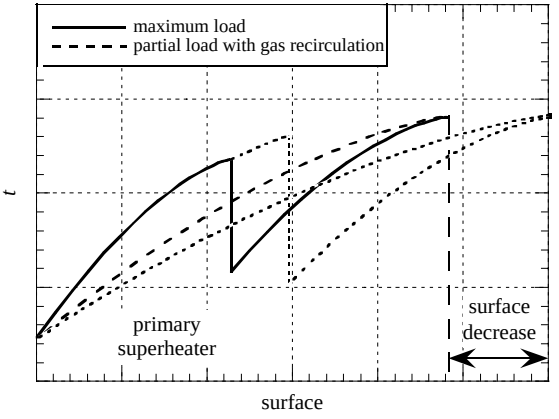


Fig. 3.43 Influence of the gas recirculation on the superheater surface

If there is just one convection stage in small power units, the superheater is generally installed at the exit of the furnace, often after the gas passes through rows of steam-generating tubes working as protective screens against the direct radiation from the flame. Sometimes two stages are preferable to desuperheat the steam as described. The primary stage can consist of a radiation superheater.

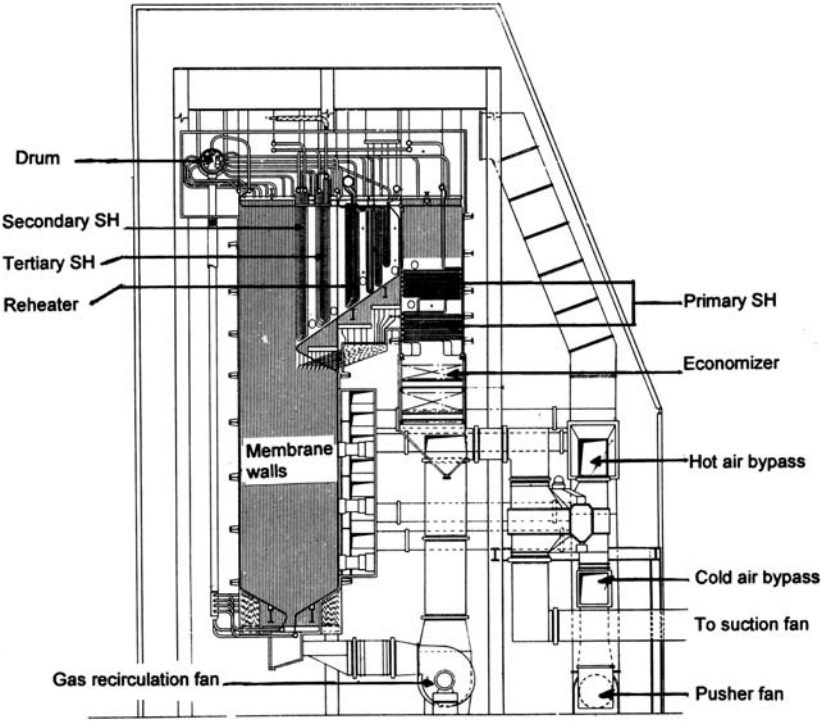


Fig. 3.44 Generator with tertiary superheater

The tubes of superheaters are subject to dirtying and corrosion, due to the presence of vanadium pentoxide and sodium in the flue gas, with fuel oil combustion. The topic will be discussed in detail in Sect. 6.2. Here it suffices to say that this phenomenon takes place more often if the fuel oil comes from the Middle East and Venezuela because they are rich in vanadium. To balance these corrosion phenomena, special additives in the oil will promote the build up of vanadium compounds with a higher melting point that are not dangerous in terms of dirt and corrosion of the coils.

To have a reference point on the temperature for the tubes, it is best to work with (3.17) and (3.18).

In the case of a radiation superheater with a thermal flux of $150\,\mathrm{kW/m^2}$, a thickness of 5 mm, and a heat transfer coefficient equal to $2300\,\mathrm{W/m^2K}$, in the first instance (average temperature)

$$\Delta t = 150{,}000\left(\frac{1}{2300}+\frac{0.005}{2\times 44}\right) = 74^{\circ}\mathrm{C}.$$

As far as the outside temperature of the tube

$$\Delta t = 150{,}000\left(\frac{1}{2300}+\frac{0.005}{44}\right) = 82^{\circ}\mathrm{C}.$$

In the case of a convection superheater with the same thickness, a heat transfer coefficient of $1700\,\mathrm{W/m^2K}$ and a flux of $58\,\mathrm{kW/m^2}$, in the first instance (average temperature)

$$\Delta t = 58{,}000\left(\frac{1}{1700}+\frac{0.005}{2\times 44}\right) = 37^{\circ}\mathrm{C}.$$

In the second instance (outside temperature of the tube),

$$\Delta t = 58{,}000\left(\frac{1}{1700}+\frac{0.005}{44}\right) = 41^{\circ}\mathrm{C}.$$

The presence of the reheater in the generator is limited to big units, where the cost of upgrading the cycle efficiency by bringing back the steam taken at the exit of the first stage of the turbine is justifiable, cost of the reheater, the piping, and the required accessories notwithstanding.

The reheater differentiates itself from the superheater by the fact that the running pressure of the former is much less compared to the latter, thus requiring thinner tubes, given equal diameter. On the other hand, the steam has a greater volume, and this leads to differences in the diameter of the tubes, the number of parallel coils, and so on.

As far as the surface of both the primary and the secondary, note that in big units the reheater is placed between them. Therefore, it is not surprising that the primary has a greater and sometimes much greater surface compared to the secondary. In fact, it is hit by the flue gas at a considerably lower temperature in comparison to the gas hitting the secondary.

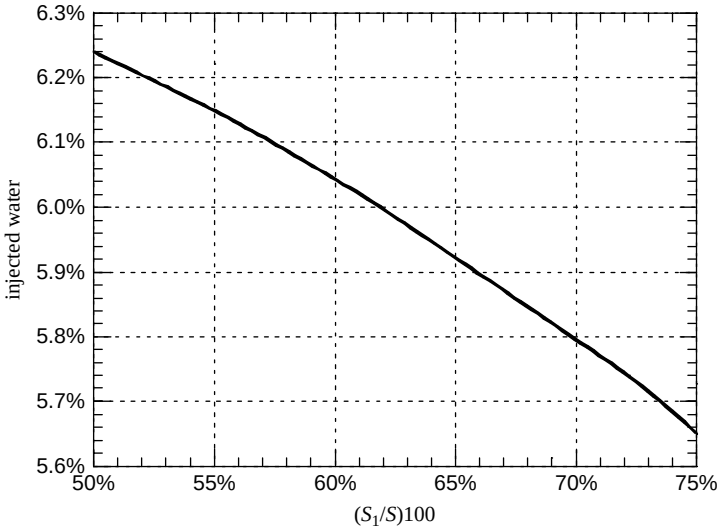


Fig. 3.45

In any case, the tendency is toward designing the primary with a larger surface even when there is no reheater in place. Note that the primary is generally built using cheaper steel, compared to the one used for the secondary, and designed to be as large as possible and compatible with the maximum temperature reached by the steam. This factor will indeed condition the choice of material.

Finally, it may be of interest to consider the impact of the surface division of the superheater between primary and secondary on the amount of water to inject in-between them. For instance, Fig. 3.45 shows the ratio between the surface of the primary and the total surface of the superheater on the abscissa, the injected water on the ordinate as a percentage of the steam output. In other words, we see that the injected water decreases with the increase of the surface of the primary.

3.8 Economizer

The function of the economizer is to heat the feed water before it enters the drum. Meanwhile the flue gas is cooled, thus positively impacting generator efficiency, given the reduced sensible heat loss of the flue gas.

We may be faced with three situations. In the first one, the economizer may be missing either because the generator is not equipped with one or because it is substituted by an air heater. In the second one, the economizer is the last stage of the generator, because the air heater is missing. In the third one, the economizer is included with the air heater and installed between the stages of the generator that precede it along the path of the flue gas and the air heater.

If the economizer and the air heater are missing, the last stage of the generator consists of the steam-generating tube bank. This structural solution may be valid from a financial point of view, under certain conditions and only under low pressure. In that case, the temperature of the steam is modest, as well as the temperature of the water–steam mixture passing in the steam-generating tubes. This way, the exit temperature of the gas from the generator can be kept relatively low, even in the absence of an economizer, thus maintaining an acceptable efficiency level.

For instance, if the relative pressure is equal to 12–15 bar, the steam temperature is equal to 190–200 °C. It is possible to reduce the flue gas temperature at the exit of the generator down to 230–240 °C with a generator efficiency of about 88.5–89.5%. This solution is frequently adopted for smoke-tube generators (where the pressure generally does not exceed 15 bar and is often around 10–12 bar) and for water-tube generators of small power. Of course, as we shall see, the installation of an air heater is not to be ruled out or considered unnecessary.

The presence of an economizer is advantageous even for the generators mentioned above because the efficiency would go up considerably from 89 to 91–92%. Note that if combustion is done using fuel oil, the economizer must have cast iron finned tubes. This is expensive, and its installation will depend on financial considerations.

The working pattern of the generator is very important in this context. Seasonal use, for instance, for heating or for seasonal technological use (tomato industry), will advise against the installation of an economizer. On-going use, on the other hand, should lead to careful consideration of the financial pros and cons of its employment. Therefore, the economizer can also be used in small- or medium-size units especially under medium or high pressure to keep up acceptable efficiency levels.

In that case, it represents the last stage of the generator, and this has consequences that will be discussed later on.

Its installation, in combination with and before the air heater, is typical of big units. In that case, the air heater represents the last stage of the generator. The economizer is hit by flue gas at relatively high temperature. The feed water enters the economizer at high temperature, as well, given that the so-called water heaters are placed before the economizer. These are heat exchangers where the water is heated by steam taken from the turbine. This clearly improves the cycle efficiency. Note that generally gas exits the economizer at a temperature ranging from 350 to 400 °C, whereas the feed water ranges from 200 to 250 °C.

Depending on its location, the economizer has different structural features. If it builds the last stage of the generator, and if combustion is done with fuel oil or coal, it is built in cast iron finned tubes because of the low temperature of the flue gas and the presence of sulfur in the fuel.

In fact, combustion with coal or fuel oil equals flue gas containing considerable amounts of SO_2 that partially transforms itself into SO_3 in certain areas of the generator. The presence of SO_3 makes the steam in the flue gas condensate at a temperature higher than its dew point. This leads to the acid dew point, so called because

the condensed steam mixing itself with sulfur trioxide creates sulfuric acid that will corrode the tube walls and rather quickly drive the economizer out of service.

The phenomenon will be discussed extensively in Chap. 6. For now, it suffices to say that the acid dew point depends on a variety of factors, such as the type of fuel, its sulfur content, the percentage of SO_3 in the flue gas, the excess air, and so on. In general terms, note that with fuel oil combustion it amounts to about 140–150 °C. The greatest danger of corrosion occurs at a temperature below 20–40 °C. Therefore, if the temperature of flue gas, in contact with the tube walls cooled down by the relatively cold water passing through them, ends up below the acid dew point, the sulfuric acid will corrode the walls. In that respect, cast iron has a greater resistance to corrosion than steel, which explains the employment of this type of economizers at low temperatures of flue gas and water when there is SO_3 in the gas itself.

For instance, let us consider an economizer designed to work at 15 bar with feed water at 60 °C and flue gas with an exit temperature of about 180 °C. If smooth steel tubes were used, the wall temperature would be about 70 °C and the temperature of the flue gas in the boundary layer in contact with the tube about 120–130 °C. This economizer with fuel oil combustion would not have a long life. Under these conditions, an economizer in cast iron can last much longer instead. First of all, because cast iron is more corrosion resistant, secondly because of the high ratio between the external finned surface and the internal surface; because of this and the resistance to heat transfer provided by the fins, these increase the temperature compared to the smooth tubes, and the flue gas in contact with them cools down less. Moreover, note that the fins considerably increase the heat exchange surface, and even though the overall heat transfer coefficient is lower than the one resulting from the same velocity but with smooth tubes, given equal volume, the heat transfer is much greater.

If the economizer is designed to be located before the air heater instead, it can be built with smooth steel tubes. This is possible given the high temperature of the flue gas and most of all the high temperature of the feed water. The latter rules out the possibility that the temperature of the boundary layer of the gas gets to levels that cause corrosion. In fact, even under low loads in which case the gas cools down more, they necessarily reach a temperature higher than the water, thus outside the area of danger.

Naturally, combustion with natural gas that does not contain sulfur does not create any of these problems. It is possible to cool the gas more and to use tubes made of steel. Usually in this case, steel tubes with helicoidal fins made of steel are preferable because they achieve a great heat exchange surface with little volume (Fig. 3.46).

The walls of the economizer get dirty because of the soot carried by the gas. It is therefore necessary to clean them with a soot blower, that is, by injecting steam into the gas channels with the help of soot blowers, consisting of tubes equipped with nozzles fed by steam at low pressure (< 20 bar). They come in different models, depending on the preferences of the designer and their purpose.

From a structural point of view, finned tubes can be made entirely of cast iron (Fig. 3.47) or of steel tubes coated with cast iron. The former has different shapes:

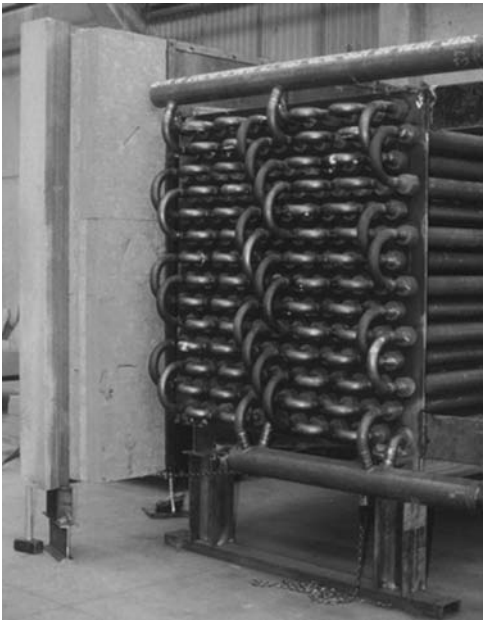


Fig. 3.46 Economizer with steel finned tubes (Courtesy of Therma-Italy)

square, rectangular, polygonal, round. The fins can be aligned at regular distances along the periphery of the tube, or discontinuously and staggered, and they can vary in terms of height, thickness, and pitch. The latter consist of an internal steel tube where the water flows and of an external finned tube of cast iron in contact with the previous one.

The primary condition for a satisfactory heat exchange through the wall is adhesion between the two tubes. A dead-air space of even a few tenth of a millimeter

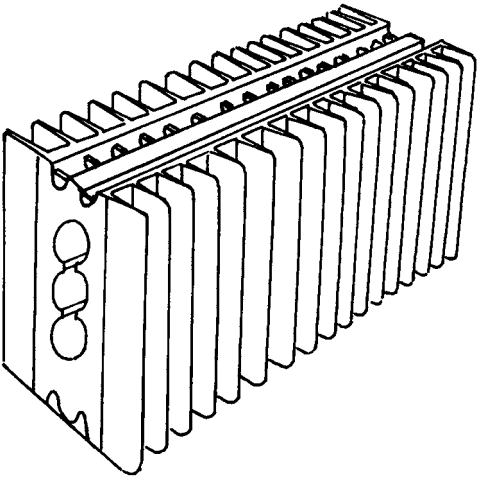


Fig. 3.47 Cast iron finned tube for economizer

can be enough to reduce the overall heat transfer coefficient to less than half the theoretical one assumed with perfect adhesion.

To that extent, the cast iron is either melted directly on the steel tube or the cast iron tube is built separately with an internal hole of smaller diameter compared to the external diameter of the steel tube. Then it is warm-forced on it. Finally, the cast iron tube can be built separately, the steel tube is inserted and expanded until it adheres to the cast iron through an expander that widens it while it moves along the tube itself.

The use of steel tubes with cast iron coating is required when the pressure is high and the cast iron tube working under traction would be unable to stand it or when the economizer is an evaporator-economizer, that is, when there is partial evaporation of the water besides its heating. In this case, the cast iron tube does not perform well under the sudden volume increase of the fluid under evaporation, and it must be lined with the steel tube.

The correct proportioning of the fins is obviously very important to achieve great heat exchange. Let us examine how the pitch, the thickness, and the height of the fins impact the heat transfer, also factoring in the other characteristics expected of a fin, such as easy cleaning, a moderate temperature difference between the top and the bottom of the fin, the weight, low cost, and so on.

A reduction of the pitch between the fins leads to an increase in heat exchange, all other conditions being equal. In fact, the heat exchange surface increases per length unit of the tube, the hydraulic diameter of the gas channels becomes smaller, and as a result the heat transfer coefficient goes up. In addition, the cross-section area of the gas becomes smaller while the resulting velocity increase leads to an increase in heat transfer coefficient. On the other hand, the pitch cannot be reduced beyond a certain limit to prevent withdrawing of the cores, a greater tendency to build deposits on the surface that could obstruct the passages over time and make the cleaning of walls more difficult because of the smaller cross-section areas.

Under equal conditions, the increased thickness of the fins increases the heat exchange. In fact, there is a reduction of the cross-section area of the gas, thus its greater velocity and a reduction of the hydraulic diameter, as we saw with respect to the reduction of the pitch. Moreover, as shown in Chap. 8 (Sect. 8.11), an increase in thickness increases the efficiency factor of the fins and the overall heat transfer coefficient as a result of it. A beneficial effect is the increase in thickness of the fin top to bottom, as shown in the Appendix (Sect. A.4). Even an increase in thickness must be limited because of cleaning-related issues and because it means additional weight and cost.

Higher fins, given equal total volume of the device, reduce the heat exchange. In fact, the velocity of gas slows down due to the greater cross-section area available. The bigger height also reduces the efficiency factor of the fins (Sects. 8.11 and A.4), resulting in a reduced overall heat transfer coefficient.

Finally, the fin becomes less rigid and more fragile during transportation and assembly, and there is an increase in the temperature difference between top and bottom of the fin that could result in breakup due to the deriving stresses. On the

other hand, the number of required tubes goes down because of their larger external surface which, in turn, reduces the price.

In conclusion, an increase or decrease of the value of each of the three-dimensional parameters of the fins has pros and cons, with respect to the discussed characteristics of the tube. The pressure drop through the economizer impacting the sizing of the fan and, as a result, both installation and running costs are additional factors to keep in mind. Therefore, there are optimal values of the three considered quantities: generally, the height varies from 20 to 40 mm, the pitch ranges from 12 to 20 mm, and the thickness at the bottom is about 5–6 mm. As far as the economizers with steel smooth tubes, there are no comments to be made in terms of construction. They consist of coils placed in horizontal banks.

3.9 Air Heater

Like the economizer, the air heater is installed to reduce the temperature of the flue gas entering the chimney and improve the generator efficiency. Note that a reduction of 20 °C of this temperature roughly corresponds to an increase in efficiency of 1%.

In powerful generators, an efficiency increase of a few points represents such a cost reduction of the kWh produced, to absolutely justify the high cost of the air heater, the cost increase of the fans, due to the greater pressure drop as far as air and flue gas resulting in greater running costs.

Small and medium power generators also face similar issues, including those at low pressure like the smoke-tube boilers. Of course, a correct financial investigation must be done, considering the cost of the air heater and the savings in fuel based on the expected and crucial load diagram. The investigation highlights the opportunity to install the air heater, and if its outcome is positive, its ideal dimensions, even taking into account potential corrosion issues. In general, the investigation will demonstrate that the cost of the air heater will be amortized within a short period of time.

While the air heater cools the flue gas, it also heats the combustion air, this way increasing the heat going into the furnace. This strongly influences the sizing of the furnace, the amount of heat radiated by the flame, as well as the exit temperature of the flue gas from the furnace. The possibility to build radiation generators completely devoid of a steam-generating tube bank also depends on the heating of the combustion air. Besides that, the warm air facilitates combustion and leads to high specific loads in the furnace.

Roughly, in big units, the flue gas enters the air heater at a temperature of about 350–400 °C and exits at a temperature of about 150–170 °C. The air enters at room temperature or at a higher temperature when it is heated by steam (we will discuss this topic later on) and exits at a temperature of about 230–300 °C.

Of course, in small- and medium-size generators, the temperatures at stake are quite different. The flue gas usually enters at a temperature of 240–300 °C and exits at a temperature of 160 ÷ 190 °C. Air exits at a temperature of 90–160 °C.

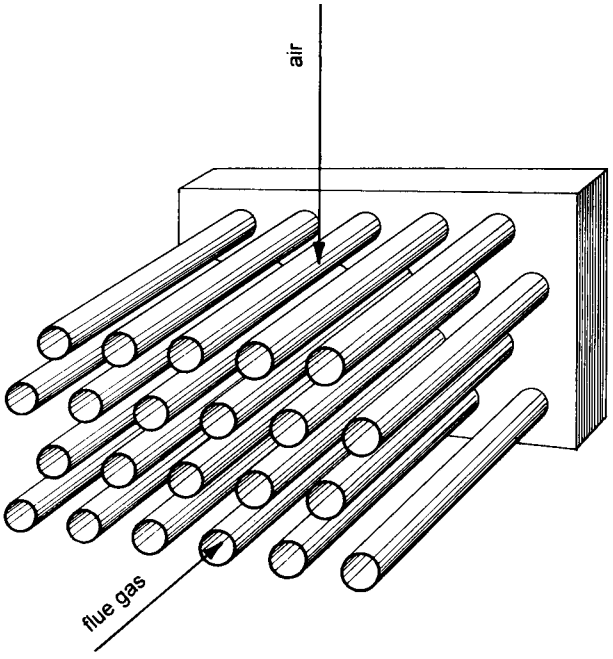


Fig. 3.48 Recuperative air heater consisting of a tube bank

Fundamentally, there are two types of air heaters, the recuperative and the regenerative ones.

The recuperative air heaters are static and keep the two fluids on both sides of the heat exchange surface. These can be done with tubes (Fig. 3.48). Generally, in that case, it is preferable to have the flue gas flow through the tubes and the bank hit by the air outside. This facilitates cleaning of the surfaces licked by flue gas that can be done with a pig.

The heat exchange surfaces may consist of plates; the plate air heaters can in turn be made of stiffened metal sheets to withstand pressure or with pockets equally made of metal welded together to have rectangular tubes for the passage of gas or air (Fig. 3.49).

Regenerative air heaters, on the other hand, alternatively exhibit the same surfaces to air and flue gas. The typical regenerative air heater was designed in Sweden by Ljungstroem (Fig. 3.50). It was named after him and is widely used throughout the world.

It consists of a rotor moving slowly (3–4 rotations per minute), consisting of various crates containing differently corrugated sheets of steel; gas and air alternatively pass through the channels in-between the steel sheets after being conveyed by the inlets of the air heater, fixed on the stator, from the exit of the generator and from the pusher fan, respectively. One part of the steel sheets hit by the gas warms up and rotates toward the area hit by air and warms it up. This way, the steel sheets function as heat-storage medium.

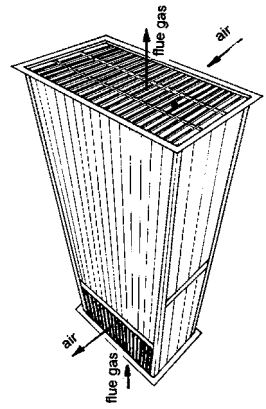


Fig. 3.49 Plate recuperative air heater

The air and the flue gas are kept separate as much as possible through appropriate seals made with special steel, but inevitably part of the air (under higher pressure) gets mixed with the gas. Usually, during the design phase, bypass leakage is factored in as 10% of the air flow rate. Depending on the seals, this value can be reduced.

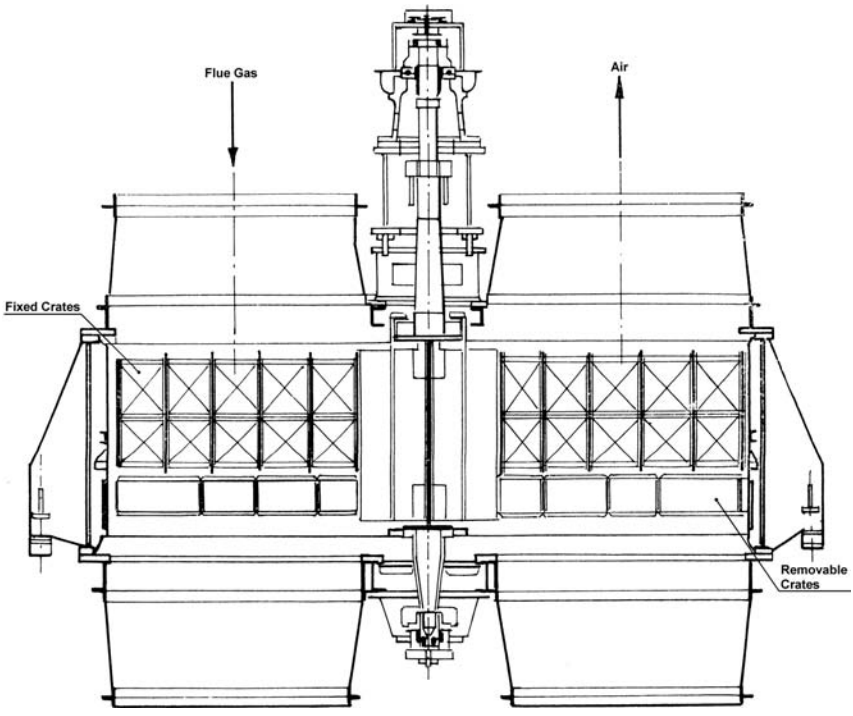


Fig. 3.50 Ljunstroem-type regenerative air heater

The bypass leakage phenomenon leads to a greater mass of flue gas in the chimney and to lower generator efficiency as a result of it. Note that the reduction amounts to a few permille at the most. Moreover, the greater gas volume requires to oversize the fan. By analogy, to provide the burners with sufficient air, the fan must be able to convey a greater volume of it to the air heater. This must be factored in during the design phase to correctly evaluate both plant and running costs. The Ljungstroem air heater typically has a vertical axis even though there are plants where it is placed horizontally.

Besides economizers, the danger of corrosion and the build up of deposits on the heat exchange surfaces represent two huge problems in air heaters too. The wall temperature must not go under a certain value that depends on the velocity of both fluids and on their minimum temperature, if their path is counterflow, as it is recommended to fully exploit the device.

The possibility to direct the fluids in parallel flow should equally be considered. This solution is less favorable in terms of heat transfer, yet more advantageous as far as corrosion issues because the minimum temperature of the flue gas is matched by the maximum air temperature (Sect. 8.11).

Approximately, we can assume that the temperature of the metal is the average between the temperature of the air and the gas, whereas the temperature of the flue gas in the boundary layer is the average between temperature of the wall and the gaseous mass. For instance, if the air enters an air heater with fluids moving counterflow at 20 °C and the flue gas exits at 190 °C, the metal will have a temperature of about 105 °C and the gas in contact with the metal a temperature of about 150 °C. This temperature still provides sufficient guarantee against corrosion through sulfur.

Usually, with fuel oil combustion, it is best if the temperature of the metal stays above 110 °C. Of course, it is possible to fulfill this condition with lower gas temperatures by working on the velocity of the fluids, that is, by increasing the velocity of the flue gas with respect to that of the air. This way, the temperature of the metal reaches a value above the average of the temperatures of both fluids.

At any rate, if we consider a regenerative air heater and wish to lower the temperature of the flue gas to 160 °C or below, we must factor in the possibility that the coldest area of the steel sheets will corrode. For this reason, the crates in the cold area are built to be extractable to quickly substitute them with new ones whenever the steel sheets are corroded. Aluminium sheets have also been used, yet with controversial results. Other materials, such as ceramic, were used with uncertain results.

It goes without saying that the necessity to substitute the steel sheets will result in cost overrun. It is a question of comparing this cost with the savings in fuel inherent to the presence of these steel sheets subject to corrosion and to draw appropriate conclusions in terms of cost optimization.

As far as cleaning, this is done through soot blowers during runtime and through washing during stops for plant maintenance. The danger of corrosion due to low temperature of the flue gas becomes more evident with reduced load and whenever the air room temperature goes down. It is possible to intervene in ways that we will briefly outline as follows.

As far as lowering the room temperature of the air, unit heaters are placed on the intake of the fans. These devices can also be used at reduced load, regardless of the room temperature to prevent excessive lowering of the flue gas temperature.

At reduced load, it is possible to intervene in yet another way. Part of the cold air can be conveyed to the exit of the air heater, thus reducing the exchanged heat taking place in it. Part of the warm air can be recirculated by picking it up at the exit of the air heater and directing it back to the intake of the fan. Part of the gas can be recirculated by mixing it with the air entering the air heater.

The desired goal to increase the exit temperature of the flue gas can be achieved through these measures. The choice of one over the other depends on technical and financial considerations tied to the type of plant, fuel, and so on.

For air heaters installed at the exit of small and medium power generators, the simplest solution consists of conveying part of the cold air to the exit of the air heater (air bypass).

3.10 The Danger of Tube Bursting

After ruling out defective materials (unpredicted inferior mechanical characteristics) or defective tubes (reduced thickness, cracks, and scoring), the settling of the tube occurs if a reduction in thickness takes place during runtime or if the working temperature is greater than the assumed one, so that the stress on the tube is no longer compatible with the mechanical characteristics of the material at the abnormal temperature it reached. Therefore, bursting takes place either because of a reduction in thickness or because of abnormal superheating of the tube.

The reduction in thickness can occur because of scaling or because of corrosion. The scaling phenomenon is connected to the working temperature of the material. The scaling temperature of carbon steel is about 500 °C; in the case of alloy steel with 0.5% Mo, this temperature is equal to about 550 °C. The scaling temperature of steel with 1% of Cr and 0.5% of Mo is 570 °C, and the one of steel with 2.25% of Cr and 1% of Mo it is about 600 °C. The scaling of the tube can occur because of design errors (mistaken estimate of the local temperature of the steam or mistaken estimate of the difference in temperature between internal fluid and tube wall) or as a result of abnormal superheating of the tube.

As far as corrosion phenomena, we already illustrated those that take place on the external side of the tube, and more precisely the one caused by vanadium and sodium occurring at high temperature of the flue gas on the walls of the superheaters and the one occurring at low temperature in economizers and air heaters because of sulfur.

Corrosion on internal side is caused by CO_2 and O_2 in the water. CO_2 causes slow and diffuse corrosion, whereas O_2 causes rapid and localized corrosion, including craters and holes with blackened edges. It was believed for a long time that boilers under low pressure (up to 8–10 bar) would not require degassing of the water.

This position is no longer sustainable, especially given the high levels of thermal flux at which we work nowadays. This high level flux is present even in small generators under low pressure and favors the onset of corrosion phenomena.

Therefore, it is advisable also for these generators to require degassing of the water before it enters into the generator.

The superheating of the tube may depend on design errors or malfunctioning of the generator. Design errors consist of not having chosen appropriate solutions to prevent the onset of film boiling or of having designed a circuit of the water–steam mixture where circulation is insufficient or highly unbalanced.

Film boiling was described in detail in Sect. 3.2. As far as circulation, it must take place under certain conditions to prevent superheating of the tube. This topic will be discussed in Chap. 10. Here it suffices to say that if the water flow rate is insufficient, the heat transfer coefficient of the water–steam mix is too low. The tube is not sufficiently cooled and there are abnormal superheating phenomena. Circulation may be inappropriate because the head is insufficient, because the pressure drop in the steam-generating tubes is excessive, because there are too few downcomers, or because their diameter is too small. In addition, sometimes the flow rate is sufficient, but there is strong circulation unbalance between the different parallel circuits, due to their geometry and due to the heat transferred to the various circuits (and as a result of the produced steam). In that case, one or more circuits may be in critical condition.

In generators with forced circulation, the water flow rate is not modifiable as it corresponds to the steam production. Thus, appropriate velocities must be chosen through a carefully designed geometry of the circuit.

Finally, the superheating of the tube may take place because of fouling on the walls that reduces its cooling.

This fouling is due to the presence of sulfates, carbonate, and silicate in the water.

- Sulfates cause hard fouling with a high density (up to $2\,\mathrm{kg/dm^3}$), scarce porosity, and a relatively high thermal conductivity of about 1 W/mK. For this reason, they are not the most dangerous.
- Carbonate causes fouling with variable density and a thermal conductivity ranging from 0.2 to 1 W/mK.
- Silicate causes fouling with low density ($\approx 0.4\,\mathrm{kg/dm^3}$) and thermal conductivity that can reach even below 0.2 W/mK.

A few examples will demonstrate how fouling can influence the temperature of the tube.

For instance, if the fouling of a tube amounts to a thickness of 0.5 mm and its thermal conductivity is 1 W/mK, assuming that the thermal flux is equal to $120\,\mathrm{kW/m^2}$, fouling brings about a difference in temperature equal to

$$\Delta t = 120{,}000\frac{0.0005}{1} = 60^{\circ}\mathrm{C}.$$

If fouling has a thickness of 0.3 mm but a thermal conductivity of 0.15 W/mK instead, even with thermal flux equal to only $60\,\mathrm{kW/m^2}$, the difference in temperature caused by fouling is as follows:

$$\Delta t = 60{,}000\frac{0.0003}{0.15} = 120^{\circ}\mathrm{C}.$$

In the first instance, the superheating of the wall can be withstood by the tube. This depends on the design temperature, the material, and so on. In the second instance, the tube can undoubtedly not withstand such a high temperature increase. These simple examples show the importance that fouling may have, even when its thickness is relatively modest.

As far as superheaters, even a smaller temperature increase will suffice to provoke the bursting of the tube. For instance, let us assume a superheater built in steel 14CrMo3 and a design temperature of 500 °C. The allowable stress is $104\,\mathrm{N/mm^2}$, and the tube was sized based on this value. If internal fouling makes the temperature go up by 90 °C, note that at 590 °C the yield strength of the material is about $105\,\mathrm{N/mm^2}$, and the tube is already in danger.

Based on the above, note how fouling can be dangerous, especially for superheaters. Adequate water treatment is indispensable to prevent its buildup, and in the case of superheaters, it is best to increase the water–steam ratio of the steam coming from the drum, as we saw before.

The tubes may also superheat if there is no water. This happens out of negligence of the stoker in the absence of automatic checks or if the latter do not work properly. In this context, note the absolute necessity of periodical checks and maintenance of automatisms overall, particularly of shutdown at lowest levels.

Finally, use caution during the starting process. In fact, during this transition, thermal shock can take place if the process is not executed with the required graduation. Note that in big generator units, thermocouples are installed in contact with the tubes in the most significant areas that allow the registration of their temperature, with particular reference to starting as it is the most delicate operation.

3.11 Boiler Settings

Boiler settings essentially depend on the structural characteristics of the tube walls.

In small units, the tubes inside the furnace are often simply lined up side by side. Generally, some of the tubes belonging to the tube bank are used to support the external walls. In that case, they may be placed side by side or at a distance from one another.

Considering the pressurized solution adopted nowadays, it is crucial to have a tight seal. There are three possible solutions.

The first one consists of installing a gastight inner skin casing made of sheet in direct contact with the tubes (Fig. 3.51). The temperature of the sheet is brought to be close to that of the water–steam mixture flowing through the tubes. Therefore, it

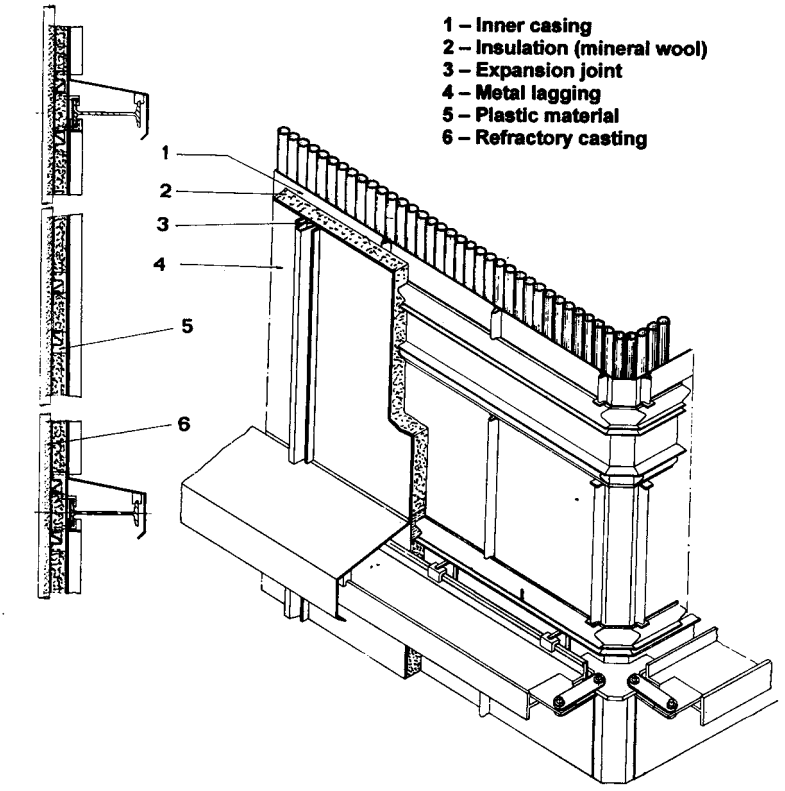


Fig. 3.51 Inner casing (skin casing)

suffices to put in place an insulation between inner casing and external metal lagging. The latter works as an insulation container. The lagging must not be gastight. The wall is reinforced with buckstays, whereas the inner casing is reinforced through stiffeners to withstand the pressure in the furnace.

The second solution involves gastight intermediate casing between a refractory-insulating coating in contact with the tubes and the insulating coating placed in contact with the metal lagging (Fig. 3.52). In that case, the casing is kept at lower temperature than before. For this reason, it creates smaller problems in terms of design to absorb its expansion and prevents undesired distortions of the sheets. Of course, this solution is preferable when the tubes are not lined up side by side.

Finally, it is possible to have single external gastight metal lagging. In that case, there are two coatings of refractory-insulating material and of insulation between it and the tubes (Fig. 3.53). The latter solution is usually not recommended because if the flue gas contains SO_3, by getting into the refractory coating through the clefts, and then hitting and burning the insulation, it gets in contact with the cold lagging corroding it through sulfuric acid. Note the existence of such generators where much

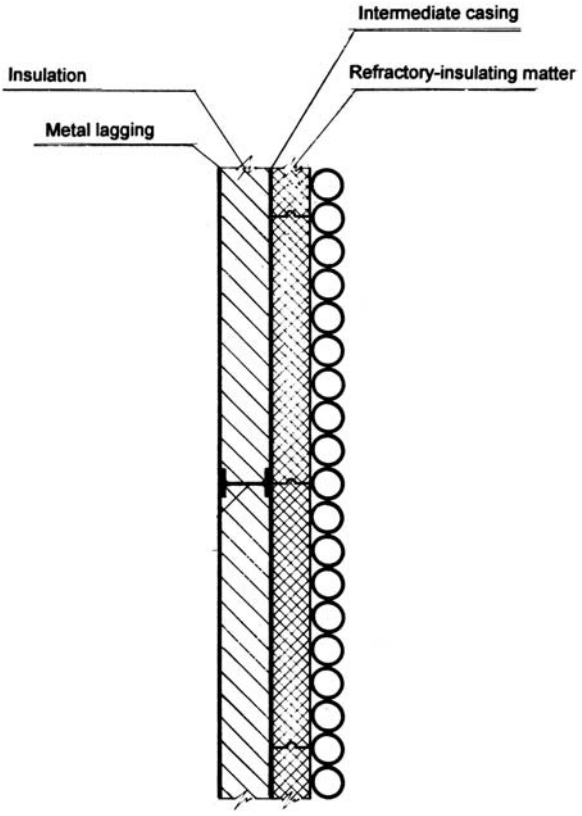


Fig. 3.52 Intermediate casing

care went into making the refractory-insulating coating that strangely enough still prevents corrosion for many years.

In high power generators, one hypothetical solution may be to factor in skin casing (Fig. 3.51). Typically, used membrane walls will not require any inner casing as the tube wall itself is gastight. Therefore, it suffices to plan for an adequate insulating coating between the tube wall and the lagging.

When the tube walls have considerable dimensions, and particularly when the tubes have a small diameter, as it happens to be the case in big radiation generators, buckstays must be included to keep the alignment of the tubes even when there are small bursts in the furnace (Fig. 3.51). The buckstays are sized even when the furnace is in depression, based on an ideal thrust exerted on the walls from the inside (generally equal to 1500–2000 Pa). If the boiler is pressurized, it is a question of considering the existing pressure and appropriately increasing it to factor in sudden pulsations and bursts.

The buckstays must be adequately spaced based on the computational pressure mentioned above and the characteristics of the tubes. In other words, the tube

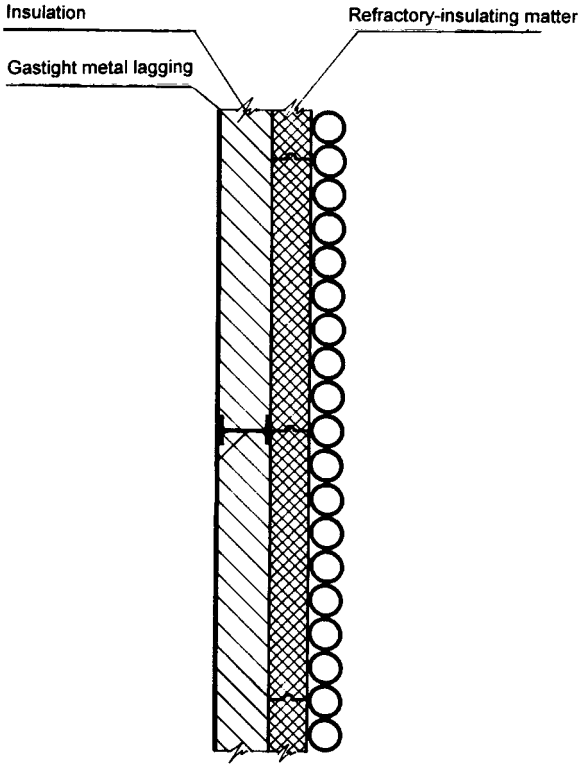


Fig. 3.53 Gastight metal lagging

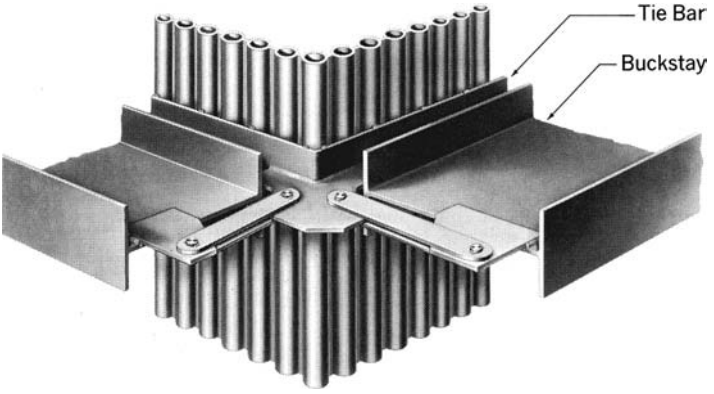


Fig. 3.54 Hinges in buckstay corner (Courtesy of Babcock & Wilcox)

behaving like a continuous beam placed on the buckstays must neither have unacceptable deflections compromising the potential refractory casting and the insulation nor exceed the allowable stress levels. Without getting into the details, note that the buckstays must be aligned closer, as the diameter of the tubes becomes smaller.

As shown in Figs. 3.51 and 3.54, the buckstays are connected to each other in the corners of the boiler through hinges. In fact, the generator swells because of the heat, whereas the buckstays outside do not expand. Therefore, it is important to compensate the expansion of the generator by joining the different buckstays together.

The correct sizing of the insulation is, of course, quite important in terms of generator efficiency. If the external walls are too warm, an excessive amount of heat is lost per radiation and convection (see Chap. 9). This causes efficiency reduction. On the other hand, a thick insulation is expensive. In the end, it is a question of identifying the optimal solution given all the different constraints.

This page intentionally left blank

Chapter 4
Smoke-Tube Boilers

4.1 Construction Characteristics

The generators of this type can be called smoke-tube boilers as they are unable to produce superheated steam, and the boiler (steam-generating tubes) is frequently, yet often inappropriately, not followed by the economizer or the air heater.

Smoke-tube boilers consist of a cylindrical flue (see Figs. 4.1, 4.2, 4.6, and 4.7) where combustion takes place (big units can have two flues), a series of tubes run through by flue gas that are split in sections, where the gas flows in the direction of the boiler front or vice versa. Both the flue and the tubes are surrounded by water and steam in a cylindrical shell; flat drilled plates are at the ends of the shell to insert the flue and the tubes.

From a constructive point of view, smoke-tube boilers can be divided into boilers with a wet end plate, with a dry end plate, or waste-heat boilers. In most commonly used boilers with a wet end plate (see Fig. 4.2), the flue is welded to the front tube sheet and to the tube sheet of the backflow chamber. The flue gas exiting the flue first enters the first backflow chamber (see Fig. 4.2) inside the boiler, therefore surrounded by water. It consists of a tube sheet welded to the flue where the tubes of the second passage of gas flow are inserted, a cylindrical metal sheet and a back flat wall. The back wall is connected to the back tube sheet through tie rods that contrast the thrust on the two walls facing each other.

The tubes of the third gas passage are connected to both tube sheets welded to the external envelope. The first backflow chamber is visibly cooled by water and contributes to the heat transfer with its entire surface. The tubes are of different lengths: the ones belonging to the second passage are shorter, whereas the ones of the third one are longer. Between the tubes of the second and third gas passage, there is a second backflow chamber (on the front of the boiler) that is in fact outside the actual boiler.

Hinge smoke-box doors are mounted on the wall of the second backflow chamber. If they are opened when the boiler is off, it is possible to inspect the tubes inside and to mechanically clean them. Access to the first backflow chamber is possible through an opening on the back tube sheet.

D. Annaratone, *Steam Generators*, DOI: 10.1007/978-3-540-77715-1_4,

© Springer-Verlag Berlin Heidelberg 2008

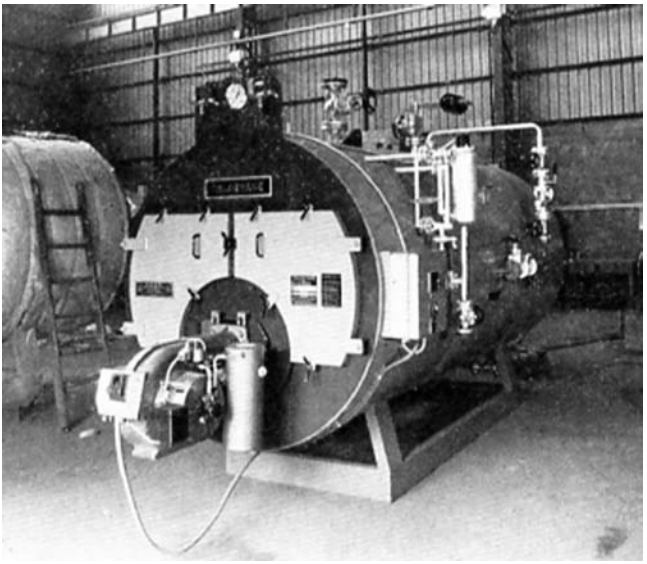


Fig. 4.1 Smoke-tube boiler with wet end plate

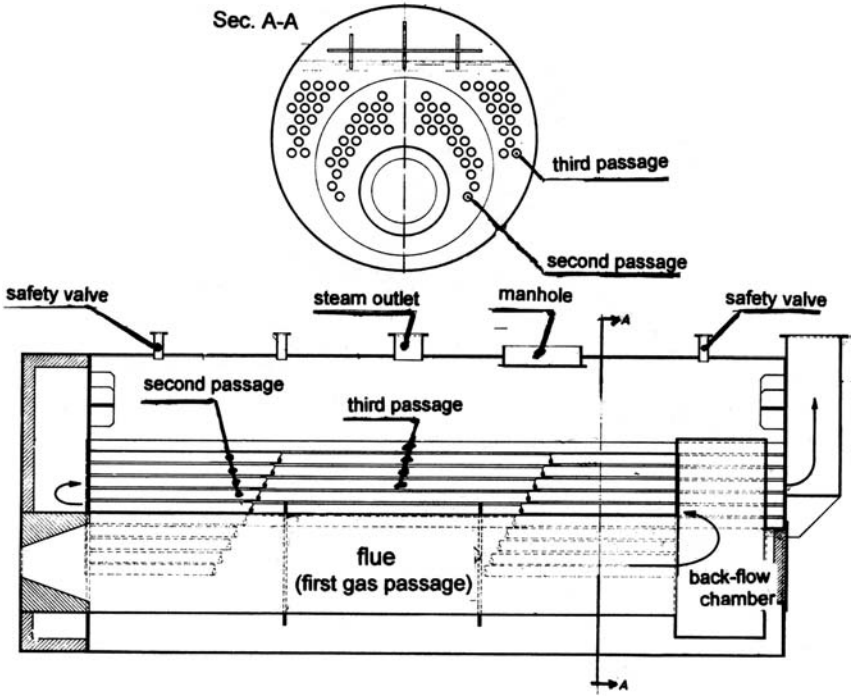


Fig. 4.2 Smoke-tube boiler with wet end plate

The flue surrounded by water, thus under pressure from the outside, is at risk for buckling. Generally, it is equipped with reinforcement rings made of flat tee bars, angle iron, or wavy elements (see Fig. 4.3) inserted between the cylindrical portions. Welding of the rings must be done with full penetration to ensure the cooling of the cylindrical envelope with the water in correspondence of the ring. Completely wavy flues are also used even though their cost usually works against them.

The cylinder of the first backflow chamber is also under external pressure, and we refer to the same guidelines provided for the flue. It is usually not reinforced with rings considering its modest length. The diameter of the flue typically ranges from a minimum of 400 mm to a maximum of 1200–1300 mm. The tubes that are also under external pressure do not pose any problem given their small diameter. The latter normally ranges from 48 to 89 mm. They are connected to the tube sheets through tube expansion (with a groove) and eventually with flaring (Sect. 3.6). They can equally be expanded, flared, and welded (see Fig. 4.4) or simply welded.

There are pros and cons to all solutions. In general, expanding with flaring and welding produces the best results.

The tube sheets can be flat and fillet weld to the flue, the shell, the cylinder of the first backflow chamber or flared. In that case we have butt welding (see Fig. 4.5). In the areas without tubes, they are reinforced with angle plates and stiffening ribs (see Figs. 4.2 and 4.7). In the remaining areas, the tubes function as tie rods contrasting the thrust produced by pressure.

A manhole is installed on the external envelope to access the inside of the boiler, or at least to inspect part of the tubes from the outside. The inside of the second backflow chamber and the smoke-box doors must be covered with refractory material, as they are not cooled by water. The boiler is insulated on the outside with material contained in an aluminum envelope.

The boiler is equipped with an optical level gauge and two faucets to check the water level. Moreover, electrical instruments or other devices fulfilling the same

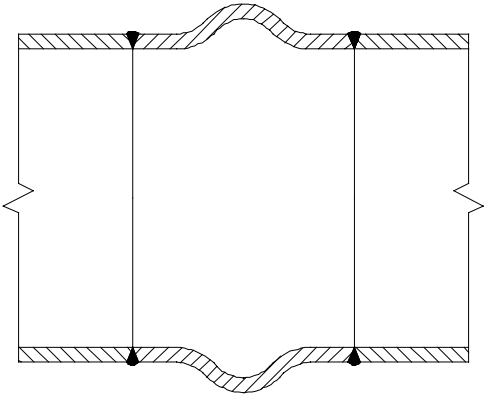


Fig. 4.3 Wavy element in the flue

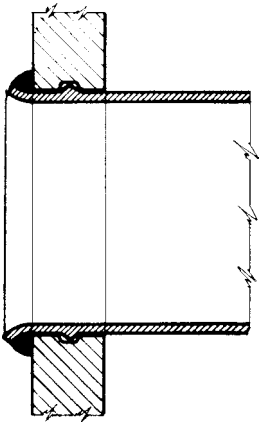


Fig. 4.4 Expanded, flared, and welded tube

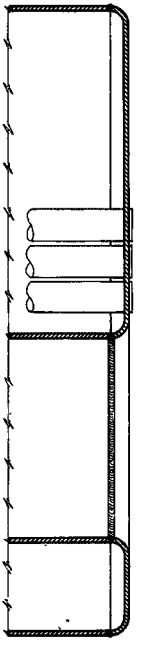


Fig. 4.5 Butt-welded tube sheet

function are installed in an external vessel connected to the areas in the boiler containing water or steam. They are expected to signal levels that are too high or too low or to shutting down the boiler if the level is dangerously low. The minimum level is normally expected to be 60–80 mm above the upper generatrix of the last row of tubes. These instruments can be used to start and stop the feed pump if the

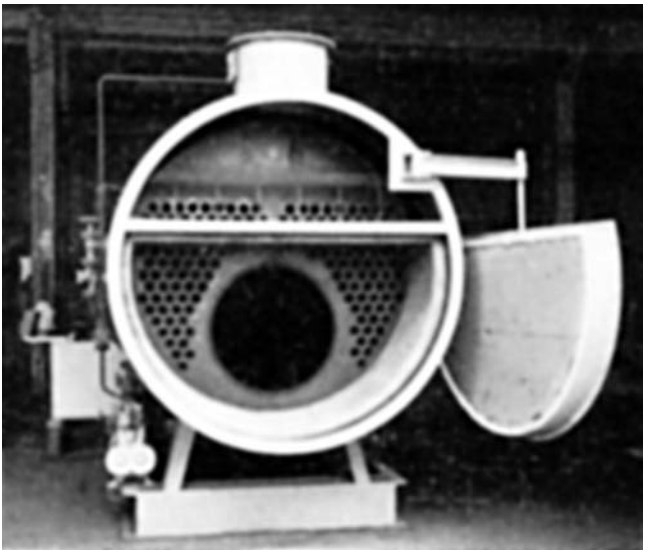


Fig. 4.6 Smoke-tube boiler with dry end plate (rear view)

"stop and go" feeding mode is chosen (Sect. 4.2). The boiler is equipped with safety valves and a pressure gauge.

The boilers with a dry end plate in Figs. 4.6 and 4.7 have many elements in common with those with a wet end plate. The former differentiate themselves by having the first backflow chamber outside the actual boiler (meaning by that the shell full of water or steam). From here, the gas enters part of the tubes connected to the front and back tube sheets. This is done with a diaphragm located in the backflow chamber and separating the different tube areas. This diaphragm is typically made with refractory casting (see Fig. 4.6).

Flue gas flows through the tubes in the lower area of the boiler. In fact, the temperature of flue gas is high, and it is best if the tubes are immersed in the area richest in water and poorest in steam.

Once the second gas passage is over, the tubes release the flue gas into the second backflow chamber outside the actual boiler, as is the case in the boiler with the wet end plate. At this point, if the boiler is designed to have three gas passages, the flue gas enters the second section of the bank performing the third passage, returning to the area of the first backflow chamber separated from the flue by the diaphragm, exiting the boiler, and releasing into the chimney. If the boiler has more than three passages, there will be a diaphragm even in the second backflow chamber, and the first one may have more than one diaphragm. These setups are out of the ordinary. In the rare case where only two passages are to be performed, there are no diaphragms and all the tubes are hit by the flue gas released by the flue.

Because the first backflow chamber is not cooled in cheaper boilers with dry end plates, there are problems caused by refractory material, wear and tear, clefts, seal,

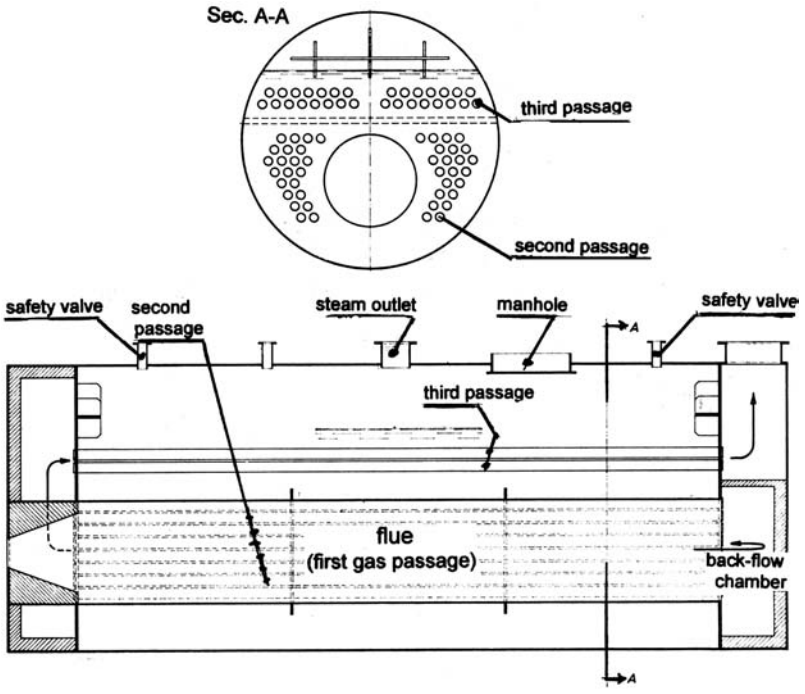


Fig. 4.7 Smoke-tube boiler with dry end plate

and so on, especially as far as the diaphragm is concerned. The boiler with a dry end plate is equipped with smoke-box doors even for the back tube sheet.

Besides these models, many more small power boilers with a wet end plate are built. For instance, Fig. 4.8 shows a Scotch boiler with only one gas passage in the tubes.

Both wet and dry end plate boilers can be relatively large. On average, boilers have a diameter up to 3 m and a length up to 7 m.

The smoke-tube boiler is typically used for modest steam output at low pressure. The pressure must be low because under high pressure the thickness of the external shell, the flue, and the tube sheets has such values to make it non-competitive. Note that it is necessary to set a limit to this thickness, to reduce the temperature of the internal side of the flue and the stresses due to thermal flux, as well as give sufficient elasticity to the tube sheet to absorb the difference of thermal expansions among flue, tubes, and external shell without any damage.

The power increase leads to a diameter increase of both the flue and the external shell that results in thickness increase. Beyond certain limits, the boiler is no longer competitive compared to water-tube boilers. On the other hand, by keeping the pressure really low (approximately below 10 bar), the cost reduction obtained with smoke-tube boilers is greater than the one with water-tube boilers.

In fact, the cost reduction with the latter is almost irrelevant. The thickness of the tubes cannot be less than a certain minimum, in turn depending on requirements

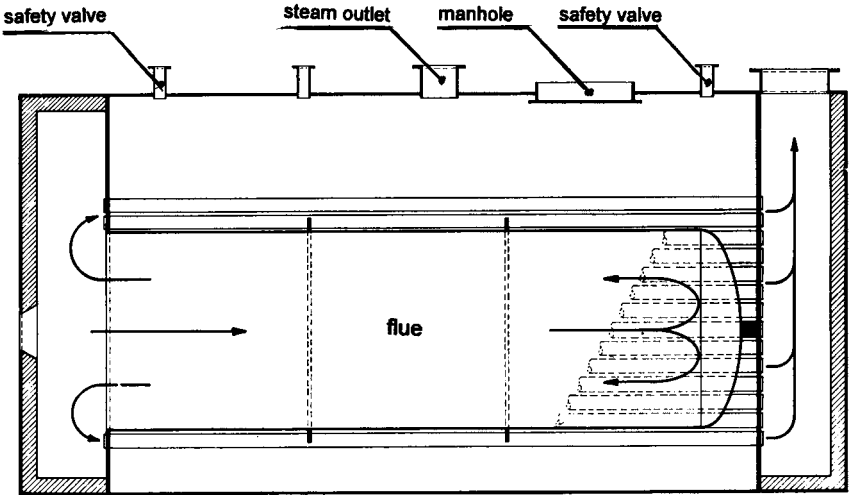


Fig. 4.8 Scotch boiler

relative to tube expanding, welding, and curvature. The thickness of the drum (or the drums), especially with expanded tubes, cannot go below a certain minimum. Valves only contribute to a little cost reduction. In smoke-tube boilers instead, it is possible to reduce the thickness of the flue and the external shell in proportion to the pressure, and minimum values required for tube expanding notwithstanding, sometimes even the thickness of the tube sheets.

In conclusion, the smoke-tube boiler can be considerably cheaper than a water-tube boiler up to 4500 kW and pressure levels up to 15 bar. For power up to 9000 kW and the same pressure, it is competitive with the water-tube boiler. Besides reliability issues with high power boilers of this kind, for greater power and pressure, it is generally more expensive than a corresponding water-tube boiler.

The smoke-tube boiler is ideal as waste-heat boiler. In reference to Fig. 4.7, it is clear that substituting the flue with a series of tubes creates a tube bank impacting the entire surface of the tube sheets except for the upper area in correspondence of the steam chamber. If the boiler produces warm or superheated water, the entire tube sheet can be drilled for the insertion of the tubes. This is basically a gas–water–steam exchanger, that is, a waste-heat boiler.

In contrast to boilers with a flue, there is only one gas passage in the waste-heat boiler. Flue gas flows through a duct to the frontal tube sheet of the boiler, continue through all the tubes, and exit from the back tube sheet. Thus, installation is quite simple without flue, backflow chamber, diaphragms, and doors. Sometimes there is a central tube of great diameter similar to the flue at the center of the boiler. Controlling the flow rate of the gas in this tube, it is possible to obtain a certain velocity distribution inside it and in the tubes of the bank, thus tuning the heat transfer within limits.

Given its construction, the smoke-tube waste-heat boiler is good at cooling gas under high pressure. In fact, gas flows through the tubes that resist pressure well due to their cylindrical shape. In this case, the water-tube waste-heat boiler is completely unsuitable instead.

4.2 Running Characteristics

The smoke-tube boiler can either deliver hot water to provide heating, or superheated water (hot water at pressure higher than atmospheric pressure) for heating and technological purposes, or steam for the same use. The thermal volumetric and superficial loads are very high in the flue. The first one is especially higher than that of a water-tube boiler. Values of 1300–1600 $\mathrm{kW/m^3}$ are normal, and values will inappropriately almost reach 2300 $\mathrm{kW/m^3}$.

Under these conditions, it is impossible to obtain high values of $|CO_2|$ while preventing the build up of unburned carbon monoxide. Combustion with fuel oil showing values of $|CO_2|$ of 12.5–13% is to be considered satisfactory. In conclusion, to prevent the build up of CO, it is necessary to factor in relatively high values of excess air. In any case, they should be higher than a corresponding water-tube generator. Of course, this has repercussions on the generator efficiency.

Considering the reduced size of the flue, the flame must be rather narrow and long in contrast to what happens in water-tube generators. It is not possible to assign very high turbulence (it would favor heat transfer by convection to the walls of the flue), and this could negatively impact mixing of fuel and air and the absence of unburned material.

In the first backflow chamber of dry end plate boilers, the flue gas at high temperature hits the smoke-box door, the diaphragm separating the tubes of the second gas passage from those of the third passage, and the refractory lining protecting the walls of the chamber itself. The refractory materials are quite stressed and must consequently be of good quality. Nonetheless, they are subject to wear and clefts, especially if they are directly radiated by the flame. Depending on the construction of the boiler and running conditions, periodical maintenance or complete overhaul must be part of the schedule at predetermined points in time.

Internal cleaning of the tubes is easily done through swabbing, given the ease of access through the doors. This must be done on a regular basis to prevent a reduction in overall heat transfer coefficient, that is, heat exchange, and an increase in pressure drop.

The smoke-tube boiler is pressurized. This does not lead to the problems described for water-tube generators because of the way the boiler is built. The only delicate point is the perfect seal of the doors, which is not always easily achievable.

This boiler is more sensitive to load variations than the water-tube boiler, as far as heat transfer and therefore boiler efficiency. It suffices to say that the heat transfer coefficient of flue gas through the tube bank of water-tube boilers is proportional to $V^{0.61}$, where V is the velocity, whereas inside the smoke tubes it is proportional to

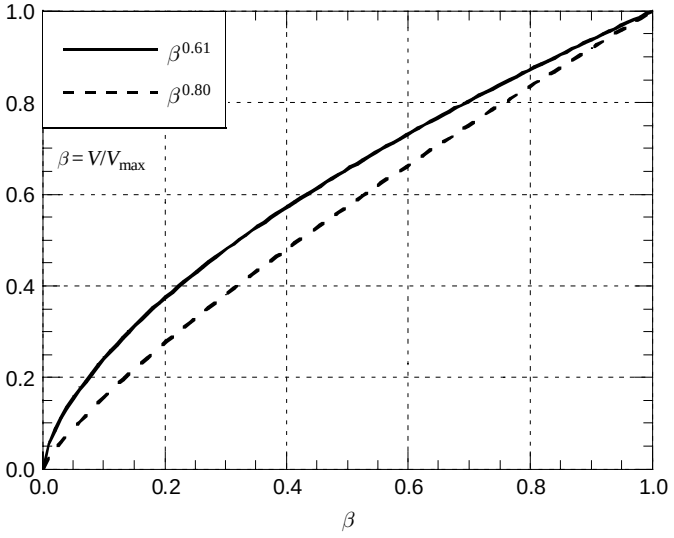


Fig. 4.9

$V^{0.8}$ (Chap. 8). Inside the latter tubes, a velocity reduction more sensibly impacts the overall heat transfer coefficient.

By indicating the ratio V/V_{max} with β, Fig. 4.9 shows the values of $\beta^{0.61}$ and $\beta^{0.8}$. Note, for instance, for $\beta = 0.5$, $\beta^{0.61} = 0.655$, whereas $\beta^{0.8} = 0.575$. The ratio between these two values that is indicative of the ratio between the respective heat transfer coefficients is equal to 1.14 in favor of the water-tube boiler.

The heat crossing the wall of the flue hits the surrounding water causing steam buildup in contact with the external surface. This steam can be condensed by heating the surrounding water, if the system is set up to produce hot or superheated water. It comes off the flue as bubbles and moves upward, given the reduced density compared to water, if the system is set up to produce steam. The same phenomenon takes place also around the tubes, albeit with less intensity due to reduced heat transfer. In the case of steam, the latter moves to the upper area of the boiler where it occupies the steam chamber, similarly to what happens in the drum of a water-tube generator. The analogy with the water-tube boiler is only apparently so because no steam is produced in the drum of the latter.

In the water-tube boiler, the presence of steam is due to the return of the mix from the steam-generating tubes and the following separation of the components. Therefore, there is clear separation between water and steam that occupy a definite portion.

In smoke-tube boilers, steam production takes place inside the cylindrical shell instead. In its lower area, there is a mix of water and steam that is more or less rich in steam, as a function of the output of the boiler per surface unit of the water content and the water surface area. The output of steam referred to the water surface area is particularly significant.

By first approximation, it is possible to compute the density of the mix above the last row of tubes (ρ_m) with the following equation:

$$\rho_m = (1 - 1.7 M_s)\,\rho_w, \tag{4.1}$$

where M_s is in fact the output referred to the water surface as kg/m^2s and ρ_w is the density of the water.

The consequence of this phenomenon is a false reading of the level (Fig. 4.10). It is higher in the boiler compared to the value shown by the level gauge, and this leads to a greater tendency of the steam to drag water while exiting the boiler. To eliminate the problem, it is possible to slightly change the design, as shown in Fig. 4.11.

In any case, in smoke-tube boilers, the danger of considerable water dragged by the steam is always present, because the steam chamber is not very large and most of all because the water surface is close to the main steam outlet. Protective screens in metal sheet are required in front of it to prevent the direct eddy of the water and to force the steam into a path along the boiler that frees it as much as possible from the water.

The position and the fluid dynamic characteristics of the often rather cold feed water entering the boiler are very important. It is crucial to prevent that it directly hits the flue, the tubes, and the tube sheets to prevent thermal shock that may cause expanding removal of the tubes and settling or cracking of the welding.

In that regard, the tendency to make these boilers run in “stop and go” mode is debatable. It consists of feeding the boiler with a heavy water flow rate provoking the intervention of the pump when the level reaches the minimum. The level goes up, and once it reaches a maximum, the pump stops automatically and stays off

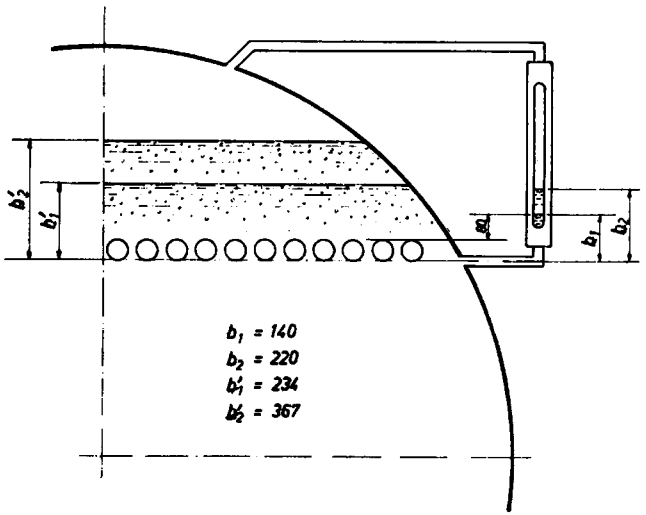


Fig. 4.10

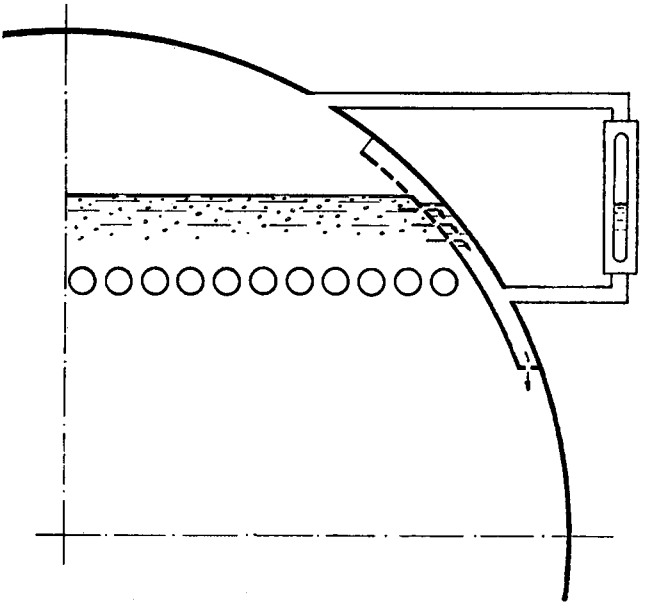


Fig. 4.11

until the level is down again. This procedure alternatively introduces a great mass of cold water above steam output or no amount of water. Obviously, these thermal unbalances do not extend the life of the boiler.

4.3 Rationalization Criteria for Construction

Smoke-tube boilers lend themselves quite well to be designed according to constructive rationalization criteria. We refer to the possibility to adopt the same elements, such as identical tube sheets, constant diameter and length of the tubes, constant diameter of the flue, identical doors, for a group of boilers of different power. This is an interesting aspect in terms of cost reductions as far as design, construction, and supplies. In practice, there are three elements to work with, that is, the diameter, the length of the tubes, and the tube sheet. The two following solutions can be applied.

The first one, we will call it option A for simplicity reasons, consists of adopting the same tube sheets, thus keeping the number and the diameter of the tubes, besides the diameter of the flue, unvaried while varying the length of the flue and of the tubes for the different boilers in the group.

The second solution called option B consists of keeping the diameter and the length of the tubes, as well as the length of the flue, the same, changing the number of tubes and the diameter of the flue instead.

From the point of view of design and construction, option A has the following advantages.

- The tube sheets are identical in various boilers carrying an obvious financial advantage, particularly if the sheets are flared, given the possibility to plan for supplies at reduced cost and to operate exchanges among different boilers in case fast stocking should be a problem.
- Moreover, the smoke-box doors are the same and make it possible to stock up, thus reducing costs.
- It is also possible to consider to stock up on standard cylinder parts to combine with cylinder parts of variable length used to build the flue.

The disadvantage as far as construction is the necessity to use tubes and flue of variable length depending on the boiler, so that stocking tubes of defined length becomes costly. On the other hand, commercial length tubes means expenses due to scraps.

Option B favors stocking up supplies of tubes of definite length with reduced extra expense. Of course, the advantages represented by identical tube sheets and smoke-box doors are gone, increasing working costs without being able to interchange parts on different boilers. As far as the tube sheets, note that if they are fillet weld, thus obtainable from a metal sheet through a simple cut, one of the negative aspects of option B becomes less important.

Both solutions evidently carry positive and negative aspects from the point of view of construction. Undoubtedly, the advantages of option A supersede those of option B.

Final evaluation on the validity of both options cannot ignore the positive and negative aspects as far as boiler performance. In other words, it is important to evaluate the impact of rationalization on the thermodynamic and fluid dynamic behavior of the boiler.

Clearly, the suggested rationalization for both options carry definite advantages in terms of working costs, but they also create problems in terms of optimization of the performance of the boiler from a thermodynamic and fluid dynamic point of view, given the imposition of constraints that condition its exploitation. To shed light on the most significant aspects of the impact of the described constructive rationalization on the performance of the boiler, we show some results achieved through investigation on different groups of boilers of different power with three gas passages and a dry end plate. In addition, note that the results obtained in this way are qualitatively transferable to boilers with a wet end plate, as well.

Three groups of boilers have been created. The first with a base power of 1000 kW includes boilers with power ranging from 700 kW up to 1300 kW. The second with a base power of 2000 kW includes boilers with a power ranging from 1400 to 2600 kW. Finally, the third one with a base power of 4000 kW includes boilers with a power ranging from 2800 to 5200 kW.

The tubes are distributed based on about 60% of the total in the second passage and 40% in the third passage, given that maximum boiler efficiency and minimum pressure drop correspond to this proportion (or at least to values in this

Table 4.1 Option A – first group

Power	kW	700	1000	1300
Flue diameter	mm	550	550	550
Boiler length	mm	3750	3900	4050
Flue superficial load	kW/m^2	125	171	214
Flue volumetric load	kW/m^3	906	1244	1557
Tubes (diameter $\times$ thickness)	mm	54×2.6	54×2.6	54×2.6
Number of tubes		$40 + 30$	$40 + 30$	$40 + 30$
Boiler specific output	kW/m^2	14.95	20.53	25.71
Pressure loss	Pa	200	416	717

neighborhood). This topic will be discussed further in Sect. 8.14. Fuel oil combustion with a net heat value equal to 40,600 kJ/kg and $|CO_2| = 13\%$ is assumed. Absolute pressure is equal to 11 bar.

Efficiency has been set to be 87%, considering miscellaneous not computable losses of 0.5%. The results are shown in Tables 4.1, 4.2, and 4.3 for option A and in Tables 4.4, 4.5, and 4.6 for option B. The examination of these tables leads to the following considerations.

Table 4.2 Option A – second group

Power	kW	1400	2000	2600
Flue diameter	mm	730	730	730
Boiler length	mm	4150	4400	4650
Flue superficial load	kW/m^2	169	228	280
Flue volumetric load	kW/m^3	926	1249	1537
Tubes (diameter $\times$ thickness)	mm	60.3×2.9	60.3×2.9	60.3×2.9
Number of tubes		$54 + 36$	$54 + 36$	$54 + 36$
Boiler specific output	kW/m^2	19.03	25.64	31.54
Pressure loss	Pa	316	664	1152

Table 4.3 Option A – third group

Power	kW	2800	4000	5200
Flue diameter	mm	1000	1000	1000
Boiler length	mm	4750	5200	5600
Flue superficial load	kW/m^2	216	282	340
Flue volumetric load	kW/m^3	863	1126	1359
Tubes (diameter $\times$ thickness)	mm	70×2.9	70×2.9	70×2.9
Number of tubes		$72 + 48$	$72 + 48$	$72 + 48$
Boiler specific output	kW/m^2	21.54	28.11	33.93
Pressure loss	Pa	364	772	1344

Table 4.4 Option B – first group

Power	kW	700	1000	1300
Flue diameter	mm	450	550	650
Boiler length	mm	3900	3900	3900
Flue superficial load	kW/m^2	146	171	188
Flue volumetric load	kW/m^3	1303	1244	1157
Tubes (diameter × thickness)	mm	54×2.6	54×2.6	54×2.6
Number of tubes		$36 + 26$	$40 + 30$	$44 + 34$
Boiler specific output	kW/m^2	16.40	20.53	23.76
Pressure loss	Pa	263	416	563

Table 4.5 Option B – second group

Power	kW	1400	2000	2600
Flue diameter	mm	600	730	860
Boiler length	mm	4400	4400	4400
Flue superficial load	kW/m^2	194	228	252
Flue volumetric load	kW/m^3	1292	1249	1170
Tubes (diameter × thickness)	mm	60.3×2.9	60.3×2.9	60.3×2.9
Number of tubes		$46 + 32$	$54 + 36$	$62 + 44$
Boiler specific output	kW/m^2	20.84	25.64	28.31
Pressure loss	Pa	427	664	800

Table 4.6 Option B – third group

Power	kW	2800	4000	5200
Flue diameter	mm	820	1000	1180
Boiler length	mm	5200	5200	5200
Flue superficial load	kW/m^2	240	282	310
Flue volumetric load	kW/m^3	1171	1126	1051
Tubes (diameter × thickness)	mm	70×2.9	70×2.9	70×2.9
Number of tubes		$56 + 38$	$72 + 48$	$88 + 62$
Boiler specific output	kW/m^2	24.98	28.11	29.42
Pressure loss	Pa	607	772	824

As far as option A, note that moving from the smallest to the biggest boiler of the group, in any case there will be a variation in the boiler specific output of about 70%. The same is true for superficial and volumetric thermal load of the flue.

The pressure drop varies greatly between the smallest and the greatest boiler. The ratio between the maximum and the minimum value exceeds 3.5 among the groups. With reference to the entire range, there is a minimum of boiler specific output equal to $14.95\,kW/m^2$. There is also a maximum of this output equal to $33.93\,kW/m^2$ combined with a high pressure loss (1344 Pa).

As far as solution B, the boiler specific output is less variable. There is a minimum of $16.40\,\mathrm{kW/m^2}$ and a maximum of $29.42\,\mathrm{kW/m^2}$. The same applies to pressure drop. The ratio between the pressure drop of the biggest and the smallest boiler is equal for all groups to 2.14, 1.87, and 1.36, respectively. The variations in superficial thermal load in the flue inside the groups are below 30%, whereas those relative to the volumetric thermal load are below 13%.

Based on the investigation, the obvious conclusion is that boilers with constant tube length (option B) are clearly preferable to those with the same tube sheet (option A) from a thermodynamic as well as a fluid dynamic point of view.

Even though option A is the most interesting solution from a construction perspective, it produces very inhomogeneous boilers, not to mention low boiler specific output for the smallest boilers in the group that leads in higher costs in terms of labor and materials. Therefore, option B is definitely preferable, regardless of the reduced advantages during construction. It works well with a vast variety of boilers bunched together in one group. Of course, there are limits relative to the length of the flame because the length of the boilers is constant. Keep in mind, though, that bigger boilers involve greater diameters of the flue and smaller volumetric thermal loads, as the tables clearly demonstrate. With an adequate shape of the flame, it is possible to include in one single group a rather wide range of boilers.

This page intentionally left blank

Chapter 5
Diathermic Fluid Boilers

5.1 Employed Fluids

The fluids used in diathermic fluid boilers are mineral oils of petroliferous origin, also used as lubricants, and certain special fluids. The most commonly used mineral oils have a paraffine base and are solvent refined with medium and high viscosity, inhibited with antioxidant and antifoaming additives. The special fluids are of organic nature and very different from one another. Silicates, diphenyl, diphenyl oxide, clorobenzene, and ethylene glycol are used.

The common characteristic to all diathermic fluids is their high boiling temperature, or the high temperature at which distillation will start (in the case of mineral oils). Consequently, they can be used at high temperature in the liquid phase under atmospheric pressure. Roughly, the maximum usage temperature ranges from fluid to fluid between 170 and 350°C.

More specifically, the main characteristics of the different fluids are as follows.

- Mineral oils can be used at temperatures up to 300–350°C without any risk of cracking.
- Their resistance to oxidation decreases as the temperature goes up.
- They have an acceptable heat transfer coefficient, even though it is generally lower compared to organic fluids, that will be higher as the viscosity goes down.
- They have great lubricating properties (as far as pumps) and no toxicity.

The silicates used as diathermic fluid can be used up to 300–340°C. They withstand oxidation and have a great heat transfer coefficient. They are also quite expensive and sensitive to humidity, potentially building up phenol and siliceous sludge deposits.

The diphenyl and diphenyl oxide mixes can be used in liquid state up to 250–280°C. The heat transfer coefficient is excellent, they are slightly toxic, stability in terms of oxidation is fairly good and viscosity is very low. They are not lubricant. At pressure above the atmospheric one, they can be used in liquid state up to 330–380°C.

D. Annaratone, *Steam Generators*, DOI: 10.1007/978-3-540-77715-1_5,

© Springer-Verlag Berlin Heidelberg 2008

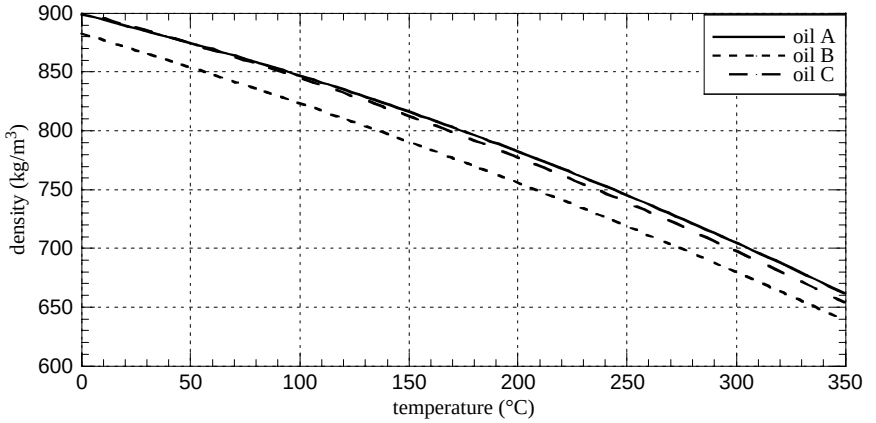


Fig. 5.1 Density of some mineral oils

Clorobenzene can be used at temperatures up to 170°C at atmospheric pressure and up to 260°C under higher pressure. It is slightly toxic.

Ethylene glycol can be used in liquid state at atmospheric pressure at temperatures ranging from 170 to 250°C. Under higher pressure, usage is possible up to 260–380°C. Its thermal conductivity is excellent. It is moderately toxic and has a tendency to polymerize.

Mineral oils are most frequently used because they cost less and are more easily available.

Figure 5.1 shows the density of three mineral oils. The quantities relative to the heat transfer are shown in Sect. 8.10. Section 8.10 also includes diagrams relative to viscosity, isobaric specific heat, and thermal conductivity of these oils. These quantities are particularly interesting for the computation of the heat transfer coefficient.

5.2 Constructive and Functional Characteristics

Fluid diathermic boilers are normally expected to function with the fluid in its liquid state, at atmospheric pressure and under forced circulation. Combustion is with fuel oil or natural gas with an automatic burner (only one burner because of the modest power).

The furnace must be screened as much as possible with tubes side by side to prevent the flame from *seeing* extended walls of refractory material. In fact, the latter maintain high temperature even in the absence of a flame due to their thermal inertia. If the absence of a flame is caused by stopping of the pump, due to mechanical failure or power failure, the tubes are radiated by the refractory material in the absence of circulation, and this implies obvious danger of superheating of themselves as well as the fluid. In that regard, it is advisable to line the refractory material with special felts, characterized by resistance to high temperatures and low thermal

inertia. The volumetric and superficial thermal loads of the furnace are modest (the second usually does not exceed 140–200 kW/m^2).

A convective tube bank is set up in the back, on top, or on the sides of the parallelepiped furnace. The diaphragms meant to direct the flue gas along the desired path are inserted among the different sections of the bank. There are also round boilers with convective coils placed helicoidally around the furnace including a burner with vertical axis.

The screens in the furnace, as well as the convective bank, can be made with differently bended, orientated, and connected coils, or with tubes inserted in headers equipped with internal diaphragms. In any case, given the flow rate, only one circuit must be created to ensure high velocity of the fluid (from 1.5 to 3 m/s).

For instance, if we consider medium oil viscosity (oil B) at 250°C, the heat transfer coefficient (expressed in W/m^2K) is about equal to $750V^{0.8}$, where V is the velocity of the fluid in m/s. If q stands for the thermal flux referred to the internal surface of the tube, the difference Δt between the wall temperature and the bulk temperature of the fluid can be obtained from Fig. 5.2. Clearly, if the flux is equal to 40–50 kW/m^2 (as in convective banks) with a fluid velocity of 1.5 m/s, the difference in temperature in question is below 50°C. On the other hand, if the flux is equal to 110–120 kW/m^2 (as is the case with the peak flux in the furnace), a velocity of 3 m/s must be adopted to limit the temperature difference under 65–70°C. It is crucial to do accurate calculations to determine the temperature of the wall inside the tubes; it should never exceed the maximum allowable working temperature of the fluid.

The piping leading to suction and delivery of the circulation pump is connected to the entry- and exit-flanged nozzles of the boiler. The expansion tank is connected to the suction piping. The expansion tank is expected to allow the thermal expansion of the fluid and to keep up a slight hydrostatic pressure to eliminate any presence of air. It is advisable to install it with a head of at least 3–4 m, with respect to the upper part of the circuit. The volume of the expansion tank must be such to absorb

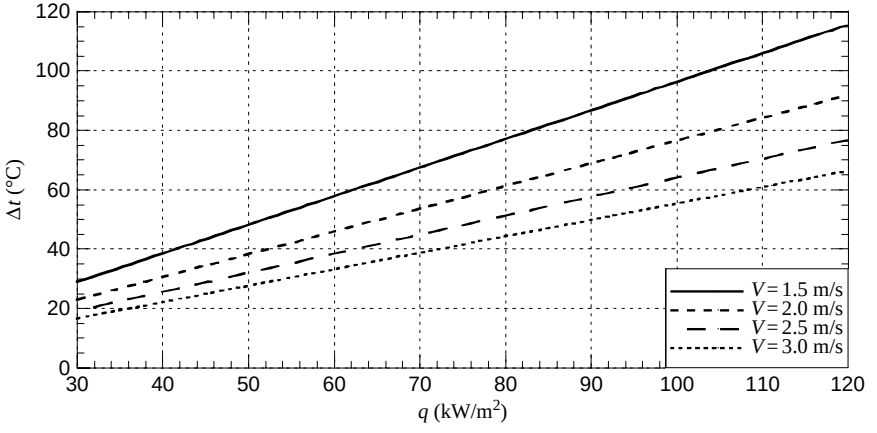


Fig. 5.2 Temperature difference between tube wall and fluid

the expansion of the fluid contained in the entire circuit (boiler, heat exchanger, and external piping). It must be approximately 30% of the total volume. Ideally, it should be tall and narrow to offer the smallest possible surface of the fluid surface in contact with air. Note that this area is the only one showing oxidation phenomena. In that respect, it is best if its temperature is kept as low as possible (50–60°C), by employing not insulated connection piping of small diameter. A good rule of thumb is to factor in a tank closed with a layer of inert gas (nitrogen) above the fluid surface. The tank can be kept under light pressure through connection of a register valve to a nitrogen bottle.

The pump can either be centrifugal or a positive displacement pump. The first type must be ruled out, if the fluid has a vapor tension at running temperature above 1/4 of suction pressure (absolute), or if viscosity is greater than 700 cS at starting. For temperatures in the 300°C range, it is best to cool the pump using water. Moreover, it is most important to plan for automatic devices that shut down the burner whenever the pump accidentally stops.

During the starting process, the pump must be turned on a certain amount of time before turning on the burner. Similarly, during shutdown of the latter, the pump will be kept working until the temperature of the fluid reduces itself to about half the running one. The temperature of the fluid at the exit of the furnace must be checked with a thermostat influencing the burner by modifying its fuel consumption.

Tuning influencing the heat transfer into the heat exchanger, in relation to the heat request (this does not rule out the previous one but it is faster and more flexible), is represented by piping to by-pass the exchanger containing a valve controlled by means of a thermostat. This way, the heat exchanger is partially short-circuited, and a part of the warm fluid is directly conveyed to the suction of the pump. Note that this piping can be used to completely cut off the heat exchanger with the help of adequate valve systems. This is required during starting to reduce the pressure drops, given the greater viscosity of the fluid.

Other solutions are obviously possible. Here we simply pointed out the fundamental requirements to provide orientation for a correct functioning of the boiler. In view of the above presentation, Fig. 5.3 shows a potential elementary setup.

The diathermic fluid boiler can produce superheated water (water under pressure greater than the atmospheric one) through a fluid–water heat exchanger. This exchanger is made with U-shaped tubes, straight tubes with fixed or floating head, and the fluid flows inside the tubes, whereas water flows outside of them. The heat exchanger is placed on the suction of the pump above the boiler, or separately in a high up location.

The boiler can also produce saturated steam (see Figs. 5.4 and 5.5). In that case, the heat exchanger is connected to a drum on the top and bottom. The upper piping discharges the water–steam mix built up in the exchanger into the drum, as in the case of return tubes of a water-tube boiler. The steam taken through the main intake valve goes to usage from the drum. As usual, the drum is equipped with levels and safety valves and is fed water by a feed pump.

Generally, the power of these boilers does not exceed 3500–5000 kW. Anyway, there are no technical impediments to units of greater power. The efficiency is not very high and ranges from 84 to 86%. It can be increased by including an air heater.

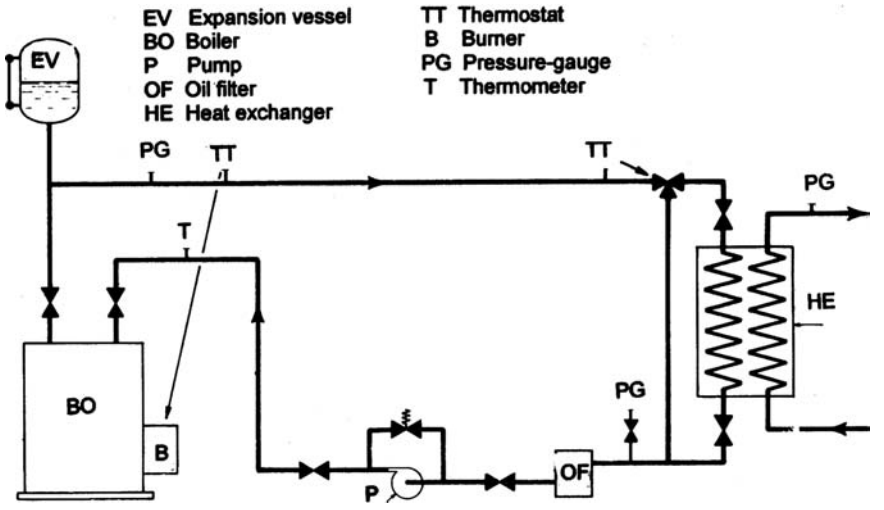


Fig. 5.3 Elementary setup for diathermic oil boiler

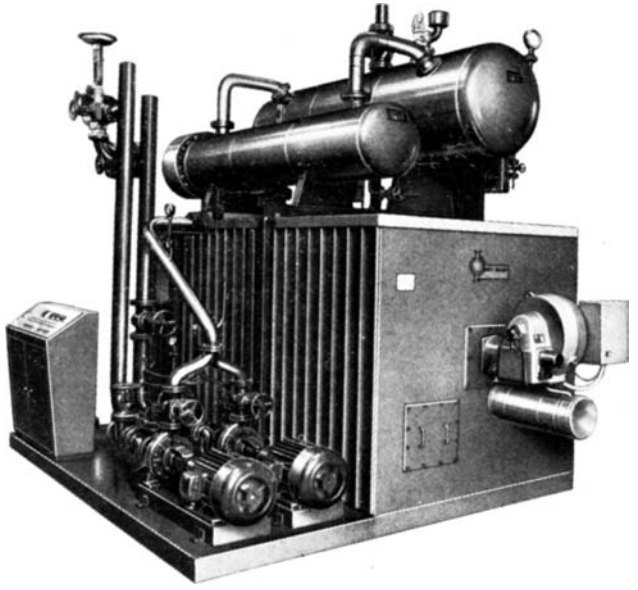


Fig. 5.4 Diathermic oil boiler

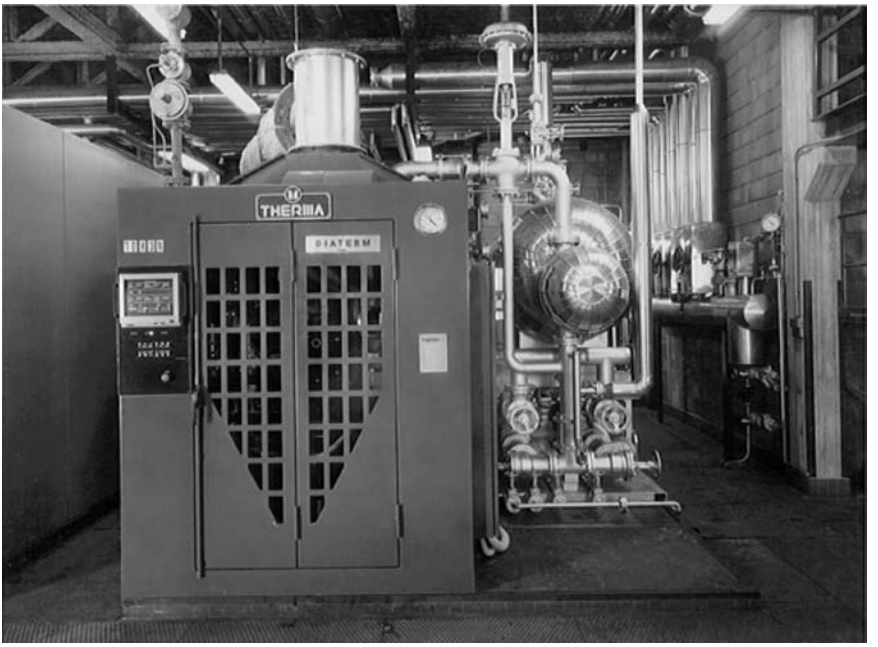


Fig. 5.5 Diathermic oil boiler (Courtesy of Therma – Italy)

5.3 Advantages and Disadvantages in Comparison with Water-Tube Boilers

Examining advantages and disadvantages of fluid diathermic boilers, one must distinguish between plant and running costs. The comparison between fluid diathermic boilers and water-tube boilers relative to each aspect leads, in fact, to diverging results.

We mentioned only water-tube boilers, as the comparison with smoke-tube boilers is meaningless. The employment of fluid diathermic boilers aims at obtaining superheated water or steam at pressure levels that are incompatible with the construction of smoke-tube boilers.

We saw that the common characteristic of all diathermic fluids is the ability to be used in their liquid state at high temperature and at atmospheric pressure. As mentioned earlier, boilers can produce superheated water through a heat exchanger, whereas it is possible to produce steam up to 40 bar through a heat exchanger and a drum. As far as costs of the plant, the situation is as follows.

One could think that the modest pressure in the boiler (due exclusively to pressure drops of the circuit) represents an advantage for the sizing of the tubes and the headers. Note, though, that this is rarely the case because tubes of standard thickness are used (minimum value for their normal production) even though it is excessive because of the actual pressure. Besides constructive issues (welding and bending), this fulfills both financial and stocking requirements. This thickness is

mostly not smaller compared to that of tubes in water-tube boilers working at the pressure obtainable for water or steam with fluid diathermic boilers. In any case, potential modest differences in thickness do not represent a crucial element.

The diathermic fluid boiler needs a heat exchanger to produce superheated water, whereas the water-tube boiler can produce it directly in the drum. The comparison is not in favor of the first, considering the higher cost of the heat exchanger. Preferably, if the water-tube boiler works with steam and is equipped with a steam–water heat exchanger for the subsequent production of superheated water instead, the comparison may favor the diathermic fluid boiler. Note, though, that the steam–water heat exchanger is much cheaper than the fluid–water heat exchanger. If steam is produced instead, the diathermic fluid boiler needs the heat exchanger missing in the water-tube boiler. Therefore, the comparison produces unfavorable results for the diathermic fluid boiler.

In addition, note that the superficial thermal load in the furnace must be rather modest in diathermic fluid boilers because of the type of fluid flowing through the tubes. In fact, high thermal flux must be avoided to rule out superheating of the tubes and most of all to prevent rapid oxidation of the fluid, as well as cracking and polymerization phenomena.

The furnace must be sized to be wider with larger radiated surfaces compared to a water-tube boiler of equal power. This leads to higher costs. The cost of the circulation pump and the deriving piping, as well as the expansion tank and its piping, must also be considered. Finally, there is the relatively high cost of the fluid for the first filling of the plant. The plant cost of a diathermic fluid boiler is clearly higher to that of a water-tube boiler of equal power.

As far as running costs, the situation is as follows. The diathermic fluid boiler is less efficient. To produce superheated water or steam at a given temperature, the fluid in the heat exchanger must necessarily be at a higher temperature. Consequently, the boiler will also register a higher temperature. The fluid in the boiler is warmer than the water–steam mix in a water-tube boiler producing superheated water or steam under the same pressure. Therefore, the exit temperature of the flue gas from the diathermic fluid boiler is higher, given equal heated surfaces and overall heat transfer coefficient.

Even ignoring the reduced heat transfer coefficient of the fluid compared to the water–steam mix, the result is either the same efficiency (assuming it is actually possible) by planning for greater heat exchange surfaces (and higher costs), or more frequently the efficiency of the diathermic fluid boiler is lower than that of a corresponding water-tube boiler. This results in higher running costs and an efficiency reduction of about 2–3%. An air heater can be used to compensate for this reduction, but its additional cost increases the overall cost of the plant.

The energy absorbed by the circulation pump and the periodical substitutions of degraded fluid must also be considered. As far as running costs, the diathermic fluid boiler would seem to be at a disadvantage, and this is true if the evaluation is based purely on technical considerations. The diffusion of this type of boiler would not be justified. The reason for it is based on a decisive element that is totally unrelated to technical issues.

Given the fact that the diathermic fluid boiler is completely automatic and that it works at atmospheric pressure, it does not require a stoker but simply personnel in charge of periodical checks. Based on the codes of industrialized countries, the water-tube boiler generally requires the uninterrupted presence of a certified stoker whose cost is not irrelevant. Therefore, the savings in running costs are often in favor of diathermic fluid boilers even though the plant and the running costs are higher.

Either way, the choice depends on the correct evaluation of all the elements at play. In general, considering that the missing cost of a stoker is invariant with respect to the output of the boiler, low power boilers with minor plant and running costs have an advantage. In fact, boilers of this type are typically low power. The opportunity to install high-power units (beyond 4000–5000 kW) must be carefully thought through and can be debatable, particularly if it is running all the time.

Chapter 6
Fuels

6.1 Solid Fuels

Solid fuels are solid materials of vegetal origin used for combustion. Natural solid fuels are wood, peat, lignite (brown coal), and coal. Artificial solid fuels are those that underwent transformation as far as their shape or through transformation caused by heat intervention, such as wood coal, coke, and briquettes made of peat, lignite, and coal.

Among artificial solid fuels, there are also residues of certain manufacturing, such as wooden shavings and saw dust, grape husk, olive husk, bagasse, and rice husk (processing residues of grapes, olives, sugar cane, and rice, respectively). Urban waste that is burnt on grates is particularly interesting.

From a geological point of view, solid fuels can be divided into recent and ancient ones. Recent fuels are wood, peat, and lignite (in chronological order), whereas pit coal (fuels rich in volatile matter are younger and those containing less of it are older) and anthracite are among the oldest fuels.

Among the most important characteristics of solid fuels are the content of volatile matter, ashes, moisture, sulfur, the melting point of ashes, heat value. Furthermore, the physical characteristics of interest are size, density and porosity, isobaric specific heat, thermal conductivity, and viscosity of the ashes. The most frequently used fuels for industrial-type steam generators are coal and lignite. Manufacturing residues directly produced by product-specific industries also belong to this category. The characteristics of coal, the most used solid fuel, will be discussed later on. As far as the other types of fuel, some of the most important characteristics are as follows.

Lignite, based on its structure that depends on age, can be divided into fibrous lignite with a structure similar to peat, xyloid lignite looking quite like wood, and pitchy lignite, morphologically quite similar to coal. Fibrous lignite consists of up to 50% of water and 30% of ashes; the water content of xyloid lignite can even reach 50%, but it is reduced to 20% if the lignite is air dried, whereas the ash content ranges from 3 to 20%; pitchy lignite contains less than 10% water and ashes ranging from 10 to 20%. The net heat value of lignite after drying ranges from 10,500 to 23,000 kJ/kg.

D. Annaratone, *Steam Generators*, DOI: 10.1007/978-3-540-77715-1_6,

© Springer-Verlag Berlin Heidelberg 2008

Peat in its natural state is very rich in water (up to 90%), but when it is exposed to air, it loses most of its moisture that is reduced to 25–35%. After air drying, the net heat value is about 12500 kJ/kg. As far as wood, its net heat value is generally equal to 13,800–15,900 kJ/kg.

It is possible to use the following equation for heat value calculation:

$$H_{\mathrm{n}} = 19,200 - 217H_2O, \tag{6.1}$$

where H_{n} represents the net heat value in kJ/kg and H_2O the water content in percentage.

As far as grape husk, olive husk, and rice husk, their moisture and ash content vary greatly, and this considerably impacts the net heat value. Examining a few typical cases where both water and ash contents are medium, it is possible to assume the following reference values.

Assuming grape husk with a water content of 10–12% (in some cases it can reach up to 30%) and ashes of about 5–8%, it was found that on average the net heat value is about 15,900 kJ/kg. The net heat value of olive husk with a water content of 20–30% and ashes equal to 6–12% is about 13,400 kJ/kg. In the case of rice husk, a water content of 8–12% and ashes of 12–15% will result in an average net heat value of about 12,500 kJ/kg.

The net heat value of urban waste is quite variable. Consider a value ranging between 4600 and 7100 kJ/kg as a reference. Also consider that the net heat value increases with the growing quality of living conditions of the population.

Coal consists of pure coal, the actual fuel, mineral matter (ashes), and water. In turn, pure coal consists of pure coke (fixed carbon) and volatile matter. The latter consists of vapor from light oil and tar, as well as gas. We already mentioned the fact that more recent coal is richer in volatile matter compared with ancient coal.

The content in volatile matter leads to a first simple classification of coal types divided into cannel, fat, lean coal, and anthracite. Cannel coal contains about 40–50% of volatile matter and has a net heat value equal to 27,200–31,400 kJ/kg. Fat coal contains about 18–36% of volatile matter, and its net heat value is equal to 29,300–33,500 kJ/kg. The content in volatile matter of lean coal is equal to 10–18%, and its net heat value is about 33,500 kJ/kg. Finally, anthracite contains about 5–10% of volatile matter and has a net heat value of about 33,500 kJ/kg.

Cannel coal and some kinds of fat coal burn with a long flame, whereas some type of fat coal, lean coal, and anthracite burn with a short flame. Even though the content of volatile matter is an important parameter in the classification of coal, it would be simplistic to base it on this parameter only.

The international classification of coal based on code numbers that identify the different kinds also includes other parameters. It considers classes, groups, and subgroups. The first code number identifies the class based solely on the content of volatile matter up to 33%; for higher values, it is based on the net heat value; there are nine different classes. Four groups represent the second code number. Inclusion in one of these groups depends on the free-swelling index. Finally, there are six sub-groups representing the third code number. Inclusion in one of the sub-groups depends on the value resulting from the Audibert–Arnu dilatometer.

The sulfur content ranging from 0.5 to 3% in coal is very important. Its presence moves up to the dew point of flue gas. The simultaneous presence of SO_3 in the flue gas, due to partial oxidation of SO_2 (present because of sulfur combustion), represents the risk of fouling of the walls and corrosion by sulfuric acid in the areas of the generator at low temperature. Further considerations on this topic are made in Sect. 6.2 relative to the sulfur contained in fuel oil. Sulfur is contained as iron sulfide (pyrite and marcasite) or rarely as other sulfide. It can be present also as calcium sulfate and sodium sulfate.

As mentioned earlier, coal also contains mineral matter and water. As far as the latter is concerned, note that some speak of moisture percentage of coal, whereas others prefer to speak of moisture of pure coal, and some others speak of kilogram of water per kilogram of pure coal. Examining the characteristics of a coal type therefore requires checking whether the moisture is referred to the coal as is, or to pure coal, that is, coal devoid of moisture and mineral matter.

As far as mineral matter and ashes, note that the amount of ashes is represented by the residue obtained by heating the coal under a series of coded conditions. The resulting values are conventional, given that they depend on trial conditions that differ from country to country.

Moreover, the content of mineral matter does not coincide with the content of ashes because it exceeds it. With reference to the amount of ashes derived according to the German trial method, the content in mineral matter can be computed with relatively good approximation with the following equation:

$$Mm = 1.11As + 0.35S, \tag{6.2}$$

where Mm is the content in mineral matter, As the content in ashes and S the one in sulfur, all expressed as percentages. As far as coal from the Ruhr, on average $Mm/As = 1.19$.

Finally, note that in the absence of experimental data the ash content can be computed by first approximation using the following equations:

$$As = 100(\rho - 1.25) \tag{6.3}$$

$$As = 100(\rho - 1.32). \tag{6.4}$$

Here, As stands for the percentage of ash content and ρ for the apparent relative density of the coal. Equation (6.3) is valid for all coal types except anthracite and (6.4) is used for anthracite. The ash content of coal usually ranges from 6 to 14%.

Ashes consist mainly of SiO_2, Al_2O_3, Fe_2O_3, and CaO. They belong to the bituminous type if the content of Fe_2O_3 is greater than that of $(CaO + MgO)$. On the other hand, if the content of $(CaO + MgO)$ is greater than Fe_2O_3, ashes belong to the lignite type. Ash fusibility is quite important as far as the evacuation of the ashes from the furnace. Fusibility is determined through standard procedures that generally use Seger cones already well known in the ceramic industry.

We obtain a series of significant temperatures representing the different stages from softening to actual fusion. Therefore, we speak of initial deformation temperature, softening temperature, hemispherical temperature, and fluid temperature. The

results can differ even by 60–80°C using the same coal, yet in different furnaces. The different procedures used in various countries add to the uncertainty. Thus, the data must be used with care and their limitations acknowledged.

The viscosity of the ashes is also very important in terms of evacuation from the furnace. The viscosity is measured with a high temperature rotating-bob viscometer. Lack of direct measurement can be addressed as follows. Note that the constituents of ashes are either basic or acidic. Fe_2O_3, CaO, MgO, Na_2O, and K_2O are basic constituents, whereas SiO_2, Al_2O_3, and TiO_2 are acidic.

As shown in Fig. 6.1, the ratio between basic and acidic constituents helps to evaluate the temperature (expressed in °C) at which the viscosity of the slag is equal to 250 Poise. If t_{250} is this temperature, the viscosity at a different temperature t can be computed using the following equation:

$$\mu = \frac{250}{\left(1.983\dfrac{t - t_{250}}{1000} + 1\right)^{6.196}}. \tag{6.5}$$

Another interesting characteristic of coal, and all fuels in general, is the fire point. Its definition is not unanimous. Generally, it is understood to be the minimum temperature at which the reaction velocity is such to produce uninterrupted combustion.

This temperature depends on the intrinsic reaction velocity of the coal, but also on size, moisture, room temperature, air velocity, and so on. Therefore, it is not at all surprising that the results of researchers vary even for the same type of coal. Note that the fire point of all types of coal, with the exception of anthracite, ranges from 215 to 300°C, whereas for anthracite it is about 480°C.

With respect to the heat value, from now on it will be indicated as H_n, if it is the net heat value, and as H_g, if it is the gross heat value. First of all, note its significance.

The net heat value represents the heat developed by complete combustion (without unburned carbon monoxide) of 1 kg or 1 Nm^3 of fuel, if the product of

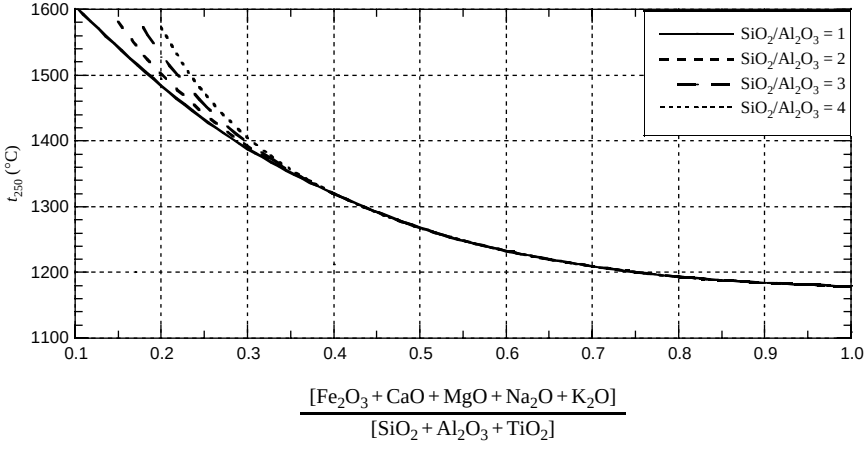


Fig. 6.1 Slag temperature for 250-Poise viscosity

combustion is cooled to the temperature of reference (generally 0 or 20°C), but imagining that the condensable product (H_2O) is not condensed. The gross heat value differs from the previous one because the heat developed by steam condensation in the flue gas is taken into account, as well.

With reference to a temperature of 0°C, with H_n and H_g in kJ/kg, we have

$$H_n = H_g - 2500M_s, \tag{6.6}$$

where M_s is the steam amount (in kg) in the flue gas for every kilogram of fuel.

In fact, if the steam is condensed, every kilogram yields 2500 kJ. Therefore, (6.6) can be written as follows:

$$H_n = H_g - 25(8.94H + H_2O), \tag{6.7}$$

where H is the hydrogen content and H_2O of water in the fuel expressed as percentages. In fact, for every kilogram of hydrogen in the fuel, there are 8.94 kg of steam in the flue gas.

Not knowing the composition of the coal, it is possible to compute the gross heat value in kJ/kg using the well-known Goutal equation:

$$H_g = 343C + \beta V, \tag{6.8}$$

where C is the percentage of fixed carbon, V the percentage of volatile matter, and β the coefficient obtained from Table 6.1 as a function of the percentage V' of volatile matter referred to pure coal.

It is given by

$$V' = \frac{100V}{C+V}. \tag{6.9}$$

Knowing the composition of coal, it is possible to use Dulong's equation with H_n in kJ/kg:

$$H_n = 339C + 105S + 1214\left(H - \frac{O}{8}\right) - 25H_2O, \tag{6.10}$$

where C, S, H, O, and H_2O are the percentages of carbon, sulfur, hydrogen, oxygen, and water, respectively. Note that Dulong's equation does not produce good results as far as young coal.

Table 6.1

V'	β	V'	β	V'	β	V'	β	V'	β
4	628	10	544	16	481	22	447	28	419
5	607	11	532	17	474	23	442	29	415
6	595	12	520	18	468	24	437	30	411
7	582	13	510	19	462	25	432	31	407
8	569	14	500	20	457	26	427	32	404
9	557	15	490	21	452	27	423	33	402

The following equation is of totally different nature because it is independent from the reaction heat of the individual components of coal:

$$H_{\mathrm{n}} = 4616C - 25.1C^2 - 176.8. \tag{6.11}$$

Equation (6.11) that includes only the carbon content has statistical character. Using (6.11) for 95% of coal types available on the market will lead to a mistake with respect to the exact value of H_{n}, equal at the most to $\pm 370\,\mathrm{kJ/kg}$, that is, equal to $\pm 1\%$.

Another equation of statistical character, where the content V' of volatile matter is referred to pure coal, that is, without ashes and moisture, is as follows:

$$H_{\mathrm{n}} = 34,068 + 154V' - 4.48V'^2. \tag{6.12}$$

As far as the size of the coal, we speak of through-and-through coal if we consider coal coming from the mine. If the average diameter of the pieces is within 30–80 mm, we speak of cob coal. If it ranges from 15 to 30 mm, we speak of nut coal. If the average diameter ranges from 0 to 8 mm instead, we speak of small coal. Coal dust obtained by pulverization has an average diameter of the pieces between 0 and 3 mm.

As far as density, one must distinguish between actual density and apparent density. The latter is given by the ratio between mass and volume; thus, it factors in the volume of the pores. The apparent density of coal with the exception of anthracite varies between 1250 and $1350\,\mathrm{kg/m^3}$, whereas it ranges from 1350 to $1500\,\mathrm{kg/m^3}$ for anthracite.

The porosity, that is, the volume of the pores as a percentage is given by:

$$P = 100\left(1 - \frac{apparent\ density}{actual\ density}\right). \tag{6.13}$$

The porosity of coal is usually below 2%, whereas lignite can exceed even 30%. The porosity of coke can amount to 50%.

As far as the other most important physical characteristics of coal, we can adopt the following values. The mean specific heat from 20 to 100°C lies within 1090 and 1300 J/kgK. Thermal conductivity at 30°C is within 0.19 and 0.23 W/mK. The value of conductivity at a different temperature can be obtained using the following equation:

$$k = k_{30}[1 + 0.002(t - 30)]. \tag{6.14}$$

6.2 Liquid Fuels

Liquid fuels are coal tar oil, distillate from oil shale and fuel oil produced from petroleum, by far the most important of them. We will discuss it in more detail later on, considering its importance for combustion in steam generators. As far as

the other two liquid fuels, we will simply highlight a few of the most significant characteristics.

Coal tar oil is the product of dry distillation of coal performed in coke plants. The by-products of this distillation are a series of substances that interest the coloring, explosives, pharmaceutical industries, as well as some oils. These oils are called coal tar oils and can be used as fuel to feed the plant itself or sold to third parties.

Coal tar oil has a relative density equal to 1–1.1, a ratio C/H (the ratio between carbon and hydrogen content in the oil) equal to 11–15, and a net heat value ranging from 32,200 to 37,700 kJ/kg.

Distillates from oil shale have a relative density equal to about 0.95, a ratio C/H ranging from 7 to 8.5, and a net heat value equal to 38,500–39,700 kJ/kg.

Among the main characteristics of fuel oil, there is its chemical composition, that is, carbon and hydrogen (the C/H ratio), sulfur, water, sediments, and ashes. Sometimes tests will also consider asphaltene.

The heat value and the different physical characteristics such as density, viscosity, pour point, specific heat, and thermal conductivity depend on the chemical composition. Finally, even the pattern of the distillation curve, the flash point, and the Conradson number depend on it. The C/H ratio of fuel oils used for industrial generators varies from 6.8 to 8.0, starting with less viscose up to more viscose oils. As we shall see, from the value of the C/H ratio one obtains the hydrogen content, taking into account the content of sulfur, water, and sediments that represent the other components of fuel oil using the following equation:

$$H = \frac{100 - (S + H_2O)}{\frac{C}{H} + 1}, \tag{6.15}$$

C, H, and S represent the percentages of carbon, hydrogen, and sulfur, and H_2O the percentage of water and sediments. After determination of the hydrogen content, it is possible to compute the carbon content using the C/H ratio.

The sulfur content varies between 2 and 5%. The presence of sulfur first reduces the heat value. In fact, while the reaction heat of hydrogen is equal to 119,620 kJ/kg and that of carbon is 33,830 kJ/kg, the reaction heat of sulfur is equal to 9253 kJ/kg only. Therefore, the presence of sulfur implies a reduction in heat value, estimated to be about 293 kJ/kg for every percentage point of sulfur, according to the typical values of the C/H ratio.

Note what we said earlier about coal in terms of higher dew point of the flue gas, buildup of SO_3, the ensuing fouling of the cold walls and corrosion caused by sulfuric acid. Fuel oil implies an even bigger danger of corrosion because of its greater content of sulfur. The dew point is even higher and the areas of the generator at risk from corrosion are consequently more extended. Specifically, if we examine the main characteristics of the phenomenon (more details will be available in specialized literature that focuses on it in-depth), note that the dew point of flue gas for fuel oil with no sulfur content would be around 40–50°C. As a result of the sulfur the dew point goes up following the pattern of the curve shown in Fig. 6.2. The upper line represents the pattern the dew point would have if SO_2 transformed itself completely into SO_3.

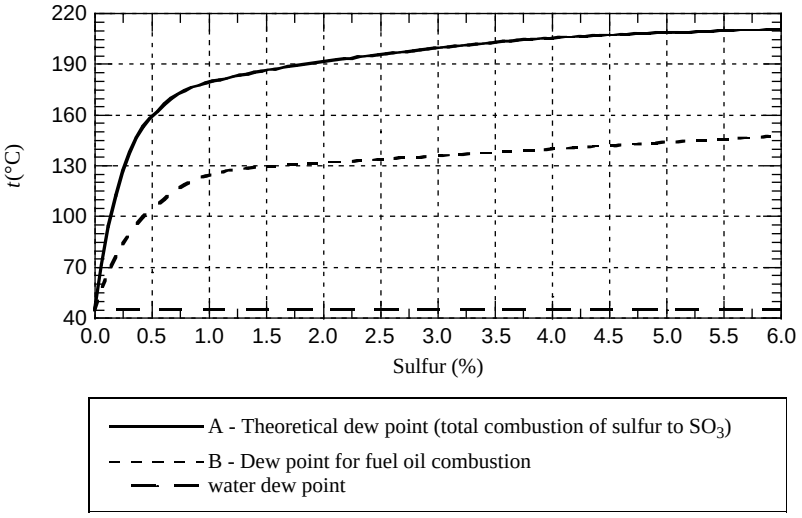


Fig. 6.2 Dew point of the flue gas

Normally, only 2–5% of the sulfur in the fuel oil causes the buildup of SO_3, otherwise sulfur combustion leads to the buildup of SO_2. In fact, the reaction

$$2SO_2 + O_2 \leftrightarrow 2SO_3 \tag{6.16}$$

is reversible and exothermic; this means that it proceeds from right to left as the temperature increases, and not vice versa. A high content of SO_3 can produce itself only at low combustion temperatures (theoretically all SO_2 oxidates into SO_3 at 400°C), therefore generally only during starting.

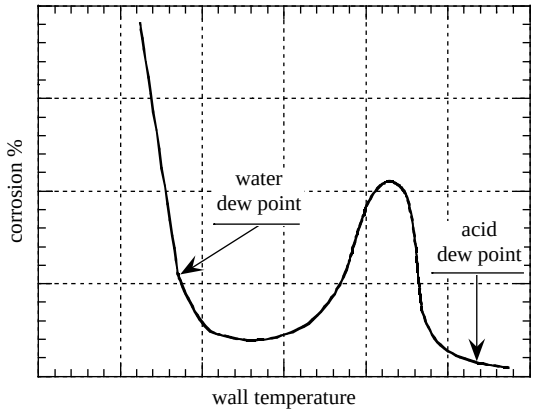
Of course, even the excess air required for combustion without unburned carbon monoxide has its impact because the more excess air, the stronger the tendency to buildup SO_3, followed by a higher dew point. The efforts of technicians are therefore focused on burners that allow full combustion with a minimum amount of excess air.

Finally, given the temperatures at play and the duration of the presence of gas in the generator [reaction of (6.16) is rather slow], the relatively high percentages of SO_3 found in the gas are not justified, unless we aim at a catalytic effect which seems to be due to ferric oxide on the tubes.

Maximum corrosion does actually not occur at the dew point, called in fact acidic dew point because of the ensuing buildup of H_2SO_4. The pattern of corrosion is qualitatively shown by the curve in Fig. 6.3. Greatest corrosion occurs at a temperature 20–40°C below the acidic dew point.

Based on this and taking into account that the temperature of the gas in direct contact with the wall (boundary layer) can be assumed to be equal to the average between the gaseous mass and the wall itself, the curves in Fig. 6.4 indicate the minimum safety values with respect to the gas temperature, and the temperature of the metallic walls in contact with them.

Fig. 6.3



In contrast to coal, the content of ashes in the fuel oil is quite modest. It is practically zero in distillates, and equal to 0.03–0.05% or at the most 0.1% in distillation or cracking residues. Their small quantity notwithstanding, the ashes are quite important because they contain variable quantities of vanadium pentoxide (V_2O_5) that corrodes at high temperature levels.

Note that while the ashes of fuel oil obtained from Texas petroleum are basically vanadium free, the ashes of fuel oil from California petroleum contain about 5% of V_2O_5, and those from the Middle East and Venezuela contain about 20 and 60% of V_2O_5, respectively. From this point of view, Middle Eastern as well as Venezuelan petroleum is the worst.

Vanadium pentoxide has a low melting point $(685°C)$ combined with a low surface tension and a high vapor tension. This is the reason for the tendency to deposits

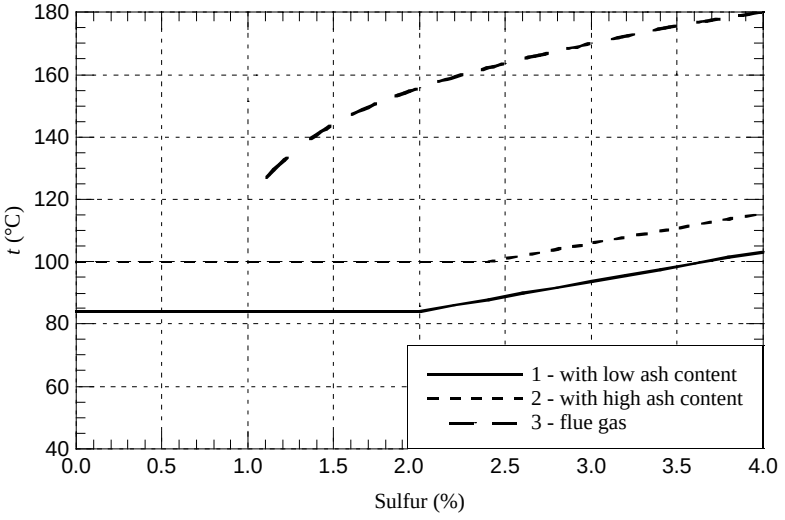


Fig. 6.4 Minimum temperatures of the flue gas (3) and of the wall (1 and 2) to avoid corrosion

on the surfaces of the superheaters, causing fouling of the walls, followed by a reduction in heat transfer, in temperature of the superheated steam, in generator efficiency and by an increasing pressure drop. Slightly reducing substances are already able to transform V_2O_5 into VO_2; this way the vanadium pentoxide acts as a catalyst for oxidation from SO_2 to SO_3. Moreover, even the presence of small quantities of V_2O_5 leads to complete oxidation from F_3O_4 to F_2O_3 with the ensuing consequences. Finally, vanadium pentoxide builds eutectic compounds with alkaline oxides and a melting point even lower than its own; with Na_2SO_4 the melting point of the eutectic compound is equal to 580°C.

Sulfur and vanadium are evidently responsible for fouling and corrosion at low and high temperature (higher than 600°C), respectively.

Special additives are available to contrast the danger of corrosion by vanadium and sulfur. Note that simply adding MgO, or rather dolomite, to the fuel already yields good results. In fact, there is buildup of a vanadium compound with a higher melting point, and also of calcium sulfate staying in the flue gas, while the calcium oxide becomes part of the ashes.

Test certificates of fuel oils usually also include the content of water and sediments through one single value that is comprehensive of both without any differentiation. The presence of water in fuel oils comes from transportation and stocking and does generally not exceed 0.1%. The presence of water up to a maximum of 0.5% does not cause any inconvenience. Greater quantities may interfere with combustion if the fuel is heated at a temperature higher than 100°C. Sediments are the non-soluble substances in benzol and are represented by coke, unstable hydrocarbon, salts. Sediments can clog both filters and nozzles. Generally, the amount of water and sediments does not exceed 0.1%.

Test certificates sometimes include the content of asphaltene. This term refers to substances that are non-soluble in heptane, yet soluble in benzol; these are brown or black substances with a high molecular weight and a high C/H ratio. The amount of asphaltene is zero in distillates and may go up to 7% for fuel oils with high viscosity. The amount of asphaltene is of interest only in very small burners, given the colloidal properties of these substances that may clog the nozzles.

The heat value of fuel oil varies in a limited way from a less viscose to a more viscose type. Considering the oils used in industrial generators, the net heat value varies between 38,900 and 41,800 kJ/kg, and more frequently between 39,800 and 41,000 kJ/kg.

Even density does not vary in any relevant way from one fuel to another. In fact, relative density at 15°C varies from 0.90 to 0.98, and more frequently from 0.93 to 0.97. In some cases the density exceeds the density of the water.

As we know, if a fluid is placed between two surfaces, one of which is mobile at velocity V, force F required to determine the movement to the mobile surface is equal to

$$F = \mu S \frac{V}{b}, \tag{6.17}$$

where S is the surface of the mobile piece, b the distance between the two pieces, and μ a coefficient, the value of which depends on the characteristics of the fluid in-between and that is called dynamic viscosity.

Therefore, dynamic viscosity has the following dimensions:

$$|\mu| = \frac{M}{L\theta}, \tag{6.18}$$

where M is the mass, L the length, and θ the time.

In the SI system, dynamic viscosity is measured in kg/ms and in g/cms in the CGS system; the SI unit has no denomination, and the CGS unit is called poise. The most commonly used part of the poise is the 100th, that is, the centipoise indicated with cp. The quantity represented by the ratio between dynamic viscosity and density is called kinematic viscosity because the mass does not show as a dimension anymore. These are the dimensions of kinematic viscosity ν:

$$|\nu| = \frac{L^2}{\theta}. \tag{6.19}$$

Therefore, in the SI system, kinematic viscosity is measured in m^2/s, and this unit does not have a name, whereas in the CGS system is measured in cm^2/s and the unit is called stokes. The most commonly used part of stokes is the 100th part, that is, the centistokes indicated with cS.

The scientific literature usually expresses the kinematic viscosity (generally the one used to characterize fuel oils or lubricants) in cS or in the corresponding SI unit. Technical literature uses the same units or the conventional units that will be discussed shortly. The latter are generally the only ones used in test reports and to classify the different fuel oils from a technical as well as commercial point of view.

Devices called viscosimeters have been set up in different countries to measure the viscosity of fuel oils and lubricants. They measure the time a certain amount of fluid needs to flow under its own weight. This is a conventional measure that depends on the characteristics of the viscosimeter providing a measuring unit tied to the viscosimeter itself. In the United States viscosity is measured in SUS (Saybolt Universal Second) or in SSF (Saybolt Furol) when the viscosity is high. Europe refers to the measurements of the Engler viscosimeter tuned up in Germany. This is why we speak of viscosity expressed in Engler degrees (°E). Of course, there are conversion tables to go from one unit to the other, such as Table 6.2 or curves.

Note, though, that unfortunately the reference temperatures adopted in various countries differ from one another. In fact, SUS viscosity of fuel oils is generally referred to 100°F and eventually even 212°F, the Saybolt Furol viscosity to 122°F, and finally the viscosity in °E in to 50°C, and sometimes even to 100°C. As the conversion tables can be used to compare the viscosity of two fuel oils expressed in different units only if the reference temperature is the same, in general it is impossible to compare two oils (or two lubricants) when their viscosity is expressed in two different conventional units. This is possible only if the respective viscosity–temperature curves are known. The diagram in Fig. 6.5 showing a few characteristic curves may be of assistance in this context. Note that the diagram refers to fuel oils originating from Middle Eastern petroleum, so it is safe to use it for this kind of petroleum only.

Table 6.2 Kinematic viscosity in cS, m^2/s, °E, and SUS

cS or m^2/s $\times 10^{-6}$	°E	SUS	cS or m^2/s $\times 10^{-6}$	°E	SUS	cS or m^2/s $\times 10^{-6}$	°E	SUS	cS or m^2/s $\times 10^{-6}$	°E	SUS
(*) 2.0	1.12	32.6	10.8	1.91	61.6	20.0	2.90	97.5	35	4.70	163.2
(*) 2.5	1.17	34.4	11.0	1.93	62.3	20.5	2.95	99.6	36	4.85	167.7
(*) 3.0	1.22	36.0	11.4	1.97	63.7	21.0	3.00	101.7	37	4.95	172.2
(*) 3.5	1.26	37.6	11.8	2.00	65.2	21.5	3.05	103.9	38	5.10	176.7
(*) 4.0	1.30	39.1	12.2	2.04	66.6	22.0	3.10	106.0	39	5.20	181.2
(*) 4.5	1.35	40.7	12.6	2.08	68.1	22.5	3.15	108.2	40	5.35	185.7
(*) 5.0	1.40	42.3	13.0	2.12	69.6	23.0	3.20	110.3	42	5.60	194.7
(*) 5.5	1.44	43.9	13.5	2.17	71.5	23.5	3.30	112.4	44	5.85	203.8
(*) 6.0	1.48	45.5	14.0	2.22	73.4	24.0	3.35	114.6	46	6.10	213.0
(*) 6.5	1.52	47.1	14.5	2.27	75.3	24.5	3.40	116.8	48	6.40	222.2
(*) 7.0	1.56	48.7	15.0	2.32	77.2	25	3.45	118.9	50	6.65	231.4
(*) 7.5	1.60	50.3	15.5	2.38	79.2	26	3.60	123.3	52	6.90	240.6
(*) 8.0	1.65	52.0	16.0	2.43	81.1	27	3.70	127.7	54	7.10	249.9
(*) 8.5	1.70	53.7	16.5	2.50	83.1	28	3.85	132.1	56	7.40	259.0
(*) 9.0	1.75	55.4	17.0	2.55	85.1	29	3.95	136.5	58	7.65	268.2
(*) 9.5	1.79	57.1	17.5	2.60	87.1	30	4.10	140.9	60	7.90	277.4
10.0	1.83	58.8	18.0	2.65	89.2	31	4.20	145.3	62	8.17	286.6
10.2	1.85	59.5	18.5	2.70	91.2	32	4.35	149.7	64	8.44	295.8
10.4	1.87	60.2	19.0	2.75	93.3	33	4.45	154.2	67	8.84	309.6
10.6	1.89	60.9	19.5	2.80	95.4	34	4.60	158.7	70	9.24	323.4

(*) passage from conventional viscosities to the viscosity in cS not allowable.
For viscosity greater than 70 cS we refer to the following conversion factors:
cS = 7.58 °E = 0.216 SUS; °E = 0.132 cS = 0.0285 SUS; SUS = 4.62 cS = 35.11°E.

The viscosity of fuel oils used in industrial boilers generally varies from 15 to 50°E referred to 50°C.

The pour point indicates a temperature at which, under certain test conditions, the oil stops or starts flowing. In Anglo-Saxon countries this name indicates the

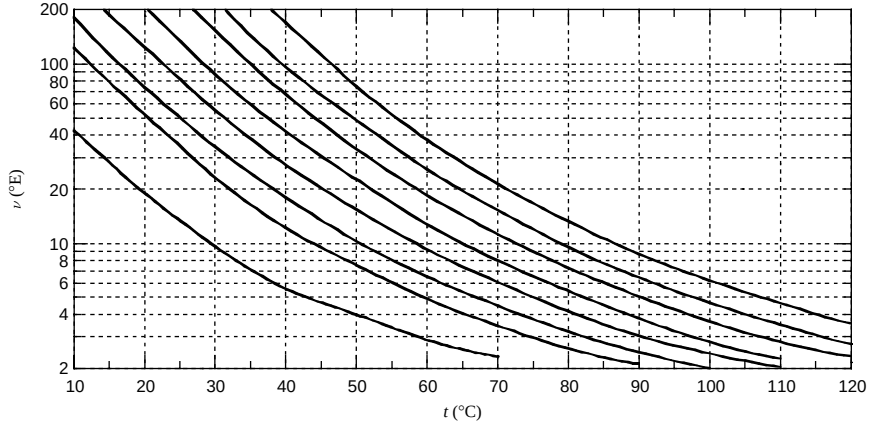


Fig. 6.5 Kinematic viscosity (°E) of the Middle Eastern fuel oils

temperature at which, under certain test conditions, the fuel oil starts flowing under its own weight. In Germany it indicates the temperature at which the fluid stops to flow (Stockpunkt). Depending on the viscosity and the origin of the petroleum, the pour point measured based on the German test method ranges from -5 to 20°C. The importance of the pour point does not exceed that of a purely reference data about the ability to pump the oil. The actual flowing conditions of the oil in the piping depending on pressure, diameter of the tubes, and so on are quite different from the test conditions leading to the identification of the pour point.

In the case of fuel oil, a mix of different hydrocarbons, one cannot speak of boiling temperature but of distillation curve instead. There is no testing method to create a completely satisfactory distillation curve. Note that this curve practically refers to distilled oils meant for evaporation burners only. It bears no interest for industrial burners.

The temperature at which the oil develops flammable vapors is called flash point. Of course, it depends on the test conditions. The Pensky Martens consisting of a closed vessel where the oil is heated from the outside can be used. The flash point is the temperature at which the vapors developed by the oil are so strong that they start burning if they get near a flame. This is the so-called P.M. flash point.

If one uses Marcusson's open vessel instead, part of the vapors drift and ignition becomes more difficult. In fact, the Marcusson flash point is about 30°C higher than the P.M. flash point. The flash point is of interest because of the risk of fire during stocking. For this reason many countries set a minimum P.M. flash point of 65°C. This regulation can be followed without any problem with industrial fuel oils (only those with low viscosity levels may have the flash point under 65°C).

When the fuel oil is heated, the heaviest fractions will progressively evaporate, and this makes it possible to build the distillation curve we mentioned earlier. One part, though, does not distill but cracks instead, and at the end of the heating test, there is a residue of coke left that represents a percentage of the oil itself. The percentage of coke in question is indicated as Conradson number. When part of the unburned oil hits the wall during combustion, a similar process will take place combined with the buildup of carbon-like deposits on the wall itself. Therefore, Conradson's number indicates the smaller or greater tendency of carbon-like deposits buildup on the walls of the furnace or on the groove of the burners. Note that this is only reference data, due to the considerable existing differences between running conditions and the lab test. Conradson's number can reach a value of up to 16% for fuel oils with high viscosity levels.

The specific isobaric heat of the fuel oil can be computed from Fig. 6.6 or using the following equation:

$$(c_{pm})_0^t = 3856 - 2345\rho_0 + 2.3t; \tag{6.20}$$

where $(c_{pm})_0^t$ is the mean specific heat between 0°C and temperature t in J/kgK, and ρ_0 is the relative density.

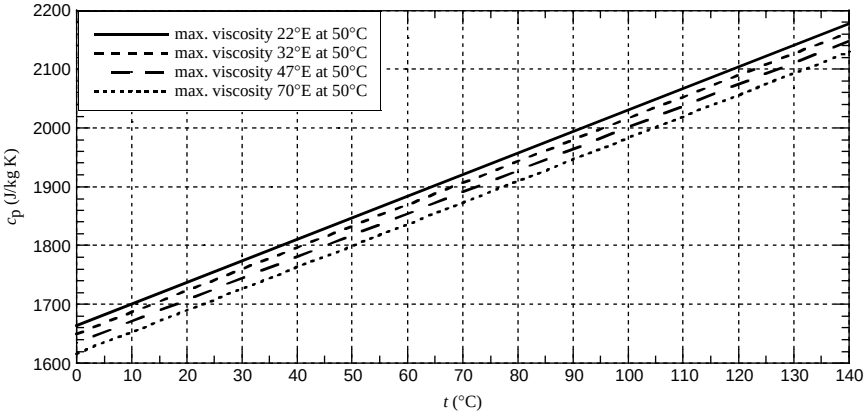


Fig. 6.6 Specific isobaric heat of fuel oils

As far as thermal conductivity, we can refer to the following equation where k is expressed in W/mK and t is the temperature in °C:

$$k = \frac{0.1172}{\rho_0}\left(1 - 0.54\frac{t}{1000}\right). \tag{6.21}$$

6.3 Gaseous Fuels

Water gas, town gas, and so on belong to the category of gaseous fuel in the widest sense, but in this case our interest is exclusively in gas used as gaseous fuel in steam generators.

Refinery gas, blast furnace gas, coke oven gas, and natural gas predominantly consisting of methane as the most used one belong to the category of gaseous fuels. Table 6.3 shows the composition of the first three gas types, based on mean percentage values of the different components and the composition of natural gas, available around the world including the net heat value. Methane is clearly the main component of natural gas, but the other components can considerably impact the heat value for natural gas depending on its origin.

Not knowing the heat value of a gas directly, its value can be computed based on its composition using the following equations:

$$H_g = 126.44CO + 127.44H_2 + 398.2CH_4 + 837.4C_aH_b, \tag{6.22}$$

$$H_n = 126.44CO + 107.35H_2 + 358CH_4 + 595.5C_aH_b. \tag{6.23}$$

H_g and H_n referred to dry gas are expressed in $\mathrm{kJ/Nm^3}$, and CO, H_2, CH_4, C_aH_b are the volumetric percentages of carbon oxide, hydrogen, methane, and generic hydrocarbons other than methane in the gas.

Table 6.3 Composition and net heat value of some gaseous fuels

	Volumetric composition (%)							H_n (kJ/Nm^3)
	CH_4	Super Hydrocarbon	N_2	CO_2	H_2	CO	H_2O	
Refinery gas	40	35			25			≈ 44000
Blast-furnace gas			54.5	10.0	3	27.5	5	≈ 4200
Coke-oven gas		34.3	1.5	1.2	55	7.0	1	≈ 16800
Natural gas								
V.Kincella (Canada)	91.9	3.2	4.9					≈ 35300
Panhandle USA)	81.8	11.2	6.9	0.1				≈ 38600
Monroe (USA)	91.3	3.0	5.4	0.3				≈ 35100
Dasawa (Russia)	97.8	0.8	1.3	0.1				≈ 35600
Lockton (U.K.)	93.7	3.5	2.6	0.2				≈ 36100
Groningen (Holland)	81.2	3.4	14.4	0.9				≈ 31400
Hassi R'Mel (Algeria)	79.6	15.1	5.1	0.2				≈ 40300

A very important characteristic of gaseous fuels is the ignition speed. It depends on the percentage of gas in the air–gas mix. The highest ignition speed does usually not correspond to the stoichiometric mix of air and gas. Figure 6.7 illustrates the values of the ignition speed with the most significant gas types, as well as the pattern of the speed with variations of the air–gas mix composition. Besides the highest value of the ignition speed, the lower and higher ignition limits are also significant, that is, the values of the gas/mix ratio below or above which combustion is impossible.

The limits of the most significant gas types are shown in Table 6.4 with reference to oxygen or air temperature of 20°C. These limits are influenced by pressure, as shown in Table 6.5 in relation to natural gas (according to Jones). The ignition speed is influenced by the Reynolds number if the air–gas mix flows in a tube and by the air temperature, too. In fact, with air at 200°C, there is an increase in ignition speed of roughly 29% and of 48% if the air temperature is equal to 400°C.

Wobbe's number modified by Bunte can be used to identify the combustion characteristics of the different gas types. It is given by:

$$K_{\text{Wobbe}} = H_{\text{g}} \sqrt{\frac{p}{\rho_0}}, \tag{6.24}$$

where H_{g} is the gross heat value, p the pressure before the burner, and ρ_0 the density related to air.

Two gas types correspond to the same number of Wobbe if they burn in the same burner (regardless of pressure) and introduce the same amount of heat into the furnace.

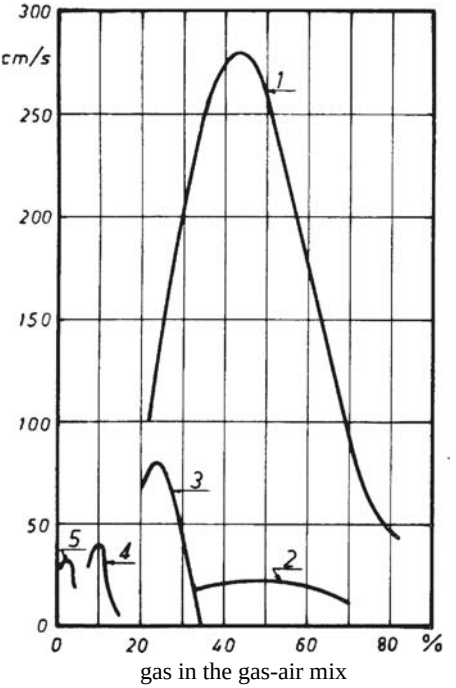


Fig. 6.7 Ignition speed: 1 – Hydrogen; 2 – Carbon monoxide; 3 – Town gas; 4 – Methane; 5 – Hexane

Table 6.4 Ignition limits (gas volumetric percentage of the air–gas mix or oxygen–air mix)

	Ignition limits			
	In air (20°C)		In oxygen (20°C)	
	Inferior	Superior	Inferior	Superior
Hydrogen	4	74	4	94
Carbon monoxide	12.5	74	15.5	94
Methane	5	15	5.1	61
Propane	2.3	9.5	–	–
Butane	1.9	8.4	–	–
Natural gas	4.5–4.8	14.2–13.5		

Table 6.5 Impact of the pressure on natural gas ignition limits (84.7% CH_4, 14.7% C_2H_6, 0.6% N_2)

Pressure (bar)	Ignition limits	
	Inferior	Superior
0	4.50	14.2
35.15	4.45	44.2
70.31	4.00	52.9
140.61	3.60	59.0
210.92	3.15	60.0

In fact, pressure p is proportional to the density of the gas and to the square of the velocity V at the exit of the burner, given that

$$p \equiv \rho_0 \frac{V^2}{2}. \tag{6.25}$$

As far as the volumetric flow rate Q that is proportional to the velocity, we can write that

$$Q \equiv V \equiv \sqrt{\frac{p}{\rho_0}}. \tag{6.26}$$

Therefore, the introduced heat q that is proportional to the multiplication product of the flow rate by the heat value is equal to

$$q \equiv QH_g \equiv H_g \sqrt{\frac{p}{\rho_0}}. \tag{6.27}$$

Thus, the introduced heat is proportional to the Wobbe number.

This page intentionally left blank

Chapter 7
Combustion

7.1 Burners

Among the most frequent industrial applications, there are gas burners (predominantly natural gas burners), fuel oil burners, and pulverized coal or pulverized lignite burners. Requirements common to all burners are as follows. The fuel or air flow rate must correspond to the heat requests within a certain tuning range. The combustion process must be such to ensure the smallest build-up of unburned carbon monoxide with minimum excess air. The characteristics of the burner must be such to allow minimal dimensions of the furnace combined with a most simple structure in order to reduce its fabrication costs. The burner must be designed to use materials fulfilling runtime parameters and requiring a minimum amount of maintenance.

Finally, it must provide the highest guarantees of correct functioning and safety under all running conditions of the generator, including starting, stops, load variations, as well as any change of fuel in the case of burners that burn different kinds of fuel.

Gaseous fuels are the easiest to burn and tune. There are no atomizing (fuel oil) or crushing and pulverization (coal) problems. Natural gas does not cause fouling and clogging or even corrosion because of the absence of sulfur. The industrial burners generally have a diffusion flame. The air and gas are not pre-mixed as they enter the furnace, and the mixing occurs through turbulent diffusion. The simplest and frequently adopted setup for small gas flow rate consists of a torus where the gas is let in equipped with a series of holes through which the gas flows into the furnace (see Fig. 7.1).

In the case of burners with higher flow rate, spuds equipped with a stainless steel head and many holes through which the gas exits are generally used. The spuds are arranged in a circle around the central flame stabilizer disc (impeller) with a cone-shape and tangential cracks (see Fig. 7.2). The spuds may also be disconnected separately from the gas-conveying pipes.

First of all, the combustion of fuel oil requires an increase of its temperature to reduce the viscosity during pumping and to facilitate atomizing. In fact, the oil must be atomized before it can burn. It is necessary to obtain a cloud of tiny drops.

D. Annaratone, *Steam Generators*, DOI: 10.1007/978-3-540-77715-1_7,

© Springer-Verlag Berlin Heidelberg 2008

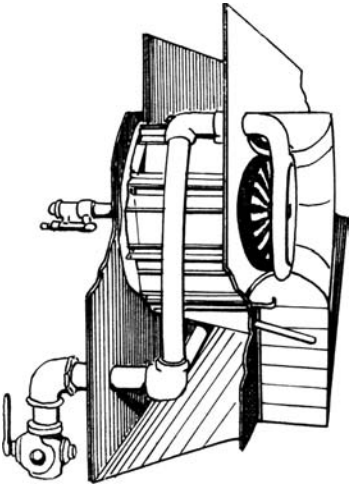


Fig. 7.1 Torus-type natural gas burner

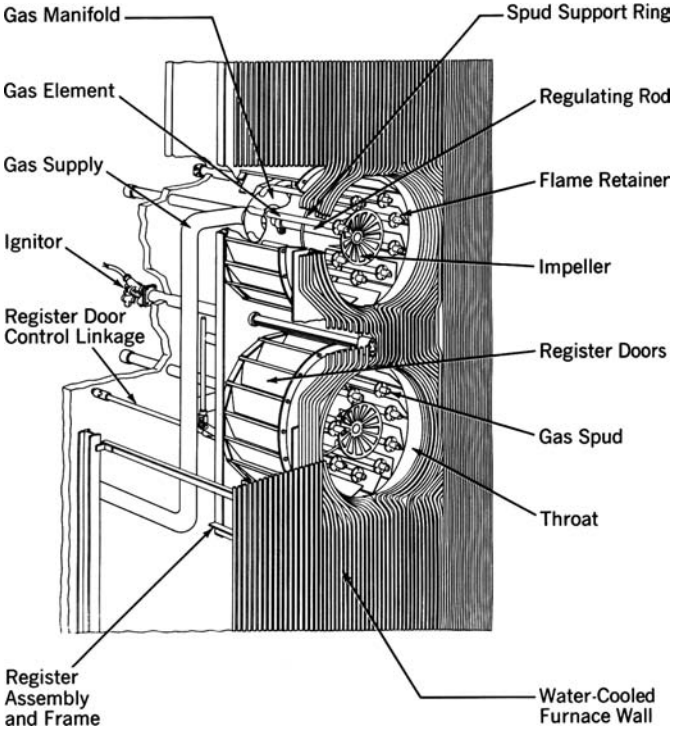


Fig. 7.2 Natural gas burners with gas spuds (Courtesy of Babcock & Wilcox)

Generally, the drops have a diameter ranging from 10 to 200 μ, even though it is possible to have drops with a larger diameter. The usual assumption for satisfactory atomizing is a diameter under 50 μ for 85% of drops.

The oil must be atomized for two reasons: to have a greater surface of liquid for evaporation during combustion and to avoid the build-up of free carbon mixed with partially cracked residues and molecules with heavy molecular weight taking place during thermal cracking. The contact with cold walls causes these products to build-up carbon deposits. Of course, rational combustion requires perfect mixing of fuel and combustion air. The air must have vortex-like motion obtained through the immission into the burner through an air register shaped like a drum with turnable blades.

The most common burners are the static ones. Completely devoid of moving mechanical parts, they are used in big generators, as well as small and medium power units. The distinction is between mechanical thrust burners with direct flow, or return flow and atomizing burners with auxiliary fluid (air or steam). In the former case with direct flow, the fuel oil is entirely pumped into the furnace. The tuning of the flow rate is done at delivery of the pump through a manually operated valve or through one included in the automatic tuning plant. The oil exits from a small hole with cone-shaped walls through specific grooves that enforce a strong rotational motion.

The volumetric flow rate Q depends on the pressure as follows:

$$p \equiv Q^n. \tag{7.1}$$

The exponent n is slightly greater than 2 for diameters of the nozzle smaller than 2 mm and slightly smaller than 2 for diameters greater than 3 mm.

By first approximation, it is safe to assume that the flow rate is proportional to the square root of the pressure. In burners of this type, the maximum pressure of the pump does not exceed 30–32 bar. On the other hand, an acceptable level of atomization requires the pressure to be at least 5–6 bar, and one can see that the tuning range of the flow rate does not exceed the value 1:2.5. In other words, without substitution of the sprayer plate with one that has a hole with smaller diameter, it is impossible to tune below 40% of the maximum load.

These simple burners are not ideally suited to work with sensible variation in load. The best atomization is obtained through high values of angular speed of the spout. Mechanical thrust burners under direct pressure show a diminished speed through the exit hole and the grooves that determine the rotational motion to the spout as the flow rate decreases. Thus, it is understandable why these burners have a relatively high limitation of the inferior value of the flow rate in order to still obtain an acceptable atomization.

This inconvenience has been resolved through mechanical atomization burners with return-flow (see Fig. 7.3). In this case the flow rate of the pump is basically constant; the oil is directed through the usual grooves into a swirl chamber where a fraction exits in the furnace and a part flows back to the suction of the pump (see Fig. 7.4). The tuning is done at return-flow through a valve that controls the flow rate.

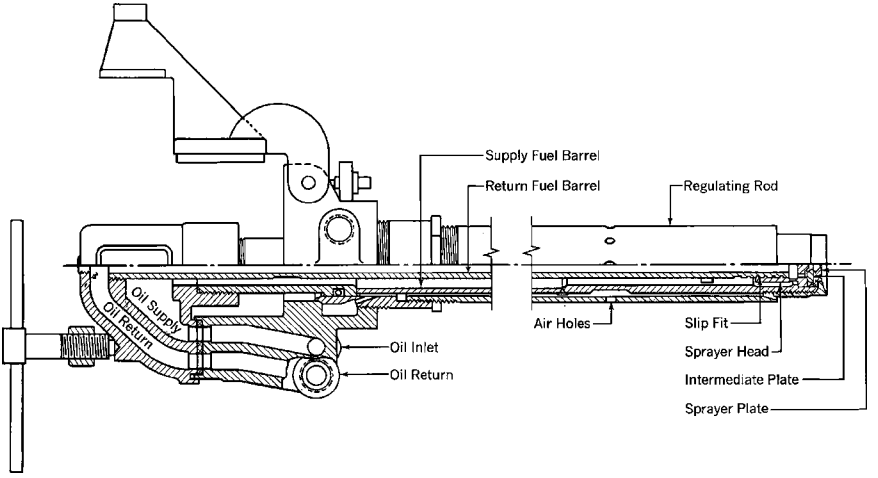


Fig. 7.3 Mechanical return-flow oil atomizer assembly (Courtesy of Babcock & Wilcox)

This is fundamental as it makes a constant or even increasing amount of oil circulate in the grooves that generate the swirling motion of the spout when the atomized oil is reduced. Figure 7.5 describes the phenomenon. Note that the return pressure is almost proportional to the atomized oil, and that facilitates tuning. High delivery pressure up to 70 bar is adopted. Under such pressure, heating the air and expecting its considerable swirling motion, followed by pressure drop through the burner up to 2000–3000 Pa, it is possible to obtain a tuning range of 1:10.

Smaller tuning ranges are also easily obtainable with this kind of burner. In any case, they will be wider than those obtained with burners under direct pressure. Return-flow burners are built to sustain fuel oil flow rates of 1.4 kg/s. In the case of

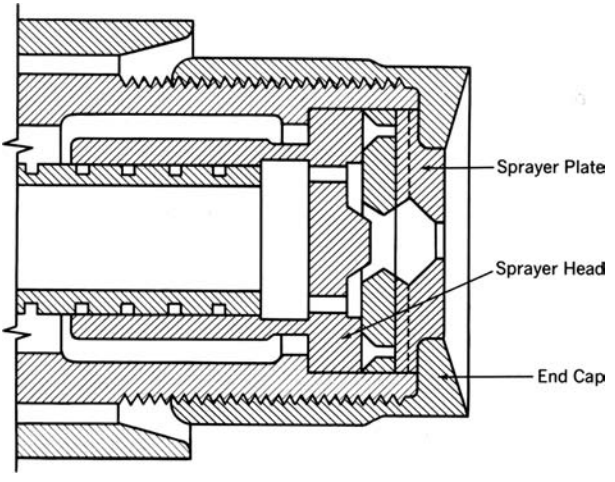


Fig. 7.4 Mechanical return-flow oil atomizer detail (Courtesy of Babcock & Wilcox)

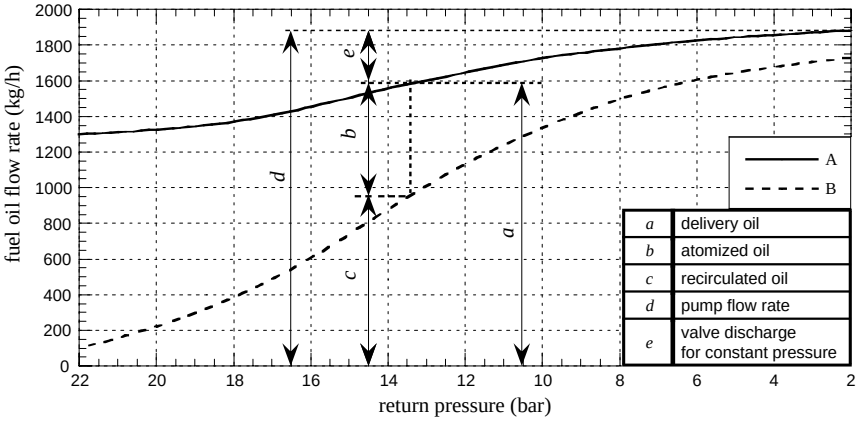


Fig. 7.5 Working characteristics of the burner with return flow

mechanical thrust burners, the viscosity of the oil must be reduced to 3–4° E through heating. In burners with steam atomizing, the level of energy required for atomizing is mostly delivered by the steam rapidly expanding as it exits the burner. In these burners (see Fig. 7.6), the steam is injected into the nozzle getting emulsified with the oil. The oil pressure is clearly lower than the one required by previous burners (it will usually not exceed 7 bar), and steam pressure exceeds oil pressure by 1.5–3 bar.

The drawback of this type of burner is steam consumption that should not exceed 0.1 kg for every kg of fuel oil at maximum load if it is well designed. Figure 7.7 indicates such consumption of both steam and air.

Note that given the predominant impact of the steam on atomization and the resulting heating of the fuel oil, the latter may be delivered to the burner even at a much higher level of viscosity of 7–10°E, compared with the one required by burners for mechanical atomization. Burners of this kind are built for an oil flow rate up to 1.4 kg/s.

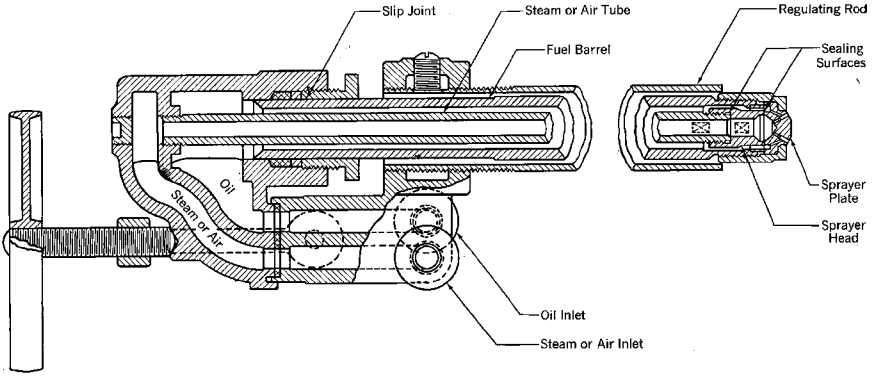


Fig. 7.6 Steam (or air) oil atomizer assembly (Courtesy of Babcock & Wilcox)

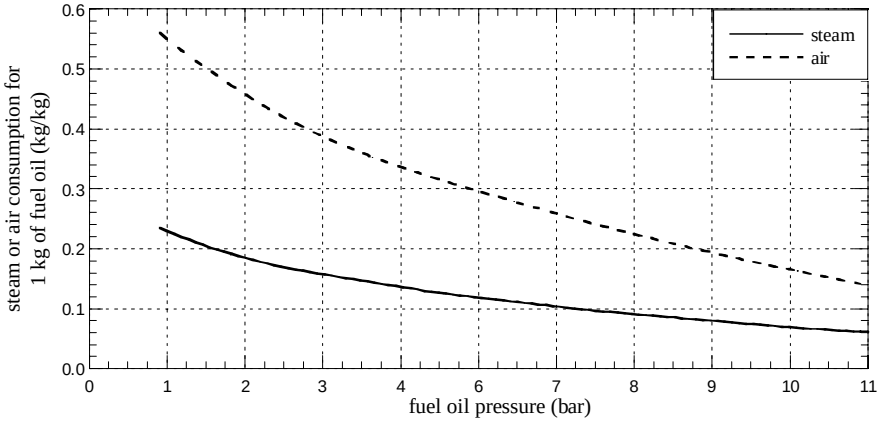


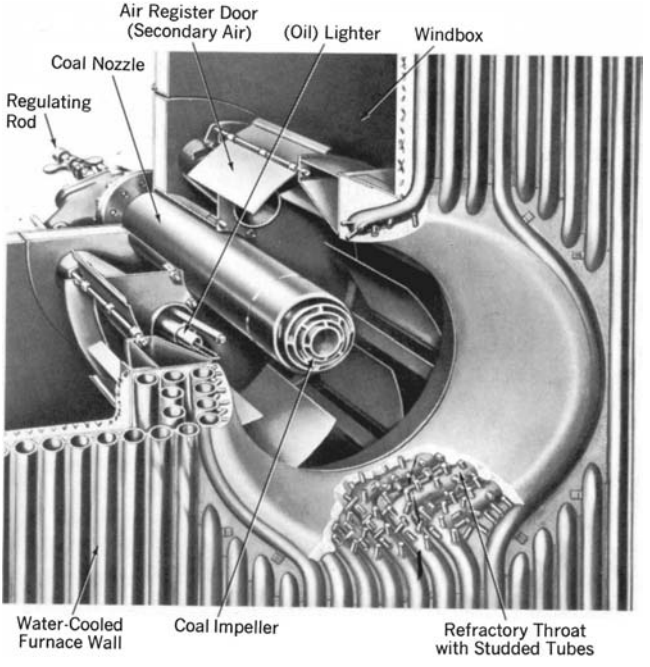
Fig. 7.7 Steam or air consumption in fuel oil burners

Finally, in the case of mechanical thrust burners with direct pressure and a modest oil flow rate, sometimes steam at low pressure is injected beyond the nozzle of the burner, in order to improve atomization under low load and to expand the tuning range.

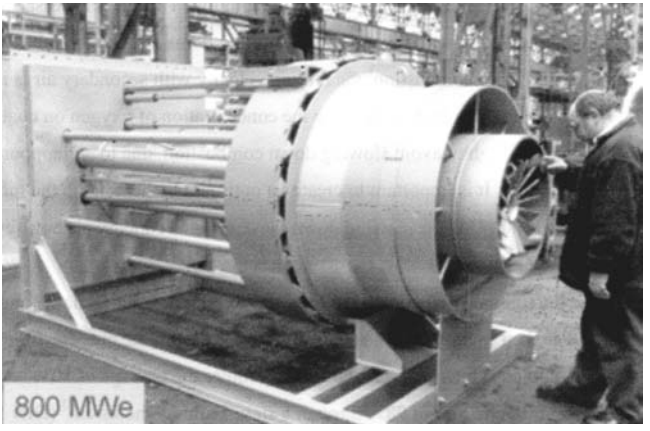
Besides steam, even air may be used as auxiliary fluid. In fact, burners of modest flow rate of this type are built. Generally, they are under high air pressure (0.5–1.5 bar), and the oil pressure has similar values. They are well suited to vary the shape of the flame by adapting it to the shape of the furnace. They are characterized, though, by more noise compared with other atomization systems. As far as installation and running costs (especially the latter), the presence of a compressor is a considerable factor. The consumption of air amounts to about 25% of the atomized oil.

The combustion of pulverized coal takes place in two intimately connected phases: ignition and combustion. Good combustion with coal requires a stable flame at a minimum ignition distance and rapid combustion in order to reduce the length of the flame. To obtain the first result, it is essential to maximize the recirculation of partially burnt gas inside the flame. The influence of primary air is negative because the temperature of the mix goes down and does not support the flash point. Therefore, it must be reduced as much as possible. The influence of very hot secondary air is also negative because it slows down the ignition. Thus, it is necessary to slow down the mixing with secondary air until the flame is stable. As far as rapid combustion, the mixing velocity with secondary air is important because it should be high to increase the concentration of oxygen on coal particles, yet not too high to avoid slowing down combustion, because of an inopportune drop in temperature. It is important to create an optimum by heating up the mix to 1500–1600°C while slowing down the entry of secondary air by a few tenths of second.

The granulometry of pulverized coal, the content in volatile matter and ashes, as well as their melting point, have a great influence on the process. In terms of granulometry, international regulations require the passage of 80% in a sieve with 6400 holes/cm^2 and of 98% through a sieve with 400 holes/cm^2 (DIN 1171). Modern pulverized coal burners reduce solid unburned matter to 2% and even 1% of burnt



(a)



(b)

Fig. 7.8 (**a**) Circular register burner for pulverized-coal firing (Courtesy of Babcock & Wilcox), (**b**) Burner for pulverized coal (Courtesy of Alstom)

coal with excess air that varies from 15 to 22%. Figure 7.8 shows two types of burner for pulverized coal.

Generally, it is possible to set a tuning range equal to 1:2.5, and within that range it is preferable to keep all burners running rather than turning some of them off. In fact, turning on a burner is more complicated than varying the amount of burnt fuel

in a running burner. Moreover, it is necessary to avoid any damage caused by flame radiation of burners that are not cooled by air. On the other hand, cooling a turned off burner through primary air is advisable in terms of its conservation, yet leads to excess air in the furnace followed by a reduction in generator efficiency.

As far as primary and secondary air, the former must be able to keep the pulverized coal in suspension in the air ducts. Therefore, its velocity is no less than 15 m/s with reference to minimum consumption of the burner. The speed of secondary air under full load ranges between 20 and 30 m/s.

Finally, pulverized coal can be burnt in the cyclone furnace as shown in Fig. 7.9. Pulverized coal mixed with primary air is introduced into a cylindrical chamber (the cyclone) where secondary air is introduced tangentially, as well. Tertiary air is introduced in the center causing counterflow phenomena, thus facilitating combustion. The cyclone can burn coal with a viscosity of the ashes not greater than 250 poise at 1400°C. The cyclone furnace has the following advantages: a smaller content of ashes in the flue gas, a reduction in fuel preparation costs given the less stringent pulverization requirements, and the reduction in furnace dimensions.

The volumetric thermal load of the cyclone is very high (up to 800 kW/m^3), as well as the gas temperature (greater than 1600°C). These temperatures are sufficient

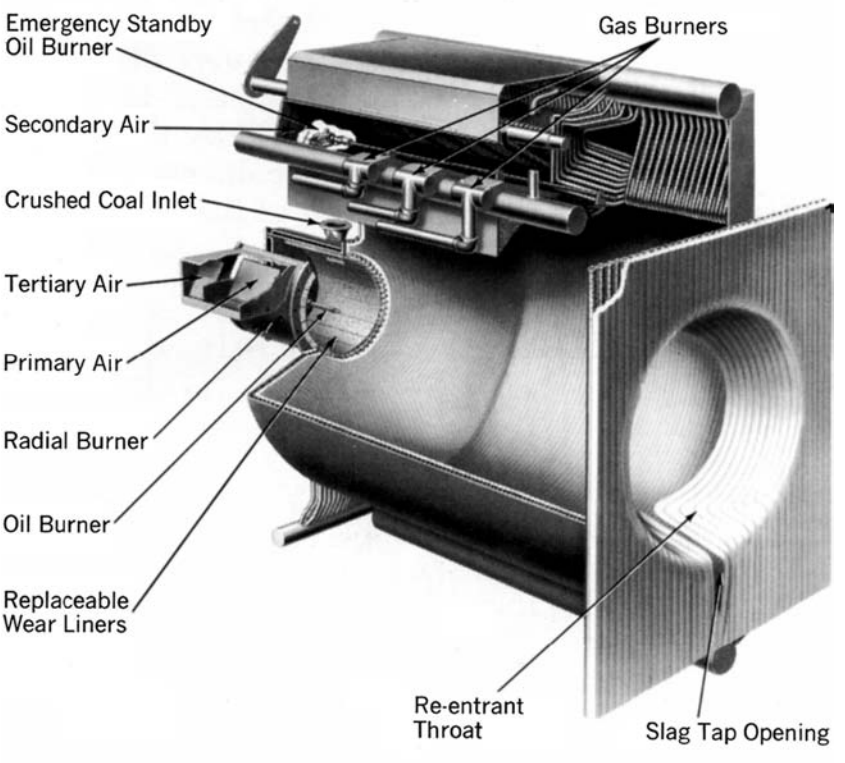


Fig. 7.9 Cyclone furnace (Courtesy of Babcock & Wilcox)

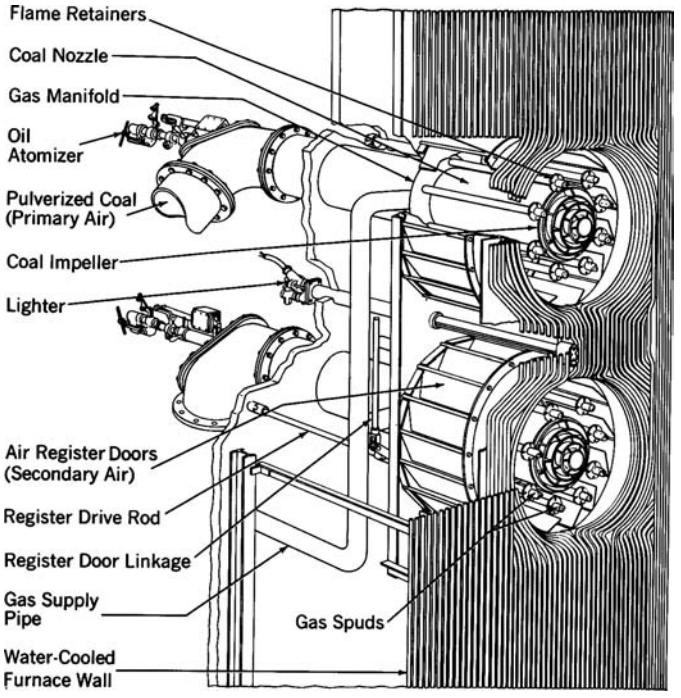


Fig. 7.10 Cell burner for pulverized coal, fuel oil, and natural gas (Courtesy of Babcock & Wilcox)

to melt the ashes that form a liquid layer on the walls of the cyclone. These special burners are built with a diameter up to 3 m. The corresponding heat introduced into the furnace reaches 100 MW.

In conclusion, note that mixed combustion is often part of the schedule. Therefore, burners are expected to alternatively burn different fuels. The setup of a burner with mixed combustion using either fuel oil or natural gas is easy. Both in the case of a torus or some spuds (with natural gas), it is always possible to design the spud of the fuel oil at the center of the burner. The installation of a burner with mixed combustion including oil, natural gas, and coal (see Fig. 7.10) is much more complex. In that case it is not advisable to run oil and pulverized coal combined for long periods of time, due to the buildup of coke on the element designed to introduce the pulverized coal into the furnace.

7.2 Flame Characteristics

Entire volumes have been written on the physical characteristics of the flame, and the present section will not be able to encompass all the complex aspects of this phenomenon. We shall only focus on a few fundamental characteristics of the flame, as

well as the different parameters influencing its nature, and refer the reader interested in a more detailed treaty to specialized literature.

From the point of view of mixing between fuel and combustion air, flames may be divided into diffusion flames and premixed flames. Premixed flames are those with components that were mixed in advance before entrance into the furnace, whereas the components of diffusion flames are mixed during combustion through diffusion. From the perspective of flow velocity of the reagents, there are laminar and turbulent flames. The components of the former are mixed and transported through molecular processes with parallel threads of the fluids and parabolic speed pattern. The latter are characterized by swirling motion with a shorter flame compared to the previous case and the Reynolds number greater than 2500–3000.

The flames of industrial burners used in steam generators are characterized by diffusion and turbulence. Moreover, they are subsonic and characterized by deflagration waves, that is, a flame front. These waves propagate at well-defined speed, typical of the fuel type and dependent on physical and environmental conditions where the flame is generated. They consist of a thin area where the chemical reaction and the release of heat take place. The reaction area divides the material that reacted from the one that did not. The speed of the front flame is in the order of a few meters per second.

The reaction area of a diffusion flame is generally more dilated than that of a premixed flame. It represents a transition area between pure fuel and pure combustion air. Combustion products are created in this area that tend to diffuse toward both the fuel and the combustion air, thus slowing down the reaction speed. Among the different physical processes occurring during combustion, the turbulence is by far the most important. It corresponds to a disorderly movement of fluids and the formation of vortexes interfering with each other. The impact of the turbulent flow is crucial for combustion because through the agitated fluids transporting portions of flame and rippling the surface, the area of the front flame is larger. The speed at which the heat is released also goes up considerably.

The turbulence of the flame can also be obtained through coaxial spouts of fuel and combustion air without swirling air, as long as the spout speed of the fuel is high. Figure 7.11 shows the geometry of a flame produced by gaseous fuel as its speed varies.

It shows that at low speed the flame is laminar, while its length increases with speed. Then there is a transition area, and finally the flame becomes turbulent. A further increase in speed causes the flame to extinguish. Stable diffusion flames may be either well anchored at the end of the burner or suspended at a certain height. Turbulent flames are always suspended. The study of turbulent flames within an enclosed volume (furnace) is quite difficult, because of the impact of the walls, and most of all because the air is not simply dragged by the fuel (free flame) but rather pushed into it.

In a furnace the spout of fuel is capable of dragging a certain air volume. If the air is less than the amount that the spout would drag in free atmosphere, even though it matches combustion requirements, a percentage of the flue gas is sucked back creating a counterflow called blow-by or recirculation (see Fig. 7.12).

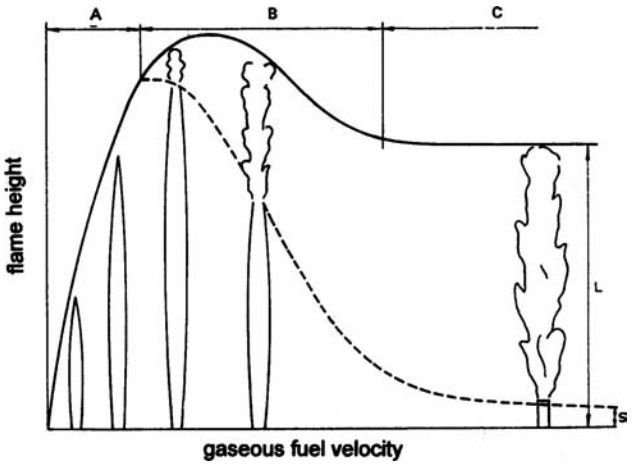


Fig. 7.11 Flame geometry for gaseous fuel (Salvi – La Combustione)

The recirculation of very hot gas favors the stabilization of flame for kinetic and thermal reasons. Both the speed of fuel and the speed of combustion air have a considerable influence on the mixing and the shape of the flame. Good mixing is particularly important in the case of solid and liquid fuels.

Figure 7.13 depicts different flame shapes that go hand in hand with speed variations of fuel oil and air, as well as the presence or not of a disk stabilizer. The comparison between case (a) and case (b) highlights the impact of the speed of the oil spout. At increasing speed the drops have smaller diameter, the flame front gets closer to the burner and has a more regular shape. The heat exchange is stronger, and the recycled flue gas rapidly brings the fuel to ignition temperature. By keeping the

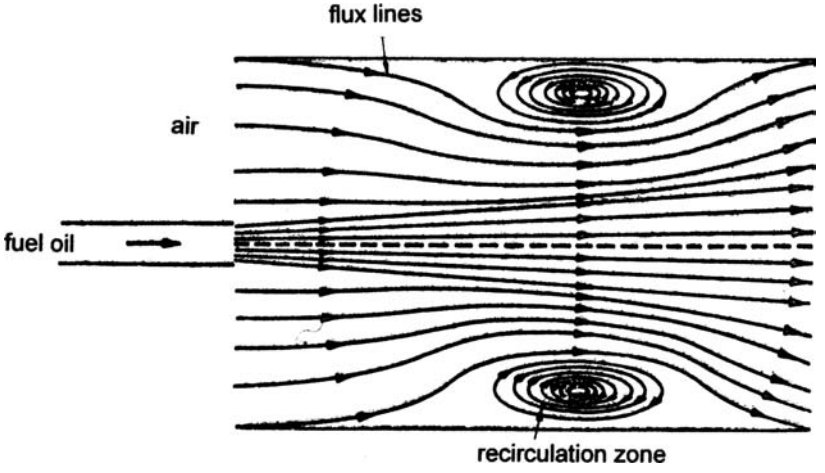


Fig. 7.12 Recirculation of flue gas (Salvi – La Combustione)

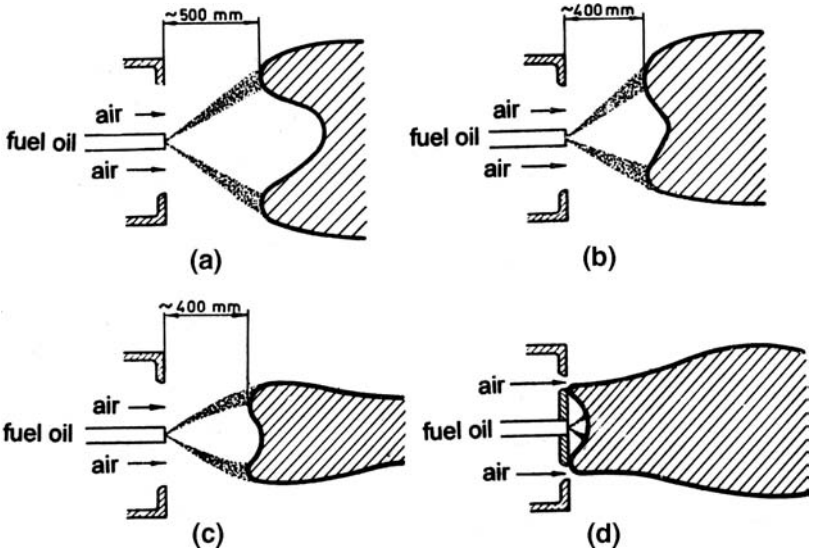


Fig. 7.13 Different flame shapes (Salvi – La Combustione)

speed of the oil unchanged and by increasing the speed of the air [case (a) and (c)], the latter is visibly able to drag even grossly atomized fuel oil. Finally, (d) shows the stabilizing impact of the disk that redirects the flame close to the burner.

In the case of axial air spouts, the mixing of fuel and combustion air is not among the best. To improve it and to reduce the length of the flame, industrial burners currently used in generators are equipped with a register with blades capable of tilting to push the air into swirls. This way, maximum speed of the gas does not occur on the axis of the burner anymore but toward the periphery of the spout instead, and the mixing is greatly improved. A conical or cylindrical vortex form and both its diameter and length can be modified through the converging–diverging exit element of the air and the variation in slant of the blades of the register. This vortex combined with the ensuing strong recirculation of hot gas has the following advantages. There is a distinct improvement in the evaporation of the little drops. The steam produced in the central section is recycled by the gas in counterflow and lead to the burner where the flame stabilizes. Thus, there is distinct internal recirculation besides the external one.

This results in good mixing given the strong speed gradients generated in the central section. There is an increase in stay time of the burning materials in the area with the highest temperature. The simultaneous adoption of strong air swirls and the disk stabilizer brings the internal recirculation to its peak with noticeable benefits for the combustion of atomized fuels. Figure 7.14 separately indicates the impact of the disk stabilizer (impeller) and of the air swirl on the internal recirculation. Figure 7.15 shows the isotherms for two different degrees of air swirl. The increase in swirling brings a reduction of the cold area on the exit of the burner where the the flame is unable to be.

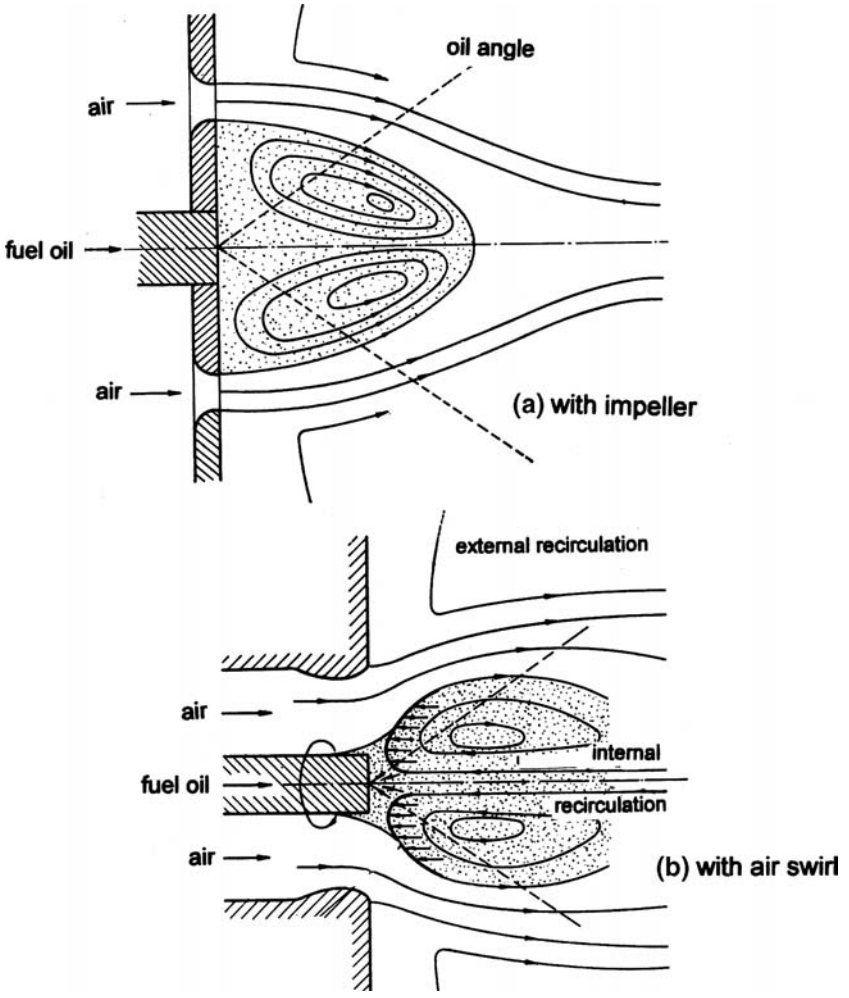


Fig. 7.14 Impact of the disk stabilizer and of the air swirl on internal recirculation (Salvi – La Combustione)

In conclusion, it is evident that the shape and length of the flame greatly depend on the flow rate of the burner, its structural features, on the way it is used, and so on. Strong turbulence and high speed of the components produce short, compact, and relatively large flames. Low turbulence and low speed produce long and soft flames. Increasing excess air tends to shorten the flame, whereas a reduction elongates it. On the other hand, different generators have different requirements. Generally a short and wide flame is desirable for a water-tube generator, as much as it is compatible with the position of the walls located on the sides of the burner.

In the case of a smoke-tube boiler, given the high ratio between length and diameter of the flue, a long and narrow flame is necessary. In general terms, burners

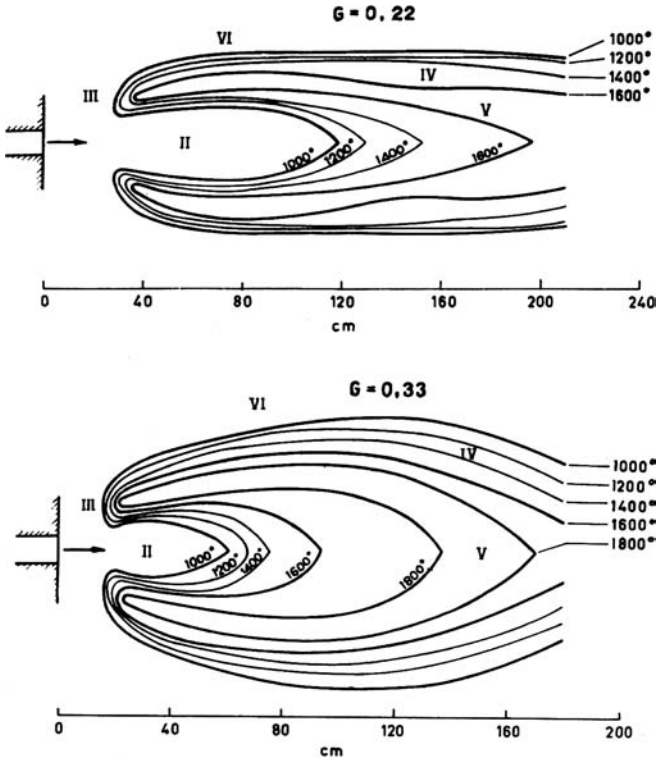


Fig. 7.15 Isotherms for different degree of air swirl (Salvi – La Combustione)

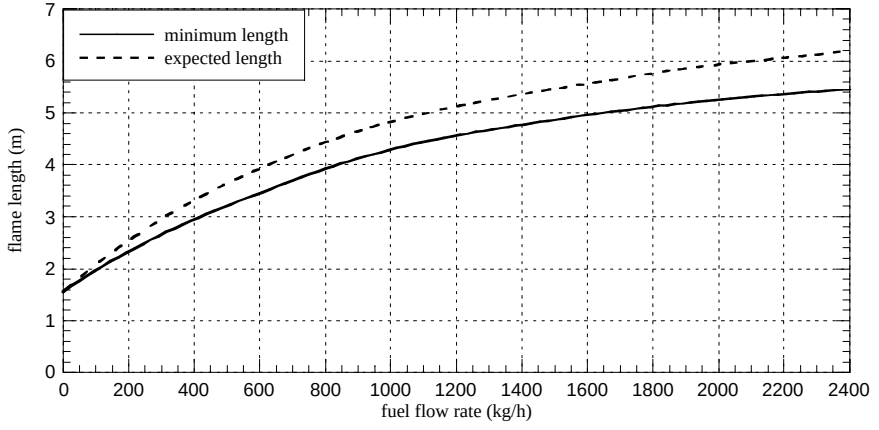


Fig. 7.16 Indicative length of the flame

designed for water-tube generators are not a good match for smoke-tube boilers and vice versa.

In the end, it is impossible to provide general guidelines as far as the length of the flames. Each burner is a story in itself. Nonetheless, Fig. 7.16 shows a diagram of a type of burner that will generally work with water-tube generators.

7.3 Grates

Grates have become less important after the spreading of coal and lignite combustion in the form of pulverized fuel. Nonetheless, the grate is still generally indispensable to burn poor fuels besides coal. The grates used for coal differentiate themselves from those used for poor fuels because of the diverse requirements, depending on the type of fuel related to the heat value, the size, the moisture, the quantity and the nature of the ashes, and so on. The common function of all grates is to support the fuel and to allow the passage of air for combustion at the same time. They consist of fire bars in pearlitic iron or special cast iron in nickel-chrome based on the temperatures the materials will have to withstand and adequately placed at a distance determined by fuel size.

The grates used for coal with natural draught or fed from underneath through a pusher fan can be stationary or mobile. The stationary grates used for ordinary coal can be flat or slightly tilted. (see Fig. 7.17). The former is suitable only for coal with little volatile matter, ashes, and moisture and is used for low power levels. They require manual loading and deliver poor combustion because of the entry of air during loading that reduces the temperature of the fire as well as the percentage

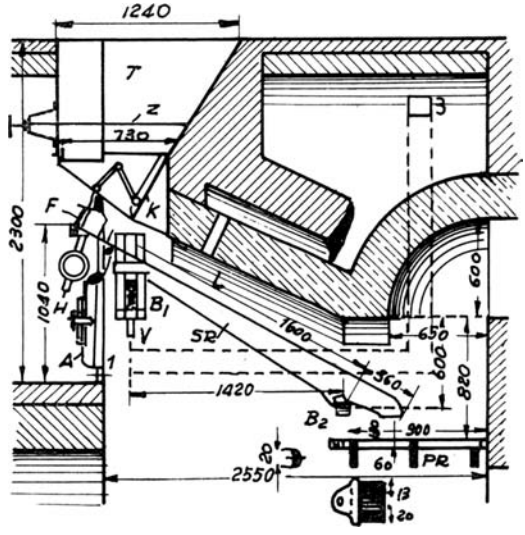


Fig. 7.17 Stationary grate for ordinary coal

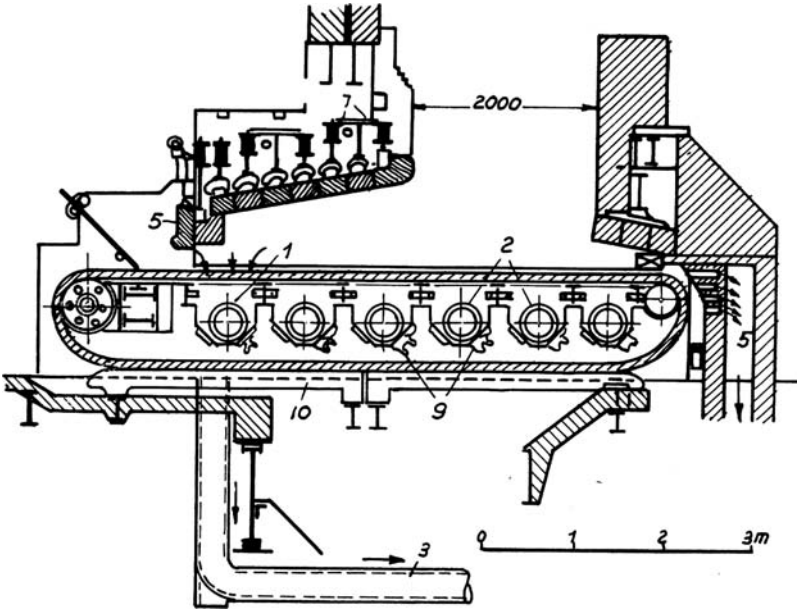


Fig. 7.18 Chain grate

of CO_2 in the flue gas. The latter has greater combustion capacity and facilitate combustion and is suited for coal in uniform size and little slag.

The most common grate is the chain grate (see Fig. 7.18). It is particularly suited for long-flaming coal and hard coal if the air is pushed. If the coal is rich and there is little space available, or if coal rich in volatile matter and little ashes is used, special types of grates will be used.

The grates used for poor fuels are usually flat stationary grates and tipping grates. The tips move in alternate fashion, the fuel moves from tip to tip and then downward (see Fig. 7.19).

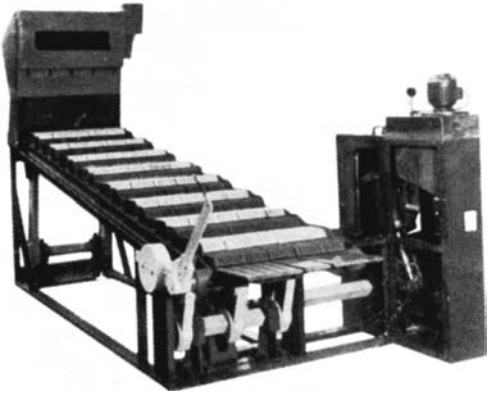


Fig. 7.19 Tipping grate

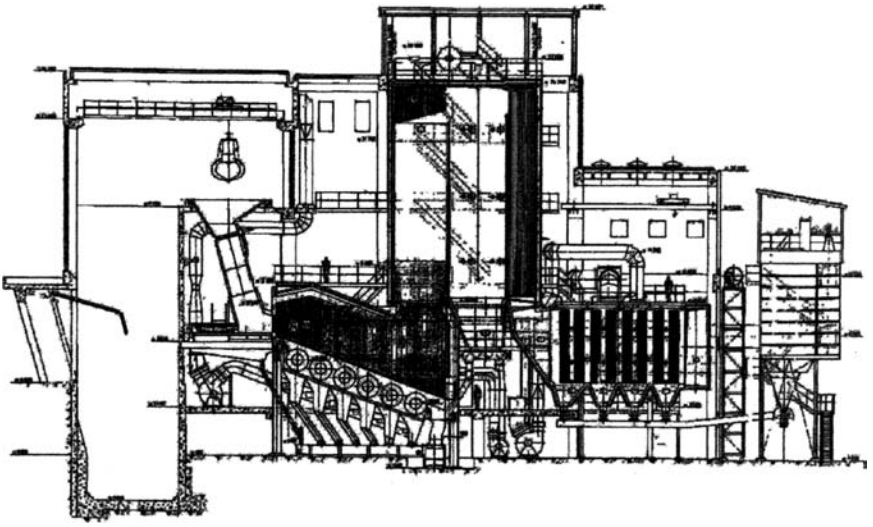


Fig. 7.20 Plant for combustion of urban waste

In terms of combustion capacity of the grates, the following approximate data about coal and lignite may be used as a reference. A good quality coal with a net heat value of 31300 kJ/kg may have a load of 0.028 kg/m^{2}s on a stationary grate and 0.039 kg/m^{2}s on a mobile grate. In the case of coal rich in slag the load may be 0.024 and 0.035 kg/m^{2}s, respectively. For anthracite on a stationary grate the load can be 0.018 kg/m^{2}s. For lignite on a tipping grate consider a load of 0.055–0.064 kg/m^{2}s, and for peat on the same type of grate a load of 0.055 kg/m^{2}s.

The characteristics of poor fuels vary so much that only experience can advise the grate combustion capacity to adopt. The combustion on a grate of urban waste is of special interest. Figure 7.20 shows a plant of this kind. This way the waste is destroyed and produces steam used for the production of electricity or to heat urban housing. Tipping grates are used in this case.

7.4 Combustion Chemistry

Combustion consists of a series of reactions that involve the different components of the fuel. The most important ones are as follows: C, S, H_2, CO, CH_4, C_mH_n (thus indicating the different hydrocarbons different from methane), O_2, N_2, CO_2, H_2O.

The first six react with oxygen contained in the air as follows:

$$C + O_2 = CO_2$$
$$S + O_2 = SO_2$$

$$\begin{aligned} 2H_2 + O_2 &= 2H_2O \\ 2CO + O_2 &= 2CO_2 \\ CH_4 + 2O_2 &= CO_2 + 2H_2O \\ C_mH_n + \left(m + \frac{n}{4}\right) O_2 &= mCO_2 + \frac{n}{2} H_2O \end{aligned} \tag{7.2}$$

The potential oxygen present in the fuel combines itself with the other components in substitution of an equivalent quantity of air. Nitrogen, carbon dioxide, and water do not burn but are present in the resulting product of combustion.

The molecular weights of the components that react with the oxygen are known to be as follows:

$$\begin{aligned} C &= 12.01 \\ S &= 32.06 \\ H_2 &= 2.016 \\ CO &= 28.01 \\ CH_4 &= 16.042 \\ C_mH_n &= 12.01m + 1.008n \end{aligned} \tag{7.3}$$

Recalling that the molecular weight of oxygen is equal to 32, based on (7.2) the combustion of 1 kg of the various components requires the following quantities of oxygen:

$$\begin{aligned} 1\,\text{kg}C &\rightarrow \frac{32}{12.01} = 2.6644\,\text{kg}\ O_2 \\ 1\,\text{kg}S &\rightarrow \frac{32}{32.06} = 0.9981\,\text{kg}\ O_2 \\ 1\,\text{kg}H_2 &\rightarrow \frac{32}{2 \times 2.016} = 7.936\,\text{kg}\ O_2 \\ 1\,\text{kg}CO &\rightarrow \frac{32}{2 \times 28.01} = 0.5712\,\text{kg}\ O_2 \\ 1\,\text{kg}CH_4 &\rightarrow \frac{2 \times 32}{16.042} = 3.989\,\text{kg}\ O_2 \\ 1\,\text{kg}C_mH_n &\rightarrow \frac{\left(m + \frac{n}{4}\right) 32}{12.01m + 1.008n} = 8\frac{4m + n}{12.01m + 1.008n}\,\text{kg}\ O_2 \end{aligned} \tag{7.4}$$

Every kilogram of air contains 0.232 kg of oxygen. Therefore, 4.31 kg of air is required to have 1 kg of O_2. The combustion of 1 kg of the examined components requires the following quantities of air:

$$\begin{aligned}
1\,\text{kg C} &\rightarrow 2.6644 \times 4.31 = 11.484\ \text{kg of air} \\
1\,\text{kg S} &\rightarrow 0.9981 \times 4.31 = 4.302\ \text{kg of air} \\
1\,\text{kg H}_2 &\rightarrow 7.936 \times 4.31 = 34.204\ \text{kg of air} \\
1\,\text{kg CO} &\rightarrow 0.5712 \times 4.31 = 2.462\ \text{kg of air} \\
1\,\text{kg CH}_4 &\rightarrow 3.989 \times 4.31 = 17.193\ \text{kg of air} \\
1\,\text{kg C}_m\text{H}_n &\rightarrow 8\frac{4m+n}{12.01m+1.008}4.31 = 34.48\frac{4m+n}{12.01m+1.008n}\ \text{kg of air}
\end{aligned} \tag{7.5}$$

In the case of gaseous fuel and in reference to volumes, based on (7.2) it is possible to quickly compute the requirement in oxygen in Nm^3 for every Nm^3 of the different components of the fuel:

$$\begin{aligned}
1\,\text{Nm}^3\ \text{H}_2 &\rightarrow \frac{1}{2} = 0.5\,\text{Nm}^3\,\text{O}_2 \\
1\,\text{Nm}^3\ \text{CO} &\rightarrow \frac{1}{2} = 0.5\,\text{Nm}^3\,\text{O}_2 \\
1\,\text{Nm}^3\ \text{CH}_4 &\rightarrow \frac{2}{1} = 2\,\text{Nm}^3\,\text{O}_2 \\
1\,\text{Nm}^3\ \text{C}_m\text{H}_n &\rightarrow \left(m+\frac{n}{4}\right)\text{Nm}^3\,\text{O}_2
\end{aligned} \tag{7.6}$$

Every Nm^3 of air contains $0.21\,\text{Nm}^3$ of oxygen. Therefore, $1\,\text{Nm}^3$ of oxygen requires $4.76\,\text{Nm}^3$ of air.

Based on (7.2), the theoretical requirement of air for combustion of $1\,\text{Nm}^3$ of the different gas types considered is as follows:

$$\begin{aligned}
1\,\text{Nm}^3\ \text{H}_2 &\rightarrow 0.5 \times 4.76 = 2.38\,\text{Nm}^3\ \text{of air} \\
1\,\text{Nm}^3\ \text{CO} &\rightarrow 0.5 \times 4.76 = 2.38\,\text{Nm}^3\ \text{of air} \\
1\,\text{Nm}^3\ \text{CH}_4 &\rightarrow 2 \times 4.76 = 9.52\,\text{Nm}^3\ \text{of air} \\
1\,\text{Nm}^3\ \text{C}_m\text{H}_n &\rightarrow 4.76\left(m+\frac{n}{4}\right)\text{Nm}^3\ \text{of air}
\end{aligned} \tag{7.7}$$

In addition, recalling the amount of oxygen in the air, if the fuel contains oxygen, this leads to a reduced requirement of air equal to $4.31\,\text{kg}$ for every kg of O_2, or $4.76\,\text{Nm}^3$ for every Nm^3 of O_2.

7.5 Combustion Air

On the basis of the previous section, the equations relative to the requirement of theoretical air can be easily computed. A_{tm} and A_{tv} indicate the theoretical air in terms

of mass and volume, respectively. Solid fuels contain carbon, hydrogen, oxygen, and sulfur plus ashes and water (and sometimes nitrogen). C, H, O, and S are the mass percentages of the components that participate in combustion. Recalling (7.5), we obtain the following equation relative to theoretical air in mass, that is, in kg per kg of fuel:

$$A_{\text{tm}} = 0.11484\text{C} + 0.34204\text{H} + 0.04302\text{S} - 0.0431\text{O kg/kg} \tag{7.8}$$

Note that for every kg of oxygen contained in the fuel, 4.31 kg less of air will be necessary. Looking for an equation to compute the volume of theoretical air, note that the air density under normal conditions is equal to 1.293 kg/Nm^3. From (7.8) it immediately follows that

$$A_{\text{tv}} = 0.08882\text{C} + 0.26453\text{H} + 0.03327\text{S} - 0.03333\text{O Nm}^3\text{/kg} \tag{7.9}$$

The same equations used for solid fuels are valid for liquid fuels.

Naturally, in the case of gaseous fuels, it is preferable to refer to Nm^3 of fuel. By indicating the percentages in volume of the different components of the gas as $\text{CO}, \text{H}_2, \text{CH}_4, \text{C}_m\text{H}_n$, and O_2, based on (7.7) the volume of the theoretical air, that is, Nm^3 for every Nm^3 of fuel, is given by

$$\begin{aligned} A_{\text{tv}} = \; & 0.0238\,(\text{CO} + \text{H}_2) + 0.0952\text{CH}_4 + 0.0476 \sum_i \left(m_i + \frac{n_i}{4} \right) \text{C}_{mi}\text{H}_{ni} \\ & - 0.0476\text{O}_2 \text{ Nm}^3/\text{Nm}^3. \end{aligned} \tag{7.10}$$

To use an equation to compute the mass of theoretical air, note the density of the latter under normal conditions. In other words:

$$\begin{aligned} A_{\text{tm}} = \; & 0.03077\,(\text{CO} + \text{H}_2) + 0.1231\text{CH}_4 + 0.06155 \sum_i \left(m_i + \frac{n_i}{4} \right) \text{C}_{mi}\text{H}_{ni} \\ & - 0.06155\text{O}_2 \text{ kg/Nm}^3. \end{aligned} \tag{7.11}$$

The amount of air stoichiometrically required for combustion given by (7.8–7.11) are basically insufficient to ensure complete combustion, that is, in the absence of unburned carbon monoxide.

The great impact of unburned carbon monoxide on generator efficiency will be discussed later on. On the other hand, even an increase in air introduced into the furnace for combustion causes a reduction in efficiency through the increase in heat loss, because of sensible heat of the flue gas at the exit of the generator. The aim of tuning the air flow rate during set up is to reach combustion without unburned matter with the minimum excess air, with respect to the theoretical one. The effort of burner designers aims at this goal, as well. Considerable progress was made in this field, and as a result in the largest plants where the most advanced techniques aimed at improving combustion are deployed, it is possible to work with an amount of air quite close to the theoretical one.

Note that in this context the air index is the ratio between required air and theoretical air. If n is this index, the required air is given by

$$A = nA_{\mathrm{t}}. \tag{7.12}$$

The percentage of excess air is therefore given by

$$e = (n-1)\,100. \tag{7.13}$$

For example, this means that an air index equal to 1.2 will have 20% of excess air. As a reference, a series of values of the air index for different fuels and combustion systems are indicated below:

Coal on grate with manual load	$n = 1.6$–2
Coal on grate with mechanical load	$n = 1.35$–1.5
Coal on chain grate	$n = 1.25$–1.4
Pulverized coal	$n = 1.10$–1.30
Lignite on mechanical grate	$n = 1.2$–1.35
Fuel oil	$n = 1.10$–1.30
Gaseous fuels	$n = 1.05$–1.20

Of course, these values are only indicative. For instance, fuel oil in small plants may have an air index greater than 1.3, whereas in large plants with particularly perfected burners it is possible to burn without unburned carbon monoxide even with n smaller than 1.1. There are plants running on fuel oil where n was reduced to 1.05. If the composition of the fuel is unknown except for its net heat value, in the case of solid or liquid fuels it is possible to use approximate equations or diagrams to determine both the theoretical and the required air. Among the approximated equations we highlight those available thanks to Rosin.

As far as solid fuels, Rosin suggests the following equation for the volume of theoretical air:

$$A_{\mathrm{tv}} = \frac{0.241 H_n}{1000} + 0.5\,\mathrm{Nm}^3/\mathrm{kg}, \tag{7.14}$$

and the following in the case of liquid fuels

$$A_{\mathrm{tv}} = \frac{0.203 H_{\mathrm{n}}}{1000} + 2\,\mathrm{Nm}^3/\mathrm{kg}. \tag{7.15}$$

H_{n} is the net heat value of the fuel expressed in kJ/kg. Moreover, it is possible to use the diagram of Fig. 7.21 for both solid and liquid fuels taken from the "Wärmetechnische Arbeitsmappe," thanks to Boie. As far as liquid fuels, the volume of theoretical air is obtained as a function of the net heat value of both fuel and air index n, or the content of CO_2 (see Sect. 7.7). As far as solid fuels, it is necessary to refer to $|CO_2|$ besides the net heat value. The first may be computed through the diagram in Fig. 7.23 based on n and the type of fuel.

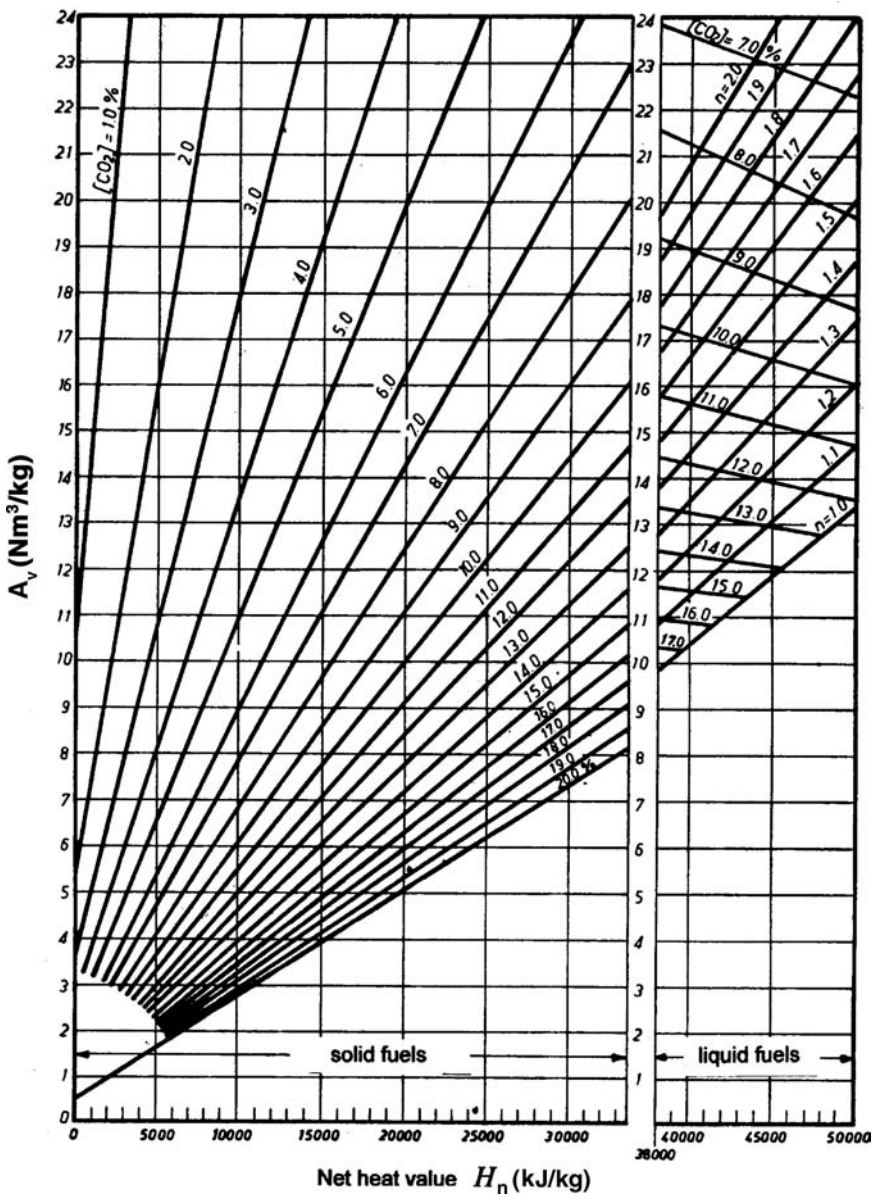


Fig. 7.21 Air requirements for solid and liquid fuels

Finally, in the case of gaseous fuels Rosin suggests the following equations. For poor gas, such as blast-furnace gas and so on

$$A_{tv} = \frac{0.209 H_n}{1000} \text{ Nm}^3/\text{kg}. \tag{7.16}$$

For rich gas, such as coke-oven gas, refinery gas, and natural gas

$$A_{tv} = \frac{0.26 H_n}{1000} - 0.25 \text{Nm}^3/\text{kg}. \tag{7.17}$$

Even in the case of gas the net heat value H_n is in reference to 1 kg of fuel.

7.6 Flue Gas

It is convenient to refer to flue gas expressed in kg per kg of fuel for solid and liquid fuel. In fact, by referring to the mass theoretic air shown in (7.8), it is easy to trace back to the products of combustion through the following equation:

$$G_m = nA_{tm} + 1 \text{ kg/kg}. \tag{7.18}$$

In fact, the required air is represented by nA_{tm} plus 1 kg of fuel to reach the amount of mass flue gas. On the other hand, if it is preferable to compute the amount of flue gas G_v as volume per kg of fuel, it is possible to proceed in two ways. If an approximate value is acceptable, it suffices to remember that the density of flue gas is equal to about 1.30–1.35 kg/Nm^3 for both solid and liquid fuels. From the value of G_m given by (7.18), it is possible to obtain the value of G_v by dividing by the density.

On the basis of the mass percentage of the content of the various components and the value of A_{tv} computed using (7.9), it is also possible to elaborate an equation leading directly to G_v. To that extent, note that fuel generally contains carbon, hydrogen, oxygen, sulfur, nitrogen, and water. Recalling that the volume of a kilomole is equal to 22.412 Nm^3, the combustion of 1 kg of carbon, sulfur, and hydrogen produces the following gas volumes, respectively:

$$1 \text{ kg C} \rightarrow \frac{22.412}{12.01} = 1.8661 \text{ Nm}^3 \text{ of } CO_2;$$

$$1 \text{ kg S} \rightarrow \frac{22.412}{32.06} = 0.699 \text{ Nm}^3 \text{ of } SO_2;$$

$$1 \text{ kg } H_2 \rightarrow \frac{22.412}{2.016} = 11.117 \text{ Nm}^3 \text{ of } H_2O.$$

In addition, for every kg of nitrogen and water in the fuel the relative volumes in the flue gas are equal to:

$$1\,\text{kg N}_2 \rightarrow \frac{22.412}{28.016} = 0.8\,\text{Nm}^3 \text{ of N}_2;$$

$$1\,\text{kg H}_2\text{O} \rightarrow \frac{22.412}{18.016} = 1.244\,\text{Nm}^3 \text{ of H}_2\text{O}.$$

Recalling that $4.76\,\text{Nm}^3$ of air contain $3.76\,\text{Nm}^3$ of nitrogen and $1\,\text{Nm}^3$ of oxygen, the volume of nitrogen in flue gas due to combustion air per kg of fuel is equal to $3.76nA_{\text{tv}}/4.76$. The volume of free oxygen is equal to $(n-1)A_{\text{tv}}/4.76$ instead.

Thus, the volume of nitrogen and oxygen in flue gas, besides potential nitrogen deriving from the fuel, is equal to

$$\frac{3.76nA_{\text{tv}}}{4.76} + \frac{(n-1)A_{\text{tv}}}{4.76} = nA_{\text{tv}} - \frac{A_{\text{tv}}}{4.76}.$$

As usual, by indicating the mass percentages of the components in the fuel with C, S, H, N, O, and H_2O, the volume of flue gas per kg of fuel is equal to

$$\begin{aligned} G_{\text{v}} = \; & nA_{\text{tv}} - \frac{A_{\text{tv}}}{4.76} + 0.018661\text{C} + 0.11117\text{H} + 0.00699\text{S} \\ & + 0.008\text{N} + 0.01244\text{H}_2\text{O}\ \text{Nm}^3/\text{kg}. \end{aligned} \tag{7.19}$$

Recalling (7.9) from (7.19), we obtain the following:

$$G_{\text{v}} = nA_{\text{tv}} + 0.05558\text{H} + 0.007\text{O} + 0.008\text{N} + 0.01244\text{H}_2\text{O}\ \text{Nm}^3/\text{kg}. \tag{7.20}$$

Given its origin, (7.20) is true only if the combustion of carbon is complete, that is, if there are no unburned carbon monoxide (see Sect. 7.7).

As far as gaseous fuels, note that the combustion of $1\,\text{Nm}^3$ of $\text{CO}, \text{H}_2, \text{CH}_4$, and C_mH_n produces the following volumes of gas, respectively:

$$1\,\text{Nm}^3\ \text{CO} \rightarrow 1\,\text{Nm}^3\ \text{CO}_2$$

$$1\,\text{Nm}^3\ \text{H}_2 \rightarrow 1\,\text{Nm}^3\text{H}_2\text{O}$$

$$1\,\text{Nm}^3\ \text{CH}_4 \rightarrow 3\,\text{Nm}^3 \text{ of flue gas } (\text{CO}_2 + 2\text{H}_2\text{O})$$

$$1\,\text{Nm}^3\ \text{C}_m\text{H}_n \rightarrow \left(m + \frac{n}{4}\right)\text{Nm}^3 \text{ of flue gas } \left(m\text{CO}_2 + \frac{n}{2}\text{H}_2\text{O}\right)$$

Moreover, for every Nm^3 of N_2, CO_2, and H_2O in the fuel, we obviously find the same volume in the flue gas. Therefore, by indicating the volumetric percentages of the components of the fuel as $\text{CO}, \text{H}_2, \text{CH}_4, \text{O}_2, \text{CO}_2, \text{H}_2\text{O}$, and C_mH_n, the volume of flue gas per Nm^3 of fuel is equal to:

$$\begin{aligned} G_{\text{v}} = \; & nA_{\text{tv}} - \frac{A_{\text{tv}}}{4.76} + 0.01\,(\text{CO} + \text{H}_2 + \text{N}_2 + \text{CO}_2 + \text{H}_2\text{O}) + 0.03\text{CH}_4 \\ & + 0.01 \sum_i \left(m_i + \frac{n_i}{4}\right)\text{C}_{mi}\text{H}_{ni}\text{Nm}^3/\text{Nm}^3 \end{aligned} \tag{7.21}$$

Recalling (7.10) from (7.21), we obtain the following:

$$G_{\mathrm{v}} = nA_{\mathrm{tv}} + 0.005\,(\mathrm{CO} + \mathrm{H_2}) + 0.01\,(\mathrm{CH_4} + \mathrm{O_2} + \mathrm{N_2} + \mathrm{CO_2} + \mathrm{H_2O}) + 0.01 \sum_i \frac{n_i}{4} \mathrm{C}_{mi}\mathrm{H}_{ni}\mathrm{Nm}^3/\mathrm{Nm}^3. \quad (7.22)$$

Observing that

$$\mathrm{CO} + \mathrm{H_2} + \mathrm{CH_4} + \mathrm{O_2} + \mathrm{N_2} + \mathrm{CO_2} + \mathrm{H_2O} + \sum \mathrm{C}_m\mathrm{H}_n = 100, \quad (7.23)$$

given that we assumed that there is no other gas present in the fuel. Equation (7.23) may be more adequately rewritten as follows:

$$G_{\mathrm{v}} = nA_{\mathrm{tv}} + 1 - 0.005\,(\mathrm{CO} + \mathrm{H_2}) + 0.0025 \sum_i (n_i - 4)\mathrm{C}_{mi}\mathrm{H}_{ni}\ \mathrm{Nm}^3/\mathrm{Nm}^3. \quad (7.24)$$

The same statement made about (7.20) as far as the complete combustion of the carbon is true for (7.24).

To dispose an equation to calculate G_{m} with reference to $1\,\mathrm{Nm}^3$ of fuel, it can be easily derived from the density of the fuel. In fact, by indicating it as ρ_{f}:

$$G_{\mathrm{m}} = nA_{\mathrm{tm}} + \rho_{\mathrm{f}}\ \mathrm{kg/Nm}^3 \quad (7.25)$$

A_{tm} is the mass theoretic air given by (7.11). Given that nA_{tm} is the mass required air per Nm^3 of fuel, it suffices to add the mass of $1\,\mathrm{Nm}^3$ of fuel to it, given in fact by ρ_{f} to obtain the products of combustion in $\mathrm{kg/Nm}^3$.

It would be possible to elaborate an equation as a function of the percentages of the components only, as was done in previous equations, but it would be complex and unpractical as a result. Equation (7.25) is definitely preferable to (7.18). Note that the density can be easily computed once the composition of the fuel is known. Even in the case of flue gas, simply knowing its net heat value instead of its composition, it is possible to use approximate equations or diagrams.

As far as solid fuels, Rosin suggests the following:

$$G_{\mathrm{tv}} = \frac{0.213H_{\mathrm{n}}}{1000} + 1.65\,\mathrm{Nm}^3/\mathrm{kg} \quad (7.26)$$

and the following in the case of liquid fuels:

$$G_{\mathrm{tv}} = \frac{0.265H_{\mathrm{n}}}{1000}\ \mathrm{Nm}^3/\mathrm{kg}. \quad (7.27)$$

H_{n} stands for the net heat value of the fuel in kJ/kg and G_{tv} is the amount of theoretic gas expressed as volume per kg of fuel.

On the basis of Fig. 7.22 and thanks to Rosin, it is also possible to obtain the amount of actual volumetric gas G_{v} as a function of the net heat value of the fuel and the air index.

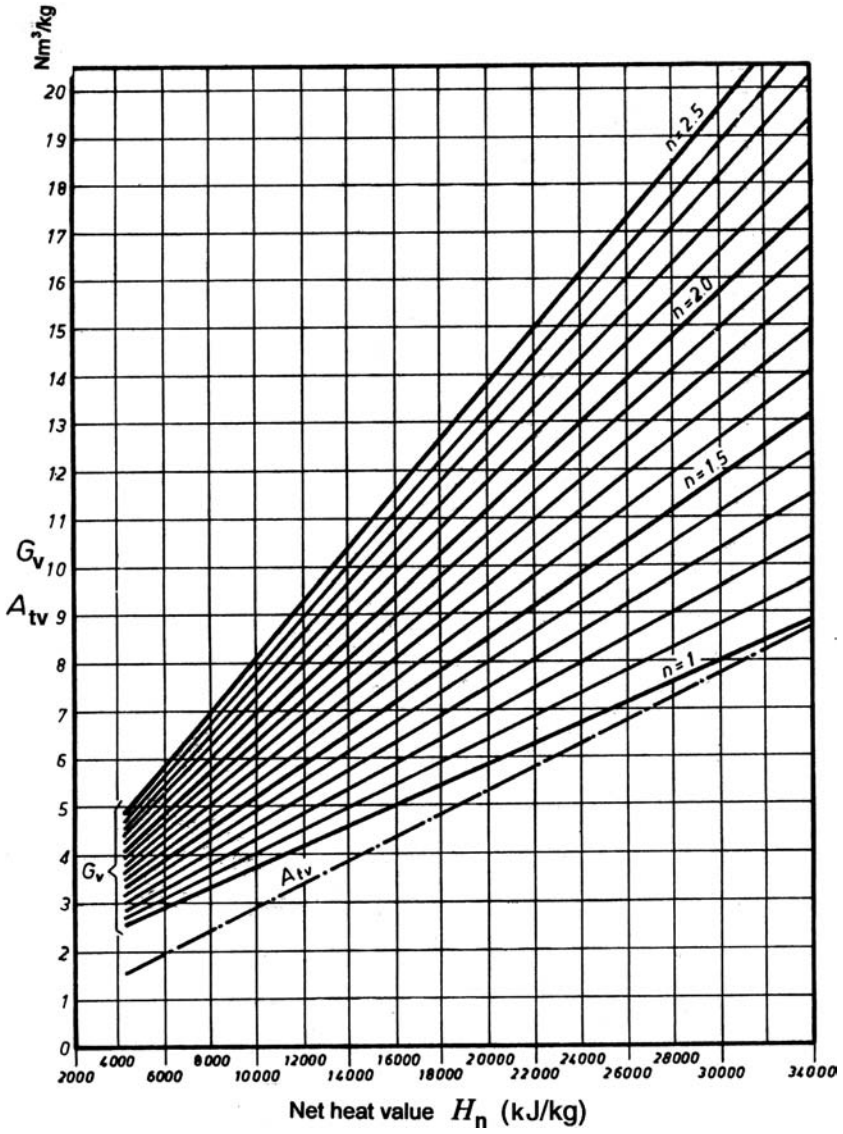


Fig. 7.22 Amount of actual flue gas as a function of net heat value and air index

Moreover, it is possible to use both Figs. 7.23 and 7.24 taken from the "Wärmetechnische Arbeitsmappe" developed by Boie. The former determines the actual volumetric gas as a function of the air index *n* (liquid fuels) or of the $|CO_2|$ (liquid and solid). The $|CO_2|$ content of solid fuels can be derived from the same diagram as a function of the air index and the type of fuel. The latter determines the actual mass of gas both for liquid and for solid fuels. Both diagrams help to determine the content of steam in the flue gas, in terms of both volume and mass. This

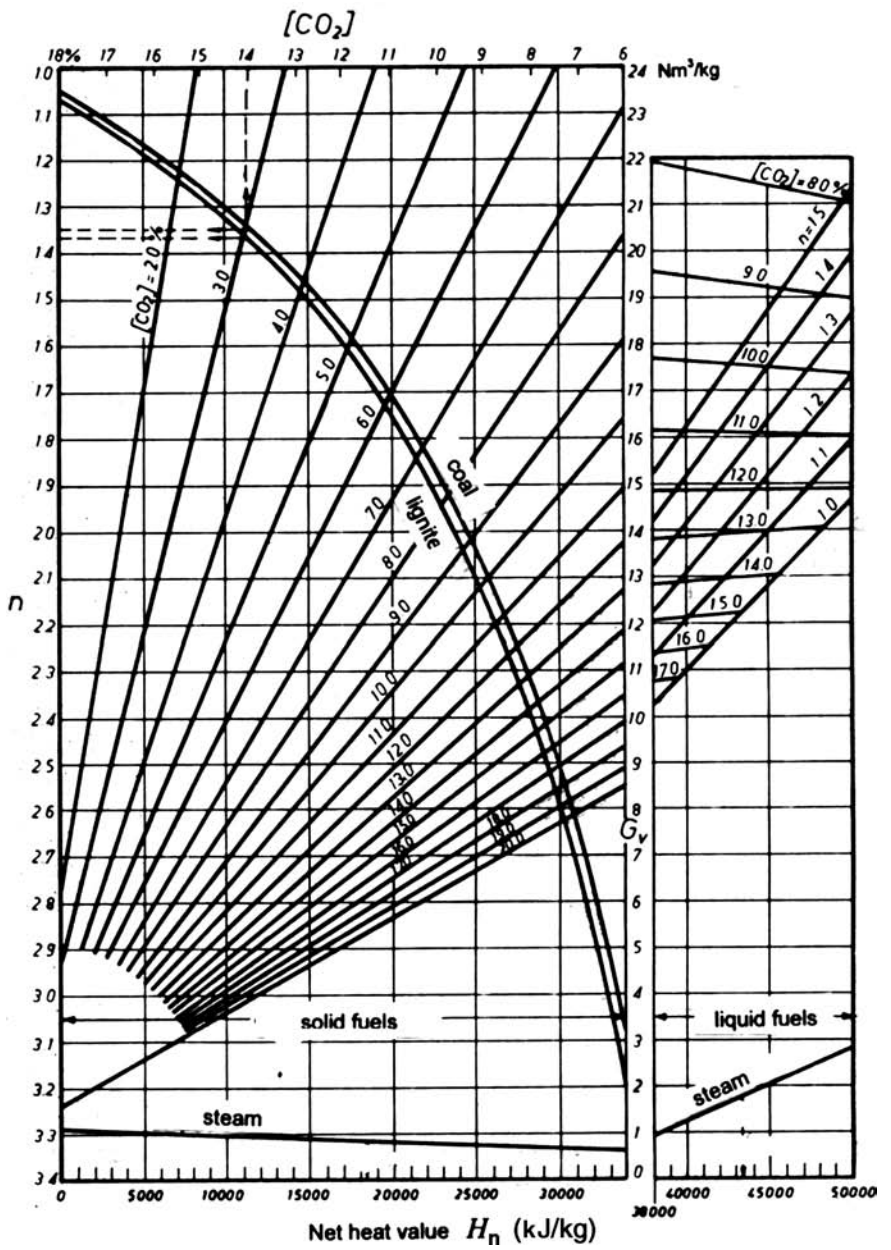


Fig. 7.23 Amount of actual flue gas for solid and liquid fuels

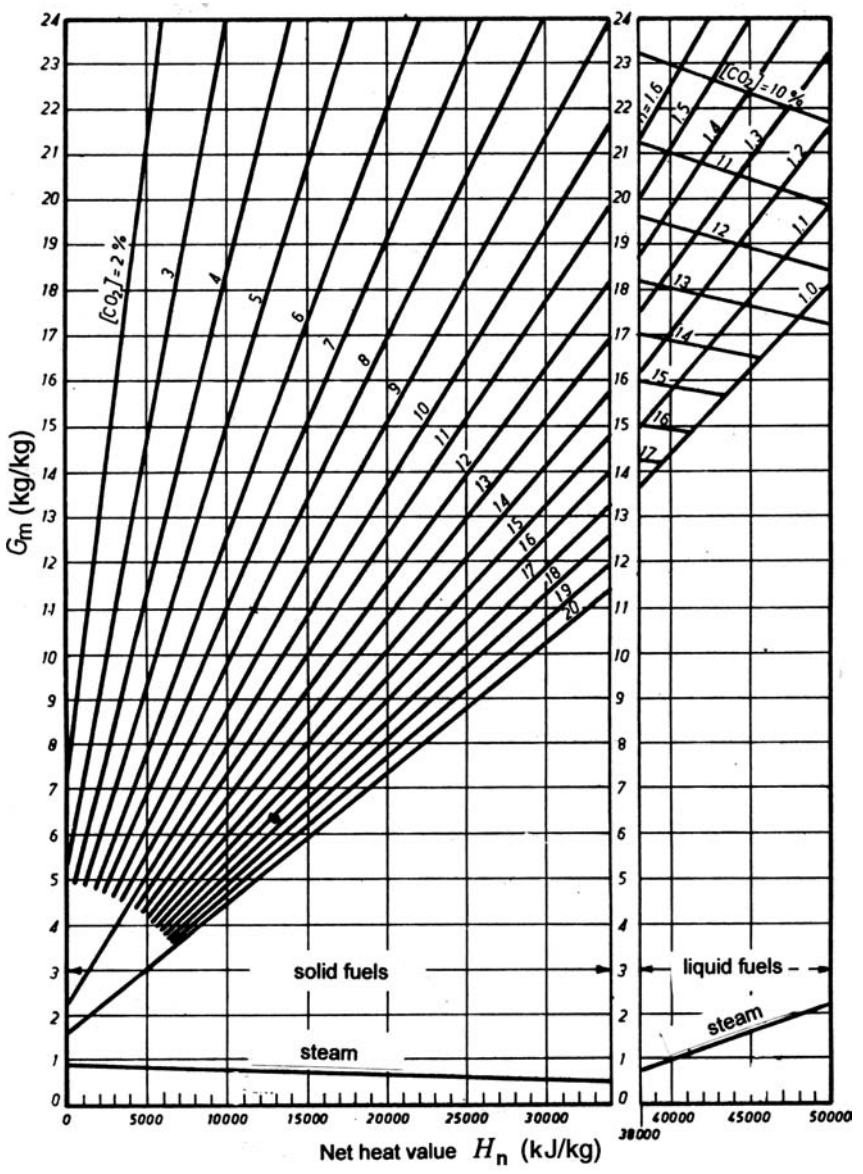


Fig. 7.24 Flue gas as mass for solid and liquid fuels

quantity is necessary to determine the specific heat of the flue gas or their enthalpy, as we shall see later on. At the most, the use of these diagrams leads to an error in the estimate of *G* that does not exceed 1.5%, plus or minus. Finally, in the case of gaseous fuels, Rosin suggests the following approximate equations to determine the volume of theoretic gas.

For poor gas (blast-furnace gas and so on)

$$G_{tv} = \frac{0.173 H_n}{1000} + 1\,\mathrm{Nm^3/kg}. \tag{7.28}$$

For rich gas (coke-oven gas, refinery gas, and natural gas):

$$G_{tv} = \frac{0.272 H_n}{1000} + 0.25\,\mathrm{Nm^3/kg}. \tag{7.29}$$

Even in this case H_n is the net heat value referred to 1 kg of fuel. Both the approximate equations and the diagrams to determine G_{tv} or G_v are true for complete combustion of carbon. Figure 7.24 is valid even in the presence of unburned carbon monoxide instead, given that it is based on mass.

7.7 $|CO_2|$ and Unburned CO

The $|CO_2|$ content in flue gas is understood to be the volumetric percentage of CO_2 in dry flue gas. If the fuel contains sulfur which means that the flue gas contains SO_2, in fact the $|CO_2|$ content in flue gas indicates the volumetric percentage content of $CO_2 + SO_2$ in dry flue gas. The maximum content of CO_2 occurs with zero excess air and, of course, in absence of unburned carbon monoxide. Assuming complete combustion, as an example we look at ways to compute $|CO_2|$ with natural gas and fuel oil. Assimilating natural gas to methane, that is, its fundamental component, based on (7.2) we know that the following types of gas are produced by stoichiometric combustion of 1 Nm^3 of methane:

$$1\,\mathrm{Nm^3}\text{ of }CO_2$$
$$2\,\mathrm{Nm^3}\text{ of }H_2O$$
$$2 \times 3.76 = 7.52\,\mathrm{Nm^3}\text{ of }N_2$$

Note that 4.76 Nm^3 of air contain 1 Nm^3 of O_2, thus 3.76 Nm^3 of N_2. The maximum $|CO_2|$ is therefore equal to:

$$|CO_2|_{max} = \frac{1}{1+7.52} 100 = 11.75\%.$$

Let us now assume that combustion takes place with excess air equal to 15% ($n = 1.15$). In that case the products of combustion for every Nm^3 of methane are as follows:

$$1\,\mathrm{Nm^3}\text{ of }CO_2$$
$$2\,\mathrm{Nm^3}\text{ of }H_2O$$
$$1.15 \times 7.52 = 8.65\,\mathrm{Nm^3}\text{ of }N_2$$
$$0.15 \times 2 = 0.3\,\mathrm{Nm^3}\text{ of }O_2$$

Therefore, the $|CO_2|$ is equal to

$$|CO_2| = \frac{1}{1+8.65+0.3}100 \approx 10\%.$$

Moreover,

$$|O_2| = \frac{0.3}{1+8.65+0.3}100 \approx 3\%.$$

In the case of natural gas which is not pure methane the values of $|CO_2|$ are slightly different from the ones that were found.

Let us now consider fuel oil with the following characteristics:

$$\frac{C}{H} = 7$$
$$S = 3.9\%$$
$$H_2O = 0.1\%$$

We have:

$$H = \frac{100-3.9-0.1}{7+1} = 12\%$$
$$C = 100-(3.9+0.1+12) = 84\%$$

Stoichiometric combustion of 1 kg of C produce

$$\frac{22.412}{12.01} = 1.8661\,\mathrm{Nm}^3 \text{ of } CO_2$$

and

$$\frac{3.76\times 22.412}{12.01} = 7.0166\,\mathrm{Nm}^3 \text{ of } N_2.$$

Combustion of 1 kg of H_2 produce

$$\frac{2\times 22.412}{4.032} = 11.117\,\mathrm{Nm}^3 \text{ of } H_2O$$

and

$$\frac{3.76\times 22.412}{4.032} = 20.9\,\mathrm{Nm}^3 \text{ of } N_2.$$

Combustion of 1 kg of sulfur produce

$$\frac{22.412}{32.06} = 0.0699\,\mathrm{Nm}^3 \text{ of } SO_2$$

and

$$\frac{3.76\times 22.412}{32.06} = 2.628\,\mathrm{Nm}^3 \text{of } N_2.$$

Moreover, as we know, 1 kg of water in the fuel equals 1.244 Nm^3 of steam in the flue gas. Thus, for 1 kg of fuel we have

$$\begin{aligned} CO_2 &= 0.84 \times 1.8661 = 1.5675\,Nm^3 \\ H_2O &= 0.12 \times 11.117 + 0.00124 = 1.3353\,Nm^3 \\ SO_2 &= 0.039 \times 0.699 = 0.0273\,Nm^3 \\ N_2 &= 0.84 \times 7.0166 = 5.8939 \\ &\quad 0.12 \times 20.9 = 2.5080 \\ &\quad 0.039 \times 2.628 = 0.1025 \\ &\quad \text{--------} \\ &\quad 8.5044\,Nm^3 \end{aligned}$$

Then

$$|CO_2|_{max} = \frac{1.5675 + 0.0273}{1.5675 + 0.0273 + 8.5044} 100 = 15.79\%.$$

With excess air of 20% ($n = 1.2$) for every kg of fuel oil, we have

$$\begin{aligned} CO_2 &= 1.5675\,Nm^3 \\ H_2O &= 1.3353\,Nm^3 \\ SO_2 &= 0.0273\,Nm^3 \\ N_2 &= 1.2 \times 8.5044 = 10.2053\,Nm^3 \\ O_2 &= \frac{0.2 \times 8.5044}{3.76} = 0.4524\,Nm^3 \end{aligned}$$

Therefore,

$$|CO_2| = \frac{1.5675 + 0.0273}{1.5675 + 0.0273 + 10.2053 + 0.4524} 100 = 13.02\%;$$

$$|O_2| = \frac{0.4524}{1.5675 + 0.0273 + 10.2053 + 0.4524} 100 = 3.69\%.$$

If the fuel contains only carbon, hydrogen, and sulfur, it is possible to obtain a general and easy equation to compute $|CO_2|$.

First of all, we know that the combustion of 1 kg of H_2 produces 11.117 Nm^3 of H_2O. Thus, based on (7.20) the amount of G'_v in terms of volume of dry flue gas in the absence of O_2, N_2, and H_2O, is given by

$$G'_v = nA_{tv} - 0.05558H \tag{7.30}$$

We also know that combustion of 1 kg of C produces 1.8661 Nm^3 of CO_2 and that combustion of 1 kg of S produces 0.699 Nm^3 of SO_2.

Therefore, $|CO_2|$ is given by

$$|CO_2| = \frac{1.8661\dfrac{C}{100} + 0.699\dfrac{S}{100}}{nA_{tv} - 0.05558H}. \tag{7.31}$$

This can be written as follows based on (7.9):

$$|CO_2| = \frac{1.8661C + 0.699S}{n(0.08882C + 0.03327S) + (0.26453n - 0.05558H)}. \tag{7.32}$$

C, S, and H are the mass percentages of the three components.

If the content of S can be neglected or assimilated to the carbon by approximation, $C = 100 - H$ and through a series of steps we obtain the following equation:

$$|CO_2| = \frac{186.61 - 1.8661H}{8.882n + \dfrac{(17.571n - 5.558)H}{100}}. \tag{7.33}$$

Table 7.1 was built based on (7.33).

The mass content of hydrogen in methane is slightly higher than 25%. The table indicates the same values of $|CO_2|$ directly computed above.

As far as the fuel oil discussed earlier, with $H = 12\%$ for $n = 1$ the table indicates that $|CO_2| = 15.91\%$, whereas through direct calculation the value was equal to 15.79%. For $n = 1.2$ the table indicates that $|CO_2| = 13.11\%$, whereas direct calculation lead to a value of 13.02%. Note that even considering sulfur like carbon the values obtained from the table match reality (for the examined fuel oil the mistakes are below 0.8%).

So far we assumed complete combustion as it should be to prevent considerable reduction in generator efficiency. In fact, if combustion is complete, the combustion of 1 kg of C frees 33830 kJ that correspond to the net heat value of carbon. But if

Table 7.1 $|CO_2|$ value in the flue gas (%)

H	*n*							
%	1.00	1.05	1.10	1.15	1.20	1.25	1.30	1.35
0	21.01	20.01	19.10	18.27	17.51	16.81	16.16	15.56
2	20.05	19.08	18.20	17.40	16.67	16.00	15.38	14.80
4	19.13	18.20	17.36	16.59	15.88	15.24	14.64	14.09
8	17.44	16.58	15.79	15.08	14.43	13.83	13.28	12.77
10	16.66	15.82	15.07	14.38	13.75	13.18	12.65	12.16
12	15.91	15.10	14.38	13.72	13.11	12.56	12.06	11.59
14	15.19	14.42	13.72	13.08	12.51	11.98	11.49	11.04
16	14.51	13.76	13.09	12.48	11.93	11.42	10.95	10.52
18	13.86	13.14	12.49	11.91	11.37	10.89	10.44	10.03
20	13.23	12.54	11.92	11.36	10.85	10.38	9.95	9.56
22	12.63	11.97	11.37	10.83	10.34	9.89	9.48	9.10
24	12.05	11.42	10.85	10.33	9.86	9.43	9.04	8.67
26	11.50	10.89	10.34	9.85	9.40	8.99	8.61	8.26

carbon is combined with oxygen to form CO, this combustion product keeps for every Nm^3 one net heat value equal to 12,644 kJ. This heat that was not developed by combustion goes to waste with the gas exiting the generator.

Thus, if $|CO|$ represents the volumetric percentage of carbon monoxide in dry flue gas, by indicating the volume of the latter per kg or per Nm^3 of fuel containing G'_v, the corresponding loss of heat is equal to

$$q = G'_v \frac{|CO|}{100} \times 12,644. \tag{7.34}$$

q is expressed as kJ/kg or kJ/Nm^3 if G'_v is expressed as Nm^3/kg or Nm^3/Nm^3, respectively.

The heat loss as percentage for unburned carbon monoxide is therefore given by

$$L_{CO} = \frac{q}{H_n} \times 100 \tag{7.35}$$

where the net heat value H_n is expressed as kJ/kg or kJ/Nm^3 as the lost heat q, respectively.

In order to highlight the great influence of unburned carbon monoxide on generator efficiency, we refer to a practical example. Let us still consider fuel oil that was already discussed earlier. Considering both solid and liquid fuels and recalling that combustion of 1 kg of H_2 produces 11.117 Nm^3 of H_2O, based on (7.20) the theoretical amount of dry flue gas G'_{tv} is given by

$$G'_{tv} = A_{tv} - 0.05558H + 0.007O + 0.008N \text{ Nm}^3/\text{kg} \tag{7.36}$$

On the other hand, the actual amount of dry flue gas is given by

$$G'_v = G'_{tv} + (n-1)A_{tv}. \tag{7.37}$$

For the fuel oil in question based on (7.9), we obtain

$$A_{tv} = 0.08882 \times 84 + 0.26453 \times 12 + 0.03327 \times 3.9 = 10.765 \text{ Nm}^3/\text{kg}.$$

Moreover, based on (7.36),

$$G'_{tv} = 10.765 - 0.05558 \times 12 = 10.098 \text{ Nm}^3/\text{kg}.$$

For sake of argument we disregard the increase in volume of gas that occurs during production of unburned flue gas (see Sect. 9.3) that does not impact G'_{tv} significantly for modest values of $|CO|$.

Assuming that $n = 1.20$ based on (7.37), we have

$$G'_v = 10.098 + 0.2 \times 10.765 = 12.251 \text{ Nm}^3/\text{kg}.$$

If the net heat value is equal to 40,450 kJ/kg, thus corresponding to the considered fuel oil based on (7.34) and (7.35), for every percentage point of $|CO|$ we have

$$q = 12.251 \times \frac{1}{100} \times 12,644 = 1549\,\text{kJ/kg}$$

$$L_{\text{CO}} = \frac{1549}{40,450} \times 100 = 3.83\%$$

As you can see, for every percentage point of |CO| 3.8 points of generator efficiency are lost. They correspond to about half the loss due to sensible heat of the flue gas in an industrial generator equipped with an economizer or air heater or both, or to 38% of all losses of a generator with an efficiency of 90%. It is crucial to prevent the presence of unburned carbon monoxide by adequately increasing the amount of combustion air.

As we discussed earlier, even an increase in air provokes a reduction in efficiency, but its influence is basically much more modest than the one caused by the presence of CO in the combustion products. This is highlighted even by the following gross calculation. The amount of flue gas can be assumed to be about proportional to the air index n if the latter does not vary considerably [note (7.18) as well as the fact that for fuel oil $A_{\text{tm}} = 13 - 14.5\,\text{kg/kg}$]. In an industrial generator with an efficiency of about 90%, the loss due to sensible heat is approximately 8–8.5%.

Now, if we assume that the temperature of the combustion products at the exit of the generator does not vary with n (of course, it is not true but may be assumed by approximation with limited variations of n), the loss due to sensible heat is proportional to G_{m} and consequently of n as far as stated. An increase in n of just 13% [going from (1.15) to (1.30)], which is a lot, leads to an increase in heat losses and the equivalent efficiency reduction of $0.13 \times 8 \approx 1\%$. Thus, we are quite far from an efficiency reduction caused by the presence of only 1% of CO in the flue gas (with $|CO_2|$ for complete combustion equal to 13%, which means that about 7.5% of carbon is not completely burned).

In terms of analytical methodology, we point out that the classic machine to measure $|CO_2|, |O_2|$, and |CO| is the Orsat apparatus by absorption.

Besides the Orsat, there are other such machines with direct or registered reading. Electro-physical machines based on the variation in thermal conductivity of gas connected to variations in the content of CO_2 and CO are also employed. The combustion products are introduced in a cell containing platinum threads heated by a battery in order to build a Wheaston bridge of great sensibility. Their composition impacts the heating of the threads, thus their electric resistance registered by a galvanometer to trace back the content of CO_2 and CO. The measurements can be occasional or on-going. In the second case the measured values are stored on taping machines.

7.8 Test of the Air Index During Runtime

The determination of the air index during runtime of the generator is essential to evaluate the loss due to sensible heat and the efficiency of the generator computed through the indirect method (see Sect. 9.4 and 9.7). In fact, to compute the loss due

to sensible heat it is necessary to determine the value of G, thus the value of the air index, as highlighted by the different equations in Sect. 7.6. To that extent it is possible to use various exact or approximate equations to compute n as a function of the data delivered by the analysis of the flue gas. The most famous one is obtained as follows, under the assumption that there is no unburned carbon monoxide.

If G'_{tv} is the minimum amount of dry flue gas, that is, the one corresponding to the combustion with theoretic air and G'_{v} the dry actual gas, and if CO_2 and SO_2 represent the volume of carbon dioxide and sulfur dioxide, the maximum value of $|CO_2|$ is given by

$$|\mathrm{CO_2}|_{\max} = \frac{\mathrm{CO_2}\,(+\mathrm{SO_2})}{G'_{\mathrm{tv}}} \times 100. \tag{7.38}$$

By analogy, the actual value of $|CO_2|$ is given by:

$$|\mathrm{CO_2}| = \frac{\mathrm{CO_2}\,(+\mathrm{SO_2})}{G'_{\mathrm{v}}} \times 100. \tag{7.39}$$

Here is equation (7.36) again in reference to both solid and liquid fuels.

$$G'_{\mathrm{tv}} = A_{\mathrm{tv}} - 0.05558\mathrm{H} + 0.007\mathrm{O} + 0.008\,\mathrm{N}\ \mathrm{Nm^3/kg}. \tag{7.40}$$

Similarly, in the case of gaseous fuels the combustion of $1\,\mathrm{Nm^3}$ of H_2 produces $1\,\mathrm{Nm^3}$ of H_2O, and $1\,\mathrm{Nm^3}$ of C_mH_n produces $n/2\,\mathrm{Nm^3}$ of H_2O. On the basis of (7.24)

$$G'_{\mathrm{tv}} = A_{\mathrm{tv}} + 1 - 0.005(\mathrm{CO} + 3\mathrm{H_2}) - 0.0025\sum_i (n_i + 4)\mathrm{C}_{mi}\mathrm{H}_{ni}. \tag{7.41}$$

Recalling (7.37) based on (7.38) and (7.39), we obtain

$$\frac{G'_{\mathrm{v}}}{G'_{\mathrm{tv}}} = 1 + (n-1)\frac{A_{\mathrm{tv}}}{G'_{\mathrm{tv}}} = \frac{|\mathrm{CO_2}|_{\max}}{|\mathrm{CO_2}|}. \tag{7.42}$$

Then

$$n = 1 + \left(\frac{|\mathrm{CO_2}|_{\max}}{|\mathrm{CO_2}|} - 1\right)\frac{G'_{\mathrm{tv}}}{A_{\mathrm{tv}}}. \tag{7.43}$$

From (7.40) about solid and liquid fuels

$$\frac{G'_{\mathrm{tv}}}{A_{\mathrm{tv}}} = 1 - \frac{0.05558\mathrm{H} - 0.007\mathrm{O} - 0.008\mathrm{N}}{A_{\mathrm{tv}}}; \tag{7.44}$$

and for gaseous fuels from (7.41)

$$\frac{G'_{\mathrm{tv}}}{A_{\mathrm{tv}}} = 1 - \frac{0.005\,(\mathrm{CO} + 3\mathrm{H_2}) + 0.0025\sum_i (n_i + 4)\,\mathrm{C}_{mi}\mathrm{H}_{ni} - 1}{A_{\mathrm{tv}}}. \tag{7.45}$$

Basically, the value of $G'_{\text{tv}}/A_{\text{tv}}$ is close to unity for almost all fuels.

As an example for methane we have

$$A_{\text{tv}} = 9.52\,\text{Nm}^3/\text{Nm}^3$$
$$G'_{\text{tv}} = 9.52 + 1 - 0.0025 \times 8 \times 100 = 8.52\,\text{Nm}^3/\text{Nm}^3$$
$$\frac{G'_{tv}}{A_{tv}} = \frac{8.52}{9.52} = 0.895$$

Refer to Sect. 7.7 for the fuel oil with $A_{\text{tv}} = 10.765\,\text{Nm}^3/\text{kg}$.

$$G'_{\text{tv}} = 10.765 - 0.05558 \times 12 = 10.098\,\text{Nm}^3/\text{kg}$$
$$\frac{G'_{\text{tv}}}{A_{\text{tv}}} = \frac{10.098}{10.765} = 0.938$$

Thus, it is an acceptable mistake to substitute $G'_{\text{tv}}/A_{\text{tv}}$ with the unity, and on the basis of (7.43) we have

$$n = \frac{|\text{CO}_2|_{\max}}{|\text{CO}_2|} \tag{7.46}$$

The mistakes made using (7.46) are modest. In the cases discussed above, one would obtain $n = 11.75/10 = 1.175$ instead of 1.15 with an error equal to 2% for methane and $n = 15.79/13.02 = 1.213$ instead of 1.20 with an error of 1% for fuel oil.

Knowing the $|\text{CO}_2|_{\max}$ content of a given fuel and the experimental measurement of $|\text{CO}_2|$ of the combustion products in the absence of unburned material leads to the rapid calculation of n through (7.46). On the other hand, note that (7.46) is cause for considerable errors if the fuel is rich in hydrogen and carbon monoxide. For instance, for hydrogen with $n = 1.2$, the mistake is in excess of 3.6%, whereas in the case of carbon monoxide and $n = 1.2$ the mistake will come short by 3.4%. Moreover, (7.46) cannot be used if the fuel is rich in nitrogen. In fact, in the case of blast-furnace gas and a volumetric percentage of nitrogen of about 60% the ratio $G'_{\text{tv}}/A_{\text{tv}}$ is about equal to 1.9. This means that the simplification of (7.43) leading to (7.46) can never be used.

In conclusion, (7.46) can be used in most cases except for fuels rich in nitrogen, including some reservation for those rich in H_2 and CO. Up to this point the combustion of carbon was assumed to be complete. In the presence of unburned carbon monoxide, it is necessary to proceed as explained below.

If CO_2^* indicates the amount of CO_2 present in flue gas with complete combustion of the carbon, we know that

$$|\text{CO}_2|_{\max} = \frac{\text{CO}_2^*}{G'_{\text{tv}}} \times 100. \tag{7.47}$$

The buildup of CO in the flue gas can be ideally regarded as a dissociation of carbon dioxide in carbon monoxide and oxygen, according to the reaction

$$2\text{CO}_2 = 2\text{CO} + \text{O}_2. \tag{7.48}$$

On the basis of (7.48), the amount of carbon dioxide in flue gas with unburned carbon monoxide is therefore given by

$$\mathrm{CO_2} = \mathrm{CO_2^*} - \mathrm{CO}. \tag{7.49}$$

And, by definition

$$|\mathrm{CO_2}| = \frac{\mathrm{CO_2}}{G'_\mathrm{v}} \times 100 = \frac{\mathrm{CO_2^*}}{G'_\mathrm{v}} \times 100 - \frac{\mathrm{CO}}{G'_\mathrm{v}} \times 100. \tag{7.50}$$

Recalling (7.47) and keeping in mind that

$$|\mathrm{CO}| = \frac{\mathrm{CO}}{G'_\mathrm{v}} \times 100, \tag{7.51}$$

it follows that

$$|\mathrm{CO_2}| = |\mathrm{CO_2}|_{\max} \frac{G'_\mathrm{tv}}{G'_\mathrm{v}} - |\mathrm{CO}|. \tag{7.52}$$

Then

$$\frac{G'_\mathrm{v}}{G'_\mathrm{tv}} = \frac{|\mathrm{CO_2}|_{\max}}{|\mathrm{CO_2}| + |\mathrm{CO}|} \tag{7.53}$$

If combustion is incomplete, based on (7.48) we determine that in flue gas the buildup of CO is matched by a volume of oxygen equal to half the volume of carbon monoxide.

Thus, instead of (7.37)

$$G'_\mathrm{v} = G'_\mathrm{tv} + (n-1)A_\mathrm{tv} + 0.5\mathrm{CO}; \tag{7.54}$$

and based on (7.53)

$$\frac{|\mathrm{CO_2}|_{\max}}{|\mathrm{CO_2}| + |\mathrm{CO}|} = 1 + (n-1)\frac{A_\mathrm{tv}}{G'_\mathrm{tv}} + 0.5\frac{\mathrm{CO}}{G'_\mathrm{tv}}. \tag{7.55}$$

On the other hand, based on (7.51) and (7.53):

$$\frac{CO}{G'_{tv}} = \frac{CO}{G'_v}\frac{|CO_2|_{\max}}{|CO_2| + |CO|} = \frac{|CO|}{100}\frac{|CO_2|_{\max}}{|CO_2| + |CO|}. \tag{7.56}$$

Thus, from (7.55)

$$(n-1)\frac{A_\mathrm{tv}}{G'_\mathrm{tv}} = \frac{|\mathrm{CO_2}|_{\max}}{|\mathrm{CO_2}| + |\mathrm{CO}|}\left(1 - 0.5\frac{|\mathrm{CO}|}{100}\right) - 1. \tag{7.57}$$

Finally,

$$n = 1 + \left[\frac{|\mathrm{CO_2}|_{\max}}{|\mathrm{CO_2}| + |\mathrm{CO}|}\left(1 - 0.5\frac{|\mathrm{CO}|}{100}\right) - 1\right]\frac{G'_\mathrm{tv}}{A_\mathrm{tv}}. \tag{7.58}$$

As usual, considering the term G'_{tv}/A_{tv} equal to unity, in the end from (7.58) we obtain

$$n = \frac{|CO_2|_{max}}{|CO_2| + |CO|}\left(1 - 0.5\frac{|CO|}{100}\right). \tag{7.59}$$

This way (7.59) substitutes (7.46) whenever there is unburned carbon monoxide.

Given that the value of $|CO|$ is always rather small, by first approximation it is possible to use even the following equation:

$$n = \frac{|CO_2|_{max}}{|CO_2| + |CO|}. \tag{7.60}$$

The use of the equations in question requires knowing $|CO_2|_{max}$. It is possible to compute n regardless of its quantity through two other equations that only use the data from the gas analysis. The first is an equation by approximation like the ones used so far, and it can be obtained by admitting the presence of unburned carbon monoxide.

The amount of free oxygen in flue gas, given that there is 21% of oxygen in the air and recalling (7.48), is as follows:

$$O_2 = (n-1)A_{tv}\frac{21}{100} + 0.5CO. \tag{7.61}$$

By definition

$$|O_2| = \frac{O_2}{G'_v} \times 100; \tag{7.62}$$

and based on (7.61) and (7.54):

$$|O_2| = \frac{21\,(n-1)A_{tv} + 50CO}{G'_{tv} + (n-1)A_{tv} + 0.5CO}. \tag{7.63}$$

Going through a series of steps based on (7.63), we obtain

$$n - 1 = \frac{|O_2|\left(1 + 0.5\frac{|CO|}{100}\frac{G'_v}{G'_{tv}}\right) - 0.5\,|CO|\,\frac{G'_v}{G'_{tv}}}{21 - O_2}\frac{G'_{tv}}{A_{tv}}. \tag{7.64}$$

Then

$$n = \frac{21 - 0.5\,|CO|\left(1 - \frac{|O_2|}{100}\right)\frac{G'_v}{G'_{tv}}}{21 - |O_2|}\frac{G'_{tv}}{A_{tv}}. \tag{7.65}$$

As usual, considering the term G'_{tv}/A_{tv} to be equal to the unity and keeping in mind that the second term in the numerator is quite small compared with 21, by ignoring the term G'_v/G'_{tv} we obtain:

$$n = \frac{21 - 0.5\,|CO|\left(1 - \frac{|O_2|}{100}\right)}{21 - |O_2|}. \tag{7.66}$$

Thus, (7.66) is an equation by approximation. The fact that it is able to disregard $|CO_2|_{max}$ is an advantage. It is based, though, on knowing $|O_2|$ which is harder to determine numerically than $|CO_2|$.

If there is no unburned carbon monoxide, (7.66) is reduced to the following:

$$n = \frac{21}{21 - |O_2|}. \tag{7.67}$$

Equations (7.66) and (7.67) may generally be used except in the case of fuels rich in nitrogen and with some reservation with those rich in H_2 and CO.

The second equation ignoring $|CO_2|_{max}$ can be obtained as shown below. We know that the volumetric content of oxygen in the air is equal to 21%, whereas the nitrogen amounts to 79%. In addition, free oxygen in flue gas is proportional to the excess air, while the amount of nitrogen is proportional to all the combustion air. Thus, with reference to (7.48) we may write that

$$|O_2| = \frac{n-1}{n}\frac{21}{79}|N_2| + 0.5|CO|; \tag{7.68}$$

then

$$3.76n(|O_2| - 0.5|CO|) = (n-1)|N_2|. \tag{7.69}$$

On the other hand,

$$|CO_2| + |N_2| + |O_2| + |CO| = 100. \tag{7.70}$$

Thus,

$$3.76n(|O_2| - 0.5|CO|) = (n-1)(100 - |CO_2| - |O_2| - |CO|). \tag{7.71}$$

Finally,

$$n = \frac{100 - |CO_2| - |O_2| - |CO|}{100 - |CO_2| - 4.76|O_2| + 0.88|CO|}. \tag{7.72}$$

In contrast to the previous ones, (7.72) is exact and therefore preferable. Moreover, it is always valid for fuels rich in H_2 and CO. Even in this case the fuels rich in nitrogen are an exception because (7.68) is true only if the nitrogen contained in the flue gas comes from the air and not from the fuel. Modest percentages of N_2 in the fuel are cause for tolerable errors. For instance, in the case of coke-oven gas containing 10% of N_2, (7.72) will underestimate n that is under 1%.

In the absence of unburned monoxide, (7.72) is reduced to the following:

$$n = \frac{100 - |CO_2| - |O_2|}{100 - |CO_2| - 4.76|O_2|}. \tag{7.73}$$

In conclusion, generally the computation of n through (7.72) is less influenced by measurement mistakes. Leaving out the details and in contrast to previous equations, note that the value of n depends on two quantities ($|CO_2|$ and $|O_2|$). The possibility exists that errors in their measurement are of opposite sign, thus annulling themselves, at least partially. This finding combined with the knowledge that the equation is exact, confirms why it is preferable compared to others.

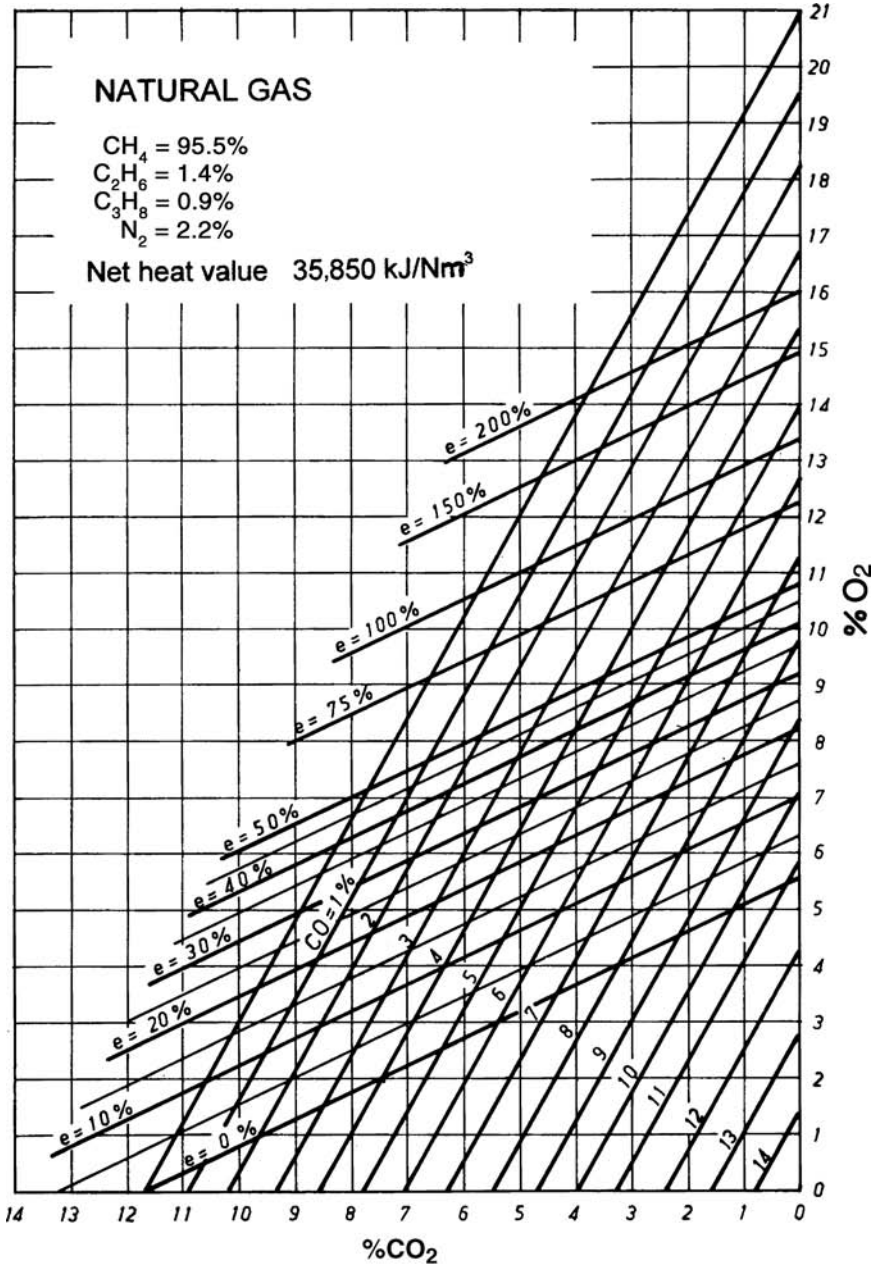


Fig. 7.25 Ostwald's triangle for natural gas

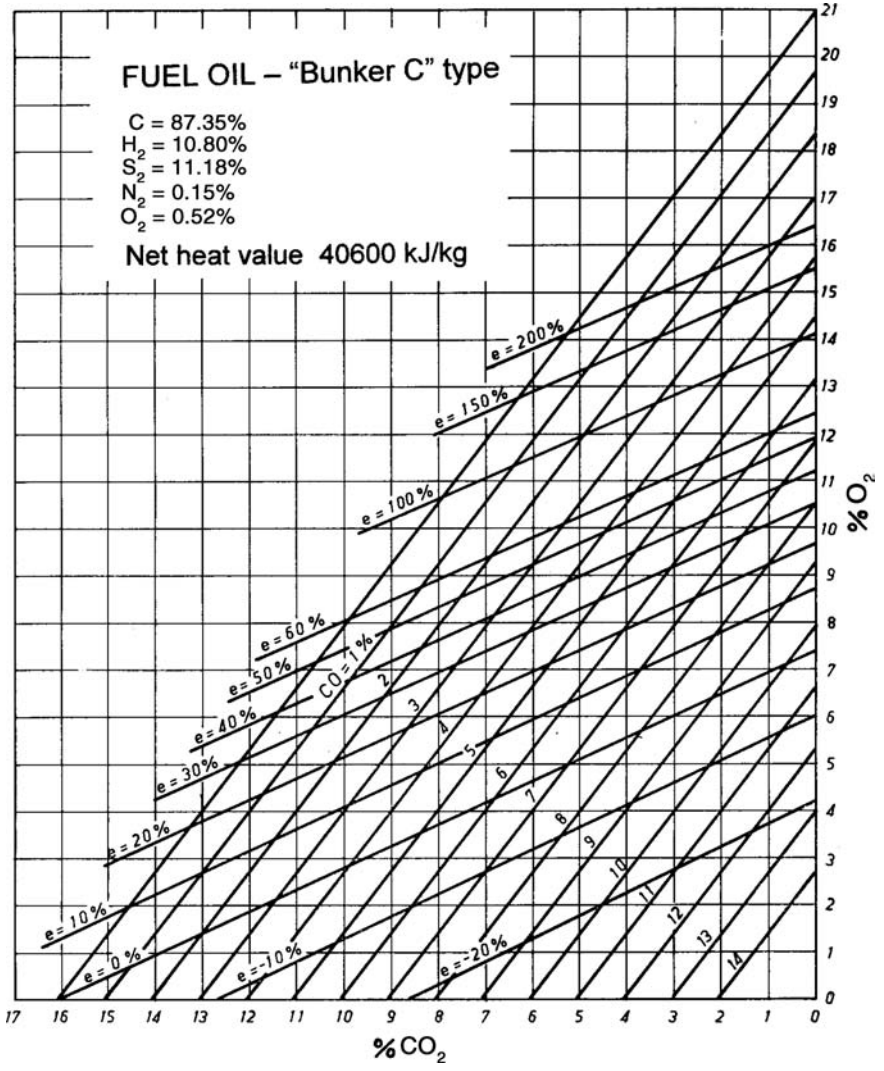


Fig. 7.26 Ostwald's triangle for fuel oil

Equation (7.72) may also be written like this:

$$n = \frac{1}{1 - \dfrac{3.76\,(|O_2| - 0.5\,|CO|)}{100 - (|CO_2| + |O_2| + |CO|)}}. \tag{7.74}$$

Many scholars developed special diagrams to determine n or the excess air graphically (Bunte, Ackermann, Ostwald). The most well-known and used models were designed according to Ostwald's criteria, and because of their shape, they are called Ostwald's triangles.

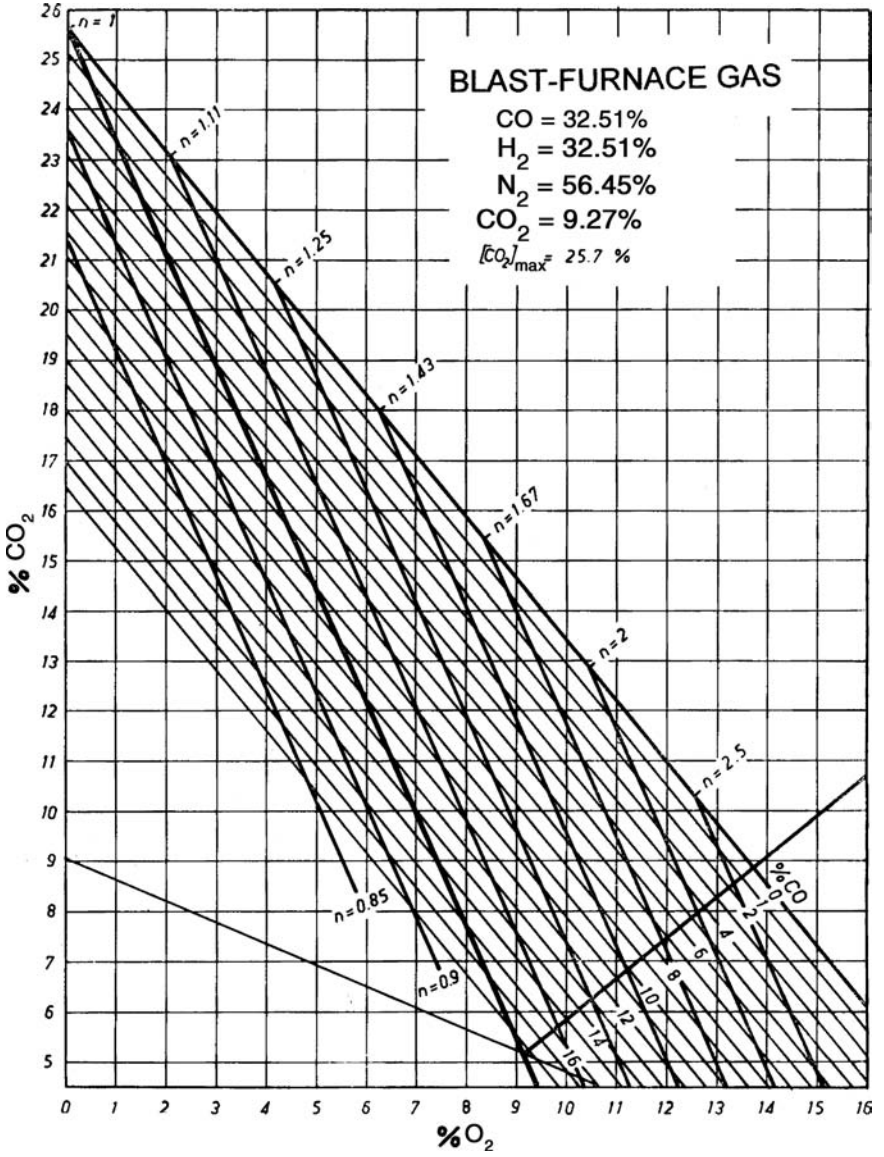


Fig. 7.27 Ostwald's triangle for blast-furnace gas

Figures 7.25, 7.26, and 7.27 show an example of triangles relative to fuel oil Bunker C, to natural gas, and to blast-furnace gas.

The diagram is to be used as follows.

On the basis of the contents value of CO_2 and O_2, one identifies a point on the diagram that may or not be on the straight line so that the content of CO is zero. In the first case combustion is complete, and depending on the position of the point, the value of excess air or air index can be read. In the second case combustion is incomplete, and the diagram helps to evaluate both the excess air and the percentage of CO. Therefore, these diagrams are easy to use and make it possible to trace back the value of n and also the potential value of $|\mathrm{CO}|$ without having to measure the carbon monoxide directly. They are actually unique to every specific fuel. Their employment for similar type fuels, for example, fuel oils of different composition, is acceptable only by initial approximation.

7.9 Physical Characteristics of Air and Flue Gas

7.9.1 Density

The density of the air under normal conditions is equal to $1.293\,\mathrm{kg/Nm^3}$. As far as flue gas it is given by

$$\rho_0 = \frac{G_\mathrm{m}}{G_\mathrm{v}}. \tag{7.75}$$

G_m and G_v are computed through (7.18) and (7.20) or through (7.25) and (7.24).

If we refer to the mass unit of the fuel, and if the fuel is a mix of hydrocarbons, based on (7.18) and (7.20):

$$\rho_0 = \frac{nA_\mathrm{tm} + 1}{nA_\mathrm{tv} + 0.05558\mathrm{H}} \tag{7.76}$$

where H is the mass percentage of the hydrogen.

Given the density of the air from (7.76), we obtain the following:

$$\rho_0 = \frac{nA_\mathrm{tm} + 1}{\dfrac{nA_\mathrm{tm}}{1.293} + 0.05558\mathrm{H}}. \tag{7.77}$$

Finally,

$$\rho_0 = 1.293\frac{nA_\mathrm{tm} + 1}{nA_\mathrm{tm} + 0.071865\mathrm{H}}. \tag{7.78}$$

We determine that the density of flue gas is greater or smaller than air density, depending on whether H is above or below 13.9%. In the case of flue gas from coal or fuel oil, it is greater than the air density (with fuel oil only slightly greater), whereas from natural gas the density of flue gas is less than the air density.

Table 7.2 Flue gas density under normal conditions (kg/Nm^3)

H	n			
%	1.0	1.1	1.2	1.3
0	1.4056	1.3954	1.3868	1.3796
5	1.3568	1.3512	1.3464	1.3424
10	1.3181	1.3160	1.3141	1.3126
15	1.2867	1.2872	1.2877	1.2881
20	1.2606	1.2633	1.2656	1.2676
25	1.2387	1.2432	1.2470	1.2503

Considering that, as expected, the fuel is a mix of hydrocarbons $C = 100 - H$ (where C is the mass percentage of carbon); thus, based on (7.8)

$$\rho_0 = 1.293 \frac{11.484n + 1 + 0.2272n\mathrm{H}}{11.484n + (0.2272n + 0.071865)\,\mathrm{H}}. \tag{7.79}$$

Table 7.2 is based on (7.79).

Note that (7.79) or Table 7.2 can also be used for fuels containing other components besides carbon and hydrogen. For instance, for fuel oil with $C = 84\%$, $H = 12\%, S = 4\%$, and $n = 1.2$, from (7.79) we obtain $\rho_0 = 1.3029\,\mathrm{kg/Nm^3}$, while the actual density is equal to $1.3031\,\mathrm{kg/Nm^3}$. The difference is irrelevant. As far as density under other than normal conditions, both the air and the flue gas may be considered as perfect gas. Thus, the density is directly proportional to absolute pressure and inversely proportional to absolute temperature.

7.9.2 Specific Isobaric Heat

Specific isobaric heat of the different types of gas and of steam can be expressed with sufficient approximation as a function of the temperature through an equation of this type:

$$c_p = X + Y\frac{t}{1000} + Z\left(\frac{t}{1000}\right)^2 \tag{7.80}$$

with temperature t in °C.

The range of temperature of air that is of interest from a practical point of view goes from 0 to 300°C; therefore,

$$c_{pa} = 1003.79 + 75.53\frac{t}{1000} + 216\left(\frac{t}{1000}\right)^2 \tag{7.81}$$

with c_{pa} in J/kgK.

To reach the specific heat of the flue gas it is possible to proceed as follows.

By examining the values of the specific heat of the air (we shall see that it is crucial in terms of the flue gas, as well), the carbon dioxide, the oxygen, and the steam

Table 7.3 Values of X, Y, and Z for the specific isobaric heat

	X	Y	Z	Error (%)
Dry air	997.69	186.68	0	± 0.8
CO_2	823.28	878.32	−416.13	± 1.1
H_2O	1838.82	503.40	115.72	± 0.6
O_2	901.97	367.55	−147.38	± 0.6

between 50 and 1200°C, we determine that using the values X, Y, and Z shown in the Table 7.3 reduces the errors plus or minus to a minimum with respect to the experimental values taken from the publication by Schack cited in the bibliography. The biggest errors are listed on the side of the table.

The mass M_c of carbon dioxide produced by the combustion of 1 kg of fuel where C stands for the mass percentage of carbon is equal to:

$$M_c = \frac{12.01+32}{12.01}\frac{C}{100} = 0.03664C. \tag{7.82}$$

Similarly, indicating the mass of H_2O produced by combustion of 1 kg of fuel as M_h where H is the mass percentage of hydrogen, we have

$$M_h = \frac{2\times 1.008+16}{2\times 1.008}\frac{H}{100} = 0.08936H. \tag{7.83}$$

The mass of oxygen M_o^* necessary for combustion of carbon and hydrogen is given by

$$M_o^* = \frac{32}{12.01}\frac{C}{100} + \frac{16}{2\times 1.008}\frac{H}{100} = 0.02664C + 0.07936H. \tag{7.84}$$

The mass of free oxygen in the flue gas indicated by M_o is therefore given by

$$M_o = (n-1)M_o^*. \tag{7.85}$$

Finally, if M_n^* is the mass of nitrogen corresponding to theoretical combustion, the mass of nitrogen M_n actually present in flue gas is equal to

$$M_n = nM_n^*. \tag{7.86}$$

The specific heat of flue gas referred to the mass unity is equal to the weighted average of the specific heat of all components. If the fuel is a mix of hydrocarbons, and the specific heat of carbon dioxide, steam, oxygen, and nitrogen are indicated as $c_{pc}, c_{ph}, c_{po}, c_{pn}$, respectively, the specific heat c_{pg} of flue gas is given by:

$$c_{pg} = \frac{M_c c_{pc} + M_h c_{ph} + M_o c_{po} + M_n c_{pn}}{G_m}. \tag{7.87}$$

Based on (7.85) and (7.86), we have

$$M_{\mathrm{o}}c_{po}+M_{\mathrm{n}}c_{pn}=(n-1)M_{\mathrm{o}}^{*}c_{po}+nM_{\mathrm{n}}^{*}c_{pn}=n\left(M_{\mathrm{o}}^{*}c_{po}+M_{\mathrm{n}}^{*}c_{pn}\right)-M_{\mathrm{o}}^{*}c_{po}. \quad (7.88)$$

If the specific heat of the air is c_{pa}, then

$$c_{pa}=\frac{M_{\mathrm{o}}^{*}c_{po}+M_{\mathrm{n}}^{*}c_{pn}}{A_{\mathrm{tm}}}. \quad (7.89)$$

Thus, in reference to (7.18), (7.87) may be written as follows:

$$c_{pg}=\frac{nA_{\mathrm{tm}}c_{pa}+M_{\mathrm{c}}c_{pc}+M_{\mathrm{h}}c_{ph}-M_{\mathrm{o}}^{*}c_{po}}{nA_{\mathrm{tm}}+1}, \quad (7.90)$$

or

$$c_{pg}=\frac{nA_{\mathrm{tm}}c_{pa}+K}{nA_{\mathrm{tm}}+1}. \quad (7.91)$$

Given that from (7.81), (7.83), and (7.84):

$$K=(0.03664c_{pc}-0.02664c_{po})C+\left(0.08936c_{ph}-0.07936c_{po}\right)H. \quad (7.92)$$

The specific heat $c_{pa},c_{pc},c_{ph},c_{po}$ is computed using the same equation (7.80) with different values of X, Y, and Z. Thus, through (7.80) it is possible to compute the specific heat c_{pg} of the flue gas by calculating the corresponding values of X,Y, and Z.

If we indicate with $X_{\mathrm{a}},X_{\mathrm{c}},X_{\mathrm{h}},X_{\mathrm{o}}$ the values of X for air, CO_2, H_2O, O_2, based on (7.91), the value X relative to the flue gas that we indicate with X_{g}, is given by:

$$X_{\mathrm{g}}=\frac{nA_{\mathrm{tm}}X_{\mathrm{a}}+K_X}{nA_{\mathrm{tm}}+1} \quad (7.93)$$

given that

$$K_X=(0.03664X_{\mathrm{c}}-0.02664X_{\mathrm{o}})C+(0.08936X_{\mathrm{h}}-0.07936X_{\mathrm{o}})H. \quad (7.94)$$

Based on the values of X of Table 7.3 relative to air, CO_2, H_2O, and O_2

$$X_{\mathrm{g}}=\frac{997.69nA_{\mathrm{tm}}+6.137C+92.737H}{nA_{\mathrm{tm}}+1}. \quad (7.95)$$

Similarly, as far as the factors Y_{g} and Z_{g} relative to the flue gas, we obtain the following equations through the values Y and Z of Table 7.3:

$$Y_{\mathrm{g}}=\frac{186.68nA_{\mathrm{tm}}+22.391C+15.785H}{nA_{\mathrm{tm}}+1}; \quad (7.96)$$

$$Z_{\mathrm{g}}=\frac{-11.321C+22.037H}{nA_{\mathrm{tm}}+1}. \quad (7.97)$$

Based on the previous assumption, $C = 100 - H$; from (7.8) we have

$$A_{\mathrm{tm}} = 11.484 + 0.2272H. \tag{7.98}$$

From (7.95–7.97), we obtain

$$X_{\mathrm{g}} = \frac{11457.5n + 226.67nH + 613.7 + 86.6H}{11.484n + 1 + 0.2272nH}; \tag{7.99}$$

$$Y_{\mathrm{g}} = \frac{2143.83n + 42.414nH + 2239.1 - 6.606H}{11.484n + 1 + 0.2272nH}; \tag{7.100}$$

$$Z_{\mathrm{g}} = \frac{-1132.1 + 33.358H}{11.484n + 1 + 0.2272nH}. \tag{7.101}$$

At this point we introduce the mass moisture percentage of the flue gas. Indicating it with m and based on (7.83):

$$m = \frac{M_{\mathrm{h}}}{G_{\mathrm{m}}}100 = \frac{8.936H}{nA_{\mathrm{tm}} + 1}. \tag{7.102}$$

If the fuel contains only carbon and hydrogen as mentioned before, based on (7.102) and factoring in (7.98) we obtain

$$m = \frac{8.936H}{11.484n + 1 + 0.2272nH}. \tag{7.103}$$

In reference to equations (7.80), (7.99), (7.100), (7.101), and (7.103), the specific heat is a function of the air index, the moisture m in addition to temperature.

In fact, while moisture is crucial for the value of c_{pg}, the air index n has a very limited direct impact (of course, it impacts the value of m), as we shall discuss later on.

Therefore, it is possible to adopt a conventional average value of n; assuming $n = 1.2$, from (7.103) we obtain:

$$H = \frac{14.781m}{8.936 - 0.2726m}. \tag{7.104}$$

In addition, with $n = 1.2$

$$X_{\mathrm{g}} = \frac{14362.7 + 358.6H}{14.781 + 0.2726H}; \tag{7.105}$$

$$Y_{\mathrm{g}} = \frac{4811.7 + 44.291H}{14.781 + 0.2726H}; \tag{7.106}$$

$$Z_{\mathrm{g}} = \frac{-1132.1 + 33.358H}{14.781 + 0.2726H}. \tag{7.107}$$

Based on (7.103) and after through a series of steps:

$$X_g = \frac{128345.1 + 1385.2m}{132.083} = 971.7 + 10.49m; \tag{7.108}$$

$$Y_g = \frac{44.997.35 - 657.01m}{132.083} = 325.53 - 4.97m; \tag{7.109}$$

$$Z_g = \frac{-10116.44 + 801.67m}{132.083} = -(76.59 - 6.07m). \tag{7.110}$$

Therefore, based on (7.80) we have

$$c_{pg} = 971.7 + 10.49m + (325.53 - 4.97m)\frac{t}{1000} - (76.59 - 6.07m)\left(\frac{t}{1000}\right)^2 \tag{7.111}$$

with c_{pg} in J/kg K.

As far as the impact of the air index, assuming $n = 1.1$ instead of $n = 1.2$, the specific heat differs at 1000°C from the one computed through (7.111) in about $+0.2\%$. For $n = 1.3$ the difference is equal to about -0.2%. At lower temperatures the differences are smaller. These differences are of no importance, and (7.111) may be used for any practical value of n. Moreover, the condition requiring the fuel to be exclusively a mix of hydrocarbons can be overcome by adopting (7.111) for any fuel. Therefore, it is a question of computing the value of m in advance with the help of (7.102) (it is influenced by the value of n); through (7.111) and based on the temperature one obtains the value of c_{pg}. Equation (7.111) is shown in Fig. 7.28.

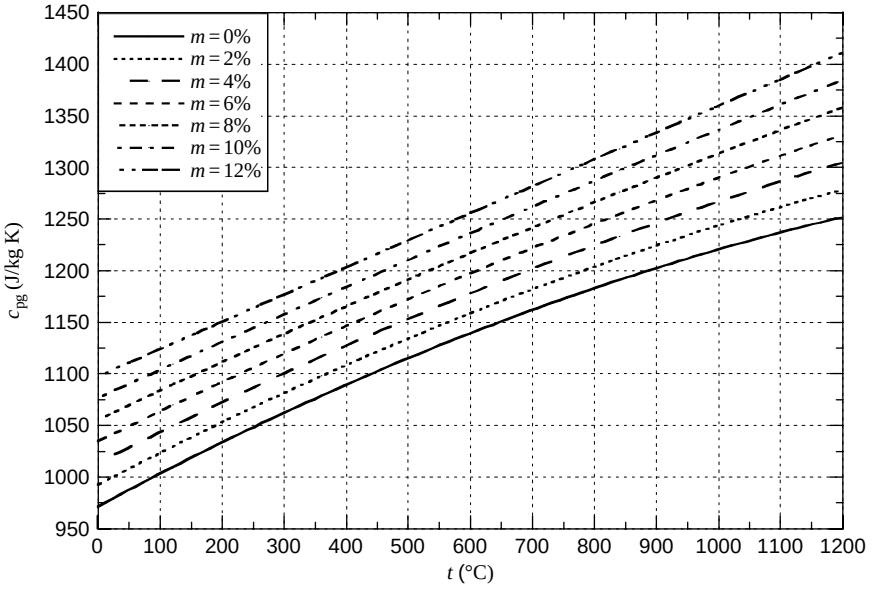


Fig. 7.28 Isobaric specific heat of flue gas

Until now we assumed that the steam contained in the flue gas originates only from combustion of the hydrogen in the fuel. In fact, a certain amount of steam comes from the air humidity. In order to factor this in, note that with a conventional value of the relative humidity in the air equal to 40% at 20°C, the content of H_2O in the air is equal to 0.0058 kg for every kg of air. The mass moisture percentage is thus equal to 0.58%. In the case of flue gas, the value of m caused by the air humidity is slightly lower than that value in the ratio of A_m/G_m. Conventionally, the moisture of flue gas can be considered to be increased by 0.5% compared with the one computed through (7.102). Finally, it is important to keep in mind that the fuel may contain H_2O. In that case it is necessary to add to the numerator of (7.102) the mass percentage of H_2O in the fuel.

7.9.3 Enthalpy

As well known, the enthalpy is given by

$$h = \int_0^t c_p \mathrm{d}t. \tag{7.112}$$

Expressing it in kJ/kg and in reference to (7.80), we generally have

$$h = X\frac{t}{1000} + \frac{Y}{2}\left(\frac{t}{1000}\right)^2 + \frac{Z}{3}\left(\frac{t}{1000}\right)^3. \tag{7.113}$$

Based on (7.81) and for air between 0 and 300°C, we have

$$h_\mathrm{a} = 1003.79\frac{t}{1000} + 37.76\left(\frac{t}{1000}\right)^2 + 72\left(\frac{t}{1000}\right)^3. \tag{7.114}$$

Equation (7.114) is shown in Fig. 7.29.

For fuel gas and based on (7.111):

$$\begin{aligned} h_\mathrm{g} = {} & (971.7 + 10.49m)\frac{t}{1000} + (162.76 - 2.49m)\left(\frac{t}{1000}\right)^2 \\ & - (25.53 - 2.023m)\left(\frac{t}{1000}\right)^3 \end{aligned} \tag{7.115}$$

Equation (7.115) is shown in Figs. 7.30, 7.31, and 7.32.

We determine that the enthalpy of any type of gas can be computed with sufficient approximation for practical application through the following equation, given that X, J, and W are characteristic factors of the gas in question.

$$h = X\frac{t}{1000} + J\left(\frac{t}{1000}\right)^2 + W\left(\frac{t}{1000}\right)^3 \tag{7.116}$$

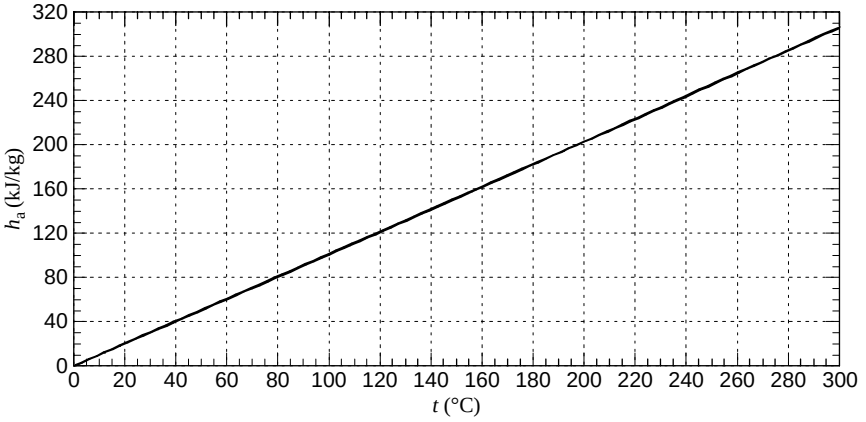


Fig. 7.29 Air enthalpy

Thus, if the mass composition of the flue gas is known, it is also possible to compute its enthalpy through the factors X_g, J_g, and W_g as follows:

$$X_g = \frac{P_1X_1 + P_2X_2 + P_3X_3 + \ldots}{100} \tag{7.117}$$

$$J_g = \frac{P_1J_1 + P_2J_2 + P_3J_3 + \ldots}{100} \tag{7.118}$$

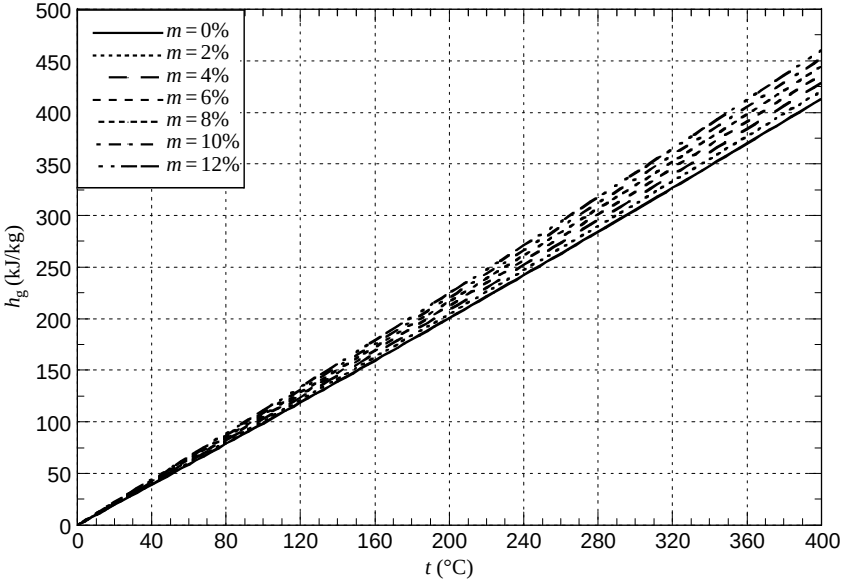


Fig. 7.30 Flue gas enthalpy

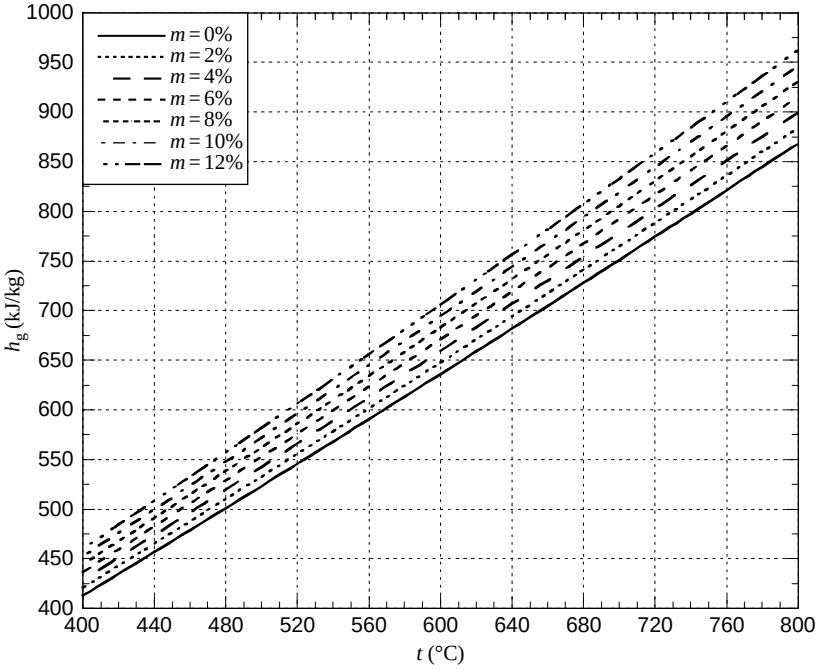


Fig. 7.31 Flue gas enthalpy

$$W_{\mathrm{g}} = \frac{P_1 W_1 + P_2 W_2 + P_3 W_3 + \ldots}{100} \tag{7.119}$$

$P_1, P_2, P_3 \ldots$ are the mass percentages of the different components, while $X_1, X_2, X_3 \ldots$, $J_1, J_2, J_3 \ldots, W_1, W_2, W_3 \ldots$ stand for the values of factors X, J, and W of the different components. They are shown in Table 7.4

7.9.4 Thermal Conductivity

As with specific heat, the thermal conductivity of the different types of gas and of steam may be expressed with sufficient approximation as follows:

$$k = X + Y\frac{t}{1000} + Z\left(\frac{t}{1000}\right)^2. \tag{7.120}$$

For air ranging from 0 to 300°C, that is, the temperature range of interest in practice, it is possible to adopt the following equation:

$$k_{\mathrm{a}} = 0.02326 + 0.06588\frac{t}{1000} \tag{7.121}$$

with k_a in W/mK.

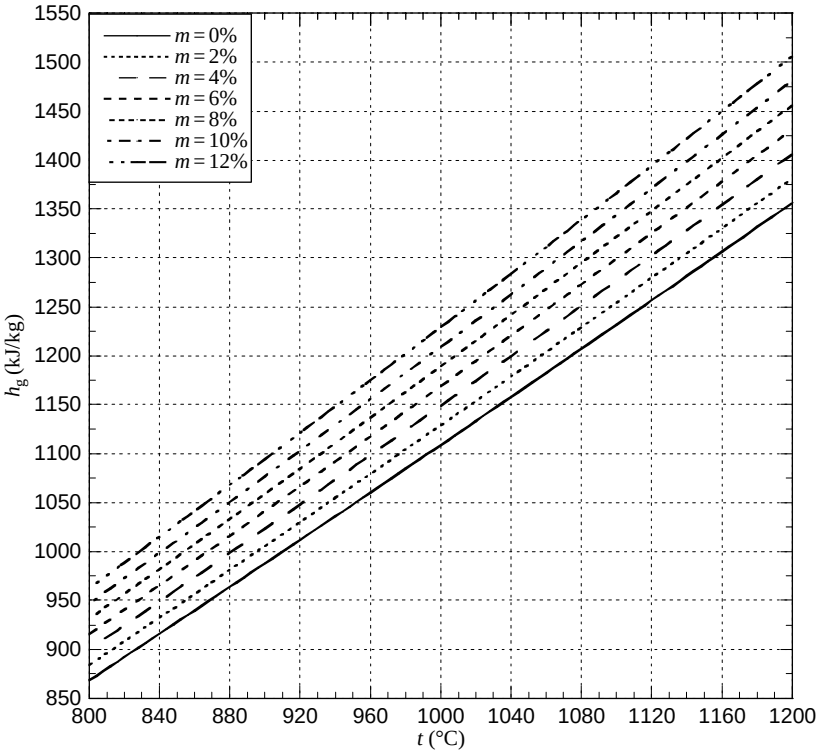


Fig. 7.32 Flue gas enthalpy

Now, considering the values of k for air, CO_2, H_2O, and O_2 ranging from 50 to 1200°C, we determine that adopting the values of X, Y, and Z shown in Table 7.5 the errors plus or minus are reduced with respect to the experimental values we obtained, as for the specific heat from Schack's publication listed in the bibliography.

Table 7.4 Factors X, J, and W for various gases

	X	J	W
CO_2	823.38	439.16	−138.71
H_2O	1838.82	251.70	38.57
N_2	1034.05	71.08	13.05
O_2	901.97	183.77	−49.13
SO_2	624.09	217.77	−56.62
CO	1031.62	100.49	0
H_2	14472.8	−50.07	369.77
NO	973.42	134.55	−25.32
OH	1747.18	−15.54	105.91
Ar	521.55	−1.56	0.43

Table 7.5 Values of X, Y, and Z for thermal conductivity

	X	Y	Z	Error (%)
Dry air	0.02373	0.06627	−0.01162	± 1.3
CO_2	0.01394	0.08699	−0.02044	± 1.7
H_2O	0.01589	0.08333	0.01940	± 3.5
O_2	0.02408	0.07444	−0.01261	± 1.2

The maximum errors are listed on the last column of the table. They are a bit high yet still acceptable for the steam, especially considering that the air conductivity remains predominant for flue gas, as well, and its errors are much more contained. To obtain the thermal conductivity of flue gas, it is reasonable to assume that it is the weighted average of the conductivities of the different components in reference to their volumes. Under normal conditions the volume of CO_2 produced by combustion of 1 kg of fuel, with C indicating the mass percentage of carbon and factoring in that the volume of a kilomole is equal to 22.412 Nm^3, will be

$$V_c = \frac{22.412}{12.01}\frac{C}{100} = 0.018661C. \tag{7.122}$$

Similarly, in case of hydrogen combustion

$$V_h = \frac{22.412}{2.016}\frac{H}{100} = 0.11117H. \tag{7.123}$$

The volume of oxygen required for combustion of carbon and hydrogen is equal to

$$V_o^* = \frac{22.412}{12.01}\frac{C}{100} + \frac{\frac{22.412}{2}}{2.016}\frac{H}{100} = 0.018661C + 0.05558H. \tag{7.124}$$

Following a similar procedure to the one applied to specific heat but in reference to volume instead of mass, we have

$$V_o = (n-1)V_o^*; \tag{7.125}$$

$$V_n = nV_n^*; \tag{7.126}$$

$$k_g = \frac{V_c k_c + V_h k_h + V_o k_o + V_n k_n}{G_v}. \tag{7.127}$$

On the other hand,

$$V_o k_o + V_n k_n = (n-1)V_o^* k_o + nV_n^* k_n = n(V_o^* k_o + V_n^* k_n) - V_o^* k_o \tag{7.128}$$

If k_a is the air conductivity,

$$k_a = \frac{V_o^* k_o + V_n^* k_n}{A_{tv}} \tag{7.129}$$

where A_{tv} is the theoretic air as volume per kg of fuel.

Furthermore, from (7.127) and (7.128),

$$k_g = \frac{nA_{\text{tv}}k_{\text{a}} + V_{\text{c}}k_{\text{c}} + V_{\text{h}}k_{\text{h}} - V_{\text{o}}^{*}k_{\text{o}}}{G_{\text{v}}}. \tag{7.130}$$

As far as the volume of flue gas under normal condition per kg of fuel, we have

$$G_{\text{v}} = nA_{\text{tv}} + V_{\text{c}} + V_{\text{h}} - V_{\text{o}}^{*}; \tag{7.131}$$

and based on (7.122–7.124)

$$G_{\text{v}} = nA_{\text{tv}} + 0.05558H. \tag{7.132}$$

Therefore, based on (7.130)

$$k_{\text{g}} = \frac{nA_{\text{tv}}k_{\text{a}} + V_{\text{c}}k_{\text{c}} + V_{\text{h}}k_{\text{h}} - V_{\text{o}}^{*}k_{\text{o}}}{nA_{\text{tv}} + 0.05558H}, \tag{7.133}$$

or

$$k_{\text{g}} = \frac{nA_{\text{tv}}k_{\text{a}} + K_X}{nA_{\text{tv}} + 0.05558H} \tag{7.134}$$

given that

$$K_X = 0.018661\,(k_{\text{c}} - k_{\text{o}})\,C + 0.11117\,(k_{\text{h}} - 0.5k_{\text{o}})\,H. \tag{7.135}$$

Following the same process applied for the specific heat, we obtain

$$K_X = (-0.1924C + 0.428H) \times 10^{-3}. \tag{7.136}$$

Finally,

$$X_{\text{g}} = \frac{23.73nA_{\text{tv}} - 0.1924C + 0.428H}{1000nA_{\text{tv}} + 55.58H}. \tag{7.137}$$

By analogy,

$$Y_{\text{g}} = \frac{66.27nA_{\text{tv}} + 0.2342C + 5.126H}{1000nA_{\text{tv}} + 55.58H}; \tag{7.138}$$

$$Z_{\text{g}} = \frac{-11.62nA_{\text{tv}} - 0.1461C + 2.857H}{1000nA_{\text{tv}} + 55.58H}. \tag{7.139}$$

Based on the same assumption that the fuel is only a mix of hydrocarbons, in other words $C = 100 - H$, from (7.9) we obtain

$$A_{\text{tv}} = 8.882 + 0.1757H. \tag{7.140}$$

Thus, from (7.137–7.139), we obtain

$$X_g = \frac{210.77n + 4.1694nH - 19.239 + 0.6204H}{8882n + 175.7nH + 55.58H} \tag{7.141}$$

$$Y_g = \frac{588.61n + 11.644nH + 23.42 + 4.892H}{8882n + 175.7nH + 55.58H} \tag{7.142}$$

$$Z_g = \frac{-103.21n - 2.0416nH - 14.61 + 3.003H}{8882n + 175.7nH + 55.58H} \tag{7.143}$$

As usual, by adopting the same conventional value of n equal to 1.2 and factoring in (7.104), we obtain the following equations:

$$X_g = \frac{21.924 + 0.2039m}{1 + 0.01084m} \times 10^{-3} \tag{7.144}$$

$$Y_g = \frac{68.467 + 0.8388m}{1 + 0.01084m} \times 10^{-3} \tag{7.145}$$

$$Z_g = \frac{-12.991 + 0.4821m}{1 + 0.01084m} \times 10^{-3} \tag{7.146}$$

It is possible to substitute with sufficient approximation the equations above with those obtained by multiplying the numerator by the denominator with the opposite sign of the term that contains m and ignoring the term to the square root. We obtain:

$$X_g = (21.924 - 0.0337m) \times 10^{-3} \tag{7.147}$$

$$Y_g = (68.467 + 0.0966m) \times 10^{-3} \tag{7.148}$$

$$Z_g = -(12.991 - 0.6229m) \times 10^{-3} \tag{7.149}$$

Based on (7.120), the thermal conductivity of flue gas is therefore given by

$$k_g = \left[21.924 - 0.0337m + (68.467 + 0.0966m)\frac{t}{1000} - (12.991 - 0.6229m)\left(\frac{t}{1000}\right)^2\right] \times 10^{-3} \tag{7.150}$$

Figure 7.33 shows the values of k_g in W/mK.

7.9.5 Dynamic Viscosity

Even dynamic viscosity can be expressed through an equation such as

$$\mu = X + Y\frac{t}{1000} + Z\left(\frac{t}{1000}\right)^2. \tag{7.151}$$

For air ranging from 0 to 300°C, that is, the range of temperature of practical interest, it is possible to adopt the following equation:

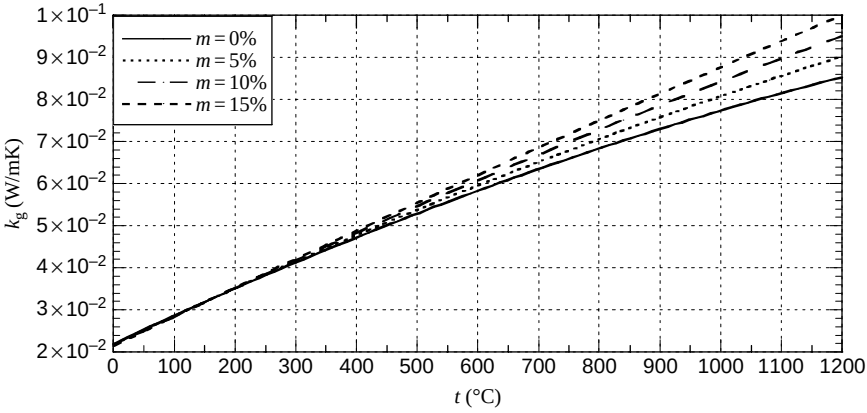


Fig. 7.33 Flue gas thermal conductivity

$$\mu_a = \left[17.069 + 47.469\frac{t}{1000} - 18.708\left(\frac{t}{1000}\right)^2\right] \times 10^{-6} \tag{7.152}$$

with μ_a in kg/ms.

As far as the different types of gas and the steam, considering a range of temperature from 50 to 1200°C, the values of X, Y, and Z that cause minimal errors compared to experimental values are listed in Table 7.6. The values relative to oxygen are missing because they are not available. To this extent the oxygen was assimilated to air, given that for the different types of gas the values of viscosity do not differ very much among each other and also given the presence of oxygen in the air.

Proceeding as with thermal conductivity because even in this case the dynamic viscosity of flue gas may be computed as weighted average, in reference to volumes, of the viscosity of single components, we obtain the following values of X_g, Y_g, and Z_g:

$$X_g = \frac{17.48nA_{tv} - 0.06597C + 0.02835H}{nA_{tv} + 0.05558H} \times 10^{-6} \tag{7.153}$$

$$Y_g = \frac{42.851nA_{tv} + 0.06378C + 1.8906H}{nA_{tv} + 0.05558H} \times 10^{-6} \tag{7.154}$$

Table 7.6 Values of X, Y, and Z for dynamic viscosity

	X	Y	Z	Error (%)
	$\times 10^{-6}$			
Dry air	17.480	42.851	−10.988	± 1.1
CO_2	13.945	46.269	−12.144	± 1.0
H_2O	8.995	38.431	−5.145	± 0.6

$$Z_{\mathrm{g}} = \frac{-10.988nA_{\mathrm{tv}} - 0.02157C + 0.03880H}{nA_{\mathrm{tv}} + 0.05558H} \times 10^{-6} \tag{7.155}$$

Recalling (7.140), we obtain the following equations:

$$X_{\mathrm{g}} = \frac{155.257n + 3.0714nH - 0.06597C + 0.02835H}{8.882n + 0.17571nH + 0.05558H} \times 10^{-6} \tag{7.156}$$

$$Y_{\mathrm{g}} = \frac{380.602n + 7.5293nH + 0.06378C + 1.8906H}{8.882n + 0.17571nH + 0.05558H} \times 10^{-6} \tag{7.157}$$

$$Z_{\mathrm{g}} = \frac{-97.595n - 1.9307nH - 0.02157C + 0.03880H}{8.882n + 0.17571nH + 0.05558H} \times 10^{-6} \tag{7.158}$$

With $n = 1.2$ and factoring in (7.104), in the end we obtain the following equations:

$$X_{\mathrm{g}} = \frac{16.861 + 0.0722m}{1 + 0.01084m} \times 10^{-6} \tag{7.159}$$

$$Y_{\mathrm{g}} = \frac{43.449 + 0.360m}{1 + 0.01084m} \times 10^{-6} \tag{7.160}$$

$$Z_{\mathrm{g}} = \frac{-11.190 + 0.02277m}{1 + 0.01084m} \times 10^{-6} \tag{7.161}$$

Similarly to the process employed for thermal conductivity, the previous equations can be simplified as follows:

$$X_{\mathrm{g}} = (16.861 - 0.1106m) \times 10^{-6} \tag{7.162}$$

$$Y_{\mathrm{g}} = (43.449 - 0.1110m) \times 10^{-6} \tag{7.163}$$

$$Z_{\mathrm{g}} = -(11.190 + 0.0985m) \times 10^{-6} \tag{7.164}$$

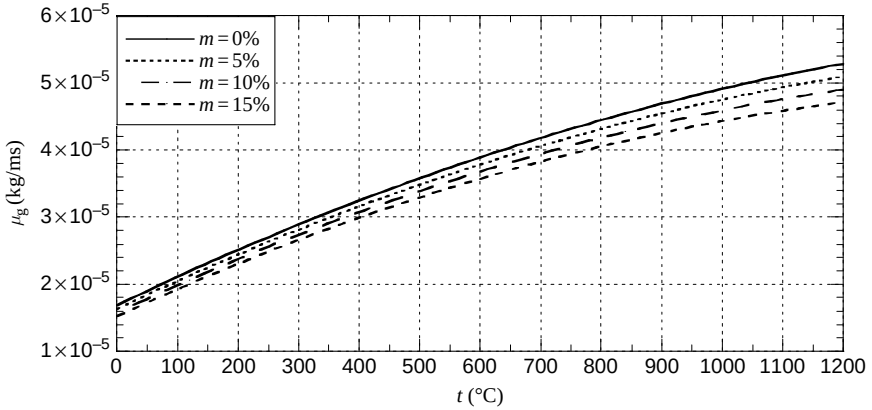


Fig. 7.34 Flue gas dynamic viscosity

Based on (7.151), the dynamic viscosity of flue gas is therefore given by:

$$\mu_g = \left[16.861 - 0.1106m + (43.449 - 0.111m)\,\frac{t}{1000} - (11.19 + 0.0985m)\left(\frac{t}{1000}\right)^2\right] \times 10^{-6} \tag{7.165}$$

Figure 7.34 shows the values of μ_g in kg/ms.

Chapter 8
Heat Transfer

8.1 General Considerations

The goal of this book does not include complete analysis of the different aspects of heat transfer phenomena, as well as fundamental concepts that are presumably known to the reader. For example, we will not perform a theoretical investigation on transmission by radiation, but limit our presentation to how to compute the radiated heat in the furnace in a satisfactory way, or how to compute the amount of radiated heat from the flue gas to the tube banks instead. This means, for instance, that we will not discuss heat transfer in the heat exchangers. This would imply the introduction of certain correction factors of the mean logarithmic temperature difference, based on the number of passages of the two fluids, as well as their direction. In fact, this topic relates more to plants (especially chemical and oil plants) than steam generators where, at the most, it may relate to a few auxiliaries (fuel oil and water heaters, heat exchangers for heating systems, and so on). In any case, this topic is dealt with extensively in specialized literature.

During computation of the heat transfer coefficient, we will ignore the laminar flow, and always refer to turbulent flow because only the latter is of interest to us. In other words, we will list only those fundamental equations and illustrate those special computation criteria that are used for thermodynamic calculation of the generator. Specifically, the next section will focus on heat transfer by conduction and convection leading to the equations on the computation of the overall heat transfer coefficient. The following sections will focus in detail on heat transfer by convection and indicate how the heat transfer coefficients relative to different fluids can be computed. Moreover, we will focus on transmission by radiation into the furnace of water-tube generators, of diathermic fluid boilers, as well as into the flue in smoke-tube boilers. We will also examine radiation by flue gas into the tube banks. Then we will examine heat transfer in specific components of the generator (economizer, air heater). Finally, we will provide some advice on the available choices to achieve the most efficient heat transfer.

D. Annaratone, *Steam Generators*, DOI: 10.1007/978-3-540-77715-1¯8,

© Springer-Verlag Berlin Heidelberg 2008

8.2 Overall Heat Transfer Coefficient

If we consider a wall with flat parallel sides of thickness x_w and consisting of material with thermal conductivity k, as shown in Fig. 8.1, the heat q transferred through the wall is given by

$$q = \frac{k}{x_w} S (t_1 - t_2) \tag{8.1}$$

where S is the surface of the sides, and t_1 and t_2 are the temperatures of the warm side and the cold side, respectively.

Figure 8.1 is valid if the assumption is based on zero heat loss along the perimeter edge of the wall. The difference in temperature between the two sides is therefore given by

$$\Delta t_2 = t_1 - t_2 = \frac{q}{S} \frac{x_w}{k}. \tag{8.2}$$

If the same wall gets in contact with a fluid at temperature t' on the warm side, and with a fluid at temperature t'' on the cold side, the heat transfer from the warm fluid at temperature t' to the wall is given by

$$q = \alpha' S \left(t' - t_1\right) \tag{8.3}$$

where α' is a quantity called heat transfer coefficient which is typical of the fluid in question, the value of which depends on the characteristics of the fluid (thermal conductivity, viscosity, specific heat), as well as its speed and the diameter, if the fluid flows through a tube or if it hits it from the outside.

The temperature difference between the fluid and the warm side of the wall is therefore equal to

$$\Delta t_1 = t' - t_1 = \frac{q}{S} \frac{1}{\alpha'}. \tag{8.4}$$

Similarly, as far as the fluid getting in contact with the cold side, we have

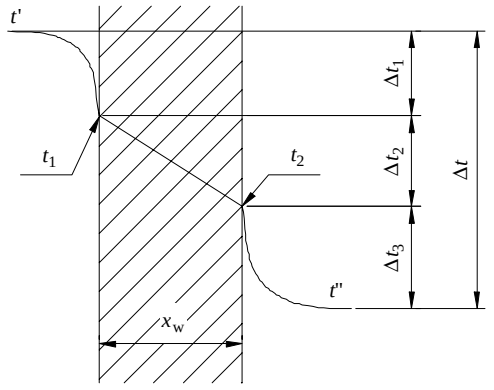


Fig. 8.1

$$q = \alpha'' \left(t_2 - t''\right); \tag{8.5}$$

$$\Delta t_3 = \left(t_2 - t''\right) = \frac{q}{S}\frac{1}{\alpha''} \tag{8.6}$$

where α'' is the heat transfer coefficient relative to the heated fluid. Given that in the absence of lateral heat loss the heat going from the heating fluid to the wall, crossing it to be subsequently transferred to the heated fluid, is the same, based on (8.2), (8.4), and (8.6).

$$\Delta t = t' - t'' = \Delta t_1 + \Delta t_2 + \Delta t_3 = \frac{q}{S}\left(\frac{1}{\alpha'} + \frac{x_\mathrm{w}}{k} + \frac{1}{\alpha''}\right). \tag{8.7}$$

On the other hand, the overall heat transfer coefficient U is the quantity in the following equation that allows the computation of the heat transferred by the heating fluid to the heated one through the wall, based on the respective temperatures.

$$q = US\left(t' - t''\right) \tag{8.8}$$

The following equation for the computation of U is obtained from (8.7) and (8.8):

$$U = \frac{1}{\dfrac{1}{\alpha'} + \dfrac{x_w}{k} + \dfrac{1}{\alpha''}}. \tag{8.9}$$

Equation (8.9) helps to calculate the overall heat transfer coefficient once the values of k, α', and α'' are known.

Generally, the overall coefficient relative to heat transfer through a series of walls of thickness $x_{\mathrm{w}1}, x_{\mathrm{w}2} \ldots x_{\mathrm{w}n}$, consisting of materials with conductivity $k_1, k_2 \ldots k_n$, is given by:

$$U = \frac{1}{\dfrac{1}{\alpha'} + \dfrac{x_{\mathrm{w}1}}{k_1} + \dfrac{x_{\mathrm{w}2}}{k_2} \cdots \dfrac{x_{\mathrm{w}n}}{k_n} + \dfrac{1}{\alpha''}}. \tag{8.10}$$

Equation (8.10) is about the external insulation walls of the generator that usually consist of various strata of different materials.

Now we consider a tube of unitary length (see Fig. 8.2) and we assume that the heating fluid is outside the tube (tube bank of water-tube generators, superheater, economizer, air heater with air flowing in the tubes).

The surface through which the heat transfer takes place in the tube is variable and equal to

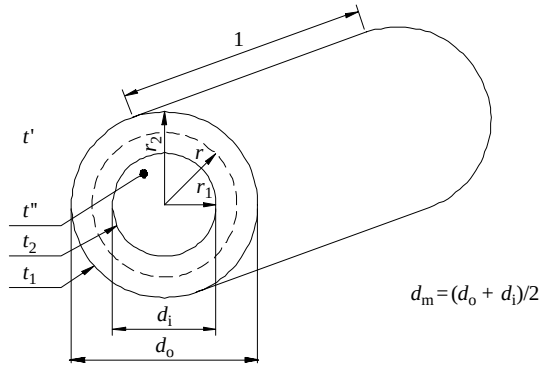
$$S = 2\pi r \tag{8.11}$$

where r is the generic radius.

Similarly to (8.2), we may write that

$$\mathrm{d}t = \frac{q}{2\pi r}\frac{\mathrm{d}r}{k}. \tag{8.12}$$

Fig. 8.2 Centripetal heat flux



By integrating (8.12) we obtain

$$\Delta t_2 = t_1 - t_2 = \frac{q}{2\pi k} \log_e \frac{r_2}{r_1}, \tag{8.13}$$

given that r_1 and r_2 are the internal and external radius of the tube, respectively.

Equation (8.13) can also be written as follows:

$$\Delta t_2 = \frac{q}{\pi d_o} \frac{d_o}{2k} \log_e \frac{d_o}{d_i}, \tag{8.14}$$

where d_i and d_o represent the inside and outside diameter. From (8.14) we obtain the following equation for the computation of q:

$$q = \frac{2\pi k}{\log_e \dfrac{d_o}{d_i}} (t_1 - t_2). \tag{8.15}$$

As far as the heat transfer from the heating fluid to the tube, based on (8.4) we have

$$\Delta t_1 = t' - t_1 = \frac{q}{\pi d_o} \frac{1}{\alpha'}. \tag{8.16}$$

As far as transmission from the wall to the heated fluid, based on (8.6) we finally have

$$\Delta t_3 = t_2 - t'' = \frac{q}{\pi d_i} \frac{1}{\alpha''}; \tag{8.17}$$

it can also be rewritten as follows:

$$\Delta t_3 = \frac{q}{\pi d_o} \frac{1}{\alpha''} \frac{d_o}{d_i}. \tag{8.18}$$

From (8.14), (8.16), and (8.18) we obtain

$$\Delta t = \frac{q}{\pi d_o} \left(\frac{1}{\alpha'} + \frac{d_o}{2k} \log_e \frac{d_o}{d_i} + \frac{1}{\alpha''} \frac{d_o}{d_i} \right). \tag{8.19}$$

If we write

$$q = U_o \pi d_o \left(t' - t''\right), \tag{8.20}$$

similarly to (8.8), we obtain the following from (8.19):

$$U_o = \frac{1}{\frac{1}{\alpha'} + \frac{d_o}{2k} \log_e \frac{d_o}{d_i} + \frac{1}{\alpha''} \frac{d_o}{d_i}}. \tag{8.21}$$

U_o is the overall coefficient, because in the case of the tube it is necessary to specify whether this quantity refers to the inside or to the outside surface. The one provided by (8.21) refers to the outside surface of the tube, as highlighted in (8.20).

If the heating fluid is inside the tube (tube bank of smoke-tube generators, air heater with air outside the tubes), through integration of (8.12) we obtain (8.13) again which can be written as follows (see Fig. 8.3):

$$\Delta t_2 = \frac{q}{\pi d_i} \frac{d_i}{2k} \log_e \frac{d_o}{d_i}. \tag{8.22}$$

In addition,

$$\Delta t_1 = t' - t_1 = \frac{q}{\pi d_i} \frac{1}{\alpha'}. \tag{8.23}$$

Finally,

$$\Delta t_3 = t_2 - t'' = \frac{q}{\pi d_o} \frac{1}{\alpha''}, \tag{8.24}$$

or

$$\Delta t_3 = \frac{q}{\pi d_i} \frac{1}{\alpha''} \frac{d_i}{d_o}. \tag{8.25}$$

From (8.22), (8.23), and (8.25) we obtain

$$\Delta t = \frac{q}{\pi d_i} \left(\frac{1}{\alpha'} + \frac{d_i}{2k} \log_e \frac{d_o}{d_i} + \frac{1}{\alpha''} \frac{d_i}{d_o} \right). \tag{8.26}$$

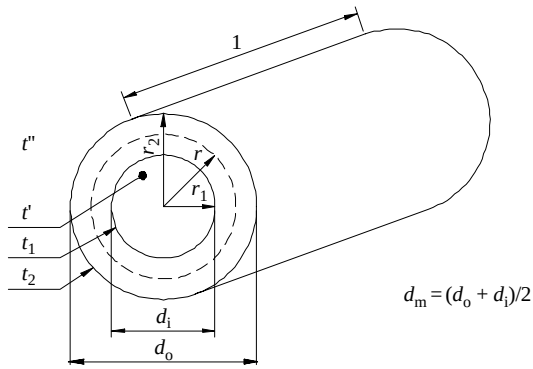


Fig. 8.3 Centrifugal heat flux

By analogy with (8.20), if we write that

$$q = U_{\mathrm{i}} \pi d_{\mathrm{i}} \left(t' - t''\right). \tag{8.27}$$

We obtain the following from (8.26):

$$U_{\mathrm{i}} = \frac{1}{\dfrac{1}{\alpha'} + \dfrac{d_{\mathrm{i}}}{2k} \log_{\mathrm{e}} \dfrac{d_{\mathrm{o}}}{d_{\mathrm{i}}} + \dfrac{1}{\alpha''} \dfrac{d_{\mathrm{i}}}{d_{\mathrm{o}}}}, \tag{8.28}$$

where the overall coefficient U_{i} refers to the inside surface of the tube, as we see from (8.27).

Recalling (8.2), we may write as far as the heat transfer through the tube wall that

$$\Delta t_2 = \frac{q}{\pi d_{\mathrm{m}}} \frac{x_{\mathrm{w}}}{k} \varphi, \tag{8.29}$$

this way referring to the mean surface, given that d_{m} is the average diameter, and introducing a corrective factor ϕ.

A comparison between (8.29) and (8.14) determines that the factor ϕ is given by:

$$\varphi = \frac{\left(\dfrac{d_{\mathrm{o}}}{d_{\mathrm{i}}} + 1\right) \log_{\mathrm{e}} \dfrac{d_{\mathrm{o}}}{d_{\mathrm{i}}}}{2\left(\dfrac{d_{\mathrm{o}}}{d_{\mathrm{i}}} - 1\right)}. \tag{8.30}$$

The values of ϕ are shown in Table 8.1.

As you can see, they considerably differ from the unity only for high values of $d_{\mathrm{o}}/d_{\mathrm{i}}$ that do not occur in steam generators. In practice, factor ϕ is neglected and (8.21) can be written as follows:

$$U_{\mathrm{o}} = \frac{1}{\dfrac{1}{\alpha'} + \dfrac{x_{\mathrm{w}}}{k} \dfrac{d_{\mathrm{o}}}{d_{\mathrm{m}}} + \dfrac{1}{\alpha''} \dfrac{d_{\mathrm{o}}}{d_{\mathrm{i}}}}. \tag{8.31}$$

Table 8.1 Corrective factor ϕ

$\frac{d_{\mathrm{o}}}{d_{\mathrm{i}}}$	ϕ	$\frac{d_{\mathrm{o}}}{d_{\mathrm{i}}}$	ϕ	$\frac{d_{\mathrm{o}}}{d_{\mathrm{i}}}$	ϕ
1.0	1.000	1.8	1.030	3.5	1.129
1.1	1.001	1.9	1.035	4.0	1.152
1.2	1.002	2.0	1.040	4.5	1.182
1.3	1.005	2.2	1.050	5.0	1.207
1.4	1.009	2.4	1.061	5.5	1.231
1.5	1.014	2.6	1.074	6.0	1.254
1.6	1.018	2.8	1.087	6.5	1.276
1.7	1.024	3.0	1.089	7.0	1.297

By analogy, (8.28) can be written as follows:

$$U_{\mathrm{i}} = \frac{1}{\dfrac{1}{\alpha'} + \dfrac{x_{\mathrm{w}}}{k}\dfrac{d_{\mathrm{i}}}{d_{\mathrm{m}}} + \dfrac{1}{\alpha''}\dfrac{d_{\mathrm{i}}}{d_{\mathrm{o}}}}. \tag{8.32}$$

Values of $d_{\mathrm{o}}/d_{\mathrm{i}}$ so high to be forced to consider the corrective factor ϕ can occur for insulated tubes outside the generator instead. In that case, keeping in mind the presence of two or more coaxial tubes of different material, we have

$$U_{\mathrm{i}} = \frac{1}{\dfrac{1}{\alpha'} + \dfrac{\varphi_1 x_{\mathrm{w1}}}{k_1}\dfrac{d_{\mathrm{i}}}{d_{\mathrm{m1}}} + \dfrac{\varphi_2 x_{\mathrm{w2}}}{k_2}\dfrac{d_{\mathrm{i}}}{d_{\mathrm{m2}}} + \ldots \dfrac{\varphi_n x_{\mathrm{wn}}}{k_n}\dfrac{d_{\mathrm{i}}}{d_{\mathrm{mn}}} + \dfrac{1}{\alpha''}\dfrac{d_{\mathrm{i}}}{d_{\mathrm{o}}}}. \tag{8.33}$$

In (8.33) $x_{\mathrm{w1}}, x_{\mathrm{w2}} \ldots x_{\mathrm{wn}}$ are the thickness of the various tubes matched by the average diameters $d_{\mathrm{m1}}, d_{\mathrm{m2}} \ldots d_{\mathrm{mn}}$, and conductivities $k_1, k_2 \ldots k_n$; the values of factors $\varphi_1, \varphi_2 \ldots \varphi_n$ must be estimated based on the ratio between outside and inside diameter of the various tubes.

Finally, as far as the tubes of the boiler, the term that corresponds to conduction through the tube wall generally has a negligible impact on the value of U. Therefore, it can be ignored, and (8.31) is as follows:

$$U_{\mathrm{o}} = \frac{1}{\dfrac{1}{\alpha'} + \dfrac{1}{\alpha''}\dfrac{d_{\mathrm{o}}}{d_{\mathrm{i}}}}. \tag{8.34}$$

By analogy, (8.32) is as follows:

$$U_{\mathrm{i}} = \frac{1}{\dfrac{1}{\alpha'} + \dfrac{1}{\alpha''}\dfrac{d_{\mathrm{i}}}{d_{\mathrm{o}}}}. \tag{8.35}$$

Given the high and conventional value of α'' (as we shall see later on), for steam generating tubes it is also possible to simplify further and write that

$$U = \frac{1}{\dfrac{1}{\alpha'} + \dfrac{1}{\alpha''}} = \frac{\alpha'\alpha''}{\alpha' + \alpha''} \tag{8.36}$$

where U is equal to U_{o} or to U_{i}, depending on whether the flue gas gets in contact with the outside or inside wall of the tubes.

For example, let us consider a steam generating tube bank where

$$\alpha' = 85\,\mathrm{W/m^2K}$$
$$\alpha'' = 12{,}000\,\mathrm{W/m^2K}$$
$$d_{\mathrm{o}} = 54\,\mathrm{mm}$$
$$d_{\mathrm{i}} = 48\,\mathrm{mm}$$
$$k = 44\,\mathrm{W/mK}$$

By calculating based on (8.31) we have

$$U_o = \frac{1}{0.01176 + \frac{0.003}{44} 1.0588 + 0.0000833 \times 1.125} = 83.85\,\mathrm{W/m^2K}$$

Through the approximate (8.36)

$$U_o = \frac{85 \times 12000}{12085} = 84.40\,\mathrm{W/m^2K}$$

By adopting the second value one makes a negligible mistake by excess equal to 0.6%, considering the greater uncertainties inherent in the computation of both α' and α'', as we shall see.

Thermodynamic computation often requires the determination of the temperature of the tube wall getting in contact with the heating or the heated fluid. Indicating the temperature of the side getting in contact with the heating fluid with t'_w, based on (8.16) and (8.20) we obtain

$$t'_w = t' - \frac{U_o}{\alpha'} \left(t' - t''\right). \tag{8.37}$$

By analogy, based on (8.23) and (8.27)

$$t'_w = t' - \frac{U_i}{\alpha'} \left(t' - t''\right). \tag{8.38}$$

Indicating the temperature of the side getting in contact with the heated fluid with t''_w, based on (8.18) and (8.20):

$$t''_w = t'' + \frac{U_o}{\alpha''} \frac{d_o}{d_i} \left(t' - t''\right), \tag{8.39}$$

and by analogy, based on (8.25) and (8.27)

$$t''_w = t'' + \frac{U_i}{\alpha''} \frac{d_i}{d_o} \left(t' - t''\right). \tag{8.40}$$

8.3 Mean Logarithmic Temperature Difference

Up to this point the temperatures t' and t'' of both fluids were assumed to be constant. In reality, as a result of heat transfer, the warm fluid is cooled and the cold fluid becomes warm. It is well known that there are two classical heat transfer types between two moving fluids: in parallel flow or in counterflow. Fluids flow in parallel when they get in contact with the wall that separates them and through which the heat transfer takes place if the fluids move in the same direction. In other words, the warm fluid is cooled along the wall, whereas the cold fluid warms up. If the fluids are in counter-flow instead, they flow in opposite directions, and the warm fluid

starts to get in contact with the wall where the cold fluid moves away after warming up, and vice versa the warm fluid stops the contact with the wall when the cold fluid starts contact with, thus getting warmer.

Of course, in practice the situation differs from the theoretical one we described. There is almost never perfect parallel flow or counterflow. For instance, in a tube bank of a superheater hit by flue gas, while the gas goes through the bank following a constant direction, the steam moving through the tubes follows the winding path of a series of pipe coils. In practice, if the steam enters the bank where the flue gas exits, one often correctly speaks of fluids in counterflow. On the other hand, one speaks of fluids in parallel flow if the steam enters the bank where this starts to be hit by the flue gas. There are, of course, instances when these definitions are incorrect because the fluids are in cross-flow. We will discuss this topic in relation to steam generators in the Appendix.

If we limit our analysis to the two typical cases mentioned earlier, the pattern of the temperatures t' and t'' is shown in both Figs. 8.4 and 8.5 where the temperatures (and generally all the quantities) referring to the heating fluid are indicated by superscript ($'$) and those referring to the heated fluid by superscript ($''$). In addition, the temperatures at the entrance are indicated with subscript 1 and those at the exit with subscript 2.

M' and M'' are the mass flow rates of both fluids, and c'_p and c''_p refer to the specific isobaric heat. The overall heat transfer coefficient U is assumed to be constant.

The heat transferred through the elementary surface dS is given by

$$dq = UdS(t' - t''). \tag{8.41}$$

On the other hand, given that t' decreases with the increase surface, the same value dq is equal to

$$dq = -M'c'_p dt'. \tag{8.42}$$

If the exchange occurs with parallel flow, given that t'' increases with S, from Fig. 8.4 we see that

$$dq = M''c''_p dt''. \tag{8.43}$$

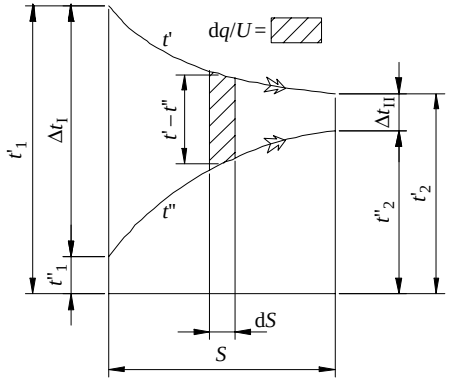


Fig. 8.4 Parallel flow

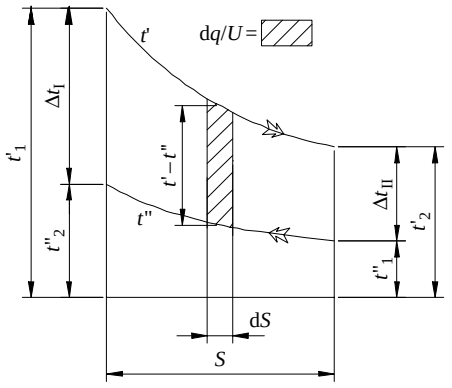


Fig. 8.5 Counterflow

Vice versa, Fig. 8.5 relative to heat transfer during counterflow shows that

$$dq = -M'' c_p'' dt''. \tag{8.44}$$

Therefore,

$$d\left(t' - t''\right) = -dq\left(\frac{1}{M' c_p'} \pm \frac{1}{M'' c_p''}\right); \tag{8.45}$$

and recalling (8.41)

$$d\left(t' - t''\right) = -U dS\left(t' - t''\right)\left(\frac{1}{M' c_p'} \pm \frac{1}{M'' c_p''}\right); \tag{8.46}$$

here the plus sign indicates parallel flow and the minus sign indicates counter-flow.

On the other hand, if there is no heat loss

$$q = M' c_p'\left(t_1' - t_2'\right) = M'' c_p''\left(t_2'' - t_1''\right). \tag{8.47}$$

Thus, with parallel flow

$$\frac{1}{M' c_p'} + \frac{1}{M'' c_p''} = \frac{1}{q}\left(t_1' - t_1'' - t_2' + t_2''\right), \tag{8.48}$$

and with counterflow

$$\frac{1}{M' c_p'} - \frac{1}{M'' c_p''} = \frac{1}{q}\left(t_1' - t_2'' - t_2' + t_1''\right) \tag{8.49}$$

The term on the right of the equal sign of both (8.48) and (8.49) (Figs. 8.4 and 8.5) is equal to

$$\frac{\Delta t_I - \Delta t_{II}}{q}. \tag{8.50}$$

Equation (8.46) can therefore be written as follows:

$$\frac{d\left(t' - t''\right)}{t' - t''} = -\frac{U dS}{q}\left(\Delta t_I - \Delta t_{II}\right); \tag{8.51}$$

and through integration we obtain:

$$\left| -\log_e\left(t' - t''\right)\right|_I^{II} = \frac{US}{q}\left(\Delta t_I - \Delta t_{II}\right); \tag{8.52}$$

then

$$\log_{\mathrm{e}} \frac{\Delta t_I}{\Delta t_{II}} = \frac{US}{q}\left(\Delta t_I - \Delta t_{II}\right). \tag{8.53}$$

Finally,

$$q = US\frac{\Delta t_I - \Delta t_{II}}{\log_{\mathrm{e}} \frac{\Delta t_I}{\Delta t_{II}}}. \tag{8.54}$$

The following quantity is the mean logarithmic temperature difference Δt_m:

$$\Delta t_m = \frac{\Delta t_I - \Delta t_{II}}{\log_{\mathrm{e}} \dfrac{\Delta t_I}{\Delta t_{II}}}; \tag{8.55}$$

then

$$q = US\Delta t_m. \tag{8.56}$$

The resulting equation is quite similar to (8.8) where instead of the difference in constant temperature between the heating fluid and the heated one, we have the mean logarithmic temperature difference given by (8.55) (of course, if it is a tube bank U represents U_{o} and U_{i}, respectively, depending on whether S is the outside or inside surface of the tubes).

Another way to proceed is suggested by the fact that if the ratio $\Delta t_I/\Delta t_{II}$ is not too high, Δt_m does not considerably differ from the mean arithmetic temperature difference equal to:

$$\Delta t = \frac{\Delta t_I + \Delta t_{II}}{2}. \tag{8.57}$$

Therefore, we can write that

$$\Delta t_m = \chi\frac{\Delta t_I + \Delta t_{II}}{2}. \tag{8.58}$$

Based on (8.55) and (8.58), the corrective factor χ is given by

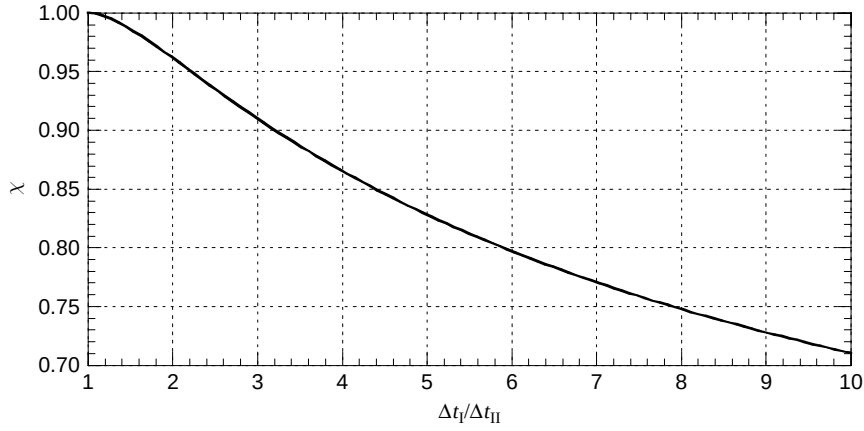


Fig. 8.6

$$\chi = \frac{2\,(\Delta t_I - \Delta t_{II})}{(\Delta t_I + \Delta t_{II})\log_e \dfrac{\Delta t_I}{\Delta t_{II}}}. \tag{8.59}$$

The value for χ obtained from Fig. 8.6 clearly shows the influence of $\Delta t_I/\Delta t_{II}$ on the reduction of Δt_m with respect to the mean arithmetic temperature difference. Note that the use of this diagram combined with (8.58) leads to the exact computation of Δt_m.

In the case of fluids in parallel flow, the value of the ratio $\Delta t_I/\Delta t_{II}$ is higher than with fluids in counterflow, thus the value of both χ and Δt_m is smaller. Based on (8.56), it follows that a greater surface with equal heat transfer is needed. The topic is addressed in more detail in Sect. 8.12.

As far as c'_p, c''_p, and U, versus temperature and pressure variations, note that pressure variations in steam generators are such to make the influence of the latter negligible. This is not true for temperature, but it is still possible to adopt constant values if we refer to values corresponding to the mean temperature of the fluids. The mean values between t'_1 and t'_2 and between t''_1 and t''_2 will be used for c'_p and c''_p, given by the ratio between the difference in enthalpy and the difference in temperature, respectively (see Sect. 7.9). As far as steam generating tube banks, this topic will be discussed in depth in the Appendix.

8.4 Heat Transfer in the Furnace of Water-Tube Generators and Diathermic Fluid Boilers

If the flame developing in the furnace did not irradiate the walls or the tube banks, it would reach the so-called adiabatic temperature of the flame, even though the name is improper considering the fact that this is actually an isobar transformation.

The heat introduced in the furnace for every kg or Nm^3 of fuel indicated with H'_n, as far as room temperature t_0, is generally given by

$$H'_n = H_n + c_{pf}\left(t_f - t_0\right) + Ac_{pa}\left(t_a - t_0\right), \tag{8.60}$$

where c_{pf} is the mean specific isobaric heat of the fuel between t_0 and t_f; c_{pa} is the mean specific isobaric heat of the air between t_0 and t_a; t_f and t_a are the temperatures of the fuel and the air at the entrance of the furnace, respectively, and A represents the amount of air for every kg or Nm^3 of fuel (see Chap. 7); finally, H_n is the net heat value of the fuel.

If H_n refers to 1 kg of fuel, this will also be true for H'_n, c_{pf}, and A. Similarly, if H_n refers to 1 Nm^3. Moreover, if A represents mass (this is A_m), c_{pa} refers to 1 kg of air, and by analogy, if A represents volume (this is A_v).

If t_{ad} is the adiabatic temperature of the flame, G is as usual the amount of flue gas per kg or Nm^3 of fuel, and c_{pg} is the mean isobaric specific heat of the flue gas between t_0 and t_{ad}, we have

$$H'_n = Gc_{pg}\left(t_{ad} - t_0\right). \tag{8.61}$$

t_{ad} can be computed through (8.61) combined with (8.60).

As far as the measuring units of G and c_{pg}, the same considerations made before about A and c_{pa} are true. Note that H'_n/G represents the heat introduced in the furnace for every kg or Nm^3 of flue gas (depending on whether G indicates G_m or G_v); Therefore, this ratio has the dimension of an enthalpy that we indicate with h_g; from (8.61) we obtain the following:

$$t_{ad} - t_0 = \frac{h_g}{c_{pg}}. \tag{8.62}$$

If we assume that $t_0 = 0°C$, the particular value of t_{ad} obtained from (8.62) represents the so-called theoretic combustion temperature; by indicating it with t_{tc} we obtain

$$t_{tc} = \frac{h_g}{c_{pg}} \tag{8.63}$$

In that case c_{pg} is the mean specific heat between 0°C and t_{tc}.

On the basis of Sect. 7.9, we know that specific heat is a function of t and the moisture of flue gas. For this reason, it would be easy to build a diagram with t_{tc} as a function of h_g and the moisture of flue gas.

Rosin preferred to put together the diagram shown in Fig. 8.7 instead. It helps to obtain t_{tc} as a function of h_g referred to 1 Nm^3 of flue gas and the air index n which is better identifiable than moisture. In general, the diagram can be used to compute t_{ad}. In fact, given that the mean specific heat between t_0 and t_{ad} differs from the mean specific heat between 0°C and t_{tc} in a negligible way, based on (8.62) it is possible to write that

$$t_{ad} = t_{tc} + t_0, \tag{8.64}$$

where t_{tc} stands for the temperature obtained from Fig. 8.7. The value of h_g to introduce is the one in (8.62), that is, the one relative to the value of H'_n in (8.60).

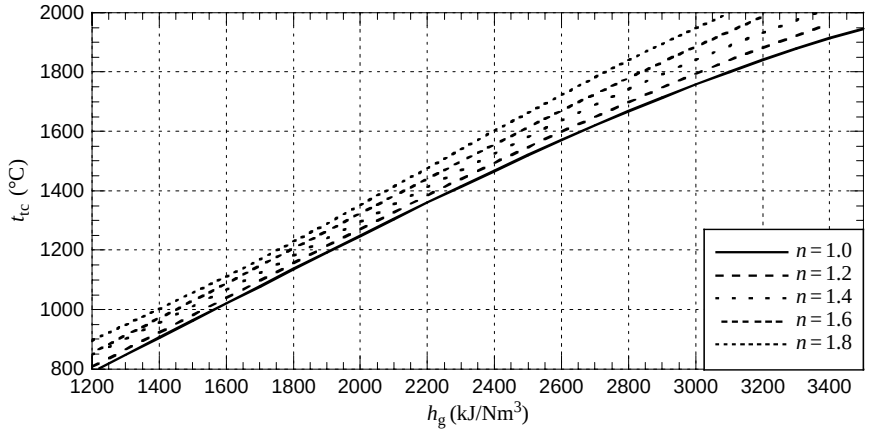


Fig. 8.7 Theoretical combustion temperature (Rosin)

In conclusion, calculation of the adiabatic temperature requires calculation of H'_n based on (8.60); by dividing this value by G_v we obtain the amount of heat h_g per Nm^3 of flue gas to introduce in Fig. 8.7; based on the air index n, it is possible to compute t_{tc} and to determine t_{ad} through (8.64). Regardless of its purely theoretical significance, the adiabatic temperature t_{ad} is interesting as a reference point on the more or less high temperature that the flame can reach. It will also help to compute the exit temperature of the gas from the furnace based on Konakow's computation method.

Note that above 1500°C there is considerable dissociation of the steam and the carbon dioxide in the flue gas that limits the development of heat as the temperature goes up because of the so-called dissociation heat. The impact of the dissociation cannot be ignored above 1500°C where (8.63) becomes incorrect. Note that Rosin's diagram (see Fig. 8.7) takes this phenomenon into account, albeit through some degrees of simplification. Therefore, the obtained temperatures t_{tc} are rather correct. The temperature in the furnace is lower than the adiabatic one because of radiation. At this point we refer to the classic equation on radiation of the blackbody based on Stefan Boltzmann's rule.

The heat radiated from a black surface at absolute temperature T_f onto a black surface at absolute temperature T_w is given by

$$q_r = \sigma S \left(T_f^4 - T_w^4\right), \tag{8.65}$$

where q_r is the radiated heat in W, S the surface in m^2 of the radiating or radiated wall, and σ the constant of Stefan Boltzmann given by

$$\sigma = 5.77 \times 10^{-8}\,\mathrm{W/m^2K^4}. \tag{8.66}$$

If we consider combustion on a grate, that is, an incandescent fuel layer, experimental results show that the radiated heat can be computed with good approximation based on the following equation:

$$q_r = 4.65S\left[\left(\frac{T_f}{100}\right)^4 - \left(\frac{T_w}{100}\right)^4\right]. \tag{8.67}$$

Here S is the radiated surface of the screens or the tube banks that "see" the flame (as we shall see later on in this section, this is an ideal surface to be computed according to special criteria), T_w is the absolute external temperature of the tubes, and T_f represents the absolute temperature registered in correspondence of the fuel layer.

On the other hand, if M_f indicates the mass flow rate of the fuel,

$$M_f G c_{pg}\left(t_f - t_0\right) = M_f H_n' - q_r \tag{8.68}$$

where c_{pg} is the mean specific heat of the gas between t_0 and t_f, t_f is the temperature of the fuel layer, and H_n' is the heat introduced in the furnace per kg of fuel provided by (8.60).

An examination of (8.67) and (8.68) shows no computation difficulties during the design phase. Once temperature t_f (thus T_f, too) is established based on M_f, G, c_{pg}, and H_n', q_r is computed through (8.68); the radiated surface S representing the unknown value is obtained through (8.67).

The computation of t_f if S is known is not as simple. One must proceed by trial and error by adopting a certain value of t_f and computing q_r based on M_f, G, c_{pg}, H_n', and S through (8.67) and (8.68). Generally, the two values of q_r will not be identical. One continues with other values of t_f until the values of q_r coincide. The corresponding value of t_f represents the unknown temperature of the fuel layer. As we shall see, it is also possible to use a diagram to avoid calculation by approximation.

If we have combustion through burners instead of combustion on grates, specifically if we have a generator with a completely screened furnace, we cannot speak of furnace temperature anymore, because the gas temperature considerably varies with the gas flow from the burner toward the exit of the furnace. In this case it is possible to use an approximated computation method (like all those that will be discussed) based on (8.65).

Based on this method, the radiated heat is given by

$$q_r = 5.77\varepsilon S\left[\left(\frac{T_\mathrm{e}}{100}\right)^4 - \left(\frac{T_\mathrm{w}}{100}\right)^4\right]. \tag{8.69}$$

As in (8.67), T_w is the absolute wall temperature, whereas T_e is the absolute gas temperature at the exit of the furnace; ε is the emissivity of the flue gas that varies according to fuel type.

Recalling the meaning of h_g and substituting t_f with t_e in (8.68), a comparison of (8.69) with (8.68) shows that

$$5.77\frac{\varepsilon S}{M_f G}\left[\left(\frac{T_e}{100}\right)^4 - \left(\frac{T_w}{100}\right)^4\right] = h_g - c_{pg}\left(t_e - t_0\right). \tag{8.70}$$

With

$$\Omega = \frac{\varepsilon S}{M_f G} \tag{8.71}$$

and recalling that c_{pg} is a function of t_0, t_e, and moisture m, we have

$$t_e = f(\Omega, h_g m, t_w, t_0). \tag{8.72}$$

Temperature t_0 can conventionally be set at 20°C. In addition, the variations of t_w have a modest impact on q_r. Therefore, it is possible to determine a mean value of t_w for any value of the pressure, thus for the temperature of the fluid inside the tubes (generally steam generating tubes). For pressures up to 100 bar, it is possible to set $t_w = 300$°C. This way t_e is a function of Ω, h_g, and m only, and it is possible to build an easy-to-use diagram like the one in Fig. 8.8 which is based on (8.70). Of course, the diagram allows the computation of the fuel layer temperature based on (8.67) and (8.68), too. It suffices to remember that the temperature obtained from the diagram is the temperature t_f in this case and to adopt $\varepsilon = 0.8$. This way (8.69) is reduced to (8.67) except for the substitution of T_e with T_f.

As far as the values of ε that turn out to be satisfactory, they are obtained according to the following:

fuel oil $\varepsilon = 0.95$
pulverized coal, wood, natural gas, refinery gas $\varepsilon = 0.75$
blast-furnace gas $\varepsilon = 0.40$

In conclusion, note that using the diagram in Fig. 8.8 it is also possible to introduce the so-called furnace efficiency that factors in the unburned fuel in the case of combustion with solid fuels. In fact, as the amount of gas developed by combustion is about proportional to this efficiency, (8.68) can be modified as follows if η_f is the cited efficiency, that is,

$$\eta_f M_f G c_{pg} (t_f - t_0) = \eta_f M_f H_n' - q_r; \tag{8.73}$$

then

$$M_f G c_{pg} (t_f - t_0) = M_f H_n' - \frac{q_r}{\eta_f}. \tag{8.74}$$

Equation (8.70) is modified as follows after the usual substitution of t_f with t_e:

$$5.77 \frac{\varepsilon S}{\eta_f M_f G} \left[\left(\frac{T_e}{100} \right)^4 - \left(\frac{T_w}{100} \right)^4 \right] = h_g - c_{pg} (t_e - t_0). \tag{8.75}$$

To use the diagram in Fig. 8.8 it suffices to refer to the following equation of Ω:

$$\Omega = \frac{\varepsilon S}{\eta_f M_f G} \tag{8.76}$$

The resulting temperature t_e is lower than the one we would have with $\eta_f = 1$.

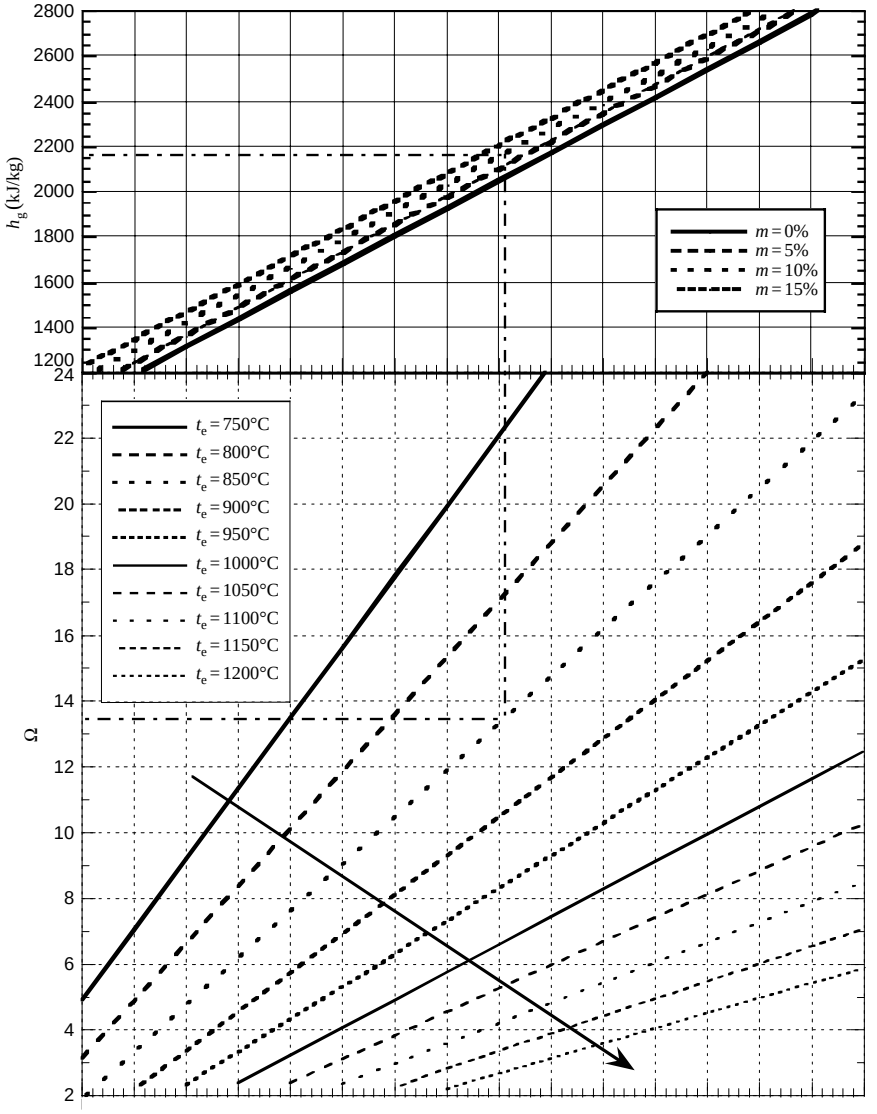


Fig. 8.8 Exit temperature of the flue gas from the furnace

Another simple computation method was first developed by Orrok and Hudson and later modified by Reid, Cohen, and Corey. On the basis of this modification that made calculation easier, the percentage of heat transferred to the furnace with respect to the introduced heat indicated with δ can be computed through the following equation:

$$\delta = \frac{100}{1 + CB\sqrt{q_s}}, \tag{8.77}$$

where C is a factor (its value will be indicated later on). B is the ratio between the gas flow rate generated by combustion and the heat introduced in the furnace during the time unit, q_s is the ratio between this heat and the radiated surface.

With the usual symbolism we have

$$B = \frac{M_f G_m}{M_f H_n'} = \frac{1}{h_g}; \tag{8.78}$$

$$q_s = \frac{M_f H_n'}{S}. \tag{8.79}$$

The difference in heat content of the gas between the exit temperature from the furnace and the room temperature (indicating with h_e and h_0 the enthalpy of the gas with respect to temperature t_e and temperature t_0), is given by

$$M_f G_m (h_e - h_0). \tag{8.80}$$

Therefore, given the significance of δ, we have

$$\left(1 - \frac{\delta}{100}\right) M_f H_n' = M_f G_m (h_e - h_0). \tag{8.80/1}$$

Then, from (8.77) and (8.78):

$$h_e - h_0 = h_g \left(1 - \frac{1}{1 + \dfrac{C}{h_g}\sqrt{q_s}}\right) = \frac{C\sqrt{q_s}}{1 + \dfrac{C}{h_g}\sqrt{q_s}}. \tag{8.81}$$

Finally,

$$h_e = h_0 + \frac{1}{\dfrac{1}{C\sqrt{q_s}} + \dfrac{1}{h_g}}. \tag{8.82}$$

Once the value of C is known, (8.82) facilitates the computation of h_e; based on the value of h_e, as illustrated in Sect. 7.9, it is then possible to calculate the unknown temperature t_e.

The authors of the method recommend the adoption of a mean value of C equal to $155.3\,\mathrm{kJ}^{1/2}\mathrm{s}^{1/2}\,\mathrm{m/kg}$ if expressing q_s in $\mathrm{kW/m^2}$ and h_e, h_0, h_g in kJ/kg.

Thus, from (8.82)

$$h_e = h_0 + \frac{1000}{\dfrac{6.439}{\sqrt{q_s}} + \dfrac{1000}{h_g}}. \tag{8.83}$$

Equation (8.77) and consequently (8.83) are usable for coal combustion (both on grates and in pulverized form) and for fuel oil combustion.

In the first case the results are closer to reality if (8.77) is modified as follows:

$$\delta = \frac{100}{1 + f_v C B \sqrt{q_s}} f_k. \tag{8.84}$$

This way (8.83) changes as follows:

$$h_e = h_0 + \frac{1000 + \dfrac{6.439\,(1 - f_k)\,h_g}{f_v\sqrt{q_s}}}{\dfrac{6.439}{f_v\sqrt{q_s}} + \dfrac{1000}{h_g}}. \tag{8.85}$$

The value of factor f_v depends on the percentage of surface covered by melted ashes and can be computed through Fig. 8.9 (for furnace with a hopper covered by melted ashes, one can assume that $f_v = 1.08$); the factor f_k is equal to unity for coal with a volatile matter content equal or greater than 20%, whereas if the content is under 20%, it is equal to

$$f_k = 1.34 - 0.017V, \tag{8.86}$$

where V is the percentage of volatile matter.

Note that

$$h_e - h_0 = c_{pg}\,(t_e - t_0)\,, \tag{8.87}$$

given that c_{pg} is the mean specific heat between room temperature t_0 and temperature t_e.

We can assume the conventional value of 20°C for t_0; moreover, c_{pg} can be assumed to be 1.164 kJ/kgK which, on average, matches actual values.

This way we obtain the following from (8.83):

$$t_e = 20 + \frac{\dfrac{1000}{1.164}}{\dfrac{6.439}{\sqrt{q_s}} + \dfrac{1000}{h_g}}. \tag{8.88}$$

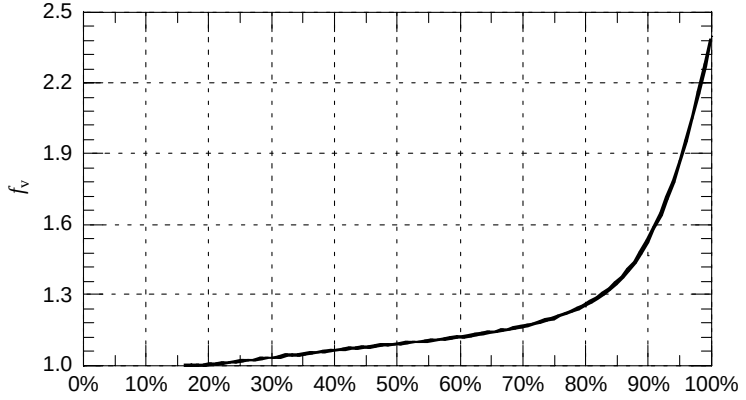


Fig. 8.9 Surface covered by melted ashes

Finally,

$$t_e = 20 + \frac{1000}{\frac{7.495}{\sqrt{q_s}} + \frac{1164}{h_g}}. \tag{8.89}$$

This highlights the temperature t_e resulting to be a function of two characteristic quantities, that is, the heat introduced per time unit and per radiated surface unit, and the heat introduced per mass unit of the flue gas.

Based on (8.89) it was possible to build the diagram shown in Fig. 8.10. Both (8.89) and the diagram corresponding to Orrok's method with the introduced simplifications; the mistakes made with respect to this method do not exceed 20°C plus or minus for $t_e = 600 - 1100$°C.

Another calculation method was developed by Konakow. According to him,

$$\left(\frac{T_e}{T_{ad}}\right)^4 - Ko\left(1 - \frac{T_e}{T_{ad}}\right) = 0, \tag{8.90}$$

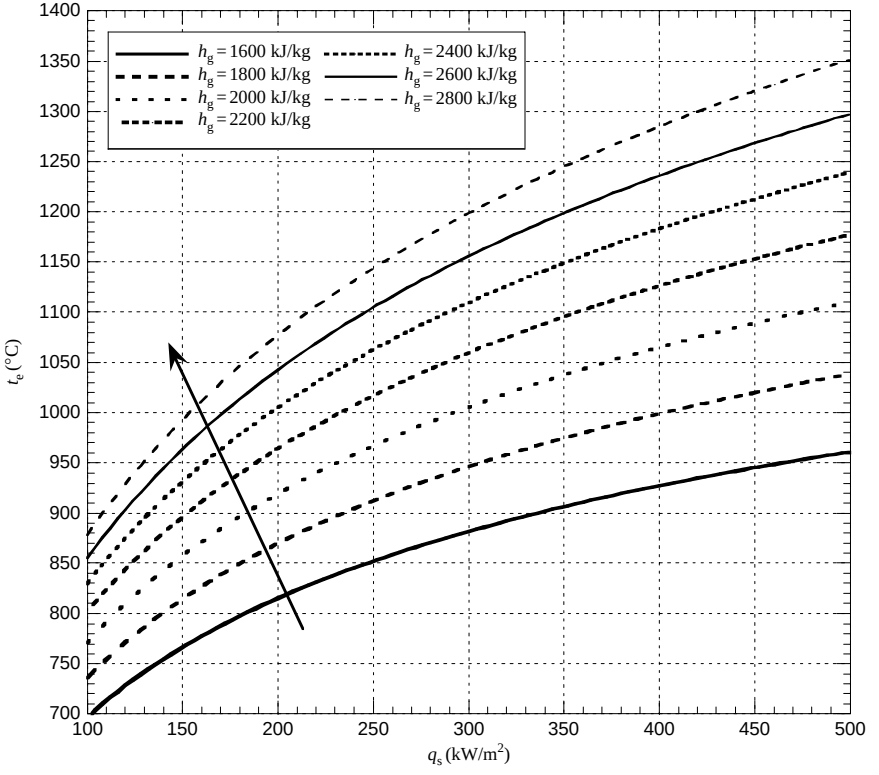


Fig. 8.10 Exit temperature from the furnace of the flue gas according to Orrok (8.89)

where T_{ad} is the adiabatic temperature of the flame estimated regardless of the dissociation and Ko is a factor that in most cases according to Gunz can be assumed to be equal to:

$$Ko = 239 \frac{q_s}{\left(\frac{T_{ad}}{100}\right)^4} \tag{8.91}$$

where q_s expressed in kW/m^2 is given by (8.79).

Equation (8.90) facilitates the project computation. In fact, after setting temperature t_e (thus T_e) and once the adiabatic temperature t_{ad} (and therefore T_{ad}) is calculated, the value of Ko is obtained from (8.90). Based on (8.91) it is possible to compute q_s and through (8.79) one obtains the unknown surface S.

The verification, that is, the computation of t_e knowing the surface S is not equally easy, and it must be done by trial and error. Even using Konakow's method it is possible to introduce the corrective factors f_v and f_k already considered as far as Orrok's method. The factor f_v reduces the involved surface. Based on (8.84), note that the introduction of f_v is equal to considering a correct value of q_s given by

$$q'_s = f_v^2 q_s. \tag{8.92}$$

Then the equation of Ko must be corrected as follows:

$$Ko = 239 \frac{f_v^2 q_s}{\left(\frac{T_{ad}}{100}\right)^4}. \tag{8.93}$$

The process is not equally straightforward to factor in f_k. In fact, looking at (8.84), note how the amount of heat transferred into the furnace is proportional to f_k.

Based on Nötzlin's research the following can be written:

$$1 - \frac{T'_e}{T_{ad}} = f_k \left(1 - \frac{T_e}{T_{ad}}\right), \tag{8.94}$$

where T_e is the value of the absolute exit temperature obtained from (8.90), whereas T'_e is the actual absolute temperature that factors in the influence of f_k.

Based on Nötzlin's measurements, f_k is equal to 1, if the content of volatile matter is equal or greater than 20%. Otherwise

$$f_k = 1.23 - 0.012V, \tag{8.95}$$

where V is the percentage of volatile matter content.

Note that (8.91) can also be written as follows:

$$Ko = 239 \frac{q_s}{\left(\frac{T_0}{100}\right)^4} \left(\frac{T_0}{T_{ad}}\right)^4. \tag{8.96}$$

Then, from (8.90)

$$\left(\frac{T_e}{T_0}\right)^4 - 239\frac{q_s}{\left(\frac{T_0}{100}\right)^4}\left(1 - \frac{T_e}{T_0}\frac{T_0}{T_{ad}}\right) = 0. \tag{8.97}$$

On the other hand, based on (8.62)

$$\frac{T_{ad} - T_0}{T_0} = \frac{T_{ad}}{T_0} - 1 = \frac{h_g}{c_{pg}T_0}. \tag{8.98}$$

Based on (8.98), from (8.97) we have:

$$\left(\frac{T_e}{T_0}\right)^4 - 239\frac{q_s}{\left(\frac{T_0}{100}\right)^4}\left(1 - \frac{T_e}{T_0 + \frac{h_g}{c_{pg}}}\right) = 0, \tag{8.99}$$

and

$$\left(\frac{T_e}{100}\right)^4 + 239q_s\left(\frac{T_e}{T_0 + \frac{h_g}{c_{pg}}} - 1\right) = 0. \tag{8.100}$$

c_{pg} represents the mean specific heat between 0°C and the theoretical combustion temperature in this case.

Note that for fuel oil without air heating $c_{pg} = 1.275 - 1.30\,\mathrm{kJ/kgK}$, whereas with air heating $c_{pg} = 1.30 - 1.32\,\mathrm{kJ/kgK}$. For coal without air heating $c_{pg} = 1.175 - 1.20\,\mathrm{kJ/kgK}$, whereas with air heating we have $c_{pg} = 1.21 - 1.235\,\mathrm{kJ/kgK}$. The values for natural gas match those for fuel oil. With reference to fuel oil and natural gas we can assume a conventional value of c_{pg} equal to 1.3 kJ/kgK; moreover, if T_0 takes the conventional value 293 K (it corresponds to 20°C), we obtain the following from (8.100).

$$\left(\frac{t_e + 273}{100}\right)^4 + 239q_s\left(\frac{t_e + 273}{0.77h_g + 293} - 1\right) = 0. \tag{8.101}$$

Equation (8.101) is shown in Fig. 8.11. The diagram can be used for fuel oil, natural gas and other gaseous fuels. Using a conventional value of c_{pg} does not introduce sensible mistakes, even though the actual value differs considerably from the assumed one. For instance, note that even with $c_{pg} = 1.13\,\mathrm{kJ/kgK}$ instead of 1.30 kJ/kgK, and with very low values of h_g (poor fuels) that represent worst conditions in terms of made errors, Fig. 8.11 leads to a value of t_e that differs from the one computed through (8.100) by about 15°C.

A comparison of Fig. 8.10 with Fig. 8.11 shows that the resulting values of t_e differ in a more or less sensible way from one another depending on the values q_s and h_g. If the difference is equal to only 18°C for $q_s = 150\,\mathrm{kW/m^2}$ and $h_g = 1800\,\mathrm{kJ/kg}$, there is a difference of 148°C for $q_s = 500\,\mathrm{kW/m^2}$ and $h_g = 2800\,\mathrm{kJ/kg}$.

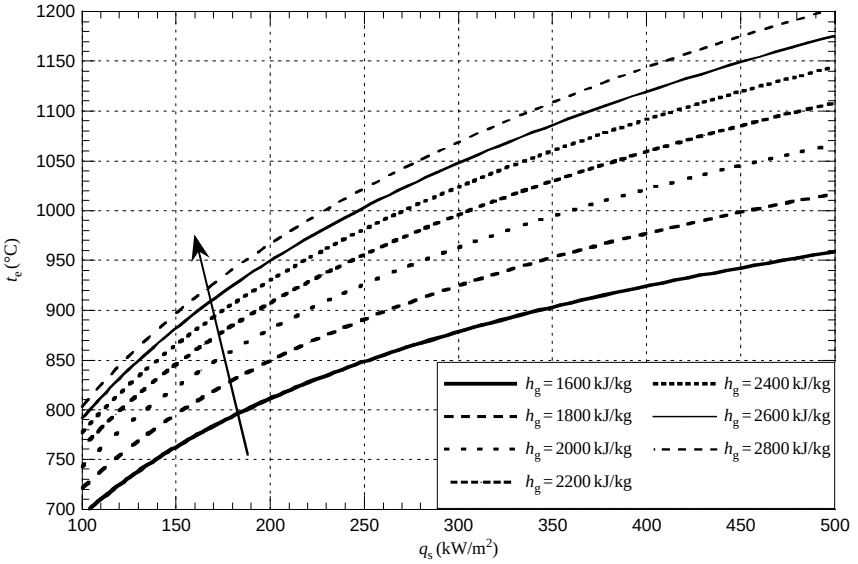


Fig. 8.11 Exit temperature from the furnace of the flue gas according to Konakow (8.101)

Note that low values of the two characteristic quantities occur when there is no heating of combustion air, and generally under reduced load, whereas the high values occur with a high superficial heat load in the furnace (referred to project requirements), as well as high air heating. These differences lead to questioning which criteria are most reliable. It is not easy to provide an answer, even though Konakow's criteria generally demonstrate more optimism about the heat transfer into the furnace, while Orrok's method is more pessimistic, especially for high values of q_s and h_g. The correct evaluation of the exit temperature of gas from the furnace should not be overestimated, given that even considerable mistakes in the estimate of t_e does not cause significant errors in the calculation of the exit temperature of gas from the generator, that is, of the efficiency.

In fact, a value of t_e in excess with respect to reality leads to a calculation of the values of the overall heat transfer coefficient relative to the tube banks in excess, as well, and as a result of it to a heat transfer greater than the real one. Consequently, the cooling of the gas is considered to be greater than the actual one, and this means that the incorrect estimate of t_e is almost completely nullified at the exit of the generator. The opposite is the case, if the value of t_e is underestimated with the same consequences as far as exit temperature of the gas from the generator which turns out to be only slightly below the actual value. Still, it would be preferable to have reliable computation criteria. Even though the correct estimate of this temperature is not very important as far as the calculation of the exit temperature of gas from the generator and as far as efficiency, this is not true for the heat transferred to the tube banks immediately following the furnace. We are specifically referring to the superheater because in this case the value of t_e is quite relevant.

With no presumption to entirely solving the problem, we elaborated a calculation process to determine t_e in a more satisfactory way, compared to Orrok's and Konakow's criteria. Undoubtedly, the Orrok-Hudson equation is structurally better suited for a quick and simple determination of t_e, because it does not require calculation by trial and error (Konakow's method). On the other hand, Orrok' equation in its original version is influenced by the value of factor C, usually assigned with a conventional value. The latter is the main cause for considerable, actual, and not completely justifiable discrepancies between the values obtained through this equation and Konakow's equation. So this is a spontaneous attempt to work on Orrok's equation through a value of C leading to values of t_e which are presumably closer to the reality of the phenomenon.

Therefore, we suggest the following value of C correlated to the value of h_g, that is,

$$C = \frac{461.9}{h_g^{0.15}}\,\mathrm{kJ}^{0.65}\mathrm{s}^{0.5}\mathrm{mkg}^{-1.15} \tag{8.102}$$

From (8.82) we obtain

$$h_e = h_0 + \frac{1000}{\dfrac{2.165h_g^{0.15}}{\sqrt{q_s}} + \dfrac{1000}{h_g}}. \tag{8.103}$$

Working as usual with the conventional value of c_{pg} equal to 1.164 kJ/kgK, we finally obtain the following equation:

$$t_e = 20 + \frac{1000}{\dfrac{2.52h_g^{0.15}}{\sqrt{q_s}} + \dfrac{1164}{h_g}}. \tag{8.104}$$

Equation (8.104) is shown in Fig. 8.12.

Note that the values of C obtained from (8.102) are lower than the conventional value relative to Orrok's criteria that is equal to 155.3, as we pointed out earlier. For $h_g = 1600\,\mathrm{kJ/kg}$ the result is $C = 152.7$, a slightly lower value; for $h_g = 2800\,\mathrm{kJ/kg}$ the outcome is $C = 140.4$ instead; the suggested equation differs from the one obtained through Orrok's criteria in a more substantial way for high values of h_g for which the differences between the values of t_e computed according to Orrok and Konakow are greater. A comparison of the diagrams in Figs. 8.10, 8.11, and 8.12 shows that the values of t_e obtained through (8.104) are generally intermediate between those resulting from Orrok's and Konakow's criteria. They also seem more realistic than the latter when taking into account the considerations we made above.

Finally, note that the value of t_e for a given fuel and a potential preset air heating depends uniquely on the air index.

The diagrams in Figs. 8.10, 8.11, and 8.12 could be substituted with diagrams valid for a given fuel and air heating with a curve bank characterized by the value

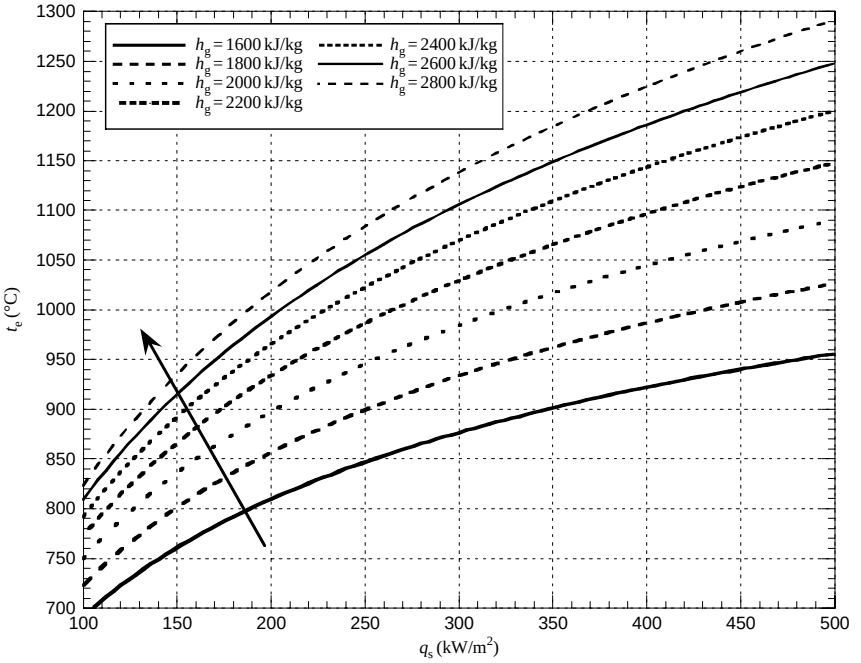


Fig. 8.12 Exit temperature from the furnace of the flue gas according to Annaratone (8.104)

of the air index or the air excess. These diagrams would look quite like the diagrams derived from experimental research in the hands of the biggest builders (e.g., Figs. 8.13 and 8.14). As far as the diagram in Fig. 8.13, note that using fuel oil with an air index $n = 1.15$, and recalling that air is heated at 300°C, the value of h_g is equal to about 2670 kJ/kg. Then it is possible to compare this experimental diagram with those in Figs. 8.10, 8.11, and 8.12, and it is evident that the one closest to the experimental diagram (often it coincides) is the diagram in Fig. 8.12. The same can be said about the diagram in Fig. 8.14 that does not include such a high air heating, thus referring to a smaller value of h_g.

All illustrated methods are of semi-empirical nature, and we cannot expect results to perfectly coincide with the reality of the phenomena. On the other hand, other methods with greater scientific pretence developed by various scholars are not more reliable than the methods described above and also bear the considerable disadvantage for practical technical purposes of being much more complex. The best solution, when possible, is to rely on experimental data registered on similar generators. This is what the biggest builders do by using these data to build tables or diagrams able to provide the exit temperature from the furnace or the heat transferred into it.

But the necessity to rely on calculation is always there to compare experimental data with theoretical ones, to study new constructive solutions not backed by experimental data, to do extrapolations of these data approximately knowing the influence

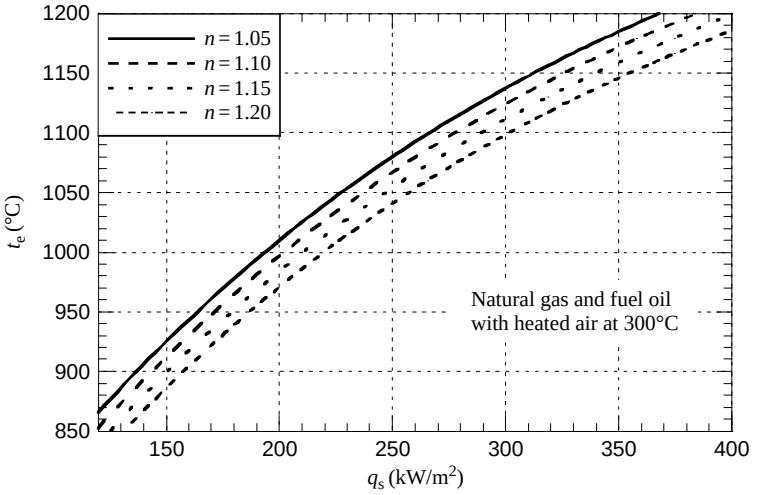
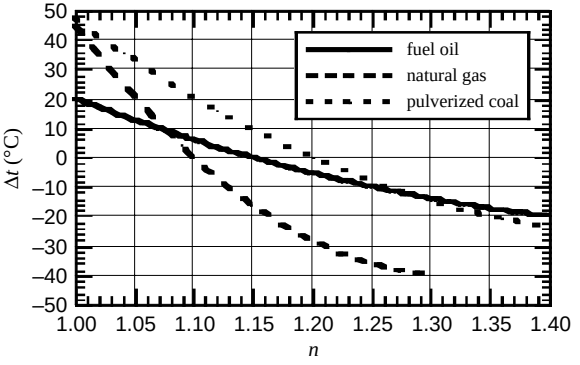


Fig. 8.13 Exit temperature from the furnace of the flue gas for power plant generators



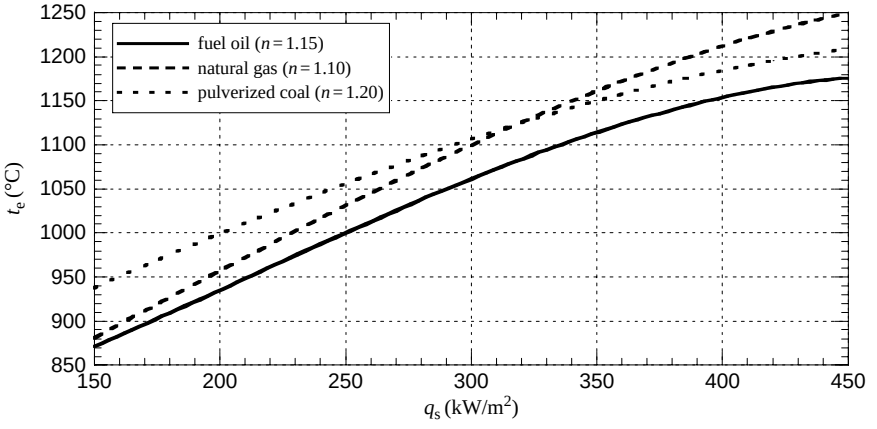


Fig. 8.14 Exit temperature from the furnace of the flue gas for various fuels

of the different parameters (e.g., moving from the smallest already proven units to bigger units yet to be designed).

The described methods can be used to this extent, yet keeping in mind that the obtained values of t_e can in some cases differ even by 30–50°C from actual values. At this point we need to determine how to compute the ideal radiated surface S. Note that in the case of a tube bank that "sees" the flame, the surface S corresponds to the projected surface of the bank. Specifically, this is the surface corresponding to the cross-sectional area of the space where the bank is lodged.

The projected surface is also the reference point for the screens on the wall made with tubes side by side or with finned tubes side by side.

If the tubes are spaced instead, S is equal to the surface of the screened wall multiplied by the factor E obtained from Fig. 8.15. This means that the value of E depends on the way the tubes are lined up on the wall and on the pitch. Curves 4 and 5 make it possible to compute the heat transferred to the first and the second row of tubes of model B. Of course, the sum of the values of E of curve 4 and 5 is equal to the value of E in curve 2.

It is interesting to know which criteria to follow if the tubes are covered with refractory material (for instance the bottom wall of the furnace). We assume that $E = 0.4$. Finally, there can be refractory walls that are not cooled by tubes, for example, the front wall or the one opposite the burners of certain small power generators. In that case $E = 0.05$.

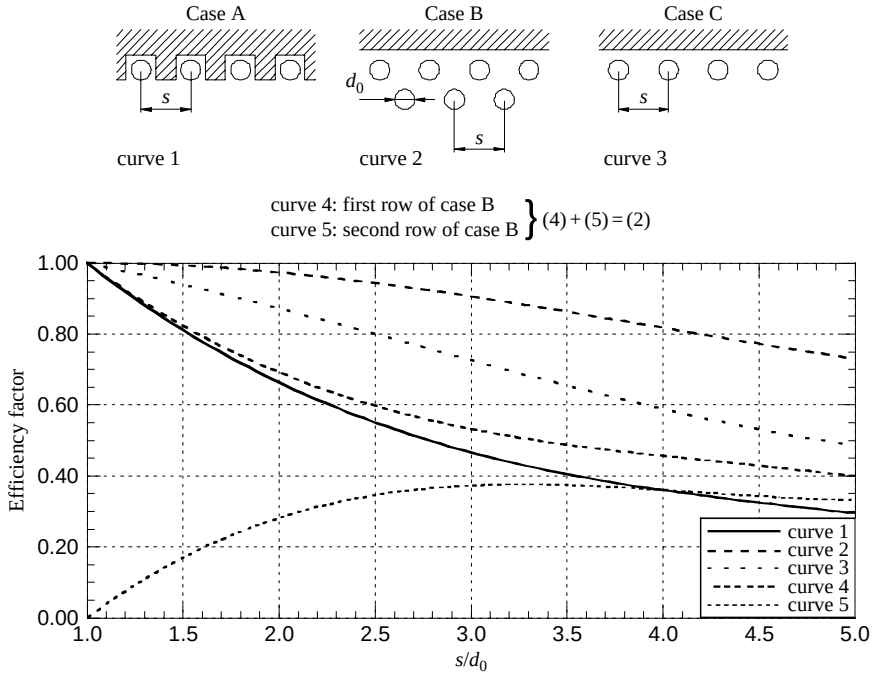


Fig. 8.15 Efficiency factor for radiated walls

As we are focussing on the furnace, we need to determine the calculation criteria for the heat transfer to the radiation superheaters located in the furnace. As far as the superheaters-dryers discussed in Sect. 3.9 and considering that they are located in the back of the furnace, that they are on its walls and not in front of the flame and that they have a limited surface, the heat transferred to the superheater can be computed through the following equation:

$$q_{SH} = 5.77 \varepsilon S_{SH} \left[\left(\frac{T_e}{100} \right)^4 - \left(\frac{T_w}{100} \right)^4 \right]; \tag{8.105}$$

q_{SH} is expressed in W, S_{SH} is the ideal radiated surface of the superheater in m^2, T_e is the absolute temperature of the flue gas at the exit of the furnace, and T_w is the absolute temperature of the wall; finally, ε is the emissivity. The value of ε can be assumed in agreement with the above, T_w can conventionally be assumed to be equal to the mean temperature of the steam plus 80–100°C.

Recalling what was said about the modest influence of T_w on q_{SH}, we can adopt a conventional value of T_w valid in approximately all cases, that is, $T_w = 673\,K$ ($t_w = 400\,°C$), after factoring in both pressure and temperature of the superheated steam typical of these cases.

Based on (8.105) we can write that

$$q_{SH} = q^*_{SH} S_{SH}, \tag{8.106}$$

given that

$$q^*_{SH} = 5.77 \varepsilon \left[\left(\frac{t_e + 273}{100} \right)^4 - 2050 \right]. \tag{8.107}$$

A check of t_w is recommended to ensure that the value assumed to compute the temperature of the external side is correct. This is required both to determine the mechanical characteristics of the material at running temperature (the reference in that case is to the temperature of the average fiber) influencing the tube resistance and to ensure that temperature t_w has a sufficient safety margin as far as the scaling temperature.

Note that the temperature difference between internal fluid and external side of the wall is given by approximation and in favor of safety as

$$\Delta t = q^*_{SH} \left(\frac{1}{\alpha''} + \frac{x_w}{k} \right), \tag{8.108}$$

where α'' is the heat transfer coefficient relative to the superheated steam flowing inside the tubes (Sect. 8.5).

The identification of the heat radiated to the superheaters on the walls of big radiation generators is obviously more complex. It must be estimated through experimental analysis of the transfer to the various areas of the furnace. It is impossible to provide guidelines of theoretical nature.

Let us now look at the impact of recirculation of flue gas on the heat transfer into the furnace. h_r will be the heat introduced per every kilogram of recirculated gas (tempering gas), given by the difference in enthalpy between inlet temperature and room temperature. χ will be the percentage of tempering gas; in addition, h'_g will be the heat introduced into the furnace per every kilogram of mixture of combustion gas and tempering gas.

Recalling the significance of h_g we will have:

$$h'_g = \frac{h_g + \frac{\chi}{100} h_r}{1 + \frac{\chi}{100}}. \tag{8.109}$$

As a result of a series of passages that are not shown here, we obtain the following:

$$\frac{h'_g}{h_g} = 1 - \frac{\chi}{100 + \chi} \left(1 - \frac{h_r}{h_g}\right). \tag{8.110}$$

Since $h_r < h_g$, we have $h'_g < h_g$.

The heat introduced into the furnace referred to 1 kg of flue gas is reduced with recirculation, as we could intuitively assume.

Figure 8.16 reproduces (8.110). As far as the introduced heat relative to the radiated surface, if q_s is the one without recirculation and q'_s is the one with recirculation,

$$q'_s = \frac{h_g + \frac{\chi}{100} h_r}{h_g} q_s. \tag{8.111}$$

Then,

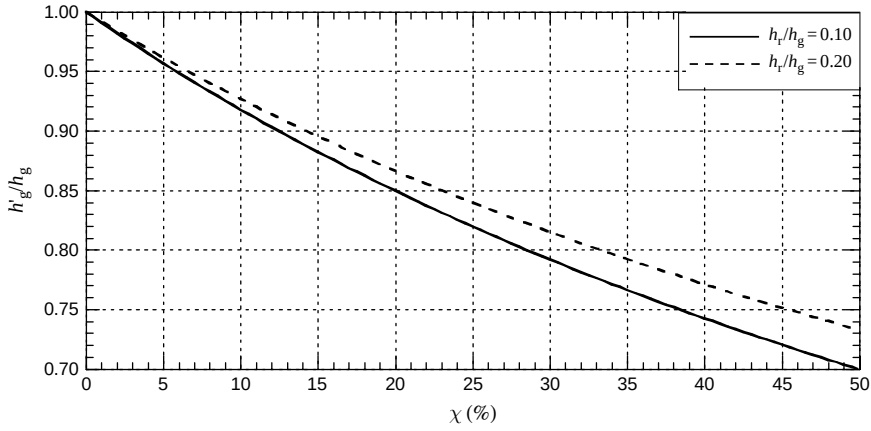


Fig. 8.16

$$\frac{q'_s}{q_s} = 1 + \frac{\chi}{100}\frac{h_r}{h_g}. \tag{8.112}$$

Note that the introduction of relatively cold gas leads to a sudden reduction of radiation in the lower area of the furnace. Actually, it is as if part of the radiated surface went missing. Consequently, the value of q'_s increases and it is possible to write that

$$\frac{q'_s}{q_s} = \psi\left(1 + \frac{\chi}{100}\frac{h_r}{h_g}\right), \tag{8.113}$$

where ψ is a factor greater than 1 which can be determined only experimentally. In any case, the value of q'_s is greater than q_s.

We now look at how recirculation may influence the exit temperature from the furnace by using an actual case as well as (8.104). Let us assume that $h_g = 2660\,\mathrm{kJ/kg}$ (combustion with fuel oil with air at $\approx 300^\circ\mathrm{C}$), that $h_r = 430\,\mathrm{kJ/kg}$ (tempering gas at $\approx 410^\circ\mathrm{C}$), and that 40% of the gas is recirculated. From (8.110) we obtain $h'_g = 2023\,\mathrm{kJ/kg}$. Assuming that $\psi = 1.4$ and $q_s = 350\,\mathrm{kW/m^2}$, from (8.113) we obtain $q'_s = 521.7\,\mathrm{kW/m^2}$. For $q_s = 350\,\mathrm{kW/m^2}$ and $h_g = 2660\,\mathrm{kJ/kg}$, based on (8.104), we obtain $t_e = 1160\,^\circ\mathrm{C}$; for $q'_s = 521.7\,\mathrm{kW/m^2}$ and $h'_g = 2023\,\mathrm{kJ/kg}$ still using (8.104) we obtain $t_e = 1106\,^\circ\mathrm{C}$.

Let us now assume that $q_s = 150\,\mathrm{kW/m^2}$ instead. Based on (8.113) we obtain $q'_s = 223.6\,\mathrm{kW/m^2}$. Referring to $q_s = 150\,\mathrm{kW/m^2}$ and $h_g = 2660\,\mathrm{kJ/kg}$, based on (8.104) we obtain $t_e = 923\,^\circ\mathrm{C}$; referring to $q'_s = 223.6\,\mathrm{kW/m^2}$ and $h'_g = 2023\,\mathrm{kJ/kg}$ we obtain $t_e = 926\,^\circ\mathrm{C}$.

The temperature variations with recirculation are evidently modest, and this confirms behavior during runtime, that is, under heavy load, temperature t_e recirculating the gas tends to decrease, while it tends to increase under reduced load.

By first approximation we can assume that temperature t_e is not subject to variations with recirculation. Δh_{e0} is the enthalpy difference between the one at temperature t_e and the one at room temperature; in other words,

$$\Delta h_{e0} = h_e - h_0. \tag{8.114}$$

Without recirculation the heat q_f transferred into the furnace is given by

$$q_f = M_g\left(h_g - h_e\right); \tag{8.115}$$

M_g is the mass flow rate of the flue gas generated by combustion.

With recirculation the radiated heat q'_f is given by

$$q'_f = M_g\left(h'_g - \Delta h_{e0}\right)\left(1 + \frac{\chi}{100}\right). \tag{8.116}$$

Recalling (8.109) we obtain

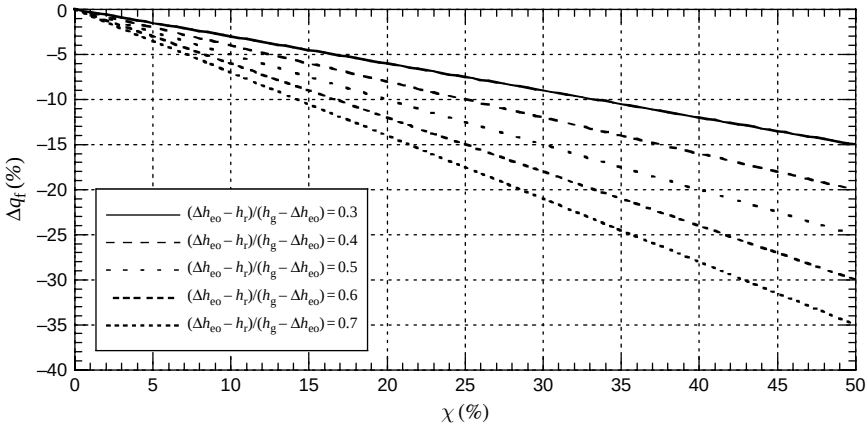


Fig. 8.17 Decrease of heat transfer in the furnace because of flue gas recirculation

$$\frac{q'_{\mathrm{f}}}{q_{\mathrm{f}}} = 1 - \frac{\chi}{100}\frac{\Delta h_{\mathrm{e}0} - h_{\mathrm{r}}}{h_{\mathrm{g}} - \Delta h_{\mathrm{e}0}}. \tag{8.117}$$

The percentage difference in absorption in the furnace Δq_{f} is therefore given by

$$\Delta q_{\mathrm{f}} = -\chi\frac{\Delta h_{\mathrm{e}0} - h_{\mathrm{r}}}{h_{\mathrm{g}} - \Delta h_{\mathrm{e}0}} \tag{8.118}$$

Figure 8.17 represents (8.118).

Recirculation clearly reduces the heat transfer by radiation (Fig. 3.42) in proportion to the percentage increase of tempering gas, and in relation to the increase of the value $\Delta h_{\mathrm{e}0}$, that is, the exit temperature of the gas from the furnace. If the latter is not subject to variations with recirculation according to our assumptions, given that both h_{g} and h_{r} are constant, the reduction in radiated heat is proportional to χ. Moreover, considering the typical values of $h_{\mathrm{g}}, \Delta h_{\mathrm{e}0}$, and h_{r}, this reduction is below the percentage of tempering gas.

8.5 Heat Transfer Coefficient of Water and Steam

In water-tube generators, the tubes carry evaporating water (steam-generating tubes), heated water (economizer), and superheated steam (superheater and reheater). In smoke-tube boilers the tubes come into contact with water on the outside. In the case of a steam boiler, the water evaporates and the steam bubbles leave the tube to move toward the upper area of the boiler (steam chamber) because of the density difference. If this is a warm water or superheated water boiler, generally steam builds up in contact with the tube after it is condensed by the colder water around it.

The heat transfer coefficient of the evaporating water inside the tubes indicated with α'' in Sect. 8.2 generally ranges from 6000 to $23,000\,\mathrm{W/m^2K}$, provided, of course, the evaporation takes place through bubble enucleation (Sect. 3.3). The influence of α'' on the overall heat transfer coefficient is quite modest, given the clear predominance of the heat transfer coefficient of the flue gas, as shown in the example in Sect. 8.2, as well. It is reasonable to adopt a mean conventional value equal to $12,000\,\mathrm{W/m^2K}$.

For smoke-tube boilers producing steam, a heat transfer coefficient equal to $6000–7000\,\mathrm{W/m^2K}$ is recommended. A value lower than the one in water-tube generators is better because in our case the steam bubbles come off the wall of the tube naturally due to the difference in density between steam and surrounding water, whereas in water-tube generators this detachment is favored by the current of the water–steam mix settling inside the tubes because of circulation.

If the generator produces warm or superheated water, it is recommended to use an even smaller value of α''. In fact, in this case there is mostly upward motion of the water potentially combined with limited local buildup of steam bubbles. The recommendation is to adopt a value of α'' equal to $2500–3500\,\mathrm{W/m^2K}$.

As far as the heat transfer coefficient of fluids flowing through the tubes in a turbulent way (as is the case in all instances of interest to us), extended experimental research was done leading to equations that differ in terms of not coinciding results, even though the tests were done using the same fluid under comparable conditions. This is because the equations refer to different investigation areas, or because of the experimented fluid, or because of the different temperature and speed ranges, and finally because the equations originate from different interpolation criteria of the experimental results.

This demonstrates that there is no scientifically valid all-purpose equation. Nonetheless, note that these equations are usually linked to the following general equation. This equation encompassing all the ones we will discuss, except for the Hansen and Schack equations, is as follows:

$$\mathrm{Nu} = \mathrm{C}\,\mathrm{Re}^{\mathrm{m}}\,\mathrm{Pr}^{\mathrm{n}}\,K. \tag{8.119}$$

In (8.119) Re stands for the Reynolds number given by

$$\mathrm{Re} = \frac{V\rho d}{\mu} = \frac{Vd}{\nu} = \frac{Gd}{\mu} \tag{8.120}$$

where V is the velocity of the fluid, G is its mass velocity, d is the inside diameter of the tube, μ and ν stand for the dynamic, as well as the kinematic viscosity, respectively, and ρ is the density.

In (8.119) Pr stands for the Prandtl number given by

$$\mathrm{Pr} = \frac{c_{\mathrm{p}}\mu}{k} \tag{8.121}$$

where c_{p} stands for the specific isobaric heat and k for the thermal conductivity.

Finally, Nu stands for the Nusselt number given by

$$\mathrm{Nu} = \frac{\alpha d}{k}, \tag{8.122}$$

where α is the heat transfer coefficient of the fluid.

C, m, and n are constants and K is a characteristic dimensionless factor.

One of the most common equations developed by Dittus and Bölter is as follows:

$$\mathrm{Nu} = 0.023\ \mathrm{Re}^{0.8}\ \mathrm{Pr}^{0.4}. \tag{8.123}$$

The values of c_p, μ, and k to be adopted are those that correspond to the mean temperature of the fluid along the tube called bulk temperature. Colburn developed the following equation:

$$\mathrm{Nu} = 0.023\ \mathrm{Re}^{0.8}\ \mathrm{Pr}^{1/3} \frac{c_\mathrm{pb}}{c_\mathrm{pf}} \tag{8.124}$$

The original Colburn equation seems to differ from (8.124) because of Stanton's number corresponding to Nu/RePr, but it actually corresponds to (8.124) that is part of (8.119).

In (8.124) c_pb is the specific isobaric heat at bulk temperature while c_pf is the specific heat at the mean temperature of the film (film temperature). The latter indicates the average between bulk temperature and wall temperature (in this case the inside of the tube). The values of c_p, μ, and k to introduce for calculation of Nu, Re and Pr refer to film temperature.

Sieder and Tate developed the following equation:

$$\mathrm{Nu} = 0.023\ \mathrm{Re}^{0.8}\ \mathrm{Pr}^{1/3} \left(\frac{\mu_\mathrm{b}}{\mu_\mathrm{w}}\right)^{0.14}. \tag{8.125}$$

The original equation by Sieder and Tate also looks different from (8.125) because it contains Stanton's number, too, but it corresponds to (8.125).

In (8.125) μ_b and μ_w stand for dynamic viscosity versus bulk temperature and wall temperature (as usual, we will adopt the average temperatures along the tube). In this case it is necessary to refer to the bulk temperature to compute Nu, Re, and Pr. Equations (8.123–8.125) are applicable when the difference in temperature between wall and fluid is modest, as is usually the case with water and steam. As far as liquids, the experiments conducted by Bernardo and Eian confirmed the reliability of (8.123). As far as the superheated steam, the literature provides other equations, such as the following one by Mac Adams:

$$\mathrm{Nu} = 0.0214 \left(1 + \frac{2.3 d_\mathrm{i}}{l}\right) \mathrm{Re}^{0.8}\ \mathrm{Pr}^{1/3} \tag{8.126}$$

where l stands for the length of the tube between inlet and outlet; it factors in the influence of phenomena taking place at the extremities of the tube.

Another equation suggested by Babcock and Wilcox is as follows:

$$\mathrm{Nu} = 0.023\ \mathrm{Re}^{0.8}\ \mathrm{Pr}^{0.4} \left(\frac{T_\mathrm{b}}{T_\mathrm{f}}\right)^{0.8} \tag{8.127}$$

where T_b is the absolute bulk temperature and T_f the absolute film temperature.

Considering that with water and steam the difference between bulk and film temperature is modest and that (8.127) includes the ratio between absolute temperatures, it does practically not differ much from (8.123).

In addition, we show Hansen's equation which does not fit in the general schematization of (8.119):

$$\mathrm{Nu} = 0.037 \left(\mathrm{Re}^{0.75} - 180\right) \mathrm{Pr}^{0.42} \left[1 + \left(\frac{d_\mathrm{i}}{l}\right)^{2/3}\right] \left(\frac{\mu_\mathrm{b}}{\mu_\mathrm{w}}\right)^{0.14} \tag{8.128}$$

This equation is reminiscent of (8.125), and factors in the impact of phenomena taking place at the extremities of the tube like (8.126).

In fact, for calmed turbulence, i.e., for l with a high value compared to d, the equation is simplified as follows:

$$\mathrm{Nu} = 0.037 \left(\mathrm{Re}^{0.75} - 180\right) \mathrm{Pr}^{0.45} \left(\frac{\mu_b}{\mu_w}\right)^{0.14} \tag{8.129}$$

Both in (8.128) and (8.129). Nu, Re, and Pr must be computed in reference to the bulk temperature.

Finally, we point out that the following equation is included in the "Wärmeatlas VDI":

$$\mathrm{Nu} = 0.024\ \mathrm{Re}^{0.8}\ \mathrm{Pr}^{0.33}. \tag{8.130}$$

It is responsible for values of α differing quite considerably from those obtainable with the Dittus Bölter equation only for high values of Pr (water at low temperature).

Equations (8.126) and (8.128) are frequently used and can be recommended without reservation, because they seem to summarize the experiments of the different researchers in a satisfactory way. Note that the equation of Dittus Bölter (8.123), which is much simpler than the latter, fulfills practical requirements in terms of water and superheated steam quite well.

The Dittus Bölter equation leads to the following equation necessary to compute α'' directly [see (8.31)]:

$$\alpha'' = 0.023\ \mathrm{Re}^{0.8}\ \mathrm{Pr}^{0.4} \frac{k}{d_\mathrm{i}}. \tag{8.131}$$

The values of μ, k, and Pr for both water and steam can be taken from the publication "Properties of water and steam in SI units."

In any case, we show the values relative to water at 50 bar in Figs. 8.18–8.20. Keep in mind that pressure has a very modest impact on the values of μ, k, and Pr relative to water. The values in the diagrams can be used for any pressure including sufficient approximation for practical purposes.

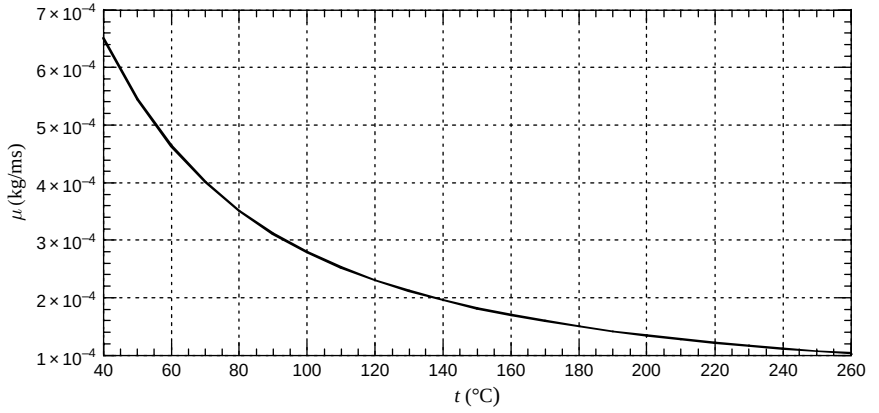


Fig. 8.18 Water dynamic viscosity

If (8.131) is used for water, recalling (8.120) and (8.121), we see that it can also be written as follows:

$$\alpha'' = 0.023 \frac{G^{0.8}}{d_{\mathrm{i}}^{0.2}} \left(\frac{c_{\mathrm{p}} k^{1.5}}{\mu} \right)^{0.4} . \tag{8.132}$$

Assuming that

$$K_{\mathrm{w}} = 0.023 \left(\frac{c_{\mathrm{p}} k^{1.5}}{\mu} \right)^{0.4} , \tag{8.133}$$

we establish that the value of K_{w} depends on pressure and temperature.

Based on the values of c_{p}, k, and μ included in the cited publication, we obtain the following approximated equation:

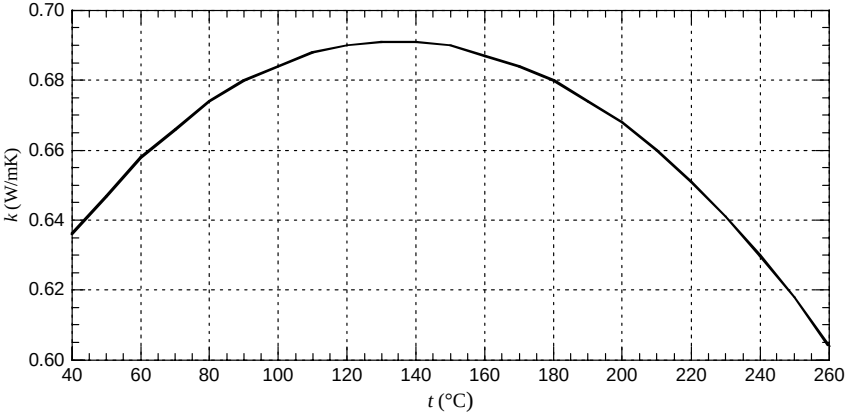


Fig. 8.19 Water thermal conductivity

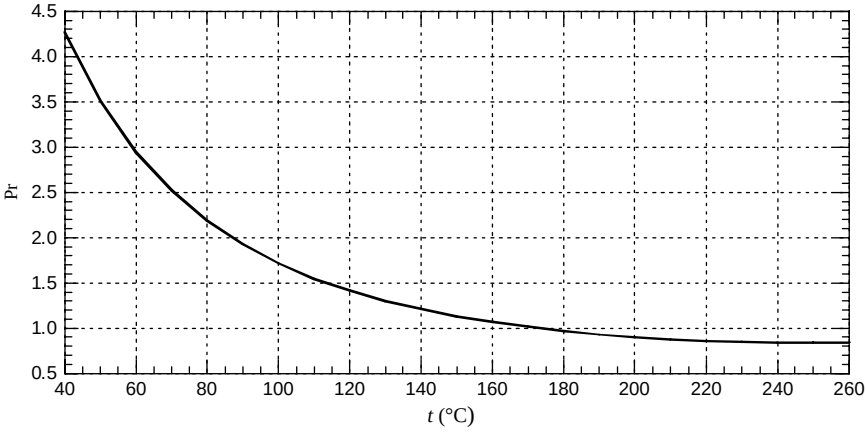


Fig. 8.20 Number of Prandtl for water

$$K_w = 5.86 + 0.018\frac{p}{100} + \left(9.41 - 0.63\frac{p}{100}\right)\frac{t_b}{100} - \left(1.542 - 0.3\frac{p}{100}\right)\left(\frac{t_b}{100}\right)^2 \tag{8.134}$$

for $p = 1 - 100$ bar and $t = 0 - 300\,^{\circ}\mathrm{C}$.

The greatest mistake using (8.134) instead of (8.133) is equal to 1.5% plus or minus, so it is acceptable given the modest influence that the heat transfer coefficient of water has on the computation of the overall heat transfer coefficient.

Finally, note that the influence of pressure is modest, so it is possible to write by first approximation that

$$K_w = 5.87 + 9.09\frac{t_b}{100} - 1.39\left(\frac{t_b}{100}\right)^2. \tag{8.134a}$$

With reference to (8.31) the heat transfer coefficient of water can therefore be computed much more easily, even based on the following equation:

$$\alpha'' = K_w \frac{G^{0.8}}{d_i^{0.2}}, \tag{8.135}$$

where α'' is in $\mathrm{W/m^2K}$, G is in $\mathrm{kg/m^2s}$, and d_i in m; factor K_w is computed through (8.134) or (8.134a).

We could proceed in a similar way for the superheated steam, but we prefer to refer to the equation suggested by Schack; using this equation in a similar way, it was used for water later on, to obtain an easy-to-use equation like (8.135).

According to Schack, the heat transfer coefficient for all types of gas and superheated steam can be computed through the following equation:

$$\alpha'' = 0.0254 c_{p1}^{0.81} k^{0.19} \frac{V_0^{0.75}}{d_i^{0.25}} \tag{8.136}$$

with α'' in $\mathrm{W/m^2K}$, k in W/mK, c_{p1} in $\mathrm{J/Nm^3K}$, and d_i in m. In addition, V_0 stands for velocity under normal conditions, that is, the velocity of the fluid at 0°C and atmospheric pressure.

Equation (8.136) is not part of (8.119); it could be included only approximately into the following equation which represents a special case of (8.119):

$$\mathrm{Nu} = C\ \mathrm{Re}^{0.75}\ \mathrm{Pr}^{0.75} \tag{8.137}$$

or

$$\mathrm{Nu} = C\ \mathrm{Pe}^{0.75} \tag{8.138}$$

where Pe is the Peclet number which is well known to be the product of Re by Pr.

Equation (8.136) would correspond to (8.138) if the exponent of c_{p1} were equal to 0.75 and the exponent of k equal to 0.25. In fact, if V is the velocity under actual running conditions, c_p the specific heat referred to the mass unit, ρ_0 the density under normal conditions and ρ the density under actual running conditions, then

$$c_{p1} = c_p \rho_0; \tag{8.139}$$

$$V_0 \rho_0 = V \rho. \tag{8.140}$$

If the exponents of c_{p1} and k were 0.75 and 0.25, (8.136) could be written as follows:

$$\alpha'' = C c_p^{0.75} k^{0.25} \frac{V^{0.75} \rho^{0.75}}{d_i^{0.25}}, \tag{8.141}$$

or

$$\alpha'' = C \left(\frac{V \rho d_i}{\mu} \right)^{0.75} \left(\frac{c_p \mu}{k} \right)^{0.75} \frac{k}{d_i} \tag{8.142}$$

that corresponds to (8.137) and (8.138).

On the other hand, c_{p1} and k are a function of the temperature; we may write

$$0.0254 c_{p1}^{0.81} k^{0.19} = A + B t_b + C t_b^2 \tag{8.143}$$

where A, B, and C are constants.

Calculating the values of A, B, and C for the superheated steam, we obtain the following equation showing only V_0, t_b, and d_i:

$$\alpha'' = \left(4.42 + 0.302 \frac{t_b}{100} \right) \frac{V_0^{0.75}}{d_i^{0.25}}. \tag{8.144}$$

Given that (8.136) is not part of (8.119), it is necessary to specify the measuring units referred to in (8.144). Note that α'' is obtained in $\mathrm{W/m^2K}$ since V_0 is expressed in m/s, d_i in m, and t_b in °C.

Clearly, velocity V_0 has no physical significance for steam, but this is the logic behind Schack's equation. Therefore, V_0 is a conventional velocity computed by considering steam as perfect gas capable of staying that way until 0°C.

Thus, if V stands for the velocity of the steam under actual running conditions

$$V = V_0 \frac{273 + t_b}{273} \frac{1.013}{p}, \tag{8.145}$$

with p in bar and keeping in mind that atmospheric pressure is equal to 1.013 bar.

Therefore, (8.144) can also be written like this:

$$\alpha'' = \frac{294 + 0.201 t_b}{(273 + t_b)^{0.75}} \frac{(pV)^{0.75}}{d_i^{0.25}}. \tag{8.146}$$

Knowing the absolute pressure, the velocity, the temperature, and the inside diameter of the tubes, (8.146) helps to compute the heat transfer coefficient α''.

If v is the specific volume of the steam

$$V = Gv, \tag{8.147}$$

given that G is, as usual, the mass velocity.

From (8.146)

$$\alpha'' = \frac{294 + 0.201 t_b}{(273 + t_b)^{0.75}} (pv)^{0.75} \frac{G^{0.75}}{d_i^{0.25}}. \tag{8.148}$$

Assuming that

$$K_s = \frac{294 + 0.201 t_b}{(273 + t_b)^{0.75}} (pv)^{0.75}, \tag{8.149}$$

we establish that this factor is a function of pressure and temperature because the specific volume is a function of these quantities. Based on the values of v, we obtain the following approximated equation of K_s:

$$K_s = 5.069 - 0.0529p + (4.467 + 0.169p) \frac{t_b}{1000} - (1.268 + 0.143p) \left(\frac{t_b}{1000}\right)^2 \tag{8.150}$$

valid for $p = 10 - 100$ bar and $t_b = 180 - 550$°C.

The greatest mistake made by using (8.150) instead of (8.149) is equal to about 1.5% plus or minus, and this is acceptable because of the modest influence of the heat transfer coefficient of steam in the computation of the overall heat transfer coefficient.

In reference to (8.31), the heat transfer coefficient of the superheated steam can be computed much more easily based on the following equation:

$$\alpha'' = K_s \frac{G^{0.75}}{d_i^{0.25}} \tag{8.151}$$

where α'' is expressed in $\mathrm{W/m^2K}$, G in $\mathrm{kg/m^2s}$, and d_i in m; factor K_s can be computed through (8.150). Note the analogy with (8.135). The value of α'' relative to the superheated steam is important especially as far as the temperature of the tube. Excessive temperatures lead to either the necessity to use higher quality steel or to the risk of bursting.

For convection superheaters the value of α'' should roughly not go under $1200\,\mathrm{W/m^2K}$. Under these conditions, with a thermal flux of $50\,\mathrm{kW/m^2}$ and a wall thickness of 5 mm, there is a temperature difference between the mean fiber of the tube and the steam of 45°C. We assume a steam pressure of 100 bar, a temperature of 500°C and an inside tube diameter of 28 mm. Based on (8.150), $K_\mathrm{s} = 6.57$; as $d_\mathrm{i}^{0.25} = 0.409$, from (8.151) we obtain $G^{0.75} = 74.70$, and finally $G = 314.6\,\mathrm{kg/m^2s}$.

As the specific volume of the steam under the given pressure and temperature conditions is equal to 0.03276 m3/kg, the velocity is equal to $V = 314.6 \times 0.03276 = 10.31\,\mathrm{m/s}$.

If $p = 25$ bar, $t = 400\,^\circ\mathrm{C}$, and $d_\mathrm{i} = 32\,\mathrm{mm}$ instead, the consequence would be $K_\mathrm{s} = 6.448$; as $d_\mathrm{i}^{0.25} = 0.423$, from (8.151) we obtain $G^{0.75} = 78.72$ and $G = 337.4\,\mathrm{kg/m^2s}$. The mass velocity is quite similar to the previous one, but the velocity is completely different. In fact, as the specific volume is equal to $0.12\,\mathrm{m^3/kg}$, we obtain $V = 337.4 \times 0.12 = 40.49\,\mathrm{m/s}$.

Worse situations happen with radiation superheaters where the thermal flux is much higher. Therefore, for low pressure superheaters and especially for the radiated ones, very high steam velocity is required. Still, there will be huge temperature differences between tube and steam that will have to be accurately computed, thus using the appropriate type of steel to build the superheater.

8.6 Heat Transfer Coefficient of Flue Gas and Air Inside the Tubes

The topic is of interest for smoke-tube boilers and recuperative air heaters. The gas produced by combustion gets in contact with the flue wall of smoke-tube boilers. Consequently, besides heat transferred by the flame through radiation, a certain amount of heat is transferred also by convection, thus the need to compute the heat transfer coefficient of the gas. This heat transfer by radiation and convection will be examined in detail within its framework in Sect. 8.7.

Moreover, flue gas flows in the tubes of the smoke-tube boiler. Thus, it is necessary to determine the calculation criteria of the heat transfer coefficient. Finally, either flue gas or air can flow in the tubes of the recuperative air heaters; therefore, it is required to determine the calculation criteria relative to the heat transfer coefficient inside the tubes.

The Dittus and Bölter equation already discussed in Sect. 8.5 can be taken into consideration for flue gas and air, as well. Here it is:

$$\mathrm{Nu} = 0.023\,\mathrm{Re}^{0.8}\,\mathrm{Pr}^{0.4} \tag{8.152}$$

It is best, though, to keep the results of other researchers into account, too, because we pointed out earlier that this equation, as much as (8.124) and (8.125), can be used only if the temperature difference between fluid and wall is modest. It is not our case, so it would not seem appropriate to refer to it.

Evans and Sarjant experimented with gas and air and then summarized it as follows:

$$\mathrm{Nu} = 0.020\ \mathrm{Re}^{0.8} \tag{8.153}$$

Experiments on warm air by Zellnick and Churchill led to the following:

$$\mathrm{Nu} = 0.0231\ \mathrm{Re}^{0.8}\ \mathrm{Pr}^{1/3} \tag{8.154}$$

Bulk temperature must be considered both in (8.153) and (8.154). A comparison between (8.153) and (8.152) for $\mathrm{Pr} = 0.76$ (value that corresponds to high temperature with flue gas) shows a difference in the value of Nu equal to 3% which is still modest. If we compare (8.154) with (8.152) the difference amounts to 2% instead. Finally, the results obtained from experiments with gas by Desmon and Sams show good correspondence with (8.152) if the reference is to film temperature.

In conclusion, in view of these results (8.152) or the corresponding (8.131) can be applied even for flue gas flowing inside the tubes, as long as the reference is to film temperature. As far as this temperature, note that it can be assumed to be equal to the average between the gas temperature (bulk temperature) and the wall temperature.

The latter can be assumed to be equal to water increased by 70–90°C for the flue of smoke-tube boilers. For the tubes of these boilers we recommend an increase of water temperature of 5–10°C if the boiler produces steam, and of 10–15°C if the boiler generates hot water or superheated water. The wall temperature of air heaters by first approximation can be assumed to be equal to the average between the temperature of flue gas and air.

Based on (8.152) we have:

$$\alpha = 0.023\ \mathrm{Re}^{0.8}\ \mathrm{Pr}^{0.4}\frac{k}{d_\mathrm{i}}; \tag{8.155}$$

it can also be written as follows, as we already pointed out in Sect. 8.5:

$$\alpha = 0.023\frac{G^{0.8}}{d_\mathrm{i}^{0.2}}\left(\frac{c_\mathrm{p}k^{1.5}}{\mu}\right)^{0.4}. \tag{8.156}$$

The values of c_p, k, and μ can be computed through (7.111), (7.150), and (7.165).

These quantities are clearly a function of the temperature and the moisture percentage by mass of the flue gas.

Now, if

$$K_\mathrm{g} = 0.023\left(\frac{c_\mathrm{p}k^{1.5}}{\mu}\right)^{0.4}, \tag{8.157}$$

even factor K_g is a function of both cited quantities; therefore, it is possible to obtain the following approximated equation for K_g based on (7.111), (7.150), and (7.165).

$$K_g = 3.00 + 0.018m + (2.161 + 0.0117m)\frac{t_f}{1000} - (0.658 - 0.0257m)\left(\frac{t_f}{1000}\right)^2 \tag{8.158}$$

with m expressed as percentage.

Equation (8.158) is valid for $t_f = 50 - 1200\,^{\circ}\mathrm{C}$ and $m = 0 - 12\%$. The biggest possible mistake using (8.158) instead of (8.157) is equal to about 0.6% plus or minus which is clearly acceptable.

Therefore, with reference to (8.32), the heat transfer coefficient of flue gas can also be easily computed through the following equation:

$$\alpha' = K_g \frac{G^{0.8}}{d_i^{0.2}} \tag{8.159}$$

where α' is expressed in $\mathrm{W/m^2K}$, G in $\mathrm{kg/m^2s}$, and d_i in m; factor K_g is computed through (8.158).

As far as moisture, based on Sect. 7.9 and (7.102), it is given by:

$$m = \frac{8.936H + H_2O}{nA_{tm} + 1} + 0.5; \tag{8.160}$$

H and H_2O are mass percentages of hydrogen and water or steam in the fuel, n is the air index, and A_{tm} the amount expressed as mass of stoichiometric air required for combustion of 1 kg of fuel (Sect. 7.5).

In (8.160) we assumed that the fuel also contains H_2O; furthermore, we conventionally factored in a certain amount of humidity of the combustion air (Sect. 7.9).

As far as air, (8.155) is still valid and we consider factor K_a given by:

$$K_a = 0.023\left(\frac{c_p k^{1.5}}{\mu}\right)^{0.4} \tag{8.161}$$

which is formally identical to factor K_g.

The values c_p, k, and μ can be computed through (7.81), (7.121), and (7.152).

Based on the values of the three quantities, it is possible to compute the following approximate equation for K_a:

$$K_a = 3.087 + 0.186\frac{t_f}{100} \tag{8.162}$$

which is valid for $t_f = 0 - 300\,^{\circ}\mathrm{C}$.

The mistakes made using (8.162) instead of (8.161) are irrelevant. With reference to (8.31), the heat transfer coefficient of air can be computed quite easily based on

$$\alpha'' = K_a \frac{G^{0.8}}{d_i^{0.2}}, \tag{8.163}$$

where α'' is expressed in W/m^2K, G in kg/m^2s, and d_i in m; factor K_a is computed through (8.162).

8.7 Heat Transfer in the Flue of the Smoke-Tube Boilers

If the transfer to the water included only radiated heat from the flame in the flue of smoke-tube boilers as in the furnace of water-tube generators, it would be possible to use the calculation criteria of the exit temperature of gas from the furnace discussed in Sect. 8.4. In fact, as we already pointed out in Sect. 8.6, besides radiated heat in the flue, there is heat transfer by convection by the flue gas getting in contact with the wall of the flue. The calculation of temperature t_e based on the criteria presented in Sect. 8.4 is in any case fundamental to determine the actual exit temperature of flue gas from the flue, too.

Note that the radiated surface S to consider in the calculation of t_e is represented by the surface of the cylinder and by the surface of the backflow chamber that "sees" the flame. For the latter, if the boiler has a wet end plate, one must consider the surface corresponding to the inside diameter of the flue minus the surface of the inspection door which is still factored in but with an efficiency factor E equal to 0.05 (Sect. 8.4). If the boiler has a dry end plate, one considers the surface corresponding to inside diameter of the flue multiplied by 0.05 because the backflow chamber does not get in contact with water.

The computation of the exit temperature of gas from the flue requires previous calculation of maximum flame temperature t_f. Note in this context that thermal flux in the flue varies considerably along the axis of the flue itself. Specifically, maximum flame temperature and maximum thermal flux is reached at close distance from the burner. This maximum value of the thermal flux is called peak flux. The mathematical model for the calculation of temperature t_f is based on the following fundamental assumptions.

The potential heat transfer by convection in the peak flow area is ignored, because it is in any case irrelevant compared with the heat transfer by radiation from the flame. The assumption is that the length of the area involved by the peak phenomenon is equal to 1 m per diameter of the flue which in turn is also equal to 1 m; for diameters other than 1 m it is assumed to be proportional to the square root of the diameter.

The mean thermal flux q_m due to flame radiation in the peak area is equal to:

$$q_m = \sigma\varepsilon\left[(t_f + 273)^4 - (t_w + 273)^4\right]; \tag{8.164}$$

σ stands for Stefan-Boltzmann constant, ε for the emissivity of the flame, t_f for the flame temperature, and t_w for the wall temperature of the flue.

The second term in square brackets can be ignored compared to the first one. In fact, if we consider a flame temperature of 1500°C and a wall temperature of 450°C, the mistake made by ignoring this term is below 3%.

Taking into account the disregard for the not very significant convective phenomena, we can use the following equation:

$$q_{\mathrm{m}} = \sigma\varepsilon\,(t_{\mathrm{f}} + 273)^4\,. \tag{8.165}$$

The Stefan-Boltzmann constant is equal to $5.77 \times 10^{-8}\mathrm{W/m^2K^4}$, and so we can write that

$$q_{\mathrm{m}} = 5.77\varepsilon\left(\frac{t_{\mathrm{f}} + 273}{100}\right)^4 \tag{8.166}$$

with q_{m} expressed in $\mathrm{W/m^2}$.

Based on the assumptions that were made, the heat radiated by the flame in the peak area indicated with q_{r} is therefore equal to:

$$q_{\mathrm{r}} = q_{\mathrm{m}}\pi D\sqrt{D} = 5.77\varepsilon\pi D^{1.5}\left(\frac{t_{\mathrm{f}} + 273}{100}\right)^4. \tag{8.167}$$

If q is the heat introduced into the flue and M_{f} is, as usual, the fuel mass flow rate (see Sect. 8.4), H'_{n} is the introduced heat per mass unit of the fuel, G is the amount of flue gas per mass unit of fuel, and c_{pg} is the average specific isobaric heat of the gas between room temperature t_0 and flame temperature, we have:

$$q = M_{\mathrm{f}}H'_{\mathrm{n}} = M_{\mathrm{f}}Gc_{\mathrm{pg}}\,(t_{\mathrm{f}} - t_0) + q_{\mathrm{r}}. \tag{8.168}$$

Assuming 20°C for temperature t_0 and recalling (8.167) we have:

$$M_{\mathrm{f}}\left[H'_{\mathrm{n}} - Gc_{\mathrm{pg}}\,(t_{\mathrm{f}} - 20)\right] = 5.77\varepsilon\pi D^{1.5}\left(\frac{t_{\mathrm{f}} + 273}{100}\right)^4; \tag{8.169}$$

then

$$q\left[1 - \frac{G}{H'_{\mathrm{n}}}c_{\mathrm{pg}}\,(t_{\mathrm{f}} - 20)\right] = 5.77\varepsilon\pi D^{1.5}\left(\frac{t_{\mathrm{f}} + 273}{100}\right)^4. \tag{8.170}$$

Note that the ratio H'_{n}/G stands for the heat introduced into the flue per mass unit of flue gas.

As usual, indicating this with h_{g}, based on (8.170) we obtain:

$$q = \frac{5.77\varepsilon\pi D^{1.5}\left(\dfrac{t_{\mathrm{f}} + 273}{100}\right)^4}{1 - \dfrac{c_{\mathrm{pg}}}{h_{\mathrm{g}}}\,(t_{\mathrm{f}} - 20)} \tag{8.171}$$

As far as emissivity, experiments show that it is equal to 0.35 for flues of 3.75 ft in diameter (1.14 m).

On the other hand, if l stands for the length of the area involved in the phenomenon (which, based on the assumption of the computation is proportional to $\sqrt{D}$), based on Mac Adams' suggestion we can write that

$$\varepsilon = 1 - \mathrm{e}^{-\mathrm{C}l}, \tag{8.172}$$

given that C is a constant.

It is therefore possible to write that

$$0.35 = 1 - \mathrm{e}^{-\mathrm{C}\sqrt{1.14}}; \tag{8.173}$$

then

$$-\mathrm{C}\sqrt{1.14} = \log_{\mathrm{e}} 0.65, \tag{8.174}$$

and finally,

$$\mathrm{C} = 0.4. \tag{8.175}$$

Then we assume the following:

$$\varepsilon = 1 - \mathrm{e}^{-0.4\sqrt{D}}, \tag{8.176}$$

and (8.171) is written as follows:

$$q = \frac{5.77\pi\left(1 - \mathrm{e}^{-0.4\sqrt{D}}\right) D^{1.5} \left(\dfrac{t_{\mathrm{f}} + 273}{100}\right)^4}{1 - \dfrac{c_{\mathrm{pg}}}{h_{\mathrm{g}}}\left(t_{\mathrm{f}} - 20\right)}. \tag{8.177}$$

The value of c_{pg} does not vary in a significant way with variations of temperature t_{f} for flame temperatures that are practically possible. A fixed value of c_{pg} corresponding to a flame temperature of 1600°C for flue gas with a moisture percentage by mass of 6% is used to simplify calculation. It is equal to 1240 J/kgK.

Thus, we can write that

$$q = \frac{5.77\pi\left(1 - \mathrm{e}^{-0.4\sqrt{D}}\right) D^{1.5} \left(\dfrac{t_{\mathrm{f}} + 273}{100}\right)^4}{1 - \dfrac{1240}{h_{\mathrm{g}}}\left(t_{\mathrm{f}} - 20\right)}. \tag{8.178}$$

Based on the heat introduced into the flue within the time unit (in W), the value of h_{g} (in J/kg), as well as the value of the diameter, it is possible to obtain temperature t_{f} by trial and error through (8.178). It is also possible to develop an approximate equation to compute t_{f} directly.

Note that expressing q in kW, h_{g} in kJ/kg and introducing cross-section area A of the flue, the following equation can be obtained from (8.178):

$$\frac{q}{A} = \frac{23.08\left(1 - \mathrm{e}^{-0.4\sqrt{D}}\right) D^{-0.5} \left(\dfrac{t_{\mathrm{f}} + 273}{100}\right)^4}{1000 - \dfrac{1240}{h_{\mathrm{g}}}\left(t_{\mathrm{f}} - 20\right)}. \tag{8.179}$$

The analysis of (8.179) shows that the influence of the diameter is quite modest, whereas the value of h_g and the value of the ratio q/A, that is, the heat introduced into the flue within the time unit and by cross-section area unit, are crucial.

We obtain the following approximate equation that does not include the diameter:

$$t_f = 775 + 0.18h_g + \left(0.048h_g - 20\right)\frac{q}{1000A} - \left(0.0017h_g + 0.2\right)\left(\frac{q}{1000A}\right)^2 \quad (8.180)$$

with $q/A = 2000 - 12,000\,\mathrm{kW/m^2}$, $h_g = 1800 - 2700\,\mathrm{kJ/kg}$ and $D = 0.6 - 1.5\,\mathrm{m}$.

The mistakes made using (8.180) instead of (8.179) do not exceed 3.5% plus or minus; these mistakes are clearly tolerable given the quantity they refer to.

At this point, note that if we could ignore the heat transfer by convection, we could write that

$$M_g c_{pg} dT = -\sigma\varepsilon\left(T^4 - T_w^4\right) dS, \quad (8.181)$$

where M_g stands for the mass flow rate of the flue gas, c_{pg} for the specific isobaric heat, T and T_w for the absolute temperatures of the flue gas and the wall of the flue, respectively.

Equation (8.181) can be written as follows:

$$\frac{dT}{dS} = -\frac{\sigma\varepsilon\left(T^4 - T_w^4\right)}{M_g c_{pg} T^4} T^4. \quad (8.182)$$

We introduce factor K_1 given by:

$$K_1 = \frac{\sigma\varepsilon\left(T^4 - T_w^4\right)}{M_g c_{pg} T^4} \quad (8.183)$$

Therefore, (8.182) is written like this:

$$\frac{dT}{dS} = -K_1 T^4. \quad (8.184)$$

Factor K_1 varies along the flue depending on variations of T, T_w, the specific isobaric heat c_{pg} and presumably the emissivity, too. We consider it like a constant, ideally referring to mean values of the different quantities. Note that it will not be necessary to compute it, as we shall see later on.

Assuming that

$$T^{-3} = -3y, \quad (8.185)$$

we obtain

$$y = -\frac{1}{3}T^{-3}; \quad (8.186)$$

$$y' = T^{-4}\frac{dT}{dS}; \quad (8.187)$$

$$\frac{\mathrm{d}T}{\mathrm{d}S} = T^4 y'. \tag{8.188}$$

Then, based on (8.184):

$$y' = -K_1. \tag{8.189}$$

The integral of (8.189) is given by:

$$y = -K_1 S + \mathrm{C} \tag{8.190}$$

where C is a constant.

From (8.190) and recalling (8.185), after a series of steps we obtain:

$$T = \sqrt[3]{\frac{1}{3K_1 S - 3\mathrm{C}}}, \tag{8.191}$$

or

$$T = \sqrt[3]{\frac{1}{3K_1 S + \mathrm{C}_1}} \tag{8.192}$$

where C_1 is a constant.

The surface S_0 of the flue is the one between the area where the flame forms and the end of the flue, while T_f and T_e^* represent the maximum absolute temperature of the flame and the temperature of the flue gas at the exit of the flue.

For $S = 0$, $T = T_\mathrm{f}$, and from (8.192) we obtain:

$$C_1 = \frac{1}{T_\mathrm{f}^3}; \tag{8.193}$$

then

$$T = \sqrt[3]{\frac{1}{3K_1 S + \dfrac{1}{T_\mathrm{f}^3}}}. \tag{8.194}$$

Moreover, for $S = S_0$:

$$T_e^* = \sqrt[3]{\frac{1}{3K_1 S_0 + \dfrac{1}{T_\mathrm{f}^3}}}. \tag{8.195}$$

Leading through a series of steps to:

$$K_1 = \frac{1}{3S_0}\left(\frac{1}{T_\mathrm{e}^{*3}} - \frac{1}{T_\mathrm{f}^3}\right). \tag{8.196}$$

If we know the temperature the flue gas would have at the exit of the flue in absence of convective phenomena and also temperature T_f, it is possible to compute the value of factor K_1 regardless of difficult considerations about the value of the emissivity.

Now, if we consider the heat transfer by convection as well, we must write that

$$M_\mathrm{g} c_\mathrm{pg} \mathrm{d}T = -\left[\sigma\varepsilon\left(T^4 - T_\mathrm{w}^4\right) + \alpha_\mathrm{g}\left(T - T_\mathrm{w}\right)\right]\mathrm{d}S, \tag{8.197}$$

where α_g stands for the heat transfer coefficient of the gas.

Equation (8.197) can be written as follows:

$$\frac{dT}{dS} = \frac{\sigma\varepsilon\left(T^4 - T_w^4\right)}{M_g c_{pg} T^4} T^4 - \alpha_g \frac{T - T_w}{M_g c_{pg} T}\ T. \tag{8.198}$$

Recalling (8.183) and introducing factor K_2 given by:

$$K_2 = \alpha_g \frac{T - T_w}{M_g c_{pg} T}, \tag{8.199}$$

Equation (8.198) is written as follows:

$$\frac{dT}{dS} = -K_1 T^4 - K_2 T. \tag{8.200}$$

Of course, factor K_2 is a function of S because the wall temperature T_w varies along the flue, while temperature T varies along the flue, followed in turn by variations as far as the specific isobaric heat and the heat transfer coefficient.

We can consider it constant and adopt mean values for the different quantities, therefore writing that:

$$K_2 = \alpha_{gm} \frac{T_m - T_{wm}}{M_g c_{pgm} T_m}; \tag{8.201}$$

This means that the specific isobaric heat will be the average between temperature T_f and temperature T_e of the gas at the exit of the flue, and that temperature T_m which represents the mean value among those mentioned above will be used for the computation of the heat transfer coefficient of the gas.

In this case the value of c_{pgm} can be assumed to be the one corresponding to the mean temperature between T_e and T_f based on (7.111) even for $t > 1200°C$.

According to the same position in (8.185) and based on (8.187) we obtain:

$$y' = -K_1 - K_2 T^{-3}. \tag{8.202}$$

Therefore, always based on (8.185):

$$y' = 3K_2 y - K_1 \tag{8.202/1}$$

Equation (8.202/1) is a linear differential equation and its integral is given by:

$$y = e^{3K_2 S}\left(-K_1 \int e^{3K_2 S} dS + C_2\right); \tag{8.203}$$

then

$$T^{-3} = e^{3K_2 S}\left(\frac{K_1}{K_2} e^{3K_2 S} - 3C_2\right). \tag{8.204}$$

Finally,

$$T = \frac{\mathrm{e}^{-K_2 S}}{\sqrt[3]{\frac{K_1}{K_2}\mathrm{e}^{3K_2 S} + C_3}}. \tag{8.205}$$

For $S = 0$ we have $T = T_\mathrm{f}$, and based on (8.205):

$$C_3 = \frac{1}{T_\mathrm{f}^3} - \frac{K_1}{K_2} \tag{8.206}$$

and

$$T = \frac{\mathrm{e}^{-K_2 S}}{\sqrt[3]{\frac{K_1}{K_2}\left(\mathrm{e}^{3K_2 S} - 1\right) + \frac{1}{T_\mathrm{f}^3}}}. \tag{8.207}$$

Thus, the exit temperature of the gas from the flue T_e is given by:

$$T_\mathrm{e} = \frac{\mathrm{e}^{-K_2 S_0}}{\sqrt[3]{\frac{K_1}{K_2}\left(\mathrm{e}^{3K_2 S_0} - 1\right) + \frac{1}{T_\mathrm{f}^3}}}. \tag{8.208}$$

Recalling (8.196) at this point and admitting that the value of K_1 may be assumed to be approximately equal to the one relative to transfer by pure radiation, we obtain:

$$T_\mathrm{e} = \frac{\mathrm{e}^{-K_2 S_0}}{\sqrt[3]{\frac{\mathrm{e}^{3K_2 S_0} - 1}{3K_2 S_0}\left(\frac{1}{T_\mathrm{e}^{*3}} - \frac{1}{T_\mathrm{f}^3}\right) + \frac{1}{T_\mathrm{f}^3}}}. \tag{8.209}$$

Equation (8.209) helps to compute T_e, once the values of T_e^* and T_f are known and by computing (potentially by trial and error) the value of factor K_2 which obviously depends on T_e.

The analysis of (8.209) shows that it can be substituted in a completely satisfactory way by the following and easier equation:

$$t_\mathrm{e} = t_\mathrm{e}^* - 4.55\sqrt[3]{t_\mathrm{f}}\sqrt{t_\mathrm{e}^*}K_2 S_0. \tag{8.210}$$

All temperatures are in °C; the exit temperature t_e of the flue gas from the flue is computed based on temperature t_e^* (this is the exit temperature of the gas computed based on the criteria in Sect. 8.4), the maximum temperature of the flame t_f (for which the calculation criteria were explained earlier), the value of factor K_2 (which depends on the entity of the convection phenomena), and surface S_0.

The latter must be computed as follows:

$$S_0 = \pi D\left(l - \sqrt{D}\right), \tag{8.211}$$

where l is the length of the flue; l and D are expressed in m.

Note that the heat transfer coefficient α_{gm} in the equation of K_2 must be computed based on the criteria in Sect. 8.6. If the heat transferred by convection cannot be ignored when the goal is to compute a value of t_e as close as possible to reality, this heat, though, is equal to a modest percentage of the heat transferred by radiation that still constitutes the predominant element of the phenomenon. Roughly, the heat transfer by convection is equal to 5–8% compared to the one by radiation. Temperature t_e generally differs from temperature t_e^* by about 50°C.

If the flue is much longer than the flame, it is advisable to proceed as follows. Consider a virtual length of the flue equal to that of the flame increased by 20%. The computation of the exit temperature is done based on this length, as indicated earlier. The remaining portion of flue is considered like a cavity, and its wall is radiated by carbon dioxide and the steam in the flue gas, as described in Sect. 8.9.

In conclusion, to prevent intolerable values of the peak flux (as far as the wall temperature of the flue, therefore its resistance, and to prevent scaling) the flue must have a sufficient diameter. The following equation is a valid reference:

$$D \geq 0.43 + 0.084 \frac{q}{1000}, \tag{8.212}$$

where D is the diameter of the flue in m and q is the heat introduced into it in kW.

8.8 Heat-Transfer Coefficient of Flue Gas and Air Hitting a Tube Bank

The topic involves tube banks of water-tube generators (steam-generating tubes, economizers, superheaters, and reheaters), convective tube banks of diathermic fluid boilers, and recuperative air heaters (the tubes are hit by either flue gas or air).

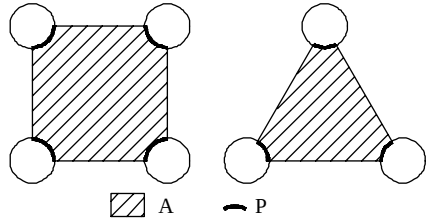
In exceptional instances the flue gas (and the air) flow parallel to the tubes, because this solution generally leads to a smaller amount of heat transferred, thus a less interesting proposition from a financial point of view. Anyway, there are no difficulties in computing the heat transfer coefficient even in this case, because the gas flows through channels consisting of space between the tubes. It is a question of computing the cross-sectional area A, as well as the wet perimeter P (Fig. 8.21), and then to compute the hydraulic diameter given by

$$d = \frac{4A}{P} \tag{8.213}$$

Based on the value of d, it is possible to compute the heat transfer coefficient, according to the criteria described in Sect. 8.6, and as long the reference to the film temperature is included.

Generally, the tube bank is hit transversally (Figs. 8.22 and 8.23). To that extent there are numerous research projects leading to very similar conclusions.

Fig. 8.21



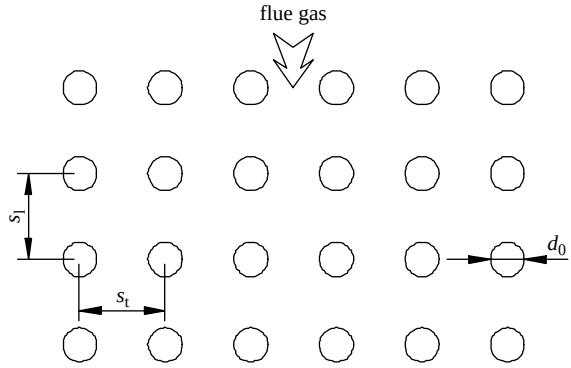


Fig. 8.22 Arrangement with inline tubes

In 1933 Colburn suggested the following equation for inline tubes (Fig. 8.22):

$$\mathrm{Nu} = 0.26\ \mathrm{Re}^{0.6}\ \mathrm{Pr}^{1/3}, \tag{8.214}$$

and the following for staggered tubes (Fig. 8.23):

$$\mathrm{Nu} = 0.33\ \mathrm{Re}^{0.6}\ \mathrm{Pr}^{1/3} \tag{8.215}$$

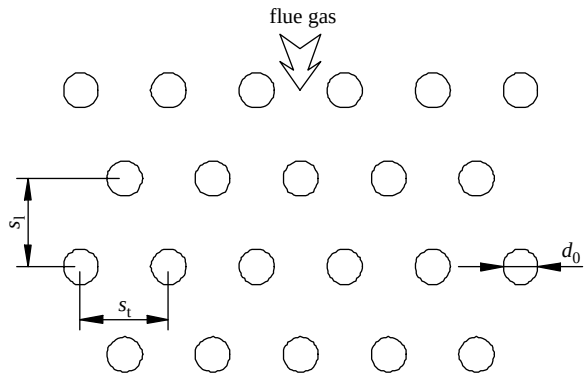


Fig. 8.23 Arrangement with staggered tubes

Equations (8.214) and (8.215) refer to film temperature. Fundamental research was done later on by Pierson and Huge at Babcock and Wilcox.

On the basis of the results of this research and after comparison with the results of other researchers, Grimison developed the following equation which is valid for a number of at least 10 rows crossed by gas:

$$\mathrm{Nu} = 0.284\, f_\mathrm{a}\, \mathrm{Re}^{0.61} \tag{8.216}$$

The reference is to film temperature.

In (8.216) f_a is an arrangement factor the value of which depends on Re, the ratio between the transverse pitch s_t and the outside diameter of the tubes d_o, and the ratio between longitudinal pitch s_l and the diameter (Figs. 8.22 and 8.23). In addition, it depends on the type of arrangement (in the case of inline and staggered tubes).

Equation (8.216) is modified as follows to factor in the influence of the number of rows (when below 10):

$$\mathrm{Nu} = 0.284\, f_\mathrm{d}\, f_\mathrm{a}\, \mathrm{Re}^{0.61} \tag{8.217}$$

where f_d does, in fact, take this influence into account; the value of depth factor f_d can be taken from Table 8.2. The values of f_a can be obtained from Figs. 8.24 and 8.25. Grimison's equation responds quite well to the reality of the phenomenon. In any case, note that Grimison's equation does not include Prandtl's number in contrast to Colburn's equations (8.214) and (8.215) and to the majority of equations in Sect. 8.5. This number is included in an equation suggested later on by Babcock and Wilcox, that is,

$$\mathrm{Nu} = 0.287\, f_\mathrm{d}\, f_\mathrm{a}\, \mathrm{Re}^{0.61}\, \mathrm{Pr}^{1/3} \tag{8.218}$$

in reference to film temperature like (8.216) and (8.217). Equation (8.218) represents a refinement compared to Grimison's equation, and we believe it to be preferable.

Highlighting the heat transfer coefficient leads from (8.217) to the following:

$$\alpha = 0.284\, f_\mathrm{d}\, f_\mathrm{a}\, \mathrm{Re}^{0.61}\, \frac{k}{d_\mathrm{o}}. \tag{8.219}$$

Similarly, from (8.218) we obtain the following:

$$\alpha = 0.287\, f_\mathrm{d}\, f_\mathrm{a}\, \mathrm{Re}^{0.61}\, \mathrm{Pr}^{1/3}\, \frac{k}{d_\mathrm{o}}. \tag{8.220}$$

The value of the Prandtl number ranges for flue gas (from 50 to 1200°C) from 0.765 to 0.795; based on the two previous equations, we determine that (8.220) leads to lower values of α by 6.5–7.5%, compared to those computed through (8.219).

Table 8.2 Depth factor f_d

Number of rows	1	2	3	4	5	6	7	8	9
f_d	0.70	0.82	0.87	0.91	0.93	0.95	0.97	0.98	0.99

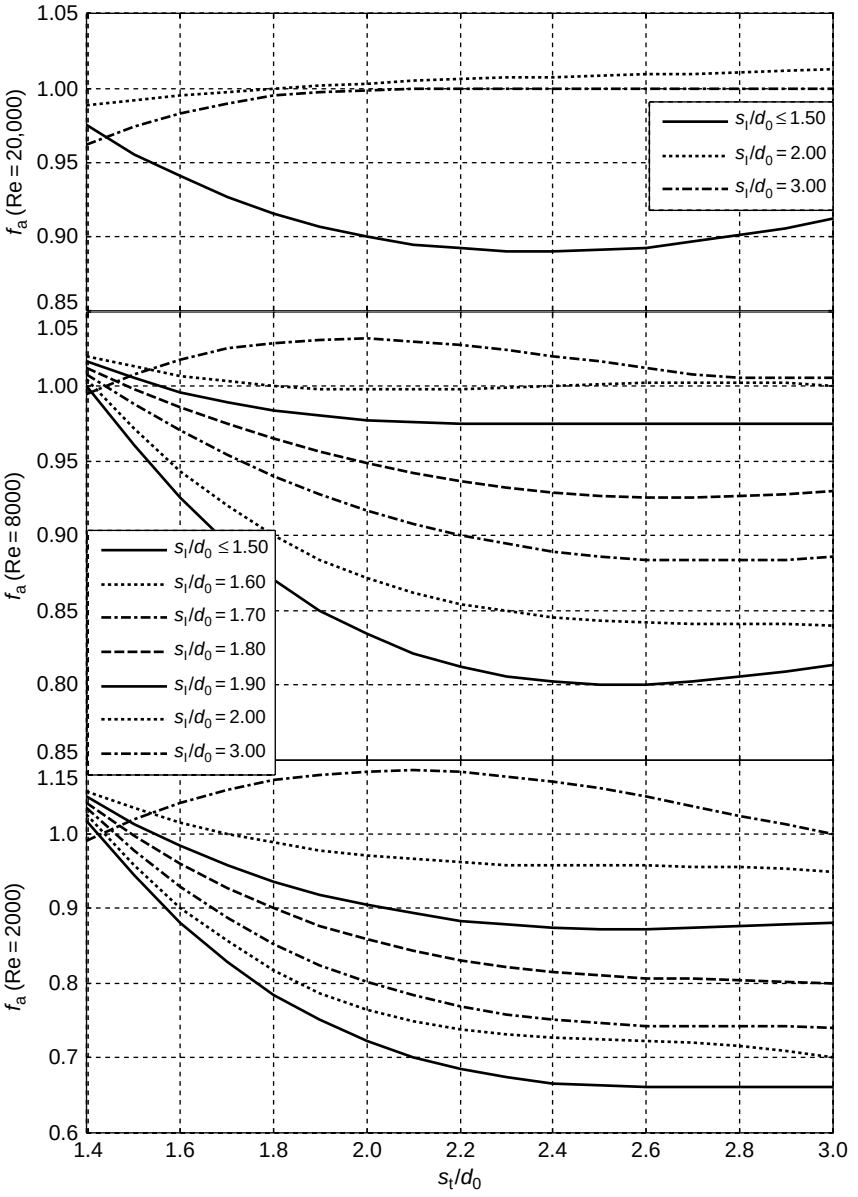


Fig. 8.24 Arrangement factor f_a for inline tubes

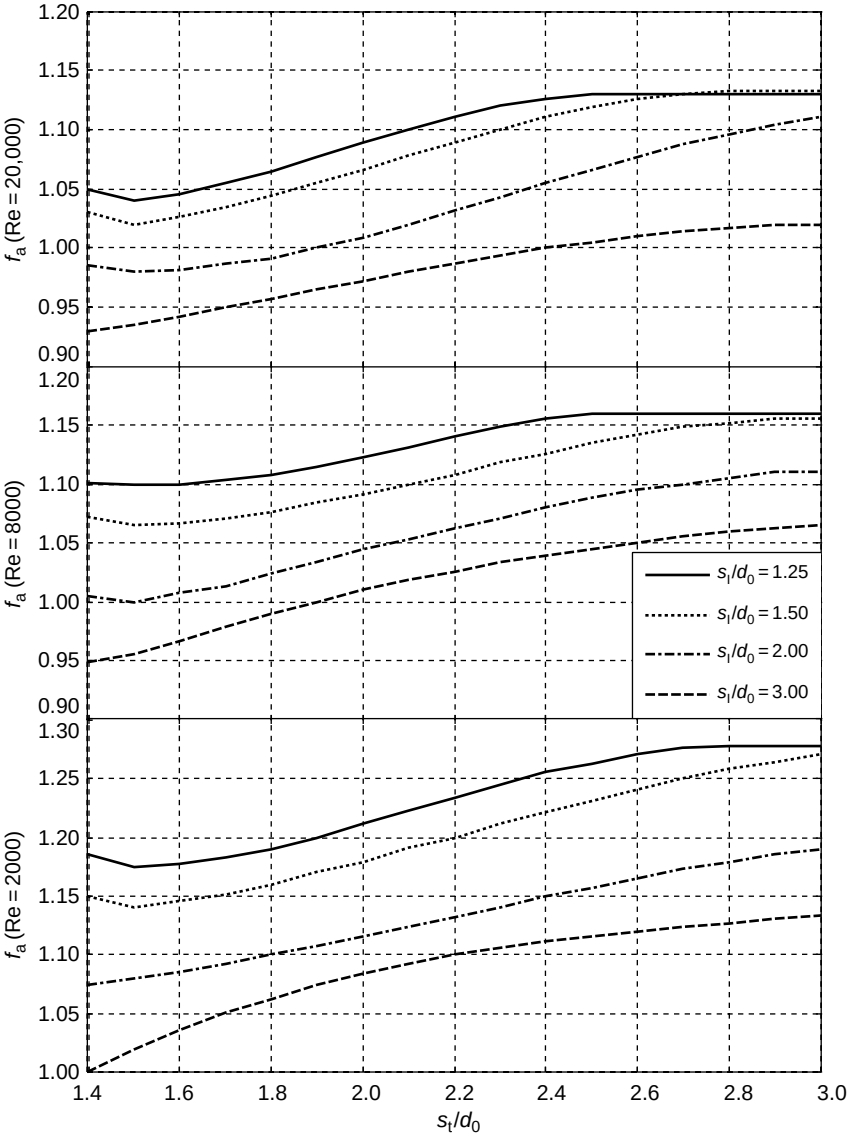


Fig. 8.25 Arrangement factor f_a for staggered tubes

For air between 0 and 300°C the Prandtl number ranges from 0.72 and 0.735, so that the difference between the values in both equations amounts to about 9%.

Equation (8.220) can also be written as follows:

$$\alpha = 0.287 f_{\mathrm{d}} f_{\mathrm{a}} \frac{G^{0.61}}{d_0^{0.39}} \frac{\left(c_{\mathrm{p}} k^2\right)^{1/3}}{\mu^{0.2767}}. \tag{8.221}$$

For flue gas the values of c_{p}, k, and μ can be computed through (7.111), (7.150), and (7.165).We determine that these quantities are a function of temperature and moisture percentage by mass of the flue gas.

Assuming that

$$K_{\mathrm{g}} = 0.287 \frac{\left(c_{\mathrm{p}} k^2\right)^{1/3}}{\mu^{0.2767}}, \tag{8.222}$$

factor K_{g} is a function of these quantities, as well; therefore, it is possible to obtain the following approximated equation for K_{g} based on (7.111), (7.150), and (7.165):

$$K_{\mathrm{g}} = 4.752 + 0.0204m + (5.553 + 0.0294m) \frac{t_{\mathrm{f}}}{1000} - (1.614 - 0.0479m) \left(\frac{t_{\mathrm{f}}}{1000}\right)^2 \tag{8.223}$$

Here m is expressed as percentage.

Equation (8.223) is valid for $t_{\mathrm{f}} = 50 - 1200°\mathrm{C}$ and $m = 0 - 12\%$.

The greatest mistake using (8.223) instead of (8.222) is equal to about 0.6% plus or minus which is definitely acceptable.

With reference to (8.31), the heat transfer coefficient of flue gas can also be easily computed based on the following equation:

$$\alpha' = K_{\mathrm{g}} f_{\mathrm{d}} f_{\mathrm{a}} \frac{G^{0.61}}{d_{\mathrm{o}}^{0.39}}, \tag{8.224}$$

where α' is expressed in $\mathrm{W/m^2K}$, G in $\mathrm{kg/m^2s}$, and d_{o} in m; factor K_{g} is computed through (8.223).

As far as moisture, we refer to (8.160) and all relative considerations. As far as air, (8.221) is naturally still valid, and we consider factor K_{a} given by

$$K_{\mathrm{a}} = 0.287 \frac{\left(c_{\mathrm{p}} k^2\right)^{1/3}}{\mu^{0.2767}} \tag{8.225}$$

which is formally identical to factor K_g.

The values of c_{p}, k, and μ can be computed through (7.81), (7.121), and (7.152). Based on the values of the three quantities, it is possible to obtain the following approximate equation for K_{a}:

$$K_{\mathrm{a}} = 4.884 + 0.545 \frac{t_{\mathrm{f}}}{100} - 0.012 \left(\frac{t_{\mathrm{f}}}{100}\right)^2 \tag{8.226}$$

valid for $t_{\mathrm{f}} = 0 - 300\,°\mathrm{C}$.

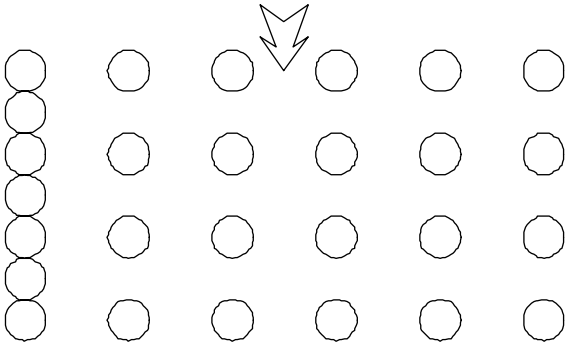


Fig. 8.26

Mistakes made using (8.226) instead of (8.225) are irrelevant. With reference to (8.32), the heat transfer coefficient of air can be computed quite easily through the following:

$$\alpha'' = K_a f_d f_a \frac{G^{0.61}}{d_o^{0.39}}; \tag{8.227}$$

α'' is expressed in W/m^2K, G in kg/m^2s, and d_o in m; factor K_a is computed through (8.226).

The determination of the value of the arrangement factor f_a is generally not difficult, given that the values of Re, $s_l/d_o, s_t/d_o$ present in the diagrams of Figs. 8.24 and 8.25 usually fulfill practical requirements, even though one cannot ignore the fact that, considering the pattern of the curves, the necessary interpolations for values of s_l/d_o and Re other than the expected ones is quite uncertain.

Generally, potential mistakes during interpolations lead to percentage errors on the value of f_a that are quite modest anyway.

The tube bank can be limited on one or both sides by a series of tangent tubes (Fig. 8.26). It is a question of establishing criteria to take it into account. We recommend adding the external surface of the tubes in the bank to the projected surface of the wall consisting of tangent tubes, and not of the surface of the half tubes.

In conclusion, note that the calculation of the heat transferred to the tube bank by convection (identified by the heat transfer coefficient of the gas) does not stand for the total heat transfer. In fact, the heat radiated by the gas, as shown in Sect. 8.9, must be factored in, too.

8.9 Heat Radiation from Flue Gas

A comparison between the actual heat transferred to the tubes of a bank with the one computed based on the heat transfer coefficient of gas (Sects. 8.6 and 8.8) shows increasingly stronger differences matching the increasing temperature of the flue gas.

This finding in 1923 lead Schack to consider the possibility that the increase in transferred heat were caused by the radiation in the infrared of the steam and the carbon dioxide in the gas. In reality, both the steam and the CO_2 possess considerable absorption bands in the infrared field, that is, for wave lengths greater than $0.8\,\mu$. Calculation of this radiation performed with appropriate equations showed that it can be such that it must be included in the computation about transferred heat.

Subsequent research was done by Thomas, Möller, Schmick, Schmidt, Hottel, Mangeldorf, and Eckert. The results made it possible to develop equations for the calculation of the heat transfer by radiation both from CO_2 and H_2O.

If T' and T_w stand for the absolute temperatures of the gas and the wall of the radiated tubes, the heat radiated by carbon dioxide can be computed through the following equation:

$$q_{CO_2} = 10.349 B \left(p_{CO_2} x_r\right)^{0.4} \left[\left(\frac{T'}{100}\right)^{3.2} - \left(\frac{T_w}{100}\right)^{3.2} \left(\frac{T'}{T_w}\right)^{0.65}\right]; \qquad (8.228)$$

q_{CO_2} is the heat expressed in W/m^2, B is the black level of the surface, p_{CO_2} is the partial pressure of CO_2 in atm and x_r, the so-called mean beam length expressed in m, the significance and values of which will be specified later.

Equation (8.228) is valid for $p_{CO_2} x_r = 0.003 - 0.4$ atm $\times$ m, and $T' = 773 - 2073\,K$ ($t' = 500 - 1800\,^\circ C$).

As far as the black level corresponding to the ratio between the heat radiated by the surface at a certain temperature and the heat radiated by the blackbody at the same temperature, we observe that, for instance, $B = 0.745$ is the result of experiments on firebricks. Most interestingly, in the case of radiation inside a tube bank, it is possible to assume that $B = 0.95$.

The partial pressure of CO_2 is equal to the volumetric ratio between CO_2 and the flue gas. For instance, if the volumetric percentage of CO_2 is equal to 10%, we have $p_{CO_2} = 0.10$ atm. It is important not to mistake this value with the $|CO_2|$ discussed in Sect. 7.7, because that referred to dry gas, whereas this one refers to moist gas.

By analogy, as far as radiation from steam, we can write the following equation:

$$q_{H_2O} = B\left(46.51 - 84.89 p_{H_2O} x_r\right)\left(p_{H_2O} x_r\right)^{0.6} \left[\left(\frac{T'}{100}\right)^{\gamma} - \left(\frac{T_w}{100}\right)^{\gamma}\right], \qquad (8.229)$$

given that

$$\gamma = 2.32 + 1.37\sqrt[3]{p_{H_2O} x_r}. \qquad (8.230)$$

In (8.229) q_{H_2O} stands for the heat radiated by H_2O expressed in W/m^2, p_{H_2O} for the partial pressure of H_2O, while the other symbols have the already known meaning.

Equation (8.229) is valid for $p_{H_2O} x_r = 0 - 0.36\,\text{atm} \times \text{m}$ and for $T' = 673 - 2173\,K$ ($t' = 400 - 1900\,^\circ C$). In the rare instances when the equations above are invalid (e.g., the large channels of certain waste-heat generators), it is possible to use Hottel's diagrams present in the literature.

The heat q_r radiated by the flue gas within the time unit and per surface unit is therefore equal to:

$$q_r = q_{CO_2} + q_{H_2O}. \tag{8.231}$$

Thus, we can compute q_r through (8.228) and (8.229).

If we introduce an ideal heat transfer coefficient α'_r that identifies the radiated heat, we may write that

$$q_r = q_{CO_2} + q_{H_2O} = \alpha'_r \left(t' - t_w\right), \tag{8.232}$$

where t' and t_w are temperatures (in °C) corresponding to T' and T_w.

From (8.232) we have

$$\alpha'_r = \frac{q_{CO_2} + q_{H_2O}}{t' - t_w}. \tag{8.233}$$

The availability of α'_r is very useful as far as computation requirements. In fact, the heat transfer by radiation is given by (8.232), whereas the one by convection is equal to:

$$q_c = \alpha'_c \left(t' - t_w\right), \tag{8.234}$$

where α'_c stands for the heat transfer coefficient computed based on Sects. 8.6 and 8.8.

The total heat transferred by the gas to the tubes is therefore equal to

$$q = q_c + q_r = \left(\alpha'_c + \alpha'_r\right)\left(t' - t_w\right). \tag{8.235}$$

At this point, if we introduce the total ideal heat transfer coefficient equal to

$$\alpha' = \alpha'_c + \alpha'_r; \tag{8.236}$$

the transferred heat is given by:

$$q = \alpha'\left(t' - t_w\right). \tag{8.237}$$

Thus, α' stands for the heat transfer coefficient to be introduced into the equations, such as (8.21) or (8.31), to compute the overall heat transfer coefficient U.

This explains why it is so practical for a computer to have the ideal heat transfer coefficient by radiation. This is, of course, a quantity called heat transfer coefficient only because of its dimension, but in fact it is not really so, because this is about the radiated heat and not the one transferred by convection.

Finally, note how the mean temperature of the flue gas through the bank, as well as t_w, can be taken as the value of t' for the computation of α'_r for the sake of simplicity, even though it is a bit incorrect. Diagrams and Tables can be useful for the rapid identification of the value of α'_r.

To that extent:

$$\Delta t_w = t' - t_w; \tag{8.238}$$

$$\beta = \frac{p_{H_2O}}{p_{CO_2}}. \tag{8.239}$$

If p is the sum of partial pressures of carbon dioxide and steam, that is,

$$p = p_{CO_2} + p_{H_2O}. \tag{8.240}$$

This results in

$$p_{CO_2} = \frac{p}{1+\beta} \tag{8.241}$$

If $B = 0.95$, (8.228) can be written as follows:

$$q_{CO_2} = 9.83 \left(\frac{px_r}{1+\beta}\right)^{0.4} \left[\left(\frac{t_w + \Delta t_w + 273}{100}\right)^{3.2} - \left(\frac{t_w + 273}{100}\right)^{3.2} \left(\frac{t_w + \Delta t_w + 273}{t_w + 273}\right)^{0.65}\right] \tag{8.242}$$

Moreover,

$$p_{H_2O} = p\frac{\beta}{1+\beta}. \tag{8.243}$$

Factoring in (8.243) and assuming that $B = 0.95$, from (8.229) we obtain:

$$q_{H_2O} = \left(44.19 - 80.65 px_r \frac{\beta}{1+\beta}\right) \left(px_r \frac{\beta}{1+\beta}\right)^{0.6} \left[\left(\frac{t_w + \Delta t_w + 273}{100}\right)^{\gamma} - \left(\frac{t_w + 273}{100}\right)^{\gamma}\right] \tag{8.244}$$

given that

$$\gamma = 2.32 + 1.37 \sqrt[3]{px_r \frac{\beta}{1+\beta}}. \tag{8.245}$$

Based on (8.232) we determine that

$$q_r = f(px_r, \beta, t_w, \Delta t_w). \tag{8.246}$$

And, by analogy, based on (8.233) we determine that

$$\alpha'_r = f(px_r, \beta, t_w, \Delta t_w) \tag{8.247}$$

Examining the pattern of α'_r as a function of the parameters influencing its value, we determine that by committing acceptable mistakes in the significant field of variability of the parameters themselves, the value of α'_r can be computed through the following equation:

$$\alpha'_r = K_r \bar{\alpha}'_r, \tag{8.248}$$

where $\bar{\alpha}'_r$ that stands for ideal heat transfer coefficient of cavity is only a function of t_w and Δt_w, whereas factor K_r is a function of px_r and β.

This has a very precise physical significance because the value of $\bar{\alpha}'_r$ depends solely on the temperatures, regardless of partial pressure from the radiating gas and of the mean beam length, while the value of factor K_r depends uniquely from the latter quantities and highlights their influence in a significant way.

Of course, the value of $\overline{\alpha}'_r$ is conventional since there are no criteria to identify the role of both K_r and $\overline{\alpha}'_r$ to obtain the value of α'_r closest to the exact one. In other words, what counts is the product of the two factors, given that the value of the single factors is arbitrary.

For $\overline{\alpha}'_r$ we adopted the values corresponding to five times the values of α'_r with $px_r = 0.02$ and $\beta = 0.4$ for which $K_r = 0.2$.

Based on this approach, we obtain the following from (8.239), (8.242), and (8.244):

$$\overline{\alpha}'_r = \frac{8.985}{\Delta t_w}\left[\left(\frac{t_w+\Delta t_w+273}{100}\right)^{3.2} - \left(\frac{t_w+273}{100}\right)^{3.2}\left(\frac{t_w+\Delta t_w+273}{t_w+273}\right)^{0.65}\right]$$

$$+\frac{9.861}{\Delta t_w}\left[\left(\frac{t_w+\Delta t_w+273}{100}\right)^{2.565} - \left(\frac{t_w+273}{100}\right)^{2.565}\right] \tag{8.249}$$

The values of $\overline{\alpha}'_r$ obtained from (8.249) are shown in Fig. 8.27.

Using the values of K_r in Table 8.3, through (8.248) it is possible to obtain values of α'_r that are very close to the exact ones.

Let us examine the following range of values of the various quantities involved, that is,

$$px_r = 0.01\text{–}0.36 \text{ atm} \times \text{m}$$
$$\beta = p_{H_2O}/p_{CO_2} = 0.3\text{–}2$$
$$t_w = 200\text{–}600^\circ\text{C}$$
$$\Delta t_w = 200\text{–}1000^\circ\text{C}$$

the most significant one.

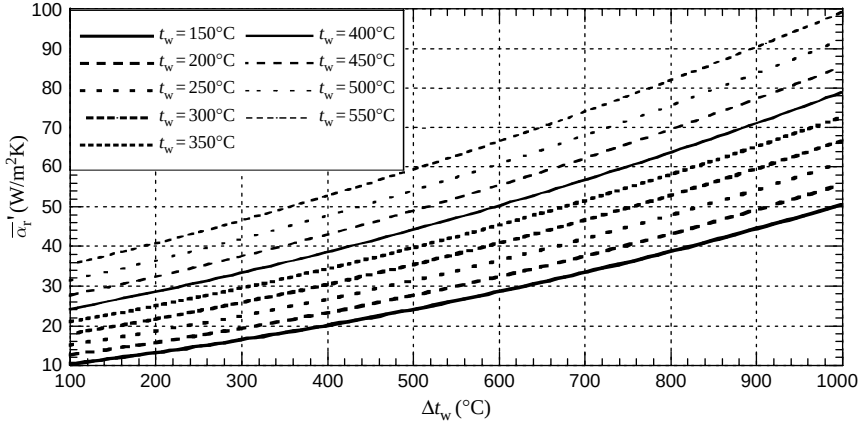


Fig. 8.27 Ideal heat transfer coefficient for the radiation in a cavity

Table 8.3 K_r factor

px_r(atm × m)	$\beta = p_{H_2O}/p_{CO_2}$							
	0.3	0.4	0.5	0.7	1.0	1.3	1.6	2.0
0.005	0.108	0.107	0.106	0.104	0.102	0.099	0.098	0.096
0.010	0.145	0.145	0.144	0.143	0.141	0.139	0.137	0.135
0.015	0.175	0.175	0.174	0.174	0.172	0.171	0.169	0.167
0.020	0.200	0.200	0.200	0.200	0.200	0.198	0.197	0.196
0.025	0.221	0.222	0.223	0.224	0.225	0.224	0.223	0.222
0.030	0.241	0.243	0.244	0.246	0.248	0.248	0.248	0.247
0.035	0.259	0.262	0.264	0.267	0.270	0.271	0.272	0.271
0.040	0.276	0.280	0.283	0.287	0.291	0.293	0.294	0.295
0.045	0.292	0.297	0.301	0.306	0.311	0.315	0.316	0.318
0.050	0.308	0.313	0.318	0.325	0.331	0.335	0.338	0.340
0.060	0.327	0.344	0.350	0.360	0.369	0.375	0.379	0.383
0.070	0.365	0.374	0.381	0.394	0.406	0.414	0.420	0.425
0.080	0.390	0.402	0.411	0.426	0.441	0.452	0.459	0.466
0.090	0.415	0.428	0.439	0.457	0.476	0.488	0.497	0.506
0.100	0.439	0.454	0.467	0.488	0.509	0.524	0.535	0.545
0.120	0.484	0.504	0.520	0.547	0.575	0.594	0.608	0.621
0.140	0.527	0.551	0.571	0.603	0.638	0.662	0.679	0.696
0.160	0.568	0.596	0.620	0.659	0.700	0.728	0.748	0.768
0.180	0.608	0.640	0.668	0.712	0.759	0.792	0.815	0.837
0.200	0.646	0.683	0.714	0.765	0.818	0.854	0.880	0.904
0.240	0.720	0.766	0.804	0.866	0.930	0.972	1.003	1.031
0.280	0.791	0.845	0.891	0.962	1.035	1.083	1.115	1.143
0.320	0.859	0.921	0.973	1.054	1.134	1.184	1.216	1.242
0.360	0.925	0.995	1.053	1.141	1.226	1.275	1.305	1.325
0.400	0.989	1.067	1.130	1.224	1.309	1.356	1.385	1.410

The mistakes range from -7 to $+5\%$ and are acceptable. Moreover, they are generally much smaller than these maximum values registered at the extremities of the range.

As far as partial pressure, note that based on (7.122), (7.123), and (7.132):

$$p_{CO_2} = \frac{0.01866C}{nA_{tv} + 0.05558H}; \tag{8.250}$$

$$p_{H_2O} = \frac{0.11117H}{nA_{tv} + 0.05558H}. \tag{8.251}$$

If the fuel is a mixture of hydrocarbons only, that is, if $C = 100 - H$, based on (8.250) and (8.251) and recalling (7.140) we obtain

$$p_{CO_2} = \frac{0.01866\,(100 - H)}{8.882n + (0.17573n + 0.05558)\,H}; \tag{8.252}$$

$$p_{H_2O} = \frac{0.11117H}{8.882n + (0.17573n + 0.0558)\,H}. \tag{8.253}$$

Table 8.4 Partial pressure of CO_2 and H_2O in the flue gas

p_{CO_2}(atm)				
H	n			
%	1.0	1.1	1.2	1.3
0	0.2101	0.1910	0.1751	0.1616
5	0.1766	0.1609	0.1478	0.1367
10	0.1500	0.1370	0.1261	0.1167
15	0.1284	0.1175	0.1082	0.1003
20	0.1105	0.1012	0.0934	0.0867
25	0.0954	0.0875	0.0808	0.0751
p_{H_2O}(atm)				
H	n			
%	1.0	1.1	1.2	1.3
5	0.0554	0.0505	0.0464	0.0429
10	0.0993	0.0907	0.0834	0.0773
15	0.1350	0.1235	0.1138	0.1055
20	0.1646	0.1508	0.1391	0.1291
25	0.1895	0.1738	0.1605	0.1490

Table 8.4 was created based on (8.252) and (8.253). It can be used even if the fuel is not made of hydrocarbons only if the percentages of the components other than carbon and hydrogen are modest. H stands for the percentage of hydrogen by mass in the fuel.

Generally, the values of p and β relative to fuel gas for the most commonly used fuels are as follows:

Pulverized coal	$p = 0.17$–0.20	atm	$\beta \approx 0.4$
Fuel oil	$p = 0.20$–0.22	atm	$\beta \approx 0.8$
Natural gas	$p = 0.24$–0.26	atm	$\beta \approx 2$

As far as the mean beam length x_r, if it is referred to a tube bank, according to Münziger it is given by (Fig. 8.28):

$$x_r = s - \frac{d_o}{2}. \tag{8.254}$$

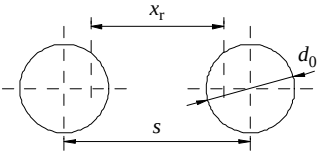
Experiments done with both arrangements (inline tubes and staggered tubes) and for different values of s_l/d_o and s_t/d_o made it possible to create the diagrams in Figs. 8.29 and 8.30. These help to compute the ratio x_r/d_o between mean beam length and outside diameter of the tube in a more accurate way, compared to Münziger's suggestion through (8.254). In air heaters the radiated heat of the flue gas can be ignored given their low temperature levels.

Gas radiation involves even those areas of generators where there is a cavity. In that case the value of the mean beam length can be assumed to be the result of

$$x_r = 3.6\frac{V_c}{S_c}, \tag{8.255}$$

where V_c is the volume of the cavity and S_c is its surface.

Fig. 8.28



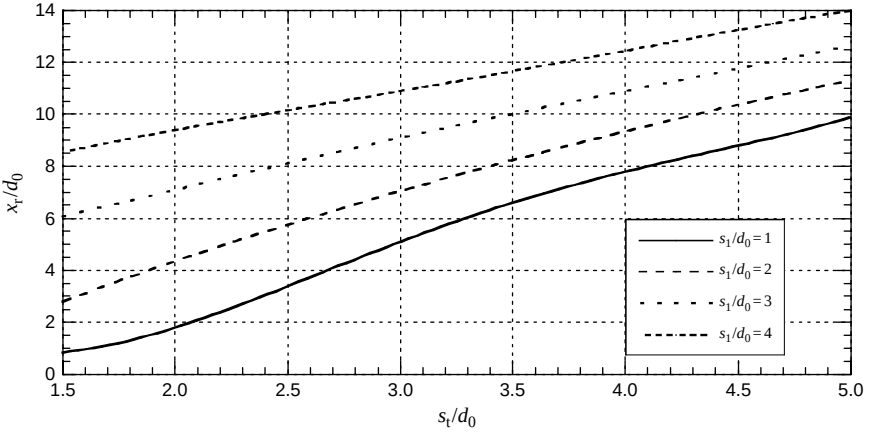


Fig. 8.29 Ratio x_r/d_0 for inline tubes

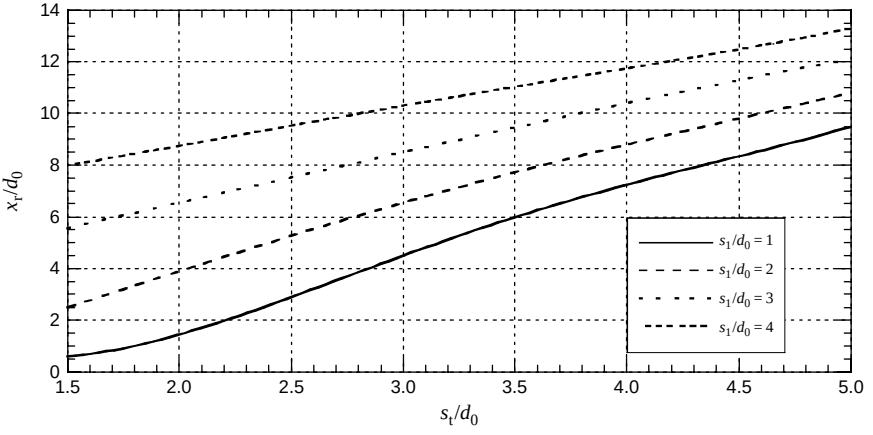


Fig. 8.30 Ratio x_r/d_0 for staggered tubes

Table 8.5 Values of γ ($x_r = \gamma a$)

	Characteristic dimension a	γ	
		Equation 8.255	Direct computing
Sphere	Diameter	0.6	0.6
Cylinder of infinite length	Diameter	0.9	0.9
Cylinder with $h = d$	Diameter	0.6	0.6
Space between parallel planes	Distance between planes	1.8	1.8
Cube	Corner length	0.6	0.6
Parallelepiped with sides in ratio 1:2:6	Shorter corner length	1.08	1.06

The values obtained through (8.255) are compared in Table 8.5 with those computed directly by various researchers. The comparison shows how they typically coincide except for one case where they are considerably close to the values computed through (8.255).

Specifically, as far as the inside of the tubes of smoke-tube generators, we have:

$$x_r = 0.9 d_i; \tag{8.256}$$

d_i stands for the inside diameter.

As far as the cavity, a few guidelines are due.

First of all, if it is a cavity it does not matter if we use (8.232) directly, or if we compute the ideal heat transfer coefficient α'_r through (8.248), and then the overall heat transfer coefficient U which, in this case, depends only on the heat radiated by the gas. Regardless, we obtain the value of the heat radiated onto the walls of the cavity per surface unit.

If it is a space between tube banks, surface S_c is obtained considering the banks facing the space like flat surfaces with an area equal to the cross-sectional area of the space occupied by the bank.

The side walls of the spaces are also factored in for the computation of S_c, regardless of their make. As far as surface S_b, to be considered in the computation of the total heat radiated by the gas within the time unit equal to $q_r S_b$, it is given by the projected surface of the banks (as was said for S_c) and by those of the side walls if they are screened. If they are not completely screened or if they are not screened at all, it is necessary to introduce efficiency factor E discussed in Sect. 8.4 (specifically Fig. 8.15).

Note that in order to avoid factoring in the gas radiation twice, during the computation of the heat transfer to the tube bank, if S_1 and S_2 generally stand for the projections of the bank (understood as stated earlier) relative to the spaces before and after it, the value of α'_r relative to the bank must be corrected by adopting the ideal heat transfer coefficient α'^*_r given by:

$$\alpha'^*_r = \alpha'_r \frac{S - S_1 - S_2}{S}, \tag{8.257}$$

where S stands for the surface of the bank.

As far as the first backflow chamber of smoke-tube boilers one must proceed as follows.

In terms of surface S_b, it is equal to the actual surface radiated by the gas. Thus, it must not be factored in the cross-sectional area of the flue and of the tubes. In addition, the surface of the backflow chamber "seen" by the flame must be taken out because it was already included in the computation of the exit temperature of the gas from the flue.

As far as S_c, one must consider the entire surface of the backflow chamber including the one corresponding to the cross-sectional area of both the flue and the tubes. Note that if the boiler has a dry end plate, when computing S_b the surfaces that do not get in contact with water must be multiplied by 0.05. The heat radiated into the second backflow chamber can be ignored because most of the surface does not get in contact with water and also because the gas temperature is already quite low. Note that the ratio between heat transfer by radiation and by convection is very small in the tubes of smoke-tube generators due to the small value of mean beam length. In terms of water-tube generators, it depends on the geometry of the bank. In very compact banks, the heat transfer by radiation has a certain weight (of course, for high temperatures of the flue gas), but the heat transfer by convection clearly prevails. On the other hand, if the bank consists of coils that are at quite a distance from each other as SH platen (see Fig. 3.35) the heat transfer by radiation is relevant and can exceed the one by convection.

In conclusion, note that in waste-heat generators installed at the exit of incinerators of solid urban waste the flue gas should not hit the tube banks at a temperature beyond 600°C. This aims at preventing the chlorine in the gas from rapidly corroding the tubes of the banks. Therefore, the banks are preceded by large channels with the walls lined with tubes where the heat is transferred by radiation of the gas that already reached high temperatures (600–1000°C). Sometimes the dimensions of the channels are such that they are not included in the validity field of Schack's equations we illustrated. In these exceptional instances it will be possible to use Hottel's diagrams available in the literature.

8.10 Heat Transfer Coefficient of Diathermic Fluids

Based on the recommendations of different producers of mineral oils or organic fluids used in diathermic fluid boilers, the heat transfer coefficient relative to heat transfer between tube wall and fluid can be computed based on the following equations.

The Dittus Bölter equation is among the recommended ones. Here it is again

$$Nu = 0.023\ \mathrm{Re}^{0.8}\ \mathrm{Pr}^{0.4}. \tag{8.258}$$

Equation (8.130) is also advisable, that is,

$$Nu = 0.024\ \mathrm{Re}^{0.8}\ \mathrm{Pr}^{0.33}. \tag{8.259}$$

It is valid for very small values of the ratio between inside diameter and tube length, as is the case in the instances we are considering, as well as for values close to unity of the ratio between the viscosity of the fluid at bulk temperature and at wall temperature (in other words for not exceedingly high thermal flux).

For mineral oils the following equation is recommended

$$Nu = 0.024\ \mathrm{Re}^{0.8}\ \mathrm{Pr}^{0.35}. \tag{8.260}$$

They are clearly very similar and differ mostly because of the exponent of Prandtl's number. Differences are greater at low temperature due to the rather high viscosity level. Of course, the equations refer to turbulent flow which occurs in boilers of this type with forced circulation. For the computation of α'' based on the included equations, it is necessary to know the specific isobaric heat, the dynamic viscosity and the thermal conductivity of the fluids.

Figures 8.31–8.33 show the curves relative to such quantities for the three mineral oils discussed in Sect. 5.1 used as diathermic fluids. As far as the specific isobaric heat, there are only slight differences from oil to oil, thus there is only one curve.

Using (8.260) and highlighting the heat transfer coefficient we obtain

$$\alpha'' = 0.024\ \mathrm{Re}^{0.8}\ \mathrm{Pr}^{0.35}\,\frac{k}{d_\mathrm{i}} \tag{8.261}$$

The producers of such fluids frequently include diagrams in their technical bulletins that make it possible to compute α'' directly based on the temperature of the fluid and the velocity with the introduction of corrective factors for the diameter and to factor in the temperature difference between wall and fluid.

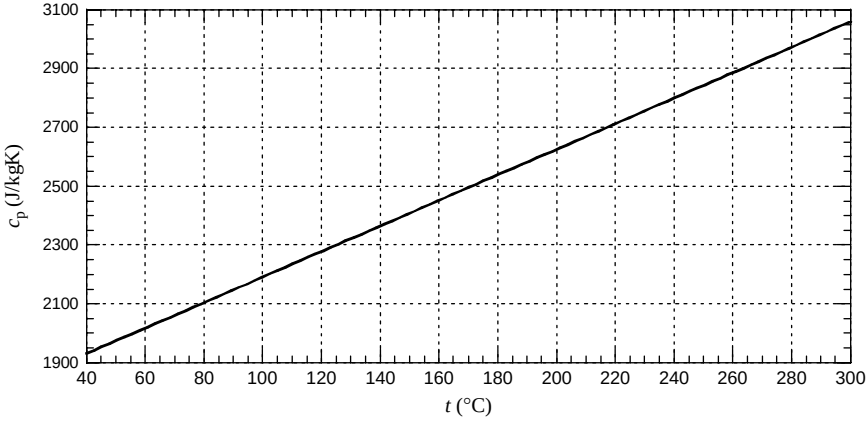


Fig. 8.31 Specific heat of mineral oils used as diathermic fluids

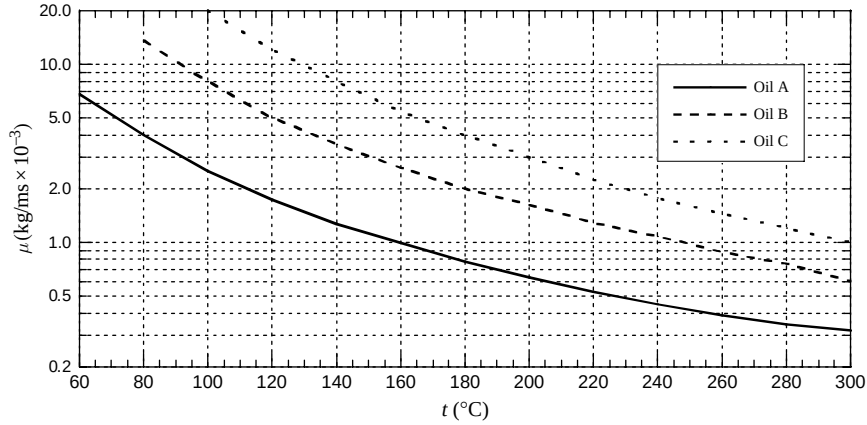


Fig. 8.32 Dynamic viscosity of some mineral oils used as diathermic fluids

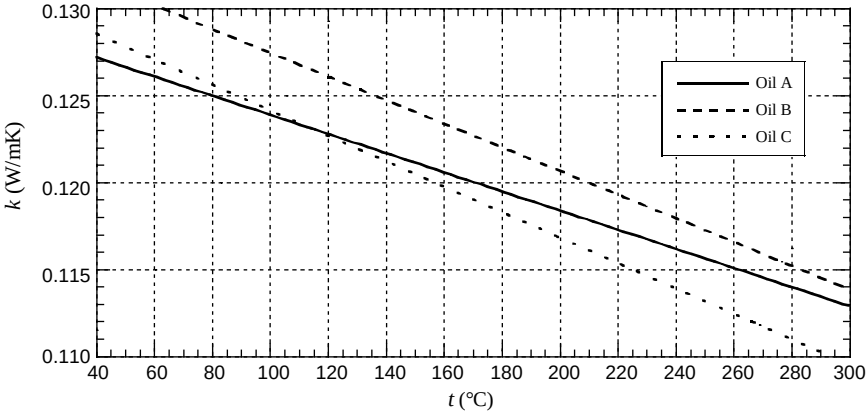


Fig. 8.33 Thermal conductivity of some mineral oils used as diathermic fluids

8.11 Heat Transfer in Economizers and Air Heaters

The computation of the heat transfer in the economizer with smooth steel tubes is not difficult. The heat transfer coefficient α' of the flue gas is calculated through (8.219), or preferably through (8.220); otherwise it can be done through (8.224), still including a reference to mean film temperature. The heat transfer coefficient α'' of water is calculated through (8.131) or (8.135) with reference to the mean bulk temperature. If the economizer is followed by the air heater, it is advisable to consider gas radiation because it could still be significant.

Economizers are often built with finned tubes. In fact, this type of regenerator is particularly suitable for this solution. Note that the adoption of finned tubes is

justified only when the heat transfer coefficient of the fluid inside the tubes is much higher than the one of the heating fluid (the flue gas) outside the tubes. In that case, the modest external heat transfer coefficient penalizing the value of the overall heat transfer coefficient is compensated by the great surface of the fins getting in contact with the gas.

The economizer is in this condition because the heat transfer coefficient of water is by far superior to that of flue gas. The fins are very tight (roughly 200 per meter), thin (generally 1.5 mm), and with a height of about 20 mm. The computation of finned tubes is discussed in Sect. A.4 of the Appendix.

As far as air heaters, if the task is to size a Ljungstroem air heater, the only possibility is to refer to experimental data, but in the case of tube air heater or a pocket air heater, it is possible to do the theoretical computation of U.

The tubes of a tube air heater are used for the passage of flue gas or air. Generally, the preference is for flue gas because this facilitates cleaning that can be done through swabbing. The heat transfer coefficient α is computed through (8.155), or in the two cases through either (8.159) or (8.163). The tube bank is hit by flue gas or air. The heat transfer coefficient α is computed through (8.219), or preferably through (8.220). The alternative in the two cases consists of either (8.224) or (8.227). The radiation of flue gas can be ignored given its low temperature. The reference temperature is always film temperature both for flue gas and for air. The wall temperature which must be known to compute the film temperature can be assumed by first approximation (except for subsequent verification) to be equal to the average between the mean gas temperature and the mean air temperature.

In the case of a pocket air heater (Fig. 3.49), both the flue gas and the air flow through channels with a rectangular cross-sectional area. Equation (8.155) is used for the computation of the heat transfer coefficients, or through (8.159) and (8.163) for flue gas and air, by introducing the hydraulic diameter and referring as usual to film temperature.

As the heat transfer occurs through flat walls, the overall heat transfer coefficient is computed through (8.9). The velocity of the fluids is very important for air heaters both in terms of overall heat transfer coefficient and wall temperature, thus corrosion. The latter can be explained best through an example.

We assume that $38\,\mathrm{W/m^2K}$ is the heat transfer coefficient of the flue gas and $38\,\mathrm{W/m^2K}$ the one for air; the air temperature will be 20°C and the temperature of gas will be 180°C, indicating a temperature difference between the two fluids of 160°C. Neglecting the thermal resistance of the wall when the heat passes through, the overall heat transfer coefficient is therefore equal to $19\,\mathrm{W/m^2K}$, and the difference between the wall temperature and the air temperature is equal to 80°C. By ignoring the resistance of the wall at the passage of heat, the wall temperature is therefore equal to 100°C and the boundary layer of the gas can be assumed to have a temperature of 140°C.

Now, by increasing the velocity of the flue gas and by decreasing the velocity of the air to obtain $\alpha' = 50\,\mathrm{W/m^2K}$ and $\alpha'' = 26\,\mathrm{W/m^2K}$, we have

$$\frac{1}{U} = \frac{1}{50} + \frac{1}{26} = 0.0585$$

Then

$$U = 17.1\,\mathrm{W/m^2K}$$

with a reduction of 10% with respect to the previous value.

The temperature difference between air and wall results in

$$\Delta t = \frac{17.1}{26}160 = 105^\circ\mathrm{C}$$

with an increase of 25% compared with the previous value.

The wall reaches 125°C and the temperature of the boundary layer of the gas 152.5°C. This means that an increase of the ratio between gas and air velocity increases the wall temperature and the temperature of the gas in contact with it. This may be desirable to prevent corrosion. In Sect. 3.9 we already pointed out the necessity to intervene in different ways whenever there is risk of corrosion under reduced loads. The simplest intervention consists of by-passing part of the air at the exit of the air heater. Figure 8.34 is an example of the pattern of the different quantities in relation to a by-pass for an air heater in counter-flow running at 50% of its maximum load.

Note that the exit temperature of the flue gas t_e increases with the increase of the by-pass, as much as the mean temperature of the boundary layer t_b increases, and this is the one that counts in terms of corrosion. Of course, the overall heat transfer coefficient U and the heat q transferred to the air decrease. In other words, to rule out corrosive phenomena it is necessary to by-pass about 50% of the air.

Note that if the same air heater were to run in parallel flow, the following results would be obtained without by-pass: $t_e = 173\,^\circ\mathrm{C}$, $t_b = 155\,^\circ\mathrm{C}$, $U = 14,3\,\mathrm{W/m^2K}$, and

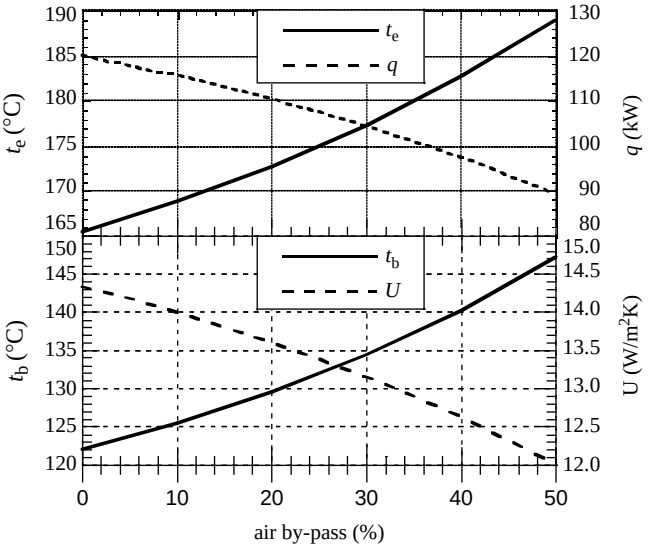


Fig. 8.34 Air by-pass in air heater with counterflow

$q = 110.5\,\text{kW}$. The value of t_b is a guarantee for the absence of corrosion. With the exception of t_b and U, we would have the same values of the air heater in counterflow with a by-pass of 20%, which is completely insufficient to guarantee the absence of corrosion. An alternative to the by-pass of cold air is the recirculation of part of the warm air. This solution has the advantage to ensure greater cooling of the flue gas leading to an increased heat transfer from the gas to the air (under safety conditions as far as corrosion).

Unfortunately, there are many disadvantages. First of all, the set-up is more complex. Moreover, the possible interventions are modest. Roughly, they are limited to cases where the by-pass of cold air would be under 20%. In more incisive interventions, the quantity of air to recirculate is enormous, and its effect is mostly nullified by the fact that high air velocity increases its heat transfer coefficient; thus, the temperature of the flue gas in the boundary layer is close to that of the air. Finally, there is a considerable pressure drop of air with the obvious consequences in terms of the sizing of the fan.

8.12 Exit Gas Temperature from a Tube Bank or a Heat Regenerator

The verification calculus of the generator requires the computation of the exit temperature of flue gas from a tube bank once the entry temperature of the heating fluid (gas) and of the heated fluid are known. A similar process takes place during verification thermodynamic calculation of an economizer or an air heater. These verification calculations are necessary to identify the behavior under reduced load, once the generator has been sized for runtime under full load. The symbolism from Sect. 8.3 will be used.

Based on (8.55) and (8.56) and considering fluids in parallel flow, we may write that

$$q = US\frac{(t_1' - t_1'') - (t_2' - t_2'')}{\log_e \dfrac{t_1' - t_1''}{t_2' - t_2''}}. \tag{8.262}$$

Note that

$$\frac{t_1' - t_1''}{t_2' - t_2''} = \frac{1 + \dfrac{t_2' - t_1''}{t_1' - t_2'}}{\dfrac{t_2' - t_1''}{t_1' - t_2'} - \dfrac{t_2'' - t_1''}{t_1' - t_2'}}. \tag{8.263}$$

Moreover, we introduce

$$\psi = \frac{t_2' - t_1''}{t_1' - t_1''}; \tag{8.264}$$

$$\beta = \frac{M' c_p'}{M'' c_p''}; \tag{8.265}$$

$$\gamma = \frac{US}{M' c'_{\mathrm{p}}}; \tag{8.266}$$

On the other hand, the transferred heat is given by

$$q = M' c'_{\mathrm{p}} \left(t'_1 - t'_2\right) = M'' c''_{\mathrm{p}} \left(t''_2 - t''_1\right). \tag{8.267}$$

Then, from (8.265)

$$\beta = \frac{t''_2 - t''_1}{t'_1 - t'_2}. \tag{8.268}$$

We introduce factor ε given by

$$\varepsilon = \frac{t'_2 - t''_1}{t'_1 - t'_2}. \tag{8.269}$$

From (8.268) and (8.269) we obtain

$$\frac{t'_1 - t''_1}{t'_2 - t''_2} = \frac{1+\varepsilon}{\varepsilon - \beta}. \tag{8.270}$$

Comparing (8.262) with (8.267) and with reference to (8.266), we have:

$$\gamma = \frac{t'_1 - t'_2}{\left(t'_1 - t''_1\right) - \left(t'_2 - t''_2\right)} \log_{\mathrm{e}} \frac{t'_1 - t''_1}{t'_2 - t''_2}. \tag{8.271}$$

Recalling (8.270) and (8.265), (8.271) leads to the following:

$$\gamma = \frac{1}{1+\beta} \log_{\mathrm{e}} \frac{1+\varepsilon}{\varepsilon - \beta}. \tag{8.272}$$

Then, from (8.272) we obtain:

$$\varepsilon = \frac{1 + \beta e^{(1+\beta)\gamma}}{e^{(1+\beta)\gamma} - 1}. \tag{8.273}$$

Based on (8.264) and (8.269):

$$\psi = \frac{\varepsilon}{\varepsilon + 1} \tag{8.274}$$

And finally,

$$\psi = \frac{\mathrm{e}^{-(1+\beta)\gamma} + \beta}{1+\beta}. \tag{8.275}$$

If the fluids are in counterflow, instead of (8.262) we have

$$q = US\frac{(t_1' - t_2'') - (t_2' - t_1'')}{\log_e \dfrac{t_1' - t_2''}{t_2' - t_1''}}. \tag{8.276}$$

Note that

$$\frac{t_1' - t_2''}{t_2' - t_1''} = \frac{\dfrac{t_1' - t_1''}{t_1' - t_2'} - \dfrac{t_2'' - t_1''}{t_1' - t_2'}}{\dfrac{t_1' - t_1''}{t_1' - t_2'} - 1}. \tag{8.277}$$

Assuming that

$$\eta = \frac{t_1' - t_1''}{t_1' - t_2'}, \tag{8.278}$$

And recalling (8.268) we have

$$\frac{t_1' - t_2''}{t_2' - t_1''} = \frac{\eta - \beta}{\eta - 1}. \tag{8.279}$$

By analogy with (8.272) we also have

$$\gamma = \frac{t_1' - t_2'}{(t_1' - t_2'') - (t_2' - t_1'')} \log_e \frac{t_1' - t_2''}{t_2' - t_1''} \tag{8.280}$$

And from that, recalling (8.265) as well as (8.268):

$$\gamma = \frac{1}{1 - \beta} \log_e \frac{\eta - \beta}{\eta - 1} \tag{8.281}$$

Equation (8.281) leads to the following:

$$\eta = \frac{\beta - e^{(1-\beta)\gamma}}{1 - e^{(1-\beta)\gamma}} \tag{8.282}$$

Observing that

$$\psi = 1 - \frac{1}{\eta} \tag{8.283}$$

we have:

$$\psi = \frac{1 - \beta}{e^{(1-\beta)\gamma} - \beta}. \tag{8.284}$$

Note that the value of ψ is undetermined if $\beta = 1$; in that case, though, we have

$$\Delta t_m = t_2' - t_1'' = t_1' - t_2'' \tag{8.285}$$

Therefore, based on (8.267) and (8.276)

$$M' c'_{\mathrm{p}} \left(t'_1 - t'_2\right) = US\left(t'_2 - t''_1\right); \tag{8.286}$$

then

$$\frac{t'_1 - t''_1}{t'_2 - t''_1} - 1 = \gamma. \tag{8.287}$$

Thus, recalling (8.264)

$$\frac{1}{\psi} - 1 = \gamma. \tag{8.288}$$

Finally,

$$\psi = \frac{1}{\gamma + 1}. \tag{8.289}$$

Figure 8.35 was built based on (8.275) and Fig. 8.36 was built based on (8.284) and (8.289). For instance, if flue gas or air in an air heater hit the tube bank with one passage only, while the fluid inside the tubes also flows one time only, the currents of both fluids cross each other and neither (8.275) nor (8.284) can be used. In this case the value of factor ψ can be taken from Tables 8.6 and 8.7. Finally, note that this factor can be computed with good approximation based on the following equation:

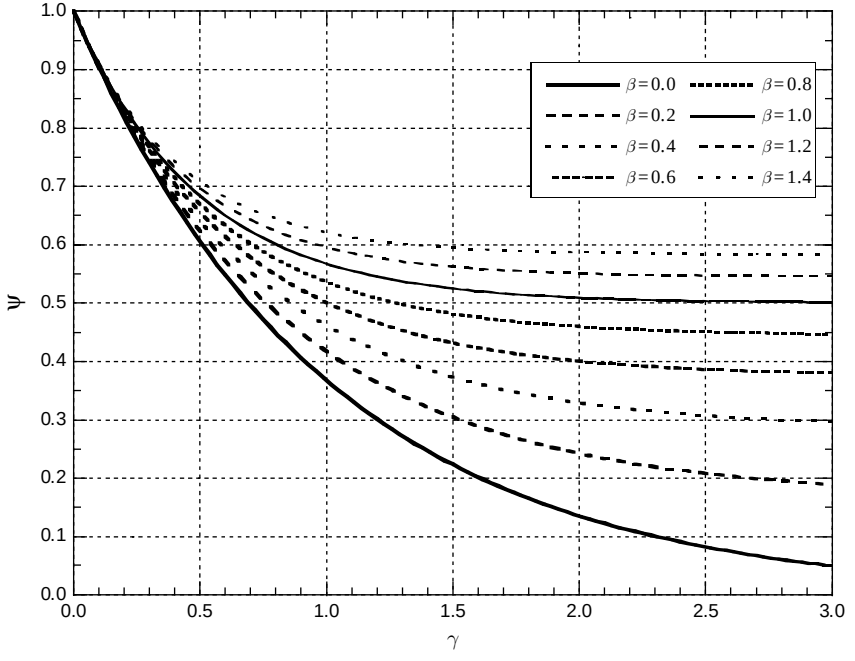


Fig. 8.35 Factor Ψ for parallel flow

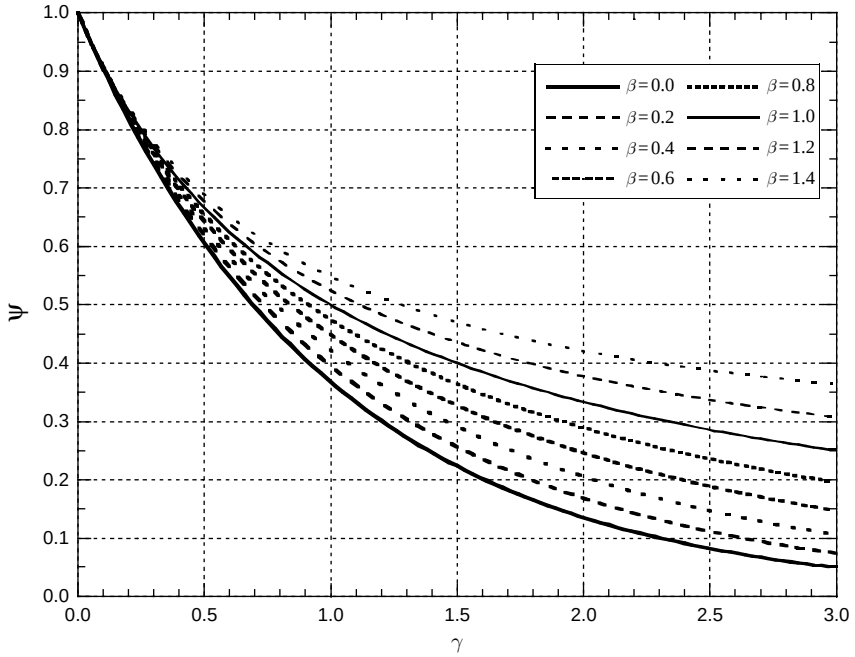


Fig. 8.36 Factor Ψ for counterflow

Table 8.6 Factor ψ for cross-flow

β	γ												
	0.30	0.40	0.50	0.60	0.70	0.80	0.90	1.0	1.1	1.2	1.3	1.4	1.5
0.20	0.747	0.681	0.621	0.568	0.520	0.477	0.438	0.403	0.372	0.343	0.317	0.294	0.272
0.30	0.751	0.686	0.628	0.577	0.531	0.490	0.454	0.420	0.390	0.363	0.338	0.316	0.295
0.40	0.754	0.691	0.635	0.586	0.542	0.503	0.468	0.437	0.408	0.382	0.359	0.338	0.318
0.50	0.757	0.696	0.642	0.595	0.553	0.516	0.482	0.453	0.426	0.401	0.379	0.359	0.340
0.60	0.760	0.701	0.649	0.603	0.563	0.528	0.496	0.468	0.442	0.419	0.398	0.379	0.362
0.70	0.763	0.705	0.655	0.612	0.573	0.539	0.509	0.483	0.458	0.437	0.417	0.399	0.382
0.80	0.766	0.710	0.662	0.620	0.583	0.551	0.522	0.497	0.474	0.453	0.435	0.418	0.402
0.90	0.769	0.714	0.668	0.627	0.592	0.562	0.535	0.511	0.489	0.470	0.452	0.436	0.421
1.0	0.771	0.719	0.674	0.635	0.602	0.572	0.547	0.524	0.503	0.485	0.469	0.454	0.440
1.1	0.774	0.723	0.680	0.642	0.610	0.583	0.558	0.537	0.517	0.500	0.485	0.471	0.458
1.2	0.777	0.727	0.685	0.650	0.619	0.593	0.569	0.549	0.531	0.515	0.500	0.487	0.475
1.3	0.780	0.731	0.691	0.657	0.627	0.602	0.580	0.561	0.544	0.529	0.515	0.503	0.491
1.4	0.782	0.735	0.696	0.663	0.635	0.612	0.591	0.572	0.556	0.542	0.529	0.518	0.507
1.5	0.785	0.739	0.702	0.670	0.643	0.621	0.601	0.584	0.568	0.555	0.543	0.532	0.522
1.6	0.788	0.743	0.707	0.676	0.651	0.629	0.611	0.594	0.580	0.568	0.556	0.546	0.537
1.7	0.790	0.747	0.712	0.683	0.658	0.638	0.620	0.605	0.591	0.580	0.569	0.560	0.551
1.8	0.793	0.751	0.717	0.689	0.666	0.646	0.629	0.615	0.602	0.591	0.581	0.573	0.565

Table 8.7 Factor ψ for cross-flow

β	γ												
	1.6	1.7	1.8	1.9	2.0	2.1	2.2	2.3	2.4	2.5	2.6	2.7	2.8
0.20	0.252	0.234	0.218	0.203	0.189	0.177	0.165	0.154	0.144	0.135	0.127	0.119	0.111
0.30	0.277	0.260	0.244	0.229	0.216	0.203	0.192	0.181	0.172	0.162	0.154	0.146	0.138
0.40	0.300	0.284	0.269	0.255	0.242	0.230	0.219	0.208	0.199	0.190	0.181	0.173	0.166
0.50	0.323	0.308	0.293	0.280	0.268	0.256	0.245	0.235	0.226	0.217	0.209	0.201	0.194
0.60	0.346	0.331	0.317	0.304	0.293	0.282	0.271	0.262	0.253	0.244	0.236	0.229	0.222
0.70	0.367	0.353	0.340	0.328	0.317	0.307	0.297	0.288	0.279	0.271	0.263	0.256	0.249
0.80	0.388	0.375	0.363	0.351	0.341	0.331	0.322	0.313	0.305	0.297	0.290	0.283	0.277
0.90	0.408	0.396	0.384	0.373	0.364	0.354	0.346	0.338	0.330	0.323	0.316	0.309	0.303
1.0	0.427	0.416	0.405	0.395	0.386	0.377	0.369	0.361	0.354	0.348	0.341	0.335	0.329
1.1	0.446	0.435	0.425	0.416	0.407	0.399	0.392	0.384	0.378	0.372	0.366	0.360	0.355
1.2	0.464	0.454	0.444	0.436	0.428	0.420	0.413	0.407	0.401	0.395	0.389	0.384	0.379
1.3	0.481	0.472	0.463	0.455	0.448	0.441	0.434	0.428	0.422	0.417	0.412	0.407	0.403
1.4	0.498	0.489	0.481	0.473	0.467	0.460	0.454	0.449	0.443	0.439	0.434	0.430	0.425
1.5	0.514	0.505	0.498	0.491	0.485	0.479	0.473	0.468	0.464	0.459	0.455	0.451	0.447
1.6	0.529	0.521	0.514	0.508	0.502	0.497	0.492	0.487	0.483	0.479	0.475	0.471	0.468
1.7	0.544	0.537	0.530	0.524	0.519	0.514	0.510	0.505	0.501	0.498	0.494	0.491	0.488
1.8	0.558	0.551	0.545	0.540	0.535	0.531	0.526	0.523	0.519	0.516	0.513	0.510	0.507

$$\psi = (1 - Z)\,\psi_c + Z\psi_p; \tag{8.290}$$

ψ_c and ψ_p are the values of ψ for counterflow and parallel flow, respectively, and factor Z is given by

$$Z = 0.5 - 0.136\,(1 + 0.24\beta)\,\sqrt[3]{\gamma} \tag{8.291}$$

Until now we assumed that all the heat is transferred by the heating fluid to the heated fluid (8.267). In reality, part of the heat is lost through the walls of the space where the bank is lodged or through the walls of either the economizer or the air heater. Therefore, it is more correct to write that

$$q = M''c_p''\left(t_2'' - t_1''\right) = \eta_b M'c_p'\left(t_1' - t_2'\right), \tag{8.292}$$

where η_b stands for thermal efficiency of the bank or the device.

Taking into account the efficiency η_b, we easily determine that based on (8.292) it suffices to multiply M' by η_b; it follows that the following corrected equations for β and γ must be adopted:

$$\beta = \frac{\eta_b M'c_p'}{M''c_p''} \tag{8.293}$$

$$\gamma = \frac{US}{\eta_b M'c_p'} \tag{8.294}$$

The calculation process is as follows.

Based on the values of β and γ, factor ψ is computed through (8.275) if the fluids are in parallel flow, or through (8.284) if they are in counterflow [possibly through (8.289) as well]. If there is cross-flow (for instance in the case of an air heater with only one passage of flue gas and air), we must adopt the values of Tables 8.6 and 8.7.

Once the value of ψ is known, and recalling (8.264), the temperature t_2' is given by

$$t_2' = t_1'' + \psi\left(t_1' - t_1''\right) \tag{8.295}$$

Knowing t_2' based on (8.268) we have

$$t_2'' = t_1'' + \beta\left(t_1' - t_2'\right) \tag{8.296}$$

Note, though, that c_{p}' and c_{p}'' depend on the unknown temperatures t_2' and t_2'', the way the heat transfer coefficients of the fluids, a.k.a. the overall heat transfer coefficient, depend on them. Therefore, it is necessary to proceed as follows.

A presumed value of temperature t_2' is set, and based on the heat balance [see (8.267) and (8.292)], the presumed temperature t_2'' is identified. At this point it is possible to compute the mean specific isobaric heat c_p' of the flue gas between t_1' and t_2' based on the values of the enthalpies (Sect. 7.9). Similarly, the mean specific isobaric heat c_{p}'' of the heated fluid is computed (for water and steam through the tables available in manuals, and for air based on the parameters in Sect. 7.9). Then the mean temperatures of both heating and heated fluid are computed; based on these, the heat transfer coefficients of both fluids and the overall heat transfer coefficient $U$are calculated.

Once the values of U, c_{p}', and c_{p}'' are known, the unknown temperature t_2' is computed based on what was previously said. It differs from the presumed temperature, and it is used to recalculate the values of U, c_{p}', and c_{p}'' and, based on these, to recalculate t_2' and so on. Note that the value of t_2' rapidly converges, so generally only one repetition of the calculation will be required.

Note that if the heated fluid is evaporating water, it is $c_{\mathrm{p}}'' = \infty$. On the basis of (8.275) and (8.284) which coincide in that case, as we cannot speak of fluids in parallel flow or counterflow, we obtain

$$\psi = \mathrm{e}^{-\gamma}. \tag{8.297}$$

As far as η_{b}, it is impossible to provide generally valid values since it is influenced by numerous factors.

In the case of tube banks if the lateral walls of the space where the bank is lodged are screened, the efficiency is equal to 1. If they are not screened, we can assume a value of η_{b} equal to 0.97–0.98, as long as the insulation of the walls is appropriate. In the case of air heaters, we can conventionally assume that $\eta_{\mathrm{b}} = 0.98 - 0.99$.

Note that sometimes, once the entry temperature of the flue gas t_1' is known, the exit temperature of the heated fluid t_2'' is set (for instance, in the case of a secondary superheater), whereas the entry temperature t_1'' is unknown. If that is the case, the latter temperature is computed through the following equation:

$$t_1'' = \frac{t_2'' - \beta t_1' (1-\psi)}{1-\beta+\beta\psi}, \tag{8.298}$$

whereas temperature t_2' is always computed through (8.295).

In conclusion, it is certainly interesting to compare fluids in parallel flow and counterflow in relation to heat transfer.

Based on (8.292) and (8.294) we have

$$q = \frac{US}{\gamma}\left(t_1' - t_2'\right). \tag{8.299}$$

Based on (8.295) and after a series of steps we have

$$q = \frac{US}{\gamma}\left(t_1' - t_1''\right)(1-\psi). \tag{8.300}$$

If we now compare two superheaters or two heat regenerators of equal surface with each other, considering that they are hit by the same amount of flue gas at the same temperature, and that the same amount of fluid enters at the same temperature, and finally that the overall heat transfer coefficient U is identical, we determine that the heat transfer depends solely on the value $(1-\psi)$.

Based on (8.284) and (8.275) the ratio between heat transferred with fluids in counterflow and in parallel flow is given by:

$$\frac{q_{\text{counter}}}{q_{\text{parallel}}} = \frac{(1+\beta)\left[\mathrm{e}^{(1-\beta)\gamma} - 1\right]}{\left[\mathrm{e}^{(1-\beta)\gamma} - \beta\right]\left[1 - \mathrm{e}^{-(1+\beta)\gamma}\right]}. \tag{8.301}$$

The values obtained from (8.301) are shown in Table 8.8. This way the influence of β and γ can be identified. First of all, note that the lowest values of β refer to the economizer (generally, $\beta = 0.3 - 0.4$), intermediate values refer to the superheater (generally $\beta = 0.4 - 0.6$), and the highest ones refer to the air heater ($\beta \approx 1.15$). The choice among fluids in parallel flow or counterflow is irrelevant until the difference in transferred heat in both instances amounts to a few percentage points, and the ratio is consequently roughly below $1.02 - 1.03$.

Table 8.8 Ratio between transferred heat with fluids in counterflow and fluids in parallel flow

β	γ				
	0.2	0.4	0.6	0.8	1.0
0.2	1.0024	1.0085	1.0172	1.0276	1.0390
0.4	1.0047	1.0165	1.0331	1.0527	1.0742
0.6	1.0069	1.0240	1.0477	1.0755	1.1056
0.8	1.0090	1.0311	1.0611	1.0958	1.1330
1.0	1.0111	1.0377	1.0733	1.1137	1.1565
1.2	1.0131	1.0439	1.0842	1.1294	1.1763

Values like these correspond to decreasing values of γ going from the economizer to the air heater. Note, though, that the values of U are quite higher in an economizer compared with an air heater. Therefore, based on (8.294) it is possible to draw the conclusion that the ratio S/M' is crucial as far as the choice between the two kinds of flow.

In other words, economizers, superheaters and air heaters with a small surface in relation to the mass flow rate of flue gas can be designed to run also in parallel flow without noticeable penalty as far as the transferred heat. This is not true if the surface is relatively large.

8.13 Comparison Between Arrangement with Inline and Staggered Tubes

At this point, a few considerations about the two kinds of arrangement of the tubes in relation to heat transfer are overdue. Let us consider two banks, one with inline arrangement and one with staggered arrangement, and tubes with the same diameter and equal values of the transverse and longitudinal pitch that are hit by the same flue gas. Under these conditions, the velocity of the gas is identical, so that both banks have the same value of Reynolds' number, as well as the same value of λ. Based on (8.220) the value of α differentiates itself in both instances only as far as the different value of f_a referred to the same values of s_t/d_o, s_l/d_o, and Re for the two types of arrangement.

Figures 8.24 and 8.25 clearly show that in most cases the values of f_a are higher with the staggered arrangement. This is especially true for low values of Re. This should lead to the conclusion that staggered arrangements are definitely preferable to inline arrangements. Nonetheless, this would be a hasty conclusion because it would neglect other aspects of the phenomenon. In fact, as we shall see in Chap. 10, pressure drop throughout the bank depends on a similar arrangement factor f_a as a function of the same parameters. For the two banks considered earlier, even a pressure drop differentiates itself solely by the different value of this arrangement factor. A comparison between the values in both arrangements shows that the inline arrangement is clearly preferable because the f_a values relative to pressure drops are lower which translates into less pressure drops.

Thus, even though the inline arrangement yields a lower value of α, the pressure drop is smaller. This equals a less favorable situation as far as heat transfer and the cost of the bank (greater surface with equal heat transfer), but a much more favorable situation as far as the cost of the fan and the energy absorbed by it.

Therefore, a comparison between the two arrangements must consider both aspects of the phenomenon and factor in the plant cost (bank and fan), as well as running costs (energy absorbed by the fan). In other words, it is a question of choosing the solution carrying the best cost optimization. The criteria to help evaluate the opportunity to of one arrangement over the other lead to a comparison of the values of α given equal pressure drops.

A complete process requires setting the other parameters keeping in mind construction and runtime constraints, such as the ability to perform steam soot blowing between the tubes correctly without making too small transverse pitches. The issue is clearly complex and requires different case by case decisions.

The following constitutes potential comparison criteria. Often the width of the space available to the tube bank is set in advance. In the case of steam generating tubes this is done because of volume, while in the case of a superheater this happens because it is inserted in substitution of a certain number of steam generating tubes. Assessing this situation and assuming that the pressure drop is the same with both arrangements leads to the following. The transverse pitch can be smaller for in-line tubes given the cross-sectional area of gas passage can be reduced, thus increasing the speed. This way the number of tubes increases per row and the number of rows decreases, leading to a more compact bank. At this point we consider the two values of the heat transfer coefficient and indicate the ratio between heat transfer coefficient with in-line and staggered tubes with $R\alpha$. This results in the diagrams of Figs. 8.37–8.39, where both Re and s_t/d_o refer to inline tubes.

Clearly, the two arrangements are only slightly different for $s_l/d_o = 1.5$, but the inline arrangement is more favorable for values higher than s_l/d_o.

The analysis above is conducted in reference to one particular situation which does not rule out other possibilities, and is independent from specific construction and runtime requirements the designer may face. Nonetheless, and with all due reservations, it is possible to conclude that the inline arrangement contrary to the simple analysis of f_a is at least to be considered very carefully to identify the best solution. The latter should also include greater ease of construction as well as cleaning of the tubes on the outside.

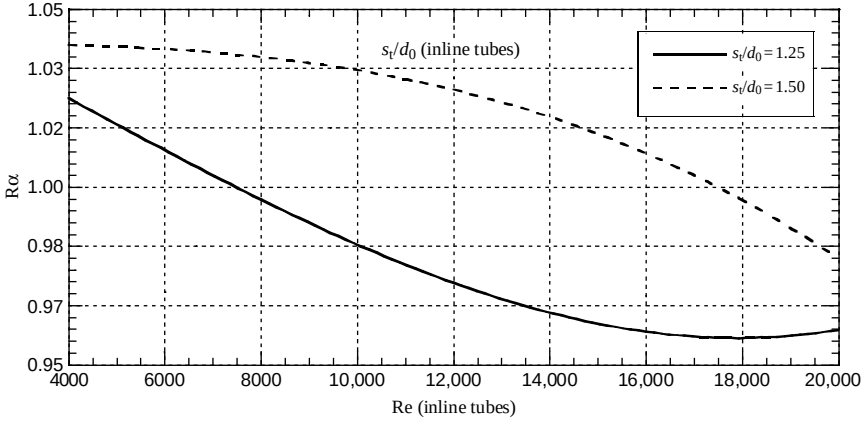


Fig. 8.37 Comparison between inline and staggered tubes ($s_l/d_0 = 1.5$)

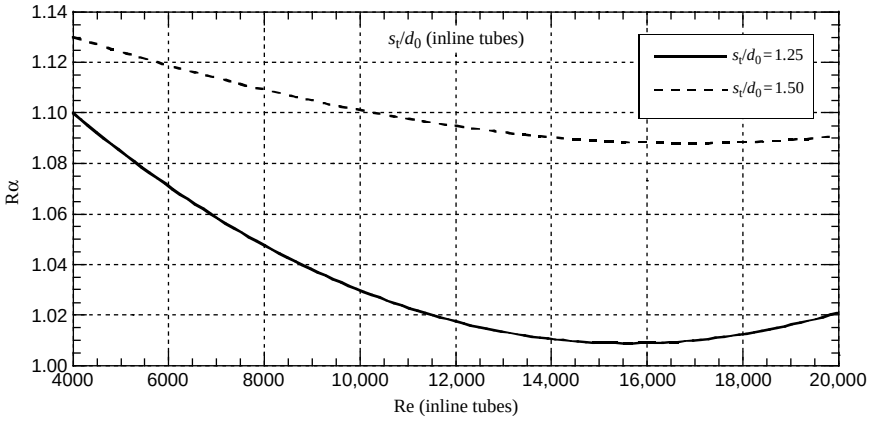


Fig. 8.38 Comparison between inline and staggered tubes ($s_l/d_0 = 2.0$)

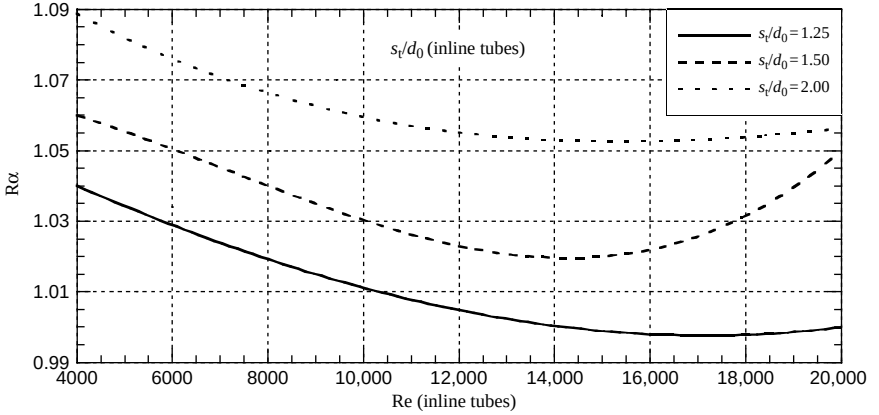


Fig. 8.39 Comparison between inline and staggered tubes ($s_l/d_0 = 3.0$)

8.14 Tube Distribution in the Passages of the Smoke-Tube Boiler

Section 8.13 focussed on the arrangement of tubes in tube banks of water-tube generators to obtain the most efficient heat transfer in relation to pressure drops. A similar problem occurs to smoke-tube boilers as far as determining the most rational arrangement of the tubes in the different passages. The topic is extensively discussed in the article "Influenza della distribuzione dei tubi nei vari giri delle caldaie a tubi da fumo" included in the bibliography. Our interest lies in the starting assumptions required to do this analysis, and in the results that can be achieved. The examined boilers have a dry end plate. The results are qualitatively valid for boilers with wet end plates, as well.

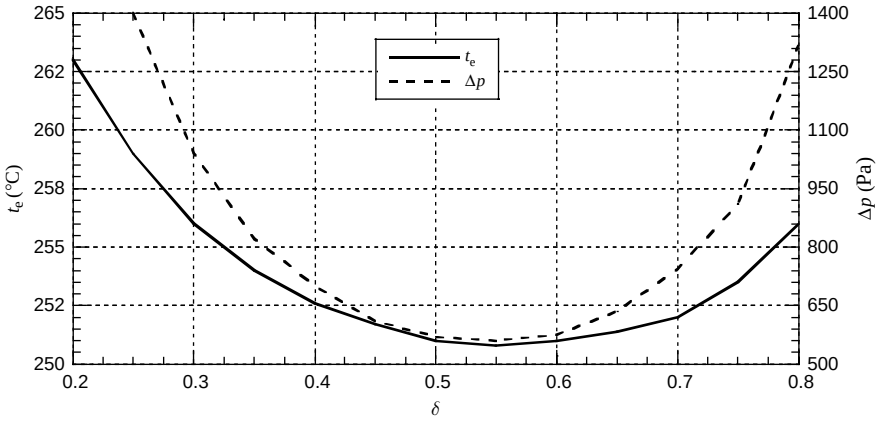


Fig. 8.40 Effects of tube distribution in the two passages ($p = 1$ bar; $q_t = 46.5\,\mathrm{kW/m^2}$; $G_m = 9.72\,\mathrm{kg/m^2 s}$; $d_i = 48.8\,\mathrm{mm}$)

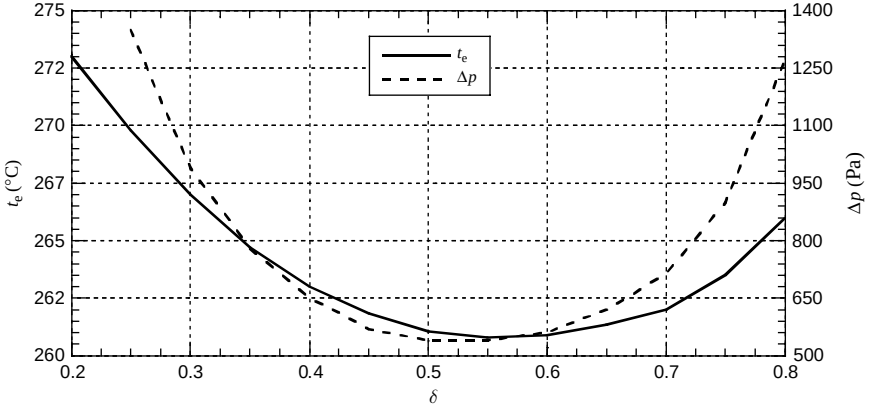


Fig. 8.41 Effects of tube distribution in the two passages ($p = 1$ bar; $q_t = 46.5\,\mathrm{kW/m^2}$; $G_m = 9.72\,\mathrm{kg/m^2 s}$; $d_i = 64.2\,\mathrm{mm}$)

The study was conducted for different values of two quantities that characterize the type of boiler under discussion. The first is the thermal load referred to the tube bank, that is, the heat introduced into the boiler per surface unit of the tubes only (we assumed a constant exit temperature of the gas from the flue). The second is the mean mass velocity in the tubes. By varying the tubes in the two passages with equal total exchange surface which means with equal total number of tubes, the mass velocity varies during the two passages, but its mean value obviously remains unchanged. Once these quantities, called q_t and G_m, are set in advance, the ratio δ between the tubes of the second passage and the total number of the tubes was varied, by calculating the exit temperature from the boiler and the pressure drop

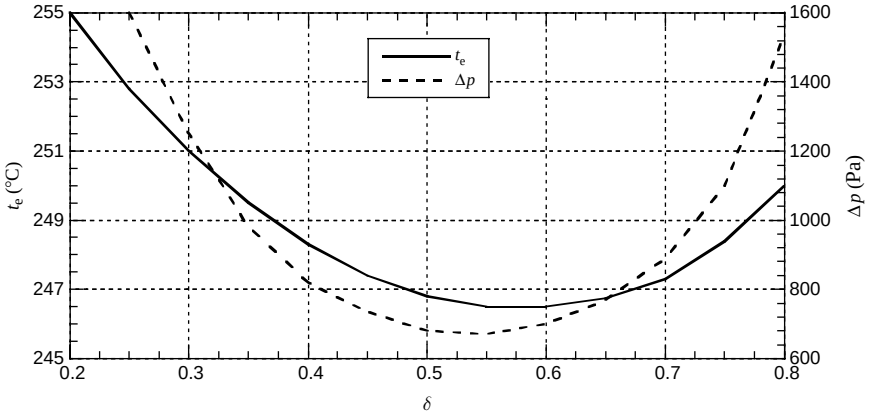


Fig. 8.42 Effects of tube distribution in the two passages ($p = 10$ bar; $q_t = 34.9\,\mathrm{kW/m^2}$; $G_m = 9.72\,\mathrm{kg/m^2 s}$; $d_i = 48.8\,\mathrm{mm}$)

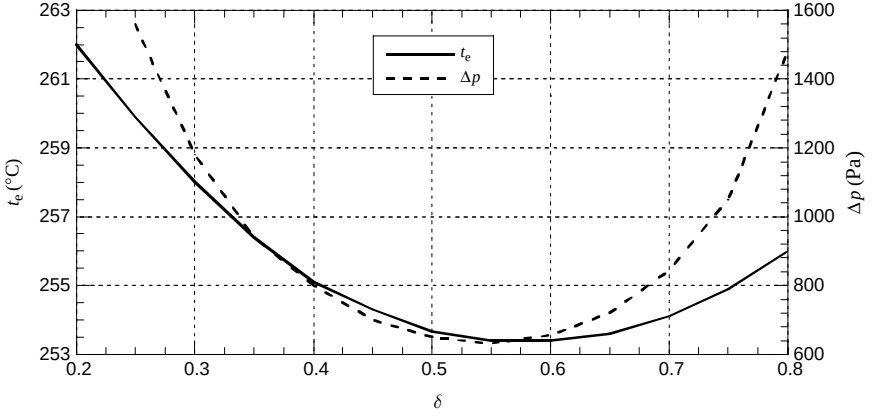


Fig. 8.43 Effects of tube distribution in the two passages ($p = 10$ bar; $q_t = 34.9\,\mathrm{kW/m^2}$; $G_m = 9.72\,\mathrm{kg/m^2 s}$; $d_i = 64.2\,\mathrm{mm}$)

in the tube bank. The analysis was done for different combinations of q_t and G_m, as well as the inside diameter of the tubes d_i and the pressure. This resulted in a series of diagrams some of which are shown in Figs. 8.40–8.43 (pressure drop Δp is expressed in Pa).

The pattern of both t_e and Δp is such that minimum values which are of interest to us correspond to values of δ that are quite close. Moreover, within the minimum range modest variations of δ are matched by modest variations of both t_e and Δp.

In conclusion, the optimization of thermal exchange and pressure drop leads to values of δ of about 0.55. In other words, 55% of the tubes will have to constitute the second passage of the flue gas while the remaining 45% will constitute the third one.

Considering the given temperatures, the often adopted method to equal the velocity of the flue gas into the two passages is incorrect. This leads to a value of δ higher than the optimal one. Finally, note that varying the diameter from 48.8 to 64.2 mm with equal q_t and G_m, the heat transfer improves slightly with the smaller diameter while the pressure drop is almost the same.

Chapter 9
Generator Efficiency

9.1 Efficiency Definition

By definition, efficiency is the ratio between energy output and energy input. In the specific case of a generator both output and input consist of heat. The question is to determine the amount of supplied heat through combustion and potential external heat, as well as the amount of heat provided by the generator in the form of steam (or warm water or superheated water). M_f stands for burned fuel. It must not necessarily be the amount burned within the time unit, because it can also be the amount burned within any time length, as long as the other quantities also refer to the same time. H_n stands for net heat value. Therefore, efficiency is referred to the net heat value. Nothing prevents the reference to the gross heat value. It is simply a convention and needs to be agreed upon by both parties, the constructor and the user.

The input to the generator supplied through combustion is equal to

$$q_\mathrm{c} = M_\mathrm{f} H_\mathrm{n}. \tag{9.1}$$

If some heat is supplied to the combustion air from a heat source outside the generator (this means that an air heater at the terminal section of the generator must be ruled out), we have

$$q_\mathrm{a} = M_\mathrm{a} c_\mathrm{pa} \left(t_\mathrm{a} - t_0\right), \tag{9.2}$$

where M_a stands for the amount of air, c_pa for the mean specific isobaric heat between t_0 and t_a, t_a for the air temperature at the entrance of the generator (if an air heater is expected to be at the exit of the generator, t_a is the temperature at the entrance of the air heater and not into the burner box) and t_0 for the room temperature.

If heat is supplied to the fuel from a heat source outside the generator (fuel heated by steam output of the generator must be ruled out), we have

$$q_\mathrm{f} = M_\mathrm{f} c_\mathrm{pf} \left(t_\mathrm{f} - t_0\right), \tag{9.3}$$

D. Annaratone, *Steam Generators*, DOI: 10.1007/978-3-540-77715-1_9,

© Springer-Verlag Berlin Heidelberg 2008

where c_{pf} stands for the specific isobaric heat between t_0 and t_f and t_f for the temperature reached by the fuel through this external heat source (for instance, a resistor, steam output from another source).

The total heat input to the generator is given by

$$q_{in} = q_c + q_a + q_f \tag{9.4}$$

or, putting it differently, by

$$q_{in} = M_f H_n + q_a + q_f. \tag{9.5}$$

We consider the most general case of a generator equipped with both superheater and reheater getting a water injection through an attemperator to keep the temperature of the steam constant as the load varies (Sect. 3.9).

The heat content of the superheated steam is given by

$$q_s = M_s h_s, \tag{9.6}$$

given that M_s stands for the steam output and h_s for its enthalpy.

The heat content of the feed-water is given by

$$q_w = M_w h_w, \tag{9.7}$$

where M_w stands for the amount of water feeding the generator and h_w for its enthalpy.

The heat content of the water injected into the attemperator is given by

$$q'_w = M'_w h'_w, \tag{9.8}$$

where M'_w stands for the amount of water supplied to the attemperator and h'_w for its enthalpy.

Of course,

$$M_s = M_w + M'_w, \tag{9.9}$$

because the test must be done at constant water level in the drum in the beginning and at the end of the test itself. In the case of a generator with forced circulation the equality in (9.9) is obvious. Now, if q''_s stands for the heat content of the reheated steam, q'_s for the heat content of the steam to be reheated, and q''_w for heat content of the water injected in the potential attemperator, we have

$$q''_s = M''_s h''_s \tag{9.10}$$

$$q'_s = M'_s h'_s \tag{9.11}$$

$$q''_w = M''_w h''_w, \tag{9.12}$$

with an obvious meaning of the symbols.

As far as the fundamental circuit (economizer, boiler, superheater), the output from the generator is given by

$$q'_{\mathrm{ou}} = q_{\mathrm{s}} - q_{\mathrm{w}} - q'_{\mathrm{w}}. \tag{9.13}$$

And, as far as the reheater, it is given by

$$q''_{\mathrm{ou}} = q''_{\mathrm{s}} - q'_{\mathrm{s}} - q''_{\mathrm{w}}. \tag{9.14}$$

The total output is equal to

$$q_{\mathrm{ou}} = q_{\mathrm{s}} + q''_{\mathrm{s}} - q'_{\mathrm{s}} - q_{\mathrm{w}} - q'_{\mathrm{w}} - q''_{\mathrm{w}}. \tag{9.15}$$

The definition of q_{ou} provided by (9.15) is correct only if the heat taken from the generator is correlated to either superheated or reheated steam. This means that there should not be water drained from the drum to keep the level of salinity in the water within safety limits. These drainages should not take place during the test. If it should happen, it is important to take it into account by summing up the heat content of the drainage itself.

The heat content q_{wd} is given by

$$q_{\mathrm{wd}} = M_{\mathrm{wd}} h_{\mathrm{wd}}, \tag{9.16}$$

where M_{wd} stands for the amount of drained water and h_{wd} for its enthalpy.

In small power generators, it is customary to simply measure the amount of supplied water instead of the produced steam.

Based on (9.9), if the de-superheating of the steam is not done through water injection (and this is the case with small power generators), M_{s} obviously coincides with M_{w}, as long as the drum is not drained. Otherwise,

$$M_{\mathrm{s}} = M_{\mathrm{w}} - M_{\mathrm{wd}}. \tag{9.17}$$

Without considering drainages, the estimate of the produced heat would exceed reality. In fact, assuming that $M_{\mathrm{s}} = M_{\mathrm{w}}$ the produced heat is computed as follows:

$$q_{\mathrm{ou}} = q_{\mathrm{s}} - q_{\mathrm{w}} = M_{\mathrm{w}} \left(h_{\mathrm{s}} - h_{\mathrm{w}} \right); \tag{9.18}$$

but in reality and based on (9.17) it is given by

$$q_{\mathrm{ou}} = \left(M_{\mathrm{w}} - M_{\mathrm{wd}} \right) h_{\mathrm{s}} + M_{\mathrm{wd}} h_{\mathrm{wd}} - M_{\mathrm{w}} h_{\mathrm{w}}; \tag{9.19}$$

in other words,

$$q_{\mathrm{ou}} = M_{\mathrm{w}} \left(h_{\mathrm{s}} - h_{\mathrm{w}} \right) - M_{\mathrm{wd}} \left(h_{\mathrm{s}} - h_{\mathrm{wd}} \right), \tag{9.20}$$

where h_{wd} is, of course, smaller than h_{s}.

Generally assuming that drainages take place (9.15) is modified as follows:

$$q_{\mathrm{ou}} = q_{\mathrm{s}} + q''_{\mathrm{s}} - q'_{\mathrm{s}} - q_{\mathrm{w}} - q'_{\mathrm{w}} - q''_{\mathrm{w}} + q_{\mathrm{wd}}. \tag{9.21}$$

M_{s} is to be measured directly or eventually obtained from the feed water and generally also from the amount of water injected into the superheater based on the following equation:

$$M_s = M_w - M_{wd} + M'_w. \tag{9.22}$$

Therefore, expressing efficiency as percentage we have

$$\eta = \frac{q_s + q''_s - q'_s - q_w - q'_w - q''_w + q_{wd}}{M_f H_n + q_a + q_f} \times 100. \tag{9.23}$$

Based on international regulations about thermal testing of generators suggested by the ISO TC 64, the definition of efficiency is slightly different from (9.23).

Using the same symbolism adopted until now, efficiency is obtained through the following equation:

$$\eta = \frac{q_s + q''_s - q'_s - q_w - q'_w - q''_w + q_{wd} - q_a - q_f}{M_f H_n} \times 100. \tag{9.24}$$

In practice the difference between the values of η computed from (9.23) to (9.24) is not relevant. For instance, if $q_a + q_f$ is equal to 7% of $M_f H_n$ (this a very high percentage) and the efficiency computed through (9.23) is equal to 92%, in both cases we have

$$\eta = \frac{98.44}{100 + 7} \times 100 = 92\%$$

$$\eta = \frac{98.44 - 7}{100} \times 100 = 91.44\%.$$

The difference is equal to 0.61%.

Undoubtedly, (9.23) is conceptually more justified than (9.24) because only the former really represents the ratio between the heat output and the heat input, according to the classical definition of efficiency. On the other hand, in actuality and besides scientific considerations, efficiency is a quantity that can be computed conventionally, as we already noted about the heat value, as long as it serves as a basis to determine, if contractual conditions are respected under running conditions. Moreover, (9.24) only showing the heat introduced through combustion in the denominator, allows comparison with the similar equation relative to the indirect computation method of efficiency that will be examined later on, and according to which the percentages of heat losses are calculated only in reference to $M_f H_n$. This is easier compared to including the contribution of external heat, as well.

Finally, note that these external contributions of heat are rather unusual. The exception is the heating of fuel oil with steam from another source which nonetheless represents a rather modest amount of heat. In practice, (9.23) generally coincides with (9.24) or differs only imperceptibly from it. Simply consider that heating fuel oil to 120 °C entails a heat quantity of 200 kJ/kg to be compared with the heat value of oil. The greater heat contribution amounts to no more than 0.5%.

Until now we spoke of steam only. The boiler can also produce warm or superheated water. Of course, in that case the quantities relative to the superheater and the water injections will be missing, as well as q_a and q_f. The heat contents q_w and q_{wd} do not change, and the same is true for the introduced heat $M_f H_n$, given that q_w

stands for the heat content of the circulation water entering the boiler. As far as q_s, it stands for the heat content of the circulation water at the exit of the boiler.

Besides the efficiency as it was defined until now, it is possible to consider the so-called useful efficiency, too. Actually, computing the efficiency of (9.23) or (9.24) highlights the greater or lesser attitude of the generator to exploit the heat developed by the fuel and potentially introduced with the heated air and the heated fuel. But this does not represent the ratio between the useful energy and the energy supplied to the generator. In fact, part of the steam is used, for instance, to heat the fuel oil, to feed a steam pump, or to feed the turbines coupled to the pumps serving the generator. This means that the steam cannot be used for the purposes assigned to the steam itself. In addition, the energy is produced as heat at the expense of electricity required to run the engines coupled to the fans and to the water and fuel pumps. In general, it is at the expense required to run the auxiliary equipment of the generator.

Therefore, if q_s^* is the heat content of the useful steam and q_{au} the energy supplied to run the auxiliary equipment, the useful efficiency is given by

$$\eta_u = \frac{q_s^* + q_s'' - q_s' - q_w - q_w' - q_w''}{M_f H_n + q_a + q_f + q_{au}} \times 100. \tag{9.25}$$

Equation (9.25), as much as (9.23), represents the scientifically correct equation in agreement with the efficiency definition. q_{wd} is not included in it because it represents lost heat as far as the useful energy. If the ongoing drainage is coupled with an exchanger that partially recuperates the heat, as is the case in bigger units, the recuperated heat must be counted in the numerator of (9.25).

Even (9.25) can be modified by following the same criteria applied to move from (9.23) to (9.24) as follows:

$$\eta_u = \frac{q_s^* + q_s'' - q_s' - q_w - q_w' - q_w'' - q_a - q_f - q_{au}}{M_f H_n} \times 100. \tag{9.26}$$

The output, besides being derived directly from the various heat contents, as shown, can also be seen as the difference between the heat input to the generator and the heat losses taking place inside it.

In other words, if $\sum q_L$ stands for the sum of the different heat losses, the output is given by

$$q_{ou} = q_{in} - \sum q_L. \tag{9.27}$$

Therefore, by recalling (9.5) we have

$$q_{ou} = M_f H_n + q_a + q_f - \sum q_L. \tag{9.28}$$

The efficiency is given by

$$\eta = \frac{M_f H_n + q_a + q_f - \sum q_L}{M_f H_n + q_a + q_f} \times 100, \tag{9.29}$$

or by

$$\eta = 100 - \sum \frac{q_{\mathrm{L}}}{M_{\mathrm{f}} H_{\mathrm{n}} + q_{\mathrm{a}} + q_{\mathrm{f}}} \times 100. \tag{9.30}$$

Equation (9.30) corresponds to (9.23).

But if we conventionally consider the output to be the numerator term in (9.24), instead of (9.29), we can simply write that

$$\eta = \frac{M_{\mathrm{f}} H_{\mathrm{n}} - \sum q_L}{M_{\mathrm{f}} H_{\mathrm{n}}} \times 100. \tag{9.31}$$

Consequently,

$$\eta = 100 - \sum \frac{q_{\mathrm{L}}}{M_{\mathrm{f}} H_{\mathrm{n}}} \times 100. \tag{9.32}$$

Equation (9.32) corresponds to (9.24).

The second term on the right of the equal sign represents the sum of heat losses expressed in percentages. If L represents the generic heat loss,

$$\eta = 100 - \sum L. \tag{9.33}$$

If the efficiency is computed according to (9.24), we say that it was computed with the direct method because output and input are computed directly. If (9.33) is used instead, we say that the efficiency was computed with the indirect method, because only heat losses are factored in without explicit reference to the two fundamental quantities constituting the foundation of efficiency, in other words heat output and heat input. In Sect. 9.6 we will discuss how to proceed operationally in both instances with a running generator including the advantages of the indirect method.

The summation in (9.33) consists of different types of losses, precisely

$$\sum L = L_{\mathrm{uf}} + L_{\mathrm{co}} + L_{\mathrm{sh}} + L_{\mathrm{er}} + L_{\mathrm{m}}, \tag{9.34}$$

where L_{uf} stands for the heat loss by unburned fuel and L_{CO} for the heat loss by unburned carbon monoxide, L_{sh} stands for heat loss by sensible heat of the flue gas and L_{er} for heat loss by external radiation. L_{m} stands for miscellaneous losses of modest entity and different origin that will be discussed in Sect. 9.5.

Figure 9.1 is an example and general reference for efficiency in generators fulfilling the following conditions.

Generators with power ranging from 1000 to 20,000 kW installed in an indoor space.
Room temperature = 20 °C.
Temperature of outside walls (except for the front) = 40–45 °C.
Temperature of front wall = 50–60 °C; absence of unburned carbon monoxide; runtime under full load.
Fuel oil combustion with a net heat value equal to 40,600 kJ/kg. Air index equal to $n = 1.2$ that corresponds to $|CO_2| = 13.4\%$.
The value for miscellaneous losses is assumed to be $L_{\mathrm{m}} = 0.5\%$ (Sect. 9.5).
The sensible heat losses as well as the external radiation losses are taken from Fig. 9.5 and from the equations in Sect. 9.5.

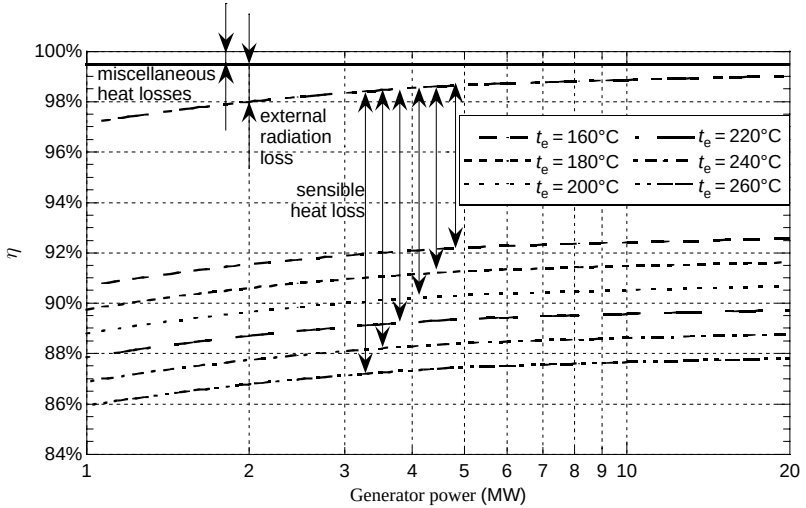


Fig. 9.1 Generator efficiency for fuel oil ($H_n = 40,600$ kJ/kg; $n = 1.2$; $|CO_2| = 13.4\%$)

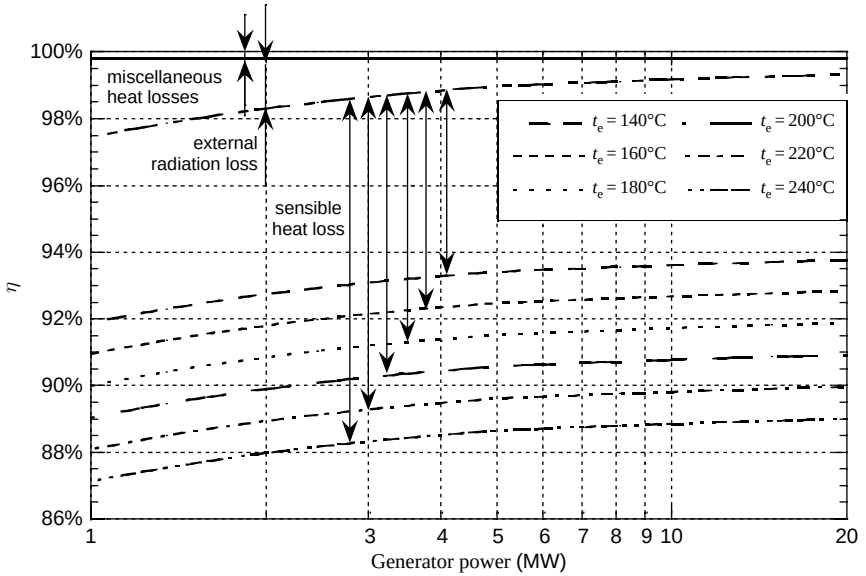


Fig. 9.2 Generator efficiency for natural gas ($H_n = 48,000$ kJ/kg; $n = 1.1$; $|CO_2| = 10.6\%$)

Figure 9.2 shows efficiency using natural gas.

The general conditions are the same as before. The specific conditions of combustion are as follows.

Natural gas combustion with a net heat value equal to 48,000 kJ/kg.
Air index $n = 1.1$ corresponding to $|CO_2| = 10.6\%$.
Miscellaneous losses equal to 0.2% (Sect. 9.6).
Sensible heat loss and external radiation loss are taken from Fig. 9.6 and from the equations in Sect. 9.5.

9.2 Heat Loss by Unburned Fuel

The heat loss relative to solid unburned fuel involves soot, furnace slag, and fuel falling under the grate. The loss caused by soot is difficult to measure. It is possible only in the case of coarse soot collected in the hoppers designed to do just that. It can be mixed with the residues of the grate and analyzed with them. The content of combustible matter of these residues consists of partially distilled carbon. In order to simplify the calculation of the heat loss, we can assume a net heat value of 33,830 kJ/kg, that is, the heat value of carbon. Given that even small percentages of oxygen determine a reduction of the heat value, it is more appropriate to adopt the conventional heat value of 33,500 or 33,000 kJ/kg. It would be even better to distinguish the grate residues from the soot collected in the hoppers because the combustible part of the former mainly consists of amorphous coal (entailing a heat value close to 33,830 kJ/kg).

The amount of soot produced in the combustion of solid fuels depends on the type of fuel, on the size, on the type of grate (if this type of combustion is intended), on the moisture level of the fuel, on its heating, and on the volume and the height of the furnace (they determine the possibility of total or partial combustion of small particles). The losses with soot are equal to 4–8% burning small coal; they decrease with cob coal and even more with nut coal (2–4%).

Considerably smaller losses occur with blind coal and with cannel coal. Lignite shows similar values going from higher values with short lignite and lower values with compact lignite. An efficient way to reduce these losses consists of taking the coarse soot from the hoppers to put it again in the furnace to burn. This way the losses will be cut in half. The same procedure with soot collected in soot precipitators is not worthwhile because the soot contains a lot of ashes. Sometimes it has been done anyway to melt the ashes together with those in the furnace to simplify their scavenging.

The heat loss caused by the presence of unburned fuel is computed through the following equation:

$$q_{\mathrm{uf}} = M_{\mathrm{r}} \frac{CM}{100} H_{\mathrm{cm}}, \tag{9.35}$$

where q_{uf} is expressed in kW, M_r stands for the amount of solid residues in kg/s, CM stands for the percentage of combustible matter in the residues and H_{cm} represents the heat value of combustible matter in kJ/kg.

The heat loss as percentage is therefore given by

$$L_{uf} = \frac{q_{uf}}{M_f H_n} \times 100; \tag{9.36}$$

M_f stands for the fuel consumption in kg/s and H_n for its net heat value. Therefore, based on (9.35):

$$L_{uf} = \frac{M_r}{M_f} CM \frac{H_{cm}}{H_n}, \tag{9.37}$$

where M_r/M_f represents the amount of residues for every kilogram of burned fuel; indicating the percentage of residues with R equal to

$$R = \frac{M_r}{M_f} \times 100, \tag{9.38}$$

and assuming that $H_{cm} = 33,000\,\text{kJ/kg}$, the loss as percentage is given by

$$L_{uf} = \frac{R \times CM}{100} \; \frac{33,000}{H_n}. \tag{9.39}$$

9.3 Heat Loss by Unburned Carbon Monoxide

Unburned carbon monoxide was already discussed in Sect. 7.7. This is the heat loss caused by incomplete combustion of the carbon contained in the fuel. If $|CO|$ is the percentage in volume of carbon monoxide in dry gas, as we know, if G'_v stands for the volume of dry gas per kg of fuel, and M_f for the fuel consumption in kg/s, the flow rate of carbon monoxide is given by

$$Q_{co} = M_f G'_v \frac{|CO|}{100} (\text{Nm}^3/\text{s}). \tag{9.40}$$

For every Nm^3 of CO, 12,644 kJ is lost. This is in fact the reaction heat of carbon monoxide that is lost because it does not develop into CO_2 during combustion.

The heat loss is given by

$$q_{co} = M_f G'_v \frac{|CO|}{100} \times 12,644, \tag{9.41}$$

where q_{CO} is expressed in kW and G'_v in Nm^3/kg.

The heat supplied to the generator is equal to $M_f H_n$, given that H_n stands for the net heat value of the fuel in kJ/kg (see Sect. 9.1).

The percentage loss for unburned carbon monoxide is given by

$$L_{\mathrm{co}} = \frac{q_{\mathrm{co}}}{M_{\mathrm{f}} H_{\mathrm{n}}} \times 100 = 12,644 \, \frac{G'_{\mathrm{v}}}{H_{\mathrm{n}}} \, |\mathrm{CO}| \, . \tag{9.42}$$

Of course, in (9.41) and (9.42) the different quantities can also be expressed in the following measuring unit: H_{n} in $\mathrm{kJ/Nm^3}$, M_{f} in $\mathrm{Nm^3/s}$, and G'_{v} in $\mathrm{Nm^3/Nm^3}$.

As far as G'_{v}, it is important to take the following into account. In Sect. 7.7 we already obtained the equation relative to dry theoretic gas for both solid and liquid fuels. Here it is again. For solid and liquid fuels

$$G'_{\mathrm{tv}} = A_{\mathrm{tv}} - 0.05558H + 0.007O + 0.008N \ \mathrm{Nm^3/kg}. \tag{9.43}$$

A_{tv} stands for theoretic air in $\mathrm{Nm^3/kg}$ and H, O, and N for the mass percentages of hydrogen, oxygen, and nitrogen in the fuel.

As far as gaseous fuels, note that the combustion of $1\,\mathrm{Nm^3}$ of H_2 produces $1\,\mathrm{Nm^3}$ of $\mathrm{H_2O}$, whereas $1\,\mathrm{Nm^3}$ of $C_{\mathrm{m}}H_{\mathrm{n}}$ produces $n/2$ $\mathrm{Nm^3}$ of $\mathrm{H_2O}$; thus, based on (7.24) we have

$$G'_{\mathrm{tv}} = A_{\mathrm{tv}} + 1 - 0.005\,(CO + 3H_2) - 0.0025 \sum_i (n_i + 4)\, C_{mi}H_{ni} \ \mathrm{Nm^3/Nm^3}, \tag{9.44}$$

where A_{tv} is in $\mathrm{Nm^3/Nm^3}$ and CO, H_2, and $C_{mi}H_{ni}$ stand for the volumetric percentages of carbon monoxide, hydrogen, and the generic hydrocarbon in the fuel.

In the absence of unburned carbon monoxide, that is, with complete combustion, and indicating the actual amount of dry gas with G'_{cv}, we also have

$$G'_{\mathrm{cv}} = G'_{\mathrm{tv}} + (n-1)A_{\mathrm{tv}}, \tag{9.45}$$

where n stands for the air index.

In the presence of unburned carbon monoxide, the flue gas increases in volume. In fact, it is as if a part of carbon dioxide dissociated into CO and $\mathrm{O_2}$ depending on the reaction

$$2\mathrm{CO_2} = 2\mathrm{CO}{+}\mathrm{O_2} \tag{9.46}$$

$1\,\mathrm{Nm^3}$ of $\mathrm{CO_2}$ generates $1\,\mathrm{Nm^3}$ of CO and $0.5\,\mathrm{Nm^3}$ of $\mathrm{O_2}$.

We know that the amount of carbon monoxide contained in dry gas per each kg or $\mathrm{Nm^3}$ of fuel is given by

$$V_{\mathrm{co}} = G'_{\mathrm{v}} \frac{|\mathrm{CO}|}{100}. \tag{9.47}$$

Based on (9.46), the increase in volume of dry gas always referred to 1 kg or $1\,\mathrm{Nm^3}$ of fuel is equal to

$$\Delta G'_{\mathrm{cv}} = 0.5 G'_{\mathrm{v}} \frac{|\mathrm{CO}|}{100}. \tag{9.48}$$

Then

$$G'_{\mathrm{v}} = G'_{\mathrm{cv}} + \Delta G'_{\mathrm{cv}} = G'_{\mathrm{cv}} + 0.5 G'_{\mathrm{v}} \frac{|\mathrm{CO}|}{100}. \tag{9.49}$$

Based on (9.49)

$$G'_{\mathrm{v}} = \frac{G'_{\mathrm{CV}}}{1 - 0.5\frac{|\mathrm{CO}|}{100}}. \tag{9.50}$$

Based on (9.50) and recalling (9.45) we obtain

$$G'_{\mathrm{v}} = \frac{G'_{\mathrm{tv}} + (n-1)A_{\mathrm{tv}}}{1 - 0.5\frac{|\mathrm{CO}|}{100}}. \tag{9.51}$$

Once |CO| and the air index n are known, A_{tv} has been computed based on the equations in Sect. 7.5, and G'_{tv} based on (9.43) and (9.44), (9.51) makes it possible to compute G'_{v} to be introduced into (9.42) for the computation of the loss by unburned carbon monoxide.

Figure 9.3 shows the curves relative to L_{CO} for fuel oil with a net heat value equal to 40,600 kJ/kg.

The diagram in Fig. 7.23 used to this extent leads to the numerator in (9.50) standing for the amount of actual dry gas per 1 kg of fuel oil in the absence of unburned fuel (9.45) which is obtained based on G_{v} and G_{wv} read on the diagram based on equation:

$$G'_{\mathrm{cv}} = G_{\mathrm{v}} - G_{\mathrm{wv}}. \tag{9.52}$$

Figure 9.4 shows the curves relative to L_{CO} for natural gas, the net heat value of which is equal to 48,000 kJ/kg.

Note that L_{CO} is a function of both |CO| and the air index and stands for very high heat loss if the value of |CO| is high. We establish once again the necessity to produce combustion in absence of unburned carbon monoxide if high generator efficiency is desired.

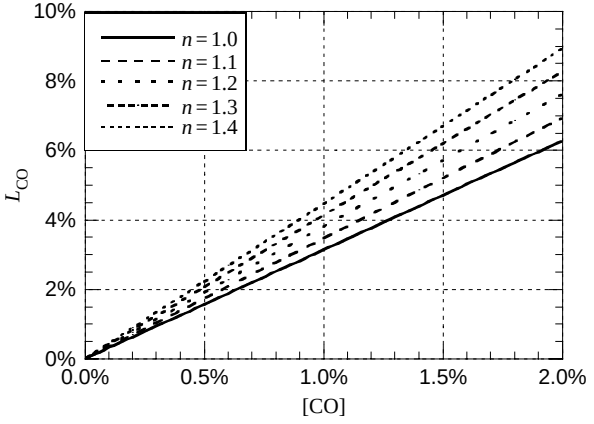


Fig. 9.3 Heat loss by unburned CO for fuel oil combustion $(\mathrm{H_n} = 40,600\ \mathrm{kJ/kg})$

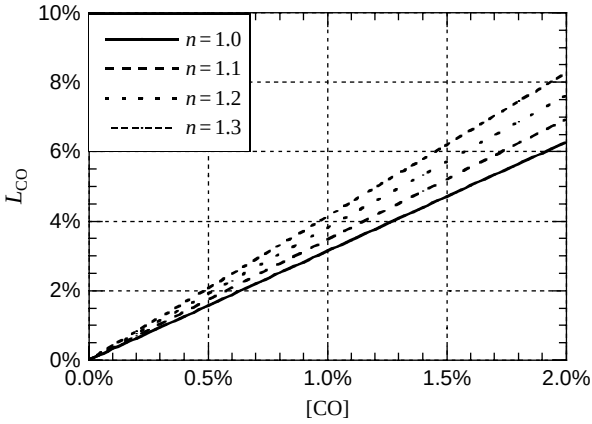


Fig. 9.4 Heat loss by unburned CO for natural gas combustion ($H_n = 48,000$ kJ/kg)

At this point, we stress that the presence of solid unburned fuel impacts the loss by unburned carbon monoxide in the sense that (9.42) is not valid anymore. In fact, (9.42) was computed assuming that all the fuel is burned. If part of it is not burned instead, the equation must be modified as follows with reference to the meaning of M_r and CM:

$$q_{co} = \left(M_f - M_r \frac{CM}{100}\right) G'_v \frac{|CO|}{100} \times 12,644. \tag{9.53}$$

Then

$$L_{co} = \frac{q_{co}}{M_f H_n} = 12,644 \frac{G'_v}{H_n} |CO| \left(1 - \frac{M_r}{M_f} \frac{CM}{100}\right). \tag{9.54}$$

Recalling (9.37) and (9.38) we may write that

$$L_{co} = 12,644 \frac{G'_v}{H_n} |CO| \left(1 - \frac{L_{uf}}{100} \frac{H_n}{33,000}\right). \tag{9.55}$$

Basically, (9.55) can be simplified as follows by committing a negligible mistake:

$$L_{co} = 12,644 \frac{G'_v}{H_n} |CO| \left(1 - \frac{L_{uf}}{100}\right). \tag{9.56}$$

Note that the value computed through (9.42) must be multiplied by the corrective factor $(1 - L_{uf}/100)$; for instance, if L_{uf} is equal to 5%, the loss L_{CO} is actually equal to 95% of the one obtained through (9.42).

9.4 Loss by Sensible Heat of the Flue Gas

The flue gas exiting the generator at a temperature higher than room temperature, that is, the temperature of fuel and combustion air entering the generator in the absence of external heating, produces heat loss called sensible heat loss. The heat loss is given by

$$q_{sh} = M_f G_m c_{pg} (t_e - t_0) = M_f G_m (h_e - h_0); \tag{9.57}$$

q_{sh} is expressed in kW, M_f stands, as usual, for the amount of burned fuel in kg/s, G_m is the mass of gas per kg of fuel in kg/kg, c_{pg} is the mean specific isobaric heat between t_0 and t_e in kJ/kgK, t_e is the exit temperature of the gas from the generator, t_0 is the room temperature, h_e and h_0 represent the enthalpies of the gas with respect to temperature t_e and t_0 in kJ/kg. The percentage loss by sensible heat is therefore equal to:

$$L_{sh} = \frac{q_{sh}}{M_f H_n} 100 = \frac{G_m}{H_n} c_{pg} (t_e - t_0) 100 = \frac{G_m}{H_n} (h_e - h_0) 100, \tag{9.58}$$

where H_n stands for the net heat value of the fuel in kJ/kg. Of course, in (9.57) and (9.58) it is possible to consider M_f in $\mathrm{Nm^3/s}$, G_m in $\mathrm{kg/Nm^3}$, and H_n in $\mathrm{kJ/Nm^3}$. Moreover, G_v can be used instead of G_m if c_{pg}, h_e, and h_0 are referred to $1\,\mathrm{Nm^3}$.

A rapid approximate computation of L_{sh} can also be done through the following equation suggested by Hassenstein:

$$L_{sh} = K \frac{t_e - t_0}{|CO_2|}, \tag{9.59}$$

given that $|CO_2|$ stands for the volume percentage of CO_2 in dry flue gas and K is a factor equal to

anthracite	$K = 0.684$
low-grade anthracite	$K = 0.648$
coke	$K = 0.702$
pitchy lignite	$K = 0.653$
xyloid lignite	$K = 0.721$
peat	$K = 0.718$
firewood	$K = 0.798$
heavy fuel oil	$K = 0.562$

For instance, for fuel oil with $H_n = 40,200\,\mathrm{kJ/kg}$ and $|CO_2| = 13.3\%$, if $t_e = 180\,^\circ\mathrm{C}$ and $t_0 = 20\,^\circ\mathrm{C}$, the diagrams in Figs. 7.24 and 7.30 lead to

$$G_m = 17.65\,\mathrm{kg/kg};\ u \approx 6\%;\ h_e = 191.5\ \mathrm{kJ/kg};\ h_0 = 20.9\,\mathrm{kJ/kg}$$

Based on (9.58), $L_{sh} = 7.49\%$; based on (9.59) $L_{sh} = 6.75\%$ instead; this simple example shows how (9.59) provides only initial orientation and approximate

calculation results. The following simple equations are closer to reality for the computation of L_{sh}, the former for fuel oil and the latter for natural gas:

$$L_{sh} = \left(0.0051 + \frac{0.548}{|CO_2|}\right)(t_e - t_0); \tag{9.60}$$

$$L_{sh} = \left(0.0066 + \frac{0.407}{|CO_2|}\right)(t_e - t_0). \tag{9.61}$$

As we already determined for L_{CO}, the presence of solid unburned fuel also impacts loss by sensible heat. A similar process to the one that led to (9.56) in substitution of (9.42) can be used to develop the following equation in substitution of (9.58) if there is solid unburned fuel:

$$L_{sh} = \frac{G_m}{H_n} c_{pg}(t_e - t_0)(100 - L_{uf}) = \frac{G_m}{H_n}(h_e - h_0)(100 - L_{uf}). \tag{9.62}$$

With reference to (9.58) Fig. 9.5 shows the curves relative to L_{sh} for fuel oil with $H_n = 40,600\,\text{kJ/kg}$ and a room temperature of 20 °C.

Figure 9.6 shows the values of L_{sh} relative to natural gas instead with $H_n = 48,000$ kJ/kg and identical room temperature of 20 °C. The loss by sensible heat is the most important heat loss. It suffices to think that in the case of combustion with fuel oil or natural gas, especially in big units, it stands almost for the entire loss (of course, in absence of unburned CO).

Only the loss by solid unburned fuel can have the same order of magnitude of the one by sensible heat if there is a considerable amount of residues. The efforts of designers are therefore aimed at reducing this loss. According to (9.58) this can be done by decreasing the value of G_m and t_e. As far as G_m, its value decreases with a decrease of excess air. This is clearly shown by Figs. 9.5 as well as 9.6. Therefore, it is a question of constructing more and more perfected burners so as to require less excess air to achieve complete combustion. This condition is essential because a reduction of air together with the buildup of CO deteriorates efficiency due to

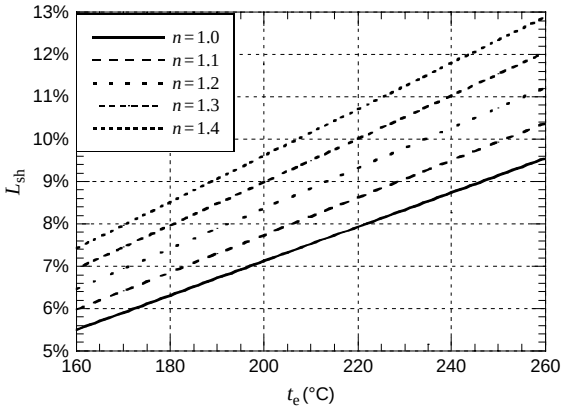


Fig. 9.5 Sensible heat loss for fuel oil combustion ($H_n = 40,600$ kJ/kg; $t_0 = 20\,°C$)

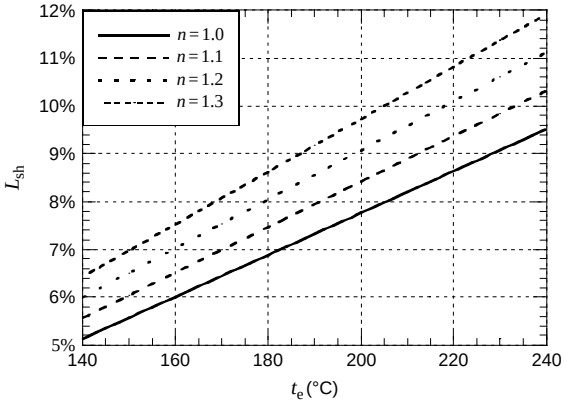


Fig. 9.6 Sensible heat loss for natural gas combustion ($H_n = 48,000$ kJ/kg; $t_0 = 20\,^{\circ}C$)

the ensuing unburned CO loss, thus abundantly nullifying the advantage represented by the reduction of G_m. This is evident in the diagrams of Figs. 9.3, 9.4, 9.5 and 9.6.

The presence of even 1% of |CO| determines a much higher loss compared with the reduction of the value of L_{sh} obtained, for instance, by passing from $n = 1.3$ to $n = 1.1$.

As far as t_e, a reduction is always possible making sure that t_e gets closer and closer to the temperature of the heated fluid in the final section of the generator (water in the case of an economizer, air in the case of an air heater, water/steam mix in the absence of both economizer, and air heater). Yet, beyond a certain limit there are two negative factors advising against further reduction of t_e. The first one is represented by the onset of potential corrosion deriving from the presence of sulfur in the fuel. This danger is out of the question if combustion occurs with natural gas.

The second one is represented by the high cost involved in cooling gas at temperatures close to the temperature of the heated fluid. The small temperature difference between the two fluids requires great surfaces to achieve modest heat transfer. The increase in efficiency and the ensuing smaller cost of energy output are obtained at the expense of a considerable increase in plant costs. The solution must therefore be the outcome of a comparative study of the different costs to identify the optimum balance. The situation is entirely different if, for instance, the generator is meant to work without interruptions, or if its runtime is seasonal, as is the case with certain technological uses of the steam. Clearly, in the second case the efficiency value is less important (of course, within limits) than the cost of the plant. On the other hand, note that nowadays the considerable cost of fuels of any kind makes optimal solutions of the past outdated in the present time.

Generally, if a boiler is not followed by a heat regenerator, it is almost always convenient to push the cooling of the flue gas up to 30–40 °C above the temperature of the produced steam. If there is a regenerator and the fuel is natural gas, a careful financial cost analysis of both plant and runtime is required to identify the optimal

surface of the regenerator. Usually, considerable cooling of the gas will be best. However, it is impossible to provide more detailed information because of the many parameters at play. In the case of fuel oil or coal, the financial analysis is conditioned by the risk of corrosion, and the cooling process of the gas cannot be pushed as far as with natural gas. Chapter 11 examines a few typical situations where it is relatively easy to generalize calculation for optimization, albeit an approximate one. Specifically, we would like to direct focus on Sects. 11.2 and 11.3.

9.5 Heat Loss by External Radiation

This is the definition of the loss corresponding to the heat transferred by the generator to the environment. Regardless of adequate insulation of the generator to reduce this loss to a minimum, a small percentage of the heat output is lost through wall radiation which make up the envelope of the generator and through the air heating getting in contact with the walls themselves.

Therefore, this is a heat loss by both radiation and convection called loss by radiation only for the sake of simplicity. Theoretically, it is not difficult to determine the entity of this loss, indicated with L_{er} from now on, through the temperature and the surface of the walls, the air temperature, the black level of the walls, and the heat-transfer coefficient of the air getting in contact with them due to the natural upward motion (or due to wind in outdoor installations). Actually, the computational uncertainties are so many and such that direct determination can be considered only in rough terms without presuming to obtain reliable values. Thus, it is preferable to estimate the loss by difference or based on the diagrams.

If the efficiency is computed with the direct method, the summation of the losses is given by

$$\sum L = 100 - \eta. \tag{9.63}$$

Once the heat losses by solid unburned matter, sensible heat, and potential unburned CO are computed, we obtain the following according to Sects. 9.2 and 9.3 as well as (9.34):

$$L_{\text{er}} + L_{\text{m}} = \sum L - L_{\text{uf}} - L_{\text{co}} - L_{\text{sh}}. \tag{9.64}$$

Then, based on (9.63)

$$L_{\text{er}} + L_{\text{m}} = 100 - \eta - L_{\text{uf}} - L_{\text{co}} - L_{\text{sh}}, \tag{9.65}$$

where L_{m} stands for miscellaneous losses which will be discussed in Sect. 9.6.

This way, the heat loss by external radiation and the miscellaneous losses are not computed but estimated based on difference according to (9.65). If efficiency is computed using the indirect method instead, it is indispensable to know L_{er}. In this case statistical data are used. Examining the different available criteria to determine the presumed value of L_{er}, specifically the criteria of the American Boiler Manufacturers Association, we recommend the following equation for generators

with power ranging from 20 to 200 MW that are completely screened (as is customary today) and located in the open

$$L_{\text{er}} = \frac{35}{P^{0.4}}, \tag{9.66}$$

with L_{er} as a percentage and P as the generator power in kW.

The equation refers to a difference in temperature between the walls and the open of about 30 °C and wind with a speed below 0.5 m/s. For completely screened water-tube generators and for smoke-tube boilers with a power equal to or greater than 5000 kW installed indoor, we recommend the following equation instead:

$$L_{\text{er}} = \frac{25}{P^{0.4}}. \tag{9.67}$$

For generators like the ones above with power ranging from 1000 to 5000 kW, we recommend the following:

$$L_{\text{er}} = \frac{210}{P^{0.65}}. \tag{9.68}$$

Both (9.67) and (9.68) for $P = 1000$–$10,000$ kW are shown in Fig. 9.7.

The values of L_{er} computed from the equations above refer to runtime of the generator under full load. If the heat output is below the maximum, that is, if the load is under 100%, the heat loss is basically equal to the one under full load. The input is reduced instead because it is proportional to the output. The loss L_{er} turns out to be inversely proportional to the load.

If we indicate the latter with γ as percentage, the loss by external radiation L'_{er} relative to reduced load is therefore given by:

$$L'_{\text{er}} = L_{\text{er}} \frac{100}{\gamma}. \tag{9.69}$$

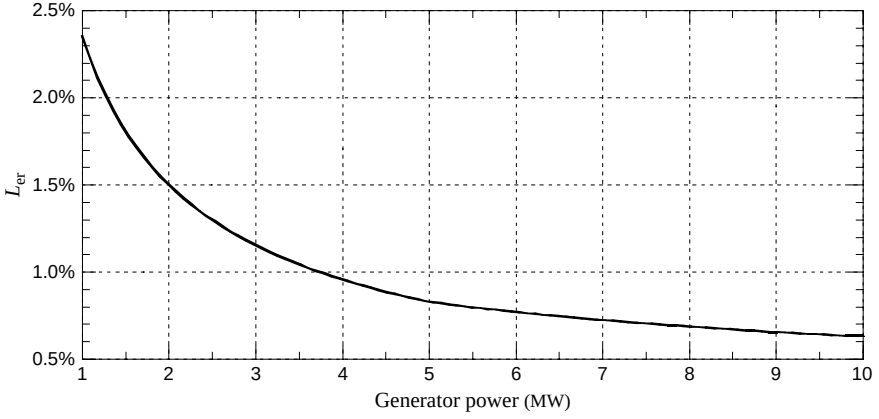


Fig. 9.7 External radiation loss ($P = 1$–10 MW)

On the basis of the recommended equations and on Fig. 9.7, we determine that except for very small power generators the loss by radiation represents a modest percentage of total losses. Thus, even a gross estimate does not really compromise the correct identification of efficiency.

9.6 Miscellaneous Heat Losses

Miscellaneous losses are those that cannot be evaluated or those that often are not determined through direct measurement because of their modest entity. These losses may be discounted if you tolerate a small difference between actual and calculated losses, or they can be factored in by introducing a term into the calculation in reference to any not explicit loss standing for a conventional value. This term will be L_{m}. Heat loss connected to soot evacuated from the chimney with the flue gas belongs to the first category. Both sensible heat loss by solid residues and sensible heat loss caused by the humidity of the combustion air belong to second category.

As far as sensible heat loss of steam contained in the air, note that if the enthalpy of the flue gas is computed according to the advice in Sect. 7.9, that is, by increasing the moisture relative to hydrogen and water in the fuel by 0.5%, one already implicitly takes the relative air humidity equal to about 40% into account. This way the value of the enthalpy h_{e} included in (9.58) turns out to be slightly higher than the one obtained without increasing the value of m. This results in a higher loss by sensible heat that factors in the humidity of the combustion air, as well. The relative humidity of the air should be taken into account only if it exceeds 40%. Let us look at the ensuing entity of the loss.

We assume relative humidity of 80%; at 20 °C the amount of steam is equal to 0.0117 kg per kg of air, in other words greater by about 0.006 kg than the corresponding one with 40% of relative humidity. We assume to burn fuel oil with a net heat value equal to 40,600 kJ/kg and an air index equal to 1.2. Figure 7.21 shows that the air requirement is equal to $12.7\,\mathrm{Nm}^3/\mathrm{kg}$ or 16.4 kg/kg. For every kilogram of oil there is a greater steam content in the air equal to $0.006 \times 16.4 = 0.0984\,\mathrm{kg}$. The specific heat of the steam at atmospheric pressure is equal to about 1.88 kJ/kgK. Assuming that the exit temperature of the flue gas from the generator is equal to 180 °C, the heat loss represented by q_{sa} is given by

$$q_{\mathrm{sa}} = 0.0984 \times 1.88\,(180 - 20) = 29.6\,\mathrm{kJ/kg}$$

The corresponding percentage loss is therefore equal to

$$L_{\mathrm{sa}} = \frac{29.6 \times 100}{40,600} = 0.07\%$$

This greater loss compared with the one due to conventional air humidity is clearly absolutely irrelevant. Heat loss by sensible heat of solid residues can be higher than the above value, still it will always be modest. For instance, if we assume that solid

residues represent 10% of burned coal, that their specific heat is equal to 1700 J/kgK, and that their temperature amounts to 800 °C, every kilogram of coal entails a heat loss equal to

$$q = 0.10 \times 1700 \times 780 = 132,600 \text{J/kg}$$

If the net heat value of coal is equal to 28,000 kJ/kg, the percentage loss is equal to

$$L = \frac{132.6 \times 100}{28,000} = 0.47\%$$

This loss is contemplated in the ISO TC/64 Code and is evaluated through the heat transferred to the water used to extinguish the residues. In fact, this is the way to proceed if an evaluation of the loss is deemed necessary (in the case of big units and specifically with melted ashes).

In conclusion, except for the loss inherent to soot eliminated from the chimney (in big units equipped with soot precipitators it is practically zero), these losses can be identified. Often they are not, and it will be appropriate to introduce a conventional value of L_{m}, which can be assumed to be 0.5–0.6% for combustion with fuel oil and 1% for combustion with coal. In the case of combustion with natural gas, it can be ignored or assumed to be 0.2%.

9.7 Generator Efficiency Test

If efficiency is computed with the direct method (Sect. 9.1), the values of the different quantities must be introduced into (9.24). To that extent the burned fuel is measured either through weighing or with a nozzle or an orifice meter, and then its net heat value is determined. This is possible either through the equations in Chap. 6 or deriving it from an analysis bulletin or through direct measurement performed with Malher's bomb calorimeter. Then the feed water and perhaps the water injected into the superheater are measured with an orifice plate or a meter. In addition, potential drainage is also measured. The steam output can be measured directly or computed based on (9.22).

Based on water temperature and pressure, its enthalpy is derived from Mollier's tables. The same is true also for superheated steam. The enthalpy of the drainages is the one of the water in the drum. If the produced steam is saturated, it is also necessary to determine its water vapor ratio. This is not an easy task often leading to considerable mistakes that can be done through an insulated water container where the steam is made to gurgle and that works as a calorimeter.

Finally, the determination of q_{a} and q_{f}, as shown by (9.2) and (9.3), requires the identification of the air flow rate (through a Venturi meter or indirectly through gas analysis and the subsequent determination of A_{v} or A_{m}), of the room temperature and the temperature of fuel and air. c_{pa} and c_{pf} are derived the way described in Sects. 6.2 and 7.9. If the reheater is included, one must also measure the flow rate of both inlet steam and injected water, temperature and pressure of the steam at

the inlet and outlet, temperature and pressure of the injected water. This way the different enthalpies can be computed, and it is possible to calculate q'_s, q''_s, and q''_w.

Finally, the computation of η_u based on (9.26) requires the measurement of energy q_{au} absorbed by the auxiliaries.

If the efficiency is computed using the indirect method, the values of all heat losses as percentage described in previous sections must be introduced in (9.34). This requires the analysis of the flue gas with a gas analyzer (Orsat, Mono, and so on). If the Ostwald triangle relative to used fuel is available, it is possible to limit the analysis to $|CO_2|$ and $|O_2|$. The potential presence of CO is highlighted by introducing these values in Ostwald's triangle. If the triangle is not available, as is often the case, direct determination of the $|CO|$ in the flue gas is required. Knowing the composition of the fuel and the values of $|CO_2|$, $|O_2|$, and $|CO|$, calculation leads to the air index, as shown in Sect. 7.8. Then, one computes the theoretic air either using the equations of Sect. 7.5 or through the diagram in Fig. 7.21 in the case of solid or liquid fuels. Knowing A_{tv} leads to the amount of dry gas per mass unit or volume of the fuel through (9.43) and (9.44). Equation (9.51) leads to G'_v.

Once G'_v, H_n, and $|CO|$ are known, the heat loss by unburned carbon monoxide is computed through (9.42) [or (9.56) if there is solid unburned fuel once the value of L_{uf} has been determined]. If solid fuel is burned, one must compute L_{uf}; the amount of solid residues compared with the burned fuel makes it possible to calculate R. The following identification of the percentage of combustible matter CM through combustion of the residues makes it possible to compute L_{uf} through (9.39). Moisture m of the flue gas is obtained through (8.160), based on what was said several times about the humidity of combustion air.

The knowledge of m and of the temperatures t_e and t_0 makes it possible to identify h_e and h_0 based on Sect. 7.9. Then L_{sh} can be computed through (9.58) or (9.62). As far as L_{er} and L_m, we already explained how to proceed in Sects. 9.5 and 9.6.

The computation of efficiency with the indirect method is clearly independent from any measurement relative to water and steam in terms of flow rate, pressure, and temperature. The same can be said for the fuel except for the calculation of L_{uf} (in the case of liquid or gaseous fuels even the consumption of fuel is uninteresting except to determine the load of the generator, but from this point of view it is not necessary to obtain a very precise measure). Therefore, liquid and gaseous fuels simply require the analysis of the flue gas and a measurement of there exit temperature to be done very accurately.

It is equally necessary to know the net heat value and the composition of the fuel (in the case of liquid fuels, the latter is not indispensable if the cited diagrams are used). This explains the reason why the indirect method is particularly advantageous for fuel oil in the first place, and second, for gaseous fuels (they require a number of computations to determine G_v and G_m). This justifies the preference for the indirect method to determine η. An example will highlight another reason intervening in favor of the indirect method. We assume a mistake of 1% in the estimate of the inlet heat and an equivalent mistake in the estimate of the heat output. If the mistakes are, respectively, one by excess and the other by defect, or vice versa, the error in

computing η with the direct method is equal to about 2%. For instance, if the actual efficiency is equal to 90.5%, the calculation leads to a value of 88.6 or 92.4%.

Now we look at how the mistakes made in the estimate of losses impact efficiency computed with the indirect method. In the absence of unburned matter with liquid or gaseous fuels, the losses are reduced to L_{sh}, L_{er}, and L_{m}. The calculation of L_{sh} can lead to somewhat precise results. Anyway, let us assume a mistake equal to 5%. If the exact value of L_{sh} is equal to 8.5%, $L_{\text{sh}} = 8.1\%$ or $L_{\text{sh}} = 8.9\%$ will result from the computation. Moreover, $L_{\text{er}} = 0.7\%$, while we assume that $L_{\text{er}} = 0.5\%$ or $L_{\text{er}} = 1\%$ with an error equal to 40% based on (9.67). Finally, $L_{\text{m}} = 0.3\%$ while we can ignore either this loss or adopt $L_{\text{m}} = 0.6\%$. Even assuming that all mistakes impact the process in the same direction, in one case we have $\eta = 89.5\%$, and in the other we have $\eta = 91.4\%$ with an error of 1.1% by defect, or 1% by excess.

This mistake is smaller than the one made using the direct method, regardless of the big mistakes made computing L_{sh}, L_{er}, and L_{m}. Of course, the most recommendable procedure consists of computing η with both methods in order to compare the resulting values (this is done in the case of big units). In addition, note that if saturated steam is produced, given the difficulty in reliable identification of the water vapor ratio, the indirect method is the only recommendable one.

Let us assume, for instance, the determination of efficiency with the direct method on a running boiler at 16 bar with feed water at 100 °C ($h = 419\,\text{kJ/kg}$). The enthalpy of saturated water is equal to 857 kJ/kg, the one of dry saturated steam is 2792 kJ/kg. We further assume a water vapor ratio of 96% which equals an enthalpy of the steam of 2715 kJ/kg.

$(2715 - 419) = 2296\,\text{kJ}$ is produced for every kilogram of steam. If the measured water vapor ratio is equal to 94 or 98%, respectively, the enthalpy of the steam is equal to 2676 or 2753 kJ/kg and the production of heat per kilogram of steam is equal to 2257 or 2334 kJ, respectively, instead of 2296 kJ. Therefore, a mistake in the water vapor ratio of the steam of only $\pm 2\%$ leads an error in the estimate of efficiency of $\pm 1.7\%$.

This page intentionally left blank

Chapter 10
Fluid Dynamics

10.1 Distributed Pressure Drops in Tubes and in Ducts

Pressure drops in tubes and ducts can be divided into distributed and concentrated drops. The former originate from the friction between fluid and wall. As we shall see, besides the fluid velocity, they are influenced by the viscosity, the diameter of the tube (or the actual or hydraulic diameter of the duct), and by the roughness of the wall. The latter originate from changes of the sections or direction along the path of the fluid. This means that they are located at inlet and outlet of a tube, in curves, elbows, valves, and so on. They are practically not influenced by the viscosity of the fluid and the roughness of the wall, yet they are by the velocity and by the geometric characteristics of the element disturbing the flow. Concentrated drops will be discussed in Sect. 10.2.

The pressure drop Δp along a straight pipe is computed through the following equation:

$$\Delta p = \lambda \frac{l}{d_\mathrm{i}} \rho \frac{V^2}{2}; \tag{10.1}$$

l stands for the length of the tube, d_i for the inside diameter, ρ for the density of the fluid, V for its velocity, and λ for a factor that will be specified later on. If l and d_i are in m, ρ in kg/m^3, and V in m/s, the pressure drop Δp is in Pa. Generally, it is more convenient to refer to mass velocity G.

Recalling that

$$G = V\rho, \tag{10.2}$$

and (10.1) can be written as follows:

$$\Delta p = \lambda \frac{l}{d_\mathrm{i}} \frac{G^2}{2\rho} \tag{10.3}$$

with G in kg/m^{2}s. As far as air and flue gas, it is very convenient to refer to density under normal conditions as ρ_0.

D. Annaratone, *Steam Generators*, DOI: 10.1007/978-3-540-77715-1_10,

© Springer-Verlag Berlin Heidelberg 2008

Note that

$$\rho = \rho_0 \frac{269.5p}{T} \tag{10.4}$$

where p stands for pressure in bar and T for the absolute temperature in K.

From (10.3) based on (10.4) we obtain

$$\Delta p = 1.855\lambda \frac{l}{d_\mathrm{i}} \frac{G^2}{p\rho_0} \frac{T}{1000}. \tag{10.5}$$

In steam generators pressure p differs only slightly from atmospheric pressure. In fact, note that a relative pressure in the air or gas circuit of 6000 Pa corresponds to 0.06 bar, and absolute pressure is equal to 1.073 bar. In addition, note that the considered value is very high and can only refer to the air duct between the pusher fan and the burners of a high power pressurized generator. Generally, values are much lower. For instance, in the tubes of a smoke-tube boiler the pressure is equal to ≈ 1000 Pa at the most.

This explains why these modest relative pressures are frequently ignored in the computation of pressure drops. By the way, by ignoring them the value of Δp will turn out higher, thus more prudent, than the actual one. From this perspective, the only exception is represented by the ducts in depression (duct of the flue gas from the generator to the suction fan of a generator with a balanced draught). With all due reservations about ducts in depression (less frequent, in any case, given widespread pressurization), pressure p can be assimilated to atmospheric pressure assuming that $p = 1.013$ bar.

Therefore, (10.5) changes into

$$\Delta p = 1.83\lambda \frac{l}{d_\mathrm{i}} \frac{G^2}{\rho_0} \frac{T}{1000}. \tag{10.6}$$

If the calculation of Δp involves a duct with a noncircular cross-sectional area, it is required to introduce the hydraulic diameter.

By indicating the cross-sectional area of the duct with A and the wet perimeter with P (in this case it coincides with the geometric perimeter of the cross-sectional area), the hydraulic diameter is given by

$$d_\mathrm{i} = \frac{4A}{P}. \tag{10.7}$$

Thus, by indicating the sides of the rectangular cross-section with a and b, we have

$$d_\mathrm{i} = \frac{2ab}{a+b}. \tag{10.8}$$

Factor λ, called friction factor, has been the object of numerous research projects. In this book we will limit our analysis to the most significant and well-known equations.

The following is the famous equation by Blasius:

$$\lambda = 0.316\mathrm{Re}^{-0.25} \tag{10.9}$$

where Re is the Reynolds number; it is valid for $\mathrm{Re} \leq 10^5$.

The following equation by Nikuradse considers the range of the high Reynolds numbers instead:

$$\lambda = 0.032 + 0.221\mathrm{Re}^{-0.237}. \tag{10.10}$$

It is valid for $\mathrm{Re} = 10^6$–10^8.

Based on these very simple equations, it is evident that λ depends only on the Reynolds number. Further equations included later on are more complete and closer to reality because they factor in the relative roughness of the walls, as well. Relative roughness stands for the ratio between the expected higher roughness of the surface in contact with the fluid and the actual or the hydraulic diameter. By indicating it with ε Fig. 10.1 makes it possible to compute it as a function of the diameter and of the type of surface.

Karmann and Nikuradse distinguish between two boundary conditions of the flow in the pipe. The first refers to turbulent flow in a practically smooth pipe. This condition occurs when

$$\mathrm{Re}\varepsilon \leq 70 - 150. \tag{10.11}$$

In that case they suggest the following equation:

$$\frac{1}{\lambda} = 2\log_{\mathrm{e}}\left(\mathrm{Re}\sqrt{\lambda}\right) - 0.8 \tag{10.12}$$

where λ is, of course, independent from ε.

The second boundary condition occurs with a perfectly rough pipe. This means that

$$\mathrm{Re}\varepsilon \geq 1000 - 2500. \tag{10.13}$$

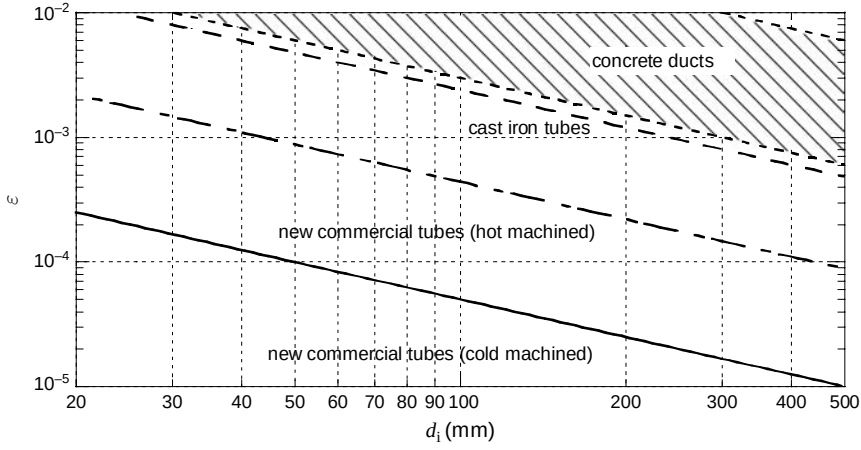


Fig. 10.1 Relative roughness ε

In that case

$$\frac{1}{\sqrt{\lambda}} = 2\log_e \frac{1}{2\varepsilon} + 1.735. \tag{10.14}$$

For values of the product Reε within 70–150 and 1000–2500, λ follows not a very well-defined rule. Karmann and Nikuradse suggested curves that are tangential to the only curve relative to the smooth pipe and to the various curves (as a function of ε) relative to the rough pipe.

Putting the equations suggested by Karmann and Nikuradse on a diagram, and following the criteria above as far as the conditions for smooth or rough pipes, we obtain a well-known diagram in the literature that we chose not to introduce in favor of Moody's diagram which is equally famous. Moody's diagram is shown in Fig. 10.2. In the case of turbulent flow (this is the only case of interest to us), the values of λ obtained from Moody's diagram can also be computed through the following equation authored by Colebrook:

$$\frac{1}{\sqrt{\lambda}} = -2\log_e \left(\frac{\varepsilon}{3.7} + \frac{2.51}{\mathrm{Re}\sqrt{\lambda}} \right). \tag{10.15}$$

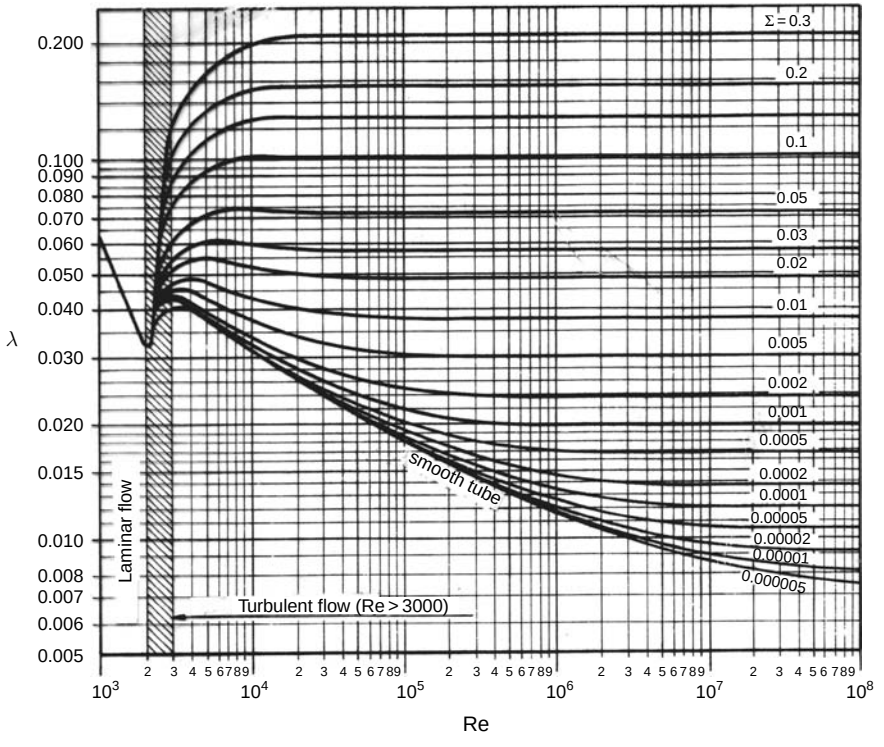


Fig. 10.2 Moody's diagram for the friction factor

The calculation of λ through (10.15) is not very straightforward because it must be done by trial and error. Still, a certain process quickly leads to a practically exact value of λ.

Note that (10.15) can be written as follows:

$$\lambda = \frac{1}{4\log_e^2\left(\frac{\varepsilon}{3.7} + \frac{2.51}{\mathrm{Re}\sqrt{\lambda}}\right)}. \tag{10.16}$$

For $\mathrm{Re} = \infty$ from 10.16, and by indicating the value of corresponding λ with λ_0, we have

$$\lambda_0 = \frac{1}{4\left(\log_e \varepsilon - 0.568\right)^2}. \tag{10.17}$$

We write (10.16) as follows:

$$\lambda_i = \frac{1}{4\log_e^2\left(\frac{\varepsilon}{3.7} + \frac{2.51}{\mathrm{Re}\sqrt{\lambda_{(i-1)}}}\right)}. \tag{10.18}$$

This is the computation process. Given that $i = 1,\ 2, \ldots$, the values of λ_i are computed as a function of ε, Re, and λ_{i-1} until the value of λ_i practically coincides with the value of λ_{i-1} [λ_0 is obtained through (10.17)]. Convergence is quick. Further considerations can be made.

The analysis of Fig. 10.2 shows that the value of λ is influenced by the value of the Reynolds number until the latter is smaller than a certain value that depends on the value of ε.

Basically, Re does not seem to influence the value of λ when

$$\mathrm{Re}\varepsilon \geq 1000. \tag{10.19}$$

In that case the value of λ_0 computed through (10.17) diagrammed in Fig. 10.3 can be taken as the value of λ.

Equation (10.17) or the diagram can be used if (10.19) is true, or committing a mistake by defect of 3–4% at the most, if

$$\mathrm{Re}\varepsilon \geq 300. \tag{10.20}$$

Among other things, note the observations made about the equations by Karmann and Nikuradse for values ranging from 150 to 1000. According to them, the values of λ are considerably lower than those obtained from Moody's diagram in this field. In our opinion, the condition expressed in (10.20) is definitely acceptable, given the uncertainty of the values of λ for $\mathrm{Re}\varepsilon < 1000$.

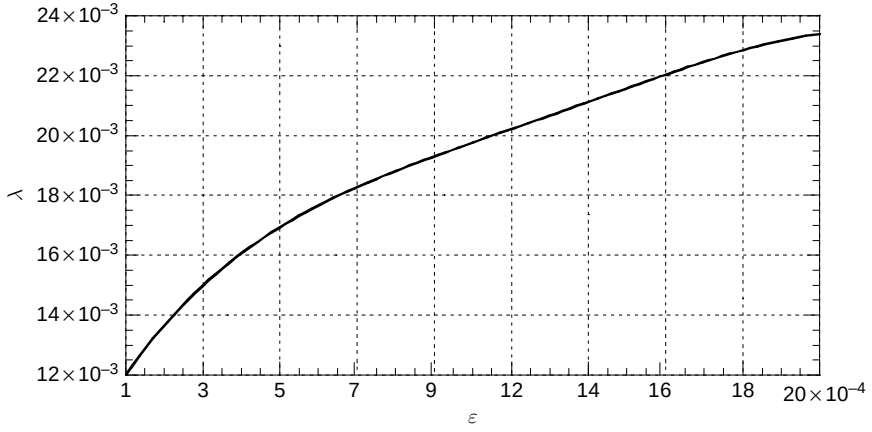


Fig. 10.3 Factor λ for a perfectly rough tube

Interestingly, for commercial warm machined steel pipes it is possible to write that

$$\varepsilon = \frac{4.4 \times 10^{-5}}{d_{\mathrm{i}}} \tag{10.21}$$

with d_{i} expressed in m.

Then, from (10.20) and recalling the significance of Re, we obtain

$$G \geq 6.8\mu \times 10^{6} \tag{10.22}$$

where G is in kg/m^{2}s, whereas the dynamic viscosity μ is expressed in kg/ms.

Figure 10.4 is obtained based on the dynamic viscosity of the water. If the mass velocity of water is equal or greater than the values obtainable from this diagram as a function of temperature, it is possible to use (10.17) or the diagram in Fig. 10.3 to compute λ. Moreover, based on the values of μ, the condition expressed in (10.22) is not verified as far as the practical values of the mass velocity of air and flue gas. Note, though, that often the values of G and μ are such that the tube can be considered to be basically smooth.

If the tube is smooth, (10.15) is reduced to the following:

$$\frac{1}{\sqrt{\lambda}} = -2\log_{\mathrm{e}} \frac{2.51}{\mathrm{Re}\sqrt{\lambda}}. \tag{10.23}$$

The diagram in Fig. 10.5 was built based on (10.23).

The tube can be assumed to be practically smooth, and factor λ can be obtained through the diagram mentioned earlier with a mistake by defect equal to 3–4% at the most if

$$\mathrm{Re}\,\varepsilon \leq 10. \tag{10.24}$$

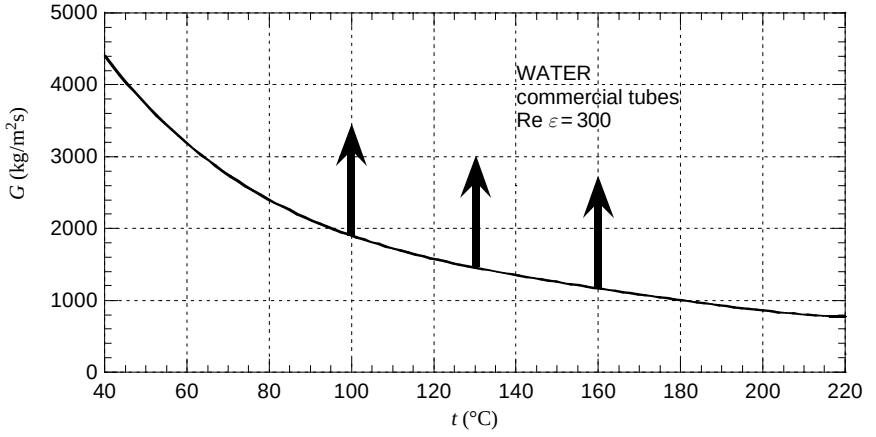


Fig. 10.4

In the case of commercial warm machined tubes, (10.24) satisfies the following condition:

$$G \leq 0.23\mu \times 10^6. \tag{10.25}$$

Figure 10.6 was built based on (10.25) and (7.91) relative to dynamic viscosity of flue gas. Figure 10.7 was built based on (10.25) and (7.78) relative to the dynamic viscosity of air. Therefore, if the mass velocity of flue gas in the tubes of the smoke-tube boiler or the air heater is smaller than the one obtainable from Fig.10.6, the value of λ can be computed through Fig. 10.5. The same is true for air flowing in the tubes of an air heater with reference to Fig. 10.7.

In terms of water and superheated steam, it is possible to refer to Mollier's tables. Nonetheless, we thought it worthwhile to show the density of water in Fig. 10.8. As

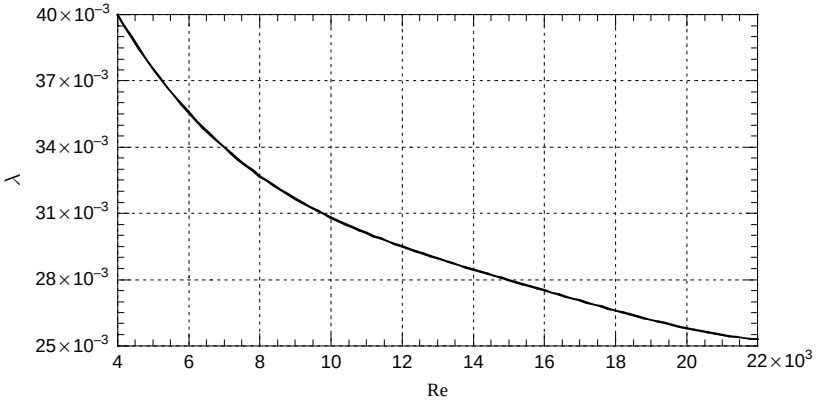


Fig. 10.5 Factor λ for a practically smooth tube

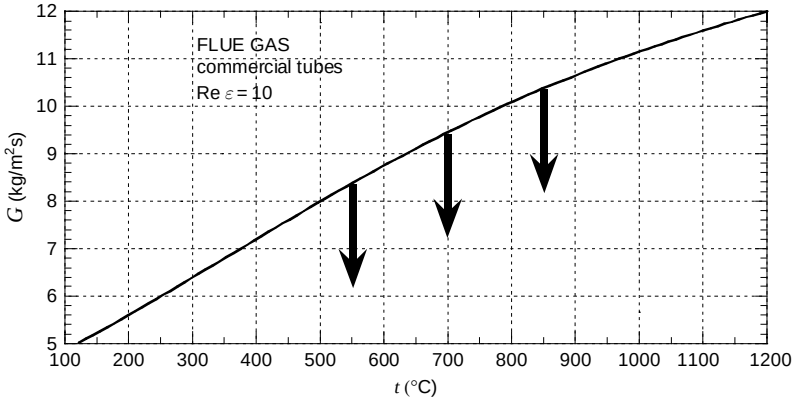


Fig. 10.6

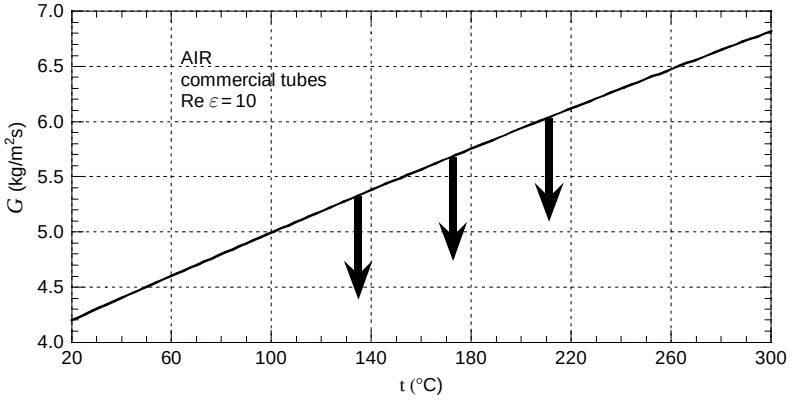


Fig. 10.7

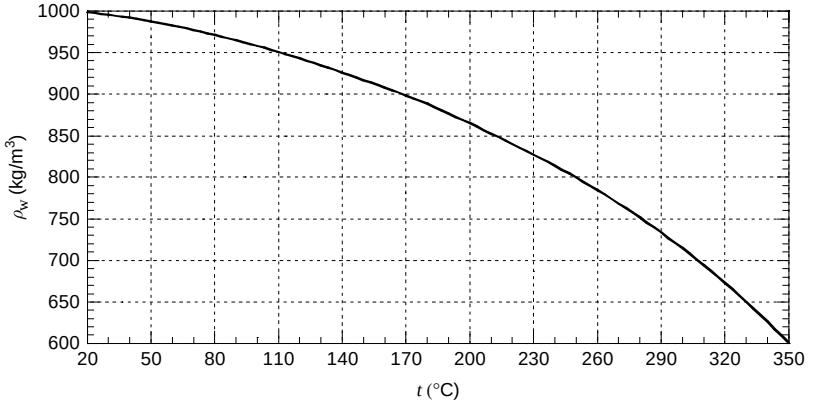


Fig. 10.8 Water density

far as flue gas and air, we already pointed out the opportunity to refer to density under normal conditions using (10.5) or (10.6) to compute Δp. The density ρ_0 of air is equal to $1.293\,\mathrm{kg/Nm^3}$. The density ρ_0 of flue gas is computed either through (7.75), or taken from Table 7.2 with sufficient approximation when the fuel is not only a mix of hydrocarbons. The value of the pressure drop Δp depends on the value of the reference temperature. In fact, the value of ρ included in (10.3) depends on this temperature. In both (10.5) and (10.6) temperature is included in an explicit way.

As far as water (economizer) or superheated steam (superheater or reheater), the average between the inlet and the outlet temperatures of the fluid from the tube bank in question can be assumed to be the reference temperature. One can proceed the same way as far as flue gas and air in air heaters. Section 10.6 illustrates the specific computation process to follow as far as steam in steam-generating tubes (mix of water and steam).

As far as flue gas flowing in the tubes of a smoke-tube boiler, it is necessary to consider the following. Because the fluid receiving the heat is at constant temperature (evaporating water), with reference to Sect. 8.12 $t_2' = t_1''$ and the factor β is zero. Thus, based on (8.34) and (8.32)

$$t_2' = t_1'' + \mathrm{e}^{-\gamma}\left(t_1' - t_1''\right) \tag{10.26}$$

where t_1' and t_2' are the inlet and outlet temperatures of the heating fluid (flue gas) and t_1'' is the inlet temperature of the heated fluid. Moreover,

$$\gamma = \frac{US_0}{M'c_p'} \tag{10.27}$$

where U stands for the overall heat transfer coefficient, M' for the mass flow rate of flue gas and c_p' for the mean specific isobaric heat, and indicating the surface of the considered passage with S_0.

Note that the presentation in Sect. 8.12 is based on U and c_p' being constant, and more specifically on the adoption of constant values for the entire temperature interval equal to the mean values. We stick to this position for now even as far as the following considerations.

Factor γ is proportional to the surface of the tubes. We may write that

$$\gamma = KS_0 \tag{10.28}$$

where K is a constant equal to $U/M'c_p'$.

Equation (10.26) can therefore be written as follows:

$$t_2' = t_1'' + \mathrm{e}^{-KS_0}\left(t_1' - t_1''\right). \tag{10.29}$$

Now, if we consider any portion of the total surface and indicate it with S, the generic temperature reached by the gas after coming in contact with surface S is given by

$$t' = t_1'' + \mathrm{e}^{-KS}\left(t_1' - t_1''\right). \tag{10.30}$$

Referring with more clarity to a numerical example with $t_1'' = 200\,^\circ\mathrm{C}$, $t_1' = 1000\,^\circ\mathrm{C}$ and $t_2' = 400\,^\circ\mathrm{C}$, the pattern of the gas temperature as a function of the surface it got in contact with is represented by curve 1 in Fig. 10.9. The temperature clearly decreases with a smaller and smaller gradient along the path of the gas.

Let us examine (10.6). Given that the mass velocity is constant and that the variations in temperature have negligible influence on factor λ, we determine that the pressure drop is proportional only to the absolute temperature of the gas. Considering the pattern of the temperature of the latter, as shown in Fig. 10.9, one makes a rather big mistake by referring to the average between the inlet and the outlet temperatures of the passage. In fact, as far as Δp, this equals substitution of curve 1 with the dashed line.

Thus, it is necessary to refer to the correctly calculated mean value of the absolute temperature. To that extent note that based on (10.30) the mean value of t' is given by:

$$t_\mathrm{m}' = \frac{1}{S_0}\int_0^{S_0}\left[t_1'' + \mathrm{e}^{-KS}\left(t_1' - t_1''\right)\right]\mathrm{d}S. \tag{10.31}$$

Then, resolving the integral

$$t_\mathrm{m}' = t_1'' - \frac{t_1' - t_1''}{KS_0}\left(\mathrm{e}^{-KS_0} - 1\right). \tag{10.32}$$

Based on (10.29)

$$\mathrm{e}^{-KS_0} = \frac{t_2' - t_1''}{t_1' - t_1''}; \tag{10.33}$$

$$KS_0 = \log_\mathrm{e}\frac{t_1' - t_1''}{t_2' - t_1''}. \tag{10.34}$$

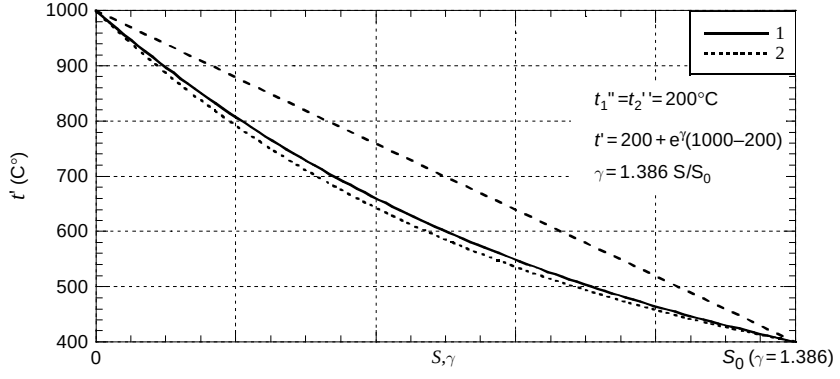


Fig. 10.9 Flue gas temperature inside smoke tubes or through a steam generating tube bank

Based on (10.32) we obtain

$$t'_{\mathrm{m}} = t''_1 - \frac{t'_1 - t''_1}{\log_{\mathrm{e}} \dfrac{t'_1 - t''_1}{t'_2 - t''_1}} \left(\frac{t'_2 - t''_1}{t'_1 - t''_1} - 1 \right); \tag{10.35}$$

and after a series of steps

$$t'_{\mathrm{m}} = t''_1 + \frac{t'_1 - t'_2}{\log_{\mathrm{e}} \dfrac{t'_1 - t''_1}{t'_2 - t''_1}}. \tag{10.36}$$

Equation (10.36) correctly computes the mean temperature of the gas, thus its mean absolute temperature to introduce in (10.5) or in (10.6) for the computation of Δp.

Note that (10.36) can also be written as follows:

$$t'_{\mathrm{m}} = t'_1 \left(\frac{t''_1}{t'_1} + \frac{1 - \dfrac{t'_2}{t'_1}}{\log_{\mathrm{e}} \dfrac{1 - \dfrac{t''_1}{t'_1}}{\dfrac{t'_2}{t'_1} - \dfrac{t''_1}{t'_1}}} \right); \tag{10.37}$$

finally,

$$t'_{\mathrm{m}} = \varphi t'_1 \tag{10.38}$$

where the dimensionless factor ϕ which corresponds to the expression in parenthesis in (10.37) can be directly taken from the diagram in Fig. 10.10 as a function of t'_2/t'_1 and t''_1/t'_1. The superior line represents the values of ϕ corresponding to the linear

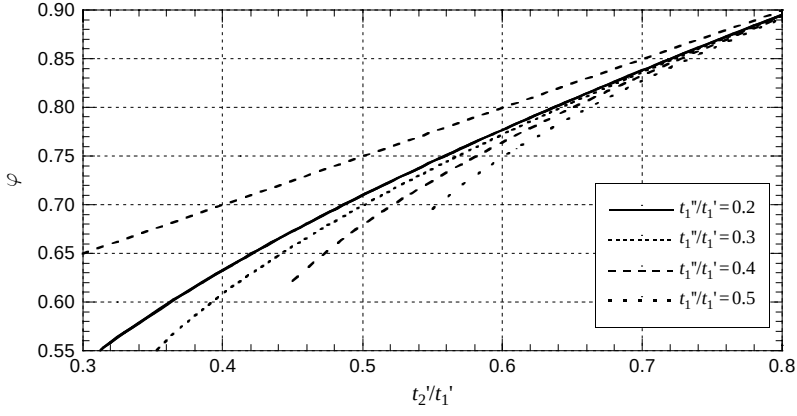


Fig. 10.10 Factor φ for the calculation of the mean flue gas temperature

pattern of the temperature (like the straight line in Fig. 10.9). This highlights the influence of the actual pattern of the temperature on the value of t'_{m}.

Of course, the mistake made by adopting the average between the extreme temperatures would be increasingly greater as the ratio between them were to farther away from one. One could argue that the computation process is invalidated by the variability of U and c'_p with the temperature. In fact, this does have a certain impact. With reference to our example, the curve that stands for the actual pattern of the temperature is represented by curve 2 in Fig. 10.9. These considerations can be applied to a steam-generating tube bank, too, as we shall be able to see in Sect. 10.3.

Thus, if it is not allowed to assimilate the theoretical curve to the dashed line in the diagram, one does not commit a sensible mistake by adopting the theoretical curve instead of the actual one. Moreover, note that the pressure drop computed this way is slightly greater than the actual one and consequently in favor of safety during runtime.

Thus, (10.38) provides good approximation to the reality of the phenomenon. Based on (10.1) and the considerations above, we determine the following. The friction factor λ depends on the type of tube or duct surface (absolute roughness). It is also a function of the diameter and, through Re, a function of the fluid velocity and its kinematic viscosity. The pressure drop per length unit of the tube is a function of the absolute roughness of the surface, of the inside diameter, of the velocity, of the dynamic viscosity, and of the density.

If R indicates absolute roughness, we have

$$\frac{\Delta p}{l} = f\left(R, V, d_{\mathrm{i}}, \mu, \rho\right). \tag{10.39}$$

On the other hand, for a given fluid μ and ρ are a function of temperature only. Thus, we can write that

$$\frac{\Delta p}{l} = f\left(R, V, d_{\mathrm{i}}, t\right). \tag{10.40}$$

We determine that once a type of surface (for instance, commercial tubes) and a reference temperature are set, the pressure drop by length unit of a given fluid is only a function of velocity and diameter.

This way it is possible to create diagrams to obtain $\Delta p/l$ directly.

The diagrams in Figs. 10.11 and 10.12 refer to commercial steel tubes and water flowing through them at 20 °C. The pressure drop referred to the length unit of the tube can be obtained based on two of the quantities Q, V, and d_i (the volumetric flow rate is expressed in m^3/h).

If the temperature is different from 20 °C, the actual pressure drop Δp can be obtained by first approximation from the following equation and by indicating the pressure drop gained from the diagrams with Δp^*, thus

$$\Delta p = \Delta p^* \left(1 - 1.04 \frac{\sqrt{t-20}}{100 V^{0.4}}\right) \frac{\rho}{1000}; \tag{10.41}$$

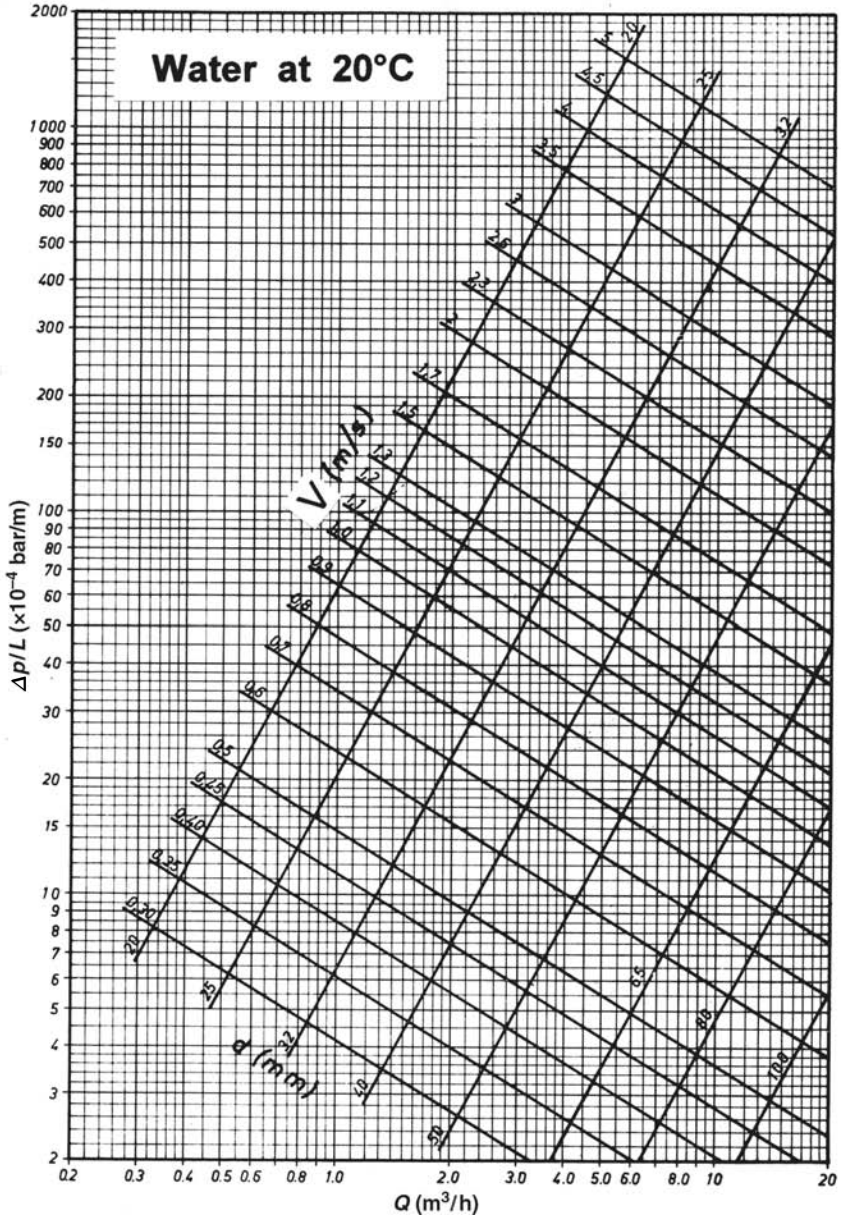


Fig. 10.11 Pressure drop for water at 20 °C ($Q = 0.2$–$20\,\mathrm{m^3/h}$)

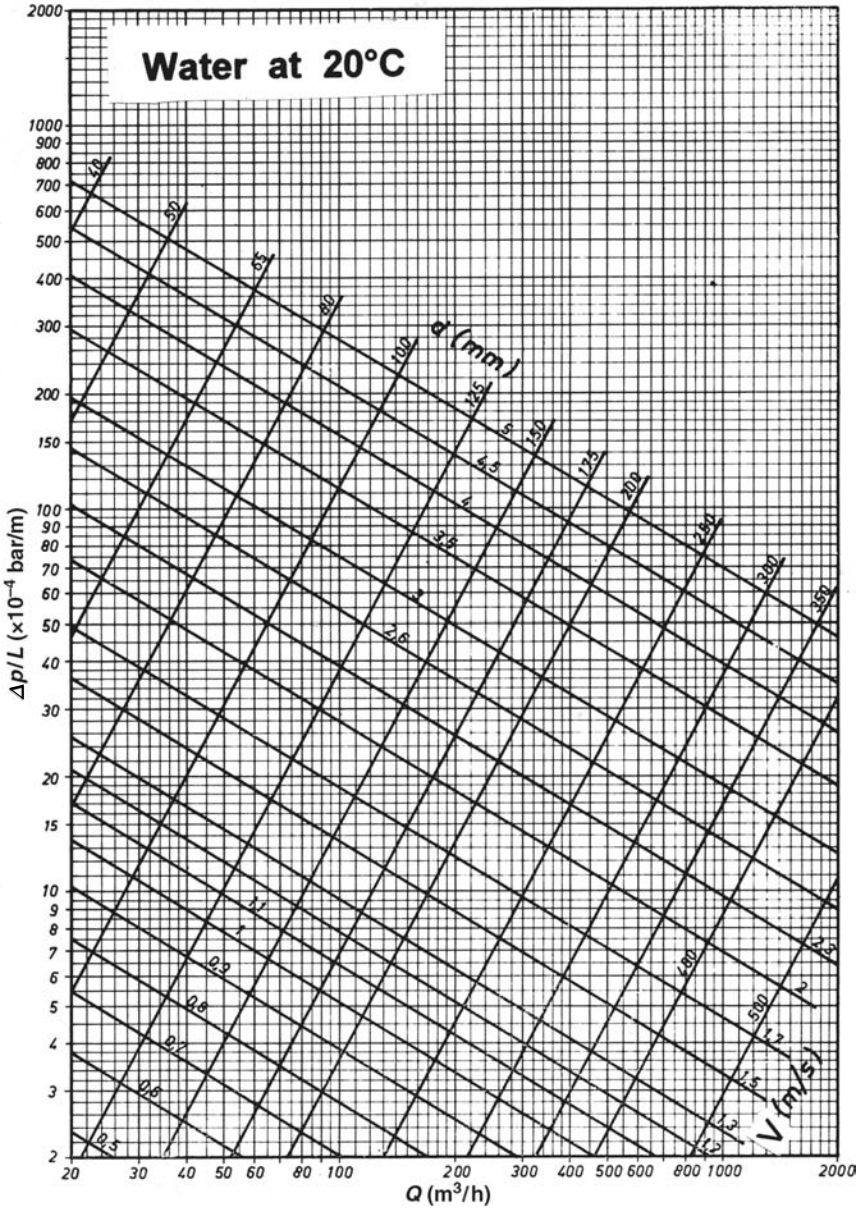


Fig. 10.12 Pressure drop for water at 20 °C ($Q = 20$–$2000\,\mathrm{m^3/h}$)

ρ stands for the water density in kg/m^3, V for the velocity in m/s, and t for the temperature in °C.

Fig. 10.13 as well as 10.14 show the diagrams relative to $\Delta p/l$ for commercial tubes or ducts in metal sheet with air under normal conditions.

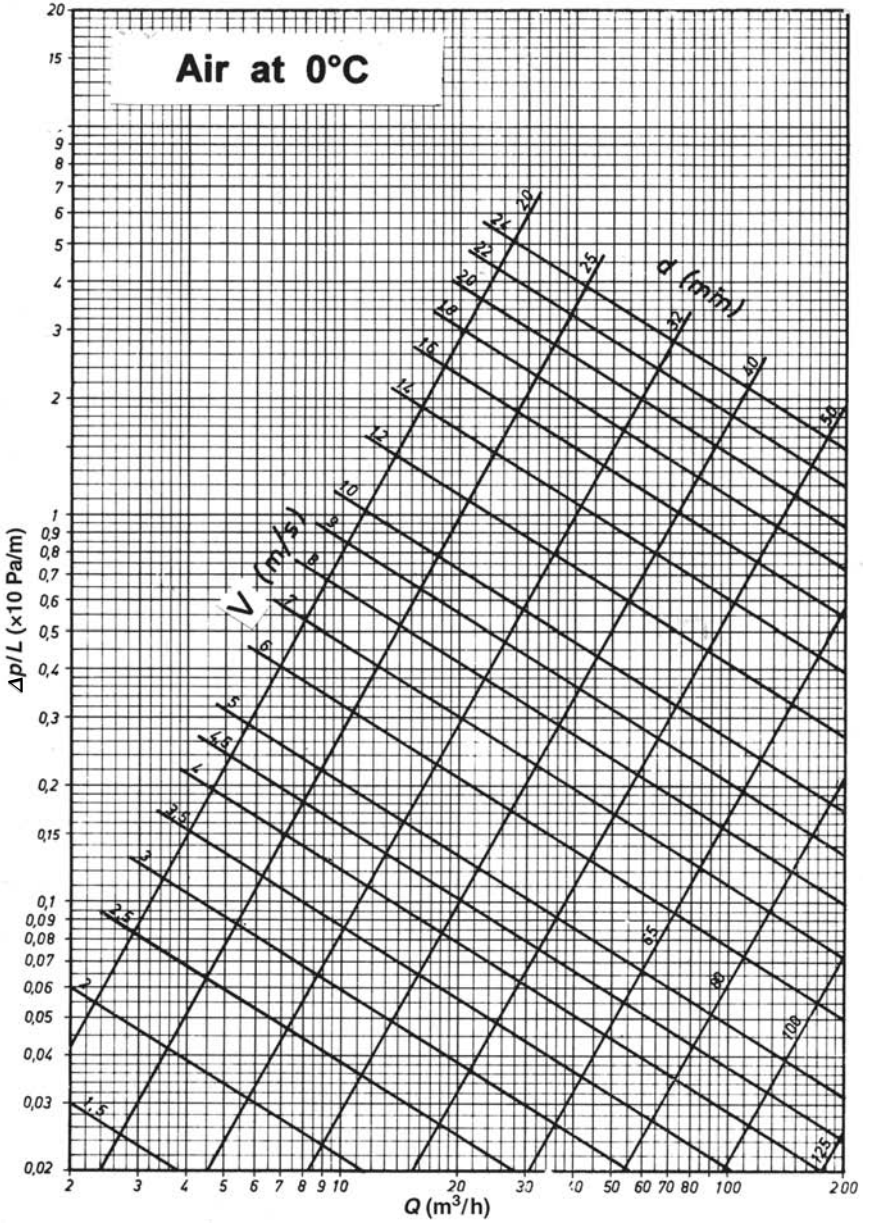


Fig. 10.13 Pressure drop for air at 0 °C ($Q = 2$–$200\,\mathrm{m}^3/\mathrm{h}$)

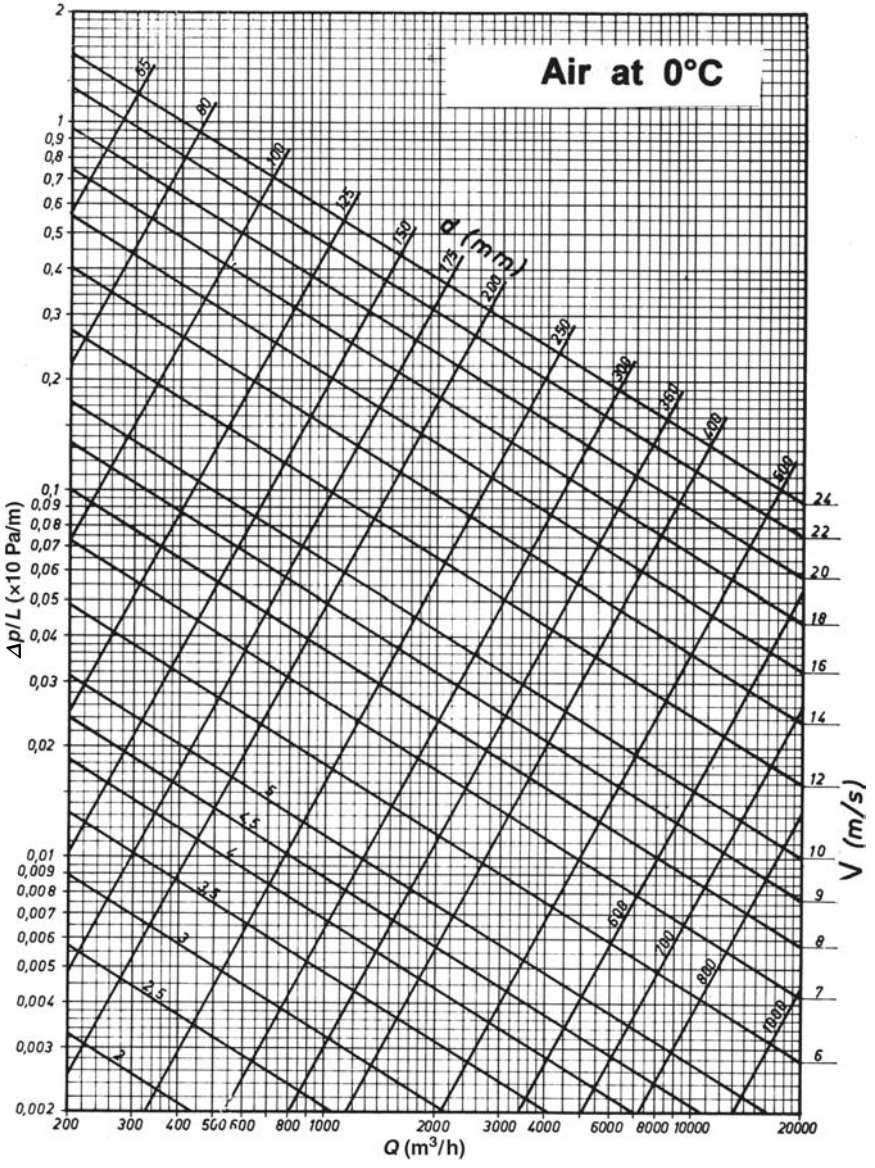


Fig. 10.14 Pressure drop for air at 0 °C ($Q = 200$–$20,000\,\mathrm{m^3/h}$)

If the temperature is different from 0 °C, the actual pressure drop Δp can be obtained by first approximation from the following equation and by indicating the pressure drop gained from the diagrams with Δp^*, thus

$$\Delta p = \Delta p * \left(1 + 2.55 \frac{\sqrt{t}}{100 V^{0.6}}\right) \frac{273}{273 + t} \tag{10.42}$$

where V stands for the velocity in m/s and t for the temperature in °C.

Note that the reference to a commercial tube indicates a new tube. If the tube shows increasing roughness during runtime caused by wear and tear, the pressure drop increases. The increase is small for low values of the Reynolds number (air and flue gas), but it can be considerable for high values of Re (superheated steam and water).

Finally, note that in the case of ducts without a round cross-section, the diagrams above must be used in reference to velocity and diameter, that is, the quantities that are crucial for the value of Δp (10.40). The value of the volumetric flow rate Q on the abscissa corresponds to the values of V and d_i only if the cross-section is round, but not if d_i is the hydraulic diameter.

10.2 Concentrated Pressure Drops

As already pointed out in the previous section, concentrated pressure drops are caused by inlets and outlets, curves, changes in the cross-sections, offtakes, and so on. They are computed as follows:

$$\Delta p = \zeta \frac{\rho V^2}{2} \tag{10.43}$$

where ζ is a factor that shall be explained later on. If ρ is in $\mathrm{kg/m^3}$ and V in m/s, the pressure drop Δp is in Pa.

Similarly to distributed pressure drops, if we refer to mass velocity G expressed in $\mathrm{kg/m^2 s}$, from (10.43) we have

$$\Delta p = \zeta \frac{G^2}{2\rho}. \tag{10.44}$$

By introducing density under normal conditions ρ_0 of both air and flue gas, from (10.44), and similarly to (10.5), we obtain

$$\Delta p = 1.855 \zeta \frac{G^2}{p\rho_0} \frac{T}{1000}. \tag{10.45}$$

By assimilating pressure p to atmospheric pressure (1.013 bar), from (10.45) we obtain the following equation:

$$\Delta p = 1.83 \zeta \frac{G^2}{\rho_0} \frac{T}{1000}. \tag{10.46}$$

Factor ζ in the previous equations can be considered to be practically independent from the Reynolds number when the latter is greater than 3000–4000, as is the case in the instances of interest to us.

For instance, Fig. 10.15 shows curves standing for ζ for the inlet and outlet of a tube from a tank for which we adopt $\zeta = 0.5$ and $\zeta = 1$, as we shall see later on.

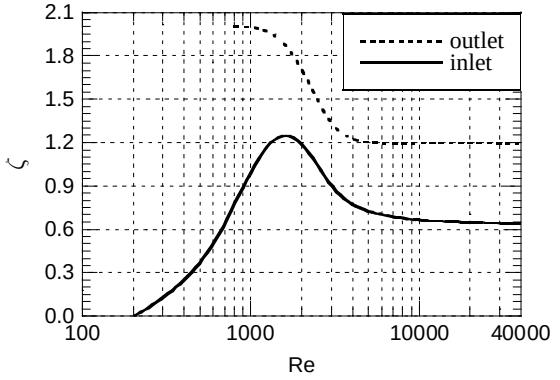


Fig. 10.15 Factor ζ for inlet and outlet in a tank

Inlet and outlet from a tank are, in fact, threshold instances of sudden sectional changes. Two cases stand out during the analysis of this issue in general terms. In the first case, the cross-section abruptly decreases along the pass of the fluid. The value of ζ is obtained from curve A of Fig. 10.16 as a function of ratio $d_\mathrm{i}/d_\mathrm{i}'$ between the diameter of the reduced cross-section and the diameter of the original cross-section. If the fluid enters the tube exiting from a tank, we may consider that $d_\mathrm{i}' = \infty$, thus $d_\mathrm{i}/d_\mathrm{i}' = 0$ which finally leads to $\zeta = 0.5$.

In the second instance the cross-section widens, the value of ζ is obtained from curve B of Fig. 10.16. If the fluid enters in a tank in a similar way, we can consider that $d_\mathrm{i}/d_\mathrm{i}' = 0$, thus $\zeta = 1$. In that case all the kinetic energy of the fluid is lost.

In both instances the velocity to consider in (10.43) is the one in the reduced cross-section. In general (here the equation can also be used with a duct with a non-circular cross-section), factor ζ for abrupt reduction of the cross section is given by

$$\zeta = 0.5\left(1 - \frac{A}{A'}\right) \tag{10.47}$$

where A stands for the smaller and A' for the greater cross-section.

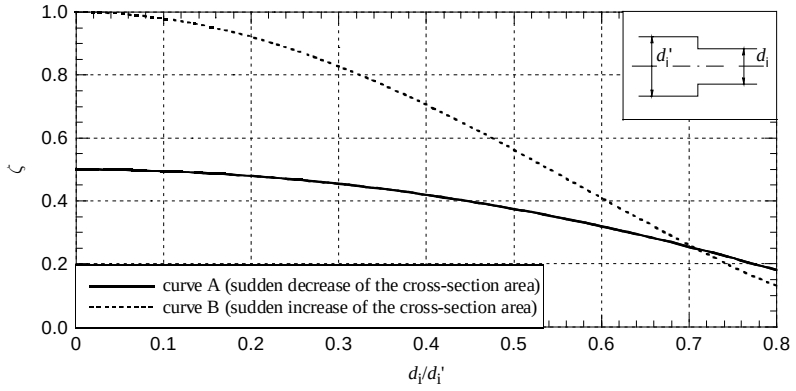
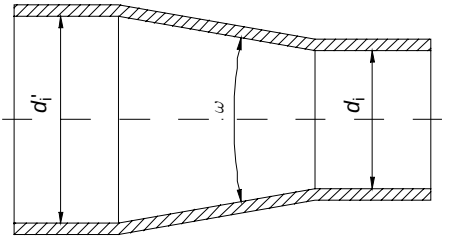


Fig. 10.16 Factor ζ for sudden variations of the cross-sectional area

Fig. 10.17



In the case of widening of the cross-section we have

$$\zeta = \left(1 - \frac{A}{A'}\right)^2, \tag{10.48}$$

including the same significance of symbols.

If the cross-section is gradually reduced with an angle ω smaller than 30° (Fig. 10.17) instead, it is possible to assume that $\zeta = 0.05$ regardless of the value of d_i/d'_i or A/A'. If the cross-section gradually widens, the values obtained from curve B in Fig. 10.16 or from (10.48) are multiplied by the corrective factor β, the values of which are shown in Table 10.1.

In the case of inlet from a tank, if the tube enters part of the tank itself (Fig. 10.18), we can assume that $\zeta = 0.8$.

As far as the pressure drop of inlet and outlet relative to tubes of smoke-tube boilers, given that flue gas has a certain kinetic energy at the tube inlet and that not all kinetic energy is lost at the outlet, it is possible to adopt the following values of ζ: for the inlet $\zeta = 0.35 - 0.4$ and for the outlet $\zeta = 0.65 - 0.7$.

Finally, it may be interesting to determine the pressure drop through a drilled diaphragm (Fig. 10.19) for the sizing of the throttling baffle plates. In that case

Table 10.1 Factor β for gradual increase of the cross-sectional area

ω	3°	5–8°	10°	14°	20°	30°	45°	60°	$\geq 90°$
β	0.18	0.14	0.16	0.25	0.45	0.70	0.95	1.10	1.00

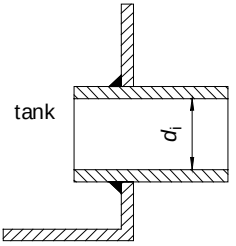
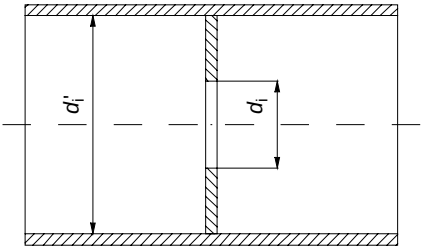


Fig. 10.18

Fig. 10.19



factor ζ is obtained with reference to curve B in Fig. 10.16 and by multiplying the value obtained this way by the corrective factor β given by

$$\beta = 2.8\left[1 - \left(\frac{d_i}{d_i'}\right)^2\right]. \tag{10.49}$$

More in general, the value of ζ computed based on (10.48) is multiplied by the corrective factor β given by

$$\beta = 2.8\left(1 - \frac{A}{A'}\right). \tag{10.50}$$

The velocity to consider in (10.43) or in the equations obtained from it is always the one referring to the reduced cross-sectional area.

Besides the bending angle, factor ζ relative to pressure drops in the curves is also a function of the ratio between the bending radius referred to the axis of the tube and its inside diameter. The diagram in Fig. 10.20 leads to its value for 45°, 90°, 135°, and 180° curves. The interpolation is done for intermediate angles. In the case of ducts it is worthwhile knowing the values relative to elbows, too (Fig. 10.21). In the absence of baffles they are taken from Table 10.2.

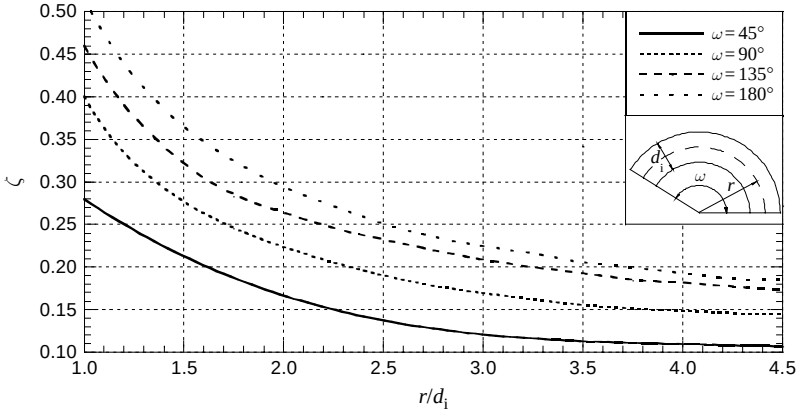


Fig. 10.20 Factor ζ for curves

Fig. 10.21

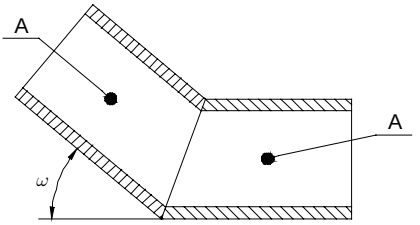


Table 10.2 Factor ζ for elbows without baffles

ω	15°	30°	45°	60°	90°
ζ	0.02	0.07	0.18	0.36	1.00

If the elbows are equipped with baffles instead, it is possible to refer to Table 10.2 by multiplying the values by 0.4.

As far as the T and Y-shaped offtakes, the values of ζ are not available for all the numerous potential instances, both in terms of the different values of volumetric flow rates in both branches of the offtake and in terms of the different diameters of the concurrent tubes. The diagram in Fig. 10.22 makes it possible to obtain ζ for T-shaped offtakes with concurrent tubes of equal diameter as a function of the ratio between the flow rates and two possible flux directions.

The diagram in Fig. 10.23, instead, makes it possible to obtain ζ for Y-shaped offtakes with concurrent tubes of equal diameter as a function of angle ω between the two spread out branches under the assumption that the flow rate in both branches is the same and for the two possible flux directions.

The velocity to consider in (10.43) and the like is the one corresponding to volumetric flow rate Q.

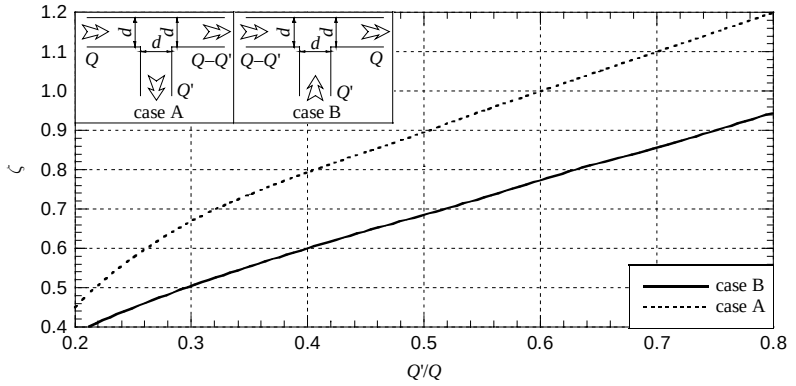


Fig. 10.22 Factor ζ for T pieces

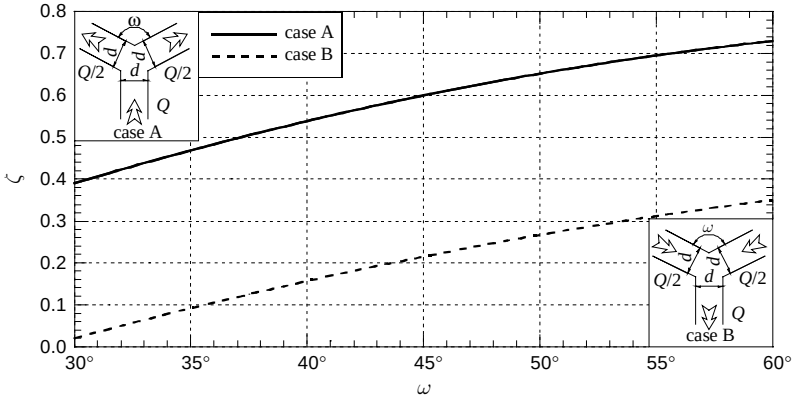


Fig. 10.23 Factor ζ for Y pieces

Other authors suggest the following values for T-shaped offtakes with equal diameters and distinguishing the two values of ζ relative to continuous piping and the one at 90° that we indicate with ζ and ζ', respectively. In case B of Fig. 10.22

$$\begin{array}{lll} \text{for } Q' = 0 & \zeta = 0.04 & \zeta' = 0 \\ \text{for } Q' = 0.5Q & \zeta = 0.40 & \zeta' = 0.30 \\ \text{for } Q' = Q & \zeta = 0 & \zeta' = 0.90 \end{array}$$

In case A of Fig. 10.22

$$\begin{array}{lll} \text{for } Q' = 0 & \zeta = 0.04 & \zeta' = 0 \\ \text{for } Q' = 0.5Q & \zeta = 0.01 & \zeta' = 0.90 \\ \text{for } Q' = Q & \zeta = 0 & \zeta' = 1.30 \end{array}$$

The values of both ζ and ζ' refer to the velocity corresponding to Q. As far as the valves, there are many more kinds. Definitely reliable data can only be obtained by consulting with the producing company. The same is true for gate valves. Finally, flow rate meters, slide regulation valves, and expansion compensators are inserted in the ducts. It is impossible to provide general information on the relative pressure drops. If the flow rate meter is a Venturi-type meter, computation is still possible by examining its shape and by applying the described values of ζ, even though in this case it is still recommended to turn to the specialist company for available experimental data on their instruments. As far as slide valves and compensators, there are experimental data, or in the lack thereof it is a question of reasonably increasing the total pressure drop in the duct.

In conclusion, note the widespread criterion to assimilate the generic concentrated drop to the one in a portion of straight tube of a certain length, called virtual

length or equivalent length. A comparison between (10.43) and (10.1) shows the requirement for equal pressure drops to be

$$\lambda \frac{l_e}{d_i} = \zeta, \tag{10.51}$$

where l_e stands for the virtual length (equivalent length).

Then

$$l_e = \frac{\zeta}{\lambda} d_i. \tag{10.52}$$

The criterion above actually consists of computing a virtual length equal to a certain number of diameters for every concentrated drop. Given that N_e is this number, from (10.52) we obtain

$$l_e = N_e d_i; \tag{10.53}$$

then

$$N_e = \frac{\zeta}{\lambda}. \tag{10.54}$$

The criterion is interesting because it simplifies the computation of the pressure drop of a tube or a duct. In fact, once the values of N_e for the different "flux perturbations" are known, one calculates a fictitious length l' given by

$$l' = l + d_i \sum N_e \tag{10.55}$$

where l stands for the length of the tube with a constant diameter d_i.

Δp is computed based on l' through one the equations in Sect. 10.1 or deriving the value of $\Delta p/l'$ directly from the diagrams. This takes both distributed and concentrated pressure drops into account. Note that to safeguard the validity of the method (i.e., to simplify computation) requires a constant value for N_e which is typical of any type of perturbation. This is what is actually done. But based on (10.54) N_e is clearly a function of λ and ζ; thus, it is influenced by the Reynolds number, as well as the roughness. Calculation based on constant values of N_e is therefore acceptable only for an approximate evaluation of Δp, especially if the concentrated pressure drops have a considerable impact on the total.

On the other hand, if the values of N_e were to be correlated to the values of ζ, Re, and ε, one would be forced to create an enormous series of diagrams for all the types of perturbations and for the different values of the quantities in question (ratios between diameters, curvature radii, and so on). At this point, the usefulness of the method would be gone. In other words, this easy calculation criterion can be recommended only for gross evaluations of Δp. These reservations notwithstanding, it can be interesting to determine some criteria to obtain approximate yet constant values of N_e. For flue gas flowing in the tubes of smoke-tube boilers the values of Re usually range from 8000 to 25000. The relative roughness ranges from 5×10^{-4} to 10^{-3}. Based on Fig. 10.2, λ ranges from 0.026 to

0.034. By adopting an average value equal to 0.030, based on (10.54) we may write that

$$N_e = 33\zeta. \tag{10.56}$$

As far as the pressure drop at the inlet, considering the extreme case of an inlet from a tank, so that $\zeta = 0.5$, the virtual length corresponds to 16.5 diameters. For the outlet with $\zeta = 1$, we have $l_e = 33d_i$ instead. Actually, the pressure drops of inlet and outlet are smaller because there is a certain kinetic energy at the inlet, and at the outlet the kinetic energy of the flue gas exiting the tubes is not completely lost, as we already pointed out before.

As far as superheated steam, the conditions vary greatly depending on pressure and temperature. For pressure ranging from 15 to 100 bar and temperatures up to 500 °C, the variability range of Re from 150,000 to 1,000,000 may be considered for the tubes of superheaters; the relative roughness may be assumed to be equal to $1–2 \times 10^{-3}$; Figure 10.2 shows that λ varies from 0.020 to 0.024. Assuming an average value equal to 0.022 we have

$$N_e = 45\zeta. \tag{10.57}$$

As far as water, and only in reference to the tubes of the economizer, the value of Re can be considered to lie between 70,000 and 1,000,000; the relative roughness can be assumed to be equal to $0.8–1.5 \times 10^{-3}$, and the same diagram leads to $\lambda = 0.0185–0.0245$. Assuming that $\lambda = 0.0215$, we have

$$N_e = 46\zeta \tag{10.58}$$

Clearly, the suggested values of N_e refer only to smoke tubes and coils of superheaters and economizers. Any extrapolation to tubes outside the generator or air and gas ducts (with much greater diameters and ensuing different values of Re and ε) is arbitrary.

10.3 Pressure Drop Through the Tube Banks

When it hits the tube banks (steam-generating bank, superheater, reheater, economizer with smooth tubes, and tube air heater with the gas on the outside), flue gas undergoes a pressure drop that can be computed through the following equation:

$$\Delta p = f_d f_a N \rho \frac{V^2}{2} \tag{10.59}$$

where f_d and f_a stand for two factors that will be discussed later on and N for a number of tube rows crossed by flue gas. With the density ρ in kg/m^3 and the velocity V in m/s, the pressure drop Δp is in Pa. Even in this case it is more convenient to refer to mass velocity G and to density ρ_0 under normal conditions.

Similarly to (10.5) and (10.45), we obtain the following:

$$\Delta p = 1.855 f_{\mathrm{d}} f_{\mathrm{a}} N \frac{G^2}{p\rho_0} \frac{T}{1000}; \tag{10.60}$$

G in $\mathrm{kg/m^2 s}$, p in bar and the absolute temperature T in K.

As usual, assimilating pressure p to atmospheric pressure we obtain the following through (10.60):

$$\Delta p = 1.83 f_{\mathrm{d}} f_{\mathrm{a}} N \frac{G^2}{\rho_0} \frac{T}{1000}. \tag{10.61}$$

It is equally possible to introduce velocity V_0 under normal conditions. In that case (10.59) leads to

$$\Delta p = 1.855 f_{\mathrm{d}} f_{\mathrm{a}} N \rho_0 \frac{V_0^2}{p} \frac{T}{1000}; \tag{10.62}$$

and assimilating pressure p to atmospheric pressure

$$\Delta p = 1.83 f_{\mathrm{d}} f_{\mathrm{a}} N \rho_0 V_0^2 \frac{T}{1000}. \tag{10.63}$$

The ability to refer to mass velocity or velocity under normal conditions is the very advantageous. Note that along the flue gas pass in the generator temperature is a constant variable which consequently varies the volumetric flow rate of the gas, whereas, of course, the mass flow rate and the volumetric flow rate under normal conditions remain constant. The simple separation of these two flow rates for the pass sections (cross-sectional areas) of the different banks makes it possible to obtain velocity G or velocity V_0 referred to normal conditions.

The different equations above are also valid for the air hitting the tube bank of the air heater. The density under normal conditions is included in (10.58), (10.61), (10.62), and (10.63). For air we have $\rho_0 = 1.293\,\mathrm{kg/Nm^3}$; for flue gas ρ_0 is computed through (7.75) or taken from Table 7.2. The considerations made in Sect. 10.1 in terms of the temperature to consider in (10.50) and (10.63) must be taken into account for steam generating tube banks, as well. In other words, one must consider the mean temperature in the bank instead of the mean temperature between inlet and outlet temperatures.

The latter can be adopted for flue gas flowing through the superheater, the economizer, and the air heater. The same is true for air hitting the tube bank of the air heater.

Factor f_{d} intervenes only if the number of crossed rows is below10. In fact, for $N \geq 10$ we have $f_{\mathrm{d}} = 1$; for $N < 10$ the values of f_{d} can be obtained through Fig. 10.24. The arrangement factor f_{a} is a function of the Reynolds number, of the outside diameter, of the transversal and longitudinal pitch of the tubes, and finally of the type of arrangement.

Let us consider Fig. 10.25 showing an arrangement with inline tubes where the transversal pitch is indicated by s_{t} and the longitudinal one by s_{l}. Figure 10.26 helps to obtain f_{a} for different values of the ratios $s_{\mathrm{t}}/d_{\mathrm{o}}$ and $s_{\mathrm{l}}/d_{\mathrm{o}}$ as a function

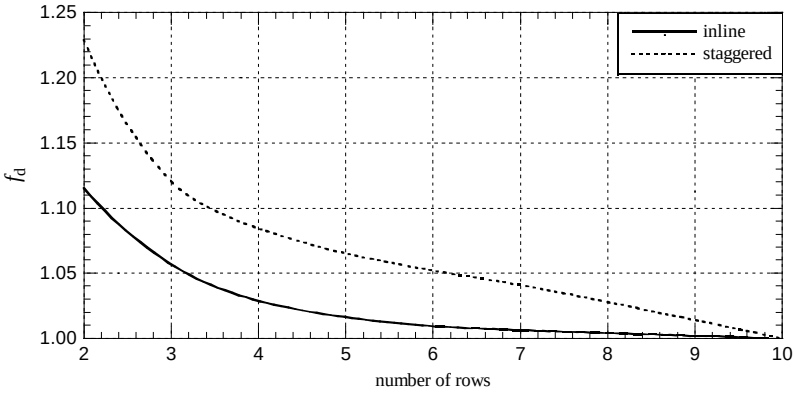
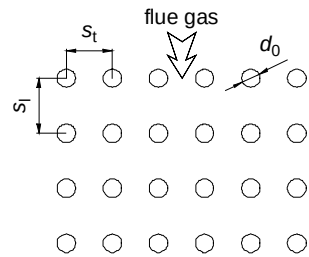


Fig. 10.24 Factor f_d for the pressure drop trough a tube bank

Fig. 10.25 Arrangement with inline tubes



of Re. Figure 10.27 shows a layout with staggered tubes instead, and the diagram in Fig. 10.28 helps to determine the arrangement factor.

Note that except for special situations, s_l/d_o, s_t/d_o, and Re being equal, the values of f_a in staggered arrangements are always higher than those relative to inline tubes. On the other hand, as we know, the staggered arrangement implies higher overall heat transfer coefficients.

The criteria for adopting one over the other arrangement was already discussed in Sect. 8.13 by highlighting the parameters to consider in order to evaluate the problem correctly and to simultaneously take both heat transfer and pressure drops into account. Certain constructive and running requirements notwithstanding, it is a question of adopting the optimal solution for a specific project. In the flue gas passage in a boiler, there are always sudden changes of direction and sometimes even throttling that cause localized pressure drops. Sect. 10.2 provides assistance in defining these drops according to cautionary criteria and by analogy. More specific information cannot be provided, but generally these pressure drops are relatively modest when compared with those deriving from the tube bank. Therefore, it may be enough to conventionally increase the latter by 5–10% in order to forecast the total pressure drop.

In conclusion, even though it is not recommended as far as heat transfer, sometimes the gas flow is parallel to the axis of the tubes and not transversal, as we

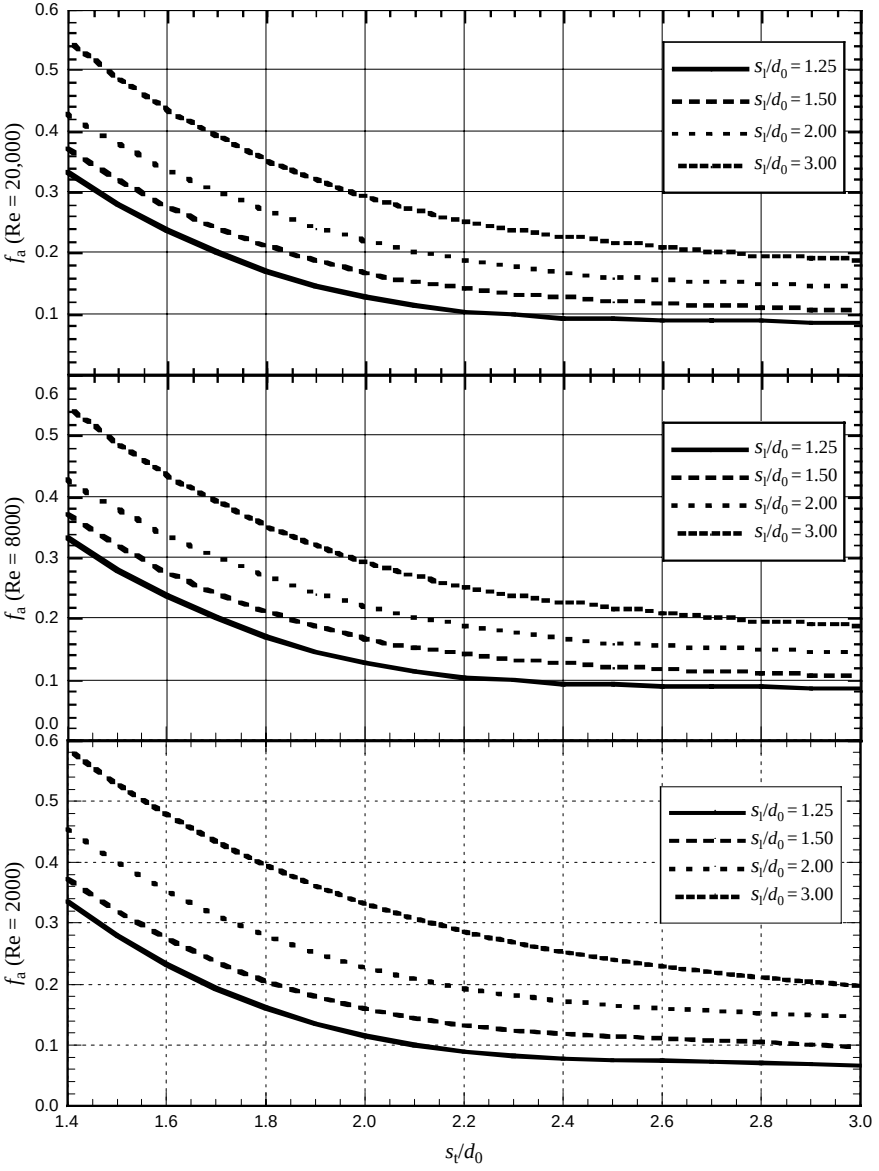


Fig. 10.26 Arrangement factor f_a for inline tubes

assumed so far. In this case we consider the cross-sectional areas shown by the dashed lines in Fig. 10.29 (with staggered arrangement an inline tubes) and the relative wet perimeter (bold line in the figure) and compute the hydraulic diameter through 10.7. The pressure drop is computed based on Sect. 10.1.

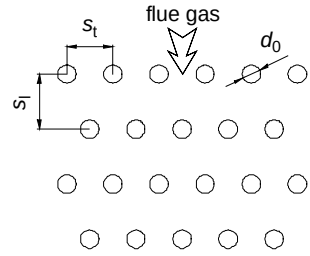


Fig. 10.27 Arrangement with staggered tubes

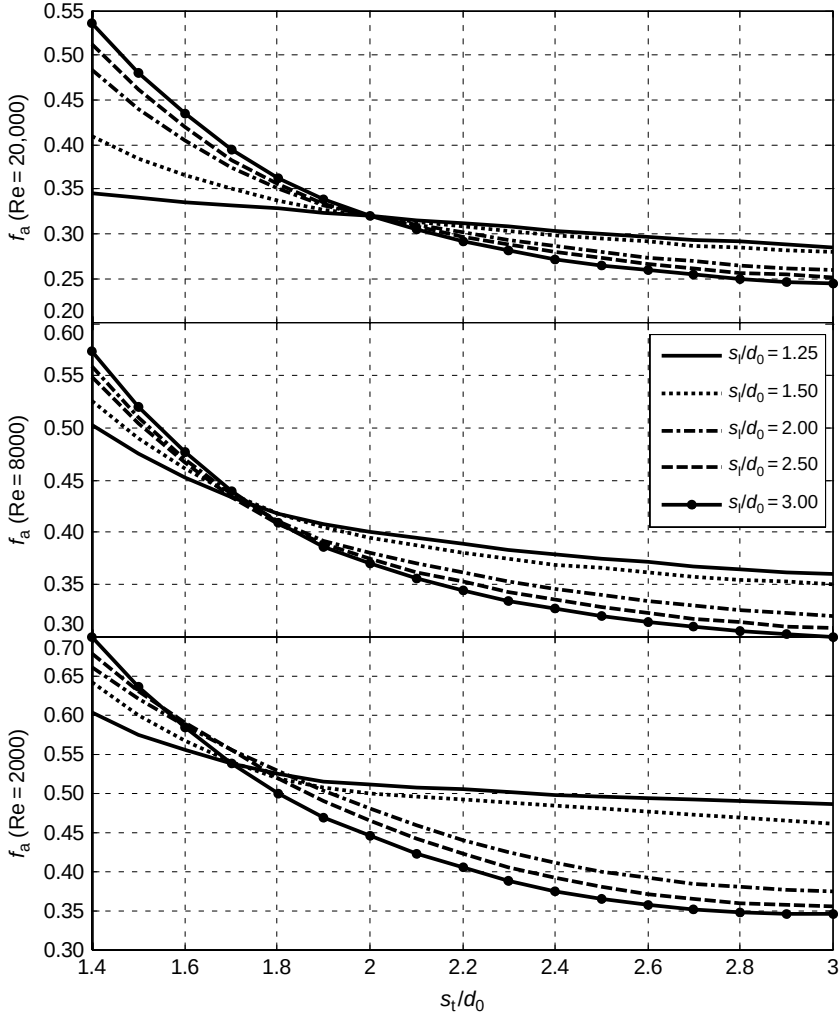
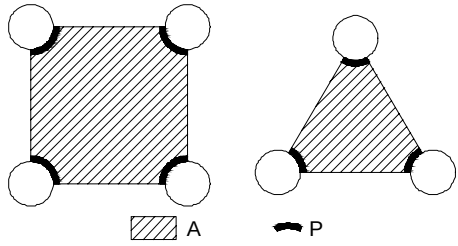


Fig. 10.28 Arrangement factor f_a for staggered tubes

Fig. 10.29



10.4 Pressure Drop in Special Equipments

We saw how to calculate pressure drops in ducts and throughout the generator, at times including an economizer with smooth tubes. This is not sufficient to complete the air and flue gas circuit. Let us look at the circuit of a radiation generator including the installation of all possible equipment in these cases (Figs. 1.6 and 1.7).

First of all, it is required to estimate the pressure drops through the air heater as far as air and flue gas. Given that it belongs to the Ljungstroem type, one is forced to base this on the experimental results of the constructor (generally, the drops amount to about 400–600 Pa for both air and flue gas).

In addition, one must consider the pressure drop due to the burners based on experimental data only. As a reference, note that the pressure difference between the burner box and the furnace required to compensate this drop and to give air the necessary velocity usually ranges from about 800 to 1800 Pa. For burners installed on convection generators, this drop usually ranges from 1200 to 1600 Pa. The pressure drop caused by soot precipitators must be established experimentally and indicated by the constructor of the equipment. Roughly, note that it typically ranges from 400 to 700 Pa.

Finally, even though its computation is quite easy, the pressure drop caused by steam unit heaters is usually indicated by the specialized constructor and mostly is about 300–500 Pa. If it is a convection generator, there could be an economizer with finned tubes after it. In this case one may refer to the general concepts in previous sections taking into account cross-sectional areas of channels (and related throttling) where water and flue gas are flowing. The literature indicates specific calculation criteria able to provide more exact data on pressure drops with finned tubes. This is indispensable during the design phase of an economizer that has not been built yet. On the other hand, if the device has already been experimented, it will be best to refer to results obtained by running plants.

There are no problems in computing pressure drops in tube air heaters. The drops relative to the fluid flowing inside the tubes are computed based on the equations in Sect. 10.1 for distributed drops and based on Sect. 10.2 for inlet and outlet drops in correspondence of the headpieces. The pressure drop relative to the fluid hitting the tube bank is computed based on the criteria described in Sect. 10.3 for tube banks.

If the air heater is a pocket heater, both air and flue gas flow in channels with a rectangular cross-section. Therefore, pressure drops are computed for both circuits

by referring to the hydraulic diameter of the channels and based on the equations in Sect. 10.1 and 10.2 (for the drops at inlet and outlet). As far as pressure drops in the cowlings which reverse the direction of both air and flue gas flowing in the tubes or channels or hit the different cross-sections of the tube bank, orientation is provided by the mass velocity corresponding to the minimum cross-section of the cowling by adopting factor ζ equal to 1.5.

Finally, the last piece of the puzzle is the pressure drop in the chimney. We refer to the equations in Sect. 10.1 for distributed drops considering the roughness of commercial tubes if the chimney is made of steel and the roughness of the masonry duct if the chimney belongs to this category. In addition, one needs to consider the pressure drop at the outlet on the top, according to Sect. 10.2.

10.5 Pumps, Fans, and Chimneys

Feed pumps of steam generators should be sized according to the following criteria. Each generator or group of generators must be fed through two feed devices, one of which is running while the other is a reserve. The two feed devices must not depend on the same energy source unless it is steam operated. Operating both feed devices with electric engines is allowable only when there are at least two independent energy sources and it is possible to rapidly switch from one source to the other. This commutation for steam generators with maximum production greater than 50 t/h must be done automatically. In any case, if the fuel feed devices operated electrically can be switched to a second energy source, it is required that even the main feed device can be switched simultaneously to the same energy source if it is operated electrically.

The flow rate of both main and backup feed pump must be at least equal to the values in Table 10.3. These stand for the percentage of the water flow rate required by the generator or the generators of the group. The latter is equal to the peak output plus the water flow rate of the continuous water drainage and of recirculation on the suction of the pump if they are included.

There are two types of pumps: centrifugal or piston pumps. The former are operated by electric engines or steam turbines, the latter by an electric engine through a reduction gear and adequate crank mechanisms, or by a steam engine. The behavior of centrifugal and piston pumps during runtime is fundamentally different and determines the use of one pump over the other. Within a certain intermediate range both can be used. Note that if a gate valve is installed on the delivery side (as is always the case), the piston pump requires a safety valve to discharge the entire flow rate of the pump.

Figure 10.30 shows the characteristic curves of a centrifugal pump. Note that the head decreases with the increase in flow rate. The efficiency which is rather low at small flow rates increases up to a maximum that usually corresponds to a head just below the maximum. Then it decreases until it reaches zero at maximum flow rate and zero head. The absorbed power grows hand in hand with the increasing flow rate.

Table 10.3 Advised pump flow rate

Maximum steam production of the generator	Pump flow rate as percentage of water flow rate	
	Without automatic regulation	With automatic regulation
Generators with natural or assisted circulation		
till 1 t/h	200%	200%
from 1 t/h to 5 t/h	160%	130%
from 5 t/h to 50 t/h	125%	115%
from 50 t/h to 100 t/h	115%	105%
from 100 t/h to 400 t/h	not allowable	105%
over 400 t/h	not allowable	100%
Generators with forced circulation		
till 1 t/h	not allowable	110%
over 1 t/h	not allowable	100%

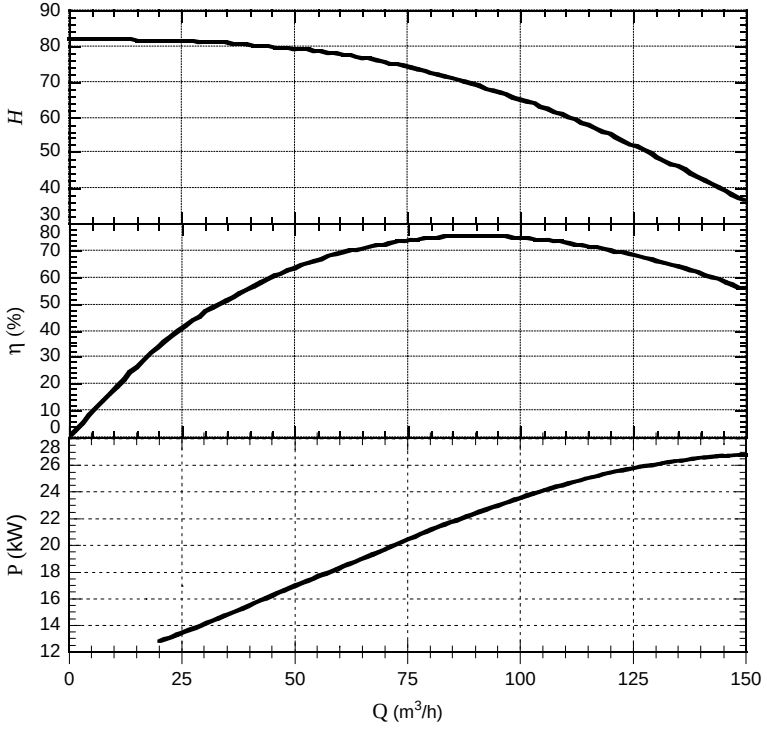


Fig. 10.30 Typical curves of centrifugal pump

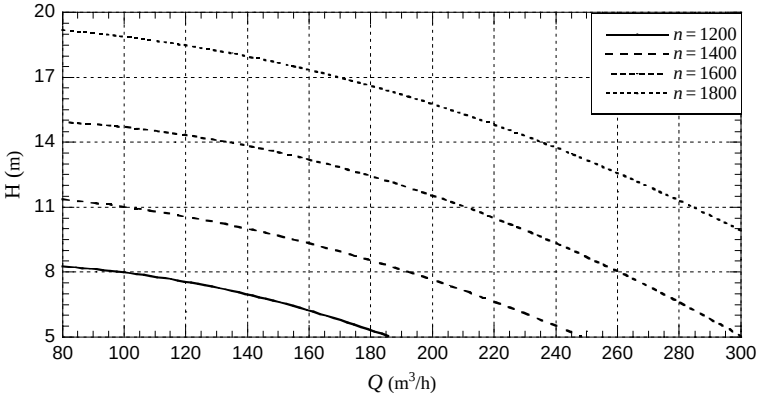


Fig. 10.31 Influence of the number of revolutions on a centrifugal pump

Figure 10.31 shows the impact of the number of revolutions on the head.

There are two types of fans: centrifugal and axial fans. In the former the fluid moving from the inside of the wheel is pushed toward the outside in a radial motion through the blades and discharges into the stator of the fan (Fig. 10.32). In the latter the fluid moves in parallel to the axis of the fan like in a common household fan, except for a collector box where the fluid discharges and generates static pressure (Fig. 10.33).

Centrifugal fans also differentiate themselves from one another by the type of blade. With respect to the radius, the exit angle can be zero, positive, or negative. In

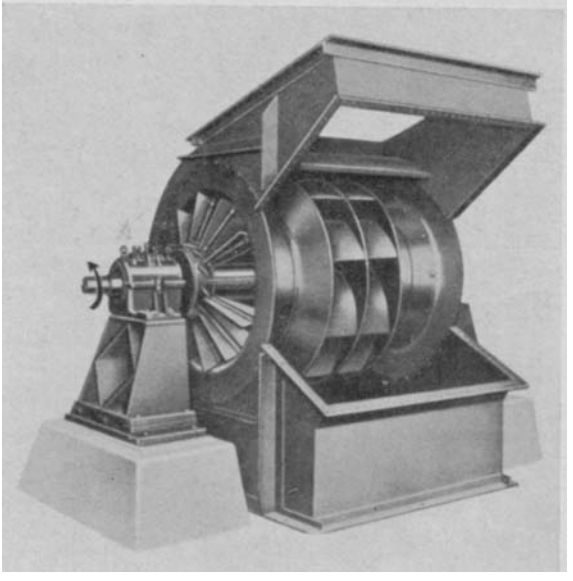


Fig. 10.32 Centrifugal fan (Courtesy of Babcock & Wilcox)

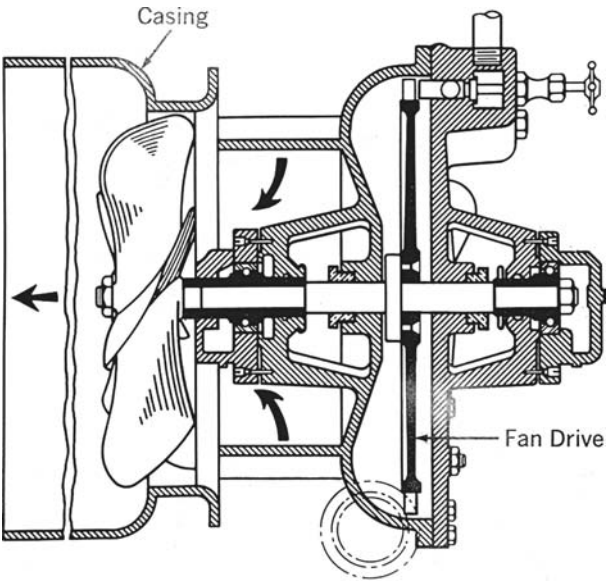


Fig. 10.33 Axial fan (Courtesy of Babcock & Wilcox)

the first case, the blades are radial and can be flat or curved. In the second case, the velocity of the fluid relative to the wheel forms an acute angle with the periphery velocity of the wheel itself. Finally, in the third case, the angle between the two velocities is obtuse (Fig. 10.34).

The first two represent quite typical constructive solutions and the blades of this kind are considered normal. The third solution involves a fan with backward-

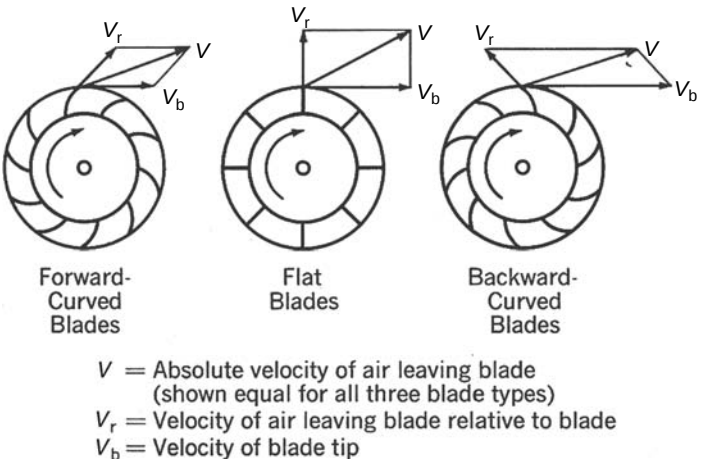


Fig. 10.34 Three general types of centrifugal fans (Courtesy of Babcock & Wilcox)

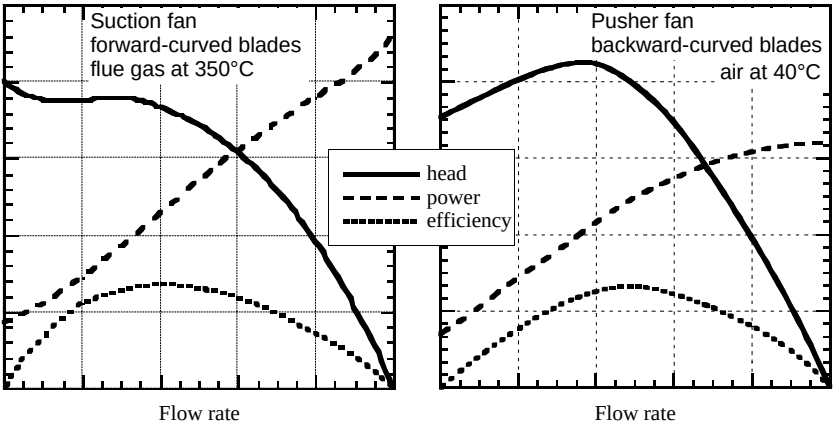


Fig. 10.35 Typical curves of two centrifugal fans

curved blades. Generally, suction fans have normal blades while pusher fans have backward-curved blades.

Figure 10.35 shows the characteristic curves of two fans with the different types of blades.

In the case of forward blades, in the initial part of the curve, the head has an inflection point that may be more or less pronounced or even missing. Regardless, the head is smaller than the one with zero flow rate. The curve representative of the absorbed power is either basically linear (straight) or demonstrates an upward concavity. The maximum efficiency value is generally shifted toward relatively low values of the flow rate.

On the other hand, backward blades imply an increase of the head from zero flow rate up to a value corresponding to the maximum of the curve. Then the head decreases rather rapidly. The absorbed power increase is less compared with the previous solution and shows a clearcut concavity downward. Its characteristics are self-limiting in the sense that it increases slightly with high flow rates. The potential reduction of pressure drop in the circuit and ensuing anomalous increase of the flow rate does not compromise the engine coupled to the fan.

On the other hand, the absorbed power at reduced loads is greater than the one relative to the previous solution. Efficiency reaches its peak in correspondence of a flow rate value that is greater in comparison with the previous case. Based on the characteristics of the circuit (pressure drops as a function of the flow rate), the running condition for the fan is identified by the crossing point of the curve characteristic of the drops with the curve of static pressure of the fan (product of the head by the density of the fluid and gravitational acceleration).

There are two ways to modify the flow rate: by introducing an additional pressure drop or by varying the speed of the fan. The first type of intervention is done through the regulation lock. Greater or lesser opening of the blades changes the pressure drop of the circuit which shifts the crossing point discussed above (Fig. 10.36).

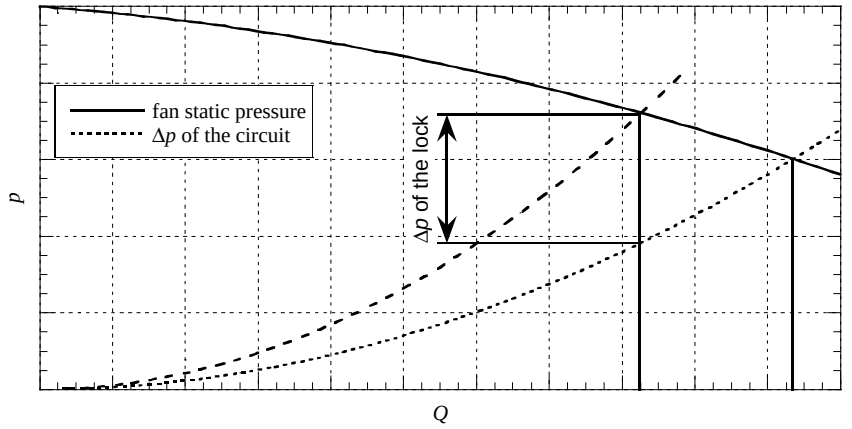


Fig. 10.36 Influence of the air lock

The lock can have rectangular blades and be inserted after the fan in the delivery duct, or it can be round with circle sector blades inserted on the suction (Fig. 10.37). In the latter solution, the dissipated power at reduced loads is less compared with the previous solution.

Flow rate regulation through a lock is the simplest and cheapest solution both in terms of regulation and the coupled engine running at constant speed. It also lends itself to quite simple solutions to set up automatic regulation. In fact, it suffices to

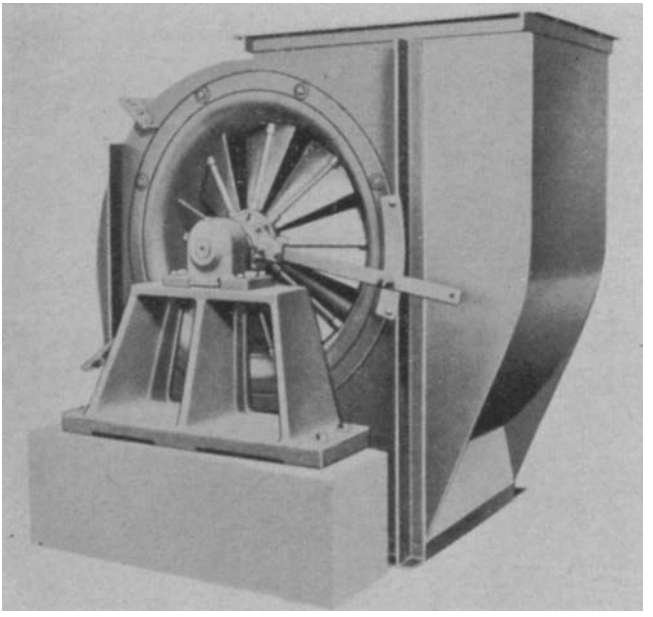


Fig. 10.37 Inlet vanes control output (Courtesy of Babcock & Wilcox)

plan for a servomotor controlled by the regulation plant that makes the blades turn. The lock is the location for dissipated energy because of the increasing pressure drops it introduces into the circuit.

The variation of the flow rate without energy dissipation can be achieved by varying of the fan speed; a lot of energy dissipation is present if the speed variation is not continuous and a regulation lock is still part of the requirements (two-speed engine). Figure 10.38 shows how speed variations modify the characteristic curve of the head (or the curve of static pressure). Thus, the characteristic curve of the circuit crosses the different curves in correspondence of variable flow rates.

Note that, efficiency being equal, variations of the speed imply that the flow rate is proportional to the speed, the head is to the root and consequently the absorbed power is to the cube. Of course, the regulation of the flow rate through speed variations of the fan is quite costly, given that in the simplest case it requires an alternate current engine with two rotation speeds, or the following features in the case of more complex and expensive solutions: magnetic coupling, hydraulic coupling, coupling with a direct current engine or with a variable speed steam turbine.

The fans servicing the generator, besides having high level safety running features because they have to run over long periods of time without interruption, must be sized with a certain leeway both as far as flow rate and head. A safety margin on the flow rate is required both because of the potential necessity to run with more excess air than expected and because of greater than expected air leaks inside the regenerative air heater. In addition, in view of emergency overload, there should be an increased air flow rate. The greater fluid flow rate requires a greater head because of the increasing pressure drops in the circuit. Moreover, their calculation may not be completely close to reality. This means that even the head requested theoretically should be increased. The rule of thumb is to increase the flow rate by at least 10–15% and the head by 15–25%.

Finally, the recommendation is to plan for a higher air temperature at the suction of the pusher fan (it reduces static pressure due to the reduction in air density). An increase by 15 °C should be considered.

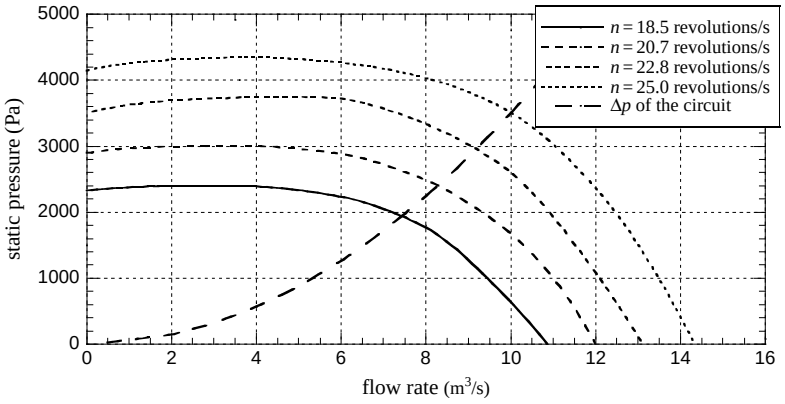


Fig. 10.38 Influence of revolution number on static pressure

The chimney is no longer important as far as suction of flue gas given the considerable pressure drops in the generator. Note that the tendency is to reduce the temperature of the flue gas at the exit of the generator as much as possible. Therefore, the draught of the chimney is modest considering the reduced difference in density between room air and flue gas. The draught p_c of the chimney expressed in Pa is given by:

$$p_c = g\left(\rho_a - \rho_{gm}\right) H_c; \tag{10.64}$$

g stands for the acceleration of gravity in $\mathrm{m/s^2}$, ρ_a and ρ_{gm} for the air density and the mean density of the flue gas in $\mathrm{kg/m^3}$, and H_c for the height of the chimney in m.

Considering the air at 20 °C, so that $\rho_a = 1.2\,\mathrm{kg/m^3}$, and adopting a value of the density of flue gas under normal conditions equal to $1.3\,\mathrm{kg/Nm^3}$, considering that the pressure is practically equal to atmospheric pressure, we have

$$\rho_{gm} = 1.3\,\frac{273}{t_{gm} + 273}. \tag{10.65}$$

From (10.64) and with $g = 9.807\,\mathrm{m/s^2}$ we have

$$p_c = \left(11.77 - \frac{3480}{t_{gm} + 273}\right) H_c. \tag{10.66}$$

With a temperature of the flue gas equal, for instance, to 180 °C the draught is equal to 4.1 Pa/m. This is clearly a modest value. Thus, the draught is quite modest even for very high chimneys in comparison to the pressure drops between furnace and chimney amounting to a several thousand Pa in big generators and to about 1000 Pa in small power ones. At any rate, the chimney has its own distributed pressure drop and exit drop at the top that reduce its useful draught. Therefore, the main purpose of the chimney is to direct the flue gas to a certain height.

It can be made of metal sheet for small units with a height ranging from 20 to 40 m. In thermoelectric plants, it is made of concrete, coated inside with refractory material, and sometimes equipped with a hollow space between the latter and the shaft made of steel concrete used for the passage of cooling air. The goal of the latter is to reduce the entity of thermal stresses in the shaft. There are also chimneys with a shaft in steel concrete and one or more cylindrical elements in metal sheet supported by the shaft, yet completely independent from it. The height of these chimneys is always considerable for ecological reasons, particularly if environmental conditions are unfavorable to dispersion of polluting substances. Some of them are 200 m tall and beyond.

Finally, note that the base of metallic chimneys can be done in such a way to contain a wheel and potentially even a regulation lock. In that case, we speak of a mechanical chimney. The simple placement of the cylinder over the base creates both the suction fan and the chimney, once the belt pulley is connected to an electric engine.

10.6 Natural Circulation

Both existing and new convection generators have natural circulation. The same is true for many existing radiation generators. Several of the new ones have natural circulation, as well. Considering that the basic principles of assisted circulation coincide with those of natural circulation except for the circulation pump in the circuits of water and saturated steam, the importance of natural circulation is quite understandable. Therefore, let us take a look at its physics laws and leave the definition of the conditions for satisfactory natural circulation to occur to the end.

First of all, we examine the simple circuit in Fig. 10.39 where the downcomers outside the flue gas pass and where warm water is passing through feed the lower header. The steam-generating tubes (also called raisers) under radiation from the flame start from here and redirect the water and steam mix forming inside them directly into the drum.

H stands for the head between the water surface in the drum and the axis of the lower header, ρ_w for water density, ρ_{mm} for the mean density of the water–steam mix, Δp_d for the pressure drop in the downcomers, and Δp_r for the pressure drop in the raisers.

With reference to the water in the downcomers, the hydrostatic pressure in correspondence of the header is equal to

$$p_d = \rho_w g H \tag{10.67}$$

where g stands for the acceleration of gravity assumed to be $9.807\,\mathrm{m/s^2}$.

Similarly, as far as the raisers, the corresponding hydrostatic pressure is equal to

$$p_r = \rho_{mm} g H. \tag{10.68}$$

The two pressures p_d and p_r are not identical, and therefore, the circuit is not balanced. This generates an anticlockwise circulation, given that $p_r < p_d$ because the density of the mix is less than that of water due to the presence of steam.

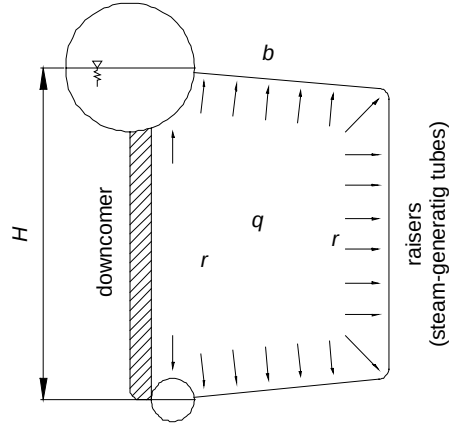


Fig. 10.39 Elementary circuit by natural circulation

Balance is reestablished when the difference between p_d and p_r is compensated by the pressure drops generated in the circuit by circulation. In other words, recalling (10.67) and (10.68) and the significance of Δp_d and Δp_r,

$$g(\rho_w - \rho_{mm})H = \Delta p_d + \Delta p_r \tag{10.69}$$

A given amount of heat transferred to the tubes generates a given amount of steam. Density ρ_{mm} is a function of the steam output and of the water flow rate feeding them through the downcomers. It goes up with the increase of the ratio between water entering the tubes and the steam output, called circulation ratio. Therefore, the term on the left hand side of the equal sign decreases with an increase in circulation ratio.

On the other hand, the pressure drops increase with the water flow rate or the water–steam mix flow rate in the downcomers and in the raisers, in other words with the circulation ratio. This determines a balance condition that can be identified through the following computation.

We indicate the heat transferred within the time unit to the raisers with q. If r stands for the vaporization heat at the running pressure set in advance, the mass flow rate of the steam at the outlet of the raisers M_{se} is given by

$$M_{se} = \frac{q}{r}, \tag{10.70}$$

where q in expressed in kW, r in kJ/kg, and M_{se} in kg/s.

If M_m stands for the mass flow rate of the steam–water mix in the raisers (of course, equal to the mass flow rate of water in the downcomers M_w) and R for the circulation ratio, the latter is given by

$$R = \frac{M_m}{M_{se}}. \tag{10.71}$$

We introduce two additional quantities, the percentage by mass and the percentage by volume of steam in the mix at the outlet of the raisers.

By indicating the former with π_m we have

$$\pi_m = \frac{M_{se}}{M_m} \times 100 = \frac{100}{R}(\text{in } \%); \tag{10.72}$$

π_v stands for the latter and v_w and v_s for the specific volume of water and steam, respectively.

The volumetric mass flow Q_{se} of the steam at the outlet of the raisers is given by

$$Q_{se} = M_{se} v_s. \tag{10.73}$$

The mass flow rate M_{we} of the water contained in the mix is equal to

$$M_{we} = M_m - M_{se}, \tag{10.74}$$

whereas the volumetric one Q_{we} is equal to

$$Q_{we} = (M_m - M_{se})\, v_w. \tag{10.75}$$

Then, in view of the significance of π_v, we have

$$\pi_v = \frac{Q_{se}}{Q_{we} + Q_{se}} \times 100 = \frac{M_{se} v_s}{(M_m - M_{se})\, v_w + M_{se} v_s} \times 100. \tag{10.76}$$

After a series of steps that are not shown here, we obtain

$$\pi_v = \frac{100}{\left(\frac{M_m}{M_{se}} - 1\right) \frac{v_w}{v_s} + 1}. \tag{10.77}$$

Finally, recalling (10.72), we have

$$\pi_v = \frac{100}{\left(\frac{100}{\pi_m} - 1\right) \frac{v_w}{v_s} + 1} (\text{in } \%). \tag{10.78}$$

By analogy, we may write that

$$\pi_m = \frac{100}{\left(\frac{100}{\pi_v} - 1\right) \frac{v_s}{v_w} + 1} (\text{in } \%). \tag{10.79}$$

If ρ_s stands for the steam density, the mass flow rate M_m of the mix is given by

$$M_m = Q_{we} \rho_w + Q_{se} \rho_s. \tag{10.80}$$

On the other hand, the volumetric flow rate Q_{me} of the mix at the outlet of the raisers is equal to

$$Q_{me} = Q_{we} + Q_{se}. \tag{10.81}$$

Then, the density of the mix at the outlet of the raisers is given by

$$\rho_{me} = \frac{Q_{we} \rho_w + Q_{se} \rho_s}{Q_{we} + Q_{se}}, \tag{10.82}$$

which can be written as follows:

$$\rho_{me} = \frac{Q_{se}}{Q_{we} + Q_{se}} \left(1 + \frac{Q_{we} \rho_w}{Q_{se} \rho_s}\right) \rho_s. \tag{10.83}$$

In other words,

$$\rho_{me} = \frac{Q_{se}}{Q_{we} + Q_{se}} \left(1 + \frac{M_{we}}{M_{se}}\right) \rho_s, \tag{10.84}$$

or

$$\rho_{me} = \frac{Q_{se} 100}{Q_{we} + Q_{se}} \frac{M_{we} + M_{se}}{M_{se} 100} \rho_s. \tag{10.85}$$

Recalling (10.72), (10.74) and (10.76), we finally have:

$$\rho_{\mathrm{me}} = \frac{\pi_{\mathrm{v}}}{\pi_{\mathrm{m}}}\rho_{\mathrm{s}}. \tag{10.86}$$

Equation (10.86) helps to compute the density of the mix at the outlet of the raisers when π_{m} and π_{v} are known (of course, ρ_{s} is known). The value of π_{m} is quickly calculated as a function of the preset circulation ratio (as we shall see later on this is indispensable to design and verification calculations) based on (10.72). The value of π_{v} is computed through (10.78) once π_{m} is known.

Knowing the value of ρ_{me}, the mean density of the water–steam mix ρ_{mm} included in (10.69) is assumed to be equal to

$$\rho_{\mathrm{mm}} = \frac{\rho_{\mathrm{w}} + \rho_{\mathrm{me}}}{2}, \tag{10.87}$$

given that at the inlet of the raisers the density of the mix matches the density of the water.

Now we introduce factor τ equal to the ratio between the mean volumetric flow rate of the steam and the mean volumetric flow rate of the mix. If Q_{sm} and Q_{mm} stand for them, respectively, by definition τ is given by

$$\tau = \frac{Q_{\mathrm{sm}}}{Q_{\mathrm{mm}}}. \tag{10.88}$$

The mean density of the steam–water mix can also be defined as the ratio between the mass flow rate M_{m} and the mean volumetric flow rate, that is,

$$\rho_{\mathrm{mm}} = \frac{M_{\mathrm{m}}}{Q_{\mathrm{mm}}}. \tag{10.89}$$

On the other hand, the mean volumetric flow rate of the water in the mix Q_{wm} is given by

$$Q_{\mathrm{wm}} = Q_{\mathrm{mm}} - Q_{\mathrm{sm}}. \tag{10.90}$$

The mass flow rate can be expressed as follows:

$$M_{\mathrm{m}} = Q_{\mathrm{sm}}\rho_{\mathrm{s}} + Q_{\mathrm{wm}}\rho_{\mathrm{w}} = Q_{\mathrm{sm}}\rho_{\mathrm{s}} + (Q_{\mathrm{mm}} - Q_{\mathrm{sm}})\,\rho_{\mathrm{w}}. \tag{10.91}$$

Thus, (10.89) can be written as follows:

$$\rho_{\mathrm{mm}} = \frac{Q_{\mathrm{sm}}\rho_{\mathrm{s}} + (Q_{\mathrm{mm}} - Q_{\mathrm{sm}})\,\rho_{\mathrm{w}}}{Q_{\mathrm{mm}}}. \tag{10.92}$$

Recalling (10.88) we obtain

$$\rho_{\mathrm{mm}} = \tau\rho_{\mathrm{s}} + (1-\tau)\,\rho_{\mathrm{w}}. \tag{10.93}$$

From (10.93) through obvious steps we obtain

$$\tau = \frac{\rho_w - \rho_{mm}}{\rho_w - \rho_s}. \tag{10.94}$$

After calculating ρ_{mm} with (10.87) it is possible to compute τ.

Factor τ is interesting in terms of the computation of the mean viscosity of the water–steam mix. In fact, this is computed as the weighted average of the viscosity of water and steam referred to the mean volumetric flow rates of both fluids. μ_w, μ_s, and μ_{mm} stand for the viscosity of water, steam, and steam–water mix average, respectively.

Note that in (10.93) even the mean density of the mix is given by the weighted average of the density of water and steam referred, of course, to the mean volumetric flow rates of the components.

Similarly, we have

$$\mu_{mm} = \tau\mu_s + (1-\tau)\,\mu_w. \tag{10.95}$$

We indicate d_i as the inside diameter of the raisers and G_r as the mass velocity. If A_r stands for the global cross-sectional area of the raisers considered in the calculation, and recalling the meaning of M_m, mass velocity is given by

$$G_r = \frac{M_m}{A_r}. \tag{10.96}$$

The Reynolds number relative to the raisers is therefore given by

$$\mathrm{Re} = \frac{G_r d_i}{\mu_{mm}} \tag{10.97}$$

with G_r in kg/m^{2}s, d_i in m, and μ_{mm} in kg/ms.

The values of μ_w and μ_s which influence the value of μ_{mm} can be obtained, for instance, from the publication "Properties of water and steam in SI-units." After computing the Reynolds number and obtaining the value of the relative roughness ε through the diagram in Fig. 10.1 or through (10.21), it is possible to compute the distributed pressure drop according to Sect. 10.1. To that extent, it is quite convenient to use (10.3) because it includes mass velocity. Of course, ρ_{mm} is introduced as the value of the density.

Then one must calculate the inlet loss in the raisers by applying the criteria discussed in Sect. 10.2. Even in this case, it will be best to refer to (10.44) and to consider the density of the water. Moreover, one needs to compute the outlet pressure drops. Density ρ_{me} relative to the outlet of the raisers must be added to (10.44). As far as the values of ζ, in both cases caution is advisable by adopting $\zeta = 0.5$ for the inlet and $\zeta = 1$ for the outlet.

Finally, one computes the drops in the curves. The criteria in Sect. 10.2 are still true and the mean value ρ_{mm} as density can be used for all curves. We see that for the computation of the pressure drops based on constant mass velocity, it suffices to consider the different values of the density in the equations. If Δp_{rd} stands for

the distributed drops and Δp_{ri}, Δp_{ro}, and Δp_{rc} stand for concentrated drops at inlet, outlet, and the curves, respectively, the total pressure drop Δp_r in the raisers is equal to

$$\Delta p_r = \Delta p_{rd} + \Delta p_{ri} + \Delta p_{ro} + \Delta p_{rc}. \tag{10.98}$$

Note that if there are deflecting plates, cyclones, and so on at the outlet of the tubes in the drum, the relative pressure drops must be considered, too. These can be implied from experimental data. The pressure drops in the downcomers are computed in a similar way. The calculation is made easier by the fact that density is constant (ρ_w).

Based on the total cross-sectional area of the water passage A_d, one computes mass velocity given by

$$G_d = \frac{M_w}{A_d} = \frac{M_m}{A_d}. \tag{10.99}$$

The distributed and concentrated drops relative again to inlet, outlet, and the curves are computed using the usual equations in Sect. 10.1 and 10.2.

Similarly, if the distributed drops are indicated as Δp_{dd} and the drops relative to inlet, outlet, and the curves as Δp_{di}, Δp_{do}, and Δp_{dc}, respectively, the total pressure drop is given by

$$\Delta p_d = \Delta p_{dd} + \Delta p_{di} + \Delta p_{do} + \Delta p_{dc}. \tag{10.100}$$

This process leads to the values of ρ_{mm}, Δp_d, and Δp_r included in (10.69).

Once the running pressure, thus the values of r, ρ_w, and ρ_s (and consequently v_w and v_s), is set and the value of the heat q transferred to the raisers is defined, the three quantities above are only a function of the circulation ratio. We already pointed out that the term on the left hand side of (10.69) decreases with the increase of R, whereas the term on the right hand side goes up. The qualitative behavior of both terms as a function of R is therefore the one included in (10.40); the crossing point of the curves identifies the balance condition matched by the characteristic value of R in the circuit.

To do the verification calculation of the circuit, one must select the different values of R and execute the computation of ρ_{mm}, Δp_d, and Δp_r for each one. This allows to trace the two curves in Fig. 10.40 and to identify the value of R relative to the circuit in question. At this point one must decide whether the resulting value is sufficient to guarantee correct functioning of the generator, that is, to rule out anomalous superheating of the tubes caused by insufficient cooling by the water–steam mix. The recommendation is to not exceed the values of π_v shown in the diagram of Fig. 10.41 as a function of absolute pressure. Based on (10.79), it is possible to compute π_m once π_v and running pressure (thus, v_w and v_s) are known. The value of R is computed through (10.72) from π_m.

Following this process, we computed R by including its values in the diagram of Fig. 10.42. They stand for minimum values. The design computation of the circulation is done as follows. The desired value of R is set based on the diagram of

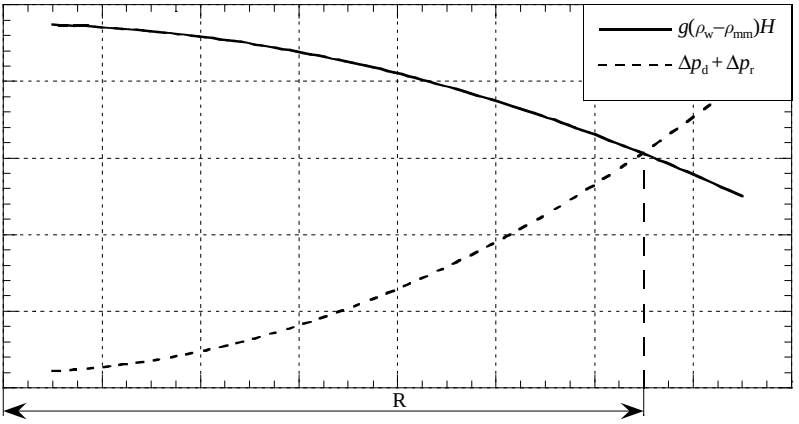


Fig. 10.40

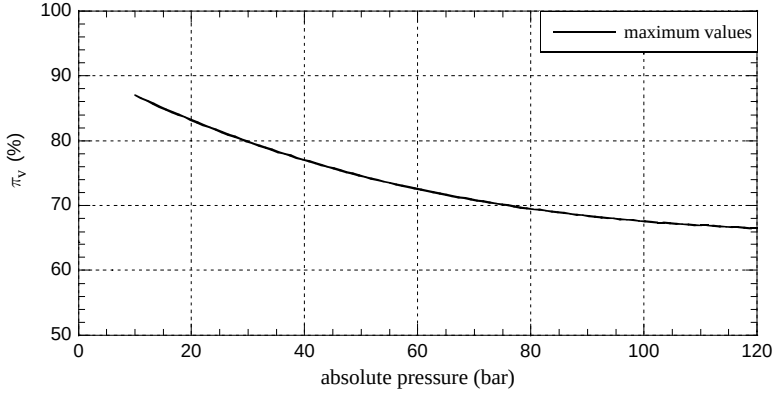


Fig. 10.41 Maximum values of π_v

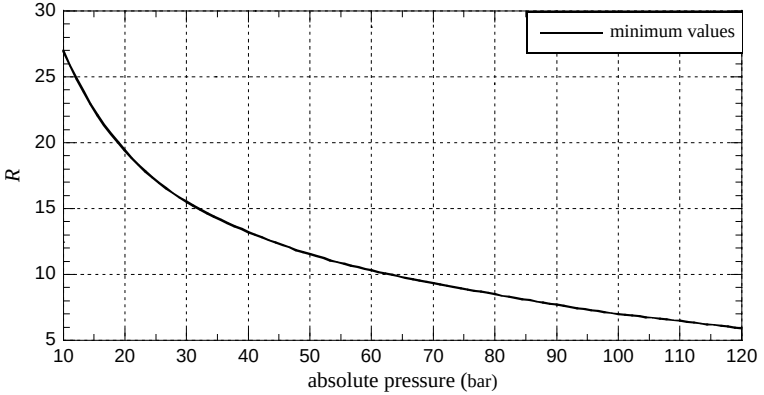


Fig. 10.42 Minimum values of R

Fig. 10.42, and ρ_{mm} and Δp_r are calculated based on this value. Based on (10.69), to ensure that the value of R is greater or equal to the set value, we must have

$$\Delta p_d \leq g\,(\rho_w - \rho_{mm})\,H - \Delta p_r. \tag{10.101}$$

It is a question of sizing the downcomers in such a way to agree with (10.101).

Note here that the global cross-sectional areas being equal, few tubes of large diameter cause a smaller pressure drop compared to many tubes of small diameter. In fact, recall (10.1) where d_i is in the denominator; as far as λ, an increase in diameter increases Re and reduces ε; Figure 10.2 demonstrates that even λ decreases. Of course, the logical tendency to plan for few tubes with a large diameter should not exasperated because it is very important to distribute the water in the raisers as evenly as possible.

Sometimes, it is preferable to have a sufficient number of downcomers in that respect. All depends on the constructive characteristics of the generator.

Note that (10.69) can be written as follows:

$$(\rho_w g H - \Delta p_d) + (-\rho_{mm} g H - \Delta p_r) = 0. \tag{10.102}$$

If we consider the difference in geodetic height between the inlet and the outlet of the fluid in the downcomers and in the raisers, given its direction, we see that the difference in height Δz_d relative to the downcomers is equal to H, whereas the one relative to the raisers (Δz_r) is equal to $-H$. Therefore, we can write (10.102) as follows:

$$(\rho_w g \Delta z_d - \Delta p_d) + (\rho_{mm} g \Delta z_r - \Delta p_r) = 0. \tag{10.103}$$

This highlights a characteristic factor of each circuit branch with the dimensions of a pressure that we call P. It is generically expressed as follows:

$$P = \rho g \Delta z - \Delta p \tag{10.104}$$

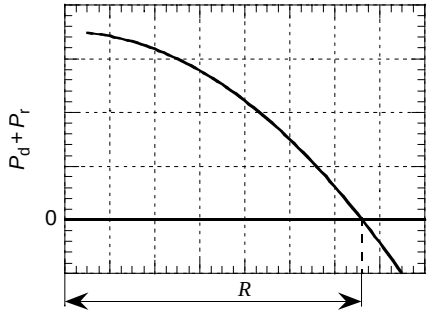
where ρ stands for the density characteristic of the branch in question, equal to the constant density of the fluid in the case of water and to the mean density in the case of a water–steam mix.

If P_d and P_r stand for the values of this factor for downcomers and raisers, (10.67) is synthesized as follows:

$$P_d + P_r = 0. \tag{10.105}$$

It is easy to establish that given zero velocity on the water surface in the drum and at the outlet of downcomers and raisers (considering that the entire kinetic energy is lost at the outlet), P_d represents the difference in pressure between the axis of the lower collector and the drum (positive) caused by the hydrostatic pressure of the water column in the downcomers minus the pressure drops. P_r represents the difference in pressure (negative) between the drum and the axis of the collector (inlet of the raisers) caused by hydrostatic pressure of the water–steam mix column minus the pressure drops.

Fig. 10.43



Therefore, (10.105) is completely justified. If we diagram the left hand term in (10.105) as a function of R, we obtain a curve shown in Fig. 10.43 with its qualitative pattern. The value of R of the circuit in question is identified by the intersection point with the axis of the abscissa.

Moreover, factor P is not only characteristic of a branch in its entirety but also of any single section of the branch (it no longer indicates the difference in pressure between extremities because of the influence of velocity).

Let us consider the generic branch shown in Fig. 10.44 characterized by a broken line. It can stand for a downcomer or a group of downcomers sharing the same geometric characteristics, or a group of identical raisers, or one or more return tubes (as we shall see later on).

Considering the generic section of the branch, we can compute its characteristic factor. With reference to (10.104), density ρ is the mean one of the fluid in the section, Δz is the difference in geodetic height between the extremity of section where the fluid enters and the extremity where the fluid exits, Δp is equal to the distributed pressure drop along the section plus the drops concentrated at the extremities, such as an inlet, outlet, or curve. Of course, concentrated pressure drops must be counted only once. In other words, if they are counted on both ends for a section, in the previous and next sections, the drops at the outlet and at the inlet, respectively, will not be counted.

After computing the factors P for all sections of the branch that we generically indicate with t, the characteristic factor of the branch is given by

$$P_t = \sum_t P \tag{10.106}$$

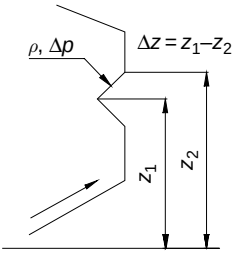


Fig. 10.44

where factor P stands for the generic section; the summation is extended to all sections of branch t.

For instance, if d and r are the branches corresponding to the downcomers and the raisers, respectively, based on (10.105) the condition of balance is represented by the following equation:

$$\sum_d P + \sum_r P = 0. \tag{10.107}$$

The calculation done through the factors P, characteristic of any section of the circuit, makes it possible, first of all, to compute circulation more accurately. Specifically, as far as the downcomers (and the return tubes, as we shall see), there is no difference between summation $\sum_d P$ and the value of factor P computed by including the entire difference in height of the circuit and the global pressure drops. In other words, recalling the significance of Δz_d and Δp_d and (10.103):

$$\sum_d P = \rho_w g \Delta z_d - \Delta p_d. \tag{10.108}$$

In fact, ρ_{w} is constant and this means that the summation of the generic terms $\rho\Delta z$ of any section corresponds to $\rho_{\mathrm{w}}\Delta z_d$. The summation of the different distributed and concentrated drops of any section necessarily corresponds to Δp_d, too. This is not true for the raisers. Previously, the computation was done considering a mean value of density (ρ_{mm}) computed as the average between the density at the inlet and outlet of the entire branch. Moreover, the pressure drops on the curves have also been computed with reference to ρ_{mm}.

But the summation of the $\rho\Delta z$ products relative to every section is not equal to the product of the mean density (not even if the exact mean value along the tube were to be computed instead of the average between extreme values) multiplied by the entire geodetic height difference of the branch. In other words,

$$\sum_r \rho\Delta z \neq \rho_{\mathrm{mm}}\Delta z_r. \tag{10.109}$$

In fact, the influence on the value of the summation of the vertical sections (with a high value of Δz) and of the less tilted sections with respect to the horizontal line is quite different. In other words, the values of ρ that count are those in the vertical sections. The value of the density that should be multiplied with Δz_r to obtain the same value of the summation is a weighted mean value that should take the geometry of the different sections into account (as in more or less tilt).

As far as pressure drops, the one at inlet and at outlet are correct. The distributed ones are equal to the summation of the various sections only if ρ_{mm} is the actual mean value, not the average between extreme values. Note that the density of the water–steam mix, especially if the circulation ratio is low, undergoes a sudden reduction at the beginning of the steam production, while the density reduction is less accentuated after that. In other words, the behavior of ρ along the branch is nothing but linear. Therefore, it is not correct to adopt the average between extremes as the mean value.

Then, as far as drops in the curves, an exact calculation is possible only based on the local density of the mix. Thus, with reference to (10.103) and (10.107):

$$\sum_r P \neq \rho_{\mathrm{mm}} g \Delta z_r - \Delta p_r. \tag{10.110}$$

Recalling that (10.101) reflects (10.69), we establish that the calculation process described at the beginning of the section is gross and is admissible only by initial approximation or for general orientation and exclusively for elementary circuits. It can absolutely not be considered for circuits with parallel braches, as we shall see later on.

The density of the water–steam mix in any point of the branch can be computed as follows.

We indicate β as the ratio between the mass flow rate of the steam M_{s} in that spot and the mass flow rate of the steam M_{se} at the outlet of the branch, that is,

$$\beta = \frac{M_{\mathrm{s}}}{M_{\mathrm{se}}}. \tag{10.111}$$

If M_{m} is the mass flow rate of the water-steam mix, we have:

$$M_{\mathrm{s}} = \beta M_{\mathrm{se}}; \tag{10.112}$$

$$M_{\mathrm{w}} = M_{\mathrm{m}} - M_{\mathrm{s}} = M_{\mathrm{m}} - \beta M_{\mathrm{se}}; \tag{10.113}$$

M_{w} stands for the mass flow rate of the water.

The specific volume v^* of the mix is equal to:

$$v^* = \frac{M_{\mathrm{s}} v_{\mathrm{s}} + M_{\mathrm{w}} v_{\mathrm{w}}}{M_{\mathrm{m}}} \tag{10.114}$$

where v_{s} and v_{w} are, usual, the specific volumes of the steam and the water.

Based on (10.112) and (10.113) we have

$$v^* = \beta \frac{M_{\mathrm{se}}}{M_{\mathrm{m}}} v_{\mathrm{s}} + \left(1 - \beta \frac{M_{\mathrm{se}}}{M_{\mathrm{m}}}\right) v_{\mathrm{w}}. \tag{10.115}$$

Recalling (10.71), we obtain the following from (10.115):

$$v^* = \frac{1}{R} \left[\beta v_{\mathrm{s}} + (R - \beta) v_{\mathrm{w}}\right]. \tag{10.116}$$

Finally, the density of the water-steam mix ρ^* is given by:

$$\rho^* = \frac{R}{\beta v_{\mathrm{s}} + (R - \beta) v_{\mathrm{w}}}. \tag{10.117}$$

The diagram in Fig. 10.45 shows the values of ρ^* for $p = 50$ bar and for various values of R as a function of β. We determine what was said earlier, that is, that the behavior of the density is not at all linear, especially for low values of R. Let us

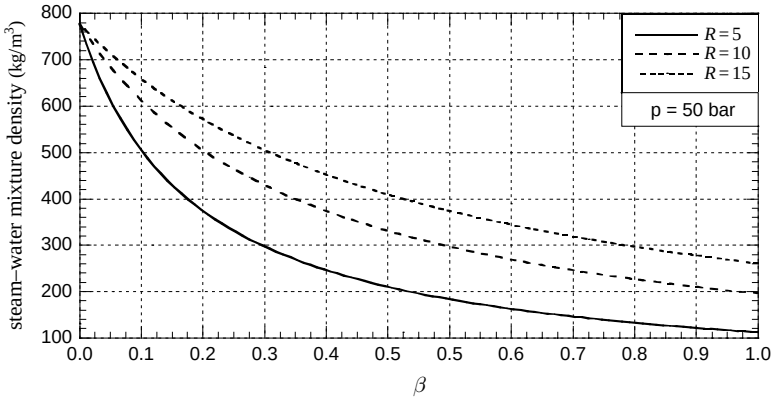


Fig. 10.45

now examine a section. β_1 stands for the value of β relative to the mass flow rate of steam entering the section, and β_2 stands for the value of β relative to the mass flow rate of steam exiting the section.

The mean density of the water–steam mix in the section simply indicated by ρ is equal to:

$$\rho = \frac{1}{\beta_2 - \beta_1} \int_{\beta_1}^{\beta_2} \rho^* d\beta. \tag{10.118}$$

Resolving the integral we obtain:

$$\rho = \frac{R}{(\beta_2 - \beta_1)(v_s - v_w)} \left| \log_e [\beta v_s + (R - \beta) v_w] \right|_{\beta_1}^{\beta_2}. \tag{10.119}$$

Therefore,

$$\rho = \frac{R}{(\beta_2 - \beta_1)(v_s - v_w)} \log_e \frac{\beta_2 v_s + (R - \beta_2) v_w}{\beta_1 v_s + (R - \beta_1) v_w}. \tag{10.120}$$

The value of ρ computed through (10.120) must be introduced in (10.104) to obtain the value of factor P relative to the section in question.

Equation (10.120) can also be written as follows, thus obtaining the equation suggested by Ledinegg:

$$\rho = \rho_w \frac{\dfrac{R}{\beta_2}}{\left(1 - \dfrac{\beta_1}{\beta_2}\right)\left(\dfrac{\rho_w}{\rho_s} - 1\right)} \log_e \frac{\dfrac{R}{\beta_2} + \left(\dfrac{\rho_w}{\rho_s} - 1\right)}{\dfrac{R}{\beta_2} + \dfrac{\beta_1}{\beta_2}\left(\dfrac{\rho_w}{\rho_s} - 1\right)}. \tag{10.121}$$

Now we take a look at the details of how to proceed. We consider the different sections of the branch and we estimate the transferred heat q. Note that it may also correspond to a thermal flux that varies from section to section. Even from this point

of view the calculation by section is much more sophisticated and makes it possible to highlight potential intensity variations of the heat transfer in the different areas of the furnace.

Based on the vaporization heat r, one computes the amount of steam output for every section indicated with m_s.

Similarly to (10.70),

$$m_s = \frac{q}{r}. \tag{10.122}$$

For the i-th generic section the mass flow rate of steam at the inlet M_{s1} is therefore equal to:

$$M_{s1} = \sum_{1}^{i-1} m_s. \tag{10.123}$$

The mass flow rate at the outlet M_{s2} is given by:

$$M_{s2} = \sum_{1}^{i} m_s. \tag{10.124}$$

If the sections are t, the mass flow rate at the outlet of the branch is equal to:

$$M_{se} = \sum_{1}^{t} m_s. \tag{10.125}$$

The values of β_1 and β_2 for the i-th section are given by:

$$\beta_1 = \frac{M_{s1}}{M_{se}}; \tag{10.126}$$

$$\beta_2 = \frac{M_{s2}}{M_{se}}. \tag{10.127}$$

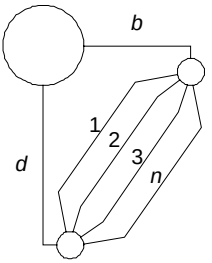
The mean density of the water–steam mix is computed through (10.120) or (10.121). Then it is possible to compute τ through (10.94) where ρ_{mm} obviously corresponds to the value of ρ calculated the way we described.

Subsequently, one computes the mean dynamic viscosity of the mix through (10.95) and the Reynolds number. The value of the friction factor λ is defined based on the value of ε, and the distributed pressure drops in the section are computed by referring, of course, to the value of ρ above.

As far as the concentrated pressure drops at inlet or outlet of the section, one proceeds as usual by considering the value of the density obtained from (10.117), where the value of β is equal to β_1 at the inlet and equal to β_2 at the outlet.

Generally, this is a curve except for the inlet of the first section where $\rho = \rho_w$ and for the outlet of the last section where $\rho = \rho_{me}$. This way one obtains the value of Δp relative to the section in question. So, once the geodetic height difference Δz between inlet and outlet of the section is computed, all quantities included in (10.104) are known. Summing up the factors P relative to the various sections making up the branch in question, one obtains the characteristic factor P of the branch.

Fig. 10.46



Let us consider the generic circuit shown in Fig. 10.46. The downcomers feed the lower collector from which n branches of raisers depart to regroup in one single collector at the outlet. From here the water–steam mix reenters the drum through the return tubes.

Practically, the circuits where the different steam generating branches in parallel regroup directly in the drum are more frequent. The raisers of every branch can also discharge the mix in one specific collector. Then, the mix reenters the drum through return tubes. This situation, though, is different from the one described in Fig. 10.46 where the outlet collector is one for all branches. If every branch has its own collector, from a functional point of view, it is as if the branches discharged directly into the drum. At any rate, when faced with the latter situations, the conclusions we will draw from the study of the schematized circuit in Fig. 10.46 are still completely valid, except for the absence of the return tubes, understood as return branch common to the steam generating branches in parallel.

We indicate d and b as the branches relative to the downcomers and the return tubes and 1, 2, 3,...n those relative to the raisers.

Let us consider the circuit consisting of $d, 1$, and b as the reference circuit.

Similarly to (10.105) we may write that

$$P_d + P_1 + P_b = 0. \tag{10.128}$$

On the other hand, we could write a similar equation for the circuit $d-2-b$, the circuit $d-3-b$, and so on, as well.

Therefore, the implication is that

$$P_1 = P_2 = P_3 ... = P_n. \tag{10.129}$$

Equation (10.129) can also be the direct outcome by observing that $P_1,\ P_2 \ldots P_n$ are nothing but the pressure differences between the inlet and outlet collectors referred to the various branches. They can only be identical. Both (10.128) and (10.129) synthesize the working conditions of the circuit in question.

The calculation process should be as follows. On the premise that the calculation is generally but not necessarily a verification, branch 1 is taken into consideration, a value R_1 of the circulation ratio is set, and P_1 is computed through the process described earlier. Then the calculation is repeated for different values of R_1 to obtain curve 1 shown in Fig. 10.47.

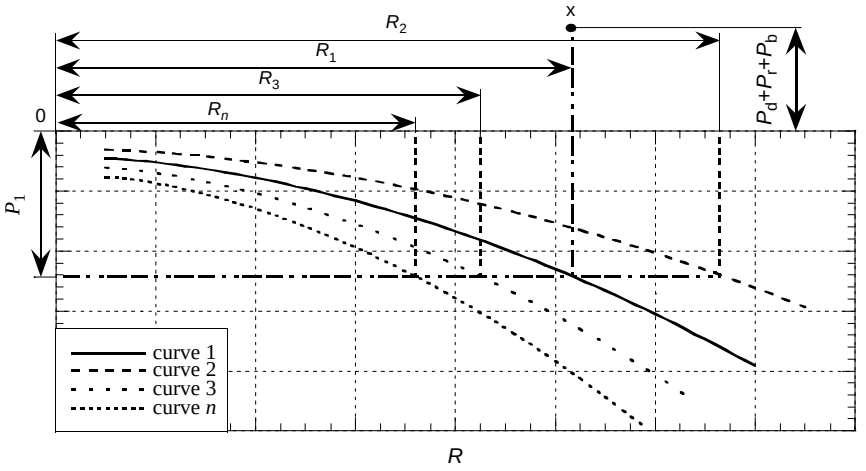


Fig. 10.47 Factor P for various parallel branches as a function of R

The process continues in a similar way for branches $2,3\ldots n$ to obtain the relative curves shown in the figure. At this point, a generic value of R_1 is selected that identifies a value of P_1 through curve 1. According to (10.127), the same value of P must be part of the other steam generating branches. Then, the parallel to the axis of the abscissa passing through P_1 is traced, and the values $R_2,\ R_3\ldots R_n$ corresponding to the value of R_1 selected in the beginning are identified through the curves $2,3\ldots n$.

If $M_{\mathrm{se}1}, M_{\mathrm{se}2}\ldots M_{\mathrm{se}n}$ stand for the mass flow rates of steam at the outlet of the different branches, and observing that based on (10.71)

$$M_{\mathrm{m}} = RM_{\mathrm{se}}, \tag{10.130}$$

based on the obtained values $R_1, R_2\ldots R_n$, the mass flow rates $M_{\mathrm{m}1}, M_{\mathrm{m}2}\ldots M_{\mathrm{m}n}$ are identified.

The flow rate of water in the downcomers and the flow rate of the water–steam mix in the return tubes is therefore equal to:

$$M_{\mathrm{w}} = M_{\mathrm{mb}} = \sum_{1}^{n} M_{\mathrm{m}}. \tag{10.131}$$

The density of the mix ρ_{mb} in the return tubes can be computed as follows.

The mass flow rate of steam M_{sb} is equal to:

$$M_{sb} = \sum_{1}^{n} M_{\mathrm{se}} = M_{\mathrm{se}_1} + M_{\mathrm{se}_2}\ldots + M_{\mathrm{se}_n}. \tag{10.132}$$

The water flow rate M_{wb} is equal to:

$$M_{\mathrm{wb}} = M_{\mathrm{mb}} - M_{\mathrm{sb}}. \tag{10.133}$$

The volumetric flow rate of the mix Q_{mb} is therefore equal to:

$$Q_{mb} = M_{sb} v_s + (M_{mb} - M_{sb})\, v_w. \tag{10.134}$$

The specific volume of the mix is given by:

$$v_{mb} = \frac{Q_{mb}}{M_{mb}} = \frac{M_{sb} v_s + (M_{mb} - M_{sb})\, v_w}{M_{mb}}, \tag{10.135}$$

or by

$$v_{mb} = \frac{M_{sb}}{M_{mb}} v_s + \left(1 - \frac{M_{sb}}{M_{mb}}\right) v_w. \tag{10.136}$$

Assuming that

$$\phi = \frac{M_{sb}}{M_{mb}}, \tag{10.137}$$

then

$$v_{mb} = \varphi v_s + (1 - \varphi)\, v_w. \tag{10.138}$$

Finally,

$$\rho_{mb} = \frac{1}{\varphi v_s + (1 - \varphi)\, v_w}. \tag{10.139}$$

Knowing $M_w = M_{mb}$, ρ_{mb} and the geometric characteristics of the downcomers and the return tubes, it is possible to compute P_d as well as P_b.

Thus, the value of the term $(P_d + P_1 + P_b)$ is put on the diagram in Fig. 10.47 in correspondence of R_1. In general, it will not be zero ("*x*" point of the diagram). The process described for different values of R_1 is repeated. This way, one creates the curve representative of the term on the left hand side of (10.128) (Fig. 10.48). Still based on (10.128), the running condition of the circuit is represented by the point where the curve mentioned above crosses the axis of the abscissa. This point

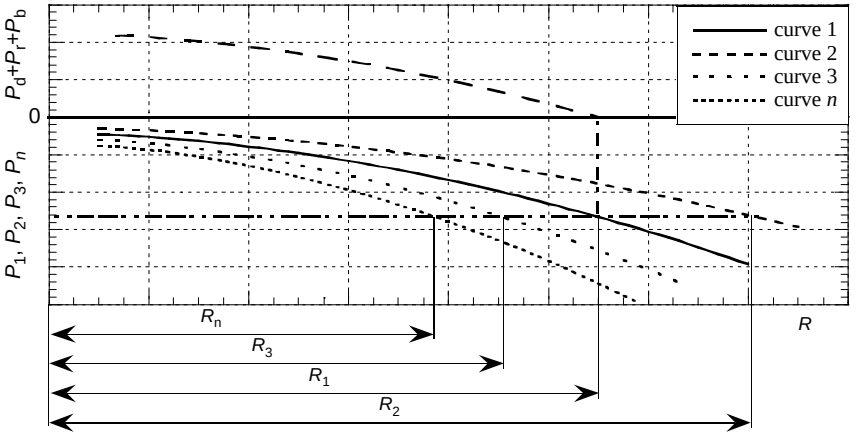


Fig. 10.48 Balance conditions of the circuit

identifies the value of R_1 characteristic of branch 1, and through curve 1 the actual value of P_1 that coincides with the one of the other branches.

The usual process leads to the values of $R_2, R_3 \ldots R_n$ relative to the different branches. At this point one takes the smallest of these values into consideration, and it is possible to judge if the circuit works correctly based on Fig. 10.42. This apparently laborious process is not problematic if the computation is done through a computer. It has repetitive characteristics which are particularly favorable in terms of programming. The calculation of P for the different sections and the subsequent summation to obtain the characteristic factor of every branch can be included in a subroutine called up by the main program as the various branches are examined.

Until now we referred to a verification calculation, given that the dimensional characteristics of the downcomers and of the return tubes are known (the dimensions of the raisers are always set for generators that are already sized from a thermodynamic point of view).

This is the way to proceed during the design phase. The curves relative to the values of $P_1, P_2 \ldots P_n$ of the various branches of the raisers in parallel (Figs. 10.47 and 10.48) must be built even in this case. After determining the minimum value of R through the diagram in Fig. 10.42 based on the running pressure which we indicate with R^*, one identifies the corresponding value of P (it is the greatest in absolute value for the different branches with reference to R^*) with reference to the least favored branch.

Based on this value of P that we indicate with P^* and that must be the same for the various branches in parallel, it is possible to determine the values of $R_1, R_2 \ldots R_n$, as well as the values of M_w, M_mb, ρ_mb through the described process.

In order to ensure the minimum circulation ratio R^* in the least favored branch (in the others the circulation ratio is obviously higher), with reference to (10.128), it must be as follows:

$$P_\mathrm{d} + P_\mathrm{b} + P^* \geq 0. \tag{10.140}$$

Given that the density of the fluid in the downcomers and in the return tubes is constant, it is possible to examine the corresponding branches in their entirety regardless of the examination of single sections.

Then

$$P_\mathrm{d} = \rho_\mathrm{w} g \Delta z_\mathrm{d} - \Delta p_\mathrm{d} \tag{10.141}$$

where Δp_d stands for the total pressure drop of the branch. As far as Δz_d, it is equal to the height difference between the axis of the drum and the axis of the lower collector at the outlet of the downcomers.

Similarly, for the return tubes

$$P_\mathrm{b} = \rho_\mathrm{mb} g \Delta z_\mathrm{b} - \Delta p_\mathrm{b} \tag{10.142}$$

where Δp_b stands for the total pressure drop of the branch. Δz_b is equal to the geodetic height difference (negative) between the axis of the inlet collector of the return tubes and the axis of the drum.

Based on (10.140) and taking into account (10.141) and (10.142), we have

$$\Delta p_{\mathrm{d}} + \Delta p_{\mathrm{b}} \leq \rho_{\mathrm{w}} g \Delta z_{\mathrm{d}} + \rho_{\mathrm{mb}} g \Delta z_{\mathrm{b}} + P^{*}. \tag{10.143}$$

The term on the right hand side in (10.143) stands for a known value once the geodetic height of the axis of the drum is defined. At this point the downcomers and the return tubes must be sized by adequately selecting number and diameter in such a way to satisfy (10.143). As the specific volume of the water and steam mix in the return tubes is clearly greater than the one of the water in the downcomers, the reference must be mostly to the return tubes to reduce pressure drops.

The illustrated computational process is the only acceptable one if there are various branches of raisers in parallel. For instance, we consider the circuit in Fig. 10.49 consisting of two branches in parallel of equal length. Furthermore, we assume that they are hit by the same amount of heat and that the only curve has the same dimensional characteristics.

We also assume that the water flowing down the downcomers distributes itself equally in the two branches.

The steam mass flow rate at the outlet of the branches is identical, and based on the assumption that was made this is true for the water–steam mix, as well. The volumetric flow rates are also identical, and so are the two values of ρ_{me}.

Adopting (10.87) the value of ρ_{mm} is also the same in the two branches. On the other hand, the value of Δz_{r} is equally the same, and because of the assumptions so is the value of Δp_{r}.

Therefore, computing P_{r} for the two branches, based on the global values [note the second term on the left hand side of the equal sign in equation (10.103)] and not in reference to the summation of the values of P of the different sections, one obtains two equal values. This agrees with (10.129), and one could draw the conclusion that the circulation ratio in the two branches is actually the same. In reality, nothing could be farther from the truth. The value of R in the left branch is lower than the one in the right branch. The following qualitative points suffice to realize it.

In the rising section of the left branch (first section), the steam starts to form as the water exits from the collector and the density of the water–steam mix decreases

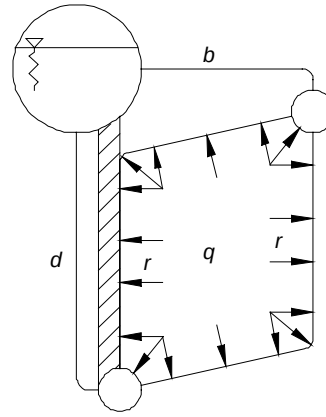


Fig. 10.49

as it moves upward. It is still rich in water, so the mean density in the rising section is relatively high.

In the right branch at the beginning of the rising section (second section), the mix is already rich in steam as a result of the steam generated in the first section. It acquires even more steam while it consequently looses water while it moves upward. The mass flow rate of the water–steam mix being equal, the mean density is therefore lower than the one relative to the rising section on the left (the difference between the two obviously depends on the value of the circulation ratio, which is assumed to be equal in both branches, and is much more sensitive as this ratio is reduced).

The hydrostatic pressure relative to mix column in the left branch is therefore greater than the one in the right branch, while the pressure drops are identical. This implies that the pressure differences between the lower and the higher collector referred to the two branches, that is, the two values of P_r, are not equal. But this is not acceptable, and to reestablish balance a greater amount of water must enter the right branch. This way both the hydrostatic pressure and the pressure drop increase, as well as the absolute value of P_r. Vice versa, the same happens in the left branch in terms of reduced amount of entering water.

The circuit is out of balance with a greater circulation ratio in the right branch, contrary to what the simplistic computation based on global mean values of ρ_{mm} lead to believe. Circulation unbalances in the circuits with parallel branches are quite frequent. Sometimes they are tolerable (if the minimum circulation ratio in the different branches is acceptable), but other times they are not. In that case, it is indispensable to intervene in some way. During the design phase, potential criteria consist of simply improving circulation globally reducing the pressure drops in the downcomers and in the return tubes. In the raisers, interventions of this kind are impossible unless the project is radically modified by adopting larger diameters. This does obviously not eliminate the unbalances, but all the circulation ratios go up which then increases the minimum value in the least fed branch, as well.

Further criteria that involve reducing the flow rate of the water–steam mix in the least fed branches in favor of the one or those poorly fed can be applied either during the design phase or after construction if unbalances are registered. This can be done through throttling plates which increase the pressure drops by reducing circulation in favor of other branches. Of course, global circulation decreases in the sense that the water flow rate in the tubes decreases, but if it is initially abundant, this reduction may not be an obstacle to the insertion of the plates.

Another widespread method consists of planning for balancing valves at the inlet of the different branches (specifically, at the inlet of headers feeding the branches). These valves are tuned as a function of the temperatures registered during runtime on the tubes through thermo-couples.

The same calculation criteria described for natural circulation are true for assisted circulation, too. It suffices to introduce the head of the circulation pump. Equation (10.128) is therefore modified as follows:

$$P_p + P_d + P_1 + P_b = 0 \tag{10.144}$$

where P_p stands for head of the pump multiplied by the density of the water and the gravity acceleration.

The value of P_p varies with the flow rate. This will be taken into account by introducing the relative value as a function of M_w computed with (10.131), thus as a function of R_1 based on the described calculation process.

Note that the latter does not include a few aspects of the phenomenon that are worth highlighting. If the steam moves faster than water, the section of the tube ideally occupied by the current of steam is smaller than the assumed one, while it is greater than the one taken up by the water flow. This means that the density of the mix is higher than the one considered up to now.

In the calculations we referred to a constant value of the water-steam density. As far as water, this is substantially correct, but in the case of steam, given the variations in pressure along the raisers, the density actually varies because it is higher than the assumed one from the drum (in fact, the adopted pressure is the drum's) to the lower collector.

The phenomenon is not really important. At the most, the increase in density can amount to 3% from the drum to the lower collector. Thus, on average the increase is 1.5% at the most in the raisers.

Pressure variations in terms of the ensuing spontaneous evaporation are more important. In fact, as the pressure decreases from the collector to the drum, the enthalpy of the water decreases. The heat freed this way generates a certain amount of steam.

The steam evaporated spontaneously may represent up to 7–8% of the steam generated by the heat transfer. Some author states that spontaneous evaporation favors circulation because the density of the water-steam mix decreases. In reality the effect is quite the opposite. Note that water flowing down the downcomers and reaching a pressure higher to that of the drum during the process, stops being saturated water. Once it enters the raisers, a certain amount of transferred heat warms up the water to bring it to evaporation temperature. Then, steam is generated as a result of the heat transfer and spontaneous evaporation. The greater amount of steam generated because of this phenomenon compensates precisely for the steam that was not generated in the initial area of the tubes where the water needed to be heated. It must obviously be this way because at the outlet of the raisers the generated steam cannot be anything but the one corresponding to the transferred heat and the evaporation heat referred to the pressure in the drum, according to the described computation process.

With reference to Fig. 10.50, the density of the water–steam mix behaves like a continuous curve instead of behaving like the dashed curve (theoretic). In the first section (heating of water) the density is practically constant, whereas in the second section (evaporation) the density decreases with a gradient higher than the theoretic one because of spontaneous evaporation.

So, the mean water–steam mix density is higher than the theoretic one, and the impact on circulation is negative. If these phenomena which always impact circulation in greater or smaller negative ways are ignored, there will be insubstantial differences between calculation and the actual phenomenon. Note that the

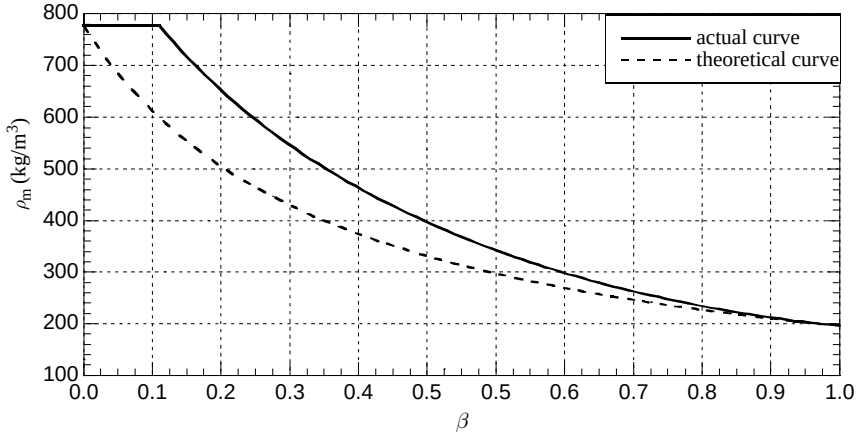


Fig. 10.50 Influence of the hydrostatic pressure and of the spontaneous evaporation

recommended values of R are based on practical experience correlated to theoretical calculation; for this reason, they implicitly factor in these negative phenomena either partially or totally.

In conclusion, we briefly consider a problem of special interest to constructors of generators of small power and pressure. Assuming, for instance, that a generator was designed to work under an absolute pressure of 25 bar and that the circulation ratio is the minimum recommended one, based on Fig. 10.42, the question is whether the same project may be used at lower or higher pressure levels after applying all due modifications to the thickness of the drum, the headers and the tubes.

Figure 10.51 shows the curve of minimum values of R from Fig. 10.42, as well as the values of the circulation ratio for the generator in question, by varying the pressure from 10 to 50 bar. Clearly, by increasing the pressure, the circulation ratio decreases, but it decreases less compared to the minimum allowable values, thus

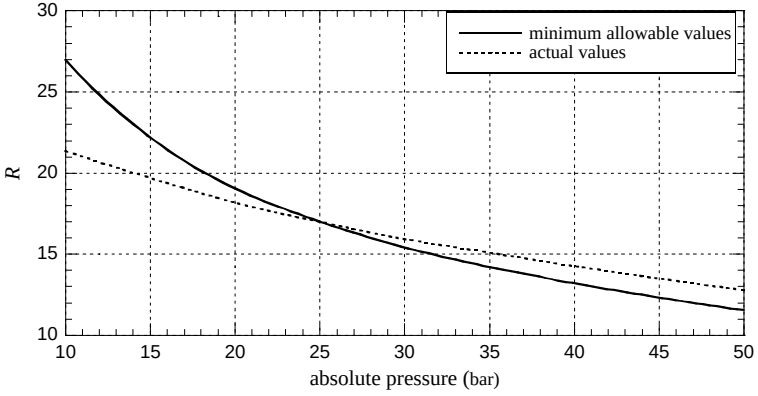


Fig. 10.51

resulting in a higher than minimum ratio at pressures above 25 bar and in a lower than minimum ratio at pressures under 25 bar.

Contrary to common assumption, taking into account the behavioral pattern of the ratio between the density of water and steam at pressure variations, for a given generator low pressure is more dangerous than high pressure.

Therefore, designing a generator that is adaptable to various pressure levels requires planning for runtime under expected minimum pressure and doing computations of circulation based on that.

This page intentionally left blank

Chapter 11
Optimization Criteria

11.1 General Information on Optimization of Convection Generators

The term optimization can encompass at least two types of investigation that will be illustrated shortly. What we call internal optimization is within the range of choices the constructor has to make. Costs being equal, it is a question of selecting the type of constructive solution that will yield the best results relative to heat exchange without neglecting the implications deriving from more or less considerable pressure drops. Another way to look at the problem is to identify the solution that, performance being equal, can be implemented at the lowest cost.

The first beneficiary of this optimization is the constructor because, performance being equal, he or she is able to offer the user a product at a lower price or because, price being equal, he or she can provide a better performing generator and be highly competitive in the marketplace. Naturally, the user profits from this situation too, but in any case this will be an indirect advantage, essentially validating a smart choice based on what the market can offer. The main player of this type of optimization is still the constructor, and we define internal optimization based on this principle.

The user must intervene at this point if he or she wishes to protect his or her interests (these largely coincide with the general interest). He or she must become the main player of another kind of optimization that we define as external, that is, outside design criteria. In fact, once the constructor has defined the fundamental dimensional characteristics that lead to internal optimization, he or she is able to provide the user with quite identical generators from a conceptual standpoint, yet with different surfaces. For instance, a generator with well-defined dimensional cross characteristics can be a more or less long, thus its surface more or less large, and its efficiency level differ. The dimensional characteristics of the section (for instance, for smoke-tube generators these are the diameter of the flue, number and diameter of the tubes in the various flue gas passages) are crucial to characterize a generator in terms of heat exchange and pressure drops. The length is free instead (within limits due to the length of the flame, acceptable volumes, etc.), and by varying it we obtain

D. Annaratone, *Steam Generators*, DOI: 10.1007/978-3-540-77715-1_11,

© Springer-Verlag Berlin Heidelberg 2008

conceptually identical generators with common constructive features that can easily be compared.

The user can choose within this range to achieve optimization. By varying the length, the cost of the generator goes up, but increasing efficiency results in fuel savings. Therefore, it is a question of identifying the solution that optimizes costs. Evidently, the choice is strongly influenced by running hours and by expected average load. This is why only the user is able to provide the constructor with those indispensable data that allow him or her to customize the best offer. This requires collaboration between constructor and user. The intervention of the latter justifies the term "external" to differentiate it from the previous optimization.

Of course, the surface of the generator is not the only variable to change the financial computation terms. A generator may be equipped with an economizer or an air heater that considerably increases efficiency. This is another well-known and important aspect of the problem that should be analyzed using the same criteria. The point is to compare the cost of the heat regenerator (in terms of yearly updated cost) with the savings achieved because of reduced fuel consumption.

The case history relative to the determination of optimal design conditions of the generator, including presence or absence of a heat regenerator, is quite rich, given the numerous parameters at play. Therefore, it is impossible to examine all possible situations facing the designer. The following sections will focus on typical situations lending themselves to general analytical evaluation by introducing a few simplifications that do not compromise the validity of the results in any way.

- Specifically, Sect. 11.2 illustrates the external optimization criteria of the boiler independently from the presence or absence of a heat regenerator.
- Section 11.3 examines the external optimization of the air heater, including the risk of corrosion due to the presence of sulfur in the fuel or the absence of such risk.
- Section 11.4 illustrates internal optimization criteria of the boiler-heat regenerator compound aiming at identifying the ideal subdivision of the heat exchange surfaces between boiler and heat regenerator, once the exit temperature of the flue gas from the generator and efficiency are set.
- Finally, Sect. 11.5 discusses the external optimization criteria for waste-heat generators with or without a heat regenerator.

All the above computation criteria are supposed to provide orientation on the best solution without the expectation to identify them exactly. Their advantage is to avoid useless and time-consuming investigations far away from the situation at hand. Moreover, note that within such a wide range, a cost higher than the minimum corresponding to the optimal solution is basically irrelevant.

11.2 External Boiler Optimization

Only considering the costs susceptible to change in relation to surface variations of the boiler (thus ruling out maintenance and personnel costs), we identify the following points:

A. plant cost

1. cost of boiler, combustion, and regulation plant and auxiliary equipment (except for the fan and its engine)
2. cost of fan and relative engine

B. running costs

1. fuel cost
2. electricity cost for auxiliary equipment.

We consider a boiler with defined geometric characteristics, except for the length. In other words, if it is a smoke-tube boiler, we define the type (dry end or wet end plate), diameter of flue, number and diameter of tubes of second and third flue gas passage, and consequently the geometric features of backflow chambers and diameter of shell. The thickness of all components will be defined based on pressure.

In the case of a water-tube boiler, we consider the type (for instance, two-drum boiler), width and height of furnace, geometric characteristics of tube bank (number of tubes in a section, diameter and length, pitches), and diameter of drum(s). Given the pressure, the thickness will be defined as well. Note that the only unknown dimension is the length. Its variation determines similar boilers with different surfaces and efficiency levels.

Under these conditions, the cost in A.1 consists of a set and a variable term, the latter of which can be considered to be proportional to the surface of the boiler. The set term encompasses combustion and regulation plant and all the auxiliaries (except for the fan), boiler accessories (water gauge, valves, etc.), including the parts of the boiler not influenced by the surface. In the case of a smoke-tube boiler, those will be the tube sheets and the backflow chambers, in the case of a water-tube boiler those will be the front and rear walls and the heads of the drums. If C_{b} stands for the yearly updated cost of the boiler, we have

$$C_{\mathrm{b}} = C_{\mathrm{bf}} + c_{\mathrm{bs}} S, \tag{11.1}$$

where C_{bf} stands for the set term, c_{bs} for the updated cost for every m^2 of surface, and S for the boiler surface.

The cost for the fan and its engine also consists of a set and a variable term, the latter of which depends on the boiler surface. In fact, the power of the fan is proportional to its head. The latter depends on the pressure drop through the burner independent from the surface, and the pressure drops in the boiler. The latter consist of inlet and outlet pressure drops in the tube bank independently from the surface and the distributed ones which are about proportional to the surface itself.

Assuming that the cost of the engine-fan device is proportional to the absorbed power, even in this case it is possible to write that

$$C_{\mathrm{v}} = C_{\mathrm{vf}} + c_{\mathrm{vs}} S. \tag{11.2}$$

C_{vf} stands for the set term and c_{vs} for the updated cost for every m^2 of boiler surface.

The yearly updated cost of the plant is given by

$$C_p = C_{pf} + (c_{bs} + c_{vs})\,S, \tag{11.3}$$

where C_{pf} stands for the set term given by the sum of C_{bf} and C_{vf}.

The value of c_{vs} is very small compared to c_{bs} (a few percentage points). For this reason, it can be ignored at first or conventionally assumed to be equal to a certain percentage of c_{bs}. Our suggestion is to substitute (11.3) with the following one:

$$C_p = C_{pf} + 1.03 c_{bs} S. \tag{11.4}$$

Now, we examine B.1. If M_f stands for the average fuel consumption within the time unit, θ for the yearly runtime of the boiler, and c_f for the unitary fuel cost, the yearly fuel cost is given by

$$C_f = M_f \theta c_f. \tag{11.5}$$

On the other hand, if P stands for the average output within the time unit of the boiler, H_n for the net heat value of the fuel, and η for efficiency

$$P = M_f H_n \eta, \tag{11.6}$$

then

$$M_f = \frac{P}{H_n \eta}. \tag{11.7}$$

Then, based on (11.5),

$$C_f = \frac{P \theta c_f}{H_n \eta}. \tag{11.8}$$

As far as the cost for the electricity consumption of the auxiliaries, it is important to distinguish between the one relative to the fan and the one relative to all other auxiliaries. The cost for the latter is not influenced by the surface (besides the irrelevant influence of efficiency, function of the surface). It naturally depends on the mean output and the annual runtime. As only the dependency from the surface actually matters, to achieve optimization the cost in question may be considered set.

There is also a set term for the energy absorbed by the fan. Its nature is equal to the previous one and its value depends on the pressure drop through the burner and on the inlet and outlet pressure drops in the tube bank. Moreover, there is a variable term depending on the distributed pressure drops in addition to burned fuel and runtime.

As the distributed pressure drops can be assumed to be about proportional to the surface, the variable term similar to C_f is given by

$$C_a = C_{af} + c_{as} S = C_{af} + K \frac{P \theta S c_e}{H_n \eta}, \tag{11.9}$$

where c_e stands for the unitary cost of electricity and K for a characteristic factor.

If C_{af} is the set cost relative to energy consumption, the running cost C_w is given by

$$C_w = C_f + C_a = C_{af} + \frac{P\theta c_f}{H_n \eta} + K\frac{P\theta S c_e}{H_n \eta} = C_{af} + \frac{P\theta}{H_n \eta}(c_f + KSc_e). \tag{11.10}$$

In conclusion, the total cost, that is, the sum of plant and running cost, is given by

$$C_t = C_{tf} + 1.03 c_{bs} S + \frac{P\theta}{H_n \eta}(c_f + KSc_e). \tag{11.11}$$

The minimum value of C_t can be identified by deriving C_t with respect to S and making the derivative equal to 0.

Considering that η is a function of S,

$$\frac{dC_t}{dS} = 1.03 c_{bs} - \frac{P\theta}{H_n \eta^2}(c_f + KSc_e)\frac{d\eta}{dS} + \frac{KP\theta c_e}{H_n \eta} = 0. \tag{11.12}$$

The third term is actually irrelevant with respect to the first one and KSc_e is irrelevant with respect to c_f.

Equation (11.12) can therefore be simplified as follows:

$$\frac{dC_t}{dS} = 1.03 c_{bs} - \frac{P\theta c_f}{H_n \eta^2}\frac{d\eta}{dS} = 0, \tag{11.13}$$

then

$$\frac{d\eta}{dS} = 1.03\eta^2 \frac{c_{bs} H_n}{P\theta c_f}. \tag{11.14}$$

This way, (11.14) solves the optimization issue. First of all, in practice, the question is to hypothesize the mean output within time unit P and runtime θ. Second, efficiency will be computed by varying the boiler surface, and by tracing the curve it will be possible to determine the corresponding curve of the derivative $d\eta/dS$.

The surface corresponding to optimal conditions is identified when (11.14) is satisfied based on the hypothesized values of P and θ, the computed value of c_{bs}, and the values of the net heat value H_n for the fuel and its cost c_f. Using (11.14), it is possible to develop an approximate calculation to generally identify optimal design conditions with sufficient reliability.

Note, in fact, that the exit temperature of the flue gas from the boiler can be expressed with good approximation through the following equation:

$$t_e = t_s + Ae^{-BS}, \tag{11.15}$$

where t_s stands for the steam temperature and A and B for constants.

Note that if $S = 0$, temperature t_e corresponds to the adiabatic temperature of the flame, so that

$$t_{ad} = t_s + A. \tag{11.16}$$

We can conventionally assume that $t_{ad} \approx 1800\,^{\circ}\mathrm{C}$ and $A \approx 1600\,^{\circ}\mathrm{C}$, then

$$t_e = t_s + 1600\mathrm{e}^{-BS}. \tag{11.17}$$

Of course, if $S = \infty$ results in $t_e = t_s$, as it should be.

Obviously, the pattern of t_e, S being equal, depends on the boiler output. Specifically, the value of t_e does not depend in absolute terms on S but from the ratio between the boiler surface and the output P. Therefore,

$$B = \frac{K_1}{P}, \tag{11.18}$$

where K_1 is a constant, the value of which will have to be determined in due time. Then,

$$t_e = t_s + 1600\mathrm{e}^{-K_1 \frac{S}{P}}. \tag{11.19}$$

Based on (11.19) and indicating the room temperature with t_0,

$$t_e - t_0 = t_s - t_0 + 1600\mathrm{e}^{-K_1 \frac{S}{P}}. \tag{11.20}$$

On the other hand, the sensible heat loss L_{sh} (9.58) is given by

$$L_{sh} = \frac{G_m c_{pg} (t_e - t_0)}{H_n}, \tag{11.21}$$

where G_m stands for the amount of flue gas for fuel mass unit, c_{pg} for mean specific heat between t_0 and t_e, and H_n for the net heat value of the fuel. Assuming that

$$K_2 = \frac{G_m c_{pg}}{H_n}, \tag{11.22}$$

from (11.20), we obtain

$$L_{sh} = K_2 \left(t_s - t_0 + 1600\mathrm{e}^{-K_1 \frac{S}{P}} \right). \tag{11.23}$$

In the absence of unburned carbon monoxide, efficiency is given by

$$\eta = 1 - L_{sh} - L_{er} - L_m, \tag{11.24}$$

where L_{er} stands for external radiation heat loss and L_m for miscellaneous heat losses.

Considering that the miscellaneous losses are constant (with respect to variations of S), we cannot ignore that the value of L_{er} is influenced by the surface of the generator. For our purposes, even the value of L_{er} can be assumed to be practically constant, as it is not crucial in terms of conclusions we draw.

Based on (11.23),

$$\eta = 1 - L_{er} - L_m - K_2 \left(t_s - t_0 + 1600\mathrm{e}^{-K_1 \frac{S}{P}} \right). \tag{11.25}$$

Then,

$$\frac{\mathrm{d}\eta}{\mathrm{d}S} = 1600\frac{K_1K_2}{P}\mathrm{e}^{-K_1\frac{S}{P}}. \tag{11.26}$$

Based on (11.14), the condition for optimization is therefore given by

$$1600\frac{K_1K_2}{P}\mathrm{e}^{-K_1\frac{S}{P}} = 1.03\eta^2\frac{c_{\mathrm{bs}}H_{\mathrm{n}}}{P\theta c_{\mathrm{f}}}, \tag{11.27}$$

then

$$\mathrm{e}^{-K_1\frac{S}{P}} = \frac{1.03\eta^2\frac{c_{\mathrm{bs}}H_{\mathrm{n}}}{\theta c_{\mathrm{f}}}}{1600K_1K_2}. \tag{11.28}$$

Moreover,

$$K_1\frac{S}{P} = \log_{\mathrm{e}}\frac{1600K_1K_2}{1.03\eta^2\frac{c_{\mathrm{bs}}H_{\mathrm{n}}}{\theta c_{\mathrm{f}}}}. \tag{11.29}$$

Finally,

$$S = \frac{P}{K_1}\log_{\mathrm{e}}\frac{1553K_1K_2}{\eta^2\frac{c_{\mathrm{bs}}H_{\mathrm{n}}}{\theta c_{\mathrm{f}}}}. \tag{11.30}$$

Equation (11.30) can be further simplified. First of all, note that the value of K_2 from (11.22) varies little in the type of boilers we are considering for rationally conducted combustion.

Presumably, $K_2 = 4.5 - 4.8 \times 10^{-4}$; conventionally, we adopt a value of K_2 equal to

$$K_2 = 4.65 \times 10^{-4}.$$

Moreover, the efficiency value under optimization conditions oscillates around 89%. Then we conventionally assume that

$$\eta = 0.89.$$

Therefore, based on (11.30)

$$S = \frac{P}{K_1}\log_{\mathrm{e}}\frac{0.912K_1\theta}{\frac{c_{\mathrm{bs}}}{c_{\mathrm{f}}}H_{\mathrm{n}}}. \tag{11.31}$$

In (11.31), all quantities are easy to calculate except for factor K_1 which is actually crucial.

Under full load, the value of K_1 is roughly equal to 70–115 kW/m^2 for smoke-tube boilers (with the exception of the smallest units) and equal to 100–135 kW/m^2 for water-tube boilers. These values become smaller under reduced loads.

Anyway, it is possible to compute K_1 directly based on the computation of a boiler of a given surface among those with a variable surface we are investigating. In fact, based on (11.19),

$$\frac{t_e - t_s}{1600} = e^{-K_1 \frac{S}{P}}, \tag{11.32}$$

then

$$K_1 \frac{S}{P} = \log_e \frac{1600}{t_e - t_s}. \tag{11.33}$$

By first approximation, we have

$$K_1 = \frac{P}{S} \log_e \frac{1600}{t_e - t_s}. \tag{11.34}$$

Once t_e is known based on the computation of a boiler with surface S and output P from (11.34), it is possible to compute K_1.

In conclusion, a first orientation about the optimal surface of the generator can be done as follows. One factors in a boiler as close as possible to the one assumed to be optimal based on the presumed mean output. The value of factor K_1 is obtained based on (11.34). The cost (of course, this refers to the cost of the buyer, not to the production cost) per m^2 of the generator is examined based on its lengthening or shortening. After establishing amortization and passive interest on the capital, the value of c_{bs} must be determined. A certain yearly time θ is assumed. Based on the net heat value H_n of the fuel and on its unitary cost c_f through (11.31), the optimal surface S is obtained based on the mean output.

As far as measuring units, c_{bs} is expressed in \$/m^2 year and c_f in \$/kg. If P is expressed in kW, the neat heat value H_n must be expressed in kJ/kg. The yearly runtime θ is expressed as s/year and, of course, S in m^2.

If the preference goes to expressing time in h/year with h, (11.31) must be written as follows:

$$S = \frac{P}{K_1} \log_e \frac{3283 K_1 h}{\frac{c_{bs}}{c_f} H_n}. \tag{11.35}$$

If we refer to a presumed diagram for the yearly load, it is possible to proceed as follows.

Based on runtime under different loads, we compute the weighted output average and assume it to be the value of P. The exit temperatures of the flue gas from the boiler in question under different loads is computed, and the weighted average is assumed to be the value of t_e. K_1 is computed based on this value t_e. This value of K_1 and the output value computed as above lead to the optimal surface.

An example will provide better insight. The goal is to optimize a water-tube boiler working under absolute pressure of 21 bar ($t_s = 215\,^\circ$C) with nominal power of 12,000 kW fed with fuel oil with $H_n = 40,600$ kJ/kg. Runtime is assumed to be 1000 h/year at full load, 800 h/year at 75% of full load (9000 kW), and 500 h/year at 50% of full load (6000 kW) for a total of 2300 h.

Examining a boiler with a surface of 320 m^2 and the following exit temperatures of the flue gas from the boiler at the different loads we have

$$\begin{aligned} P &= 12,000\,\text{kW} & t_e &= 270\,^\circ\text{C} \\ &= 9000\,\text{kW} & &= 252\,^\circ\text{C} \\ &= 6000\,\text{kW} & &= 236\,^\circ\text{C}. \end{aligned}$$

Then,

$$P = \frac{12000 \times 1000 + 9000 \times 800 + 6000 \times 500}{2300} = 9652\,\text{kW}$$

$$t_e = \frac{270 \times 1000 + 253 \times 800 + 236 \times 500}{2300} = 256.7.^\circ\text{C}$$

Based on (11.34):

$$K_1 = \frac{9652}{320} \log_e \frac{1600}{256.7 - 215} = 110\,\text{kW/m}^2.$$

The ratio between the updated yearly cost of the boiler (in \$/m^{2}year) and the cost of the fuel (in \$/kg) is assumed to be 350. Then,

$$S = \frac{9652}{110} \log_e \frac{3283 \times 110 \times 2300}{350 \times 40600} = 357\,\text{m}^2.$$

Roughly, we can assume that the optimal surface value lies within 340 and 375 m^2. Even the surface of 340 m^2 (smaller by 5% than the computed one) is most likely to represent a practically optimal solution.

We now look at the influence of the load diagram. We assume a runtime for the same boiler of 500 h/year at full load, 600 h/year at 75% of full load, and 900 h/year at 50% of full load for a total of 2000 h. Runtime at low loads is clearly predominant.

We have

$$P = \frac{12000 \times 500 + 9000 \times 600 + 6000 \times 900}{2000} = 8400\,\text{kW}$$

$$t_e = \frac{270 \times 500 + 253 \times 600 + 236 \times 900}{2000} = 249.6\,^\circ\text{C}$$

$$K_1 = \frac{8400}{320} \log_e \frac{1600}{249.6 - 215} = 100\,\text{kW/m}^2$$

$$S = \frac{8400}{100} \log_e \frac{3283 \times 100 \times 2000}{350 \times 40600} = 322\,\text{m}^2.$$

Note that the calculation produces a value of the optimal surface that is 10% smaller than the previous one. Roughly, the optimal surface may be assumed to be within 310 and 335 m^2. Presumably, even the surface of 310 m^2 represents a practically optimized solution.

In conclusion, note the great impact of the fuel cost. If it increases, boilers with greater surfaces become more interesting. For instance, if the ratio between the yearly updated cost of the boiler and the fuel cost decrease to 250 with a runtime of 2300 h/year (first case), the computation of the optimal surface leads to a surface of 386 m^2 with an increase of 8%.

11.3 External Optimization of Air Heaters

The analysis involves a tube air heater with fluids in counterflow with the flue gas inside the tubes and air outside. We look at the solution for fuel containing sulfur requiring special attention. In that case, the temperature of the boundary layer of the gas must be kept under control during any load variations to redirect part of the air after the air heater when necessary. Then we see how to do the calculation, which is easier when there is no risk of corrosion.

The exit temperature of the flue gas t'_2 from the air heater is given by (8.295):

$$t'_2 = t''_1 + \psi\left(t'_1 - t''_1\right). \tag{11.36}$$

t'_1 stands for the inlet temperature of the gas, t''_1 for the inlet temperature of the air which coincides with room temperature, and the dimensionless factor ψ for heat exchange in counterflow is given by (8.284):

$$\psi = \frac{1-\beta}{e^{(1-\beta)\gamma} - \beta}. \tag{11.37}$$

As

$$\beta = \frac{M' c'_{\mathrm{p}}}{M'' c''_{\mathrm{p}}}, \tag{11.38}$$

$$\gamma = \frac{US}{M' c'_{\mathrm{p}}}. \tag{11.39}$$

M' and M'' stand for the mass flow rates of flue gas and air, respectively, c'_{p} and c''_{p} for the mean specific isobaric heat of flue gas and air, U for the overall heat transfer coefficient, and S for the surface of the air heater.

M'^* and M''^* represent the mass flow rates of flue gas and air, respectively, under full load, and factor δ is given by

$$\delta = \frac{M'}{M'^*}. \tag{11.40}$$

Assuming the air index remains constant as the load varies, factor δ is basically the load of the generator.

ϕ stands for the ratio between the air flowing through the air heater and the air required for combustion. Values of ϕ below one indicate that part of the air is redirected after the heater without flowing through it.

We have

$$M' = M'^* \delta \quad \text{and} \tag{11.41}$$

$$M'' = M''^* \delta \phi, \tag{11.42}$$

then

$$\beta = \frac{M'^{*}\,\delta c'_{\mathrm{p}}}{M''^{*}\,\delta\phi c''_{\mathrm{p}}}. \tag{11.43}$$

Ignoring the modest variations of the specific isobaric heat at load variations, we may write that

$$\beta = \frac{\beta^{*}}{\phi}, \tag{11.44}$$

given that β^{*} is the value that factor β takes under full load given by

$$\beta^{*} = \frac{M'^{*}c'_{\mathrm{p}}}{M''^{*}c''_{\mathrm{p}}}. \tag{11.45}$$

With sufficient approximation for practical purposes, we can assume that

$$\beta^{*} \approx 1.15,$$

then

$$\beta = \frac{1.15}{\phi}. \tag{11.46}$$

The overall heat transfer coefficient U is given with sufficient approximation for our analysis by

$$U = \frac{\alpha'\alpha''}{\alpha' + \alpha''}, \tag{11.47}$$

where α' and α'' stand for the heat transfer coefficients of gas and air, respectively.

On the other hand, if the flue gas flows in the tubes, based on (8.156) we may write that

$$\alpha' \equiv M'^{0.8}. \tag{11.48}$$

By indicating the heat transfer coefficient under full load with α'^{*}, we have

$$\alpha' = \alpha'^{*}\delta^{0.8}. \tag{11.49}$$

For the air hitting the tube bank from outside, we may write that

$$\alpha'' \equiv M''^{0.61}. \tag{11.50}$$

With α''^{*} of air standing for the heat transfer coefficient under full load and complete passage of air through the heater, we have

$$\alpha'' = \alpha''^{*}(\phi\delta)^{0.61}. \tag{11.51}$$

Therefore, we may write that

$$U = \frac{\alpha'^{*}\alpha''^{*}\delta^{0.8}(\phi\delta)^{0.61}}{\alpha'^{*}\delta^{0.8} + \alpha''^{*}(\phi\delta)^{0.61}} = \frac{\alpha''^{*}(\phi\delta)^{0.61}}{1 + \dfrac{\alpha''^{*}}{\alpha'^{*}}\dfrac{\phi^{0.61}}{\delta^{0.19}}}. \tag{11.52}$$

Also, if U^* stands for the value of U under full load, based on (11.47) we obtain the following:

$$U^* = \frac{\alpha''^*}{1+\dfrac{\alpha''^*}{\alpha'^*}}. \tag{11.53}$$

Then,

$$\frac{U}{U^*} = (\phi\delta)^{0.61}\,\frac{1+\dfrac{\alpha''^*}{\alpha'^*}}{1+\dfrac{\alpha''^*}{\alpha'^*}\dfrac{\phi^{0.61}}{\delta^{0.19}}}. \tag{11.54}$$

Assuming that

$$\varepsilon^* = \frac{\alpha''^*}{\alpha'^*}, \tag{11.55}$$

we obtain

$$U = U^*\,(\phi\delta)^{0.61}\,\frac{1+\varepsilon^*}{1+\varepsilon^*\dfrac{\phi^{0.61}}{\delta^{0.19}}}. \tag{11.56}$$

Recalling (11.39) and (11.41), through a series of steps we obtain:

$$\gamma = \frac{U^*S}{M'^*c'_{\mathrm{p}}}\,\frac{(1+\varepsilon^*)\,\phi^{0.61}}{\delta^{0.39}+\varepsilon^*\phi^{0.61}\delta^{0.2}}. \tag{11.57}$$

By indicating the value of γ under full load ($\phi = 1$) with γ^*, the latter is given by

$$\gamma^* = \frac{U^*S}{M'^*c'_{\mathrm{p}}}. \tag{11.58}$$

From (11.57),

$$\gamma = \gamma^*\,\frac{(1+\varepsilon^*)\,\phi^{0.61}}{\delta^{0.39}+\varepsilon^*\phi^{0.61}\delta^{0.2}}. \tag{11.59}$$

Once the values of ε^* and γ^* based on the values of δ and ϕ are known, the values of β and γ are obtained through (11.46) and (11.59). The value of ψ is computed through (11.37), whereas the exit temperature of the flue gas from the air heater is obtained through (11.36).

Now, we examine the minimum film temperature of the flue gas in contact with the tubes. By indicating it with t_{f}, it may be assumed to be equal to

$$t_{\mathrm{f}} = \frac{t'_2 + t_{\mathrm{w}}}{2}, \tag{11.60}$$

where t_{w} stands for the wall temperature.

On the other hand, by adopting (11.47) we have

$$U\left(t'_2 - t''_1\right) = \alpha'\left(t'_2 - t_{\mathrm{w}}\right) = \alpha''\left(t_{\mathrm{w}} - t''_1\right). \tag{11.61}$$

After a series of steps

$$t_{\mathrm{f}} = \left(\frac{U}{\alpha''} + \frac{U}{2\alpha'}\right)\left(t'_2 - t''_1\right) + t''_1, \tag{11.62}$$

then

$$t'_2 - t''_1 = 2\left(t_{\mathrm{f}} - t''_1\right)\frac{\alpha' + \alpha''}{2\alpha' + \alpha''}. \tag{11.63}$$

Based on (11.49), (11.51), as well as (11.55),

$$t'_2 - t''_1 = 2\left(t_{\mathrm{f}} - t''_1\right)\frac{1 + \varepsilon^* \dfrac{\phi^{0.61}}{\delta^{0.19}}}{2 + \varepsilon^* \dfrac{\phi^{0.61}}{\delta^{0.19}}}. \tag{11.64}$$

Assuming that

$$\chi = \frac{t'_1 - t''_1}{t_{\mathrm{f}} - t''_1}, \tag{11.65}$$

based on (11.36), the outcome is

$$\chi = \frac{1}{\psi}\frac{t'_2 - t''_1}{t_{\mathrm{f}} - t''_1} \tag{11.66}$$

and based on (11.64),

$$\psi = \frac{2}{\chi}\frac{1 + \varepsilon^* \dfrac{\phi^{0.61}}{\delta^{0.19}}}{2 + \varepsilon^* \dfrac{\phi^{0.61}}{\delta^{0.19}}}. \tag{11.67}$$

Equation (11.67) keeps the minimum film temperature under control.

In fact, once the minimum allowable value of t_{f} and consequently the maximum value of χ are set, and once the value of ε^* is known and the one of δ (load) is pre-set, for every value of ϕ we obtain a value of ψ which must match the values resulting from (11.46), (11.59), and (11.37). In other words, generally there is only one value of ϕ simultaneously satisfying (11.37) and (11.67). Therefore, the value of ϕ represents the maximum allowable value to prevent temperature t_{f} from decreasing below the set value.

Note that even with $\phi = 1$ (complete passage of air through the heater), the value of ψ obtained through (11.67) may be below the one computed through (11.37). This means that even with $\phi = 1$, the film temperature is higher than the value set in advance. So, obviously this is a valid working condition.

In synthesis, the allowable working conditions of the heater can be expressed through the following equations:

$$\chi = \frac{t'_1 - t''_1}{t_f - t''_1} \tag{11.65 bis}$$

$$\varepsilon^* = \frac{\alpha''^*}{\alpha'^*} \tag{11.55 bis}$$

$$\gamma^* = \frac{U^* S}{M'^* c'_{\mathrm{p}}} \tag{11.58 bis}$$

$$\beta = \frac{1.15}{\phi} \tag{11.46 bis}$$

$$\gamma = \gamma^* \frac{(1+\varepsilon^*)\,\phi^{0.61}}{\delta^{0.39} + \varepsilon^* \phi^{0.61} \delta^{0.2}} \tag{11.59 bis}$$

$$\psi = \frac{1-\beta}{e^{(1-\beta)\gamma} - \beta} \geq \frac{2}{\chi} \frac{1 + \varepsilon^* \dfrac{\phi^{0.61}}{\delta^{0.19}}}{2 + \varepsilon^* \dfrac{\phi^{0.61}}{\delta^{0.19}}}. \tag{11.68}$$

Therefore, once ε^* and γ^* are known and the value of t_f (and therefore of χ) is set in advance, the value of ϕ satisfying (11.68) must be calculated as a function of δ. This yields the value of ψ and through (11.36) to the exit temperature of the flue gas from the heater which varies with the load. At this point, it is possible to set up financial calculations.

In fact, note that based on (11.36)

$$t'_1 - t'_2 = t''_1 - t''_1 - \psi\left(t'_1 - t''_1\right) = (1-\psi)\left(t'_1 - t''_1\right). \tag{11.69}$$

The recuperated heat through the heater within yearly runtime θ is given by

$$q = M' c'_{\mathrm{p}} \left(t'_1 - t'_2\right) \theta = M_{\mathrm{f}} G' c'_{\mathrm{p}} \left(t'_1 - t'_2\right) \theta, \tag{11.70}$$

where M_{f} stands for the burned fuel per time unit and G' for the amount of flue gas per mass unit of fuel.

If M^*_{f} stands for the fuel consumption under full load, recalling (11.69) we have:

$$q = M^*_{\mathrm{f}}\, \delta G' c'_{\mathrm{p}} (1-\psi) \left(t'_1 - t''_1\right) \theta. \tag{11.71}$$

The amount of saved fuel indicated by ΔF, if its net heat value is H_{n}, is given by

$$\Delta F = \frac{q}{H_{\mathrm{n}}} = M^*_{\mathrm{f}}\, \delta \frac{G' c'_{\mathrm{p}}}{H_{\mathrm{n}}} (1-\psi) \left(t'_1 - t''_1\right) \theta. \tag{11.72}$$

Equation (11.72) can be simplified by assuming with sufficient approximation for flue gas from fuel oil that

$$\frac{G' c'_{\mathrm{p}}}{H_{\mathrm{n}}} = 4.8 \times 10^{-4}. \tag{11.73}$$

Thus, we have

$$\Delta F = 4.8 \times 10^{-4} M^*_{\mathrm{f}}\, \delta (1-\psi) \left(t'_1 - t''_1\right) \theta. \tag{11.74}$$

Assuming that

$$\tau = 4.8\delta\,(1-\psi)\,, \tag{11.75}$$

the outcome is

$$\Delta F = \tau M_{\mathrm{f}}^{*}\left(t'_1 - t''_1\right)\theta \times 10^{-4}. \tag{11.76}$$

Factor τ depends on the load (δ) and on the value of ψ obtained through the process explained above.

The optimization of the heater is achieved by examining different solutions with different surfaces. The results are various values of ΔF minus the amount of fuel equivalent to the greater cost of the fan, the engine, the ducts, the structures, and the increased cost of electricity. Naturally, working conditions, that is, the value δ, and the expected runtime are crucial.

If the fuel contains no sulfur, the limitation in (11.68) has no reason to be and the value of ϕ is equal to one for any value of the load (all the air flows through the air heater). Thus, based on (11.46), $\beta = 1.15$. In addition, (11.59) and (11.37) are reduced to the following:

$$\gamma = \gamma^{*}\frac{1+\varepsilon^{*}}{\delta^{0.39}+\varepsilon^{*}\delta^{0.2}}, \tag{11.77}$$

$$\psi = \frac{0.15}{1.15 - \mathrm{e}^{-0.15\gamma}}. \tag{11.78}$$

This way the calculation is considerably simplified.

Once the values of ε^{*} and γ^{*} are computed through (11.55) and (11.58), γ is calculated based on the value of load δ and finally the value of ψ. The value of t'_2 is obtained through (11.36).

As far as the value of τ, if the fuel is natural gas, it is necessary to substitute (11.75) with the following:

$$\tau = 4.6\delta\,(1-\psi)\,. \tag{11.79}$$

The value of ΔF is again computed with (11.76) and then one proceeds as above.

Here is an example. A water-tube generator of nominal power equal to 12,000 kW working under absolute pressure of 13 bar shows the following exit temperatures of the flue gas, depending on load variations that correspond to entry temperatures t'_1 in the planned air heater.

Load 100%	$t'_1 = 248\,^{\circ}\mathrm{C}$
70%	$= 226^{\circ}\mathrm{C}$
40%	$= 205.5^{\circ}\mathrm{C}$.

The fuel oil consumption under full load M_{f}^{*} is equal to 0.33 kg/s.

Initially, the plan includes a heater with a surface of 80 m^2 and an overall heat transfer coefficient U^{*} equal to 22 $\mathrm{W/m^2K}$. Moreover, $M'^{*} = 5.8$ kg/s and $c'_{\mathrm{p}} = 1110$ J/kgK. Then,

$$\gamma^{*} = \frac{22 \times 80}{5.8 \times 1110} = 0.2733.$$

In addition,

$$\varepsilon^* = \frac{\alpha''^*}{\alpha'^*} = 0.8.$$

Finally, the minimum film temperature t_f is set at 145°C to prevent the risk of corrosion.

Given that $t''_1 = 20°\text{C}$ and based on (11.65), we have

$$\delta = 1 \qquad \chi = \frac{248-20}{145-20} = 1.824$$

$$\delta = 0.7 \qquad \chi = \frac{226-20}{145-20} = 1.648$$

$$\delta = 0.4 \qquad \chi = \frac{205.5-20}{145-20} = 1.484.$$

Based on (11.46), (11.59), (11.67), (11.74), and (11.76)

$$\begin{array}{llll} \delta = 1 & \phi = 1 & \tau = 1.043 & t'_2 = 198.4 \\ \delta = 0.7 & \phi = 0.9 & \tau = 0.739 & t'_2 = 180.7 \\ \delta = 0.4 & \phi = 0.43 & \tau = 0.400 & t'_2 = 172.7. \end{array}$$

The plan is to run 400 h/year at 40% of the capacity, 1000 h/year at 70% of the capacity, and 800 h/year under full load.

Given that time is indicated in s, based on (11.76) we have

$$\begin{aligned} \Delta F &= 0.400 \times 0.33 \times 185.5 \times 1.44 \times 10^6 \times 10^{-4} = 3,526 \\ &= 0.739 \times 0.33 \times 206 \times 3.60 \times 10^6 \times 10^{-4} = \ 18,085 \\ &= 1.043 \times 0.33 \times 228 \times 2.88 \times 10^6 \times 10^{-4} = \ \underline{22,601} \\ &\qquad\qquad\qquad\qquad\qquad\qquad\qquad\qquad\qquad\qquad 44,212\,\text{kg/year}. \end{aligned}$$

We consider the updated yearly cost (in \$/m^2 year) of the air heater, the ducts, the structures, and the greater yearly updated cost of both fan and engine, as well as the greater yearly cost of electricity. We also factor in the unitary cost of the fuel (in \$/kg). Assuming that the ratio between the two costs is 170, for the heater with 80 m^2 surface, the greater plant costs correspond to the cost of $170 \times 80 = 13,600$ kg of fuel. The actual saving is therefore equal to $44,212 - 13,600 = 30,612$ kg of fuel.

Now we consider a heater with a surface of 100 m^2, assuming that the values of U^* and ε^* remain the same.

We obtain γ^*, and proceeding the way we did before, we obtain the following values for the significant quantities.

$$\begin{array}{llll} \delta = 1 & \phi = 1 & \tau = 1.20 & t'_2 = 191.0 \\ \delta = 0.7 & \phi = 0.72 & \tau = 0.791 & t'_2 = 177.5 \\ \delta = 0.4 & \phi = 0.37 & \tau = 0.359 & t'_2 = 170.7 \end{array}$$

$$\Delta F = 48525.$$

The greater updated yearly plant cost corresponds to $170 \times 100 = 17,000$ kg of fuel. This translates into an actual saving corresponding to the cost of $48,525 - 17,000 = 31,525$ kg of fuel.

Now let us examine heater of $120\,\mathrm{m}^2$ matched by $\gamma^* = 0.41$, and

$$\begin{aligned}
&\delta = 1 \quad \phi = 1 \quad \tau = 1.366 \quad t'_2 = 183.1\\
&\delta = 0.7 \quad \phi = 0.615 \quad \tau = 0.829 \quad t'_2 = 175.2\\
&\delta = 0.4 \quad \phi = 0.335 \quad \tau = 0.372 \quad t'_2 = 169.5\\
&\Delta F = 53167.
\end{aligned}$$

The greater yearly updated plant cost corresponds to $170 \times 120 = 20,400$ kg of fuel, and the actual saving is equal to the cost of $53,167 - 20,400 = 32,767$ kg of fuel.

Following the same process, a heater with a surface of $140\,\mathrm{m}^2$ leads to

$$\begin{aligned}
&\delta = 1 \quad \phi = 0.90 \quad \tau = 1.452 \quad t'_2 = 179.0\\
&\delta = 0.7 \quad \phi = 0.545 \quad \tau = 0.856 \quad t'_2 = 173.5\\
&\delta = 0.4 \quad \phi = 0.310 \quad \tau = 0.381 \quad t'_2 = 168.6\\
&\Delta F = 55769.
\end{aligned}$$

The greater yearly updated cost of the plant corresponds to $170 \times 140 = 23,800$ kg of fuel, so that the actual saving is equal to the cost of $55,769 - 23,800 = 31,969$ kg of fuel.

In summary:

$$\begin{aligned}
&S = 80\,\mathrm{m}^2 && \text{Saving} = 30,612\,\text{kg of fuel}\\
&S = 100 && \text{Saving} = 31,525\\
&S = 120 && \text{Saving} = 32,767\\
&S = 140 && \text{Saving} = 31,969.
\end{aligned}$$

Clearly, the optimal solution involves an air heater with a $120\,\mathrm{m}^2$ surface. Note, though, that the difference in savings between the $120\,\mathrm{m}^2$ air heater and the $100\,\mathrm{m}^2$ heater is minimal. Therefore, it is preferable to adopt the $100\,\mathrm{m}^2$ surface heater to reduce additional plant costs and also to reduce the dimensions of the heater. Finally, this analysis was done considering fluids in counterflow to particularly highlight the necessity to bypass part of the air under small loads.

Note that as far as corrosion under small loads, the solution with fluids in parallel flow has advantages. First of all, even though the heat transfer is less efficient, if there is sulfur in the fuel it is worthwhile considering this solution, which may turn out be the more profitable one.

At this point, it is worthwhile examining the same generator with natural gas combustion to compare the two situations.

We assume that $M_\mathrm{f} = 0.375\,\mathrm{Nm}^3/\mathrm{s}$ and that the ratio between the greater yearly updated cost of the plant and the unitary cost of the fuel is equal to 200. For the sake of simplicity (even though it is not exact), we assume that the values of γ^*

Table 11.1 Combustion with natural gas

S	100			120			140			160			180		
	δ			δ			δ			δ			δ		
	1.0	0.7	0.4	1.0	0.7	0.4	1.0	0.7	0.4	1.0	0.7	0.4	1.0	0.7	0.4
γ	0.342	0.381	0.451	0.410	0.457	0.540	0.479	0.534	0.631	0.547	0.610	0.721	0.616	0.686	0.811
ψ	0.750	0.730	0.696	0.716	0.694	0.658	0.684	0.661	0.624	0.656	0.632	0.594	0.630	0.605	0.567
τ	1.15	0.870	0.559	1.31	0.986	0.629	1.45	1.09	0.692	1.58	1.19	0.747	1.70	1.27	0.797
t'_2	191	170	149	183	163	142	176	156	136	169	150	130	164	145	125
ΔF^*	58112			65954			73104			79470			85265		
ΔC^*	20000			24000			28000			32000			36000		
Saving	38112			41954			45104			47470			49265		

$^* = \mathrm{Nm}^3$/year of fuel

and ε^* and of the exit temperatures of the flue gas from the boiler are the same as before. Considering heaters of 100, 120, 140, 160, and 180 m^2 and using (11.36), (11.76), (11.77), (11.78), and (11.79), we obtain the values of the different quantities shown in Table 11.1, where ΔC indicates the greater yearly updated cost of the plant expressed in Nm^3/year of fuel.

Clearly, the savings are always increasing, regardless of the cost increase caused by the heater. Of course, the increased savings resulting from an increase of the surface by 20 m^2 decreases while the surface becomes bigger. It is equal to 3842 Nm^3/year when moving from 100 to 120 m^2, but it is reduced to 1795 Nm^3/year when passing from 160 to 180 m^2.

Theoretically, the optimal surface would be very high, about 300 m^2, with very low values as far as temperature t'_2, especially under small loads (about 100°C). This would also lead to a huge heater in relation to the boiler, an absurdity from the point of view of construction. It would also imply a considerable capital investment compensated by a modest saving only compared to the solutions included in Table 11.1. Based on these considerations, a surface of about 160 m^2 should satisfy all the different requirements.

11.4 Optimal Distribution of the Surfaces of the Boiler Tube Bank and of the Heat Regenerator

If the design of a steam generator, regardless of whether it is a water-tube or a smoke-tube generator, requires the installation of a heat regenerator (economizer or air heater) after the boiler, one must decide at which temperature the flue gas exits the boiler and hits the regenerator. Generally, this choice is made empirically, for instance by setting a certain difference in temperature between flue gas and steam temperature in advance and by leaving aside a critical analysis of the resulting boiler and regenerator surfaces. In fact, this is an optimization problem that depends, among other things, on the cost per surface unit of the bank of steam-generating tubes and of the regenerator. Of course, other significant quantities are at stake, such as the overall heat transfer coefficients relative to the steam-generating bank and the regenerator, the temperature of both steam and flue gas at the inlet of the steam-generating bank and at the exit of the regenerator.

Next, we will develop a calculation method of absolutely general validity to identify the optimal value of the inlet temperature of the flue gas in the regenerator. Specifically, the calculation is structured to set the exit temperature of the gas from the regenerator in advance and obtain the value of this inlet temperature to minimize the total cost of the tube bank in the boiler and of the regenerator. Naturally, the issue may be considered from another angle, in the sense that this optimal solution makes it possible to achieve minimum exit temperature of the gas from the regenerator, thus maximum generator efficiency, at equal total cost of the bank and the regenerator.

If t'_1 and t'_2 stand for the temperature of the flue gas at the inlet and the exit of the steam-generating bank in the boiler, respectively, and if t_s stands for the steam temperature, we know that (8.295)

$$t'_2 = t_s + \psi_b \left(t'_1 - t_s\right), \tag{11.80}$$

where (8.297)

$$\psi_b = e^{-\gamma_b}, \tag{11.81}$$

with (8.266)

$$\gamma_b = \frac{U_b S_b}{M' c'_{pb}}, \tag{11.82}$$

where U_b stands for the mean overall heat transfer coefficient relative to the steam-generating bank, S_b for the surface of the bank, M' for the mass flow rate of the flue gas, and c'_{pb} for mean specific isobaric heat of the gas.

Similarly, if t'_3 indicates the exit temperature of the gas from the regenerator and t''_1 the inlet temperature of the heated fluid

$$t'_3 = t''_1 + \psi_r \left(t'_2 - t''_1\right), \tag{11.83}$$

given that for fluids in counterflow (8.284)

$$\psi_r = \frac{1-\beta}{e^{(1-\beta)\gamma_r} - \beta} \tag{11.84}$$

with

$$\gamma_r = \frac{U_r S_r}{M' c'_{pr}}, \tag{11.85}$$

$$\beta = \frac{M' c'_{pr}}{M'' c''_p}. \tag{11.86}$$

U_r stands for the overall heat transfer coefficient relative to the regenerator, S_r for its surface, c'_{pr} for the mean specific isobaric heat of the flue gas in the regenerator, M'' and c''_p for the mass flow rate and the mean specific isobaric heat of the heated fluid, respectively.

From (11.83) based on (11.80), we obtain

$$t'_3 - t''_1 = \psi_r \left[t_s + \psi_b \left(t'_1 - t_s\right) - t''_1\right]. \tag{11.87}$$

Therefore,

$$\psi_r = \frac{t'_3 - t''_1}{t_s + \psi_b \left(t'_1 - t_s\right) - t''_1}. \tag{11.88}$$

We assume that

$$\tau_1 = \frac{t'_1}{t_s}, \tag{11.89}$$

$$\tau_3 = \frac{t'_3}{t_s}, \tag{11.90}$$

$$\tau_r = \frac{t''_1}{t_s}. \tag{11.91}$$

Equation (11.88) can be written as follows:

$$\psi_r = \frac{\tau_3 - \tau_r}{1 + \psi_b(\tau_1 - 1) - \tau_r}. \tag{11.92}$$

From (11.84) through a series of steps, we obtain:

$$\gamma_r = \frac{1}{1-\beta} \log_e \left(\frac{1-\beta}{\psi_r} + \beta \right). \tag{11.93}$$

Thus, based on (11.92)

$$\gamma_r = \frac{1}{1-\beta} \log_e \left[(1-\beta) \frac{1 + \psi_b(\tau_1 - 1) - \tau_r}{\tau_3 - \tau_r} + \beta \right]. \tag{11.94}$$

Note that if c_r indicates the cost per surface unit of the regenerator and C_r its total cost

$$C_r = c_r S_r, \tag{11.95}$$

and, based on (11.85) and (11.94)

$$C_r = \frac{c_r M' c'_{pr}}{U_r(1-\beta)} \log_e \left[(1-\beta) \frac{1 + \psi_b(\tau_1 - 1) - \tau_r}{\tau_3 - \tau_r} + \beta \right]. \tag{11.96}$$

From (11.81), we obtain

$$\gamma_b = -\log_e \psi_b. \tag{11.97}$$

If c_b indicates the cost per surface unit of the steam-generating bank and C_b its total cost, then

$$C_b = c_b S_b. \tag{11.98}$$

Then, based on (11.82) and (11.97)

$$C_b = -\frac{c_b M' c'_{pb}}{U_b} \log_e \psi_b. \tag{11.99}$$

We introduce the dimensionless factor A given by

$$A = \frac{c_b U_r c'_{pb}}{c_r U_b c'_{pr}}. \tag{11.100}$$

The total cost of the bank and of the regenerator is therefore given by

$$C = C_r + C_b = \frac{c_r M' c'_{pr}}{U_r} \left\{ \frac{1}{1-\beta} \log_e \left[(1-\beta) \frac{1 + \psi_b(\tau_1 - 1) - \tau_r}{\tau_3 - \tau_r} + \beta \right] - A \log_e \psi_b \right\}. \tag{11.101}$$

By computing the derivative of C with respect to ψ_b and setting the derivative equal to 0, we obtain

$$\frac{1}{1-\beta}\frac{1}{(1-\beta)\dfrac{1+\psi_\mathrm{b}(\tau_1-1)-\tau_\mathrm{r}}{\tau_3-\tau_\mathrm{r}}+\beta}\frac{(1-\beta)(\tau_1-1)}{\tau_3-\tau_\mathrm{r}}-\frac{A}{\psi_\mathrm{b}}=0. \tag{11.102}$$

Then,

$$\frac{\tau_1-1}{(1-\beta)[1+\psi_\mathrm{b}(\tau_1-1)-\tau_\mathrm{r}]+\beta(\tau_3-\tau_\mathrm{r})}=\frac{A}{\psi_\mathrm{b}}. \tag{11.103}$$

After a series of steps that are not shown here, based on (11.103) we obtain the following equation for ψ_b:

$$\psi_\mathrm{b}=A\frac{1-\tau_\mathrm{r}+\beta(\tau_3-1)}{(\tau_1-1)[1-A(1-\beta)]}. \tag{11.104}$$

We introduce factors δ and ε given by

$$\delta=\frac{1-\tau_3}{\tau_1-1}=\frac{t_\mathrm{s}-t'_3}{t_\mathrm{s}}\frac{t_\mathrm{s}}{t'_1-t_\mathrm{s}}=\frac{t_\mathrm{s}-t'_3}{t'_1-t_\mathrm{s}}, \tag{11.105}$$

$$\varepsilon=\frac{1-\tau_\mathrm{r}}{\tau_1-1}=\frac{t_\mathrm{s}-t''_1}{t_\mathrm{s}}\frac{t_\mathrm{s}}{t'_1-t_\mathrm{s}}=\frac{t_\mathrm{s}-t''_1}{t'_1-t_\mathrm{s}}. \tag{11.106}$$

From (11.104),

$$\psi_b=A\frac{\varepsilon-\beta\delta}{1+A(\beta-1)}. \tag{11.107}$$

Moreover, based on (11.92)

$$\psi_\mathrm{r}=\frac{\varepsilon-\delta}{\varepsilon-\psi_\mathrm{b}}. \tag{11.108}$$

Once the values of t'_1 and t_s are known and the desired value of t'_3 is set in advance, it is possible to compute the values of δ and ε based on (11.105) and (11.106).

After calculation of the values of A and β based on the unitary costs c_b and c_r and the presumable values of $U_\mathrm{b}, U_\mathrm{r}, c'_\mathrm{pb}$, and c'_pr (values that need to be checked and refined later on based on the results of the calculation for optimization), from (11.107) we obtain the optimal value of ψ_b that makes it possible through (11.80) to compute the corresponding temperature t'_2 of the flue gas at the inlet of the regenerator. Moreover, surface S_b of the bank is obtained through (11.97) and (11.82), whereas surface S_r of the regenerator is obtained through (11.108), (11.93), and (11.85). Note that based on (11.108), $\varepsilon > \delta$ is a requirement. In addition, the values of ψ_b greater than one are insignificant because in that case based on (11.80) $t'_2 > t'_1$.

Finally, some values have theoretical significance, yet no practical validity, as far as logical criteria to construct the plant. In that case, the results simply highlight a tendency to be followed. However, they do not provide concrete data to optimize the distribution of the two surfaces in question. The following is an example.

We assume a water-tube generator with a 14,000 kW power working under absolute pressure of 21 bar that should be equipped with an air heater. The inlet temperature of the gas in the tube bank is equal to 1000°C, and the exit temperature of the gas from the heater is equal to 180°C. Moreover, given the pressure, the steam temperature is equal to 215°C, whereas the room temperature is 20°C. Therefore,

$$\begin{aligned} t'_1 &= 1000\,^\circ\mathrm{C} \\ t'_3 &= 180\,^\circ\mathrm{C} \\ t_s &= 215\,^\circ\mathrm{C} \\ t''_1 &= 20\,^\circ\mathrm{C} \\ \delta &= \frac{215-180}{1000-215} = 0.0446 \\ \varepsilon &= \frac{215-20}{1000-215} = 0.2484. \end{aligned}$$

The mass flow rates of gas and air are equal to

$$\begin{aligned} M' &= 6.48\,\mathrm{kg/s} \\ M'' &= 6.111\,\mathrm{kg/s}. \end{aligned}$$

As far as the specific heat, we can assume the following values:

$$\begin{aligned} c'_{\mathrm{pb}} &= 1218\,\mathrm{J/kgK} \\ c'_{\mathrm{pr}} &= 1109\,\mathrm{J/kgK} \\ c'' &= 1009\,\mathrm{J/kgK}. \end{aligned}$$

We also assume that the overall heat transfer coefficients are, respectively, equal to

$$\begin{aligned} U_{\mathrm{b}} &= 70\,\mathrm{W/m^2K} \\ U_{\mathrm{r}} &= 22\,\mathrm{W/m^2K}. \end{aligned}$$

Finally, we assume that the ratio between unitary cost of surface of both bank and heater is as follows:

$$\frac{c_{\mathrm{b}}}{c_{\mathrm{r}}} = 0.8.$$

Based on (11.100)

$$A = 0.8\frac{1218\times 22}{1109\times 70} = 0.276.$$

Based on (11.86)

$$\beta = \frac{6.48\times 1109}{6.111\times 1009} = 1.165.$$

Therefore, based on (11.107)

$$\psi_{\mathrm{b}} = 0.276\frac{0.2484 - 1.165\times 0.0446}{1+0.276\,(1.165-1)} = 0.05186.$$

Table 11.2 Influence of ratio c_b/c_r

c_b/c_r	0.6	0.8	1.0	1.2
A	0.207	0.276	0.345	0.414
ψ_b	0.0393	0.0519	0.0641	0.0761
ψ_r	0.7084	0.6787	0.6522	0.6280
t'_2	245.8	255.7	265.3	274.7
S_b	364.9	333.6	309.8	290.4
S_r	139.2	161.0	182.3	203.6

Moreover, based on (11.108)

$$\psi_r = \frac{0.2484 - 0.0446}{0.2484 + 0.05286} = 0.6787$$

Then, based on (11.80)

$$t'_2 = 215 + 0.05186\,(1000 - 215) = 255.7^\circ\text{C}.$$

The optimal exit temperature of the flue gas from the boiler is therefore higher by about 40°C than the steam temperature.

Now, let us determine which surfaces are necessary. For the bank, based on (11.97) and (11.82)

$$\gamma_b = -\log_e 0.05186 = 2.939$$

$$S_b = \frac{2.959 \times 6.48 \times 1218}{70} = 333.63\,\text{m}^2.$$

For the heater, based on (11.93) and (11.85)

$$\gamma_r = \frac{1}{1 - 1.165} \log_e \left(\frac{1 - 1.165}{0.6787} + 1.165 \right) = 0.4929$$

$$S_r = \frac{0.4929 \times 6.48 \times 1109}{22} = 161.01\,\text{m}^2.$$

It may be interesting to analyze the impact of ratio c_b/c_r on the value of temperature t'_2 and on surfaces S_b and S_r of tube bank and air heater. Table 11.2 below highlights its influence.

11.5 Optimized Sizing of the Waste-Heat Generator

In the case of a traditional steam generator, optimization consists of minimizing costs with respect to a set and constant energy output. The costs consist of the yearly cost for fuel and energy required to run the auxiliaries of the generator, plus the

yearly updated cost of the plant. Thus, it is a question of selecting the generator (with or without a regenerator, economizer, or air heater) to minimize them.

As we pointed out in Sect. 11.2, to achieve this goal it is crucial to find out either the known or the presumed yearly load diagram. This implies collaboration between constructor and user to identify actual working conditions of the generator itself. On the other hand, in the case of a waste-heat generator consisting only of a boiler, or a boiler combined with a heat regenerator after the boiler, optimization is to maximize profits.

In the case of a traditional steam generator, the produced energy is an invariant. Thus, the derived financial profit is an invariant. The issue to resolve consists of achieving this profit at minimum cost, especially through a reduction of burned fuel conditioned by the ensuing greater cost of the plant.

In the case of a waste-heat generator, the warm gas making up the heat source used to produce energy costs zero instead. Greater or smaller exploitation of their latent heat produces a bigger or smaller amount of energy matched by a certain gross yearly variable profit. This production of energy has a cost represented for by the yearly updated cost of the plant. The difference between the gross profit from the energy output and this cost of the plant represents the net profit. The issue is to maximize the latter.

Generally, we do our analysis in reference to a waste-heat generator consisting of a boiler and a regenerator (usually an economizer). In that case, the analysis must be done with reference to the regenerator. The conclusions we will draw are easily transferable to a boiler without a regenerator (simplified computation). As usual, t'_1 and t'_2 stand for the temperatures of the heating fluid at inlet and exit of a generic regenerator, respectively, whereas t''_1 and t''_2 stand for the temperatures of the heated fluid at inlet and exit, respectively. Furthermore, M' and M'' stand for the mass flow rates of both heating and heated fluids, c'_{p} for the mean specific isobaric heat of the heating fluid between t'_1 and t'_2, and c''_{p} for the mean specific isobaric heat of the heated fluid between t''_2 and t''_1.

Finally, U stands for the overall heat transfer coefficient, S for the surface of the regenerator, and η_{he} for the efficiency of the heat exchange. In our specific case, the value of the latter is very close to one, as it is influenced only by the heat loss by radiation and convection through the outside walls of the regenerator itself.

Assuming that (Sect. 8.12)

$$\psi = \frac{t'_2 - t''_1}{t'_1 - t''_1}, \tag{11.109}$$

$$\beta = \frac{\eta_{\mathrm{he}} M' c'_{\mathrm{p}}}{M'' c''_{\mathrm{p}}}, \tag{11.110}$$

$$\gamma = \frac{US}{\eta_{\mathrm{he}} M' c'_{\mathrm{p}}}, \tag{11.111}$$

we know that with fluids in parallel flow

$$\psi = \frac{\mathrm{e}^{-(1+\beta)\gamma} + \beta}{1+\beta}. \tag{11.112}$$

Considering the value of β practically constant as surface S and therefore γ vary

$$\frac{\mathrm{d}\psi}{\mathrm{d}\gamma} = -\mathrm{e}^{-(1+\beta)\gamma} = \beta - (1+\beta)\,\psi. \tag{11.113}$$

As variations of S imply variations of exit temperature of the gas from regenerator t'_2, recalling (11.109) we have

$$\frac{\mathrm{d}\psi}{\mathrm{d}\gamma} = \frac{1}{t'_1 - t''_1}\frac{\mathrm{d}t'_2}{\mathrm{d}\gamma}. \tag{11.114}$$

A comparison of (11.113) and (11.114) leads to

$$\frac{\mathrm{d}t'_2}{\mathrm{d}\gamma} = \left(t'_1 - t''_1\right)\left[\beta - (1+\beta)\frac{t'_2 - t''_1}{t'_1 - t''_1}\right]. \tag{11.115}$$

After a series of steps from (11.115), we obtain

$$\frac{\mathrm{d}t'_2}{\mathrm{d}\gamma} = -\left(t'_2 - t''_1\right)\left(1 - \beta\frac{t'_1 - t'_2}{t'_2 - t''_1}\right). \tag{11.116}$$

Recalling (11.110) and assuming that

$$\varepsilon = 1 - \frac{\eta_{\mathrm{he}} M' c'_{\mathrm{p}}}{M'' c''_{\mathrm{p}}}\frac{t'_1 - t'_2}{t'_2 - t''_1} \tag{11.117}$$

from (11.116), we obtain

$$\frac{\mathrm{d}t'_2}{\mathrm{d}\gamma} = -\varepsilon\left(t'_2 - t''_1\right). \tag{11.118}$$

As far as fluids in counterflow, we know that

$$\psi = \frac{1-\beta}{\mathrm{e}^{(1-\beta)\gamma} - \beta}. \tag{11.119}$$

Then,

$$\frac{\mathrm{d}\psi}{\mathrm{d}\gamma} = -\psi^2 \mathrm{e}^{(1-\beta)\gamma} = -\beta\,\psi^2 - (1-\beta)\,\psi. \tag{11.120}$$

Recalling (11.114), we have

$$\frac{\mathrm{d}t'_2}{\mathrm{d}\gamma} = \left(t'_1 - t''_1\right)\left[-\beta\,\psi^2 - (1-\beta)\,\psi\right]. \tag{11.121}$$

From (11.121) through a series of steps we obtain

$$\frac{\mathrm{d}t'_2}{\mathrm{d}\gamma} = -\left(t'_2 - t''_1\right)\left(1 - \beta\frac{t'_1 - t'_2}{t'_1 - t''_1}\right). \tag{11.122}$$

Recalling (11.110) and assuming that

$$\varepsilon = 1 - \frac{\eta_{\text{he}} M' c'_{\text{p}}}{M'' c''_{\text{p}}} \frac{t'_1 - t'_2}{t'_1 - t''_1}, \tag{11.123}$$

from (11.122), we obtain

$$\frac{\mathrm{d}t'_2}{\mathrm{d}\gamma} = -\varepsilon \left(t'_2 - t''_1\right). \tag{11.118 bis}$$

Both in the case of fluids in parallel flow and counterflow, the derivative of t'_2 with respect to γ is given by (11.118), of course by varying the equation of the dimensionless factor ε.

Considering the value of η_{he} and of the ratio U/c'_{p} practically constant with respect to variations of the surface, and recalling (11.111), we obtain

$$\frac{\mathrm{d}\gamma}{\mathrm{d}S} = \frac{U}{\eta_{\text{he}} M' c'_{\text{p}}}. \tag{11.124}$$

Therefore, based on (11.118)

$$\frac{\mathrm{d}t'_2}{\mathrm{d}S} = \frac{\mathrm{d}t'_2}{\mathrm{d}\gamma} \frac{\mathrm{d}\gamma}{\mathrm{d}S} = -\frac{\varepsilon U}{\eta_{\text{he}} M' c'_{\text{p}}} \left(t'_2 - t''_1\right). \tag{11.125}$$

The heat per time unit $\mathrm{d}q$ transferred by the gas, due to a variation in temperature $\mathrm{d}t'_2$ and indicating the specific heat at temperature t'_2 with c'_{p2}, is given by

$$\mathrm{d}q = M' c'_{\text{p2}} \mathrm{d}t'_2. \tag{11.126}$$

Thus, recalling (11.125)

$$\frac{\mathrm{d}q}{\mathrm{d}S} = \frac{\varepsilon U c'_{\text{p2}}}{\eta_{\text{he}} c'_{\text{p}}} \left(t'_2 - t''_1\right). \tag{11.127}$$

Factoring in efficiency η_{he} and indicating the regenerated energy/year with E, we have

$$\frac{\mathrm{d}E}{\mathrm{d}S} = \int \eta_{\text{he}} \frac{\mathrm{d}q}{\mathrm{d}S} \mathrm{d}\theta, \tag{11.128}$$

where θ stands for time and the integral is extended to a year.

Then, based on (11.117)

$$\frac{\mathrm{d}E}{\mathrm{d}S} = \int \frac{\varepsilon U c'_{\text{p2}}}{c'_{\text{p}}} \left(t'_2 - t''_1\right) \mathrm{d}\theta. \tag{11.129}$$

For fluids in parallel flow

$$\phi = \frac{U c'_{\text{p2}}}{c'_{\text{p}}} \left(1 - \frac{\eta_{\text{he}} M' c'_{\text{p}}}{M'' c''_{\text{p}}} \frac{t'_1 - t'_2}{t'_2 - t''_1}\right) \left(t'_2 - t''_1\right), \tag{11.130}$$

and for those in counterflow

$$\phi = \frac{Uc'_{\mathrm{p}2}}{c'_{\mathrm{p}}}\left(1 - \frac{\eta_{\mathrm{he}} M' c'_{\mathrm{p}}}{M'' c''_{\mathrm{p}}} \frac{t'_1 - t'_2}{t'_1 - t''_1}\right)\left(t'_2 - t''_1\right). \tag{11.131}$$

If the generator consists only of a boiler without regenerator, the reference must obviously be to the boiler, and the fluid receiving heat is evaporating water, so $c''_{\mathrm{p}} = \infty$; by indicating the steam temperature with t_{s}, instead of (11.130) and (11.131), we obtain

$$\phi = \frac{Uc'_{\mathrm{p}2}}{c'_{\mathrm{p}}}\left(t'_2 - t_{\mathrm{s}}\right). \tag{11.132}$$

In any case, we may write that

$$\frac{\mathrm{d}E}{\mathrm{d}S} = \int \phi \mathrm{d}\theta. \tag{11.133}$$

If V_E indicates the global financial value of energy E produced per year and v_{E} the marginal financial value of this energy, we have

$$\frac{\mathrm{d}V_E}{\mathrm{d}S} = \frac{\mathrm{d}V_E}{\mathrm{d}E}\frac{\mathrm{d}E}{\mathrm{d}S} = v_E \frac{\mathrm{d}E}{\mathrm{d}S} = v_E \int \phi \mathrm{d}\theta. \tag{11.134}$$

Now, if c_{s} stands for the yearly marginal updated cost of the surface unit of the regenerator, we have

$$c_{\mathrm{S}} = \frac{\mathrm{d}C_{\mathrm{S}}}{\mathrm{d}S}, \tag{11.135}$$

where C_{s} stands for the yearly updated cost of the waste-heat generator.

Therefore, the marginal profit u_{s} of the plant is given by

$$u_{\mathrm{S}} = \frac{\mathrm{d}\left(V_E - C_{\mathrm{S}}\right)}{\mathrm{d}S} = v_E \int \phi \mathrm{d}\theta - c_{\mathrm{S}}. \tag{11.136}$$

The maximization of profits is achieved when the marginal profit is zero. Thus, based on (11.136), the condition for maximizing profits is represented by

$$\int \phi \mathrm{d}\theta = \frac{c_{\mathrm{S}}}{v_E}. \tag{11.137}$$

Equation (11.137) synthesizes the parameters for maximum profits. We now discuss how to proceed in practice.

If the issue is optimization of a waste-heat boiler not equipped with an air heater or an economizer, the process is as follows.

After defining the size of a boiler with surface S as well as determining its working pressure, the value of t_{s} is known, and depending on the mass flow rate of the gas M' and on their inlet temperature t'_1, it is possible to determine the values of U, t'_2, c'_{p}, and $c'_{\mathrm{p}2}$. Then, it is possible to compute the value of ϕ as a function of M' through (11.131). Once the diagram of M' as a function of time θ during the

year is known, it is possible to correlate the value of ϕ to time and to execute the integration in (11.137).

The value of c_s must be determined at this point. Generally, it is possible to adopt a constant value because the updated yearly cost of the boiler can be expressed according to the following:

$$C_S = C_f + c_S S. \tag{11.138}$$

The cost consists of the term C_f that is independent from the surface and from a term proportional to the surface itself.

Besides the actual boiler and its auxiliaries, the cost must, of course, include the structures required to its layout and the necessary connections, the chimney or the gas duct between boiler and existing chimney, and so on. Specifically, the cost of the fan may be expressed with sufficient approximation with a binomial equation comprehensive of a fixed term and a term proportional to the surface of the boiler. Equation (11.138) can generally be considered appropriate to represent C_s and makes it possible to compute the constant value of c_s. As far as the marginal financial value of the energy output, it may be possible to adopt a constant value if it is independent from the output. More frequently, the marginal value will be decreasing with the output, and for certain values of the latter it may even be zero, because there will be no interest in producing energy beyond a certain level.

To use (11.137), we must assume that the value of v_E can be correlated to the total yearly output of the waste-heat generator.

Note that the energy in this case is given by

$$E = \int \eta_{he} M' c'_p \left(t'_1 - t'_2\right) \mathrm{d}\theta. \tag{11.139}$$

Once the values of M' and t'_1 versus time variations are known, the values of η_{he} are defined and the values of t'_2 and c'_p are computed, it is possible to calculate the output through (11.139).

At this point, after identifying the correlation between v_E and E, it is possible to compute the ratio c_s/v_E included in (11.137). If the integral included in it has a higher value compared to this ratio, surface S is insufficient to maximize profits. Obviously, if the value is smaller, the boiler has an excessive surface. So the issue is to adopt a different value of the surface and to repeat calculations until the equality of the two terms of (11.137) is achieved. This will be easy to accomplish through diagrams where they are a function of the surface.

If the generator is equipped with an air heater or an economizer and the goal is to determine their optimal surface, this is the regenerator of reference. The heat regenerator with surface S is defined geometrically. U, t'_2, c'_p, and c''_p are computed by varying the mass flow rate M' of the gas and the corresponding mass flow rate M'' of the air or the water, once the value t'_1 of the gas temperature at the inlet of the regenerator (exit temperature from the boiler) and the value t''_1 of the inlet temperature of air or water are known.

Based on the value of η_{he}, ϕ is subsequently computed based on (11.130) or (11.131) depending on M'.

After the M' diagram as a function of time is known, it is possible to correlate ϕ to the time and to calculate the integral shown in (11.137). Otherwise, one follows the procedure described above, keeping in mind that c_s stands for the updated marginal cost of the unit surface of the regenerator and that v_E must be correlated to its output if (11.139) is used. Nothing prevents the designer from referring to total output from boiler and from the regenerator because this is the marginal value. Only the definition of v_E will be different but, of course, the value to introduce into the calculation of c_s/v_E does not change. As far as the value of v_E, it is worthwhile noting that by increasing the value of S (and this is true, of course, even in the case of a boiler), the pressure drops will increase as well. Therefore, an increase in output is matched by an increase in energy input to run the fan. This must be factored in by adequately decreasing the value of v_E. In any case, the influence is modest, so that even relatively gross evaluation criteria may be applied. Equation (11.137) also lends itself to a first orientation about the optimal surface (this being the most significant practical aspect), thus allowing the designer to avoid the sizing and computation of boilers and regenerators outside the optimal range.

In the case of a waste-heat regenerator without economizer and without air heater, it is possible to proceed as follows.

Based on the variations over time of the values of M' and t'_1, it is possible to identify the mean yearly values. After setting the expected values of U and η_{he} in advance, one adopts an arbitrary value for t'_2. ϕ is computed based on (11.130) and ignoring the ratio c'_{p2}/c'_p. Assuming that θ_0 is the yearly runtime of the boiler, the output is equal to

$$E = \eta_{he} M' c'_p \left(t'_1 - t'_2\right) \theta_0, \tag{11.140}$$

where M' and t'_2 are the mean values mentioned above.

The value of v_E is determined based on E. Once the value of c_s is known, boiler optimization requires that

$$\phi \theta_0 = \frac{c_S}{v_E}. \tag{11.141}$$

If this is not the case, one varies the value of t'_2 until (11.141) is verified.

At this point, when the values of t'_1, t'_2, and t''_1 are defined, we know that the mean logarithmic temperature difference is given by

$$\Delta t_m = \frac{t'_1 - t'_2}{\log_e \dfrac{t'_1 - t''_1}{t'_2 - t''_1}}. \tag{11.142}$$

In addition, the regenerated heat by the time unit is equal to

$$q = \frac{E}{\theta_0}. \tag{11.143}$$

Then,

$$S = \frac{q}{U \Delta t_m} = \frac{E}{U \theta_0 \Delta t_m}. \tag{11.144}$$

The surface S computed in this way is certainly quite close to the optimal one. It also helps to refine the analysis by examining the values in its proximity, as described above.

In the case of an economizer or air heater, the methodology is substantially identical except for all appropriate adjustments.

This page intentionally left blank

Chapter 12
Computation Examples

12.1 General Considerations

The author developed a series of computation programs based on the topics presented in previous chapters.

The simplest programs are about physical characteristics of water, steam, flue gas, and air. Moreover, they compute the heat transfer coefficient of the different fluids both inside and outside the tubes, as well as the heat radiated by the flue gas, and so on.

More articulated programs do thermodynamic (and fluid dynamic, if necessary) computation of the different parts of a generator, such as furnace, flue, steam-generating bank, superheater, economizer, and air heater. Various constructive scenarios (smooth tubes, finned tubes, and cast-iron finned tubes) are considered for the two heat regenerators.

Finally, complex programs were developed to compute the entire generator (water-tube generators, smoke-tube generators, and waste-heat generators) including potential superheater, economizer, or air heater.

The following sections show some computation examples using these programs.

12.2 Water-Tube Generator

This is a two-drum generator fed by fuel oil for the output of 13 t/h of superheated steam at 36 bar and 420°C (Fig. 12.1). The furnace with entirely screened walls is followed by a cavity preceding the superheater. The latter consists of two banks (secondary and primary with water injection between them) and occupies the first section of the second passage of the flue gas. The second section of this pass is occupied by the steam-generating tube bank. Finally, the third passage of the gas is entirely occupied by the steam-generating bank. The boiler is equipped with an economizer with steel tubes coated with a cast-iron finned tube.

D. Annaratone, *Steam Generators*, DOI: 10.1007/978-3-540-77715-1_12,

© Springer-Verlag Berlin Heidelberg 2008

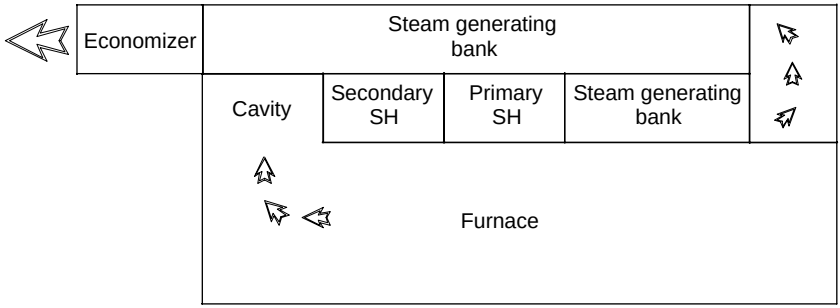


Fig. 12.1 Scheme of two-drum convection generator

```
Water-tube generator (boiler and economizer with
cast iron finned tubes)

   Generator nominal power                          (kW)      =   10200.
   Absolute pressure in the drum                    (bar)     =   37.1
   Absolute pressure at the outlet                  (bar)     =   36.0
   Load                                             (%)       =   100.
   Steam output                                     (kg/h)    =   12995.
   Room temperature                                 (°C)      =   20.

   Number of burners                                          =   1
   Fuel = fuel oil
   Composition (% in mass) :
   C=85.5 - H=11.7 - S= 2.8
   Net heat value                                   (kJ/kg)   =   40600.
   Fuel consumption                                 (kg/h)    =   982.9
   Fuel temperature                                 (°C)      =   100.
   Air flow rate                                    (kg/s)    =   4.568
   Air index                                                  =   1.20
   Air temperature at the burner                    (°C)      =   20.0

   Flue gas flow rate                               (kg/s)    =   4.841
   Density under normal conditions                  (kg/Nm3)  =   1.305
   Moisture in mass                                 (%)       =   6.40
   Partial pressure of CO2                          (atm)     =   .1174
   Partial pressure of H2O                          (atm)     =   .0957

   Feed water temperature                           (°C)      =   105.0
   Feed water enthalpy                              (kJ/kg)   =   442.83
   Saturated water enthalpy                         (kJ/kg)   =   1065.73
   Saturated steam temperature                      (°C)      =   245.9
   Dry saturated steam enthalpy                     (kJ/kg)   =   2801.43
   Water-vapor ratio                                (%)       =   98.0
   Saturated steam enthalpy                         (kJ/kg)   =   2766.71

   Furnace:

   Furnace length                                   (m)       =   5.426
   Furnace width                                    (m)       =   1.927
   Furnace mean height                              (m)       =   2.743
   Bank wall length                                 (m)       =   4.980
   Useful length of bank tubes                      (m)       =   2.300
   Length of bottom, external wall, top             (m)       =   6.438
   Efficiency of the horizontal bottom wall                   =   .400
   Efficiency of the burner wall                              =   .850
   Efficiency of the rear wall                                =   1.000
```

Furnace radiated surface	(m^2)	=	49.89
Superficial thermal load	(kW/m^2)	=	223.0
Cross-section thermal load	(kW/m^2)	=	2104.8
Furnace volume	(m^3)	=	28.68
Volumetric thermal load	(kW/m^3)	=	387.9
Flame length	(m)	=	4.80
Furnace exit temperature	(°C)	=	976.8
Heat transfer in the furnace	(kW)	=	5637.1

Cavity:

Cavity wall surface	(m^2)	=	2.28
Bank projected surface	(m^2)	=	1.21
Fluid temperature in the bank	(°C)	=	415.
Mean beam length of the flue gas	(m)	=	.410
Cavity exit temperature of flue gas	(°C)	=	967.7
Heat transfer to the walls	(kW)	=	38.73
Heat transfer to the superheater	(kW)	=	17.46
Heat transfer in the cavity	(kW)	=	56.19

Tube banks		:	1	2	3	4
Bank type (steam generating, SH)		:	SH	SH	S.G	S.G
Outside diameter of the tubes	(mm)	=	38.0	38.0	51.0	51.0
Tube thickness	(mm)	=	3.60	3.60	3.20	3.20
Outside surface of the bank	(m^2)	=	20.06	36.10	46.17	71.95
Lateral walls surface (steam generating)	(m^2)	=	1.68	3.78	6.90	12.74
Total surface of the steam generating tubes	(m^2)	=	.00	.00	53.07	84.69
Cross-section area for flue gas flow	(m^2)	=	.538	.538	.691	.537
Actual or conventional length of the tubes	(m)	=	2.100	2.100	.000	.000
Tube number per row		=	8/ 8	8/ 8	5/ 5	4/ 4
Row number		=	10	18	25	50
Arrangement type (in-line, staggered)		:	LINE	LINE	LINE	LINE
Transversal pitch	(mm)	=	70.0	70.0	105.0	105.0
Longitudinal pith	(mm)	=	80.0	80.0	100.0	100.0
Arrangement factor f_a (heat transfer)		=	1.006	1.006	.998	1.003
Depth factor f_d (heat transfer)		=	1.000	1.000	1.000	1.000
Ratio x_r/d_o for gas radiation		=	4.207	4.207	4.420	4.420
Fluids (parallel-, counterflow) (for SH)		:	COUNT	COUNT		
Cross-section area for steam (for SH)	(m^2)	=	.0119	.0119	.0000	.0000
Heat transfer coefficient (convection)	(W/m^2K)	=	110.64	102.06	70.54	78.90
Heat transfer coefficient (radiation)	(W/m^2K)	=	10.81	7.93	6.32	4.15
Total heat transfer coefficient of flue gas	(W/m^2K)	=	121.44	109.99	76.87	83.05
Heat transfer coefficient of internal fluid	(W/m^2K)	=	1060.	954.	12000.	12000.
Overall heat transfer coefficient	(W/m^2K)	=	106.41	96.29	75.87	81.89
Flue gas inlet temperature	(°C)	=	967.7	772.7	538.4	389.3
Flue gas outlet temperature	(°C)	=	772.7	538.4	389.3	286.4
Heat transfer in the bank	(kW)	=	1195.1	1377.9	842.1	564.5
Number of rows		=	10	18	25	50
Arrangement factor f_a (pressure drop)		=	.280	.279	.210	.208
Depth factor f_d (pressure drop)		=	1.000	1.000	1.000	1.000

Mass velocity of the flue gas	(kg/m^{2}s)	=	9.00	9.00	7.01	9.01
Mean flue gas velocity	(m/s)	=	28.81	23.29	14.41	15.39
Number of Reynolds		=	7721.	8796.	10727.	15770.
Pressure drop of the flue gas	(Pa)	=	362.2	523.4	263.1	711.4
Pressure drop of the steam	(bar)	=	.339	.519	.000	.000

Mass of the steam generating banks	(kg)	=	2781.
Mass of the superheater tubes	(kg)	=	1437.

Superheater:

Superheater outside surface	(m^2)	=	56.16
Steam flow rate in the primary SH	(kg/h)	=	12230.0
Inlet pressure in the primary SH	(bar)	=	36.9
Outlet pressure in the primary SH	(bar)	=	36.4
Exchange efficiency in the primary SH	(%)	=	88.22
Outlet steam temperature	(°C)	=	358.7
Outlet steam enthalpy	(kJ/kg)	=	3124.51
Heat transfer to the primary SH	(kW)	=	1215.54
Heat transfer to the lateral walls	(kW)	=	162.36
Steam flow rate in the secondary SH	(kg/h)	=	12995.4
Inlet pressure in the secondary SH	(bar)	=	36.4
Outlet pressure from the generator	(bar)	=	36.0
Exchange efficiency in the secondary SH	(%)	=	89.73
Inlet steam temperature	(°C)	=	297.2
Inlet steam enthalpy	(kJ/kg)	=	2966.55
Exit steam temperature from the generator	(°C)	=	420.0
Exit steam enthalpy	(kJ/kg)	=	3268.44
Heat transfer to the secondary SH	(kW)	=	1089.92
Heat transfer to the lateral walls	(kW)	=	122.83
Density of the exit steam	(m^3/kg)	=	.0849
Velocity of the exit steam	(m/s)	=	25.7
Pressure drop in the superheater	(bar)	=	.858
Injection water temperature	(°C)	=	105.0
Injection water enthalpy	(kJ/kg)	=	442.83
Flow rate of the injection water	(kg/h)	=	765.4

Generator efficiency:
Generator without economizer:

Sensible heat loss	(%)	=	12.59
External radiation heat loss	(%)	=	.62
Miscellaneous heat losses (umburned matter)	(%)	=	.50
Boiler efficiency	(%)	=	86.28

Generator with economizer:

Sensible heat loss	(%)	=	6.74
Boiler heat loss by external radiation	(%)	=	.62
Miscellaneous heat losses (unburned matter)	(%)	=	.50
Economizer heat loss by external radiation	(%)	=	.12
Generator efficiency	(%)	=	92.02

Pressure drops of the flue gas:

Flue gas pressure drop in the boiler	(Pa)	=	1860.1
Flue gas pressure drop in the economizer	(Pa)	=	276.7
Total pressure drop in the generator	(Pa)	=	2136.8

Fan required power by pressure drops	(kW)	=	8.101

Economizer with steel internal tubes and external cast iron finned tubes

Tubes outside surface	(m^2)	=	221.03
Steel tube outside diameter	(mm)	=	38.0
Steel tube thickness	(mm)	=	4.0
Steel type		=	carb.st.

Steel tube mean temperature	(°C)	=	147.1
Steel thermal conductivity	(W/mK)	=	49.52
Presumed thermal resistance between steel tube and cast iron finned tube	(m^2K/W)	=	.00100
Cast iron tube outside diameter	(mm)	=	52.0
Cast iron tube thickness	(mm)	=	7.0
Fin height	(mm)	=	23.0
Bottom fin thickness	(mm)	=	5.0
Top fin thickness	(mm)	=	2.5
Fin pitch	(mm)	=	12.0
Fin mean temperature	(°C)	=	170.1
Fin maximum temperature at the top	(°C)	=	220.7
Cast iron thermal conductivity	(W/mK)	=	40.00
Fin efficiency factor		=	.783
Isolated fin theoretical efficiency factor		=	.834
Finned tubes length	(m)	=	2.000
Number of tubes per row		=	8
Number of rows		=	13
Transversal pitch	(mm)	=	105.
Longitudinal pitch	(mm)	=	105.
Fluids (parallel-, counterflow)		:	COUNT
Tube arrangement (in-line, staggered)		:	LINE
Heat exchange efficiency	(%)	=	98.0

Flue gas:

Flow rate	(kg/s)	=	4.841
Density in normal condition	(kg/Nm^3)	=	1.305
Moisture in mass	(%)	=	6.40
Cross-section area for gas flow	(m^2)	=	.618
Heat transfer coefficient of flue gas	(W/m^2K)	=	64.82
Inlet temperature	(°C)	=	286.4
Outlet temperature	(°C)	=	164.9
Mass velocity	(kg/m^2s)	=	7.83
Mean velocity	(m/s)	=	10.97
Number of Reynolds		=	16300.
Flue gas pressure drop	(Pa)	=	276.7

Water:

Flow rate	(kg/s)	=	3.397
Absolute pressure	(bar)	=	37.1
Tube number in parallel regarding the flow		=	8
Cross-section area for water flow	(m^2)	=	.0057
Water heat transfer coefficient	(W/m^2K)	=	5102.
Inlet temperature	(°C)	=	105.0
Inlet water enthalpy	(kJ/kg)	=	442.8
Outlet temperature	(°C)	=	149.0
Outlet water enthalpy	(kJ/kg)	=	630.0
Mass velocity	(kg/m^2s)	=	600.76
Exit water density	(kg/m^3)	=	919.6
Maximum velocity at exit	(m/s)	=	.65
Water pressure drop	(bar)	=	.050

Overall heat transfer coefficient	(W/m^2K)	=	30.81
Heat transfer in the economizer	(kW)	=	635.63

Mass of steel tubes of the economizer	(kg)	=	698.
Mass of the cast iron finned tubes	(kg)	=	4297.
Total tube mass of the economizer	(kg)	=	4995.

Stop - Program terminated.

Clearly, without the economizer, the efficiency of the generator would equal to 86.28%. The presence of the economizer increases efficiency up to 92%, that is, by almost 6 points.

12.3 Smoke-Tube Generator

This is a wet end plate generator fed by natural gas for the output of 7.8 t/h of saturated steam at 15 bar. The boiler is followed by an economizer made of steel finned tubes.

Smoke-tube generator (boiler and economizer with finned tubes)

Generator nominal power	(kW)	=	5000.
Boiler total outside surface	(m2)	=	211.46
Absolute pressure	(bar)	=	15.0
Load	(%)	=	100.
Steam output	(kg/h)	=	7793.
Type (wet end plate, dry end plate)		:	W.P.
Room temperature	(°C)	=	20.
Fuel: natural gas			
Fuel temperature	(°C)	=	20.
Composition (% in mass):			
C=72.4 - H=23.9 - N= 3.7			
Mass net heat value	(kJ/kg)	=	48000.
Volumetric net heat value	(kJ/Nm^3)	=	35941.
Mass consumption	(kg/h)	=	404.3
Volumetric consumption	(Nm^3/h)	=	539.9
Air temperature to the burner	(°C)	=	20.0
Air index		=	1.10
Air flow rate	(kg/s)	=	2.037
Flue gas flow rate	(kg/s)	=	2.149
Moisture in mass	(%)	=	11.66
Partial pressure of CO_2	(atm)	=	.0880
Partial pressure of H_2O	(atm)	=	.1730
Feed water temperature	(°C)	=	105.0
Feed water enthalpy	(kJ/kg)	=	441.19
Saturated water enthalpy	(kJ/kg)	=	844.66
Steam temperature	(°C)	=	198.3
Water vapor ratio	(%)	=	98.0
Steam enthalpy	(kJ/kg)	=	2750.99
Flue:			
Flue inside diameter	(mm)	=	1050.
Flue thickness	(mm)	=	15.
Flue length	(mm)	=	3737.
Back-flow chamber diameter	(mm)	=	1789.
Back-flow chamber length	(mm)	=	600.
Flue surface	(m^2)	=	12.33
Back-flow chamber surface	(m^2)	=	7.10
Superficial load of the flue	(kW/m^2)	=	437.3
Volumetric load of the flue	(kW/m^3)	=	1665.8

Load on the flue cross-section	(kW/m^2)	=	6225.
Flame length	(m)	=	3.53
Flame temperature	(°C)	=	1678.4
Flue exit temperature of the gas	(°C)	=	1140.2
Radiated heat in the flue	(kW)	=	2278.1
Convective heat in the flue	(kW)	=	100.4
Total heat transfer in the flue	(kW)	=	2378.5
Heat transfer in back-flow chamber	(kW)	=	233.18

Flue gas convective sections		:	1	2
Tube number		=	170	142
Tube outside diameter	(mm)	=	54.0	54.0
Tube thickness	(mm)	=	2.90	2.90
Tube length	(mm)	=	3737.	4457.
Tube inside surface	(m^2)	=	96.20	95.84
Cross-section area for gas passage	(m^2)	=	.3102	.2591
Heat transfer coefficient (convection)	(W/m^2K)	=	36.12	37.68
Heat transfer coefficient (radiation)	(W/m^2K)	=	3.95	1.65
Total heat transfer coefficient	(W/m^2K)	=	40.07	39.33
Evaporating water heat transfer coefficient	(W/m^2K)	=	6000.	6000.
Over-all heat transfer coefficient	(W/m^2K)	=	39.73	39.01
Flue gas inlet temperature	(°C)	=	1061.6	415.3
Flue gas outlet temperature	(°C)	=	415.3	248.1
Heat transfer in the section	(kW)	=	1789.1	424.8
Flue gas mass velocity	(kg/m^2s)	=	6.93	8.29
Gas mean velocity	(m/s)	=	20.60	14.74
Number of Reynolds		=	8267.	13302.
Flue gas pressure drop	(Pa)	=	237.8	223.7

Mass of the flue	(kg)	=	1472.
Mass of the boiler tubes	(kg)	=	4635.

Generator efficiency:

Boiler (generator without economizer) :

Sensible heat loss	(%)	=	10.28
External radiation heat loss	(%)	=	.83
Miscellaneous heat losses (unburned matter)	(%)	=	.20
Boiler efficiency	(%)	=	88.70

Generator with economizer:

Sensible heat loss	(%)	=	6.17
External radiation heat loss (boiler)	(%)	=	.83
Miscellaneous heat losses (unburned matter)	(%)	=	.20
External radiation heat loss (economizer)	(%)	=	.04
Generator efficiency	(%)	=	92.76

Gas pressure drop in the boiler	(Pa)	=	461.5
Gas pressure drop in the economizer	(Pa)	=	92.3
Total pressure drop in the generator	(Pa)	=	553.8
Required fan power for pressure drops	(kW)	=	.936

Economizer with finned tubes:

Outside tube surface	(m^2)	=	96.46
Outside tube diameter	(mm)	=	48.0
Tube thickness	(mm)	=	3.00
Tube steel		=	carb.st.
Tube mean temperature	(°C)	=	131.2

```
   Tube steel thermal conductivity            (W/mK)  =   49.92
   Fin height                                 (mm)    =   19.0
   Fin thickness                              (mm)    =   1.5
   Fin number per meter                               =   200
   Fin steel                                          =   carb.st.
   Fin mean temperature                       (°C)    =   142.3
   Fin steel thermal conductivity             (W/mK)  =   49.64
   Fin maximum temperature (at the top)       (°C)    =   172.2
   Fin efficiency factor                              =   .824
   Isolated fin theoretical efficiency factor         =   .843
   Finned tube length                         (m)     =   1.800
   Number of tubes per row                            =   6
   Number of rows                                     =   5
   Transversal pitch s_t                      (mm)    =   92.
   Longitudinal pitch s_l                     (mm)    =   114.
   Fluids (parallel-, counterflow)                    :   COUNT.
   Tube arrangement (in-line, staggered)              :   LINE
   Heat exchange efficiency                   (%)     =   99.00


   Flue gas:

   Flow rate                                  (kg/s)  =   2.149
   Density in normal condition                (kg/Nm3)=   1.246
   Moisture in mass                           (%)     =   11.66
   Cross-section area for gas passage         (m2)    =   .352
   Heat transfer coefficient of flue gas      (W/m2K) =   40.46
   Gas inlet temperature                      (°C)    =   248.1
   Gas outlet temperature                     (°C)    =   158.4
   Flue gas mass velocity                     (kg/m2s)=   6.10
   Flue gas mean velocity                     (m/s)   =   8.55
   Number of Reynolds                                 =   12464.
   Gas pressure drop                          (Pa)    =   92.3

   Water:

   Flow rate                                  (kg/s)  =   2.165
   Absolute pressure                          (bar)   =   15.0
   Number of tubes in parallel for water flow         =   6
   Cross-section area for water passage       (m2)    =   .0083
   Water heat transfer coefficient            (W/m2K) =   2370.
   Inlet temperature                          (°C)    =   105.0
   Inlet water enthalpy                       (kJ/kg) =   441.2
   Outlet temperature                         (°C)    =   128.9
   Outlet water enthalpy                      (kJ/kg) =   542.4
   Mass velocity                              (kg/m2s)=   260.41
   Water density at the exit                  (kg/m3) =   936.2
   Maximum velocity at the exit               (m/s)   =   .28
   Water pressure drop                        (bar)   =   .003

   Overall heat transfer coefficient          (W/m2K) =   27.70
   Heat transfer in the economizer            (kW)    =   219.05

   Mass of the tubes of the economizer        (kg)    =   688.

Stop - Program terminated.
```

If the boiler were not followed by the economizer, its efficiency would be 88.7%. The presence of an economizer increases the efficiency up to 92.8%, that is, by 4 points. Note that because of combustion with natural gas, it is possible to considerably cool the flue gas in the economizer. In fact, the exit temperature of the gas is equal to 158.4°C.

12.4 Waste-Heat Generator

This generator is installed after a gas turbine (Fig. 12.2). 20 t/h of saturated steam at 55 bar and 460°C are produced by exploiting the sensible heat of the flue gas exiting the turbine and by the contribution of natural gas burned in the post-combustion chamber.

The flue gas coming from the turbine hits one superheater that is tertiary as far as the path of the steam. Then, there is a completely screened post-combustion chamber where natural gas is burned. This amount is equal to 55% of the burned fuel before the turbine. A small-steam generating tube bank and a superheater with two banks (secondary and primary) follow the post-combustion chamber. Finally, we have the main steam-generating tube bank with finned tubes. The final section of the generator consists of an economizer with finned tubes as well.

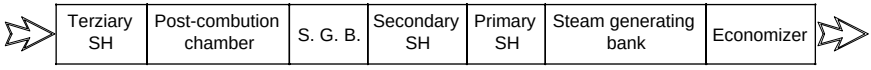


Fig. 12.2 Scheme of waste-heat generator with post-combustion chamber

```
Waste-heat generator installed after a gas turbine
(with post-combustion chamber)

Gas turbine:

Fuel burned before the gas turbine          (kg/h)   =   1300.0
Fuel mass composition:                      C (%)    =   72.40
                                            H (%)    =   23.92
                                            N (%)    =   3.68
Air index                                            =   3.00
Air relative humidity at 20 °C              (%)      =   40.0
Gas mass flow rate after the turbine        (kg/h)   =   66010.
Gas volumetric flow rate                    (Nm3/h)  =   51990.
Density under normal conditions             (kg/Nm3) =   1.270
Moisture in mass                            (%)      =   4.779
Partial pressure of CO2                     (atm)    =   .0338
Partial pressure of H2O                     (atm)    =   .0755
Gas exit temperature from gas turbine       (°C)     =   521.

Steam output and characteristics of water and steam:

Steam output                                (kg/h)   =   20115.
Absolute pressure in the drum               (bar)    =   57.5
Feed water temperature                      (°C)     =   105.0
Feed water enthalpy                         (kJ/kg)  =   444.34
Saturated water enthalpy                    (kJ/kg)  =   1199.73
Saturated steam temperature                 (°C)     =   272.8
Dry saturated steam enthalpy                (kJ/kg)  =   2787.50
Water vapor ratio                           (%)      =   99.0
Saturated steam enthalpy                    (kJ/kg)  =   2771.62
Water/steam mixture heat transfer coefficient(W/m2K) =   12000.
Global heat exchange efficiency             (%)      =   99.0

Superheater before the post-combustion chamber
(tertiary superheater):

Tube outside diameter                       (mm)     =   38.0
Tube thickness                              (mm)     =   4.00
```

Tube steel		:	carb.st.
Tube mean temperature	(°C)	=	454.0
Steel thermal conductivity	(W/mK)	=	41.88
Actual or conventional tube length	(m)	=	3.585
Number of tubes per row		=	21/21
Number of rows		=	6
Bank outside surface	(m^2)	=	53.93
Cross-section area for flue gas flow	(m^2)	=	3.398
Arrangement type (in-line, staggered)		:	STAGG.
Transversal pith	(mm)	=	81.2
Longitudinal pitch	(mm)	=	60.0
Arrangement factor f_a (heat transfer)		=	1.122
Depth factor f_d (heat transfer)		=	.950
Ratio x_r/d_0 for gas radiation		=	3.231
Fluids (parallel-, counterflow)		:	COUNT.
Number of tube in parallel for steam flow		=	21
Cross-section area for steam flow	(m^2)	=	.0148
Heat transfer coefficient (convection)	(W/m^2K)	=	77.71
Heat transfer coefficient (radiation)	(W/m^2K)	=	4.24
Total heat transfer coefficient	(W/m^2K)	=	81.95
Steam heat transfer coefficient	(W/m^2K)	=	1220.
Overall heat transfer coefficient	(W/m^2K)	=	76.83
Gas inlet temperature	(°C)	=	521.0
Gas outlet temperature	(°C)	=	508.5
Steam inlet temperature	(°C)	=	440.3
Steam inlet enthalpy	(kJ/kg)	=	3286.35
Steam temperature at the generator exit	(°C)	=	460.0
Steam exit enthalpy	(kJ (kg)	=	3334.20
Heat transfer to the tertiary superheater	(kW)	=	267.3
Number of rows		=	6
Arrangement factor f_a (pressure drop)		=	.414
Depth factor f_d (pressure drop)		=	1.051
Flue gas mass velocity	(kg/m^2s)	=	5.40
Flue gas mean velocity	(m/s)	=	21.89
Number of Reynolds		=	5813.
Flue gas pressure drop	(Pa)	=	86.4
Steam pressure drop	(bar)	=	.704
Mass of the tertiary superheater tubes	(kg)	=	1515.

Post-combustion chamber :

Tube wall surfaces (steam generating)	(m^2)	=	25.00
Smaller side of the chamber cross-section	(m)	=	1.500
Greater side of the chamber cross-section	(m)	=	3.500
Chamber length	(m)	=	2.500
Cross-section area for gas flow	(m^2)	=	5.250
Hydraulic diameter	(m)	=	2.100
Mean beam length of the flue gas	(m)	=	1.331
Fuel consumption	(kg/h)	=	710.
Fuel net heat value	(kJ/kg)	=	48000.
Fuel composition in mass:	C (%)	=	72.40
	H (%)	=	23.92
	N (%)	=	3.68
Flue gas flow rate	(kg/h)	=	66720.
Moisture in mass	(%)	=	7.00
Partial pressure of CO_2	(atm)	=	.051
Partial pressure of H_2O	(atm)	=	.110
Density in normal condition	(kg/Nm^3)	=	1.260
Flue gas mass velocity	(kg/m^2s)	=	3.530
Flue gas mean velocity	(m/s)	=	8.00
Flue gas adiabatic temperature	(°C)	=	1243.9
Flue gas exit temperature	(°C)	=	836.3
Heat transfer to the tube walls	(kW)	=	1469.67

Radiated bank surface	(m^2)	=	5.25
Heat transfer to the radiated bank	(kW)	=	308.63

Tube bank		:	1	2	3	4
Bank type (steam-generating, SH)		:	S.G	SH	SH	S.G
Gas mass flow rate	(kg/s)	=	18.53	18.53	18.53	18.53
Tube outside diameter	(mm)	=	51.0	38.0	38.0	51.0
Tube thickness	(mm)	=	4.00	4.00	4.00	4.00
Tube steel		:	carb.s	carb.s	carb.s	carb.s
Tube mean temperature	(°C)	=	279.2	385.9	375.8	288.6
Tube steel thermal conductivity	(W/mK)	=	46.23	43.57	43.83	46.00
Fining type (continuous, discontinuous)		:	-----	-----	-----	CONT.
Fin height	(mm)	=	.0	.0	.0	19.0
Fin thickness	(mm)	=	.00	.00	.00	1.50
Number of fins per meter		=	0	0	0	200
Fin steel		:	---	---	---	carb.s
Fin mean temperature	(°C)	=	.0	.0	.0	329.8
Maximum temperature at fin top	(°C)	=	.0	.0	.0	428.5
Fin efficiency factor		=	.000	.000	.000	.685
Isolated fin theoretical efficiency factor		=	.000	.000	.000	.715
Available cross-section area for tube bank	(m^2)	=	.000	.000	.000	5.798
Actual or conventional tube length	(m)	=	3.720	3.585	3.635	3.514
Number of tubes per row		=	16/17	21/21	21/21	16/16
Number of rows		=	2	6	10	12
Bank outside surface	(m^2)	=	19.67	53.93	91.13	1259.9
Lateral walls surface (steam generating)	(m^2)	=	.00	4.27	7.12	.00
Total surface of steam generating tubes	(m^2)	=	19.67	4.27	7.12	1259.9
Cross-section area for flue gas flow	(m^2)	=	3.383	3.398	3.445	2.290
Arrangement type (in-line, staggered)		:	STAG.	STAG.	STAG.	STAG.
Transversal pitch	(mm)	=	103.0	81.2	81.2	100.0
Longitudinal pitch	(mm)	=	100.0	60.0	60.0	100.0
Arrangement factor f_a (heat transfer)		=	1.072	1.134	1.130	.000
Depth factor f_d (heat transfer)		=	1.000	1.000	1.000	.000
Ratio x_r/d_o for gas radiation		=	3.855	3.231	3.231	.000
Fluids (parallel-, counterflow) (for SH)		:	----	COUNT	COUNT	----
Number of tubes in parallel for steam flow (SH)		=	0	21	21	0
Cross-section area for steam flow (for SH)	(m^2)	=	.0000	.0148	.0148	.0000
Gas heat transfer coefficient (convection)	(W/m^2K)	=	74.13	89.49	85.00	81.16
Gas heat transfer coefficient (radiation)	(W/m^2K)	=	6.77	7.24	6.07	.96
Total heat transfer coefficient	(W/m^2K)	=	80.90	96.73	91.07	82.12
Heat transfer coefficient of internal fluid	(W/m^2K)	=	12000.	1244.	1107.	12000.
Over-all heat transfer coefficient	(W/m^2K)	=	79.66	87.27	81.79	51.17
Gas inlet temperature	(°C)	=	836.3	799.7	714.6	601.0
Gas outlet temperature	(°C)	=	799.7	714.6	601.0	289.5
Heat transfer to the bank	(kW)	=	853.9	1966.5	2570.7	6740.3
Number of rows		=	2	6	10	12
Arrangement factor f_a (pressure loss)		=	.403	.429	.424	.000
Depth factor f_d (pressure loss)		=	1.000	1.000	1.000	.000

Flue gas mass velocity	(kg/m^2s)	=	5.48	5.45	5.38	8.09
Flue gas mean velocity	(m/s)	=	17.37	16.32	14.53	16.46
Number of Reynolds		=	6491.	4987.	5245.	12850.
Flue gas pressure drop	(Pa)	=	38.3	114.3	165.4	816.6
Steam pressure drop	(bar)	=	.000	.678	.854	.000

Mass of the smooth steam generating tubes	(kg)	=	569.
Mass of the finned steam generating tubes	(kg)	=	9767.
Mass of the superheater tubes	(kg)	=	4075.

Superheater after the post-combustion chamber
(primary and secondary superheater)
(tubes perpendicular to gas flow)

Superheater surface	(m^2)	=	145.05
Absolute pressure at superheater exit	(bar)	=	55.7
Steam density at superheater exit	(m^3/kg)	=	.0555
Steam flow rate in the primary superheater	(kg/h)	=	18228.1
Inlet pressure in the bank	(bar)	=	57.5
Absolute pressure at the bank exit	(bar)	=	56.6
Heat exchange efficiency in the primary SH	(%)	=	90.48
Steam temperature at primary superheater exit	(°C)	=	418.0
Steam enthalpy at primary superheater exit	(kJ/kg)	=	3230.99
Heat transfer to the primary superheater	(kW)	=	2326.07
Heat transfer to the lateral walls	(kW)	=	244.69
Steam flow rate in the secondary superheater	(kg/h)	=	20114.6
Inlet pressure in the bank	(bar)	=	56.6
Outlet pressure from the secondary superheater	(bar)	=	55.7
Heat exchange efficiency in the secondary SH	(%)	=	90.02
Steam temperature at inlet of secondary SH	(°C)	=	321.2
Steam enthalpy at inlet of secondary SH	(kJ/kg)	=	2969.55
Steam temperature at secondary SH exit	(°C)	=	440.3
Steam enthalpy at secondary superheater exit	(kJ/kg)	=	3286.35
Heat transfer to the secondary superheater	(kW)	=	1770.14
Heat transfer to the lateral walls	(kW)	=	196.44
Steam velocity at the secondary SH exit	(m/s)	=	20.9
Steam pressure drop in the superheater	(bar)	=	1.839
Injection water temperature	(°C)	=	105.0
Injection water enthalpy	(kJ/kg)	=	444.34
Injection water flow rate	(kg/h)	=	1886.5

Generator efficiency and pressure losses:

Generator without economizer:

Available heat	(kW)	=	19549.59
Heat transfer to the generator	(kW)	=	13968.35
Boiler efficiency	(%)	=	71.45
Flue gas pressure drop in the boiler	(Pa)	=	1134.6

Generator with economizer:

Heat transfer to the generator	(kW)	=	16146.74
Generator efficiency	(%)	=	82.59
Flue gas pressure drop in the economizer	(Pa)	=	267.5
Flue gas total pressure drop in the generator	(Pa)	=	1488.5

Economizer with finned tubes:

Tubes outside surface	(m^2)	=	775.19
Tube outside diameter	(mm)	=	48.3
Tube thickness	(mm)	=	3.68

```
        Tube steel                                          :   carb.st.
        Tube mean temperature                    (°C)       =   167.5
        Tube steel thermal conductivity          (W/mK)     =   49.01
        Fining with annular continuous fins
        Fin height                               (mm)       =   19.0
        Fin thickness                            (mm)       =   1.5
        Number of fins per meter                            =   200
        Fin steel                                           :   carb.st.
        Fin mean temperature                     (°C)       =   181.7
        Fin maximum temperature at the top       (°C)       =   243.6
        Fin steel thermal conductivity           (W/mK)     =   48.66
        Fin efficiency factor                               =   .766
        Isolated fin theoretical efficiency factor          =   .790
        Available cross-section area for the bank (m²)      =   5.643
        Finned tube length                       (m)        =   3.000
        Number of tubes per row                             =   16
        Number of rows                                      =   9
        Transversal pitch                        (mm)       =   114.
        Longitudinal pitch                       (mm)       =   99.
        Fluids (parallel-, counterflow)                     :   COUNT.
        Tube arrangement (in-line, staggered)               :   STAGG.
        Heat exchange efficiency                 (%)        =   99.00


        Flue gas:
        Flow rate                                (kg/h)     =   66720.
        Density in normal condition              (kg/Nm³)   =   1.260
        Moisture in mass                         (%)        =   7.002
        Cross-section area for gas flow          (m²)       =   2.777
        Flue gas heat transfer coefficient       (W/m²K)    =   57.32
        Inlet temperature                        (°C)       =   289.5
        Outlet temperature                       (°C)       =   182.7
        Mass velocity                            (kg/m²s)   =   6.67
        Mean velocity                            (m/s)      =   9.88
        Number of Reynolds                                  =   12715.
        Flue gas pressure drop                   (Pa)       =   267.5


        Water:
        Flow rate                                (kg/h)     =   18228.
        Absolute pressure at water inlet         (bar)      =   57.6
        Number of tubes in parallel for water flow          =   16
        Cross-section area for water flow        (m²)       =   .0211
        Water heat transfer coefficient          (W/m²K)    =   2486.
        Inlet temperature                        (°C)       =   105.0
        Water inlet enthalpy                     (kJ/kg)    =   444.3
        Outlet temperature                       (°C)       =   204.5
        Water outlet enthalpy                    (kJ/kg)    =   874.1
        Mass velocity                            (kg/m²s)   =   240.67
        Water density at exit                    (kg/m³)    =   862.7
        Maximum velocity at exit                 (m/s)      =   .28
        Water pressure drop                      (bar)      =   .0076

        Overall heat transfer coefficient        (W/m²K)    =   34.55
        Heat transfer to the economizer          (kW)       =   2178.39

        Mass of the tubes of the economizer      (kg)       =   5836.

Stop - Program terminated.
```

Clearly, with the economizer, efficiency goes from 71.45 to 82.59%. Therefore, its presence is crucial.

12.5 Air Heater

This program shows the computation for an air heater under full load where the flue gas comes from the combustion of fuel oil. To rule out the danger of corrosion by sulfur, minimum temperature of the boundary layer is set not to go below 145°C. This condition is visibly respected. On the other hand, when the air heater runs under reduced load, the danger of corrosion becomes real and part of the air must be bypassed to reduce the heat exchange and the cooling of the gas. Therefore, we include the computation relative to running at 64% of the maximum load to demonstrate how necessary it is to bypass 33% of air.

```
Air heater with smooth tubes (full load)

Tube inside surface                                (m²)      =   59.93
Computation surface                                (m²)      =   59.93
Tube outside diameter                              (mm)      =   60.3
Tube thickness                                     (mm)      =   2.90
Fluids (parallel-, counterflow, cross flow)                  :   COUNT.
Tube arrangement (in-line, staggered)                        :   LINE
Fluid at inside of the tubes                                 :   GAS
Thermal exchange efficiency                        (%)       =   98.0

Flue gas:

Flow rate                                          (kg/h)    =   7800.
Density in normal condition                        (kg/Nm³)  =   1.304
Moisture in mass                                   (%)       =   6.46
Partial pressure of CO2                            (atm)     =   .1170
Partial pressure of H2O                            (atm)     =   .0970
Tube length by each passage                        (m)       =   3.500
Number of passages                                           =   1
Cross-section area by gas flow                     (m²)      =   .233
Heat transfer coefficient (convection)             (W/m²K)   =   37.60
Heat transfer coefficient (radiation)              (W/m²K)   =   .91
Total heat transfer coefficient                    (W/m²K)   =   38.51
Inlet temperature                                  (°C)      =   290.0
Outlet temperature                                 (°C)      =   195.6
Minimum temperature of boundary layer              (°C)      =   145.5
Allowable temperature of boundary layer            (°C)      =   145.0
Mass velocity                                      (kg/m²s)  =   9.29
Mean velocity                                      (m/s)     =   13.46
Number of Reynolds                                           =   19601.
Total number of entrance/exit                                =   1
Pressure drops:                distributed         (Pa)      =   111.0
                             entrance/exit         (Pa)      =   62.4
                                     total         (Pa)      =   173.4

Air:

Flow rate                                          (kg/h)    =   7363.
Number of tubes per row                                      =   10
Number of passages                                           =   4
Number of row by each passage                                =   10
Transversal pitch                                  (mm)      =   100.0
Longitudinal pitch                                 (mm)      =   100.0
Cross-section area for air flow                    (m²)      =   .347
Arrangement factor fa (heat transfer)                        =   .961
Depth factor fd (heat transfer)                              =   1.000
Heat transfer coefficient                          (W/m²K)   =   46.34
Inlet temperature                                  (°C)      =   20.0
Outlet temperature                                 (°C)      =   127.5
Mass velocity                                      (kg/m²s)  =   5.89
```

```
   Mean velocity                                    (m/s)    =   5.78
   Number of Reynolds                                        =   17346.
   Arrangement factor f_a (pressure drop)                    =   .275
   Depth factor f_d (pressure drop)                          =   1.000
   Number of back-flow caps                                  =   3
   Minimum cross-section area of the caps           (m²)     =   .600
   Pressure drops :                distributed      (Pa)     =   187.5
                                          caps      (Pa)     =   25.7
                                         total      (Pa)     =   213.1

   Overall heat transfer coefficient                (W/m²K)  =   21.96
   Heat transfer to air heater                      (kW)     =   222.27
   Pressure drop (flue gas + air)                   (Pa)     =   386.5

   Mass of the air heater tubes                     (kg)     =   1437.

   Air heater sizes (with possible caps)      =     3500x1000x2200

   ********************************************************

   Working conditions by reduced load (about 64 %)
   (with air bypass)

   Flue gas:

   Flow rate                                        (kg/h)   =   5000.
   Heat transfer coefficient (convection)           (W/m²K)  =   26.31
   Heat transfer coefficient (radiation)            (W/m²K)  =   .85
   Total heat transfer coefficient                  (W/m²K)  =   27.16
   Inlet temperature                                (°C)     =   270.0
   Outlet temperature                               (°C)     =   189.9
   Minimum temperature of boundary layer            (°C)     =   145.2
   Allowable temperature of boundary layer          (°C)     =   145.0
   Mass velocity                                    (kg/m²s) =   5.95
   Mean velocity                                    (m/s)    =   8.41
   Number of Reynolds                                        =   12801.
   Total number of entrance/exit                             =   1
   Pressure drops :                distributed      (Pa)     =   48.7
                                 entrance/exit      (Pa)     =   25.0
                                         total      (Pa)     =   73.7

   Air:

   Flow rate                                        (kg/h)   =   4720.
   Arrangement factor f_a (heat transfer)                    =   .941
   Depth factor f_d (heat transfer)                          =   1.000
   Air bypass                                       (%)      =   33.0
   Heat transfer coefficient                        (W/m²K)  =   27.39
   Inlet temperature in air preheater               (°C)     =   20.0
   Outlet temperature from air preheater            (°C)     =   155.4
   Inlet temperature in the generator               (°C)     =   111.0
   Mass velocity                                    (kg/m²s) =   2.53
   Mean velocity                                    (m/s)    =   2.58
   Number of Reynolds                                        =   7231.
   Arrangement factor f_a (pressure drop)                    =   .278
   Depth factor f_d (pressure drop)                          =   1.000
   Pressure drops :                distributed      Pa)      =   36.3
                                          caps      (Pa)     =   4.9
                                         total      (Pa)     =   41.2

   Over-all heat transfer coefficient               (W/m²K)  =   14.31
   Heat transfer to the air heater                  (kW)     =   120.42
   Pressure drop (flue gas + air)                   (Pa)     =   114.9


Stop - Program terminated.
```

12.6 Natural Circulation

To illustrate the computation of natural circulation, we referred to the elementary circuit shown in Fig. 12.3 where a downcomer and a return tube correspond to 10 tubes with an outside diameter of 54 mm placed on the walls. The program can be used for the computation of much more complex circuits, including the combination with differently fed steam-generating tubes connected in various ways to the drum.

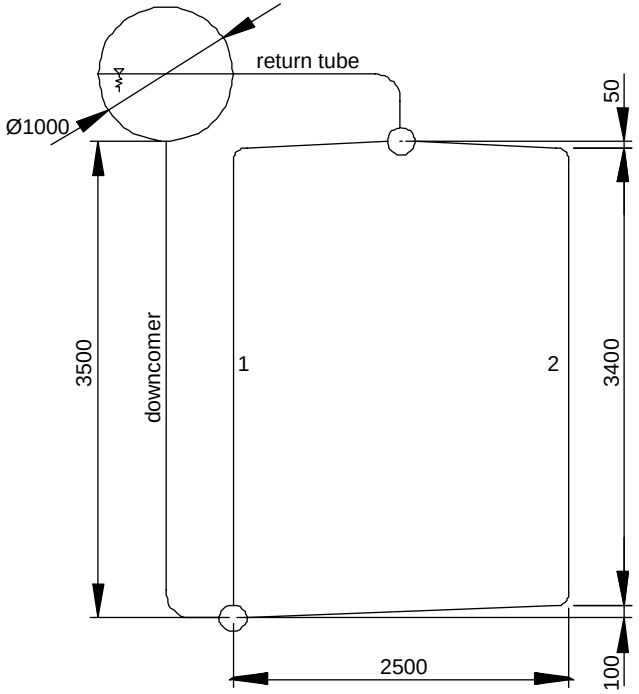


Fig. 12.3

```
Calculation of the natural circulation in the circuit of Fig. 12.1

General data :

Absolute pressure                          (bar)  =    41.
Steam temperature                          (°C)   =   252.
Vaporization heat                          (kJ/kg)= 1705.3
Water specific volume                      (m³/kg)= .00126
Water density                              (kg/m³)=  793.7
Steam specific volume                      (m³/kg)=  .0485
Steam density                              (kg/m³)= 20.619
Water dynamic viscosity                    (kg/ms)=  107.0 *10⁻⁶
Steam dynamic viscosity                    (kg/ms)=  17.50 *10⁻⁶
Minimum allowable circulation ratio               =  13.02
```

Downcomer :

Section		:	1	2	3
Tube outside diameter	(mm)	=	.0	88.9	88.9
Tube thickness	(mm)	=	.00	3.60	3.60
Cross-section area for water flow	(m^2)	=	.00000	.00524	.00524
Section length	(mm)	=	0.	3500.	300.
Level difference between entrance and exit	(mm)	=	500.	3500.	0.
Water density	(kg/m^3)	=	793.65	793.65	793.65
Hydrostatic factor	(Pa)	=	3892.	27242.	0.
Water velocity	(m/s)	=	.000	2.839	2.839
Distributed pressure drop	(Pa)	=	0.	2377.	204.
Drop factor by section inlet		=	.00	.50	.00
Pressure drop by section inlet	(Pa)	=	0.	1599.	0.
Drop factor by section outlet		=	.00	.28	1.00
Pressure drop by section outlet	(Pa)	=	0.	895.	3198.
Characteristic factor P	(Pa)	=	3892.	22371.	-3401.

Steam generating tubes (raiser) - Branch N. 1:

Section		:	1	2
Tube outside diameter	(mm)	=	54.0	54.0
Tube thickness	(mm)	=	2.60	2.60
Tube pitch	(mm)	=	55.	55.
Cross-section area for mixture flow	(m^2)	=	.01870	.01870
Section length	(mm)	=	3500.	1250.
Thermal flux	(kW/m^2)	=	175.00	175.00
Radiated surface	(m^2)	=	1.925	.688
Level difference between entrance and exit	(mm)	=	-3500.	-50.
Mixture mean density	(kg/m^3)	=	426.38	228.13
Hydrostatic factor	(Pa)	=	-14635.	-112.
Mixture mean velocity	(m/s)	=	.439	.821
Distributed pressure drop	(Pa)	=	63.	41.
Drop factor by section inlet		=	.50	.00
Pressure drop by section inlet	(Pa)	=	11.	0.
Drop factor by section outlet		=	.28	1.00
Pressure drop by section outlet	(Pa)	=	19.	86.
Characteristic factor P	(Pa)	=	-14728.	-238.

Steam generating tubes (raiser) - Branch N. 2:

Section		:	1	2	3
Tube outside diameter	(mm)	=	54.0	54.0	54.0
Tube thickness	(mm)	=	2.60	2.60	2.60
Tube pitch	(mm)	=	55.	55.	55.
Cross-section area for mixture flow	(m^2)	=	.01870	.01870	.01870
Section length	(mm)	=	2500.	3400.	1250.
Thermal flux	(kW/m^2)	=	175.00	175.00	175.00
Radiated surface	(m^2)	=	1.375	1.870	.688
Level difference between entrance and exit	(mm)	=	-100.	-3400.	-50.
Mixture mean density	(kg/m^3)	=	614.04	389.08	298.39
Hydrostatic factor	(Pa)	=	-602.	-12973.	-146.
Mixture mean velocity	(m/s)	=	.723	1.141	1.488
Distributed pressure drop	(Pa)	=	168.	355.	169.
Drop factor by section inlet		=	.50	.00	.00
Pressure drop by section inlet	(Pa)	=	62.	0.	0.
Drop factor by section outlet		=	.28	.28	1.00
Pressure drop by section outlet	(Pa)	=	57.	87.	351.
Characteristic factor P	(Pa)	=	-889.	-13416.	-666.

Return tube:

Section		:	1	2
Tube outside diameter	(mm)	=	114.3	114.3
Tube thickness	(mm)	=	3.60	3.60
Cross-section area for mixture flow	(m^2)	=	.00901	.00901
Section length	(mm)	=	400.	1050.

```
Level difference between entrance and exit  (mm)    =   -400.      -50.
Mixture mean density                        (kg/m3)=  253.31    253.31
Hydrostatic factor                          (Pa)    =   -994.     -124.
Mixture mean velocity                       (m/s)   =  5.172     5.172
Distributed pressure drop                   (Pa)    =    206.      540.
Drop factor by section inlet                        =     .50       .00
Pressure drop by section inlet              (Pa)    =   1694.        0.
Drop factor by section outlet                       =     .28      1.00
Pressure drop by section outlet             (Pa)    =    949.     3389.
Characteristic factor P                     (Pa)    = -3843.    -4053.



Results:

Branch                                :      DOWN       1       2     RET
Mixture flow rate              (kg/s)=    11.805   3.502   8.303  11.805
Water flow rate at inlet       (kg/s)=    11.805   3.502   8.303  11.134
Steam flow rate at inlet       (kg/s)=     .0000   .0000   .0000   .6717
Water flow rate at outlet      (kg/s)=    11.805   3.234   7.900  11.134
Steam flow rate at outlet      (kg/s)=     .0000   .2681   .4036   .6717
Circulation ratio                     =       .00   13.06   20.58   17.58
Hydrostatic factor             (Pa)   =    31133. -14747. -13722.  -1118.
Pressure drop                  (Pa)   =     8272.    219.   1249.   6777.
Characteristic factor P        (Pa)   =    22861. -14966. -14971.  -7895.
Error                          (%)    =       .00     .00    -.02     .00

The verification is affirmative because all the circulation ratios are higher
than the minimum allowable circulation ratio that is equal to 13.02


Stop - Program terminated.
```

Appendix

A.1 Accurate Calculation of the Heat Exchange in the Steam-Generating Tube Bank

When flue gas flows through a steam-generating tube bank, it cools off while the temperature of the fluid inside the tubes (the water–steam mix) is constant. The computation of the exit temperature of flue gas from the bank is particularly easy. It can be done using (8.295) where factor ψ is simply computed from (8.297).

The above calculation, though, is based on the incorrect assumption that γ is constant. In fact, the overall heat transfer coefficient U_o and the isobaric specific heat c'_p vary depending on variations of the flue gas temperature. They require criteria to take these variations into account. One of the frequently used criteria consists of computing the average value of c'_p given by the ratio between the difference of enthalpy and the difference in temperature between entrance and exit and of computing the overall heat-transfer coefficient referred to the average temperature between entrance and exit. Factor γ is computed based on these values of U_o and c'_p. This procedure is incorrect because it assumes that the variation in temperature along the bank is linear, which it is not by far.

A better and more realistic result can be obtained by referring to the logarithmic mean temperature given by (A.1) and by using this temperature to compute U_o as well as c'_p, and consequently γ, too.

$$t'_\mathrm{m} = \frac{t'_1 - t'_2}{\log_\mathrm{e} \dfrac{t'_1}{t'_2}}. \tag{A.1}$$

We suggest a more elaborate computation that leads to basically exact values of t'_2.

Note that

$$\mathrm{d}q = U_\mathrm{o}\mathrm{d}S\left(t' - t_\mathrm{s}\right), \tag{A.2}$$

where t' stands for the generic temperature of the flue gas, t_s for the temperature of both the saturated water and the steam, and S for the generic surface.

We may also write that

$$\mathrm{d}q = -M' c'_p \mathrm{d}t', \tag{A.3}$$

given that M' is the mass flow rate of the flue gas.

Assuming that

$$y = t' - t_\mathrm{s}, \tag{A.4}$$

we obtain

$$\frac{\mathrm{d}y}{\mathrm{d}S} = -\frac{U_\mathrm{o}}{M' c'_p} y. \tag{A.5}$$

In order to factor in variations of U_o and c'_p with temperature variations, at this point we assume that

$$\frac{U_\mathrm{o}}{M' c'_p} = A + B y^\delta, \tag{A.6}$$

where A, B, and δ are constant.

Therefore,

$$\frac{\mathrm{d}y}{\mathrm{d}S} = -Ay - By^{\delta+1}. \tag{A.7}$$

The differential equation (A.7) is a Bernoulli equation of the following type:

$$y' = \phi y + \psi y^n. \tag{A.8}$$

Resolving the equation we obtain

$$y^{-\delta} = -\delta \mathrm{e}^{-\delta \int -A \mathrm{d}S} \left(\int -B \mathrm{e}^{\delta \int -A \mathrm{d}S} \mathrm{d}S + C \right), \tag{A.9}$$

where C is a constant; from (A.9) we obtain

$$y^\delta = -\frac{\mathrm{e}^{-\delta AS}}{\frac{B}{A}\mathrm{e}^{-\delta AS} + C\delta} \tag{A.10}$$

As far as the constant C, note that for $S = 0$ is $t' = t'_1$; therefore, $y = t'_1 - t_\mathrm{s}$, as a result. From (A.10) we obtain

$$\left(t'_1 - t_\mathrm{s}\right)^\delta = -\frac{1}{\frac{B}{A} + C\delta}; \tag{A.11}$$

then

$$C = -\frac{1}{\delta}\left[\frac{B}{A} + \left(t'_1 - t_\mathrm{s}\right)^{-\delta}\right]. \tag{A.12}$$

From (A.10) and factoring in (A.12) we obtain

$$y = \frac{\left(t'_1 - t_\mathrm{s}\right)\mathrm{e}^{-AS}}{\left[1 + \frac{B}{A}\left(1 - \mathrm{e}^{-\delta AS}\right)\left(t'_1 - t_\mathrm{s}\right)^\delta\right]^{\frac{1}{\delta}}}. \tag{A.13}$$

Thus, given that S_0 is the bank surface, the exit temperature t_2' of the gas from the bank is given by:

$$t_2' = t_s + \left(t_1' - t_s\right) \frac{e^{-AS_o}}{\left[1 + \frac{B}{A}\left(1 - e^{-\delta AS_o}\right)\left(t_1' - t_s\right)^{\delta}\right]^{\frac{1}{\delta}}}. \tag{A.14}$$

Note that if in (A.6) $B = 0$, thus $\gamma = AS_o$, (A.14) would be reduced to the following equation, one that is well known in relation to Sect. 8.12:

$$t_2' = t_s + \left(t_1' - t_s\right) e^{-\gamma}. \tag{A.15}$$

Standard procedures are as follows.

First of all, consider the following temperature t_0', intermediate between t_1' and t_2':

$$t_0' = t_s + \sqrt{\left(t_1' - t_s\right)\left(t_2' - t_s\right)}. \tag{A.16}$$

Also, compute the values γ_1, γ_0, and γ_2 provided by (A.17):

$$\begin{aligned} \gamma_1 &= \frac{U_o S_o}{M' c_p'} \text{ for } t' = t_1' \\ \gamma_0 &= \frac{U_o S_o}{M' c_p'} \text{ for } t' = t_0' \\ \gamma_2 &= \frac{U_o S_o}{M' c_p'} \text{ for } t' = t_2' \end{aligned} \tag{A.17}$$

On the basis of (A.16) we establish that

$$A = \frac{1}{S_o} \frac{\gamma_1 \gamma_2 - \gamma_0^2}{\gamma_1 + \gamma_2 - 2\gamma_0}; \tag{A.18}$$

$$\delta = \frac{\log_e \frac{\gamma_1 - AS_o}{\gamma_0 - AS_o}}{\log_e \sqrt{\frac{t_1' - t_s}{t_2' - t_s}}}; \tag{A.19}$$

$$B = \frac{\gamma_1 - AS_o}{\left(t_1' - t_s\right)^{\delta}}. \tag{A.20}$$

All elements required to compute t_2' through (A.14) are available this way. Note that the calculation procedure assumes advance knowledge of t_2' which is the final result of the calculation. Therefore, it is necessary to proceed by trial and error up

to agreement between the assumed value of t_2' and the one resulting from the computation. The values of the exit temperature of the flue gas from the bank obtained through this method are practically exact.

A.2 Accurate Calculation of the Heat Exchange in both Superheaters and Economizers

In Sect. 8.3 we already pointed out that as far as the coils of the economizer or of the superheater we cannot strictly talk about parallel flow or counterflow. In fact, each section of the coil is hit by flue gas in such a way that we have cross-flow. In other words, the coil is the sum of elements in which there is cross-flow. In reality, though, if the heated fluid enters the coils in correspondence of the entry into the bank of the flue gas (see Fig. A.1), it is possible to speak of parallel flow.

If the heated fluid enters the coils in correspondence of the exit of the flue gas instead, it is possible to speak of counterflow (see Fig. A.2).

We discuss this topic in more detail by starting to consider the coils in Fig. A.1.

With respect to pure parallel flow, there are differences in the heat transfer that is worth highlighting. Our recommendation is to introduce a corrective factor of the ψ value obtained from (8.275). Recalling that transferred heat is proportional to

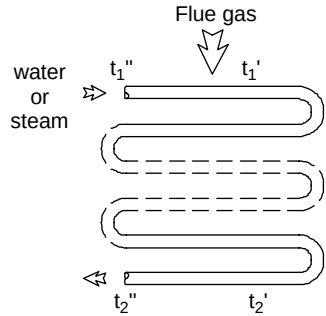


Fig. A.1 Coils - parallel flow

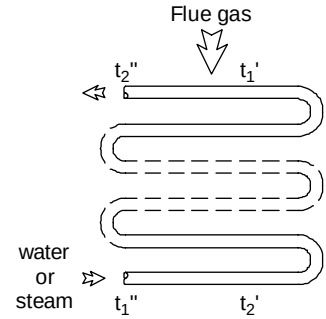


Fig. A.2 Coils - counterflow

Table A.1 Coil with two sections – Parallel flow – Correction factor for ψ

β	γ									
	0.8	1.0	1.2	1.4	1.6	1.8	2.0	2.2	2.4	2.6
0.4	–	–	–	0.983	0.980	0.978	0.976	0.976	0.977	–
0.6	–	0.990	0.987	0.984	0.983	0.983	0.984	–	–	–
0.8	–	0.990	0.988	0.987	0.987	–	–	–	–	–
1.0	0.993	0.991	0.990	0.990	–	–	–	–	1.012	1.019
1.2	0.993	0.992	0.992	–	–	–	–	1.014	1.021	1.028
1.4	0.994	0.993	–	–	–	1.007	1.014	1.021	1.028	1.035

$(1-\psi)$, we ignored the instances where the difference between the actually transferred heat and the one transferred through pure parallel flow is less than $\pm 1\%$, because we consider this difference insignificant. Considering the coil with two sections, the corrective coefficient above can be taken from Table A.1. To generalize the analysis, we always examined values of β between 0.2 and 1.4, and values of γ ranging from 0.2 to 2.6, even though many of these values are unlikely or impossible for economizer and superheater coils.

Evidently, in some cases (the most likely ones) the value of the corrective factor is below unity, that is, the transferred heat is greater compared with pure parallel flow. In other situations the opposite is the case.

If we now consider coils with three or more sections, we see that the difference in transferred heat is always below $\pm 1\%$. Given that a coil with only two branches is exceptional and unlikely, it is safe to state that coils in parallel flow actually behave as such.

We now examine coils in counterflow shown in Fig. A.2.

Proceeding the same way as before, the corrective factors of ψ [computed with (8.284) or (8.289)] are shown in Tables A.2, A.3, A.4, and A.5, respectively, for coils with two, three, four, and five sections.

As expected, the corrective factor is always greater than 1, that is, the transferred heat is less compared with the one in pure counterflow. Clearly, the cases to consider are less and less going from 2 to 5 sections. Moreover, note that cases with 4 or 5 sections are out of the ordinary or even unlikely, given the high value of both β and

Table A.2 Coil with 2 sections – counterflow – correction factor for ψ

β	γ										
	0.6	0.8	1.0	1.2	1.4	1.6	1.8	2.0	2.2	2.4	2.6
0.2	–	–	–	–	–	–	1.042	1.057	1.076	1.099	1.127
0.4	–	–	–	1.021	1.033	1.048	1.067	1.090	1.118	1.152	1.191
0.6	–	–	1.016	1.027	1.040	1.057	1.078	1.104	1.133	1.167	1.207
0.8	–	1.010	1.019	1.030	1.043	1.060	1.080	1.104	1.130	1.160	1.193
1.0	–	1.011	1.020	1.030	1.044	1.059	1.076	1.096	1.117	1.140	1.165
1.2	1.006	1.012	1.020	1.030	1.042	1.055	1.069	1.084	1.100	1.117	1.134
1.4	1.006	1.012	1.020	1.029	1.038	1.049	1.060	1.071	1.082	1.093	1.104

Table A.3 Coil with three sections – counterflow – correction factor for ψ

β	γ								
	1.0	1.2	1.4	1.6	1.8	2.0	2.2	2.4	2.6
0.4	–	–	–	–	–	1.040	1.052	1.067	1.085
0.6	–	–	–	1.026	1.035	1.047	1.061	1.077	1.095
0.8	–	–	1.020	1.028	1.037	1.048	1.061	1.076	1.092
1.0	–	1.014	1.020	1.027	1.036	1.046	1.056	1.068	1.081
1.2	1.009	1.014	1.019	1.026	1.033	1.041	1.049	1.058	1.067
1.4	1.009	1.013	1.018	1.024	1.029	1.035	1.041	1.047	1.053

Table A.4 Coil with four sections – counterflow – correction factor for ψ

β	γ					
	1.6	1.8	2.0	2.2	2.4	2.6
0.6	–	–	–	–	1.044	1.055
0.8	–	–	1.028	1.035	1.044	1.054
1.0	–	1.021	1.027	1.033	1.040	1.048
1.2	1.015	1.019	1.024	1.029	1.034	1.040
1.4	1.014	1.017	1.021	1.024	1.028	1.032

Table A.5 Coil with five sections – counterflow – correction factor for ψ

β	γ		
	2.2	2.4	2.6
0.8	–	–	1.035
1.0	–	1.026	1.031
1.2	1.019	1.022	1.026
1.4	1.016	1.018	1.021

γ. If the number of sections is equal or greater than 6, the mistake made considering the coils in counterflow is always below $\pm 1\%$.

In conclusion, for an even or higher than six number of sections, as is usually the case, the computation made for pure counterflow is correct. For a smaller number of sections, the corrective factor may be introduced when necessary.

A.3 Accurate Calculation of the Heat Exchange in the Air Heater

In Sect. 8.3 we already considered the possibility that the flue gas and the air do one passage only. In that case there is cross-flow and the value of ψ can be taken from Tables 8.7 and 8.8 or be computed with the help of the approximated (8.290). This situation, though, is rare. The flue gas more frequently flows through the tubes once, whereas the air flows through several times (Figs. A.3 and A.4). The figures consider three passages.

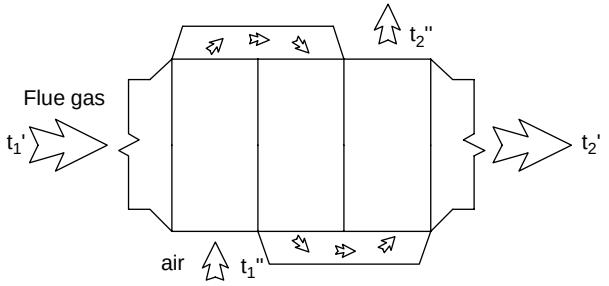


Fig. A.3 Air heater - parallel flow

As for coils, we speak of fluids in parallel flow if the air enters the air heater in correspondence of the entry of the flue gas (see Fig. A.3), whereas we speak of counterflow if the entry of air occurs in correspondence of the exit of the gas (see Fig. A.4). In fact, for every passage of air there is a section of the air heater where the fluids cross flow, and the air heater is the sum of these sections. A more correct computation of the heat transfer requires the introduction of a corrective factor of factor ψ to take into account what actually happens. During the investigation we ignored the cases where the difference between the actual transferred heat and the one corresponding to pure parallel flow or pure counterflow was less than $\pm 1\%$ because we considered it insignificant. Finally, given that these are air heaters, we limited the value of β to a range between 0.9 and 1.4, whereas the range for γ lies between 0.2 and 2.6.

Let us examine the air heater in Fig. A.3 and consider that the air flows through twice. The corrective factor of ψ, computed based on (8.275), can be taken from Table A.6.

As expected, the value of the corrective factor is always below unity (except for unlikely cases), and this means that the heat transfer is greater than pure parallel flow. Chances of two air passages are high; therefore, the corrective factors shown in the Table are interesting, if the case is within the considered group of instances. Note that if the number of passages is equal or greater than 3, it is never necessary to apply a corrective factor of ψ.

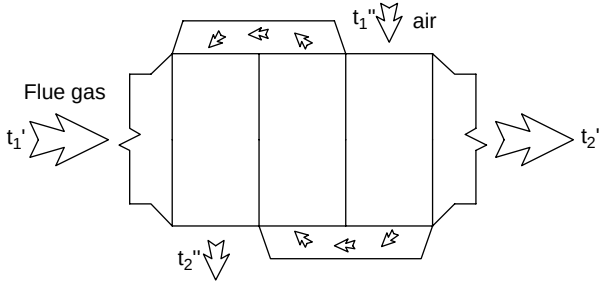


Fig. A.4 Air heater - counterflow

Table A.6 Air heater with two passages – parallel flow – correction factor for ψ

β	γ										
	0.6	0.8	1.0	1.2	1.4	1.6	1.8	2.0	2.2	2.4	2.6
0.9	–	0.991	0.986	0.982	0.979	0.978	0.979	0.981	0.984	0.989	–
1.0	–	0.990	0.986	0.983	0.981	0.980	0.981	0.984	0.988	–	–
1.1	0.995	0.990	0.987	0.984	0.982	0.982	0.984	0.987	–	–	–
1.2	0.994	0.990	0.987	0.984	0.984	0.984	0.985	0.990	–	–	–
1.3	0.994	0.991	0.987	0.985	0.985	0.986	0.989	–	–	–	1.009
1.4	0.994	0.991	0.988	0.986	0.986	0.988	0.991	–	–	–	1.011

Now we examine the air heater in Fig. A.4, formally in counterflow, and we proceed as before by considering the corrective factor of ψ computed based on (8.284) or (8.289). Considering that the air may go through 2, 3, or 4 times, we obtain the values of the corrective factor shown in the Tables A.7, A.8 and A.9.

The corrective factor is always greater than the unity. This means that there is less heat transfer compared with pure counterflow. There is no need to introduce a corrective factor for 5 or more passages of air (actually unlikely). Note, though, that as far as coils, coils with less than six sections are quite rare and unlikely, whereas for an air heater in counterflow the solution with 2, 3, or 4 passages is quite frequent. The use of corrective factors mentioned earlier is recommended, considering that there is less heat transfer compared with pure counterflow. This is especially true for air heaters with only two passages of air and a large surface.

Table A.7 Air heater with two passages – counterflow – correction factor for ψ

β	γ									
	0.8	1.0	1.2	1.4	1.6	1.8	2.0	2.2	2.4	2.6
0.9	–	1.014	1.021	1.030	1.040	1.052	1.064	1.077	1.091	1.106
1.0	1.009	1.014	1.021	1.030	1.039	1.050	1.061	1.072	1.085	1.097
1.1	1.009	1.014	1.021	1.029	1.038	1.047	1.057	1.067	1.077	1.088
1.2	1.009	1.014	1.021	1.028	1.036	1.045	1.053	1.061	1.070	1.078
1.3	1.009	1.014	1.020	1.027	1.034	1.042	1.049	1.056	1.063	1.069
1.4	1.009	1.014	1.020	1.026	1.032	1.039	1.045	1.050	1.056	1.061

Table A.8 Air heater with three passages – counterflow – correction factor for ψ

β	γ							
	1.2	1.4	1.6	1.8	2.0	2.2	2.4	2.6
0.9	–	–	1.020	1.026	1.033	1.040	1.048	1.057
1.0	–	1.015	1.020	1.025	1.032	1.038	1.045	1.053
1.1	–	1.015	1.019	1.024	1.030	1.036	1.042	1.048
1.2	–	1.014	1.018	1.023	1.028	1.033	1.038	1.043
1.3	1.010	1.014	1.018	1.022	1.026	1.030	1.034	1.038
1.4	1.010	1.013	1.017	1.020	1.024	1.027	1.031	1.034

Table A.9 Air heater with four passages – counterflow – correction factor for ψ

β	γ			
	2.0	2.2	2.4	2.6
0.9	–	–	1.030	1.035
1.0	–	1.023	1.028	1.033
1.1	1.018	1.022	1.026	1.030
1.2	1.017	1.020	1.024	1.027
1.3	1.016	1.019	1.021	1.024
1.4	1.015	1.017	1.019	1.021

Another option for the air heater is shown in Figs. A.5 and A.6. The flue gas goes through twice, whereas the air does it 2 or 3 times.

These solutions can be adopted for two reasons. First of all, they create a very compact air heater. Then they have an advantage as far as corrosion because they have cold air in correspondence of warm gas like an air heater in parallel flow, but with a heat transfer halfway between parallel flow and counterflow, as we shall see. These air heaters cannot be defined in terms of parallel flow or counterflow. Nonetheless, given that air enters the air heater in correspondence of the entrance

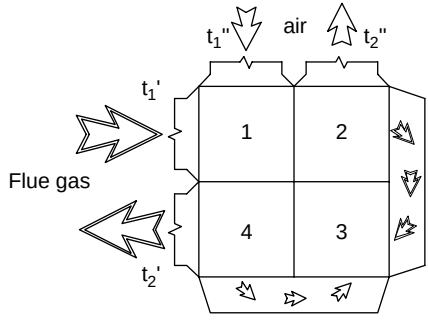


Fig. A.5 Air heater - cross-flow 4 sections

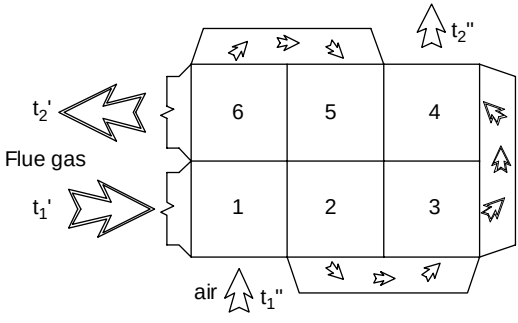


Fig. A.6 Air heater - cross-flow 6 sections

Table A.10 Air heater – cross-flow with four sections – correction factor for ψ (parallel flow)

β	γ										
	0.6	0.8	1.0	1.2	1.4	1.6	1.8	2.0	2.2	2.4	2.6
0.9	0.986	0.973	0.959	0.945	0.932	0.922	0.915	0.911	0.910	0.911	0.913
1.0	0.985	0.972	0.959	0.946	0.935	0.927	0.921	0.919	0.919	0.921	0.924
1.1	0.984	0.972	0.959	0.947	0.938	0.931	0.927	0.926	0.927	0.930	0.934
1.2	0.984	0.972	0.960	0.949	0.941	0.936	0.933	0.933	0.935	0.938	0.944
1.3	0.984	0.972	0.961	0.951	0.944	0.940	0.938	0.939	0.942	0.946	0.952
1.4	0.984	0.972	0.962	0.953	0.947	0.944	0.944	0.945	0.949	0.953	0.959

Table A.11 Air heater – cross-flow with six sections – correction factor for ψ (parallel flow)

β	γ										
	0.6	0.8	1.0	1.2	1.4	1.6	1.8	2.0	2.2	2.4	2.6
0.9	0.984	0.969	0.952	0.935	0.919	0.906	0.895	0.887	0.881	0.877	0.876
1.0	0.983	0.968	0.952	0.936	0.922	0.910	0.901	0.894	0.890	0.888	0.888
1.1	0.982	0.968	0.952	0.938	0.925	0.915	0.907	0.902	0.899	0.898	0.899
1.2	0.982	0.968	0.953	0.939	0.928	0.919	0.913	0.909	0.907	0.907	0.909
1.3	0.982	0.968	0.954	0.941	0.931	0.924	0.919	0.916	0.915	0.916	0.918
1.4	0.981	0.968	0.955	0.943	0.935	0.928	0.925	0.923	0.923	0.924	0.927

of flue gas, we start from a condition of parallel flow and consider the value of ψ provided by (8.275). If we consider the air heater in Fig. A.5, the corrective factor of ψ has the value shown in Table A.10.

We see that the value of the corrective factor is always below the unity, which means that the transferred heat is greater than that equivalent to pure parallel flow. As far as the air heater in Fig. A.6, the corrective factors of ψ are shown in Table A.11.

A comparison of the values in Table A.11 with those in Table A.10 shows that with six sections the gap between the behavior of the air heater and the one in pure parallel flow is even more noticeable, particularly for high values of γ, that is, when there is a large surface. Knowing the corrective factors is therefore very useful to do an accurate calculation of the air heaters of this kind. The corrective factor can be ignored only if $\gamma < 0.6$.

A.4 Finned Tubes

Finned tubes are widely used in the banks of steam-generating tubes of waste-heat generators and in economizers. Close finning with fins made of steel of constant thickness is possible only if the flue gas is "clean" and there is no risk of corrosion. This is true for flue gas created by combustion of natural gas. In economizers that represent the last stage of the generator and that are run through by flue gas created

by combustion of fuel oil, cast iron finned tubes or steel tubes with cast iron finned muffs can be used. In this case the fins have variable thickness from the bottom to the top.

Note that the use of finned tubes makes sense only if the heat-transfer coefficient of the internal fluid (evaporating water or heated water) is clearly higher than the one of the external fluid (flue gas). This rules out the use for air heaters where the heat transfer coefficients are comparable. We are generally referring to tapered fins (Fig. A.7) because the fins with constant thickness constitute a special case within this category.

Because of the thermal gradient along the fin and the following increase in temperature from the bottom to the top, the fin is hit by less heat flux compared with the one hitting the tube. An efficiency factor of the fin ideally reducing its surface is introduced to take this into account. This is possible as follows.

With reference to Fig. A.7 the generic thickness x_f of the fin is given by

$$x_f = x_{f_2}\left[1+\frac{\dfrac{x_{f_1}}{x_{f_2}}-1}{1-\dfrac{r_1}{r_2}}\left(1-\frac{r}{r_2}\right)\right]. \tag{A.21}$$

We introduce factor ϑ given by:

$$\vartheta = \frac{\dfrac{x_{f_1}}{x_{f_2}}-1}{1-\dfrac{r_1}{r_2}}. \tag{A.22}$$

Therefore, the generic thickness of the fin is given by

$$x_f = x_{f_2}\left[1+\vartheta\left(1-\frac{r}{r_2}\right)\right]. \tag{A.23}$$

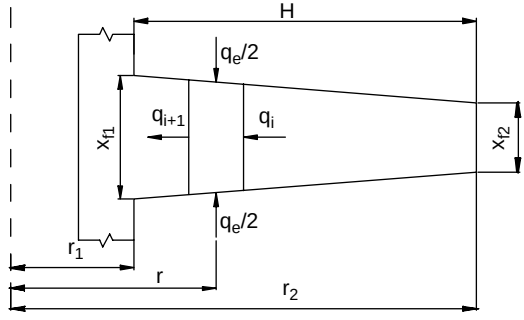


Fig. A.7

Consider the i-th section of radius r_i; the heat q_i crossing the section is given by

$$q_i = 2\pi r_i k x_{f_2} \left[1 + \vartheta\left(1 - \frac{r}{r_2}\right)\right] \left(\frac{\mathrm{d}t}{\mathrm{d}r}\right)_i, \tag{A.24}$$

where t is the generic temperature of the fin and k the thermal conductivity of the material. The temperature of the fluid transferring heat to the fin is t', while r_1 and r_2 are the radius at the bottom and the top of the fin. We assume that

$$\chi = \frac{r}{r_2} \tag{A.25}$$

$$\phi = \frac{t' - t}{t' - t_2}, \tag{A.26}$$

where t_2 as the temperature of the fin in position 2 $(r = r_2)$.

Equation (A.24) can be written as follows.

$$q_i = -2\pi k x_{f_2} \left[1 + \vartheta\left(1 - \chi_i\right)\right] \left(t' - t_2\right) \chi_i \left(\frac{\mathrm{d}\phi}{\mathrm{d}\chi}\right)_i. \tag{A.27}$$

By analogy, if we consider the $(i+1)$-th section where its smaller radius differs from the radius r_i of Δr, we may write that

$$q_{i+1} = -2\pi k x_{f_2} \left[1 + \vartheta\left(1 - \chi_{i+1}\right)\right] \left(t' - t_2\right) \chi_{i+1} \left(\frac{\mathrm{d}\phi}{\mathrm{d}\chi}\right)_{i+1}. \tag{A.28}$$

On both circular crowns of width Δr that make up the sides of the fin, the external fluid transfers the heat q_e given by

$$q_\mathrm{e} = 4\pi r_i \Delta r \alpha \left(t' - t_i\right) = 4\pi r_2^2 \alpha \left(t' - t_2\right) \chi_i \phi_i \Delta\chi, \tag{A.29}$$

where α is the heat-transfer coefficient of the external fluid.

Thermal balance requires that

$$q_{i+1} = q_i + q_\mathrm{e}. \tag{A.30}$$

Then, through a series of steps we obtain

$$\left(\frac{\mathrm{d}\phi}{\mathrm{d}\chi}\right)_{i+1} = \left\{\left[1 + \vartheta\left(1 - \chi_i\right)\right] \left(\frac{\mathrm{d}\phi}{\mathrm{d}\chi}\right)_i - A\phi_i \Delta\chi\right\} \frac{\chi_i}{\chi_{i+1}\left[1 + \vartheta\left(1 - \chi_{i+1}\right)\right]}, \tag{A.31}$$

given that

$$A = \frac{2\alpha r_2^2}{k x_{f_2}}. \tag{A.32}$$

We introduce factor B given by

$$B = \sqrt{\frac{2\alpha H^2}{k x_{f_2}}}, \tag{A.33}$$

where H is the height of the fin.

Then

$$A = \left(\frac{B}{1 - \dfrac{r_1}{r_2}} \right)^2 . \tag{A.34}$$

Note that at the top of the fin ($r = r_2$) we have $\chi = 1$ and $\varphi = 1$. In addition,

$$q_2 = -2\pi k x_{f_2} \left(t' - t_2\right) \left(\frac{\mathrm{d}\phi}{\mathrm{d}\chi} \right)_2 = 2\pi r_2 x_{f_2} \alpha \left(t' - t_2\right), \tag{A.35}$$

given that q_2 is the heat transferred to the fin through the circular crown with a width equal to the thickness.

From (A.35) we obtain

$$\left(\frac{\mathrm{d}\phi}{\mathrm{d}\chi} \right)_2 = -\frac{\alpha r_2}{k} = -C. \tag{A.36}$$

The sequence is as follows.

Presetting a very small value of $\Delta\chi$ and knowing the values of ϕ and $(\mathrm{d}\phi/\mathrm{d}\chi)$ for $\chi = 1$ (top of the fin), we proceed toward its bottom by computing $(\mathrm{d}\phi/\mathrm{d}\chi)_{i+1}$ through (A.31), the new value of $\chi_{i+1} = \chi_i - \Delta\chi$, the new value of $\phi_{i+1} = \phi_i - (\mathrm{d}\phi/\mathrm{d}\chi)_i \Delta\chi$, and so on and so forth down to the bottom.

The heat q_1 exiting the fin that corresponds to the heat that the external fluid transfers to the fin is equal to

$$q_1 = -2\pi k x_{f_1} \left(t' - t_2\right) \left(\frac{r_1}{r_2} \right) \left(\frac{\mathrm{d}\phi}{\mathrm{d}\chi} \right)_1 . \tag{A.37}$$

If the entire fin were at temperature t_1, that is, the one at the bottom, the transferred heat q_0 would be equal to

$$q_0 = 2\pi \left(r_2^2 - r_1^2 + r_2 x_{f_2}\right) \alpha \left(t' - t_1\right). \tag{A.38}$$

The efficiency factor of fin E_f, equal to the ratio q_1/q_0 is therefore given by

$$E_f = \frac{-2 \left(\dfrac{r_1}{r_2} \right) \left(\dfrac{\mathrm{d}\phi}{\mathrm{d}\chi} \right)_1}{A\phi_1 \dfrac{x_{f_2}}{x_{f_1}} \left[1 - \left(\dfrac{r_1}{r_2} \right)^2 + 2\dfrac{C}{A} \right]}. \tag{A.39}$$

Table A.12 Efficiency factor for fins ($x_{f_1}/x_{f_2} = 1$)

B	r_2/r_1	E_f	B	r_2/r_1	E_f
0.20	1.20	0.979	0.80	1.20	0.813
	1.40	0.972		1.40	0.797
	1.60	0.965		1.60	0.784
	1.80	0.959		1.80	0.771
	2.00	0.954		2.00	0.760
0.40	1.20	0.940	1.00	1.20	0.741
	1.40	0.930		1.40	0.724
	1.60	0.922		1.60	0.708
	1.80	0.914		1.80	0.693
	2.00	0.907		2.00	0.680
0.60	1.20	0.881	1.20	1.20	0.672
	1.40	0.869		1.40	0.653
	1.60	0.858		1.60	0.636
	1.80	0.848		1.80	0.620
	2.00	0.839		2.00	0.606

We see that the value of E_f depends on $r_2/r_1, B, C$, and the ratio x_{f_1}/x_{f_2}. As far as C, its influence is modest and we can conventionally assume that $C = 0.05$.

Tables A.12, A.13, A.14 and A.15 show the values of E_f for $x_{f_1}/x_{f_2} = 1$, 1.5, 2, and 2.5, respectively. A comparison of the values of E_f in the four tables highlights the beneficial effect of the variability in thickness of the fins. In fact, the value of E_f increases with an increase of x_{f_1}/x_{f_2}. Note, though, that the thickening of the heat flux lines in correspondence of the tube reduces the efficiency factor with respect to the above. Taking this phenomenon into account, we determine that the computation

Table A.13 Efficiency factor for fins ($x_{f_1}/x_{f_2} = 1.5$)

B	r_2/r_1	E_f	B	r_2/r_1	E_f
0.20	1.20	0.984	0.80	1.20	0.855
	1.40	0.979		1.40	0.842
	1.60	0.973		1.60	0.831
	1.80	0.969		1.80	0.820
	2.00	0.964		2.00	0.811
0.40	1.20	0.955	1.00	1.20	0.795
	1.40	0.948		1.40	0.780
	1.60	0.941		1.60	0.766
	1.80	0.935		1.80	0.753
	2.00	0.930		2.00	0.742
0.60	1.20	0.910	1.20	1.20	0.734
	1.40	0.900		1.40	0.717
	1.60	0.891		1.60	0.701
	1.80	0.883		1.80	0.687
	2.00	0.876		2.00	0.675

Table A.14 Efficiency factor for fins ($x_{f_1}/x_{f_2} = 2$)

B	r_2/r_1	E_f	B	r_2/r_1	E_f
0.20	1.20	0.987	0.80	1.20	0.881
	1.40	0.983		1.40	0.870
	1.60	0.978		1.60	0.860
	1.80	0.974		1.80	0.851
	2.00	0.971		2.00	0.843
0.40	1.20	0.964	1.00	1.20	0.829
	1.40	0.958		1.40	0.816
	1.60	0.952		1.60	0.804
	1.80	0.947		1.80	0.793
	2.00	0.943		2.00	0.783
0.60	1.20	0.927	1.20	1.20	0.775
	1.40	0.919		1.40	0.760
	1.60	0.911		1.60	0.746
	1.80	0.905		1.80	0.733
	2.00	0.898		2.00	0.722

procedure shown below makes it possible to obtain the values of E_f that correspond well to reality for fins with constant thickness.

We have

$$W = B\left(1 + \frac{x_{f_2}}{2H}\right), \tag{A.40}$$

where B, x_{f_2}, and H are previously considered quantities.

Then

$$V = \frac{\tanh W}{W}; \tag{A.41}$$

$$Z = V\left(0.7 + 0.3V\right). \tag{A.42}$$

Table A.15 Efficiency factor for fins ($x_{f_1}/x_{f_2} = 2.5$)

B	r_2/r_1	E_f	B	r_2/r_1	E_f
0.20	1.20	0.989	0.80	1.20	0.899
	1.40	0.985		1.40	0.889
	1.60	0.982		1.60	0.881
	1.80	0.978		1.80	0.873
	2.00	0.975		2.00	0.866
0.40	1.20	0.970	1.00	1.20	0.853
	1.40	0.965		1.40	0.841
	1.60	0.960		1.60	0.830
	1.80	0.956		1.80	0.821
	2.00	0.952		2.00	0.812
0.60	1.20	0.938	1.20	1.20	0.805
	1.40	0.931		1.40	0.790
	1.60	0.925		1.60	0.778
	1.80	0.919		1.80	0.766
	2.00	0.914		2.00	0.756

Finally,

$$E_f = Z\left(1+0.02W^3\right)\left[0.45\,(Z-1)\log_{\mathrm{e}}\left(\frac{d_0+2H}{d_0}\right)+1\right], \tag{A.43}$$

where d_0 is the external diameter of the tube without fins.

For fins with variable thickness, it is recommended to compute E_f based on A.43 and to multiply the resulting value for the following corrective factor.

$$1+0.12\left(\frac{x_{f_1}}{x_{f_2}}-1\right)W^{1.75}. \tag{A.44}$$

At this point, we need to determine how to compute the heat transfer coefficient of the flue gas, as well as the overall heat transfer coefficient in relation to the finned tubes. We recommend the following.

We calculate

$$C_1 = 0.25\ \mathrm{Re}^{-0.35}; \tag{A.45}$$

$$C_3 = 0.2+0.65\mathrm{e}^{-0.25H/b} \tag{A.46}$$

for inline tubes or

$$C_3 = 0.35+0.65\mathrm{e}^{-0.25H/b} \tag{A.47}$$

for staggered tubes.

In (A.46) and (A.47), b is the space between the fins (equal to the pitch minus the average thickness).

Then

$$C_5 = 1.1-\left(0.75-1.5\mathrm{e}^{-0.7N}\right)\mathrm{e}^{-2s_l/s_t} \tag{A.48}$$

for inline tubes, otherwise

$$C_5 = 0.7+\left(0.70-0.8\mathrm{e}^{-0.15N^2}\right)\mathrm{e}^{-s_l/s_t} \tag{A.49}$$

for staggered tubes.

In (A.48) and (A.49), N is the number of rows run through by the gas, s_l and s_t are the longitudinal and transversal pitches. If $N \geq 6$, $N = 6$ will be used.

Then we compute

$$J = C_1C_3C_5\left(\frac{d_0+2H}{d_0}\right)^{0.5}\left(\frac{t'_m+273}{t_c+273}\right)^{0.25}, \tag{A.50}$$

where t'_m is the average temperature of the flue gas, and t_c is given by

$$t_c = t''_m+0.3\left(t'_m-t''_m\right), \tag{A.51}$$

where t''_m is the average temperature of the internal fluid; all temperatures are expressed in °C.

The heat transfer coefficient α' of the flue gas is equal to

$$\alpha' = J \,\mathrm{Re}\,\mathrm{Pr}^{1/3}\frac{k}{d_o}. \tag{A.52}$$

Re and Pr stand for the Reynolds and Prandtl numbers, k for the thermal conductivity of the material and d_0 for the external diameter of the tube without fins.

Recalling the significance of Re and Pr, (A.52) can be written as follows:

$$\alpha' = JG\frac{c_p^{1/3}k^{2/3}}{\mu^{2/3}}, \tag{A.53}$$

where G is the mass velocity.

Recalling the equations for c_p, k, and μ in Chap. 7, we determine that (A.53) can also be written as follows:

$$\alpha' = K_g JG, \tag{A.54}$$

given that

$$K_g = 1200 + 8.251m + (317.23 + 3.063m)\frac{t_b}{1000} - (76.14 - 9.687m)\left(\frac{t_b}{1000}\right)^2, \tag{A.55}$$

where m is the mass moisture percentage of the gas and t_b the bulk temperature (of course, the average temperature) expressed in °C.

Now, referring to a meter of tube, we indicate the surface of the fins with S_f, the external tube surface not related to the fins with S_b, the total surface of the finned tube ($S_f + S_b$) with S_0, the average surface with S_m and the internal surface of the tube with S_i, the overall heat-transfer coefficient relative to S_0 is given by

$$U_\mathrm{o} = \frac{1}{\left(\frac{1}{\alpha'} + f_\mathrm{o}\right)\frac{S_\mathrm{o}}{E_f S_f + S_b} + \frac{x}{k}\frac{S_\mathrm{o}}{S_\mathrm{m}} + \left(\frac{1}{\alpha''} + f_\mathrm{i}\right)\frac{S_\mathrm{o}}{S_\mathrm{i}}}. \tag{A.56}$$

In this case x is the thickness of the tube, α'' the heat transfer coefficient of the internal fluid, f_o and f_i the potential fouling factors relative to both the outside and inside of the tube.

If these are steel tubes covered by finned cast iron muffs, (A.56) changes as follows.

$$U_\mathrm{o} = \frac{1}{\left(\frac{1}{\alpha'} + f_\mathrm{o}\right)\frac{S_\mathrm{o}}{E_f S_f + S_\mathrm{b}} + \frac{x_\mathrm{c}}{k_\mathrm{c}}\frac{S_\mathrm{o}}{S_\mathrm{mc}} + R\frac{S_\mathrm{o}}{S_\mathrm{e}} + \frac{x_\mathrm{s}}{k_\mathrm{s}}\frac{S_\mathrm{o}}{S_\mathrm{ms}} + \left(\frac{1}{\alpha''} + f_\mathrm{i}\right)\frac{S_\mathrm{o}}{S_\mathrm{i}}}. \tag{A.57}$$

In (A.57) x_c and x_s represent the thickness of the cast iron tube and the steel tube, k_c and k_s represent the thermal conductivity of cast iron and steel, S_mc and S_ms

the average surfaces of the cast iron and steel tubes. S_i and S_e are the internal and external surface of the steel tube. R stands for thermal resistance that should be expected, assuming that the adherence between steel and cast iron tube will not be perfectly tight. Its value can be assumed to be equal to $0.7–1.4 \times 10^{-3}\,\mathrm{m^2K/W}$.

Bibliography

Annaratone D., *Pressure Vessel Design*, Springer Verlag, Heidelberg
Babcock & Wilcox, *Steam*, B & W, New York
Boussicaud A., *Le calcul des pertes de charge*, Chaud Froid, Plomberie
Canali E., *L'acqua delle caldaie a vapore e il suo trattamento*, Hoepli, Milano
Combustion Engineering, C. E., New York
Dornig M., *Macchine termiche ed idrauliche*, C. Tamburini, Milano
Giambelli G., *Lezioni di fisica tecnica*, Tamburini, Milano
Gumz W., *Kurzes Handbuch der Brennstoff- und Feuerungstechnik*, Springer Verlag, Berlin
Guzzoni, Storace, *Corrosione dei metalli e loro protezione*, Hoepli, Milano
Hansen W., *Heizöl Handbuch für Industriefeuerungen*, Springer Verlag, Berlin
ISO TC/64, *Code d'essai pour les générateurs de vapeur fixes équipant les centrales productrices d'énergie*
Kern O., *Process Heat Transfer*, Mc Graw Hill, New York
Kreith F., *Principi di trasmissione del calore*, Liguori Editore
K.S.B., *Manuale sulle pompe*
Ledinegg M., *Dampferzeugung*, Springer Verlag, Berlin
Lorain P., *Les chaudières à vapeur*
Loschge A., *Dampfkessel*, Springer Verlag, Berlin
Mac Adams W., *Heat Transmission*, Mc Graw Hill, New York
Medici M., *La costruzione delle macchine termiche*, Cedam, Padova
Muenziger F., *Dampfkraft*, Springer Verlag, Berlin
Necati M., Ozisik, *Heat transfer, a basic approach*, Mc Graw Hill, New York
Nicolò R.S., *Impianti di caldaie a vapore*, La Goliardica, Milano
Nuber F., *Calcolo termodinamico per impianti di focolari e caldaie a vapore*, Mursia, Milano
Salvi G., *La combustione*, Tamburini, Milano
Schack A., *La trasmissione industriale del calore*, Hoepli, Milano
Setti B., *La caldaia a vapore*, Hoepli, Milano
Shell, *The Petroleum Handbook*
Shields C.D., *Boilers*, F.W. Dodge Corporation, New York
Smith, Stinson, *Fuels and combustion*, Mc Graw Hill, New York
Spiers H.M., *Technical data on fuel*, British National Committee, London
Wärmetechnische Arbeitsmappe, Verlag des Vereines Deutscher Ingegneure
Wolf F., Dietrich, *Das Kalt-Biegen von Rohren*, Springer Verlag, Berlin
Zinzen A., *Dampfkessel und Feuerungen*, Springer Verlag, Berlin
Ancona G., Scavizzi G., *Moderni orientamenti nella combustione del carbone polverizzato*, Convegno ATI, 1963
Anglesio P., *Focolari sperimentali per bruciatori a combustibili liquidi egassosi*, La Termotecnica, 1975

Anglesio P., Gramondi M., *Analisi di caratteristiche termiche nel funzionamento di bruciatori*, La Termotecnica, 1976
Annaratone D., *Alcune considerazioni sulla circolazione naturale nelle caldaie*, Il Calore, 1965
Annaratone D., *Confronto fra le disposizioni a quinconce e in fila dei fasci tubieri dei generatori di vapore*, Il Calore, 1966
Annaratone D., *Alcune considerazioni sulle formule usate per il calcolo dell'indice d'aria*, Il Calore, 1968
Annaratone D., *Influenza della distribuzione dei tubi nei vari giri delle caldaie a tubi da fumo*, Il Calore, 1971
Annaratone D., *Considerazioni sul falso livello nelle caldaie a tubi da fumo*, Il Calore, 1972
Annaratone D., *Criteri di unificazione delle caldaie a tubi da fumo*, La Termotecnica, 1972
Annaratone D., *Trasmissione del calore e perdita di carico nei fasci tubieri vaporizzatori*, La Termotecnica, 1975
Annaratone D., *Influenza della pressione sulla circolazione naturale nei generatori di vapore*, La Termotecnica, 1976
Annaratone D., *Influenza della temperatura dell'acqua nei tubi di caduta dei generatori a circolazione naturale*, La Termotecnica, 1977
Annaratone D., *Indagine sulle condizioni ottimali di progettazione delle caldaie a tubi d'acqua per la produzione di vapor saturo*, La Termotecnica, 1977
Annaratone D., *Influenza degli incombusti gassosi sulla determinazione dell'indice d'aria e del rendimento*, La Termotecnica, 1978
Annaratone D., *Superficie ottimale dei riscaldatori d'aria*, La Termotecnica, 1981
Annaratone D., *Suddivisione ottimale della superficie fra fascio vaporizzatore in caldaia e ricuperatore di calore*, Ingegneria, 1981
Annaratone D., *Preriscaldatore d'aria: fluidi in equicorrente o in controcorrente*, Ingegneria, 1981
Annaratone D., *Ottimizzazione "esterna" dei generatori di vapore industriali*, Energia e Calore, 1981
Annaratone D., *Dimensionamento ottimale dei generatori a ricupero*, La Termotecnica, 1982
Annaratone D., *Sul flusso di picco nelle caldaie a tubi da fumo*, La Termotecnica, 1983
Annaratone D., *Trasmissione del calore per convezione nei focolari delle caldaie a tubi da fumo*, La Termotecnica, 1984
Annaratone D., *Proposta di una formula di calcolo della temperatura di uscita dei gas di combustione dalla camera*, La Termotecnica, 1984
Annaratone D., *Grandezze fisiche fondamentali dei gas di combustione*, La Termotecnica, 1985
Annaratone D., *Sull'irraggiamento dei gas di combustione*, Termotecnica, 1986
Annaratone D., *Qualche considerazione sulla mandrinatura dei tubi*, La Termotecnica, 1986
Annaratone D., *Convenienza del riscaldatore d'aria in equicorrente per generatori di vapore funzionanti ad olio combustibile*, La Termotecnica, 1989
Annaratone D., *Temperatura di uscita dei gas di combustione da un fascio tubiero vaporizzatore*, La Termotecnica, 1991
Annaratone D., *Economizzatore o riscaldatore d'aria?* La Termotecnica, 1997
Annaratone D., *Surriscaldatori in uno o due stadi*, La Termotecnica, 1998
Annaratone D., *Indice d'aria e perdite per calore sensibile e incombusti gassosi*, La Termotecnica, 1998
Annaratone D., *Entalpia dei gas*, La Termotecnica, 1999
Annaratone D., *Adduttanza dell'acqua, del vapor d'acqua, dell'aria e dei gas di combustione*, La termotecnica, 2001
Armoni C.A., Caruso S., Gregorio P., *An investigation on the instability occurring in a pressurized natural circulation water loop*, Politecnico, Torino
Beer J.M., *Untersuchungen der Internationalen Gemeinschaft für Flammenforschung über die Verbrennung von Heizöl*, BWK, 1963
Bombarda E., *Intercambiabilità di gas combustibili: paragone fra due criteri di intercambiabilità*, La Termotecnica, 1985
Boow J., *Viscosity/temperature characteristics of some Australian coal-ash slags in the range 1100–1600˚C*, J. Inst. Fuel, 1965

Brossa G., *Comportamento termodinamico e funzionale dei generatori di vapore in relazione ai combustibili utilizzati*, XIII congresso ATI
Caffo O., Padovani C., *Stabilità di fiamma in bruciatori di aria preriscaldata*, La Termotecnica, 1965
Campolonghi F., Cuneo M., Urbani G., Vaccaro G., *Scambio termico in elementi tubolari di generatori di vapore ad un solo passaggio*, La Termotecnica, 1974
Casagrande A., Piantanida A., *La combustione tangenziale nei moderni generatori di vapore*, Convegno ATI, 1969
Cereda W., *Versatilità e sicurezza nei sistemi di protezione contro la mancanza di fiamma*, Honeywell, 1970
Chedaille J., *La fondation des recherches internationales sur les flammes*, Rev. Gen. de Termique, 1965
Cleve K., *Ölfeuerungen mit Rauchgasrücksaugung*, VGB, 1963
Codegone C., *La correlazione dei coefficienti di convezione termica libera e forzata*, XVII Congresso ATI
Cuneo M., Farello G.E., Ferrari G., Palazzi G., *Influenza di vorticatori a nastro avvolto in generatori di vapore ad un solo passaggio riscaldati in contro-corrente*, La Termotecnica, 1974
Dauer S., *Heizwert und Brennstoffkenngrössen*, Öl und Gasfeuerungen, 1966
De Graaf J.G.A., *Über den Mechanismus der Verbrennung von festem Kohlenstoff*, BWK, 1965
De Lecaux P., *La combustion des fuels sulfureux avec faible excès d'air*, Rev. Gen. de Termique, 1965
Diamant W., *La mécanique des suspensions et la longueur des flammes des brûleurs à mazout*, Rev. Gen. de Thermique, 1965
Dumex P., Delcroix J., *Etude thermique concernant les tubes à aillettes longitudinales*, 1963
Engler O., *Dampfkesselfeuerungen*, BWK, 1965
Estevenon P., *Mise au point de générateurs de vapeur à foyers-cyclones*, Rev. Gen. de Termique, 1965
Froelich P., *Auslegung von Brennkammer grosser Dampferzeuger*, Convegno ATI-VGB, 1973
Gilli P.V., Edler A., Halozan H., Schaup P., *Probleme des Wärmenüberganges, Druckverlustes und der Strömungstabilität in thermisch hochbeanspruchten Dampferzeugerrohren*, Convegno ATI-VGB, 1973
Grenlich H.S., *Combustione di carbone e di polverino di carbone nelle caldaie industriali*, Convegno ATI, 1969
Grimison E.D., *Correlation and utilization of new data on flow resistance and heat transfer for cross of gases over tube banks*, Trans. Amer. Soc. Mech. Engrs., 1937
Guglielmini G., Nannei E., *Sulle oscillazioni di temperatura superficiale in ebollizione nucleata*, Congresso ATI, 1972
Guidi L., *I vantaggi della caldaia a circolazione controllata e il suo sviluppo nel mercato italiano*, La Termotecnica, 1964
Gumz W., *Die Vorgänge in den Feuerungen bei hohen Temperaturen*, Mitt. WGB, 1955
Gupta V.S., *Solve heat transfer by nomograph*, Power, 1961
Hedley A.B., Brown T.D., *Low excess air protects boiler*, Power, 1963
Jarach F., *Le temperature in un preriscaldatore d'aria*, La Termotecnica, 1959
Konakow P.K., *Wärmeübertragung in Kesselfeuerungen*, Acad, Wiss. URSS, 1952
Manzi A., Noferini A., *Problema della riduzione dei depositi nelle zone ad alta temperatura delle caldaie alimentate con olio combustibile denso*, XIX Congresso ATI
Mirkovic Z., *Heat transfer and flow resistance correlation of helical finned tubes in cross flow of staggered tube banks*, Int. Seminar on Heat Exchanger, 1972
Niepenberg H., *Neue Untersuchungen und Betriebserfahrungen an ölgefeuerten Dampferzeuger*, VGB, 1963
Profos P., Sharan H.N., *L'influence du pas des tubes et leur arrangement surl'encrèssement des faisceaux tubulaires*, Rev. Tech. Sulzer, 1960
Sharan H., *HGE/HGK: Un nuovo sistema di combustione per la generazione di calore e vapore*, La Termotecnica, 1974

Thring M.W., *Il progetto di bruciatori con vortice d'aria*, Convegno ATI, 1969
Todd J., *Why boilers explode*, Power, 1964
Upmalis A., *Die Bemessung der Rippenhöhe bei Rippenrohren für Lufterhitzer*, BWK, 1962
Yudin V.F., Tokhtarova L.S., *Heat transfer and resistance of staggered bundles of tubes with transverse fin in a transverse flow*, Thermal Engineering, 1973
Zanchi C, *Considerazioni sulla regolazione automatica della combustione di grandi generatori di vapore*, Congresso ATI, 1962

Index

Absorption band, 242
Additive, 69, 103
Adiabatic temperature, 198
Air
  air drill, 61
  air index, 163, 171, 199, 211, 227, 276, 279, 286, 360
  air register, 131
  combustion air, 17, 30, 75, 167, 209, 227, 269, 281, 286
  compressed air, 28
  pushed air, 144
  swirl, 131, 138, 141
  theoretic air (stoichiometric air), 148, 151, 163, 278, 288
Anchorage, 24
Angle iron, 89
Antifoaming, 103
Antioxidant, 103
Ash, 2, 111, 117, 205, 287
Asphaltene, 117
Atomizing, 1, 129
Attemperator, 19, 65, 270
Automatic regulation, 321

Back-flow chamber, 388–389, 397
Baffle plate, 13
Balanced draught, 292
Blackbody, 200, 242
Black level, 242, 284
Blade, 12, 43, 131, 140, 322
Bomb calorimeter, 287
Boundary layer, 41, 72, 78, 118, 253, 360, 396
Branch, 335–342, 344–346
Bubble, 37, 217
Buckling, 89
Bulk temperature, 219, 226, 251, 252
Burner box, 269, 319
Burst, Bursting, 2, 8–9, 31, 38, 44, 63, 79, 81, 83
Butt welding, 89
Bypass, 367

Cast iron, 26, 47, 71–74, 143, 383, 384–387
Catalytic effect, 118
Cavity, 244–245, 247, 249, 383–385
Channel, 235
Chemical elements and compound
  benzol, 120
  calcium oxide, 120
  calcium sulfate, 113, 120
  carbon, 112, 148
  carbonate, 80
  carbon dioxide, 46, 146, 163, 172–173, 200, 242, 278
  carbon monoxide, 94, 118, 157, 163, 270–278
  chrome, 143
  clorobenzene, 103–104
  diphenyl, 103
  diphenyl oxide, 103
  dolomite, 120
  ethylene glycol, 103–104
  ferric oxide, 118
  heptane, 120
  hydrogen, 115, 148
  iron sulfide, 113
  marcasite, 113
  nickel, 143
  nitrogen, 106, 146, 158, 167, 173, 278
  oxygen, 151, 167, 172
  pearlitic iron, 143
  phenol, 103
  pyrite, 113

silicate, 80
silicon dioxide, 43–46
sodium, 69, 79
sodium sulphate, 113
sulfate, 43, 80
sulfric acid, 72, 82, 113, 117
sulfur, 78, 148, 360, 790
sulfur dioxide, 163
sulfur trioxide, 72
vanadium, 79
vanadium pentoxide, 69, 119
Chimney, 10–12, 28, 50, 286, 320–327, 379
Circulation
assisted circulation, 5–9, 19–23, 25, 328
circulation ratio, 41, 43, 329
forced circulation, 5, 20, 25, 80, 104, 251, 270
natural circulation, 5–8, 18, 25, 41, 398–399
recirculation, 3, 8, 17, 66–68
Clamping, 57
Coil, 25, 56, 61, 75, 105, 195, 250, 314, 404
Coke plant, 117
Cold rolled, 33
Collar, 14, 24–25
Combustion plant, 353, 357
Control board, 14
Conveyor belt, 2, 4
Corrosion, 360, 366–367
Cracking, 103, 109, 119, 131
Crate, 76, 78
Cyclone, 44, 136–137, 333
Cyclone burner, 2

Deflagration wave, 138
Dew point, 71, 113, 117–119
Diaphragm, 50, 91–93, 94, 105, 309
Diesel engine, 5, 26
Direct current motor, 326
Dissociation heat, 200
Downcomer, 7, 13, 19, 41–43, 48, 80, 328–329, 333, 335–337, 341–347, 398
Draught, 28, 327
Drum, 5–9, 13–50, 61, 66, 70, 81, 93, 95, 106, 108, 109, 271, 328, 353, 398

Elbow, 291, 310–311
Electrical conductivity, 47
Electric energy, 1, 353–355, 365
Emissivity, 2, 201, 228, 229, 231, 232
End plate, 87–88, 91, 92, 94, 98, 228, 250, 265, 353, 388
Enthalpy, 9, 48, 64, 177–180, 198, 199, 216, 270–271, 287, 289, 401
Erecting yard, 15
Expansion compensator, 312
External radiation, 48, 274–276, 284, 356
Eyepiece, 12, 24

Failure, 104–105
Fan, 10–12, 14, 33, 75, 78–79, 263, 273, 353
axial fan, 322–323
centrifugal fan, 322–324
pusher fan, 10–12, 17–18, 143, 292, 324, 326
recirculation fan, 17–18
suction fan, 10, 17, 28, 292, 324, 327
Felt, 104
Fillet weld, 89, 98
Film boiling, 31, 38–41, 80
Film temperature, 219, 220, 226, 235, 237, 363, 366
Fin, 29, 33–37, 74, 411–413
Fire point, 114
Fixed head, 106
Flame front, 138–139
Flash point, 117, 123, 134
Floating head, 106
Fluids
counterflow, 78, 136, 138, 140, 194–196, 255–256, 360, 370, 404–409
cross-flow, 195, 259–261, 404, 406, 409–410
fluid dynamic, 96, 98, 101, 383
fluid surface, 106
friction factor, 292, 294, 302, 340
laminar flow, 187, 294
parallel flow, 78, 194, 255, 367, 404–405, 407–410
turbulence, 1–2, 94, 138, 141, 220
turbulent flow, 41, 138, 187, 251, 293–294
Fouling, 80–81, 117, 120, 129
Framework, 24, 25
Fuel bed, 4
Fuels
anthracite, 111–114, 116, 145
bagasse, 3, 111
blast-furnace gas, 125, 151, 157, 164, 170, 202
blind coal, 276
cannel coal, 112
coal tar oil, 25, 116–117
coke, 111–112
coke oven gas, 2, 124–125, 167
fat coal, 112
fibrous lignite, 111
fuel oil, 1–3, 14, 25, 31–32, 48, 69, 71–72, 78, 99, 104, 113, 116–124, 129, 131–134, 137, 157–162, 169, 171, 181,

211, 247, 272–273, 279, 281, 286, 364–365, 383, 396
grapes (by-product of), 3, 111
lean coal, 112
lignite, 1–2, 25, 30, 111, 143, 149, 276
long-flaming coal, 144
low-grade fuel, 1, 3–4
methane, 145
natural gas, 1–3, 25–26, 31, 33, 72, 104, 124–126, 129–130, 157, 158, 171, 208, 212, 247, 279, 280, 365, 388, 391
oil shale, 116–117
olive (by-product of), 3, 111–112
peat, 111–112, 145
pitchy lignite, 111
pit coal, 111
process gas, 26
pulverized coal, 2–3, 25, 30, 61, 129, 134–137, 202, 212, 247
pulverized lignite, 25, 129
refinery gas, 2, 25, 125, 202
rice (by-product of), 3, 111
rich coal, 143–145
sawdust, 3, 111
town gas, 124, 126
water gas, 124
wood coal, 111
wooden shaving, 3, 111
xyloid lignite, 111
Full penetration, 35, 89

Galvanometer, 162
Gas network, 2
Gate valve, 312, 320
Glass furnace, 5, 26, 28
Gradient, 140, 300
Grate, 2–4, 143–145, 149, 201, 276
chain grate, 144, 149
tipping grate, 144–145
Gravitational acceleration, 324
Groove, 60, 89, 123, 131–132

Head, 6, 80, 105, 320, 322, 324, 326, 353
Header, 13, 19, 41–42, 48, 328
Heat balance, 261
Heat content, 48, 67, 204, 270–271, 273
Heat exchanger, 5, 25, 28, 47, 65, 71, 106, 108–109, 187
Heat of reaction, 277
Heat regenerator, 352, 369, 375, 379–380
Heat value, 4, 111–112, 117, 124, 143, 149, 151, 153, 157, 160, 199, 269, 272, 274, 276–277, 279, 281, 286, 287–288, 354, 356, 358
Heat of vaporization, 5, 40, 61, 329
Hopper, 2, 28, 205, 276
Hydraulic coupling, 326
Hydraulic diameter, 320
Hydrocarbon, 124–125, 145, 171, 278
Hydrostatic, 105
Hydrostatic pressure, 328
Hypercritical, 8, 25

Ignition limit, 125–126
Infrared, 242
Inspection door, 228
Insulating coating, 193
Interference, 58–59

Kinetic energy, 308–309, 314, 335

Latent heat, 375
Level, 96, 106
Level gauge, 46–47, 96
Liquid phase, 103
Load, 8–9, 18, 19–30, 63–64, 75, 94, 129, 209, 255, 326, 352, 357–359, 396
Load diagram, 75, 359
Lubricant, 103

Magnetic coupling, 326
Manhole, 89
Mean beam length, 61, 242, 244, 247, 249–250
Mean logarithmic temperature difference, 187, 194–197, 380
Melting point, 69, 111, 119–120, 134
Membrane wall, 13, 29, 33, 49
Mill, 2–3
Modular, 15, 25, 48
Moisture, 2, 48, 111–114, 116, 143–144, 175, 199, 227, 230, 240, 276, 286
Molecular weight, 120, 131, 146
Moving grate, 143–145

Natural draught, 10, 143
Nozzle, 78, 105, 120, 131, 287
Number of Nusselt (dimensionless), 218–220, 223, 237, 250–251
Number of Prandtl (dimensionless), 218, 222, 237, 240, 251
Number of Reynolds (dimensionless), 218–220, 223, 237, 241, 263–265, 293–298, 314, 316–318

One-trough generator, 6
Open-heart furnace, 26
Optical gauge, 89
Organic base, 103
Organic fluid, 250
Oxidation, 103, 106, 109

Paraffin base, 103
Partial pressure, 242, 244, 246–247
Peak flux, 228
Phosphate, 43, 46
Pig, 76
Plasticization, 56
Pocket, 76
Poisson's ratio, 53
Polymerization, 109
Porosity, 80, 111, 116
Post-combustion chamber, 391–392, 394
Pour point, 117, 122–123
Pressure gauge, 91
By-product, 2–3
Pump
  centrifugal pump, 320–322
  circulation pump, 6–8, 19, 105, 109, 328
  feed pump, 6–7, 41, 90, 106, 320
  piston pump, 320
  positive displacement pump, 106
  pumping plant, 1
  steam pump, 273

Refractory casting, 24, 49, 85, 91
Refractory material, 1, 4, 13, 89, 91–92, 104–105, 213, 327
Resistance welding, 26
Return tube, 8, 15, 19, 42, 48, 106, 336–337, 341–346, 398
Ring, 89
Roller, 56–57
Room temperature, 12, 48, 75, 78–79, 114, 199, 204–205, 215–216, 269, 281, 287, 356, 360
Rotor, 76
Roughness, 23, 291, 320, 332
Row, 14, 31, 90, 264

Safety valve, 320
Salinity, 43, 271
Scaling, 34, 37, 79, 214
Scaling temperature, 214
Seal, 12, 28, 49–50, 59, 77, 81, 91, 94
Self-limiting, 324
Sensible heat, 26, 70, 148, 162–163, 274–276, 281–283, 284, 286, 356, 391
Service gangway, 24
Servomotor, 326
Setup, 8, 30
Shutdown, 47, 81, 90, 106
Sludge, 9, 47, 103
Smoke-box door, 87, 89, 92, 94
Softening, 113–114
Solvent, 103
Soot, 12, 28, 72, 276, 286
Soot blower, 12, 24, 28, 72, 78, 264
Soot precipitator, 12, 17, 276, 287, 319
Specific heat, 104, 111, 116–117, 156, 172–176, 188, 199, 201, 205, 208, 219, 223, 286–287, 356, 373, 401
Specific volume, 224–225, 329
Starting, 1, 8, 9, 64, 81, 106, 129
Stator, 76
Steady-state condition, 8
Steam
  condensing steam, 65
  reheated steam, 25
  saturated steam, 4, 16, 17, 47, 61, 106, 289, 328, 384
  steam accumulator, 9
  steam bubble, 217–218
  steam chamber, 42–44, 93, 95–96
  steam dryer, 8
  steam engine, 320
  superheated steam, 7, 18, 29, 32, 63–64, 66, 120, 214, 382
Steel
  alloy steel, 79
  austenitic steel, 25
  carbon steel, 79
  lowalloy steel, 25
  refractory steel, 14
  stainless steel, 129
Steel concrete, 327
Stiffening rib, 89
Stocking, 1–2
Stocking tank, 1
Stoker, 47, 81, 110
Stress, 34, 52–54, 56–59, 79, 81, 327
Sub-critical, 25
Sugar cane, 3
Surface tension, 119
Swabbing, 94, 253

Tangential combustion, 30
Tank, 307–309
Taper fin, 36–37
Tee bar, 89
Tempering gas, 215–217
Theoretic gas, 278
Thermal conductivity, 34, 37, 80–81, 104, 111, 117, 124, 162, 179–186, 188, 218, 251–252
Thermal expansion, 34, 105
Thermal flux, 22–23, 31, 35, 37, 38–40, 50, 69, 80, 92, 109, 228, 251, 339, 399
Thermal inertia, 104–105
Thermal load, 30, 100, 101, 105, 109, 136, 266

Thermal shock, 96
Thermocouple, 23, 81
Thermodynamic, 2, 98, 255, 344, 383
Thermoelectric power plant, 1, 17
Thermostat, 66, 106
Tie rod, 14, 24, 87
Toxicity, 103
Tubes
  arrangement, 236–239, 241, 263–264, 265, 315–318
  arrangement factor, 237–239, 263, 316–318
  depth factor, 237
  expanded tube, 48
  expander, expanding machine, 56–57, 61, 74
  finned tube, 26, 47, 49, 71–73, 252–253, 319, 383–384, 386–390, 391, 394–395, 410–411, 417
  in-line tubes, 236, 247–248, 264–265, 315–317
  pitch, 60, 73–75, 213, 237, 263, 315, 353
  staggered tubes, 48, 73, 236–237, 248, 263, 316–318
  tube expanding, 56–61, 93
Tubesheet, 60, 87, 89, 91–99, 96, 97–98, 101, 353
Turbines
  back-pressure turbine, 26–27
  closed-cycle turbine, 26
  gas turbine, 5, 26
  steam turbine, 26, 273

Unburned carbon monoxide, 48, 114, 129, 148, 149, 157, 161, 273, 274, 277–280, 288, 356
Unburned fuel, 202, 274, 276–277, 282, 288
Unburned material, 94, 164
Unit heater, 11–12, 18, 79, 319

Vapor tension, 106, 119
Venturi meter, 287
Viscosity, 1, 103, 105–106, 111, 133, 136, 188, 251, 291, 332
  dynamic viscosity, 120–121, 183–186, 219, 251, 296–297, 340
  kinematic viscosity, 121–122, 218, 302
  viscosimeter, 121
Volatile matter, 2, 111–112, 115–116, 134, 143–144, 205, 207

Water
  evaporating water, 37
  evaporation temperature, 347
  feed water, 14, 46, 71–72, 96, 270
  hot water, 226
  saturated water, 347, 401
  superheated water, 106, 226, 269
  water content, 9–10
  water drainage, 43, 271, 273, 287, 320
  water evaporation, 61
  water gauge, 353
  water heater, 71
  water injection, 65, 21, 270–27
  water level, 42, 47, 89
  water surface, 42, 328, 495–496
  water vapor ratio, 8, 38–41, 43–45, 289
Wave length, 242
Wear, 91, 94, 307
Wet perimeter, 235, 292
Wheel, 12, 28, 322

Yield strength, 57, 60